



449722

pgs 228

Unsteady High Turbulence Effects on Turbine Blade Film Cooling Heat Transfer Performance Using a Transient Liquid Crystal Technique

J.C. Han, S.V. Ekkad, H. Du, and S. Teng
Texas A&M University, College Station, Texas

The NASA STI Program Office . . . in Profile

Since its founding, NASA has been dedicated to the advancement of aeronautics and space science. The NASA Scientific and Technical Information (STI) Program Office plays a key part in helping NASA maintain this important role.

The NASA STI Program Office is operated by Langley Research Center, the Lead Center for NASA's scientific and technical information. The NASA STI Program Office provides access to the NASA STI Database, the largest collection of aeronautical and space science STI in the world. The Program Office is also NASA's institutional mechanism for disseminating the results of its research and development activities. These results are published by NASA in the NASA STI Report Series, which includes the following report types:

- **TECHNICAL PUBLICATION.** Reports of completed research or a major significant phase of research that present the results of NASA programs and include extensive data or theoretical analysis. Includes compilations of significant scientific and technical data and information deemed to be of continuing reference value. NASA's counterpart of peer-reviewed formal professional papers but has less stringent limitations on manuscript length and extent of graphic presentations.
- **TECHNICAL MEMORANDUM.** Scientific and technical findings that are preliminary or of specialized interest, e.g., quick release reports, working papers, and bibliographies that contain minimal annotation. Does not contain extensive analysis.
- **CONTRACTOR REPORT.** Scientific and technical findings by NASA-sponsored contractors and grantees.

- **CONFERENCE PUBLICATION.** Collected papers from scientific and technical conferences, symposia, seminars, or other meetings sponsored or cosponsored by NASA.
- **SPECIAL PUBLICATION.** Scientific, technical, or historical information from NASA programs, projects, and missions, often concerned with subjects having substantial public interest.
- **TECHNICAL TRANSLATION.** English-language translations of foreign scientific and technical material pertinent to NASA's mission.

Specialized services that complement the STI Program Office's diverse offerings include creating custom thesauri, building customized data bases, organizing and publishing research results . . . even providing videos.

For more information about the NASA STI Program Office, see the following:

- Access the NASA STI Program Home Page at <http://www.sti.nasa.gov>
- E-mail your question via the Internet to help@sti.nasa.gov
- Fax your question to the NASA Access Help Desk at (301) 621-0134
- Telephone the NASA Access Help Desk at (301) 621-0390
- Write to:
NASA Access Help Desk
NASA Center for Aerospace Information
7121 Standard Drive
Hanover, MD 21076



Unsteady High Turbulence Effects on Turbine Blade Film Cooling Heat Transfer Performance Using a Transient Liquid Crystal Technique

J.C. Han, S.V. Ekkad, H. Du, and S. Teng
Texas A&M University, College Station, Texas

Prepared under Grant NAG3-1656

National Aeronautics and
Space Administration

Glenn Research Center

Available from

NASA Center for Aerospace Information
7121 Standard Drive
Hanover, MD 21076
Price Code: A11

National Technical Information Service
5285 Port Royal Road
Springfield, VA 22100
Price Code: A11

Table of Contents

	Page
1.0 Project Summary	1
2.0 Introduction	4
2.1 Background.....	4
2.2 Objective.....	9
3.0 Test Apparatus and Data Analysis	12
3.1 Test Apparatus and Instrumentation	12
3.2 Test Conditions and Data Analysis.....	21
4.0 Results and Discussion	24
4.1 Detailed Film Cooling Effectiveness Measurements over A Film-Cooled Gas Turbine Blade (Steady Flow).....	24
4.2 Effect of Unsteady Wake on Film Cooling Performance for A Film-Cooled Gas Turbine Blade.....	33
4.3 Effect of Unsteady Wake with Trailing Edge Coolant Ejection on Detailed Heat Transfer Coefficient for A Uncooled Gas Turbine Blade.....	45
4.4 Effect of Unsteady Wake with Trailing Edge Coolant Ejection on Film Cooling Performance for A Film-Cooled Gas Turbine Blade.....	50
4.5 Unsteady Wake Effect on Film Temperature and Effectiveness Distributions for A Gas Turbine Blade with Only One Row of Film Holes Near the Gill Hole Portion.....	61
4.6 Detailed Film Cooling Measurements on A Cylindrical Leading Edge Model: Effect of Free-Stream Turbulence and Coolant Density.....	69
4.7 Film Temperature Measurements on A Cylindrical Leading Edge Film Cooling Model.....	78
5.0 Conclusions	81
5.1 Conclusions on Gas Turbine Blade Models.....	81
5.2 Conclusions on Cylindrical Leading Edge Models.....	83
6.0 References	85
7.0 Appendix	92
7.1 Figures 1 – 64.....	92
7.2 Tabulated Spanwise-Averaged Data.....	160

NOMENCLATURE

C_x	blade axial chord length (17cm)
d	wake generator rod diameter
D	film hole diameter
DR	coolant-to-mainstream density ratio, ρ_c/ρ_m
h	local heat transfer coefficient
I	coolant to mainstream momentum flux ratio, $\rho_c V_c^2/\rho_m V^2$
k	thermal conductivity of blade material (0.159 W/m•°C)
k_{air}	thermal conductivity of mainstream air
L	film cooling delivery length
M	coolant-to-mainstream mass flux ratio or blowing ratio, $\rho_c V_c/\rho_m V$
M_t	trailing edge coolant-to-mainstream mass flux ratio or blowing ratio, $\rho_j V_j/\rho_m V$
n	number of rods on wake generator
N	speed of rotating rods
Nu	local Nusselt number based on axial chord, hC_x/k_{air}
\bar{Nu}	spanwise-averaged Nusselt number
P	film hole pitch
PL	streamwise length on the pressure surface (25.6 cm)
Re	Reynolds number based on exit velocity and axial chord, $V_2 C_x/\nu$
S	wake Strouhal number, $2\pi N d n/(60 V_1)$
SL	streamwise length on the suction surface (33.1cm)
t	liquid crystal color change time
T_c	coolant temperature
T_f	film temperature
T_i	initial temperature of blade surface
T_m	mainstream temperature
Tu	free-stream turbulence intensity
$\tilde{T}u$	Ensemble-averaged turbulence intensity
$\bar{T}u$	time-mean averaged free-stream turbulence intensity
T_w	liquid crystal color change from green to red

V	local mainstream velocity along the blade pressure or suction surface
$V(t)$	instantaneous velocity at cascade inlet
\tilde{V}	Ensemble-averaged cascade inlet velocity
V_1	cascade inlet velocity
V_2	cascade exit velocity
V_c	coolant hole exit velocity
VR	coolant-to-mainstream velocity ratio, V_c/V
X	streamwise distance from blade leading edge; streamwise distance from centerline of film cooling holes
Y	radial distance from blade surface
α	thermal diffusivity of blade material ($0.135 \times 10^{-6} \text{ m}^2/\text{s}$)
δ_2	local momentum thickness
η	local film cooling effectiveness
$\bar{\eta}$	spanwise-averaged film cooling effectiveness
ν	kinematic viscosity of cascade inlet mainstream air
ρ_c	coolant density
ρ_j	density of trailing edge jet
ρ_m	mainstream flow density

1.0 PROJECT SUMMARY

Unsteady wake effect on detailed heat transfer coefficient and film cooling effectiveness distributions is presented for a downstream film-cooled gas turbine blade. The detailed heat transfer coefficient and film effectiveness distributions on the blade surface are obtained using a transient liquid crystal technique. The blade surface is coated with a thin layer of thermochromic liquid crystal and transient tests are run to obtain the heat transfer coefficients and film cooling effectiveness. Upstream unsteady wakes are simulated using a spoke-wheel type wake generator. Tests were performed on a five-blade linear cascade at an axial chord Reynolds number of 5.3×10^5 at cascade exit. The test blade has three rows of film holes on the leading edge and two rows each on the pressure and suction surfaces. Air and CO_2 were used as coolants to simulate different coolant-to-mainstream density ratio effect. Coolant blowing ratio is varied from 0.4 to 1.2. Results show that Nusselt numbers for a film-cooled blade are much higher compared for a blade without film injection. Particularly, film injection causes earlier boundary layer transition on the suction surface. Unsteady wake slightly enhances Nusselt numbers but significantly reduces film cooling effectiveness on a film-cooled blade compared with a film-cooled blade without wake. Nusselt numbers increase slightly but film cooling effectiveness increases significantly with an increase in blowing ratio for CO_2 injection. Higher density coolant (CO_2) provides higher effectiveness at higher blowing ratios ($M=1.2$) whereas lower density coolant (Air) provides higher effectiveness at lower blowing ratios ($M=0.8$).

The effect of unsteady wakes with trailing edge coolant ejection on surface heat transfer coefficients and film cooling effectiveness is also presented for the same downstream film-cooled turbine blade. The coolant jet ejection is simulated by ejecting coolant through holes on the hollow spokes of the wake generator. For a blade without film holes, unsteady wake increases both pressure side and suction side heat transfer levels due to early boundary layer transition. Adding trailing edge ejection to the unsteady wake further enhances the blade surface heat transfer coefficients particularly near the leading edge region. For a film-cooled blade, unsteady wake effects slightly enhance surface heat transfer coefficients but significantly reduces film effectiveness. Addition of trailing edge ejection to the unsteady wake has a small effect on surface heat transfer coefficients compared to other significant parameters such as film injection, unsteady wakes, and grid generated turbulence, in that order. Trailing edge ejection has more effect on film effectiveness distribution than on the heat transfer coefficients.

The film effectiveness and coolant jet temperature profile on the suction side of a gas turbine blade were measured over a turbine blade using a transient liquid crystal and a cold-wire technique, respectively. The blade has only one row of film holes near the gill hole portion on the suction side of the blade. Tests were performed on a five-blade linear cascade in a low-speed wind tunnel. The mainstream Reynolds number based on cascade exit velocity was 5.3×10^5 . Upstream unsteady wakes were simulated using a spoke-wheel type wake generator. Coolant blowing ratio was varied from 0.6 to 1.2. Wake Strouhal number was kept at 0 and 0.1. Results show that unsteady wake reduces film cooling effectiveness. Results also show that film injection enhances local heat

transfer coefficient while the unsteady wake promotes earlier boundary-layer transition. The development of coolant jet mean temperature and temperature fluctuation profiles could be used to explain the film cooling performance.

Detailed heat transfer coefficient and film effectiveness distributions as well as film temperature profiles are presented on a cylindrical leading edge model. Tests were done in a low speed wind tunnel on a cylindrical model in a crossflow with two rows of injection holes. Mainstream Reynolds number based on the cylinder diameter was 100,900. The two rows of injection holes were located at $\pm 15^\circ$ from stagnation. The film holes were spaced 4-hole diameters apart and were angled 30° and 90° to the surface in the spanwise and streamwise directions, respectively. Heat transfer coefficient and film effectiveness distributions are presented on only one side of the front half of the cylinder. Film coolant temperature distributions are taken at 20° , 30° , 50° , and 70° from stagnation and presented as mean temperature and temperature fluctuation. Air and CO_2 were used as coolant to simulate coolant-to-mainstream density ratio effect. The effect of coolant blowing ratio was studied for blowing ratios of 0.4, 0.8, and 1.2. Results show that Nusselt numbers downstream of injection increase with an increase in blowing ratio for both coolants. Air provides highest effectiveness at blowing ratio of 0.4 and CO_2 provides highest effectiveness at a blowing ratio of 0.8. Higher density coolant (CO_2) provides lower Nusselt numbers at all blowing ratios compared to lower density coolant (air). An increase in free-stream turbulence has very small effect on Nusselt numbers for both coolants. However, an increase in free-stream turbulence intensity (up to 7%) reduces film effectiveness significantly at low blowing ratios for both coolants.

2.0 INTRODUCTION

2.1 Background

A continuing trend towards higher gas turbine inlet temperatures has resulted in higher heat loads on turbine components. Sophisticated cooling techniques are employed to cool the components to maintain the performance requirements. Some turbine blades are cooled by ejecting cooler air from within the blade through discrete holes to provide a protective film on the surface exposed to hot gas path.

Many studies have presented heat transfer measurements on turbine blades with film cooling. Nirmalan and Hylton (1990) and Abuaf et al. (1995) studied heat transfer on film cooled turbine vanes. Camci and Arts (1990) studied heat transfer coefficients on film cooled turbine blades. Takeishi et al. (1992) compared the film effectiveness values for a stationary cascade under 4% mainstream turbulence intensity and for a rotor blade using the heat-mass transfer analogy. Ito et al. (1978) and Haas et al. (1992) studied the effect of coolant density on film effectiveness on turbine blades under low mainstream turbulence levels. Ito et al. (1978) found that an increase in coolant-to-mainstream density ratio causes an increase in film effectiveness on both pressure and suction surfaces for a blowing ratio of 1.0. Haas et al. (1992) found their results show the same trends as that of Ito et al. (1978). They reported that an increase in density ratio for a low blowing ratio of 0.5 causes a decrease in film effectiveness on the suction surface. However, an increase in density ratio causes an increase in film effectiveness at higher blowing ratios. Ames (1998) reported the influence of high free-stream turbulence on turbine vane heat transfer coefficient and film effectiveness distribution.

The effect of unsteady wakes produced by upstream vane trailing edges has a strong effect on rotor blade surface heat transfer distributions. Several studies have focused on the effect of unsteady wake on the downstream blade heat transfer coefficient distributions without film cooling. Many researchers, for example, Abhari et al. (1994), Blair et al. (1989), Blair (1994), Doorly (1988), Dullenkopf et al. (1991), Dullenkopf and Mayle (1994), Dunn et al. (1989, 1994), Han et al. (1993), Liu and Rodi (1992), O'Brien and Capp (1989), Wittig et al. (1987) have studied the effect of unsteady wakes caused by trailing edges of the vanes and the blade rotation on the surface heat transfer coefficient of the downstream blades. Ashworth et al. (1985), Doorly and Oldfield (1985), and Zhang and Han (1995) studied the combined effect of free-stream turbulence and wake passing on turbine blade heat transfer. They all reported that unsteady wake enhanced turbine blade heat transfer and caused earlier and longer laminar-turbulent boundary layer transition on the suction surface. Few studies have focused on the effect of unsteady wakes on film cooled turbine blades. Abhari and Epstein (1994) conducted heat transfer experiments on a fully cooled transonic turbine stage in a short duration turbine facility. They measured steady and time-resolved chord-wise heat flux distributions at three spanwise locations. They concluded that film cooling reduces the time-averaged heat transfer by about 60% on the suction surface compared to the uncooled rotor blade. However, the effect is relatively low on the pressure surface. Ou et al. (1994), and Mehendale et al. (1994) simulated unsteady wake conditions over a linear turbine blade cascade with film cooling. They studied the effects of unsteady wake on a model turbine blade with multiple-row film cooling using air and CO₂ as coolants. They measured heat transfer coefficients and film cooling effectiveness at discrete

locations using thin foil heating and multiple thermocouples. They concluded that heat transfer coefficient increases and film cooling effectiveness decreases with an increase in unsteady wake strength. They also concluded that the higher density (CO_2) coolant provides better film cooling effectiveness at higher blowing ratios than lower density coolant (air).

In gas turbine engines the unsteady wakes generated by the trailing edges of the upstream vanes and the blade rotation significantly influence the downstream rotor blade heat transfer. The upstream vanes are internally cooled and hence some coolant is ejected through ejection holes located at the trailing edge. This coolant ejection combined with the unsteady wake further affects heat transfer coefficients on the downstream rotor blade. Heat transfer coefficients on downstream blades under the effects of unsteady wake and trailing edge ejection are important for design considerations. Dunn (1986) measured heat flux for the rotor blade of a Garrett TFE 731-2 hp full stage rotating turbine with upstream nozzle guide vane (NGV) trailing edge injection. They found that the NGV injection effect is to significantly increase the local blade heat transfer up to 20 percent of the streamwise distance from the leading edge on the suction surface and ten percent on the pressure surface.

The leading edge of the turbine blade is the most critical heat transfer region as some of the highest heat transfer occurs in that region. So, film cooling near the turbine blade leading edge is essential to protect the blade from the hot gases and prevent failure. The inlet high temperature gases from the combustor to the turbine inlet are highly turbulent. Also, since the coolant is cooler than the mainstream, the coolant is at a higher density than the mainstream. The influence of free-stream turbulence and coolant density

on the turbine blade leading edge film effectiveness and heat transfer coefficients are important. The leading edge region of the turbine blade has been a focus for many film cooling studies. Luckey and L'Ecuyer (1976) and Bonnice and L'Ecuyer (1983) studied a circular cylinder with several rows of spanwise injection holes to model the leading edge region. They reported that the surface heat flux was very much dependent on the injection geometry and coolant blowing ratio. Mick and Mayle (1988) studied film cooling on a blunt body with a semi-circular leading edge and flat after body. They concluded that leading edge injection reduces the surface heat load for lower blowing ratios. They also determined that the regions of high effectiveness do not necessarily correspond to the regions having a high heat transfer coefficient. Karni and Goldstein (1990) used the naphthalene sublimation technique to study the effects of surface injection on local mass transfer from a circular cylinder in crossflow with one row of inclined holes. Mehendale and Han (1992) studied the effect of free-stream turbulence on leading edge film effectiveness and heat transfer coefficient. They reported that high free-stream turbulence reduced film effectiveness and enhanced heat transfer coefficient. Ou et al. (1992) studied the effect of film hole row location on the same test model as that of Mehendale and Han (1992). They reported that film cooling effectiveness was higher for injection farther downstream from the true leading edge. Ou and Han (1992) studied the effect of slot injection and free-stream turbulence on the blunt body model. Salcudean et al. (1994) studied the effect of coolant density on film effectiveness on a semi-circular leading edge with a flat afterbody. They reported that higher density fluid (CO_2) provides highest effectiveness at a higher blowing ratio compared to a lower density fluid (air), particularly farther downstream of injection. Lee et al. (1994) studied the effect of free-

stream turbulence and horse-shoe vortices on mass transfer on a film cooled cylinder. They reported that an increase in free-stream turbulence reduces the effects of horse-shoe vortex structure. Funazaki et al. (1995) studied the effects of periodic wake passing on film effectiveness around the leading edge of a blunt body. They reported a decrease in film effectiveness with an increase in wake strength.

In recent years, liquid crystal techniques have been used extensively for heat transfer measurements. The two main advantages of this technique over the classical techniques are high spatial resolution and good geometrical adaptability. In addition to those advantages, Hippensteele et al. (1983) indicated that, unlike thermocouples, liquid crystal coatings are non-intrusive and cheaper and, therefore, could be a superior alternative to thermocouples for the low temperature tests. Vedula and Metzger (1991) presented a transient liquid crystal technique for detailed measurements of both heat transfer coefficients and film cooling effectiveness over a flat surface with one row of simple angle injection holes. Martinez-Botas et al. (1995) presented detailed heat transfer coefficient distributions on a non-film cooled blade in an annular transonic cascade using a transient liquid crystal technique. Hoffs et al. (1997) measured heat transfer coefficients in a linear cascade without film cooling using a transient liquid crystal technique and compared the results with measurements using the naphthalene sublimation mass transfer technique. Other studies such as Ekkad et al. (1997a-b) presented detailed heat transfer coefficient and film effectiveness distributions on a flat surface with compound angle injection. They used a transient liquid crystal technique for detailed heat transfer coefficient and film effectiveness measurement. Drost and Bölcs

(1998) also reported detailed heat transfer coefficient and film effectiveness distributions on a turbine vane using a transient liquid crystal technique.

The measurement of coolant jet temperature field using cold-wire is well described in the study of Kohli and Bogard (1998). Their study has focused on temperature measurements in a film cooling flow field on the flat plate. A high-frequency-response temperature sensor was used, which provided information about film cooling flow in terms of actual turbulence levels and probability density functions of the thermal field. They concluded that film cooling jets tend to lift off the surface with higher blowing ratio and lateral injection yields a more uniform distribution of effectiveness immediately downstream of injection.

2.2 Objective

The objectives of this study are:

- (1) **The effect of unsteady wake on turbine blade heat transfer coefficient and film cooling effectiveness distributions.** Tests were performed on a five-blade linear cascade in a low speed wind tunnel at an axial chord Reynolds number of 5.3×10^5 at cascade exit. Upstream unsteady wakes are simulated using a spoke-wheel type wake generator. The test blade has three rows of film holes on the leading edge and two rows each on the pressure and suction surfaces. Air and CO₂ were used as coolants to simulate different coolant-to-mainstream density ratio effect. Coolant blowing ratio is varied from 0.4 to 1.2. The detailed heat transfer coefficient and film

effectiveness distributions on the blade surface are obtained using a transient liquid crystal technique.

- (2) **The effect of unsteady wake with trailing edge coolant ejection on the downstream blade heat transfer coefficient and film cooling effectiveness distributions.** Tests were performed on a five-blade linear cascade in a low speed wind tunnel. The test blade has three rows of film holes on the leading edge and two rows each on the pressure and suction surfaces. The exit Reynolds number based on the blade axial chord is varied from 5.3×10^5 to 7.6×10^5 for the heat transfer coefficient measurement and is 7.6×10^5 for the film cooling effectiveness measurement. Unsteady wakes are produced by a spoked wheel-type wake generator upstream of the five-blade linear cascade. The coolant jet ejection is simulated by ejecting coolant through holes on the hollow spokes of the wake generator.
- (3) **The effect of unsteady wake on film temperature and effectiveness distributions for a gas turbine blade with only one row of film holes near the gill hole portion.** Tests were performed on a five-blade linear cascade in a low-speed wind tunnel. The mainstream Reynolds number based on cascade exit velocity was 5.3×10^5 . Upstream unsteady wakes were simulated using a spoke-wheel type wake generator. Coolant blowing ratio was varied from 0.6 to 1.2. Wake Strouhal number was kept at 0 and 0.1. The film temperature distributions are measured at $X/D=1, 5, 10$ and 15 from the centerline of the film cooling holes. The film mean temperature and temperature fluctuation profiles are measured using a cold-wire technique.
- (4) **The effect of free-stream turbulence on leading edge region heat transfer coefficient and film cooling effectiveness distributions and film temperature**

profiles. Tests were done in a low speed wind tunnel on a cylindrical model in a crossflow with two rows of injection holes. Mainstream Reynolds number based on the cylinder diameter was 100,900. The two rows of injection holes were located at $\pm 15^\circ$ from stagnation. The film holes were spaced 4-hole diameters apart and were angled 30° and 90° to the surface in the spanwise and streamwise directions, respectively. Heat transfer coefficient and film effectiveness distributions are presented on only one side of the front half of the cylinder. Air and CO_2 were used as coolant to simulate coolant-to-mainstream density ratio effect. The effect of coolant blowing ratio was studied for blowing ratios of 0.4, 0.8, and 1.2. Film coolant temperature distributions are taken at 20° , 30° , 50° , and 70° from stagnation and presented as mean temperature and temperature fluctuation.

3.0 TEST APPARATUS AND DATA ANALYSIS

3.1 Test Apparatus and Instrumentation

Figure 1 shows the schematic of the test section and camera locations for the detailed film cooling measurements over a gas turbine blade model without wake effect. The test apparatus consists of a low speed wind tunnel with a suction type blower. The five-blade linear cascade is shown in the figure. The mainstream turns 107.49° and the flow is accelerated 2.5 times from inlet to exit of cascade.

A 25-HP AC motor powers the suction blower. The rotation speed of the motor is varied by adjusting a frequency controller to obtain the different Reynolds numbers. The mainstream Reynolds number based on axial chord length of the blade is 5.3×10^5 . The blade configuration is designed to produce a similar velocity ratio (V/V_2) distribution as in a typical advanced high pressure turbine blade cascade. The selected blade has a 107.49° turning with relative flow angles of 35° and -72.49° at the blade inlet and outlet, respectively. Each blade in the linear cascade has an axial chord length of 17 cm and radial span of 25.2 cm. The blade-to-blade spacing is 17.01 cm at the cascade inlet and the blade throat-to-span ratio is 5. The blade configuration, scaled up five times, produces a velocity distribution typical of an advanced high pressure turbine blade row.

A calibrated, single hot wire is used to measure the instantaneous velocity from which the time mean turbulence intensity and ensemble-averaged velocity and the turbulence intensity can be evaluated. The hot wire sensor is vertically oriented at the inlet of the pressure side passage of the test blade, 8.82cm downstream of the spokes, and connected to a three-channel TSI IFA 100 constant Temperature Anemometer (CTA).

The analog signal from the anemometer is converted to digital by a 250kHz Data Translation DT2831G A/D board installed in a PC.

A heater box, shown in Figure 1 (Figure 3(c) shows the schematic diagram of its cross section), is used to preheat the middle test blade prior to the transient test. The same blade is coated with a thin layer of thermochromic liquid crystals. The blade surface color changes during the transient test is analyzed using a high-speed, high-resolution image processing system. The image processing system consists of four cameras individually connected to a color frame grabber board inside the PC. The cameras are focused using a color monitor. A software is used to digitize the liquid crystal color changes. During a transient test, only one camera is operational. Since the color changes are processed real time and no frames are stored in the PC, the frame speed will be reduced if all the four cameras are operated at the same time. Hence, four separate tests are required to map the entire blade surface using four different camera locations as shown in the figure.

The surface of the center blade is painted black and uniformly coated with liquid crystals (BM/R32C5W/17-10). The temperatures at which liquid crystal color changes from colorless to red, red to green, and green to blue are 31.6°C, 32.7°C, and 37.2°C, respectively. In the experiment the test blade was heated uniformly using a box-type heater. The transient test requires that the blade be heated to a temperature higher than the liquid crystal color range (37.2°C). During the transient test, the hot blade surface is suddenly cooled by exposing it to a cooler mainstream flow. The heater box has the blade profile and is slightly larger than the test blade. A gap of 10 mm exists between the blade outside surface and the heater box inner surface. The insides of the heater box are instrumented with thin foil heaters and controlled using several variacs to provide a near

uniform blade surface temperature. The heater box is lowered to completely cover the test blade during heating. The blade surface temperature is monitored using embedded thermocouples during heating. The uniformity of surface temperature with heating is within 1.2°C . An interpolation scheme was used to further reduce the temperature variation in the initial surface temperature to within 0.2°C . When the surface is heated to the required uniform temperature, the suction type blower is switched on. The mainstream reaches full flow within 20-30 seconds. Once the mainstream has reached required flow, the heater box is lifted up completely to expose the test blade to the mainstream. The coolant flow and the image processing system are automatically triggered at the same instant the test surface is exposed to the mainstream. The color changes during the transient test are monitored by the system. The times of color change on the blade surface to red at every pixel location is measured.

Before the blade surface is heated, the camera is focused on the particular region of the blade. The blade is uniformly illuminated such that the entire region the camera is focused on indicates uniform background intensity. This intensity and light settings help in correcting camera angles and blade curvature problems indicated by other studies using liquid crystal techniques. Once the heater box is lifted, the color intensity profiles at each pixel on the region are analyzed during the transient test. Once the required color intensity is matched, the actual time of color change for a particular color band appearance is noted. This color change time is used in the data analysis explained in the next section.

Figure 2 shows the schematic of the test section and camera locations for the detailed film cooling measurements over a gas turbine blade model with wake effect.

The test apparatus is the same as that in Figure 1 except for the spoked wheel type wake generator. The wake generator, similar to the one used by Ou et al. (1994), simulated the upstream unsteady wake. The wake generator has 32 rods, each 0.63cm in diameter, to simulate the trailing edge of an upstream vane. It is covered with a casing to prevent leakage flow, and the center is located below the bottom wall of the wind tunnel. The blade cascade is installed downstream of the wake generator. The wake generator is driven by a 2.2 kW DC motor. The wake Strouhal number is adjusted by controlling the motor speed (N). The wake generator rotation speed is measured by a DT-36M digital photo tachometer. The error caused by using nonparallel rotating rods with a linear blade cascade was small and is discussed by Ou et al. (1994).

Figure 3(a) - (e) present the section of the film cooled turbine blade model. The coolant is supplied to various locations on the blade surface through five cavities. The first cavity supplies coolant to the three leading edge film hole rows and each of the other four cavities supply coolant to each row on the pressure and suction surfaces. Coolant is fed into each cavity from the bottom of the blade and flow rate into each cavity is controlled using a flowmeter. The coolant flow from each flowmeter is passed through a solenoid-controlled three-way diverter valve before the flow enters the coolant cavity inside the blade. Each solenoid controlled valve is connected to a switch which triggers the coolant flow into the cavities at the instant the transient test is initiated. The blade film hole row geometry and configuration are shown in the figure. Figure 3(a) also presents a 3-dimensional view of the pressure and suction surfaces of the test blade. The liquid crystal coated surface area is 15.2 cm wide and the data acquiring area is 7.6 cm wide along the midspan region of the test blade as shown in Figure 3(b).

Figure 4 shows the schematic of the test section and camera arrangement for the heat transfer and film cooling measurements on a gas turbine blade with the combined effect of unsteady wake and trailing edge coolant ejection. For the heat transfer coefficient measurement, a smooth-surface blade model has been used. For the film cooling measurement, a film-cooled turbine blade model as shown in Figure 3 has been used. The spoked wheel-type generator has 32 hollow rods to simulate the trailing edge of an upstream blade row. There are 32 ejection holes opening towards the downstream blade to simulate the trailing edge ejection on each rod. The ejection holes have the diameters of 0.16cm and are evenly spaced at three hole diameters apart from one another. Figure 5(a) presents a detailed sketch of the rotating rod. The compressed air source is connected to the rotation union, through which the air is transported to the hub and then to the ejection holes on the hollow rods. Figure 5(b) shows the conceptual view of the unsteady wakes generated by the rotating rods with coolant ejection passing the blade cascade in which the inlet velocity direction of the free-stream and the coolant jet velocity direction are indicated.

A turbulence grid is installed 60cm upstream of the test blade to generate free-stream turbulence. A turbulence intensity of five percent at the inlet of the pressure passage of the test blade is obtained without the spokes. The grid is made of hollow brass tubes 1.2cm square in cross section and 4.8cm in pitch. The width and the height of the grid are the same as that of the wind tunnel. The open area ratio of the grid is 54 percent.

Figure 6 presents the experiment setup for studying unsteady wake effect on the film temperature and effectiveness distributions on a turbine blade model with only one row of film holes near the gill hole portion on the suction side of the blade. There is

one cavity used to supply coolant to the row of film holes on the suction side. The film holes, 1.905mm in diameter and 10.16mm apart from one another ($P/D=5.3$), have a radial angle of 90° and a tangential angle of 40° . The film hole length is 15mm ($L/D=7.9$). Flow rate is controlled by a flowmeter. The heated coolant flow is passed through a solenoid-controlled three-way diverter valve before the flow enters the coolant cavity inside the blade. The solenoid-controlled valve is connected to a switch that triggers the heated coolant flow into the cavity at the instant the transient test is initiated.

For the film cooling effectiveness measurements, the liquid crystal coated surface area is 7.2cm wide and the data acquisition area is 2.5cm wide along the midspan region of the test blade. The system consists of 2 cameras individually connected to a color frame grabber board in the PC and a monitor. Software is used to measure the time of color change of liquid crystals. During one test, only one camera is operational. Hence, we require 2 different runs with 2 different camera locations to measure one set of data on the suction side for a particular condition.

The film temperature distributions are measured at $X/D=1, 5, 10, 15$ from the centerline of the film cooling holes as shown in Figure 7. The measuring plane is perpendicular to the oncoming mainstream. When measuring film temperature field, the blade model is not heated and only the coolant is heated and ejected. The coolant has been heated to maintain a temperature difference from free-stream at about 18°C . The temperature field is measured using a cold-wire system. The cold-wire system includes a tungsten wire probe, $5\mu\text{m}$ in diameter and 1.5mm in length, and a temperature bridge. The temperature bridge is designed to restrict the current applied to the wire at less than 1mA to ensure negligible sensitivity to velocity. The wire current is typically maintained

at about $70\mu\text{A}$. The frequency response of the cold-wire is about 800Hz. The signal from the cold-wire system is directed to an A/D converter installed in a PC. The A/D converter has 12-bit resolution and maximum gain of 8. Resulting temperature measurement accuracy is 0.1°C .

Figure 8 presents the experimental setup for the film temperature and effectiveness measurement on the cylindrical leading edge model. The setup consists of a suction type blower that has a straight section with the test cylinder and an upstream nozzle. The flow enters through the nozzle into the test tunnel. The test tunnel is 25.4 cm x 76.2 cm in cross-section and is 183 cm long with the test cylinder placed 77.5 cm downstream of the nozzle exit. A tailboard is placed at the rear of the cylinder to reduce wake effects on the upstream heat transfer. The image processing system used for measuring the detailed heat transfer coefficient and film effectiveness distributions consists of a RGB camera, monitor, and a PC with a color frame grabber board. A turbulence grid is placed between the nozzle and the test tunnel to generate higher levels of free-stream turbulence intensity. Two different size grids were used to generate the turbulence levels of 4.1% and 7.1%. The coolant flow loop is also shown in the figure. Compressed air or CO_2 is routed through an orifice meter for the coolant flow. The coolant is initially directed away from the test cylinder using a three-way ball diverter valve. The valve is switched as the transient test is initiated. A heater heats the coolant flow for the film effectiveness test.

Figure 9 shows the test cylinder. The cylinder is 7.62 cm in diameter and 25.4 cm long. The cylinder is hollow with a polycarbonate exterior and copper interior. The copper interior has six heaters embedded along the circumference to heat the cylinder

uniformly. The six cartridge heaters are 25.4 cm long and 0.32 cm in diameter. There is no air space between the copper interior and the polycarbonate exterior. The polycarbonate layer is 0.64 cm thick and has low thermal conductivity and diffusivity. Film holes are drilled through the copper and polycarbonate layers. Coolant is sent into the hollow of the cylinder from the bottom of the cylinder and ejected out of the film holes. The front half of the polycarbonate exterior can be replaced as a smooth or film holed surface. Film holes, placed 15° from the leading edge of the cylinder, are 0.475 cm in diameter and are inclined 30° and 90° in the spanwise and streamwise directions, respectively. Ten holes in each row are spaced four-hole diameters apart ($P/d=4$). The film hole-to-cylinder diameter ratio (d/D) was 0.063 and the film hole length-to-diameter ratio (L/d) was 3.1. The measured region is limited to one side of the front half of the cylinder from stagnation (0°) to about 70° from stagnation. A total of 7000 points were measured on the test surface.

The test surface is heated uniformly using the cartridge heaters. Cartridge heater power inputs are controlled using a variac for each heater and surface temperature is monitored by placing several thermocouples on the surface. Uniformity of the surface temperature is within 0.6°C when the test surface is heated to a temperature above the liquid crystal range. Thermochromic liquid crystals are sprayed uniformly on the surface using an air gun. Liquid crystal (Hallcrest: BM/R32C5W/C17-10) color change temperatures for appearance of red, green, and blue were 31.6°C , 32.7°C , and 37.2°C , respectively. In the present experiment, the surface is heated to a temperature above the blue color. The test surface is suddenly cooled by inducing the mainstream flow by the fast starting blower. The blower takes less than three seconds from initiation for full flow

rate. The liquid crystal color changes from blue to green to red, and then becomes colorless during the transient test. The coolant flow is initiated by a solenoid controlled three-way diverter valve. The earliest color changes during the transient test occur around 15-20 seconds from initiation. The frame grabber board is programmed to capture data 10 frames per second in real time. The time of color change at every pixel location is analyzed and stored in a file on the computer.

For the cylindrical leading edge model, the coolant jet temperature profiles are measured at 20°, 30°, 50°, and 70° from stagnation as show in Figure 10. When measuring the coolant jet temperature profiles, the leading edge model is not heated and only the coolant is heated and injected. The temperature difference between free-stream and the coolant is maintained at about 15°C. The temperature field is measured using a cold-wire system. The cold-wire system includes a tungsten wire probe, 5 μ m in diameter and 1.5mm in length, and a temperature bridge. The temperature bridge is designed to restrict the current applied to the wire less than 1 mA to ensure negligible sensitivity to velocity. The wire current is typically maintained at about 70 μ A. The frequency response of the cold-wire is about 800Hz. The measurement of temperature using cold-wire is well described in the study of Kohli and Bogard (1996). The signal from the cold-wire system is directed to an A/D converter installed in a PC. The A/D converter has 12-bit resolution and maximum gain of 8. Resulting temperature measurement accuracy is 0.1°C.

3.2 Test Conditions and Data Analysis

A transient liquid crystal technique was used to measure the detailed heat transfer coefficients and film effectiveness on the blade surface. The technique is similar to the one described by Ekkad et al. (1997a,b). A one-dimensional transient conduction model into a semi-infinite solid with convective boundary condition is assumed. The solution for surface temperature is obtained as

$$\frac{T_w - T_i}{T_m - T_i} = [1 - \exp(-\frac{h^2 \alpha t}{k^2}) \operatorname{erfc}(\frac{h \sqrt{\alpha t}}{k})] \quad (1)$$

where T_w is the wall temperature when liquid crystals change to red from green (32.7°C) at time t , T_i is the initial surface temperature, T_m is the oncoming mainstream flow temperature, and α and k are the thermal diffusivity and conductivity of the blade material respectively. The heat transfer coefficient is obtained from Equation (1). For film cooling tests, the mainstream temperature (T_m) in Equation (1) is replaced by the local film temperature (T_f) which is a mixture of the coolant (T_c) and mainstream temperatures. The film temperature is defined in terms of η , which is the film effectiveness.

$$\eta = \frac{T_f - T_m}{T_c - T_m}; \text{ or } T_f = \eta T_c + (1 - \eta) T_m \quad (2)$$

For the film cooling test, we obtain an equation similar to Equation (1)

$$\frac{T_w - T_i}{T_f - T_i} = \frac{T_w - T_i}{\eta T_c + (1 - \eta) T_m - T_i} = [1 - \exp(\frac{h^2 \alpha t}{k^2}) \operatorname{erfc}(\frac{h \sqrt{\alpha t}}{k})] \quad (3)$$

Two similar transient tests are run to obtain the heat transfer coefficient (h) and film effectiveness (η). In the first test, the blade surface is heated and the coolant and mainstream temperatures are nearly the same. In this case, there is only one unknown, h , in the equation. For the second test, the coolant is heated to a temperature close to blade initial temperature. The calculated local heat transfer coefficient from the first test is substituted in the equation to obtain the local film effectiveness. The above equation is solved at each point on the blade surface to obtain the detailed heat transfer coefficient and film effectiveness distributions.

The experimental uncertainty in the measurement of the local heat transfer coefficient (h), based on Kline and McClintocks (1953) methodology, is about 4.5%. The individual uncertainties of all the parameters in Equation (1) have been included. The uncertainty in the film effectiveness measurement includes the additional uncertainty in heat transfer coefficient measurement and was estimated to be about 6.8%. It should be noted that the uncertainty in the immediate vicinity of the hole (less than 1 diameter around the hole) and close to blade trailing edge could be as high as 17% due to invalidation of the semi-infinite model assumption. However, the semi-infinite solid assumption can be applied where thickness of material is higher than 0.51 cm. The uncertainty in the velocity measurement using the single hot wire was estimated to be 4%.

A well-established cold-wire technique was used to measure the detailed temperature and temperature fluctuation profiles on the blade suction side. The mean temperature fields are presented as a non-dimensional temperature defined similar to film effectiveness, i.e.,

$$\theta = \frac{T - T_m}{T_c - T_m} \quad (4)$$

The temperature fluctuation is normalized as

$$\theta' = \frac{T'}{T_c - T_m} \quad (5)$$

Here, T' represent the root mean squared temperature fluctuation. 1200 data points are measured at each measurement plane at different X/D locations. At each data point, 36,864 samples are acquired and averaged to get time averaged and fluctuation temperature. The uncertainty in the coolant jet temperature field measurement using cold-wire was estimated to be 5.8%.

4.0 RESULTS AND DISCUSSION

4.1 Detailed Film Cooling Effectiveness Measurements over A Film-Cooled Gas Turbine Blade (Steady Flow)

Experiments were performed at a cascade exit Reynolds number of 5.3×10^5 . The corresponding flow velocity at the cascade exit was 50 m/s. Two different coolants, air and CO_2 , are used to simulate coolant-to-mainstream density ratios of $\text{DR}=1.0$ and $\text{DR}=1.5$, respectively. Air as coolant was tested at blowing ratios of 0.8 and 1.2 and CO_2 was tested at blowing ratios of 0.4, 0.8, and 1.2. The flow conditions for the film cooling tests are summarized in Table 1. For all the results presented in this study, the oncoming free-stream turbulence intensity was measured to be about 0.75% at the cascade inlet.

Table 1 Test Conditions for Film Cooling Measurement

Case	Re	Coolant	M	VR	DR	I
1	5.3×10^5	None				
2		CO_2	0.4	0.27	1.5	0.11
3		CO_2	0.8	0.53	1.5	0.42
4		CO_2	1.2	0.8	1.5	0.96
5		Air	0.8	0.8	1.0	0.64
6		Air	1.2	1.2	1.0	1.44

- **Effect of blowing ratio on Nusselt number distribution**

Figure 11 presents the detailed Nusselt number distributions on the blade suction and pressure surfaces for CO_2 injection and blowing ratios of 0.4, 0.8, and 1.2. Case 1 is for a smooth surface (no film holes); case 2 is for $M=0.4$; case 3 is for $M=0.8$; case 4 is

for $M=1.2$ for a blade with film holes. The blades with and without film cooling holes have same shape and flow angles. The blades are also made from the same material (Ren Shape).

Effect on Suction Surface The smooth surface Nusselt number (case 1) levels drop significantly from the leading edge with increasing streamwise distance on the suction surface. Nusselt numbers are lowest around $X/SL=0.5$ after which the Nusselt numbers increase again. This is due to boundary layer transition to turbulence. Nusselt numbers are higher towards the trailing edge as the transition is not complete. For a film cooled blade (case 2) with $M=0.4$, Nusselt number show streaks due to film cooling jets downstream of leading edge holes. High Nusselt numbers immediately downstream of injection decrease rapidly and the jet effect is non-existent upstream of the first film hole row on the suction surface (S1). Downstream of the row S1, jet streaks of higher Nusselt numbers are obtained along the holes. The streaks extend all the way up to the next film hole row S2. However, the jets do not cause any Nusselt number enhancement between the holes for row S1. Downstream of film hole row S2, the Nusselt numbers are significantly higher than for case 1. Some streaks of high Nusselt numbers are obtained along the holes. Such high levels of Nusselt number downstream of row S2 may be explained as follows. Film injection may cause boundary layer instabilities which cause earlier laminar to turbulent boundary layer transition. This may produce higher heat transfer coefficients downstream of injection. After transition, the effect of coolant jets disappears. Nusselt numbers decrease after transition with growth of the turbulent

boundary layer. With an increase in blowing ratio ($M=0.8, 1.2$) (case 3 and 4), Nusselt numbers downstream of injection after every row show slight increases. The streaks downstream of hole row S1 become stronger and appear to mix downstream with hole row S2. The effect of blowing ratio after hole row S2 is to increase Nusselt number slightly. With an increase in blowing ratio, the jet-mainstream interaction increases causing more turbulence downstream. This may be the cause for higher Nusselt numbers with an increase in blowing ratio.

Effect on Pressure Surface For case 1, the Nusselt numbers drop rapidly till $X/PL=-0.15$ and then increase a little bit over the entire surface. For case 2, film injection has a very small effect immediately downstream of leading edge row injection. However, Nusselt numbers are enhanced between the leading edge row and first row P1 over case 1. Downstream of rows P1 and P2, film injection enhances Nusselt numbers over case 1. The effect of film injection on the pressure surface is more in the region immediately downstream of injection. Since the boundary layer on the pressure surface is thicker than on the suction surface, the effect on Nusselt numbers due to film injection is lesser. Jet streaks are not evident on the pressure surface. With further increase in blowing ratio from $M=0.4$ to $M=1.2$, Nusselt numbers are not significantly affected. The increase in injectant mass into a thicker boundary layer does not appear to disturb the boundary layer as significantly as in the case of the thinner boundary layer on the suction surface.

Nusselt numbers with film injection are significantly enhanced due to the boundary layer disturbance cause by injection. Earlier studies on film cooling have

shown that film injection can create local turbulence intensities as high as 15-20% depending on blowing ratio. With such high local turbulence, heat transfer coefficients downstream of injection are significantly enhanced as seen in the figure.

Figure 12 presents the span-averaged Nusselt number distribution for cases 1-4. The Nusselt number distribution for case 1 are the lowest on both pressure and suction surfaces. Laminar-turbulent boundary layer transition on suction surface occurs at about $X/SL=0.55$. Nusselt numbers are enhanced significantly with addition of film injection (case 2-4). As explained earlier, film injection disturbs boundary layer and causes earlier transition to a turbulent boundary layer. Higher Nusselt numbers are obtained downstream of injection row S1. Further increase in Nusselt numbers occurs with transition and addition of coolant at row S2. On the pressure surface, film injection produces higher heat transfer coefficients from leading edge injection location to downstream of hole row P2. Higher blowing ratio produces higher Nusselt numbers downstream of injection for both pressure and suction surfaces.

The present results are compared to results for the same cases from Ou et al. (1994). The results for the smooth surface blade are in good agreement with the present data. Ou et al. (1994) show much higher Nusselt numbers downstream of injection hole on the suction surface. However, the pressure surface Nusselt numbers with film injection are in good agreement with present results. There may be two reasons for the differences in the results. The study by Ou et al. (1994) had the same coolant cavity feeding the hole rows P2 and S2. This may cause more coolant to exit out of hole row S2 and causing higher heat transfer coefficients. However in the

present study, two different cavities feed coolant to the hole rows. This may explain the lower Nusselt numbers obtained on the suction surface. Also, it is difficult to estimate the heat loss to the coolant during the steady state test by Ou et al. Since the heat loss to coolant was not estimated, that could add to the error. Ou et al. (1994) measured four thermocouple locations in the spanwise direction at every axial location.

- **Effect of blowing ratio on film effectiveness distribution**

Figure 13 presents the detailed film effectiveness distributions for cases 2, 3 and 4.

Effect on Suction Surface For case 2, film effectiveness immediately downstream of leading edge holes is as high as 0.5 but drops rapidly. The coolant protection might dissipate rapidly in this high curvature region. Effectiveness is high along the holes for row S1. The film streaks are clearly evident along the injection holes. The film streaks extend up to the next hole row S2. However, the film effectiveness between the holes is lower due to lack of spanwise mixing of jets. Effectiveness downstream of injection from row S2 shows shorter streaks with the jets coalescing downstream. The high curvature of the blade and the boundary layer transition to turbulence in this region (Figure 11) may be the reason for the shorter streaks. As blowing ratio increases from $M=0.4$ to $M=1.2$, film effectiveness downstream of each injection hole row increases. Effectiveness is higher downstream

of leading edge hole rows with short jet streaks. The effectiveness downstream of row S1 show significant increase in film effectiveness values along the hole. The streaks of high effectiveness are stronger and appear to mix with downstream row S2. Downstream of S2 also, the effectiveness is higher. As blowing ratio increase, more coolant is injected into the mainstream providing more protection to the surface. The effectiveness is as high as 0.2 at about $X/SL=0.6$ for $M=1.2$.

Effect on Pressure Surface Effectiveness on the pressure surface do not show strong jet like streaks as on the suction surface. Effectiveness levels are also not very high downstream of injection holes. As blowing ratio increases, film effectiveness in the entire injection region increases. The effect is significant downstream of LE holes. Effectiveness also increases around injection hole rows P1 and P2. Higher blowing ratio for CO_2 injection produces higher effectiveness on the blade surface. More coolant is injected into the boundary layer with an increase in blowing ratio providing more protection and thus higher effectiveness.

Figure 14 presents the span-averaged film effectiveness distributions for cases 2-4. Effectiveness increases with increase in blowing ratio on the suction surface. Effectiveness drops rapidly downstream of leading edge holes on the suction surface, then increases immediately downstream of hole row S1, drops again, and increases immediately downstream of hole row S2 and then decreases gradually towards the trailing edge for all three blowing ratios. Effectiveness decreases gradually over the entire pressure surface for all three blowing ratios with intermittent highs downstream of hole rows P1 and P2. Results from Mehendale et al. (1994) for the same coolant

and flow conditions are also presented at $M=0.8$. The data are closer away from the injection holes. However, in the injection region, there are differences in the measured effectiveness levels between the studies. The reason for this could be similar to the reason explained for heat transfer coefficient data.

- **Effect of coolant density**

Figure 15 presents the detailed Nusselt number distributions for air injection at blowing ratios of $M=0.8$ (case 5) and $M=1.2$ (case 6). On the suction surface, the Nusselt number distributions downstream of LE holes and row S1 are similar to the cases for CO_2 injection. Downstream of row S2, the Nusselt number distributions are also similar except that the highest Nusselt numbers at the end of transition are higher for air for both blowing ratios than for CO_2 injection. Nusselt numbers downstream of injection rows show a slight increase with an increase in blowing ratio for air injection. On the pressure surface, the effect of film injection is not as significant as on the suction surface. The Nusselt number distributions are similar to that for CO_2 injection. The effect of blowing ratio on the pressure side is insignificant. There are no streaklines of high Nusselt number downstream of injection holes for air injection also.

Figure 16 presents effect of coolant density on span-averaged Nusselt number distributions for $M=0.8$ and $M=1.2$ (cases 3-4, 5-6). Air injection simulates a density ratio of 1.0 whereas CO_2 injection simulates a density ratio of 1.5. Film injection causes earlier boundary layer transition on the suction surface and enhances Nusselt

numbers over the entire surface, as indicated earlier. Effects of coolant density are limited to regions downstream of injection holes. Higher density coolant produces higher Nusselt numbers downstream of injection at the same blowing ratio. This effect is stronger on the suction surface. On the pressure surface, the density ratio effect vanishes immediately downstream of injection. Changes in coolant density ratio has only a small effect on the already high Nusselt numbers produced by film injection.

Figure 17 presents the detailed film effectiveness distributions for the same cases as shown in Figure 15 (cases 5-6). The cases 5-6 are for $M=0.8$ and $M=1.2$ with air injection. Effectiveness distributions for air injection are similar on both pressure and suction surfaces. High effectiveness streaks are evident downstream of suction side rows S1 and S2. Effectiveness is very high downstream of LE holes on the pressure surface. However, the main difference is that air provides higher effectiveness at $M=0.8$ compared to $M=1.2$. However, CO_2 injection provides higher effectiveness at highest blowing ratio of 1.2. This may be due to the reason that air at $M=1.2$ produces high momentum jets ($I=1.44$) which tend to penetrate the boundary layer and provide reduced protection. At a lower blowing ratio of 0.8 ($I=0.64$), the jets have lower momentum and tend to stay closer to the surface and provide better protection.

Figure 18 presents the span-averaged film effectiveness distributions for the same cases as for Figure 16 (cases 3-4, 5-6). Film effectiveness on the suction surface is higher for CO_2 injection at $M=1.2$. At a lower blowing ratio of $M=0.8$, air provides higher effectiveness than CO_2 injection. At low blowing ratio of 0.8, air has higher but optimum momentum ($I=0.64$) compared to CO_2 ($I=0.42$) and protects the surface

better. At $M=1.2$, air possess very high momentum ($I=1.44$) and coolant jets blow into the mainstream penetrating the boundary layer and do not provide good protection compared to CO_2 injection ($I=0.96$). Overall, CO_2 injection at $M=1.2$ provides highest effectiveness downstream of injection. But in the injection hole region, it is difficult to distinguish the blowing ratio and density ratio effects.

Figure 19 provides more detailed Nusselt number distributions for CO_2 injection at $M=0.8$ in the region between LE and S2 rows on the suction surface. This figure provides a magnified version of the results shown earlier. It also provides more insight into the results that have been explained earlier. The detailed distributions show streaks of higher Nusselt numbers downstream of each injection row as indicated earlier. High effectiveness is obtained along the holes downstream of injection as indicated earlier. Also, this figure shows clearly the lack of coolant jet-to-jet interaction in the spanwise direction. The phenomena have been explained in the earlier figures. Such detailed information will be useful for validating CFD predictions for film cooling on curved surfaces.

4.2 Effect of Unsteady Wake on Film Cooling Performance for A Film-Cooled Gas Turbine Blade

Experiments were performed at a cascade exit Reynolds number of 5.3×10^5 . The corresponding flow velocity at the cascade exit was 50 m/s. Two different coolants, air and CO₂, are used to simulate density ratios of DR=1.0 and DR=1.5, respectively. For CO₂ as coolant, the blowing ratio was varied from 0.4 to 1.2. For air as coolant, the blowing ratio was varied from 0.8 to 1.2. Wake Strouhal number is varied from 0.0 (no rod, no wake) to 0.1. Table 2 lists the test conditions.

Table 2 Test Conditions

Case No.	S	Coolant	M	VR	DR	I
1	No Wake	None				
2	0.1	None				
3	No Wake	Air	0.8	0.8	1.0	0.64
4	0.1	Air	0.8	0.8	1.0	0.64
5	0.1	Air	1.2	1.2	1.0	1.44
6	0.1	CO ₂	0.4	0.27	1.5	0.11
7	0.1	CO ₂	0.8	0.53	1.5	0.42
8	0.1	CO ₂	1.2	0.80	1.5	0.96

Figure 20 presents the local-exit velocity ratio (V/V_2) distribution around the blade. A pressure tap instrumented blade was used to measure the surface static pressure distributions which was then converted to local mainstream velocity distribution around the blade (Ou et al., 1994). Figure 20 also presents the instantaneous velocity ($V(t)$), ensemble-averaged velocity (\bar{V}) and ensemble-averaged turbulence (\tilde{T}_u) profiles at the cascade inlet for strouhal number, $S=0.1$.

The instantaneous velocity profile shows the periodic unsteady fluctuations caused by the upstream passing wakes. The unsteady wakes are actually velocity deficiencies caused by the blockage of mainstream flow by the rotating rods. The ensemble-averaged velocity distribution shows the time-dependent mean velocity defect caused by the upstream passing wakes. The ensemble-averaged turbulence intensity profiles show that intensity could be as high as 20% inside the wake. The time mean averaged turbulence intensity is about 10.4%.

- **Effect of unsteady wake**

Figure 21 presents the detailed Nusselt number distributions on the blade suction and pressure surfaces for cases 1-4. Case 1 is for a smooth surface (no film holes) without rods ($S=0$); case 2 is for a smooth surface with $S=0.1$; case 3 is for a film cooled turbine blade with air injection at $M=0.8$ and no rods ($S=0$); case 4 is for a film cooled turbine blade with air injection at $M=0.8$ and $S=0.1$.

Effect on Suction Surface Nusselt number For a smooth surface without wake (case 1), the Nusselt numbers drop rapidly from the leading edge to about $X/SL=0.5$ on the suction surface and then increase due to boundary layer transition to turbulent flow. For a smooth surface with wake (case 2), the Nusselt numbers decrease along the suction side but transition occurs ($X/SL=0.25$) earlier for this case than for case 1. Also the spanwise variation in the Nusselt number distribution in the transition region reduces. For a blade with film cooling (case 3), Nusselt numbers are higher than for

the case 1 comparing only the effect of film cooling. On the suction surface, Nusselt numbers are higher downstream of injection from the leading edge. High Nusselt number streaks are obtained along the film holes. Nusselt numbers decrease towards the first film hole row S1. Nusselt numbers are higher along the holes immediately downstream of injection from S1 row. Between the film holes of S1 row, Nusselt numbers are not enhanced over case 1. Downstream of film hole row S2, Nusselt numbers are significantly higher than for both cases 1 and 2. Some streaks of high Nusselt numbers are observed immediately downstream between the film holes from S2 row. Film injection may cause transition to occur even earlier than for case 2 (smooth blade with unsteady wake condition). Further addition of an unsteady wake to the film cooled blade (case 4) does not appear to cause a significant effect on the suction surface over case 3. The Nusselt number distributions are similar with slight variations downstream of injection row S2. It appears that unsteady wake has little effect on Nusselt numbers which are already enhanced by film injection. Comparing cases 2 and 4 for at $S=0.1$, it can be seen that film injection enhances Nusselt numbers significantly after injection hole rows S1 and S2.

Effect on Pressure Surface Nusselt number For case 1, the Nusselt numbers drop rapidly to about $X/PL=-0.15$ and increases a little bit over the entire surface. Nusselt numbers are enhanced with the addition of wake (case 2) over the entire pressure surface. For case 3, film injection has little effect immediately downstream of leading edge row injection. However, Nusselt numbers are enhanced between the leading edge row and first row P1 over case 1. Downstream of rows P1 and P2, film

injection enhances Nusselt numbers over case 1. Compared to case 2, Nusselt numbers for case 3 are not affected significantly by film injection as in the case for suction surface. The effect of film injection on the pressure surface is more in the region immediately downstream of injection. Nusselt numbers for case 3 are lower than for case 2 in the region far away from P2 ($-0.35 < X/PL < -0.6$). Since the boundary layer on the pressure surface is thicker than on the suction surface, the effect on Nusselt numbers due to film injection is lesser. Nusselt numbers for case 4 are not significantly different from case 3 except in the region $-0.35 < X/PL < -0.6$, where Nusselt numbers for case 4 are higher. This region is far away from injection holes. It may be concluded that this may be due to unsteady wake effect. Comparing cases 2 and 4 for same $S=0.1$, it may be noticed that film injection has some additional effect on pressure surface Nusselt numbers downstream for leading edge film row.

Nusselt numbers with film injection are significantly enhanced due to the boundary layer disturbance cause by injection. Earlier studies on film cooling have shown that film injection can create local turbulence intensities as high as 15-20% depending on blowing ratio. With such high local turbulence, heat transfer coefficients downstream of injection are significantly enhanced as seen in the figure. Further addition of unsteady wake elevates free-stream turbulence. This addition in free-stream turbulence has only a slight effect on blade surface Nusselt numbers already greatly enhanced by the high turbulence produced by jet-mainstream interactions. Also, the local jet-mainstream boundary layer interaction causes earlier transition on the suction surface and higher heat transfer coefficients.

Figure 22 presents the span-averaged Nusselt number distribution for cases 1-4.

The Nusselt number distribution for case 1 are the lowest on both pressure and suction surfaces. Transition on suction surface occurs at about $X/SL=0.55$. For case 2, Nusselt numbers are higher than for case 1. Transition location on the suction surface moves upstream to $X/SL=0.25$. With film injection (cases 3 and 4), the boundary layer transition location moves further upstream to immediately downstream of the first row on the suction surface (S1 at $X/SL=0.15$). Nusselt numbers are enhanced with addition of film injection without unsteady wake (case 3). On the suction surface, Nusselt numbers with film injection are much higher than for the smooth surface with unsteady wake (case 2). Boundary layer is disturbed by film injection downstream of row S1. This causes higher heat transfer coefficients immediately downstream of injection and causes the boundary layer to undergo transition to turbulence. The transitional boundary layer is further disturbed by the second row S2. Nusselt numbers are enhanced downstream of both rows S1 and S2 on the suction surface. Based on the results, it can be concluded that boundary layer transition with film injection begins around $X/SL=0.15$ (around row S1). Nusselt numbers are significantly affected by film injection on the suction surface. However, further addition of unsteady wake does not significantly affect the Nusselt number distribution with film injection (case 4 vs. case 3). On the pressure surface, unsteady wake with $S=0.1$ (case 2) enhances Nusselt numbers up to 35% at $X/PL=-0.5$ over no rod, no wake case (case 1). It is evident that unsteady wake has a significant effect on Nusselt numbers on the pressure surface for a smooth surface blade. For case 3, Nusselt numbers are enhanced in the injection region by film injection over a smooth surface. However further downstream the effect is dissipated. Unsteady wake

imposed on film injection (case 4) does not seem to have a significant effect on the pressure surface over a surface without film injection but with unsteady wake.

The present results are compared to results for the same cases from Ou et al. (1994). The results for the smooth surface blade without or with wake are in good agreement with the present data. However, the Nusselt numbers for the film injection cases do not agree well in the film hole regions on the pressure and suction surfaces. Ou et al. (1994) presented much higher Nusselt numbers downstream of injection hole on both pressure and suction surfaces. Ou et al. (1994) measured four locations in the spanwise direction at every axial location. This limited measurement could be the reason for overprediction in their study. Film cooling causes strong spanwise variations, particularly near the film hole region, as seen in Figure 21 which may be difficult to measure using discrete thermocouples.

Figure 23 presents the detailed film cooling effectiveness distributions for air injection at $M=0.8$ for cases 3 and 4.

Effect on Suction Surface Film Cooling Effectiveness For case 3, film cooling effectiveness immediately downstream of leading edge holes is very high but drops rapidly. The leading edge holes are located in the high curvature region. The coolant protection might be dissipating rapidly. This may be the reason for the rapid drop in effectiveness. Effectiveness is high along the holes for row S1. The film streaks are clearly evident downstream of the injection holes. The film streaks extend up to the next hole row S2. However, the film cooling effectiveness between the holes is very

low due to lack of spanwise mixing of jets. Effectiveness downstream of injection from row S2 is also streaklike along the holes. However, the streaks are shorter and the jets appear to coalesce a little distance downstream. This may be due to two reasons. One is the high curvature of the blade in this region. Another reason may be due to the boundary layer transition to turbulence in this region (Figure 21). Effectiveness is higher than 0.2 up to $X/SL=0.7$. For the case with unsteady wake (case 4), the turbulence levels in the free-stream are higher. On the suction surface leading edge, effectiveness is reduced compared to case 3. The oncoming free-stream disturbed by passing wakes might cause the jets to breakdown. Effectiveness along the holes for hole row S1 are also significantly reduced due to the unsteady wake effect. The streaks of higher effectiveness are still evident. However, the effectiveness levels are much lower. Downstream of hole row S2, the unsteady wake reduces effectiveness significantly. It may be important to note here that unsteady wake imposed on film injection has very small effect on Nusselt numbers on the suction surface, but the effect on film cooling effectiveness is significant.

Effect on Pressure Surface Film Cooling Effectiveness For case 3, effectiveness is again very high immediately downstream of leading edge row injection. However, the positive curvature can cause the jets to protect the surface better in this region. There is no significant drop in effectiveness after injection on the pressure surface. Also, the row P1 is closer to the leading edge rows. Effectiveness is very high in the hole region and drops to about 0.2~0.3 immediately downstream of injection. Effectiveness is high around the hole region for row P2 also. However, the values

drop below 0.2 after $X/PL=-0.3$. This may be due to film dilution. For case 4 on the pressure surface, the effect of unsteady wake has slightly lesser effect on the film cooling effectiveness in the injection hole region. The film cooling effectiveness in the hole region is slightly reduced. Further downstream, the effect shows reduced effectiveness. Effectiveness drops below 0.2 immediately downstream of row P2.

Although, the addition of unsteady wake has a very small effect on heat transfer coefficients with film injection, the effect is significant on the film cooling effectiveness distributions. Without unsteady wake, the film cooling jets protect the surface better with limited mixing with the mainstream. Addition of unsteady wake causes disturbances in the mainstream which result in more mixing between the mainstream and coolant jets and reduce protection of the surface by the coolant jets. This causes significantly reduced film cooling effectiveness with unsteady wake.

Figure 24 presents the span-averaged film cooling effectiveness distributions for cases 3 and 4. Effectiveness is higher for case 3 compared to case 4 over the entire turbine blade surface. Effectiveness on the suction surface near the leading edge is high immediately downstream of injection and decreases rapidly and again increases for rows S1 and S2. Effectiveness is as high as 0.55 immediately downstream of row S2. Further downstream effectiveness decreases gradually. On the pressure side, effectiveness is high near the leading edge, decreases downstream with locally high effectiveness immediately downstream of the injection row, P1 and P2. Effectiveness is lower on the pressure surface compared to that for the suction surface after the second row of holes. The present results are compared to results for the same cases from Mehendale et al. (1994). The data are closer away from the injection holes but

in the injection region, there is significant differences in the effectiveness levels. The same explanation holds for the effectiveness measurements as for the Nusselt number measurements.

- **Effect of blowing ratio**

Figure 25 presents the effect of blowing ratio on detailed Nusselt number distributions for a given wake condition, $S=0.1$. Blowing ratio is varied from 0.4 to 0.8 to 1.2 (cases 6-8) for CO_2 injection ($\text{DR}=1.5$). The case for smooth surface with $S=0.1$ is also presented (case 2). On the suction surface, Nusselt numbers, downstream of injection, slightly increase with an increase in blowing ratio. This is true downstream of leading edge film row and row S1. Downstream of row S2, the blowing ratio effect is very small. This may be due to boundary layer transition to turbulence in this region. An increase in blowing ratio does not seem to significantly affect the Nusselt numbers which are already significantly high due to the boundary layer transition. On the pressure surface, the detailed Nusselt number distributions show very little effect of an increase in blowing ratio. An increased blowing ratio causes increase in jet penetration and lesser cumulative effects. The thick boundary layer on the pressure surface does not seem to be further affected by the increasing coolant blowing.

Figure 26 presents the span-averaged Nusselt number distributions for the same cases as for Figure 25 (case 2, cases 6-8). The no rod no wake case is also shown for comparison. On the suction surface, film injection ($M=0.4$, case 6) enhances Nusselt

numbers and causes earlier transition than for a smooth surface (case 2) as explained earlier. However, there is very little additional effect of blowing ratio (cases 7 and 8 for $M=0.8, 1.2$) on the Nusselt number distributions except in the regions immediately downstream of injection rows S1 and S2. On the pressure surface also, the effect of blowing ratio is very little except in the film injection region. In the film injection region on both surfaces, the Nusselt numbers are slightly higher with increasing blowing ratio.

Figure 27 presents detailed film cooling effectiveness distributions for the effect of blowing ratio under an unsteady wake condition of $S=0.1$ with CO_2 injection ($\text{DR}=1.5$) for cases 6-8. It can be observed that effectiveness increases with an increase in blowing ratio on the suction surface. On the suction surface, effectiveness streaks downstream of injection holes become stronger with an increase in blowing ratio. Effectiveness is as high as 0.2 at $X/\text{SL}=0.5$ for a high blowing ratio of 1.2. Effectiveness streaks are not seen for row S2. Effectiveness downstream of row S2 appears to be affected by boundary layer transition causing the jets to coalesce downstream of injection. Effectiveness immediately downstream of the leading edge holes on the pressure surface increase significantly with an increase in blowing ratio. Effectiveness streaks are not evident on the pressure surface. However, at $M=1.2$, effectiveness appears to be higher around the holes with small streaks. An increase in blowing ratio for CO_2 injection produces increased effectiveness on the blade surface. More coolant is injected into the boundary layer with an increase in blowing ratio providing more protection and thus higher effectiveness.

Figure 28 presents the span-averaged film cooling effectiveness distributions for cases 6-8. Effectiveness increases with increase in blowing ratio on the suction surface. Effectiveness drops rapidly downstream of leading edge holes on the suction surface, then increases immediately downstream of hole row S1, drops again, and increases immediately downstream of hole row S2 and then decreases gradually towards the trailing edge for all three blowing ratios. Effectiveness decreases gradually over the entire pressure surface for all three blowing ratios. Effectiveness is similar for $M=0.4$ and 0.8 on the pressure surface.

- **Effect of coolant density**

Figure 29 presents effect of coolant density on span-averaged Nusselt number distributions for $M=0.8$ and $M=1.2$ for an unsteady wake condition of $S=0.1$ (cases 4-5, 7-8). Air injection simulates a density ratio of 1.0 whereas CO_2 injection simulates a density ratio of 1.5. Nusselt numbers on both the surfaces are not affected significantly by coolant density. Film injection enhances Nusselt numbers over the entire surface and causes earlier boundary layer transition on the suction surface, as indicated earlier. Increase in coolant density causes small effects immediately downstream of injection holes. Higher density coolant produces higher Nusselt numbers downstream of injection at the same blowing ratio. Nusselt numbers downstream of injection are greatly enhanced by film injection over the blade surface. Changes in coolant density ratio has only a small effect on the already high Nusselt numbers.

Figure 30 presents the span-averaged film cooling effectiveness distributions for the same cases as for Figure 29 (cases 4-5, 7-8). Film cooling effectiveness on the suction surface is higher for higher density coolant for both blowing ratios ($M=0.8$ and 1.2). Since CO_2 is heavier (lower momentum flux ratio I), the coolant jets tend to stay closer to the surface and provide better protection compared to air. Air jets also possess higher momentum than CO_2 at same blowing ratio. Higher effectiveness is obtained at $M=1.2$ for CO_2 injection whereas higher effectiveness is obtained at $M=0.8$ for air injection on the suction surface. On the pressure surface, CO_2 injection at $M=0.8$ produces the lowest effectiveness. Air injection provides higher effectiveness closer to the leading edge. However, CO_2 injection at $M=1.2$ produces highest effectiveness after row P2. On the pressure surface also, effectiveness is higher for $M=1.2$ for CO_2 injection compared to $M=0.8$ and is higher at $M=0.8$ for air injection compared to $M=1.2$ for same coolant. Heavier coolant (CO_2) stay closer to boundary layer and protects better. At low blowing ratio of 0.8 , air has higher momentum ($I=0.64$) than CO_2 ($I=0.42$) and protects the surface better. At $M=1.2$, air possess very high momentum ($I=1.44$) and coolant jets blow into the mainstream and do not provide good protection than CO_2 ($I=0.96$).

4.3 Effect of Unsteady Wake with Trailing Edge Coolant Ejection on Detailed Heat Transfer Coefficient for A Uncooled Gas Turbine Blade

Table 3 Flow conditions for heat transfer measurement

Case No.	Re	Tu	S	M _t	\overline{Tu}
1	5.3×10^5	0.7%	No wake	0.0	0.7%
2		0.7%	0.1	0.0	10.4%
3		5.0%	0.1	0.0	13.7%
4		5.0%	0.1	0.25	13.4%
5		5.0%	0.1	0.50	13.0%
6		5.0%	0.1	1.00	12.7%
7	7.6×10^5	0.7%	No wake	0.0	0.7%
8		0.7%	0.1	0.0	10.4%
9		5.0%	0.1	0.0	13.7%
10		5.0%	0.1	0.25	13.4%
11		5.0%	0.1	0.50	13.0%

A time-mean averaged turbulence intensity (\overline{Tu}) is used in this study to describe the total turbulence level of the mainstream at the blade cascade inlet edge ejection. The time-mean averaged turbulence intensity definition is based on the integration of the ensemble-averaged turbulence intensity over a rod passing period. The methodology is described in detail by Zhang and Han (1995).

Figure 31(a) presents the effect of the unsteady wake on the spanwise-averaged Nusselt number distributions on the blade surface for a $Re=5.3 \times 10^5$. For Case 1 (No wake) the suction surface Nusselt number decreases monotonically with increasing streamwise distance (X/SL) from the blade leading edge and then increases sharply due to the transition to turbulent flow around $X/SL=0.55$. The heat transfer coefficients near

the trailing edge on the suction surface are high. This may be attributed to the unsteadiness of the flow near the trailing edge. The pressure surface Nusselt number decreases sharply with increasing streamwise distance from the blade leading edge; it has the lowest at $X/PL=-0.05$ and then increases slightly with increasing streamwise distance. This may be due to the acceleration of the flow on the pressure side. The Nusselt numbers on both the suction and pressure surfaces increase with an increase in the wake Strouhal number from 'no wake' (case 1) to $S=0.1$ (Case 2). The suction surface boundary layer transition to turbulence starts earlier, with an increase in the Strouhal number. The increase in the suction surface heat transfer coefficients is much higher than that on the pressure surface for increasing wake Strouhal numbers. The present results compare well with results from Han et al. (1993) using a thin foil-thermocouple technique for 'no wake' and $S=0.1$. Their inlet Reynolds number 3×10^5 , based on the cascade inlet velocity and the blade geometric chord length, is equivalent to the exit Reynolds number 5.3×10^5 that is based on the cascade exit velocity and the axial chord length used in the present study.

Figure 31(b) compares the results for the cases with $Re=5.3 \times 10^5$ for (1) clear wind tunnel, (2) wake only, (3) grid and wake, (4) grid, wake and jet $M_t=0.25$, (5) grid, wake and jet $M_t=0.5$, and (6) grid, wake and jet $M_t=1.0$. Results show that the blade surface Nusselt numbers increase with adding unsteady wake and free-stream turbulence. Boundary layer transition to turbulence on the suction surface occurs earlier with an increase in mainstream turbulence level. Transition on the suction surface occurs at $X/SL=0.55$ for Case 1, at $X/SL=0.3$ for Case 2, and at $X/SL=0.25$ for Case 3.

For Cases 2 and 3 the Nusselt number increases on the suction surface with the onset of transition and then decreases further downstream after the boundary layer becomes fully turbulent. On the pressure surface Nusselt numbers increase with an increase in mainstream turbulence level. For Case 1 the Nusselt number is lowest at $X/PL=-0.05$. There could be a small separation bubble which causes a very low Nusselt number in that region. Further downstream, Nusselt numbers increase with an increase in streamwise distance. For the higher mainstream turbulence cases the Nusselt numbers are flatter in that region. The increases levels of mainstream turbulence might tend to reduce the flow separation in that region and thus reduces the effect on the heat transfer coefficients. For the cases with trailing edge jets (Cases 4, 5, and 6) the effect of jets on Nusselt number is different at different locations on the blade surface. On the suction side before transition ($X/SL<0.25$) the jets enhance Nusselt number, and the higher the mass flux ratio of the jets, the greater the magnitude of these effects. The jets can enhance heat transfer up to 25 percent near the leading edge region ($X/SL<0.2$) for $M_t=0.5$ (Case 5). In this region the effect of jet increased mainstream velocity and more uniformly disturbed turbulence intensity profile enhances heat transfer compared to 'no jet' (Case 3). Further downstream ($X/SL>0.25$) there is not much effect of the jets on the heat transfer distributions. This may be because the jet effect decays in the transition and fully turbulent regions. On the pressure side of the blade the Nusselt number shows an increase in the region near the leading edge ($X/PL<-0.1$), but further downstream the effect is negligible. This may be due to the strong pressure gradient diminishing the jet effect. The magnitude of the jet effect on heat transfer is higher on the suction surface compared to the pressure surface.

Figure 31(c) compares Cases 7 through 11 for $Re=7.6 \times 10^5$ for (7) clear wind tunnel, (8) wake only, (9) grid and wake, (10) grid, wake and jet $M_t=0.25$, and (11) grid, wake and jet $M_t=0.5$. For this Reynolds number, transition on the suction surface occurs at $X/SL=0.5$ for Case 7 and at $X/SL=0.25$ for higher mainstream turbulence cases. The trend for the effect of coolant ejection on heat transfer for $Re=7.6 \times 10^5$ is similar to that for $Re=5.3 \times 10^5$. The jet effect on the suction side heat transfer before transition can be up to 25 percent, as compared to the case without jet injection. Again, the jet effect diminishes in transition and fully turbulent regions. As explained earlier, heat transfer on the transition and fully turbulent regions is already high, and adding jets to the unsteady wake does not seem to cause any further effect. Therefore, the jet effect (Cases 10 and 11) on suction side heat transfer is limited to the region before the transition location compared with the case without jet injection (Case 9). Also, the jet effect on the pressure surface heat transfer for $Re=7.6 \times 10^5$ is significant and can be up to 15 percent, compared with the case without jet injection (Case 9).

Figure 32(a) to 32(c) shows the detailed distributions of the local Nusselt number for $Re=5.3 \times 10^5$. The detailed contour distributions are presented for three flow conditions of (a) 'No grid, no wake and no jet', Case 1; (b) combined 'grid and wake', Case 3; and (c) combined 'grid, wake and jet', Case 5. For the 'no grid, no wake' condition ($\bar{T}u=0.7$ percent) in the region where $X/SL < 0.6$, there is no spanwise variation in the Nusselt number distribution. In transition region ($0.6 > X/SL > 0.8$) the Nusselt number in the spanwise direction shows significant variations. In fully turbulent regions ($X/SL > 0.8$), the Nusselt number is higher, with some spanwise variation. On the pressure surface there is a very small spanwise and streamwise variation on the pressure

surface. For the combined 'grid and wake', Case 3, and the combined 'grid, wake and jet', Case 5, the Nusselt numbers on the blade surfaces are significantly enhanced. The addition of unsteady wake and an elevated free-stream turbulence reduces spanwise variations on the blade surface and promotes earlier transition on the suction side of the blade.

Figure 33(a) and 33(c) presents detailed Nusselt number distributions on the blade surface for a $Re=7.6 \times 10^5$. The detailed contour distributions are presented for three flow conditions of (a) 'no grid, no wake and no jet', Case 7; (b) combined 'grid and wake', Case 9; and (c) combined 'grid, wake and jet', Case 11. Results show that the Nusselt numbers in general are higher than for $Re=5.3 \times 10^5$ on the entire blade surface. There is less spanwise variation and earlier transition for unsteady wake and higher mainstream turbulence cases compared with the low mainstream turbulence case.

4.4 Effect of Unsteady Wake with Trailing Edge Coolant Ejection on Film Cooling Performance for A Film-Cooled Gas Turbine Blade

Table 4 Test Conditions

Case No.	Tu	S	M _t	M	$\overline{T_u}$
1	0.7%	No Wake	0.0	No holes	0.7%
2	0.7%	No Wake	0.0	0.8	0.7%
3	0.7%	0.1	0.0	0.8	10.4%
4	0.7%	0.1	0.5	0.8	10.0%
5	5.0%	0.1	0.0	No holes	13.7%
6	5.0%	0.1	0.5	No holes	13.0%
7	5.0%	0.1	0.0	0.8	13.7%
8	5.0%	0.1	0.5	0.8	13.0%

Tests were performed at the chord Reynolds number of 7.6×10^5 at the cascade exit. The corresponding velocity at the cascade exit is 75 m/s. Unsteady wake strength is defined by wake Strouhal number ($S = 2\pi N d n / (60 V_1)$). It can be achieved by the combination of the number of rods (n), diameter of rod (d), and wake rod rotation speed (N). Table 4 presents the test cases for which heat transfer measurements were obtained for this study. Case 1 is for a no wake case and no-film holes blade. Case 2 is for a film cooled blade with cooling blowing ratio (M) of 0.8 with no wake effect. Case 3 is for a cooled blade under the effect of wake Strouhal number $S=0.1$. Case 4 is for the cooled blade under the effect of unsteady wakes and trailing edge ejection with jet blowing ratio (M_t) of 0.5. Case 5 is for an uncooled blade with grid generated turbulence and unsteady wake. Case 6 is for an uncooled blade with grid generated turbulence and unsteady wake with trailing edge ejection ($M_t=0.5$). Case 7 is for a cooled blade under the effects of grid generated turbulence and unsteady wake. Case 8 is for the cooled blade under the effects

of grid generated turbulence and unsteady wake with trailing edge ejection. The grid generated turbulence (Tu) and the time-mean averaged turbulence intensities ($\tilde{T}u$) for each case are shown in the table. The parameters are chosen in this study to simulate typical of engine conditions. The cascade exit mainstream Reynolds number of 7.6×10^5 represented the non-dimensional engine flow conditions. An unsteady wake Strouhal number of $S=0.1$ simulates the blade rotation frequency and velocity defect effects. As indicated earlier, the combustor generated free-stream turbulence levels downstream of the nozzle guide vanes are of the order of 5-6% which is generated using an upstream grid. The trailing edge ejection jet blowing ratio (M_t) of 0.5 and film cooling blowing ratio (M) on the blade of 0.8 are in the range of typical coolant flow conditions.

- **Free-stream Flow Measurements**

Figure 34(a) presents the local-to-exit velocity ratio (V/V_2) distribution around the blade. A pressure tap instrumented blade was used to measure the surface static pressure distributions which was then converted to local mainstream isentropic velocity distribution around the blade (Ou et al., 1994). Figures 34(b) and 34(c) present the instantaneous velocity profiles for cases 7 and 8. Case 7 is for a free-stream with grid generated turbulence ($Tu=5.0\%$) and unsteady wake ($S=0.1$) and case 8 is for a free-stream with grid generated turbulence ($Tu=5.0\%$) and unsteady wake ($S=0.1$) with trailing edge ejection ($M_t=0.5$). Comparing both figures, it is evident, that in Fig. 34(b), the velocity deficit is clearly seen with the passing of the unsteady wake and this deficit appears slightly reduced in Fig. 34(c). This indicates

that the trailing edge jets enhance the mean value of mainstream velocity. Figure 34(d) presents the ensemble-averaged velocity (\tilde{V}) and turbulence intensity ($\tilde{T}u$) profiles at the cascade inlet for the same cases as in Figures 34(b) and 34(c). The turbulence intensity profile for the trailing edge ejection case is more uniformly disturbed in the time period. Based on these measurements, it is evident that the addition of trailing edge ejection to unsteady wake profile produces increased mainstream velocity and slightly reduced but more uniformly disturbed turbulence intensity profile.

- **Film Cooling**

For all film cooled cases, air was used as coolant to simulate coolant-to-mainstream density ratio of $DR=1.0$ at a blowing ratio of 0.8. Air was used for trailing edge ejection ($M_t = 0.5$).

Nusselt Number Distributions

Figures 35 and 37(a) present the detailed and spanwise averaged Nusselt number distributions on the blade suction and pressure surfaces for cases 1-4, respectively. All cases are with no grid-generated turbulence intensity of $Tu=0.7\%$. The figure compares the no-wake, no-film holes blade (case 1) to no-wake film cooled blade with $M=0.8$ (case 2); film cooled blade with $M=0.8$ and wake $S=0.1$ (case 3); and

film cooled blade with $M=0.8$, wake $S=0.1$, and trailing edge ejection $M_t=0.5$ (case 4).

Effect on Suction Surface The no-film holes surface Nusselt number (case 1) levels drop significantly from the leading edge with increasing streamwise distance on the suction surface. Nusselt numbers are lowest around $X/SL=0.5$ after which the Nusselt numbers increase again. This is due to boundary layer transition to turbulence. Nusselt numbers are higher towards the trailing edge as the transition is not completed. For a film cooled blade (case 2) with no wake, Nusselt numbers are high due to film cooling jets immediately downstream of leading edge holes. Further downstream of LE row injection, Nusselt numbers decrease rapidly and the injection effect is dissipated upstream of the first film hole row on the suction surface (S1). Downstream of the hole row S1, jet streaks of higher Nusselt numbers are obtained along the holes. The streaks extend all the way up to the next film hole row S2. However, the jets do not cause Nusselt number enhancement between the holes for row S1 due to lack of spanwise mixing between the jets. Downstream of film hole row S2, the Nusselt numbers are significantly higher than for case 1. Film injection from row S2 causes boundary layer instabilities which promote earlier laminar to turbulent boundary layer transition. This also produces higher heat transfer coefficient downstream of injection. Nusselt numbers decrease after transition with growth of the turbulent boundary layer and dissipation of coolant jet effect. Further addition of unsteady wake to the film cooled blade (case 3) shows small effect on the blade surface Nusselt numbers compared to case 2. Nusselt number distributions appear to

be similar to case 2 except in the region downstream of hole row S2. It appears that the additional effect of unsteady wakes is small due to the reason that surface Nusselt numbers are already significantly enhanced by film injection. Addition of trailing edge ejection to the unsteady wake (case 4) on the film cooled blade does not affect the Nusselt number distributions.

Effect on Pressure Surface For case 1, the Nusselt numbers drop rapidly till $X/PL=0.15$ and then increase a little bit over the entire surface. For case 2, film injection has a very small effect immediately downstream of leading edge row injection. However, Nusselt numbers are enhanced between the leading edge row and first row P1 over case 1. Downstream of rows P1 and P2, film injection enhances Nusselt numbers slightly over case 1. The effect of film injection on the pressure surface is not as significant as on the suction surface. Since the boundary layer on the pressure surface is thicker than on the suction surface, the effect on Nusselt numbers due to film injection is less. Jet streaks are also not evident on the pressure surface. Addition of unsteady wake (case 3) causes slight increases over case 2 in the region between LE holes and hole row P1. Further addition of trailing edge ejection to case 3 (case 4) causes only slight increases in Nusselt numbers on the pressure surface in the region downstream of hole row P1.

Nusselt numbers with film injection are significantly enhanced due to the boundary layer disturbance cause by film injection. Earlier studies on film cooling have shown that film injection can create local turbulence intensities as high as 15-20% depending on blowing ratio. With such high local turbulence, heat transfer

coefficients downstream of injection are significantly enhanced as seen in the figure. This may cause significantly reduced effects of other factors such as unsteady wakes and trailing edge ejection on film cooled blades. The spanwise-averaged results in Figure 37(a) present the same trends as discussed above.

Figure 36 and 37(b) presents the detailed and span-averaged Nusselt number distribution for cases 5-8. All the cases are for a grid generated turbulence of $Tu=5.0\%$. The figure compares an uncooled blade with wake $S=0.1$ (case 5) with an uncooled blade with wake $S=0.1$ and trailing edge ejection, $M_t=0.5$ (case 6); a film cooled blade with wake $S=0.1$, $M=0.8$ (case 7); and a film cooled blade with wake $S=0.1$, $M=0.8$, and trailing edge ejection, $M_t=0.5$ (case 8).

Effect on Suction Surface The no-film holes surface Nusselt number (case 5) levels drop significantly from the leading edge to $X/SL=0.25$ and then increases due to transition to turbulent boundary layer toward the trailing edge. Comparing to case 1, case 5 has both grid generated turbulence and unsteady wake effects included. The added influence of both the unsteady wake and grid generated turbulence can cause transition location to move upstream towards the leading edge. The differences in cases 5 and 6 are in the region downstream of leading edge on the suction surface. Nusselt numbers are enhanced up to 20% in the region from leading edge to $X/SL<0.3$ on the suction surface. The effect of trailing edge ejection on the uncooled blade is also strongly evident over the entire pressure surface and in the transition region on the suction surface. For a film cooled blade (case 7) with wake and grid

generated turbulence, Nusselt numbers are significantly enhanced in the region between LE holes and the suction side second row holes S2. Additional effect of film injection is to cause local instabilities in the boundary layer and causing higher heat transfer region immediately downstream of hole rows. Further downstream of hole row S2, the Nusselt numbers are only slight enhanced compared to case 6. Further addition of trailing edge ejection to case 7 (case 8) causes very small changes in the detailed heat transfer coefficient distributions. The trailing edge ejection effect is not as significant as the other effects of film injection, unsteady wakes, and grid generated turbulence, in that order.

Effect on Pressure Surface For case 5, the Nusselt numbers drop rapidly till $X/PL=0.15$ and then increase a little bit over the entire surface. For case 6, Nusselt numbers are enhanced from leading edge to $X/PL<0.1$ on the pressure surface compared to case 5. For case 7, the effect of film injection on the pressure surface is more in the region immediately downstream of injection holes. Further addition of trailing edge ejection to case 7 (case 8) causes slight decreases in Nusselt numbers on the pressure surface just downstream of LE hole rows.

The trailing edge ejection jets for a low $Tu=0.7\%$ may be attached to the unsteady wake generated by the rods. However, with grid generated turbulence, the trailing jets may not be uniformly impinging on the LE region. This may cause slight changes in the heat transfer distributions as compared to the no-grid case. The grid turbulence effect seems to be stronger on the pressure surface. Overall effect of trailing edge ejection imposed on a free-stream disturbed by unsteady wakes and grid generated turbulence on the film-cooled blade heat transfer is slightly incremental.

Film Effectiveness Distributions

Figures 38 and 40(a) present the detailed and spanwise-averaged film effectiveness distributions for cases 2, 3 and 4, respectively. The figure compares the no-wake film cooled blade with $M=0.8$ (case 2) to film cooled blade with $M=0.8$ and wake $S=0.1$ (case 3); and film cooled blade with $M=0.8$, wake $S=0.1$, and trailing edge ejection $M_t=0.5$ (case 4).

Effect on Suction Surface For case 2, film effectiveness immediately downstream of leading edge holes is as high as 0.5 but drops rapidly. The coolant protection dissipates rapidly in this high curvature region. Effectiveness is high along the holes for row S1. The film streaks are clearly evident along the injection holes. The film streaks extend up to the next hole row S2. However, the film effectiveness between the holes is lower due to lack of spanwise mixing of jets. Effectiveness downstream of injection from row S2 shows shorter streaks with the jets coalescing downstream. The high curvature of the blade and the boundary layer transition to turbulence in this region (Figure 35) may be the reason for spanwise mixing of jets. With addition of unsteady wake to the mainstream flow (case 3), effectiveness is significantly reduced. The effectiveness downstream of the LE rows is lower as coolant jets dissipate rapidly. The oncoming free-stream disturbed by passing wakes breaks down the jets. Also the advancement of the boundary layer transition location can cause more spanwise mixing of jets specially for the coolant downstream of hole

row S1. Also, effectiveness reduces far downstream of the last injection row S2. For case 4 with trailing edge ejection, effectiveness distributions are similar to that for case 3. Film effectiveness distribution on the suction surface appears to be slightly affected by the further addition of trailing edge ejection to a free-stream already affected by unsteady wakes.

Effect on Pressure Surface For case 2, effectiveness distributions on the pressure surface do not show strong jet like streaks as on the suction surface. Effectiveness levels are also not very high downstream of injection holes but decrease rapidly downstream of hole row P2 and any coolant protection is not evident for distance $X/PL > 0.5$. Addition of unsteady wake (case 3) reduces effectiveness downstream of hole row P2. However, upstream of P1, the effectiveness values are similar to case 2. Addition of trailing edge ejection seems to produce some variations in the effectiveness distributions (case 4). The effectiveness in the LE region decreases significantly. However, downstream of the LE hole row, the effectiveness values are higher for case 4. This may be due to the reason that some of the trailing edge coolant may be convected downstream into the low velocity region thus providing more protection.

Figure 39 and 40(b) presents the detailed and span-averaged film effectiveness distributions for cases 7-8. The figure compares a film cooled blade with wake $S=0.1$, $M=0.8$ (case 7) and a film cooled blade with wake $S=0.1$, $M=0.8$, and trailing edge ejection, $M_t=0.5$ (case 8).

Effect on Suction Surface Case 7 is for a turbine blade with film cooling under the effect of grid turbulence and unsteady wakes. Effectiveness is high immediately downstream of LE row holes. Effectiveness decreases rapidly to hole row S1. Weak jets streaks are observed downstream of hole row S1 due to the unsteady wake affected free-stream. Downstream of hole row S2, effectiveness is greatly reduced due to spanwise mixing of jets in the transition and fully turbulent boundary layer region. With an addition of trailing edge ejection (case 8), effectiveness reduces downstream of LE and S1 holes. However, effectiveness levels are not significantly affected over the rest of the suction surface. Some of the trailing ejection coolant might penetrate the coolant jets from the LE row holes and disturb the already weak protection thus reducing the film effectiveness. Further downstream, the effect of the trailing edge jets might be weaker and hence the lack of reduction in film effectiveness.

Effect on Pressure Surface For case 7, effectiveness downstream of LE rows is as high as 0.4 but rapidly decreases downstream. Some high effectiveness is observed upstream of hole row P2 due to accumulation of coolant in the low velocity region. For case 8, effectiveness levels are similar but lower than that for case 7. The effect of trailing edge jets is noticeable on the pressure surface.

On the suction surface, case 8 provides lower effectiveness values downstream of LE film hole rows. Downstream of hole row S1, both cases provide similar

effectiveness values. Case 8 provides lower effectiveness over the entire pressure surface.

4.5 Unsteady Wake Effect on Film Temperature and Effectiveness

Distribution for a Gas Turbine Blade with Only One Row of Film Holes

Experiments were performed at a cascade exit Reynolds number of 5.3×10^5 . The corresponding flow velocity at the cascade exit was 50m/s. Air as coolant was tested at blowing ratios of 0.6, 0.8, and 1.2 for no rod no wake cases ($S=0$, $\bar{T}_u=0.7\%$) and cases with wake ($S=0.1$, $\bar{T}_u=10.4\%$).

- **Coolant Jet Temperature Field Measurements**

Effect of Unsteady Wake Figures 41 and 42 present the result of heated coolant jet temperature profile development for the cases of $M=0.8$, with and without wake effect ($S=0.0$ and $S=0.1$, respectively). Temperature profiles are measured at planes at $X/D=1, 5, 10$, and 15 along the streamwise direction. Due to the delicacy of cold wire, we couldn't approach it very close to the blade wall surface (in the Y direction). The closest measurement location is about 0.5mm away from the surface ($Y \geq 0.5\text{mm}$, $Y/D \geq 0.25$). Temperature contours dilute as the heated coolant jet moves away from the eject location due to mixing between heated jet and cold free stream air for both steady and unsteady flow cases. However, the unsteady cases dilute faster. Higher mean temperature (θ) can be seen at the center of the heated jet trajectory. Both the strength and the area of this central hotter region are also reduced along the streamwise direction. There's no significant interference between two adjacent

coolant jets. Higher temperature fluctuation (θ') can be found at the mixing region of the jet and the free-stream, where the mean temperature varies greatly. The fluctuation intensity is also gradually weakened along the streamwise direction. The results show that the unsteady wake produces slightly higher temperature fluctuations than the steady flow case. Meanwhile, at the same locations, the case with wake effect has larger areas of temperature fluctuations than the case without. This indicates that the unsteady wake has expanded the mixing region by bringing more free-stream air into it and thus enhanced the diffusion of the jet.

Figure 43 shows the enlarged coolant jet temperature contours at $X/D=10$ for both steady and unsteady cases of a blowing ratio of $M=0.8$. For the case with unsteady wake effect, both the coolant jet mean temperature (θ) and temperature fluctuation (θ') contour have been expanded to a larger area. The dimensionless mean temperature at jet center is 0.27 for the steady case and is reduced to 0.19 for the unsteady case. The central hotter region of the coolant jet for the case with wake effect is smaller than that of the case without wake effect and it has somewhat drifted away from the blade surface. The temperature fluctuation level is of the same range (from 0 to 0.08) for both cases, but the unsteady case has a much larger temperature fluctuation area. All this implies that the unsteady wake enhances the mixing between the heated coolant jet and the cold free-stream, and more heated jet is diffused into the free-stream.

Effect of Blowing Ratio Figure 44 presents the result of enlarged coolant jet contours for two different blowing ratios ($M=0.8$ and $M=1.2$) at location $X/D=10$ and without wake effect ($S=0$). The dimensionless mean temperature (θ) at jet center is 0.27 for the case $M=0.8$ and is reduced to 0.15 for the case $M=1.2$. For the case $M=0.8$, we observe a fairly large center region of higher mean temperature, and the jet center is still attached to the blade surface. For the case $M=1.2$, the central hotter region is smaller than the case $M=0.8$ and the coolant jet has lift off the blade surface and is barely attached to the wall. Only part of the periphery of the jet has touched the blade wall. This indicates that the higher the blowing ratio, the further the jet would lift off the blade surface, which reduces the film cooling coverage. The case $M=1.2$ has a much larger temperature fluctuation area than the case $M=0.8$, but the temperature fluctuation level is decreased due to its lower jet temperature. The temperature fluctuation range is from 0 to 0.05 for the case $M=1.2$, and from 0 to 0.08 for the case $M=0.8$. All this shows that for the higher blowing ratio, there is more mixing between the heated coolant jet and the cold main stream. The coolant jet dilutes faster as the jet goes away along the streamwise direction.

- **Film Cooling Measurements**

Effect of Unsteady Wake on Film Cooling Effectiveness Figure 45 presents the detailed film cooling effectiveness distributions for air injection at three different blowing ratios ($M=0.6, 0.8, 1.2$) with and without unsteady wakes, respectively. Since there are no film cooling holes at leading edge of the blade, the film streaks

start where the row of film cooling holes (the only row of holes in this study) is located. From Figure 45, one can see that the film streaks extend along the streamwise direction fairly straightly. The streaks are gradually weakened the further they extend away from the film cooling holes. The film cooling effectiveness between streaks is very low due to the lack of spanwise mixing of jets, which we can also clearly observe from the coolant jet temperature contour measurements. For cases without the effect of unsteady wakes, the streaks remain clearly evident downstream of the injection holes, except for the very high blowing ratio of 1.2, in which the jet has apparently lift off from the blade surface because of its high momentum. With the effect of unsteady wake, the turbulence level in the free-stream is higher. The figure shows that the streaks are evidently weakened but expanded further down in the streamwise direction. Observation of coolant jet temperature contour tells us that, due to the effect of unsteady wake, the coolant jet has more mixing with the mainstream, which widens the jet streak yet weakens the cooling jet much faster than the cases without unsteady wake.

In Figure 46, the film cooling effectiveness distribution along film hole centerline shows that centerline film effectiveness decreases along the streamwise direction due to the continuous mixing between coolant jet and mainstream. The higher the blowing ratio, the lower its centerline film effectiveness at the same location. Among all the cases, the case $M=0.6$ and without wake effect has the highest centerline effectiveness. It has a high value of 0.33 at the location right behind the film hole and then decreases to and remains at about 0.2 afterwards. Addition of unsteady wake decreases the centerline film effectiveness for the same blowing

ratios. Compared to the case $M=0.8$, unsteady wake has a greater effect on the case of lower ($M=0.6$) and higher blowing ratios ($M=1.2$), especially at the region right behind the film hole, where both of the latter two cases have a sharp drop in centerline effectiveness.

In the spanwise-averaged film effectiveness distribution shown in Figure 46, for blowing ratios of 0.6 and 0.8, film cooling effectiveness with the effect of unsteady wake is significantly lower than that without unsteady wake at areas immediately downstream of the film cooling holes. However, this trend doesn't last long. Starting from $X/D=5$, the spanwise-averaged cooling effectiveness with wake effect is about the same as that without wake effect. The possible explanation for this phenomenon is that before $X/D=5$, the wake effect is mainly manifested in the reduction of the spanwise-averaged effectiveness; after $X/D=5$, another aspect of wake effect, expansion of the coolant jet to cover more blade surface area, begins to show its beneficial part and thus keeps the spanwise-averaged effectiveness from decreasing. For a blowing ratio of 1.2, the spanwise cooling effectiveness with wake effect is generally only slightly lower than that without wake effect. In this case, the expanding of the coolant jet won't make much difference because the jet has lift off the blade surface anyway. So the wake effect is mainly the decrease of the film cooling effectiveness.

All this indicates that unsteady wake has a strong effect on the film cooling effectiveness distributions. Without unsteady wake, the film cooling jets protect the surface better within limited areas. Addition of unsteady wake causes disturbances in the mainstream which result in more mixing between the mainstream and coolant

jets. This results in two effects: on the one hand, the film coolant jet has been diluted and produced smaller cooling effectiveness; on the other hand, the film coolant jet has been expanded along the spanwise direction and more area is covered by film cooling, and thus could contribute to the increase of spanwise-averaged cooling effectiveness. However, generally, unsteady wake has caused the film cooling effectiveness to decrease.

Effect of Unsteady Wake on Nusselt number Figure 47(a1) — (a4) are for cases without wake effect and (b1) — (b4) for cases with wake effect. Among them, (a1) and (b1) are for the smooth surface and the other three in each group have blowing ratios of 0.6, 0.8 and 1.2. Unlike the film effectiveness distribution measurements, here we have gathered data on the whole suction surface in order to get information on the film cooling jet's effect on the blade surface heat transfer right behind the film cooling holes as well as its effect on boundary-layer transition.

For a smooth surface without wakes (case a1), the Nusselt numbers drop rapidly from the leading edge to about $X/SL=0.5$ on the suction surface and then increase again due to boundary-layer transition to turbulent flow. For a smooth surface with wakes (case b1), the Nusselt numbers also decrease along the streamwise direction but transition occurs much earlier ($X/SL=0.25$) for this case than for case a1. Also, its spanwise-averaged Nusselt number is higher than that of case a1 before the transition begins.

With film cooling, the Nusselt numbers at locations right behind the film cooling holes increase significantly and traces of high Nusselt numbers are formed right

behind the holes. The higher the blowing ratio, the longer this trace of highly-increased Nusselt numbers. Due to the film injection, boundary-layer transition occurs slightly earlier in cases a2 to a4 than in case a1. As soon as boundary transition begins, the Nusselt numbers increase at about the same rate as in case a1, and they keep increasing much further down the blade before they begin to decrease again. The same is true for cases with both film cooling and unsteady wake effect, as we compare the cases b2 to b4 with case b1. However, as we have noticed, no matter with or without film cooling, the addition of an unsteady wake has caused boundary transition to occur significantly earlier than the cases without unsteady wake. Also, for cases with wake effect, the streaks of high Nusselt numbers right after the film holes are a little shorter compared with cases without wake effect. The reason for this is that, due to the unsteady wake, the cooling jet is diluted faster along the streamwise direction than in cases without unsteady wake.

Figure 48 presents the spanwise-averaged Nusselt number distributions for both steady and unsteady flow with wake effect. The small arrows indicate where the film injection is. The results for the smooth surface blade with and without wake are in good agreement with those for the same cases from Ou et al. (1994), who used the thin-foil-thermocouple technique to study the heat transfer over a model turbine blade. The figure shows that, for both cases with and without unsteady wake, the spanwise-averaged Nusselt number shows a peak increase right downstream of the jet ejection location. It then decreases along the streamwise direction till it reaches the boundary-layer transition location, where it begins to increase again to reach its second peak value. The second peak value is higher than the first one. However, for

the cases with wake effect, the spanwise-averaged Nusselt number doesn't drop as low as the cases without wake effect before it begins to increase again due to much earlier boundary-layer transition. In Figure 48 we also observe that, the higher the blowing ratio, the greater both of its peak values. Blowing ratio has a comparatively greater effect on the first peak value. Higher blowing ratio pushes the transition front only slightly ahead. The blowing ratio effect is very small compared to the effect of unsteady wake as far as the boundary-layer transition is concerned.

It indicates that film cooling enhances the surface heat transfer along the blade while the unsteady wake causes earlier boundary-layer transition. However, the results show that both film cooling and wake effect can't affect much on the maximum spanwise-averaged Nusselt number (the second peak value at the end of boundary-layer transition) achieved on the suction surface.

4.6 Detailed Film Cooling Measurements on A Cylindrical Leading Edge Model: Effect of Free-Stream Turbulence and Coolant Density

Tests were conducted in a low speed wind tunnel for a Reynolds number of 100,900 based on cylinder diameter. Air is used as coolant to simulate a coolant-to-mainstream density ratio (DR) of 1.0 and CO₂ is used to simulate a density ratio of 1.5. The coolant-to-mainstream momentum flux ratio (I) is a function of the blowing ratio and the density ratio, $I=M^2/DR$. The mainstream inlet velocity and density is used for evaluating the blowing and density ratios. Heat transfer coefficient results are presented on a smooth surface for three turbulence levels of 1%, 4.1%, and 7.1%. Film effectiveness and heat transfer coefficient distributions are presented for three blowing ratios of 0.4, 0.8, and 1.2 and two coolant density ratios of 1.0 (air) and 1.5 (CO₂) at a low free-stream turbulence intensity of 1%. Film effectiveness and heat transfer coefficient distributions are also presented at $M=0.4$ and 1.2 for both coolants at $Tu=4.1\%$ and 7.1%.

The coolant-to-mainstream density ratio for the heat transfer coefficient and film effectiveness tests are almost equal. The heat transfer coefficient test is run with both mainstream and coolant at room temperature whereas in the film effectiveness test, the coolant is slight hotter ($T_c-T_\infty \sim 6^\circ\text{C}$) than the mainstream. Such a small difference in temperatures does not produce significant variation in the density ratios between the two tests.

Velocity and turbulence measurements were measured along the wind tunnel. Incident mainstream velocity (U_∞) was obtained to be 21 m/s at $X/D=9.5$ from the grid location. Figure 49 presents the centerline streamwise turbulence intensity distributions for the three turbulence levels. As the distance from the nozzle increases, the streamwise turbulence decays and reaches a low just upstream of the cylinder. This low value is defined as the oncoming free-stream turbulence intensity and is obtained to be 1% for no grid case, 4.1% for grid 1, and 7.1% for grid 2. Corresponding streamwise dissipation length scales at the same location were estimated to be about 1.3 cm for grid 1 and 1.5 cm for grid 2.

- **Smooth Surface Heat Transfer**

Heat transfer coefficients were measured on a smooth surface with no film holes under the three free-stream turbulence levels. Local Nusselt numbers are normalized by the mainstream Reynolds number and presented as $Nu/Re^{1/2}$. The viscosity and conductivity used to evaluate the $Nu/Re^{1/2}$ values are based on the oncoming mainstream inlet flow. Figure 50(a) presents the span-averaged $Nu/Re^{0.5}$ distributions under free-stream turbulence effects. Results are presented on one side of the front half of the cylinder from geometric stagnation (0°) to about 70° downstream from the stagnation point. The $Nu/Re^{0.5}$ values over the entire measurement region increases with an increase in free-stream turbulence. Stagnation point heat transfer is enhanced up to 50% for $Tu=7.1\%$ over low turbulence level of $Tu=1\%$. The enhancement for $Tu=4.1\%$ is about 30%. The $Nu/Re^{0.5}$ values decreases with increase in angle from

stagnation. The Frössling theoretical solution for zero-turbulence is also shown for comparison. Results from Mehendale et al. (1991) are also presented for comparison. Turbulence levels used in the study by Mehendale et al. (1991) were 0.75%, 5.07%, and 9.67%. Their results agree well with the present results closer to the leading edge. However, farther from the leading edge, the present results are lower than that from Mehendale et al. (1991).

Figure 50(b) compares the stagnation point heat transfer results from the present study with established correlations by Smith and Keuthe (1966), Kestin and Wood (1971) and Lowery and Vachon (1975). The present data agree most closely with the Kestin and Wood correlation. Comparison with other two correlations is not good at $TuRe^{1/2}$ values over 20. All the three correlations are close to each other at low $TuRe^{1/2}$ values. In the present study, the Reynolds number is constant and the free-stream turbulence is varied to obtain different $TuRe^{1/2}$ values.

• Film Cooling

Figure 51 presents the detailed $Nu/Re^{0.5}$ distributions for the three blowing ratios for both coolants at $Tu=1\%$. For both coolants, an increase in blowing ratio produces higher $Nu/Re^{0.5}$ values. For low blowing ratio of 0.4, the $Nu/Re^{0.5}$ values are higher near the top edge of the film holes. As blowing ratio increase, the $Nu/Re^{0.5}$ values are higher downstream of the entire hole. The coolant has limited interaction with the mainstream for low blowing ratios. However, as blowing ratio increase, the interaction with mainstream increases producing more turbulent mixing thus

enhancing downstream heat transfer coefficients. The $Nu/Re^{0.5}$ distributions for the same blowing ratio for both coolants appear similar. However, the higher density coolant produces slightly lower $Nu/Re^{0.5}$ values due to lower momentum flux ratio (I).

Figure 52 presents the detailed film effectiveness distributions at the three blowing ratios for both coolants at $Tu=1\%$. Effectiveness in the axial direction along the hole decreases with an increase in blowing ratio. However, effectiveness appears to be highest for $M=0.8$ with CO_2 injection. It is clearly evident that the coolant streaks show more angle away from the mainstream as blowing ratio increases. At higher blowing ratios, coolant jets have a higher momentum into the mainstream which may cause the angled coolant streaks. Higher density coolant (CO_2) provides higher effectiveness near the hole at a blowing ratio of $M=0.8$ compared to lower density coolant (air). However, at $M=0.4$, air provides better effectiveness. Air as coolant possesses higher momentum than CO_2 at the same blowing ratio. At low blowing ratio, air has optimum momentum to provide higher effectiveness on the surface. The coolant density effect appears to be reduced at higher blowing ratios of $M=1.2$. At higher blowing ratios, coolant jets shoot into the mainstream and disturb the thin boundary layer without providing enough protection.

Figure 53 presents the span-averaged $Nu/Re^{0.5}$ distributions for both coolants at all three blowing ratios. The momentum flux ratios (I) for each coolant at different blowing ratios are presented in the figure. Span-averaged results are presented from the upstream edge of film hole location (10°) to about 70° from leading edge stagnation point. The $Nu/Re^{0.5}$ values are high at the hole location and decrease

downstream for all blowing ratios and both coolants. Far downstream (70°), the effect of film injection is reduced and $Nu/Re^{0.5}$ values are closer to a value of 1.0. The no-grid turbulence case for smooth surface is also presented for comparison. An increase in blowing ratio produces an increase in $Nu/Re^{0.5}$ values for both coolants. An increase in coolant density produces lower $Nu/Re^{0.5}$ values for same blowing ratio. CO_2 as coolant has lower momentum flux ratio compared to air at the same blowing ratio. The coolant-to-mainstream momentum flux ratio is also an important parameter in film cooling situations. Higher density coolant is heavier than the oncoming mainstream fluid. This reduces coolant jet to mainstream interaction, thus reducing turbulent mixing, which in turn produces lower heat transfer coefficients compared to a coolant which has same density as mainstream. Figure 53 also presents the span-averaged film effectiveness distributions for all three blowing ratios and both coolants. Results are presented from upstream edge of film hole location. Effectiveness value decrease slightly with increase in distance from hole location. An increase in blowing ratio produces lower film effectiveness for air injection. However, the effect of blowing ratio for an increase from $M=0.8$ to $M=1.2$ does not produce much variation for $\bar{\eta}$ values with air as coolant. It should be noted that the detailed film effectiveness distributions at the two blowing ratios are different. CO_2 as coolant provides highest effectiveness at $M=0.8$. Film effectiveness with CO_2 as coolant is lower than for air as coolant at blowing ratios of 0.4. However, at higher blowing ratios ($M=1.2$), the effect of coolant density disappears. Both air and CO_2 produces similar $\bar{\eta}$ values for $M=1.2$.

- **Effect of Free-Stream Turbulence**

The effect of free-stream turbulence is also an important parameter that effects airfoil leading edge film effectiveness and heat transfer coefficients. Figure 54 presents the detailed $Nu/Re^{0.5}$ distributions for air injection at blowing ratios of 0.4 and 1.2 under increased free-stream turbulence. Two higher levels of turbulence at 4.1% and 7.1% are presented for both blowing ratios. Free-stream turbulence does not appear to significantly affect the $Nu/Re^{0.5}$ distributions downstream of injection. Free-stream turbulence intensity may be lower than the large-scale turbulence generated immediately downstream of film holes by coolant-mainstream mixing. This may be the reason for the small effect of free-stream turbulence on heat transfer coefficients.

Figure 55 presents the detailed $Nu/Re^{0.5}$ distributions for CO_2 injection at blowing ratios of 0.4 and 1.2 under increased free-stream turbulence. Two higher levels of turbulence at 4.1% and 7.1% are presented for both blowing ratios. Free-stream turbulence does not seem to significantly alter the $Nu/Re^{0.5}$ distributions for both blowing ratios as in the case for air injection. However, an increase in free-stream turbulence appears to reduce the spanwise variations downstream compared to the no-grid case ($Tu=1\%$) for both blowing ratios. Higher free-stream turbulence enhances coolant-mainstream mixing which may be the reason for reduced spanwise variations of Nusselt numbers.

Figure 56 presents the span-averaged $Nu/Re^{0.5}$ distributions for both air and CO_2 injection under the effects of increase free-stream turbulence. It can be seen that free-

stream turbulence has little effect for most of the surface for both coolants at both blowing ratios. However, in the region immediately (1 hole diameter) downstream of the holes, the free-stream turbulence causes significant variations of span-averaged Nusselt number values.

Figure 57 presents detailed film effectiveness distributions for air injection at blowing ratios of 0.4 and 1.2 under increased free-stream turbulence. Free-stream turbulence reduces film effectiveness significantly for $M=0.4$ ($I=0.16$). Higher free-stream turbulence breaks down low momentum coolant jets ($I=0.16$) and decreases surface protection. The reduction in the film effectiveness is clearly evident in the detailed distributions. At higher blowing ratio of 1.2 ($I=1.44$), the effect of free-stream turbulence is not so significant. However, the effectiveness is slightly reduced immediately downstream of injection. There is more uniform effectiveness over the entire surface at higher free-stream turbulence. The stronger momentum jets at $M=1.2$ ($I=1.44$) are not affected significantly by free-stream turbulence as in the case for $M=0.4$.

Figure 58 presents the detailed film effectiveness distributions for CO_2 injection at blowing ratios of 0.4 and 1.2 under increased free-stream turbulence. Free-stream turbulence reduces film effectiveness significantly for $M=0.4$ from $Tu=1\%$ to $Tu=7.1\%$. Higher free-stream turbulence breaks down coolant jet structure ($I=0.107$) at low blowing ratio. At higher blowing ratio of 1.2 ($I=0.96$), the effect of free-stream turbulence is not so significant with more uniform effectiveness over the entire surface at higher free-stream turbulence. Effectiveness downstream of the hole is reduced with an increase in free-stream turbulence.

Figure 59 presents the span-averaged film effectiveness distributions for both air and CO_2 injection under the effects of increase free-stream turbulence. For a low blowing ratio of 0.4, the film effectiveness value drop significantly with an increase in free-stream turbulence for air and CO_2 injection. The free-stream turbulence effect is not so significant at $M=1.2$ for both coolants. There is a slight reduction in the region immediately downstream of the holes. But the effectiveness values are not affected by an increase in free-stream turbulence at such high blowing ratios.

Local Nusselt numbers (Nu) with film injection are normalized by local Nusselt numbers (Nu_0) without film injection. The local Nusselt number ratios (Nu/Nu_0) are regionally averaged to produce a single spatially averaged Nusselt number ratio for each blowing ratio for each coolant at each free-stream turbulence. The spatial averaging is done for the spanwise length encompassing four-hole spacing as shown in the detailed distributions and for the axial distance from 20° to 70° (downstream of injection hole) from leading edge. Similarly, the local film effectiveness values are averaged over the same region to produce a single spatially averaged film effectiveness. The spatially averaged Nusselt number ratios and film effectiveness values are plotted against the momentum flux ratios in Figure 60. The open symbols represent I values with air injection and closed symbols represent I values with CO_2 injection. The Nusselt number with film injection are normalized by Nusselt number without film injection at the same free-stream turbulence intensity. The Nusselt number ratios show a continuing increase with an increase in momentum flux ratio. With increasing I, there is more coolant-to-mainstream interaction causing higher heat transfer coefficients downstream of injection. This may be the reason for the

increase in Nusselt number ratio with increasing I . With an increase in free-stream turbulence, Nusselt number ratio at the same I value decreases. As indicated earlier, Nusselt number downstream of injection (Nu) are not affected by increases in free-stream turbulence intensity. However, Nusselt numbers without film injection (Nu_0) increase with an increase in free-stream turbulence intensity. This is the reason for lower Nusselt number ratios for higher free-stream turbulence intensity. Film effectiveness values at low turbulence (1.0%) increase from $I=0.1$ to a peak at $I=0.16$ and then decrease to $I=0.96$ and are maintained at about same level at $I=1.44$. With an increase in free-stream turbulence intensity, film effectiveness at low I decrease significantly. At low I , film effectiveness is very low at $Tu=7.1\%$. At high I ($I>0.96$), free-stream turbulence has little effect on film effectiveness. The high momentum jets are not easily broken down by higher free-stream turbulence as in the case for low momentum jets. The results obtained from this study using two different coolants at same blowing ratios correlate well with the dependent parameter I . From the results, it can be interpreted that momentum flux ratio can be used a parameter to correlate the effects of coolant density and coolant blowing ratio.

4.7 Film Temperature Measurements on A Cylindrical Leading Edge Film Cooling Model

Tests were conducted in a low speed wind tunnel for a Reynolds number of 100,900 based on a cylinder diameter. Film effectiveness and the temperature field measurement results are presented for two blowing ratios (M) of 0.4 and 1.2 and two turbulence intensities (Tu) of 1% and 7.1%.

Figures 61-64 present the results of film temperature field measurements. Figures 61 and 62 represent the case of a small blowing ratio, $M=0.4$. Low turbulence level results are presented in Figure 61. The results at 20° and 30° show the clear shape of the injected jet. Maximum temperature can be obtained at the center of a jet trajectory. Very high temperature fluctuation can be found at the mixing region of the jet and free-stream where the mean temperature varies greatly. The results at 50° and 70° show a very small region of high temperature. According to Figure 54(a), the film effectiveness is still high at 50° and 70° along with jet trace. These results imply that the jet approaches very close to the wall as it progresses downstream due to the curvature and pressure gradient effect. The jet trajectories taken from Figure 54 appear to be different from that of Figures 61 and 62. It seems that the bottom part of the jet is in the relatively low momentum part of the boundary layer, and thus the amount of deflection is different for the top and bottom parts of the jet. The cold-wire probe cannot approach the cylinder wall close enough to reveal very thin jet at these angles. The nearest measurement point is 0.5mm from the cylinder surface. High free-stream turbulence results are shown in Figure 62. Since high free-stream

turbulence enhances the diffusion of a jet, the jet is mixed with free-stream and spread out much more when compared with low free-stream turbulence. Thus the maximum temperature of a jet is slightly lower than the low free-stream turbulence for the near hole region such as the angle of 20° and 30° . As shown in Figure 54(a), free-stream turbulence reduces the film effectiveness significantly. At 50° and 70° angle, there remains little of the jet and both the mean temperature and the temperature fluctuations are very small. It implies that most of the jet is diffused and provides little effectiveness there. For a small blowing ratio, the jet momentum is small and it follows the main stream immediately after injection regardless of the turbulence intensity, thus the spanwise displacement of a jet is very small and is also clearly seen in Figure 54(a).

The results of a high blowing ratio are depicted in Figures 63-64. As previously presented, low turbulence is shown in Figure 63 and high turbulence in Figure 64. From the figure, a kidney shaped vortex just downstream of the injection can be clearly seen. The effect of curvature and pressure gradient makes the coolant jet deflect closer to downstream and accelerate. The jet deflection in the direction of injection for the leading edge is much larger than that for the flat plate when comparing the results with Ekkad et al. (1997a). Thus the development of secondary motion in the deflecting jet is increased and results in the formation of a kidney shaped vortex. This kind of formation does not occur in lateral injection flat plate film cooling (Han et al., 1997). In the study of Han et al. (1997), only one dominating vortex can be found. The kidney vortex formation results in low film cooling effectiveness along the centerline of the jet passage and high effectiveness at

the edge region of jet passage as can be found in Figure 54(b). For low free-stream turbulence, both sides of the vortex contact the surface and provide high film cooling effectiveness along the edge of the jet passage near the cooling hole region as can be found in Figure 54(b). Temperature distribution cannot show this clearly because the probe cannot measure closely enough to reveal this near wall jet behavior. For high free-stream turbulence, the jet also forms a kidney shaped vortex but only one side of the jet touches the surface and show the high film cooling effectiveness as can be seen in Figure 54(b). The temperature distributions are not greatly affected by the turbulence intensity. As the jet proceeds downstream, it approaches the wall and provides better film coverage over the downstream region compared to the low blowing ratio. AT the downstream region, such as 50° and 70° angle, the mean temperature distribution and temperature fluctuation is affected little by a free-stream turbulence. Due to the large momentum of the jet, the jet trajectories are more deflected when compared to the results of a small blowing ratio. As can be seen in Figure 54, the deflection is reduced by a high free-stream turbulence. Turbulent mixing transfers the momentum of a jet into a free-stream and the deflection is reduced.

5.0 CONCLUSIONS

5.1 Conclusions on gas turbine blade models

1. Detailed Nusselt number and film effectiveness distributions using a transient liquid crystal technique were obtained on the entire turbine blade mid-span region. The strong spanwise and axial variations due to film injection are clearly evident in the detailed distributions that provide valuable insight into the film cooling process.
2. It is important to note that unsteady wake, trailing edge coolant jets, free-stream turbulence, coolant density and flow Reynolds numbers are all important parameters affecting the blade surface heat transfer coefficient and film cooling effectiveness.
3. Nusselt numbers are significantly enhanced for a film cooled blade compared to a non-film cooled blade. Film injection also causes earlier boundary layer transition on the suction surface.
4. Higher film effectiveness streaks are observed downstream of injection holes on the suction surface. However, the streaks are not evident on the pressure surface.
5. Nusselt numbers increase with an increase in blowing ratio, particularly in the region immediately downstream of holes. Film effectiveness significantly increases with an increase in blowing ratio for CO₂ injection.
6. An increase in coolant density has little effect except in the regions immediately downstream of injection where CO₂ injection provides higher Nusselt numbers

than air injection. CO_2 injection provides highest effectiveness at $M=1.2$ compared to air injection. Air injection provides higher effectiveness at $M=0.8$ compared to CO_2 as coolant.

7. Unsteady wake promotes mainstream turbulence and thus enhances the heat transfer coefficient on blade surface. However, unsteady wake significantly reduces film effectiveness. Unsteady wake also induces earlier boundary layer transition to turbulence on the suction surface and reduces spanwise variations of the heat transfer coefficients over the entire blade surface.
8. For the blade model with only one row of cooling holes near the gill hole region on the suction surface, unsteady wake plays a dominate role in determining the boundary –layer transition location. Single-row of film injection does not affect much on the location of boundary-layer transition.
9. A grid-generated turbulence imposed on an unsteady wake further enhances the heat transfer coefficient on the blade surface and also promotes early transition on the blade suction surface.
10. The trailing edge jets compensate the defect of the velocity profile caused by the rod passing, and hence velocity is slightly increased for the mainstream flow while the turbulence intensity profile is more uniformly disturbed. The net effect of trailing edge jets is to increase both the pressure surface heat transfer near blade leading edge region and the suction surface heat transfer before boundary layer flow transition. The net effect diminishes in transition and fully turbulent regions on suction surface or far away from the blade leading edge on pressure surface.

11. For a film cooled blade, trailing edge ejection has only a small effect on blade surface heat transfer coefficients compared to other significant parameters such as film injection, unsteady wakes, and grid generated turbulence, respectively in that order of decreasing effect. Film effectiveness decreases with the addition of trailing edge ejection in the leading edge region on both pressure and suction surfaces. However, the effect decreases further downstream.
12. The development of coolant jet mean temperature and its fluctuation profiles provides better understanding of the film cooling process and can be used to explain the film cooling performance.

5.2 Conclusions on cylindrical leading edge models

1. On a cylindrical leading edge model without film cooling hole, heat transfer coefficient is enhanced up to 30% for $Tu=4.1\%$ and up to 50% for $Tu=7.1\%$ over a $Tu=1\%$.
2. On a cylindrical leading edge model with film cooling, high free-stream turbulence enhances the diffusion of a jet into a free stream. For a small blowing ratio, free-stream turbulence largely affects film cooling effectiveness. Free stream turbulence significantly reduces film effectiveness.
3. Increase in blowing ratio increases Nusselt numbers downstream of injection. Effectiveness for air injection is higher at low blowing ratio $M=0.4$ and decreases with an increase in blowing ratio. Effectiveness for CO_2 injection is highest at

$M=0.8$. Higher heat transfer coefficient region does not necessarily correspond to high film effectiveness as seen in the detailed distributions.

4. Increase in coolant density causes a decrease in heat transfer coefficients at all blowing ratios. Air provides better effectiveness at low blowing ratios. Higher density coolant (CO_2) provides highest effectiveness at $M=0.8$. However, at even higher blowing ratios, an increase in coolant density has little effect on film effectiveness distributions.
5. Higher free-stream turbulence has only a small effect on Nusselt numbers at all blowing ratios for both coolants. However, higher free-stream turbulence reduces film effectiveness significantly at $M=0.4$ for both coolants but has little effect on film effectiveness for $M=1.2$.
6. Overall averaged Nusselt number ratios for film injection show a continual increase with increase in coolant-to-mainstream momentum flux ratio. However, overall averaged film effectiveness varies with different momentum flux ratios. Momentum flux ratio may be used to correlate the results obtained for different coolant densities and coolant blowing ratios.

6.0 REFERENCES

Abhari, R. S., Guenette, G. R., Epstein, A. H., and Giles, M. B., 1992, "Comparison of Time-Resolved Measurements and Numerical Calculations," *ASME Journal of Turbomachinery*, Vol. 114, pp. 818-827.

Abhari, R. S., and Epstein, A. H., 1994, "An Experimental Study of Film Cooling in a Rotating Transonic Turbine," *ASME Journal of Turbomachinery*, Vol. 116, pp. 63-70.

Abuaf, N., Bunker, R., and Lee, C. P., 1995, "Heat Transfer and Film Cooling Effectiveness in A Linear Airfoil Cascade," ASME paper 95-GT-3.

Ames, F. E., 1998, "Aspects of Vane Film Cooling with High Turbulence: part I - Heat Transfer, part II - Adiabatic Effectiveness," *ASME Journal of Turbomachinery*, Vol. 120, pp. 768-784.

Ashworth, D. A., LaGraff, J. E., Schultz, D. L., and Grindrod, K. J., 1985, "Unsteady Aerodynamic and Heat Transfer Processes in a Transonic Turbine Stage," *ASME Journal of Engineering for Gas Turbines and Power*, Vol. 107, pp. 1022-1030.

Blair, M. F., 1994, "An Experimental Study of Heat Transfer in A Large-Scale Turbine Rotor Passage," *ASME Journal of Turbomachinery*, Vol. 116, pp. 1-13.

Blair, M. F., Dring, R. P., and Joslyn, H. D., 1989, "The Effects of Turbulence and Stator/Rotor Interactions on Turbine Heat Transfer: Part I – Design Operating Conditions; Part II – Effects of Reynolds Number and Incidence," *ASME Journal of Turbomachinery*, Vol. 111, pp. 87-103.

Bonnice M.A., and L'Ecuyer, M. T., 1983, "Stagnation Region Gas Cooling – Effects of Dimensionless Coolant Temperature," NASA CR-168197.

Camci, C., and Arts, T., 1990, "An Experimental Convective Heat Transfer Investigation Around a Film-Cooled Gas Turbine Blade," *ASME Journal of Turbomachinery*, Vol. 112, pp. 497-503.

Doorly, D. J., 1988, "Modeling the Unsteady Flow in a Turbine Rotor Passage," *ASME Journal of Turbomachinery*, Vol. 110, pp. 27-37.

Doorly, D. J., and Oldfield, M. L. G., 1985, "Simulation of the Effects of Shock-Waves Passing on a Turbine Rotor Blade," *ASME Journal of Engineering for Gas Turbines and Power*, Vol. 107, pp. 998-1006.

Drost, U., and Böls, A., 1998, "Investigation of Detailed Film Cooling Effectiveness and Heat Transfer Distributions on A Gas Turbine Airfoil," ASME paper 98-GT-20.

Dullenkopf, K., and Mayle, R. E., 1994, "The Effect of Incident Turbulence and Moving Wakes on Laminar Heat Transfer in Gas Turbines," *ASME Journal of Turbomachinery*, Vol. 116, pp. 23-28.

Dullenkopf, K., Schulz, A., and Wittig, S., 1991, "The Effect of Incident Wake Conditions on the Mean Heat Transfer on an Airfoil," *ASME Journal of Turbomachinery*, Vol. 113, pp. 412-418.

Dunn, M. G., 1986, "Heat Flux Measurements for the Rotor of a Full-Stage Turbine: Part I – Time-Averaged Results," *ASME Journal of Turbomachinery*, Vol. 108, pp. 90-97.

Dunn, M. G., Kim, J., Civiskas, K. C., and Boyle, R. J., 1994, "Time-Averaged heat Transfer and Pressure Measurements and Comparison with Prediction for a Two-Stage Turbine," *ASME Journal of Turbomachinery*, Vol. 116, pp. 14-22.

Dunn, M. G., Seymour, P. J., Woodward, S. H., George, W. K., and Chupp, R. E., 1989, "Phase-Resolved Heat Flux Measurements on the Blade of a Full-Scale Rotating Turbine," *ASME Journal of Turbomachinery*, Vol. 111, pp.8-19.

Ekkard, S. V., Zapata, D., And Han J. C., 1997a, "Heat Transfer Coefficients Over a Flat Surface with Air and CO₂ Injection Through Compound Angle Holes Using a Transient Liquid Crystal Image Method," *ASME Journal of Turbomachinery*, Vol. 119, No. 3, pp. 580-586.

Ekkard, S. V., Zapata, D., And Han J. C., 1997b, "Film Effectiveness Over a Flat Surface with Air and CO₂ Injection Through Compound Angle Holes Using a Transient Liquid Crystal Image Method," *ASME Journal of Turbomachinery*, Vol. 119, No. 3, pp. 587-593.

Funazaki, K., Yokota, M., Yamawaki, S., 1995, "The effect of periodic wake passing on film effectiveness of discrete cooling holes around the leading edge of a blunt body," ASME Paper No. 95-GT-183.

Han, B., Sohn, D. K., and Lee, J. S., 1997, Flow and Heat Transfer Measurements of Film injectant from a Row of Holes with Compound Angle Orientations, *International Journal of Rotating Machinery*, accepted for publication.

Han, J. C., Zhang, L., and Ou, S. H., 1993, "Influence of Unsteady Wake on Heat Transfer Coefficient From a Gas Turbine Blade," *ASME Journal of Heat Transfer*, Vol. 115, pp. 184-189.

Haas, W., Rodi, W., and Schöning, B., 1992, "The Influence of Density Difference Between Hot and Coolant Gas on Film Cooling by a Row of Holes: Predictions and Experiments," *ASME Journal of Turbomachinery*, Vol. 114, pp. 747-755.

Hippensteele, S. A., Russell, L. M., and Stepka, F. S., 1983, "Evaluation of a Method for Heat Transfer Measurements and Thermal Visualization Using a Composite of a Heater Element and Liquid Crystals," *ASME Journal of Heat Transfer*, Vol. 105, pp. 184-189.

Hoffs, A., Bölcs, A, and Harasagama, S. P., 1997, "Transient Heat Transfer Experiments in a Linear Cascade Via an Insertion Mechanism Using a Liquid Crystal Technique," *ASME Journal of Turbomachinery*, Vol. 119, pp. 9-13..

Ito, S., Goldstein, R. J., and Eckert, E. R. G., 1978, "Film Cooling of a Gas Turbine Blade," *ASME Journal of Engineering for Power*, Vol. 100, pp. 476-481.

Karni, J. and Goldstein, R.J., 1990, "Surface Injection Effect on Mass Transfer from a Cylinder in Crossflow: A Simulation of Film Cooling in the Leading Edge Region of a Turbine Blade," *ASME Journal of Turbomachinery*, Vol. 112, pp. 418-427.

Kestin, J. and Wood, R.T., 1971, "The Influence of Turbulence on Mass Transfer from Cylinders," *ASME Journal of Heat Transfer*, Vol. 93, pp. 321-327.

Kline, S. J., and McClintock, F. A., 1953, "Describing Uncertainties in Single Sample Experiments," *Mechanical Engineering*, Vol. 75, pp. 3-8.

Kohli, A. and Bogard, D. G., 1998, "Fluctuating Thermal Field in the Near-Hole Region for Film Cooling Flows," *ASME Journal of Turbomachinery*, Vol.120, pp. 86-91.

Lee, J.S., Ro, S.T., Seo, H.J., 1994, "Mass transfer effects of free-stream turbulence and horseshoe vortex formed at the upstream edge of film cooling jets about a cylindrical surface," ASME Paper No. 94-GT-18.

Liu, X., and Rodi, W., 1992, "Measurements of Unsteady Flow and Heat Transfer in a Linear Turbine Cascade," ASME paper No. 92-GT-323.

Lowery, G.W. and Vachon, R.I., 1975, "The Effect of Turbulence on Heat Transfer from heated Cylinders," *International Journal of Heat and Mass Transfer*, Vol. 18, pp. 1229-1242.

Luckey, D.W. and L'Ecuyer, M.R., 1976, "Stagnation Region Gas Film Cooling - Spanwise Angled Coolant Injection," Thermal Sciences and Propulsion Center, Purdue University, W. Lafayette, IN, Technical Report No. TSPC-TR-76-2.

Martinez-Botas, R. F., Lock, G. D., and Jones, T. V., 1995, "Heat Transfer Measurements in an Annular Cascade of Transonic Gas Turbine Blades Using a Transient Liquid Crystal Technique," *ASME Journal of Turbomachinery*, Vol. 117, pp. 425-431.

Mehandale, A. B., Han, J. C., and Ou, S., 1991, "Influence of High Mainstream Turbulence on Leading Edge Heat Transfer," *ASME Journal of Heat Transfer*, Vol. 113, pp. 843-850.

Mehandale, A. B., and Han, J. C., 1992, "Influence of High Mainstream Turbulence on Leading Edge Film Cooling Heat Transfer," *ASME Journal of Turbomachinery*, Vol. 114, pp. 707-715.

Mehandale, A. B., Han, J. C., Ou, S., and Lee, C. P., 1994, "Unsteady Wake Over a Linear Turbine Blade Cascade with Air and CO₂ Film Injection: Part II - Effect on Film Effectiveness and Heat Transfer Distributions," *ASME Journal of Turbomachinery*, Vol. 116, pp. 730-737.

Mick, W.J. and Mayle, R.E., 1988, "Stagnation Film Cooling and Heat Transfer, Including Its Effect Within the Hole Pattern," *ASME Journal of Turbomachinery*, Vol. 110, pp. 66-72.

Nirmalan, V., and Hylton, L., 1990, "An Experimental Study of Turbine Vane Heat Transfer with Leading Edge and Downstream Film Cooling," *ASME Journal of Turbomachinery*, Vol. 112, pp. 477-487.

O'Brien, J. E., and Capp, S. P., 1989, "Two-Component Phase-Averaged Turbulence Statistics Downstream of a Rotating Spoked-Wheel Wake Generator," *ASME Journal of Turbomachinery*, Vol. 111, pp. 475-482.

Ou, S., and Han, J. C., 1992, "Influence of Mainstream Turbulence on Leading Edge Film Cooling Heat Transfer Through Two Rows of Inclined Film Slots," *ASME Journal of Turbomachinery*, Vol. 114, pp. 724-733.

Ou, S., Han, J. C., Mehendale, A. G., and Lee, C. P., 1994, "Unsteady Wake Over a Linear Turbine Blade Cascade with air and CO₂ Film Injection: Part I - Effect on Heat Transfer Coefficients," *ASME Journal of Turbomachinery*, Vol. 116, pp. 721-729.

Salcudean, M., Gartshore, I., Zhang, K., and Barnea, Y., 1994, "Leading Edge Film Cooling of a Turbine Blade Model Through Single and Double Row Injection: Effects of Coolant Density," ASME Paper No. 94-GT-2.

Smith, M.C. and Keuthe, A.M., 1966, "Effects of Turbulence on Laminar Skin Friction and Heat Transfer," *Physics of Fluids*, Vol. 9, pp. 2337-2344.

Takeishi, K., Aoki, A., Sato, T., and Tsukagoshi, K., 1992, "Film Cooling on a Gas Turbine Rotor Blade," *ASME Journal of Turbomachinery*, Vol. 114, pp. 828-834.

Vedula, R. J., and Metzger, D. E., 1991, "A Method for Simultaneous Determination of Local Effectiveness and Heat Transfer Distributions in Three-Temperature Convection Situations," ASME Paper No. 91-GT-345.

Wittig, S., Dullenkopf, K., Schulz, A., and Hestermann, R., 1987, "Lase-Doppler Studies of the Wake-Effectuated Flow Field in a Turbine Cascade," *ASME Journal of Turbomachinery*, Vol. 109, pp. 170-176.

Zhang, L. and Han, J. C., 1995, "Combine Effect of Free-Stream Turbulence and Unsteady Wake on Heat Transfer Coefficients from a Gas Turbine Blades," *ASME Journal of Heat Transfer*, Vol. 117, pp. 296-302.

7.0 Appendix

7.1 Figures 1~64

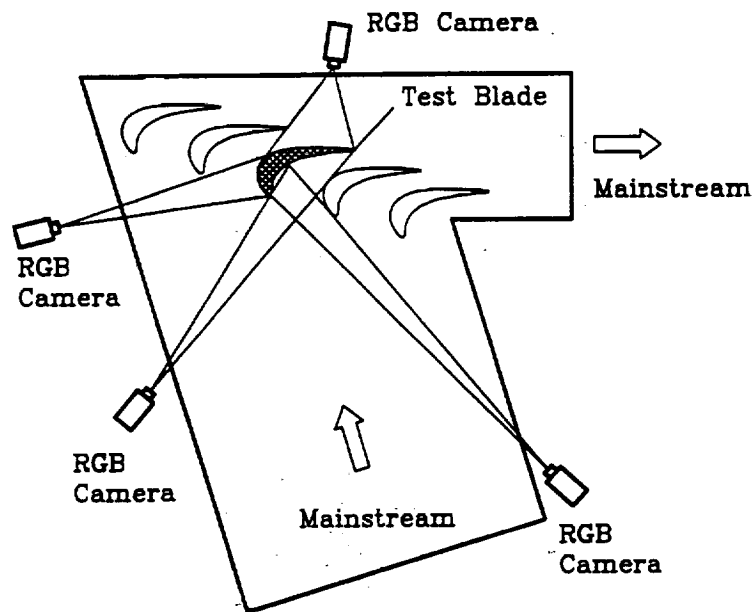
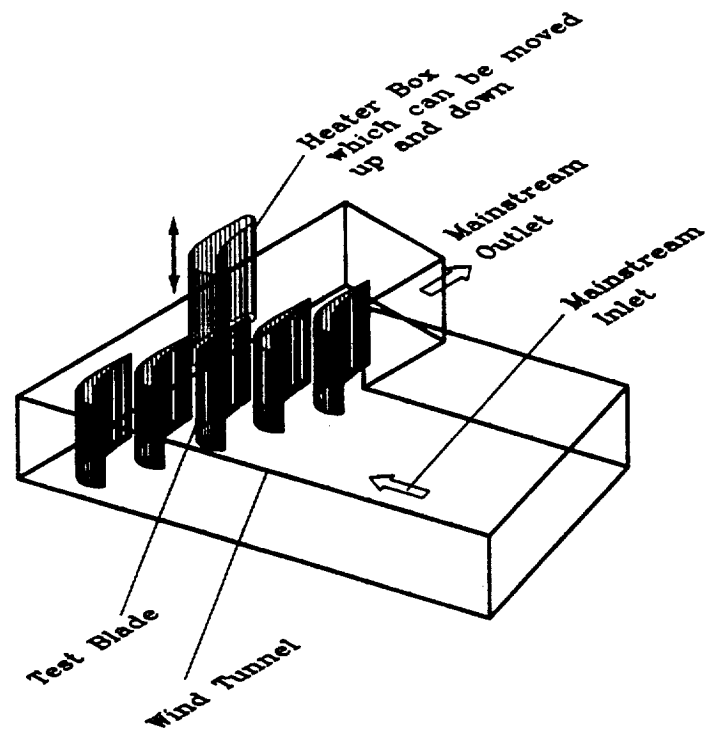


Fig.1 Experiment setup 1: schematic of test section and camera arrangement for film cooling measurement over a gas turbine blade (without wake effect)

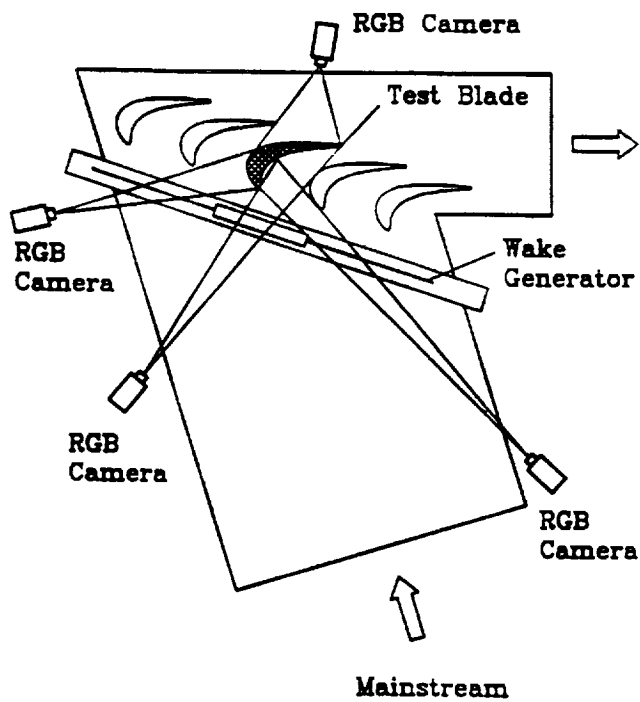
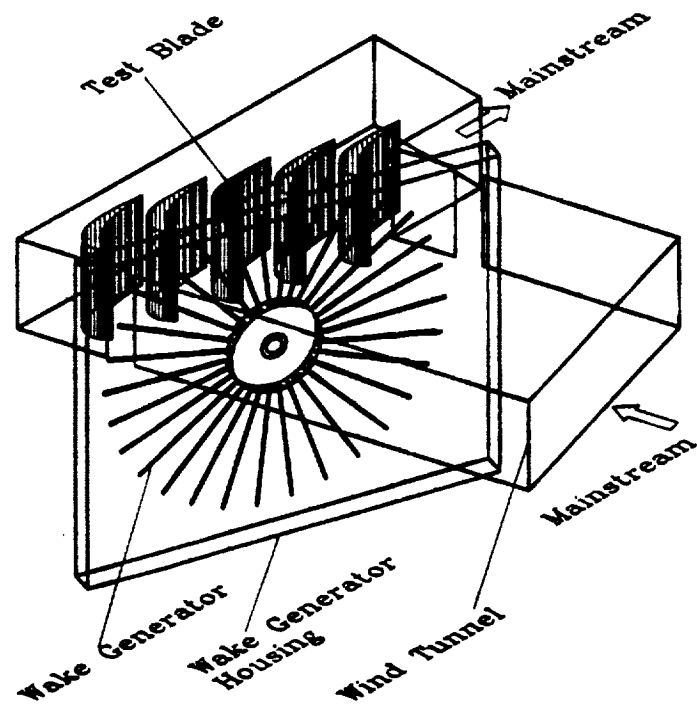
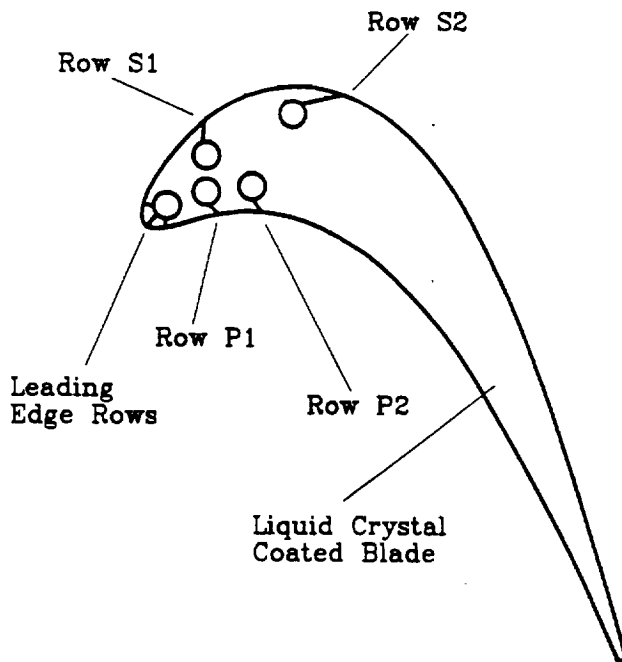


Fig.2 Experiment setup 2: schematic of test section and camera arrangement for film cooling measurement over a gas turbine blade (with wake effect)



Film Hole Location	P/D	L/D	Axial Angle	Radial Angle	Tangential Angle
LE	7.31	2.7	90°	27°	—
S1	4.13	7.6	—	90°	45°
S2	5.71	12.8	—	90°	30°
P1	6.79	4.2	—	32°	55°
P2	5.00	6.7	—	35°	50°

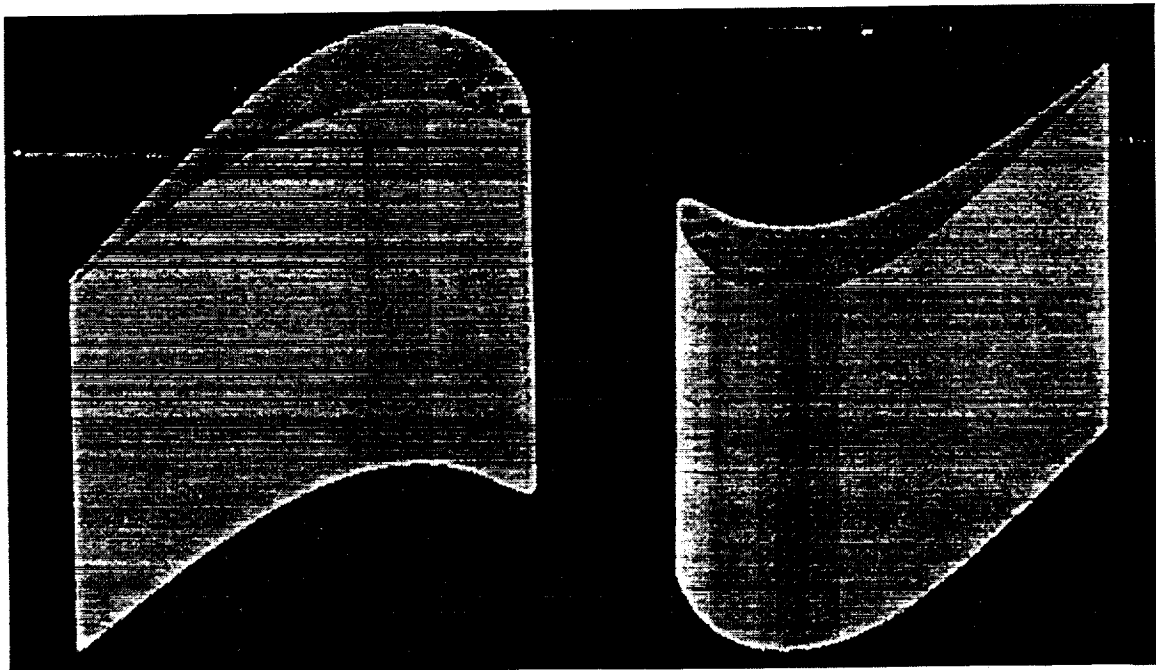


Fig.3(a) Film-cooled turbine blade model

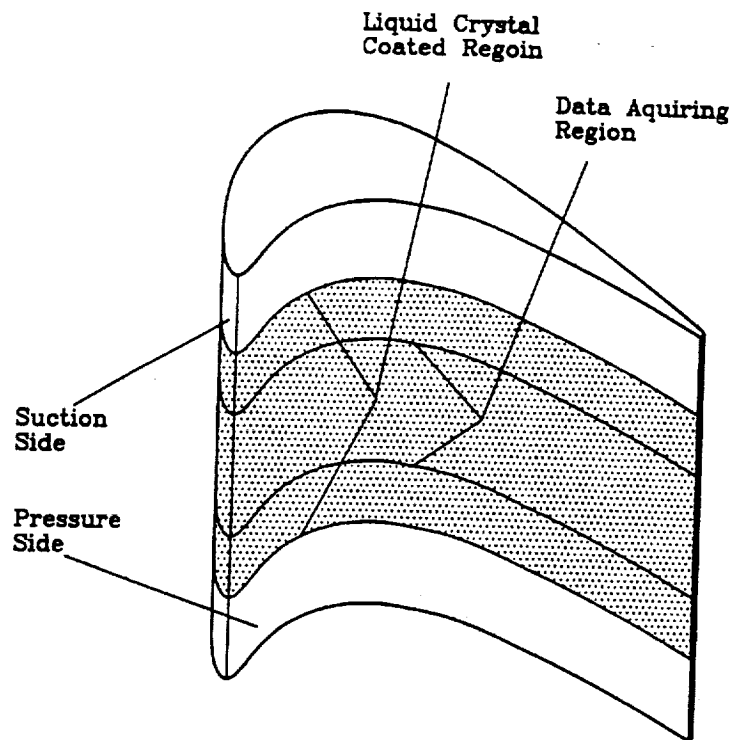


Fig.3(b) The Liquid Crystal Coated Surface Area

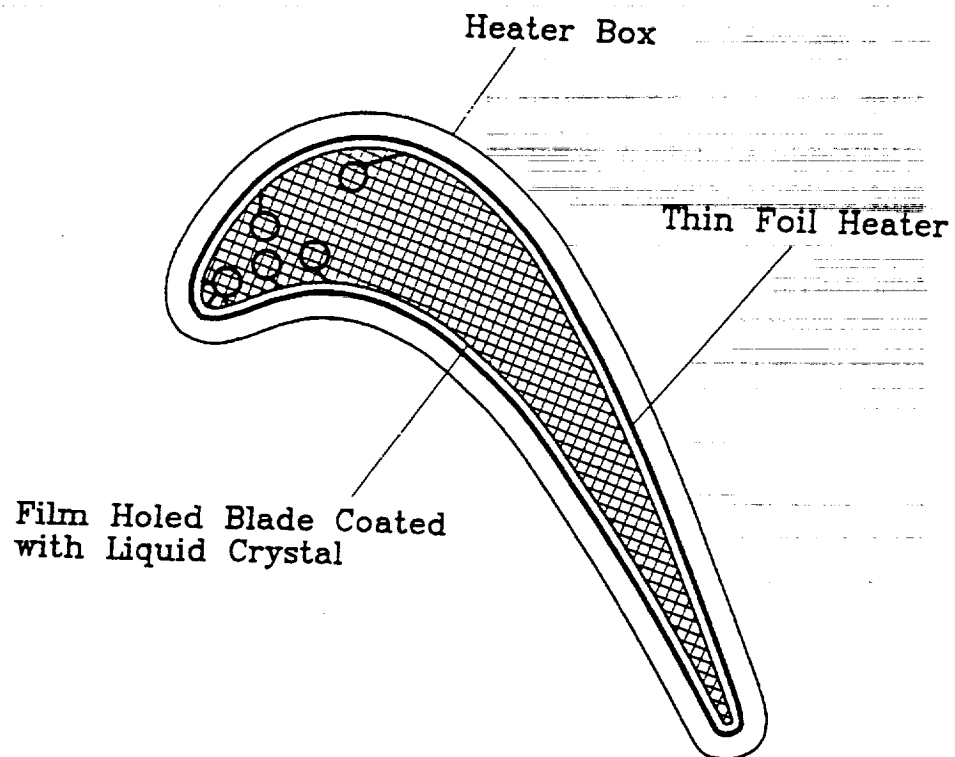


Fig.3(c) Heater Box Cross Section

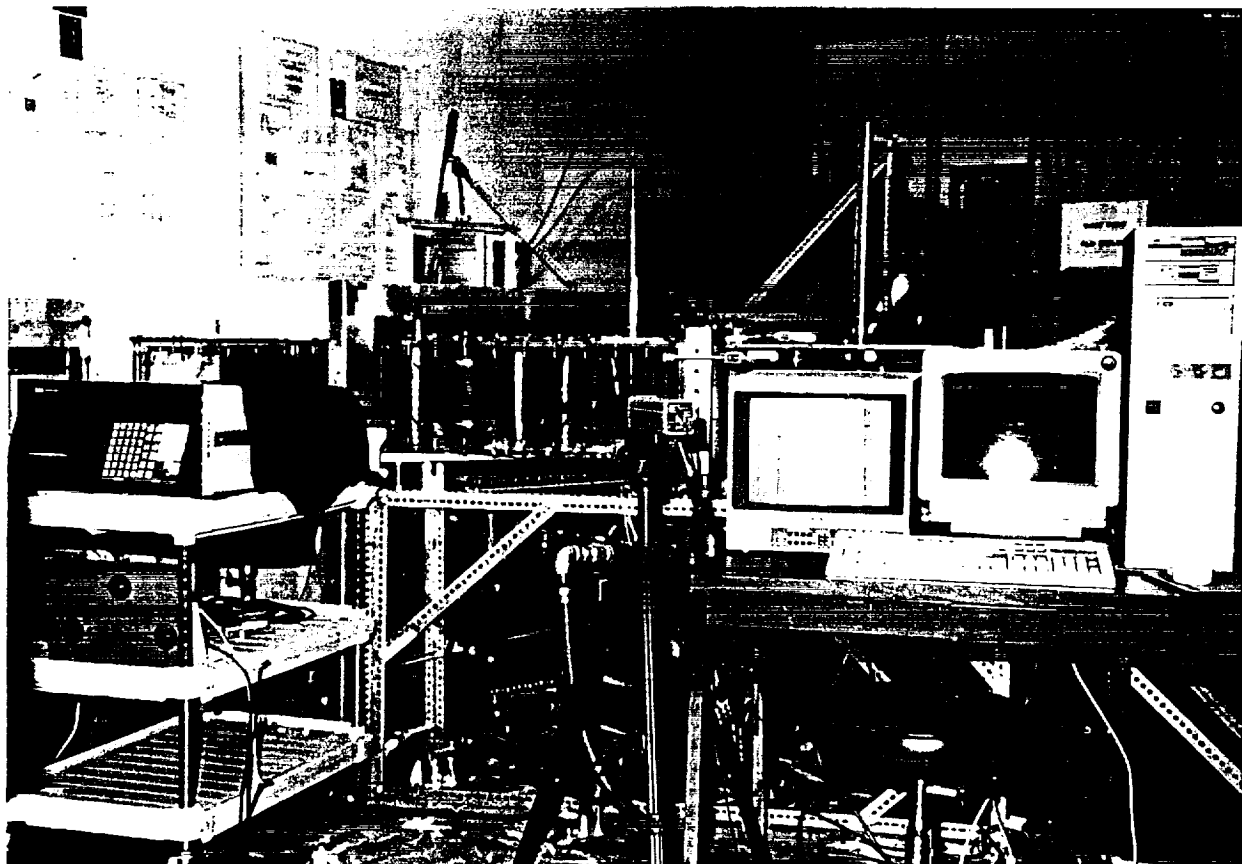


Fig.3(d) Photo of the unsteady flow test facility

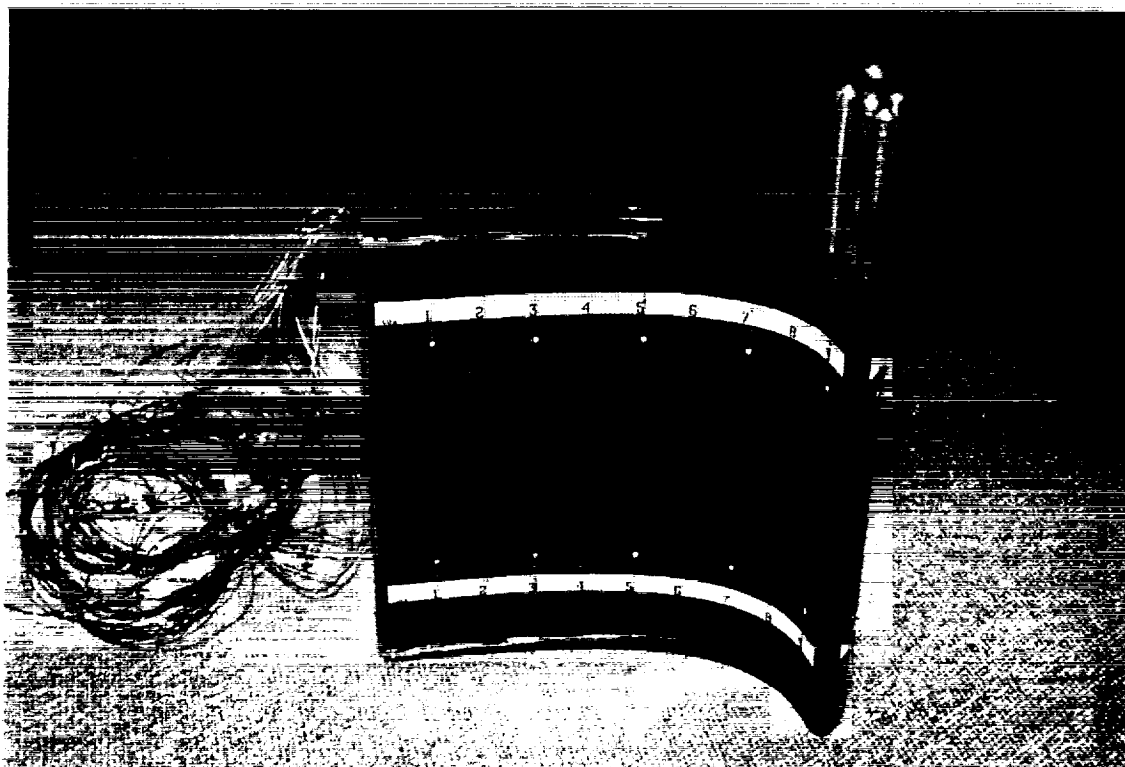
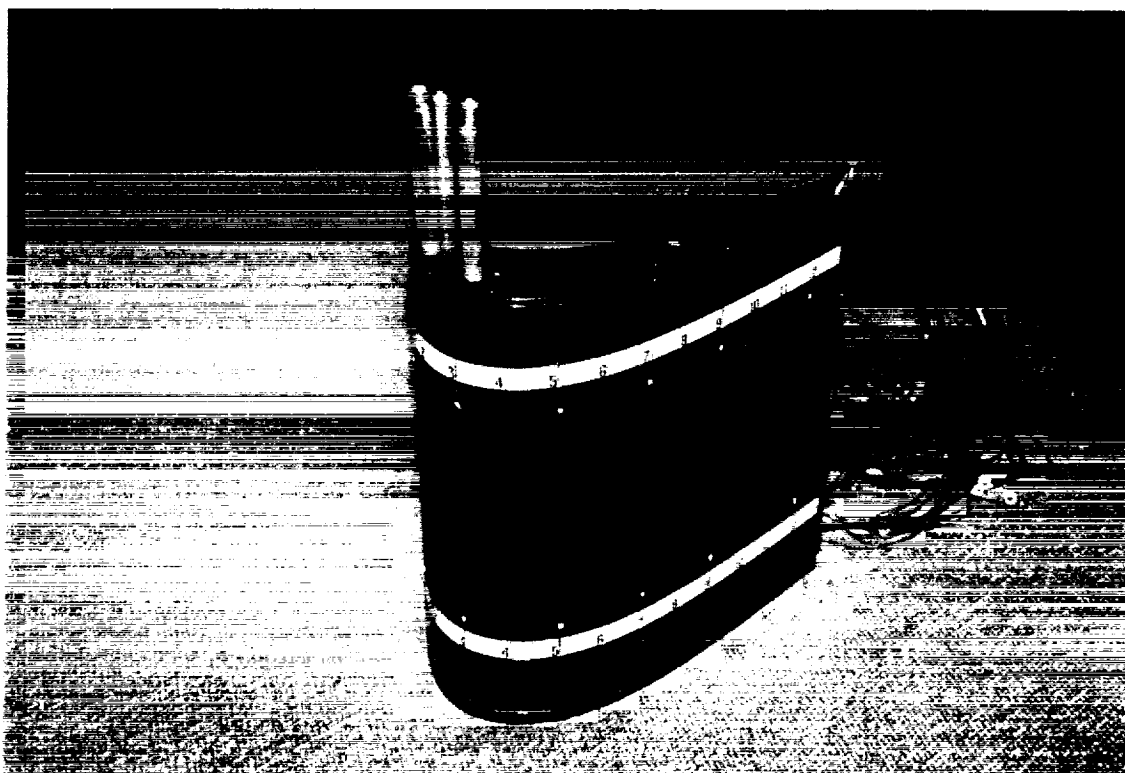


Fig.3(e) Photo of the test blade

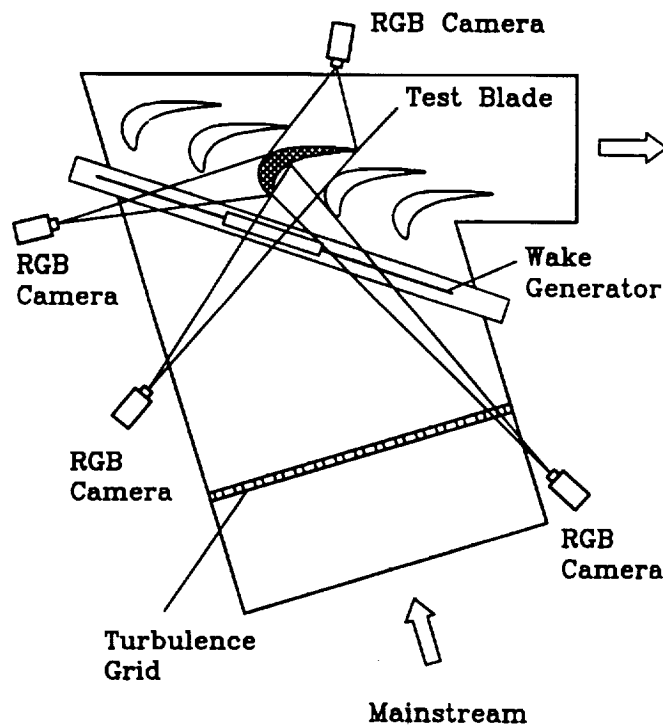
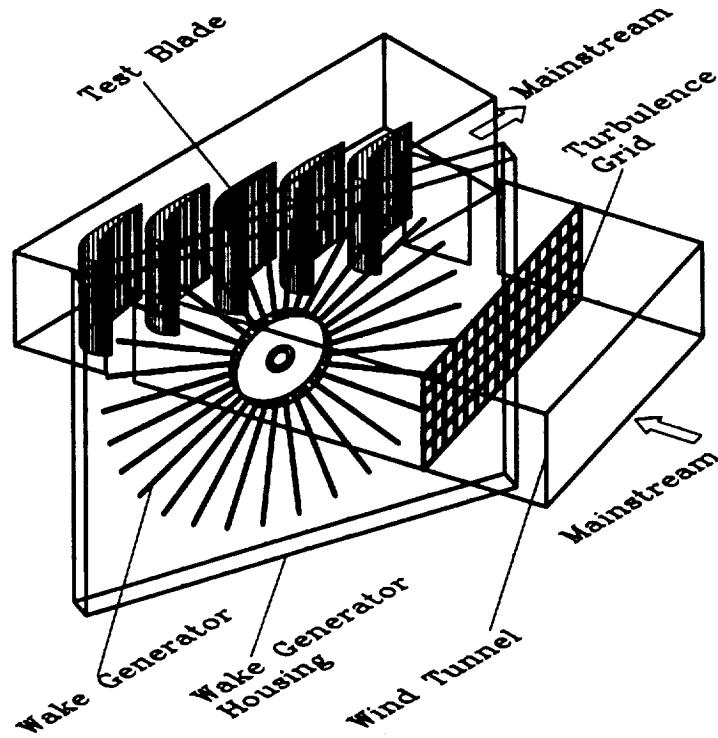


Fig.4 Experiment setup 3: schematic of test section and camera arrangement for the heat transfer and film cooling measurement over a gas turbine blade (with the combined effect of unsteady wake and trailing edge coolant ejection)

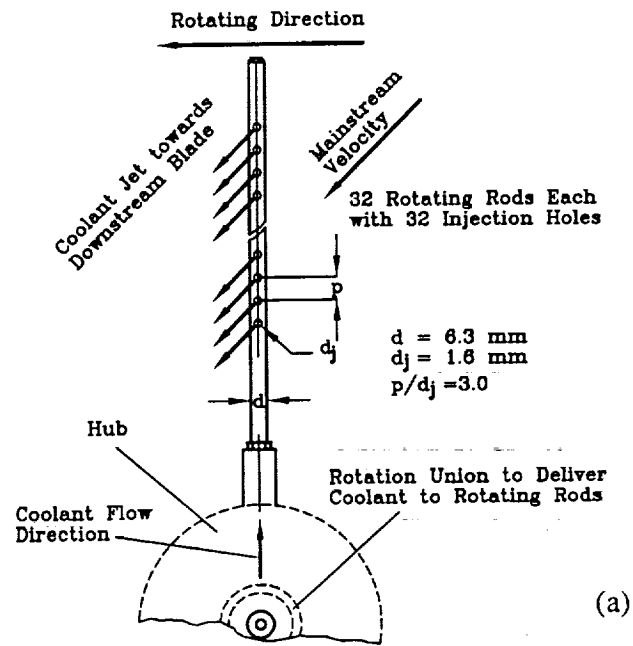


Fig. 5(a) Detailed sketch of a rotating rod

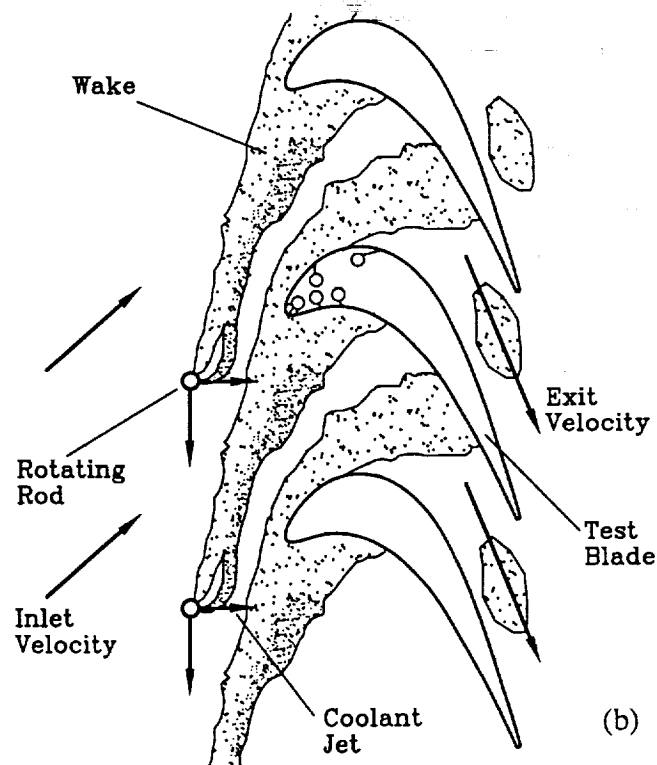


Fig. 5(b) Conceptual view of effects of unsteady wake with coolant ejection on turbine heat transfer

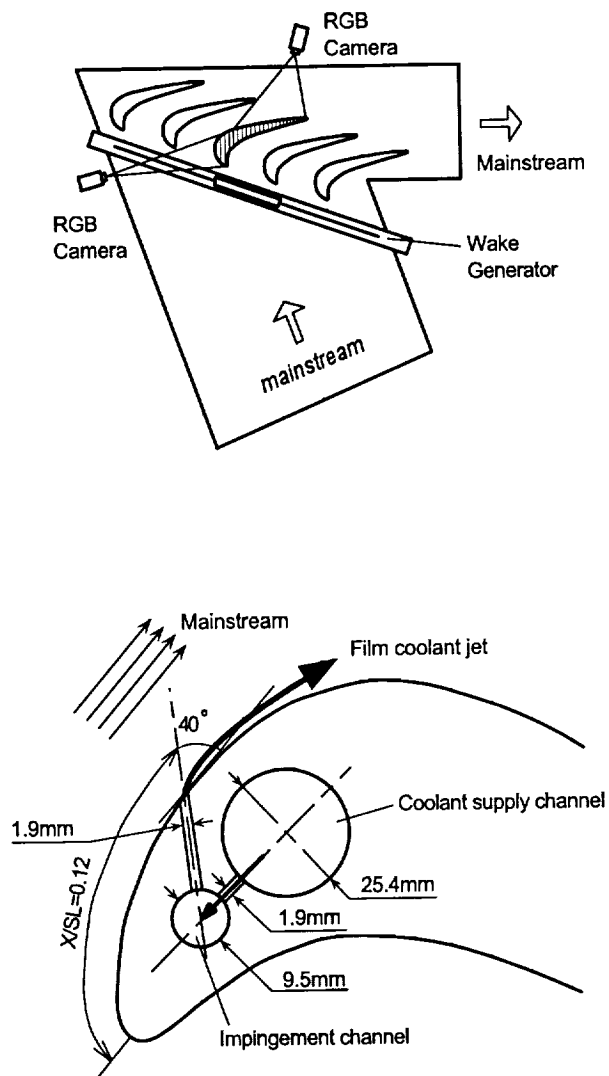


Fig. 6 Experiment setup 4: film temperature and effectiveness measurement on a turbine blade with only one row of film holes on the suction side
 (a) Five blade cascade with center blade coated with liquid crystal and viewed by two cameras
 (b) A 2-D view of the film-cooled blade model

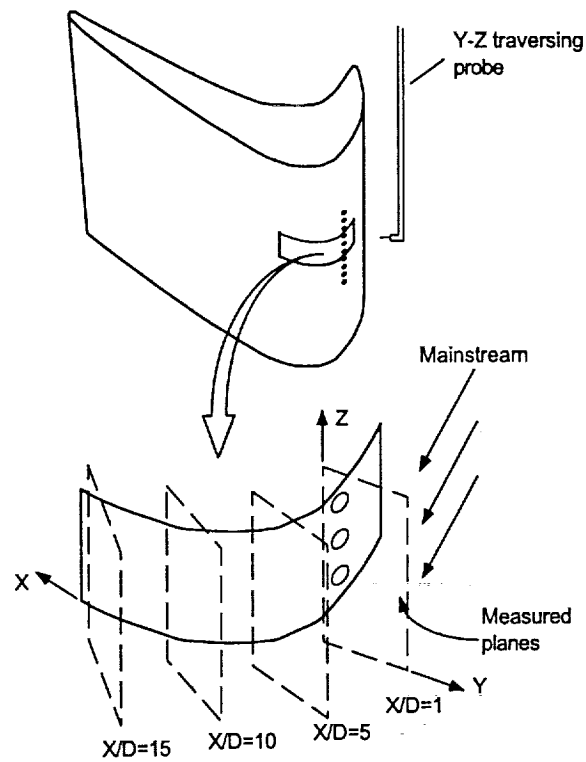


Fig. 7 Measurement planes at selected locations with a cold-wire probe (experiment setup 4)

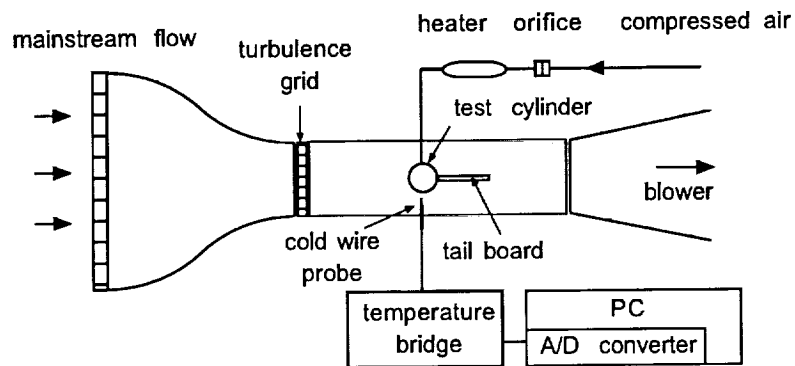


Fig. 8 Experiment setup 5: film temperature and effectiveness measurement on a cylindrical leading edge model

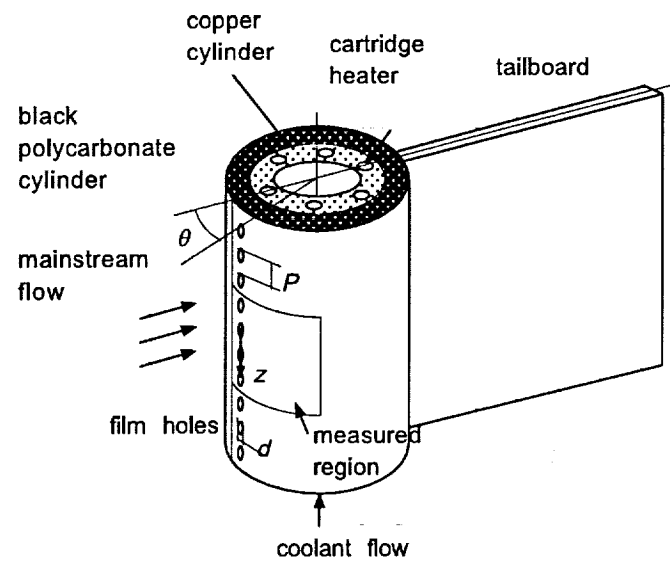


Fig. 9 The cylindrical leading edge model

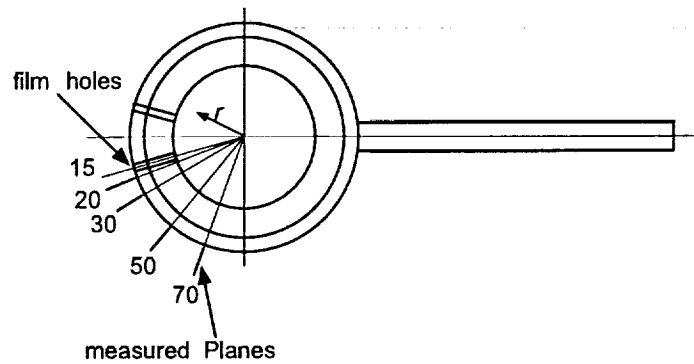


Fig. 10 The measuring planes for the cylindrical leading edge model

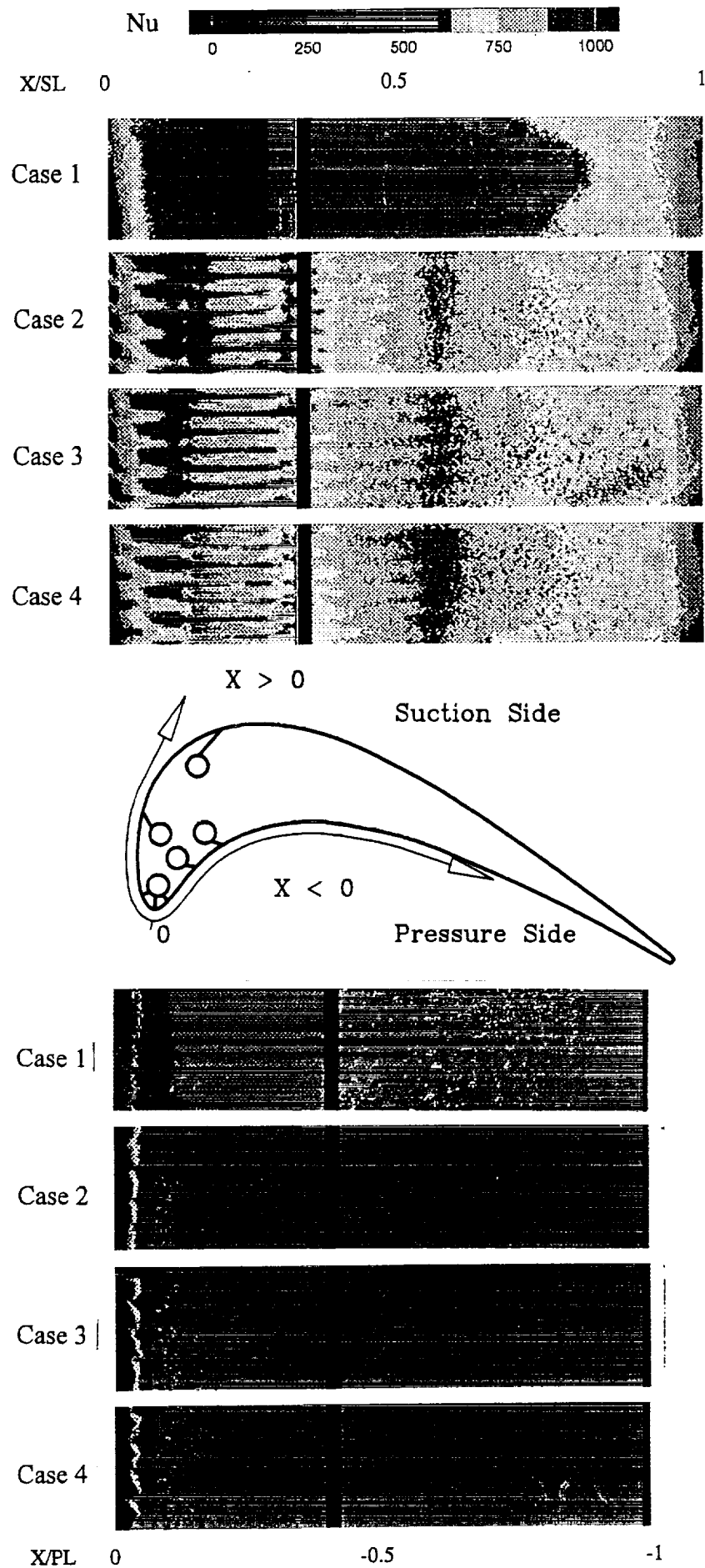


Fig.11 Effect of blowing ratio on detailed Nusselt number distributions for CO_2 injection (Experiment setup 1)

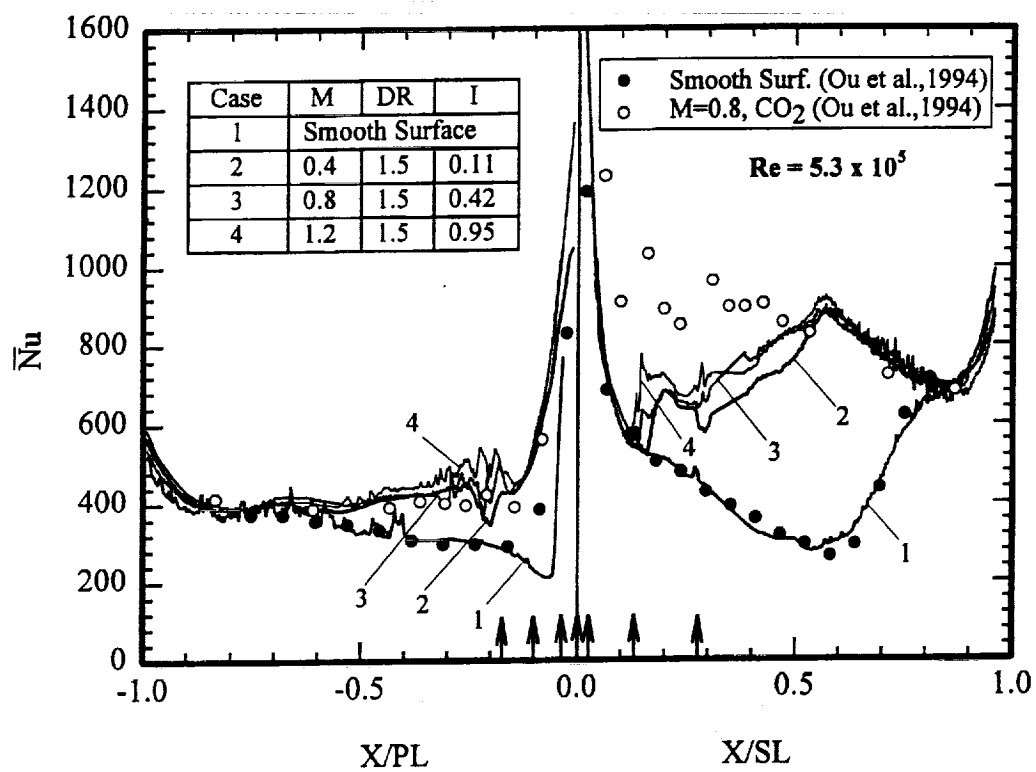


Fig.12 Effect of blowing ratio on spanwise-averaged Nusselt number distributions for CO₂ injection (Experiment setup 1)

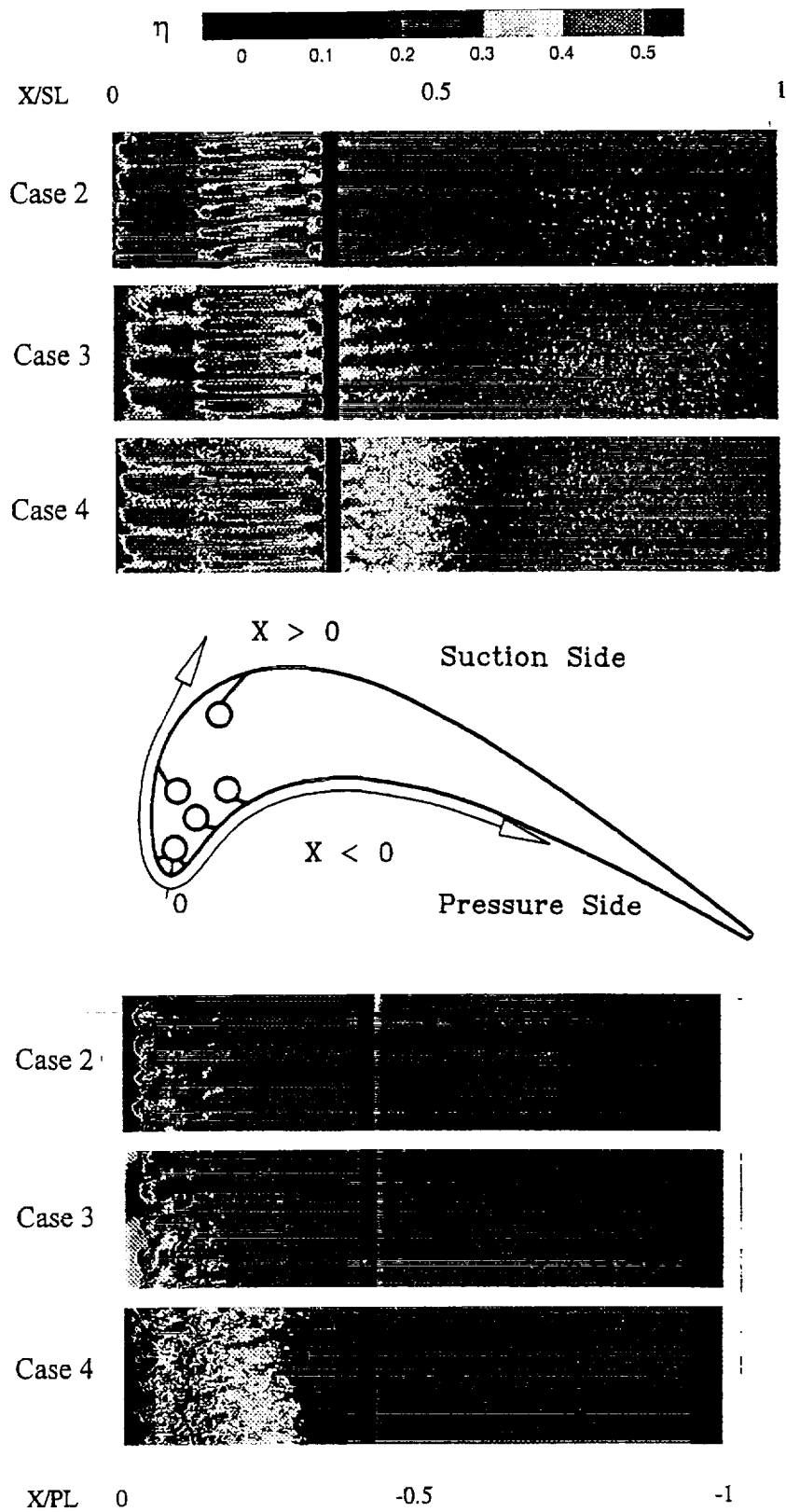


Fig.13 Effect of blowing ratio on detailed film effectiveness distributions for CO_2 injection (Experiment setup 1)

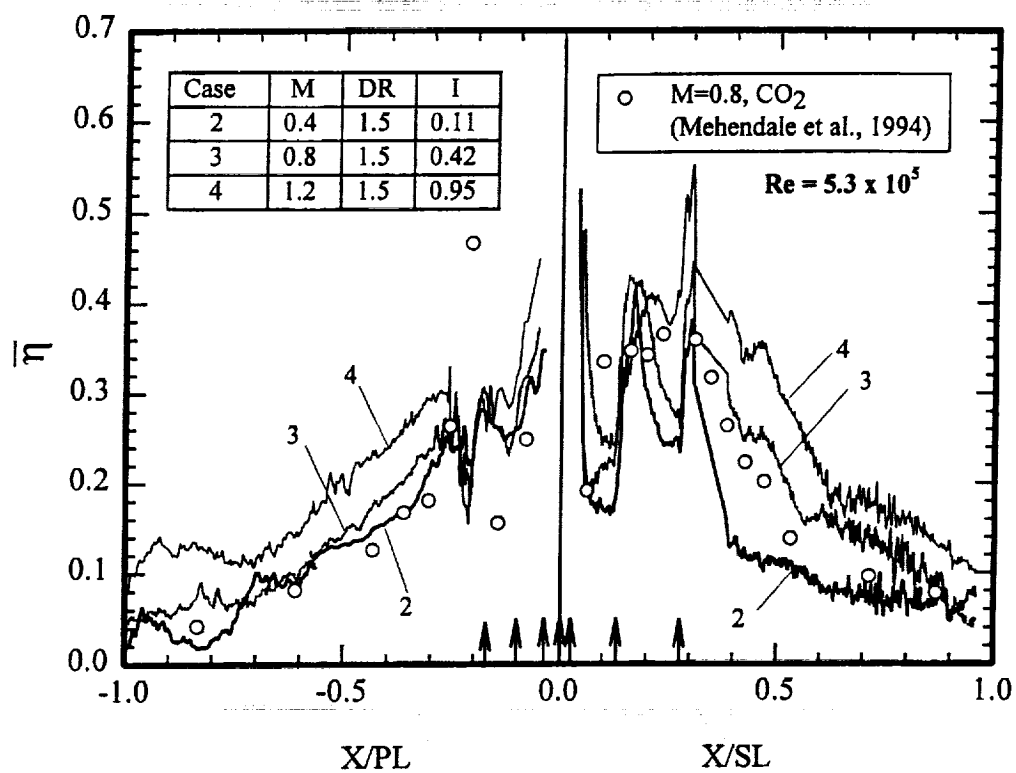


Fig.14 Effect of blowing ratio on spanwise-averaged film effectiveness distributions for CO₂ injection (Experiment setup 1)

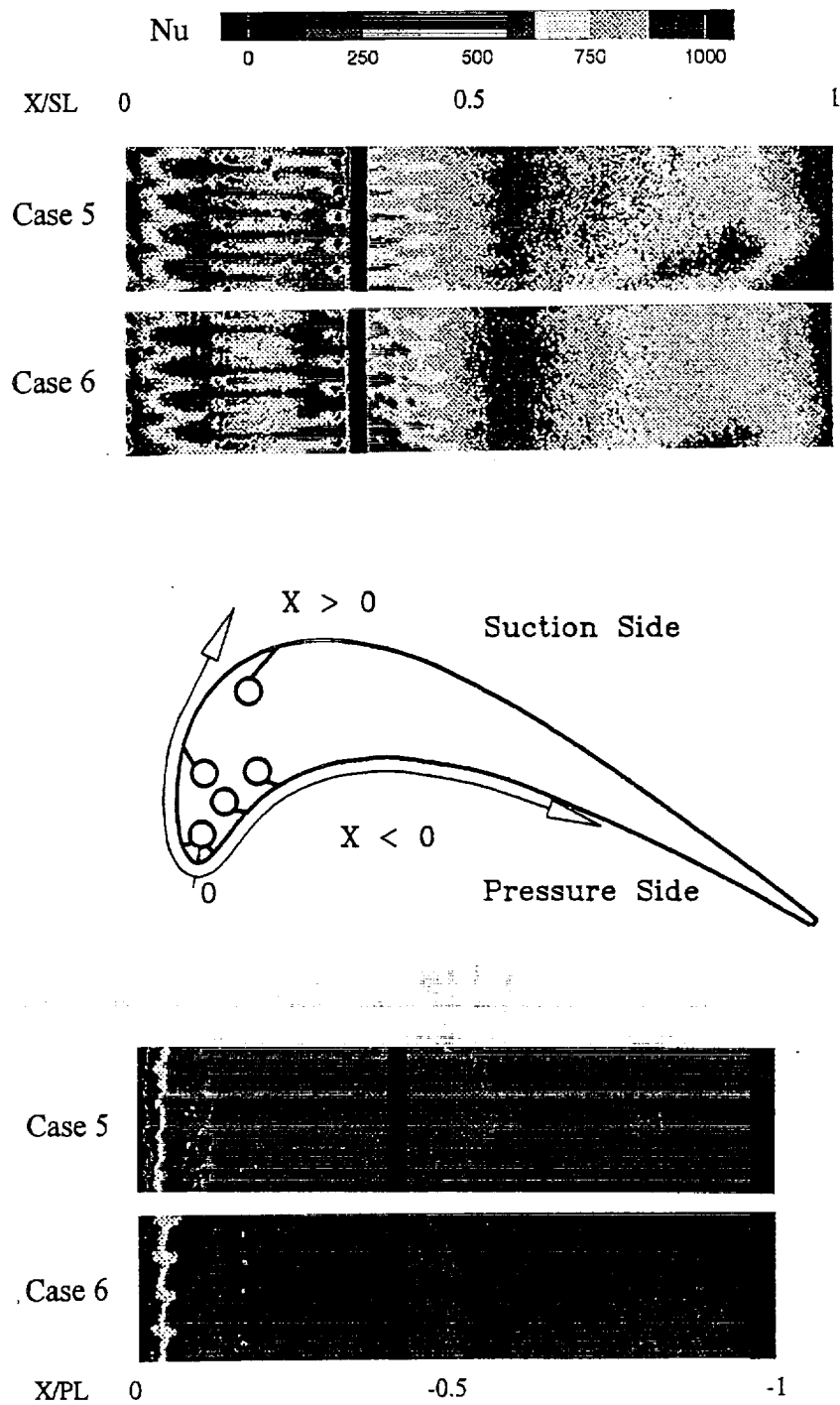


Fig.15 Effect of blowing ratio on detailed Nusselt number distributions for air injection (Experiment setup 1)

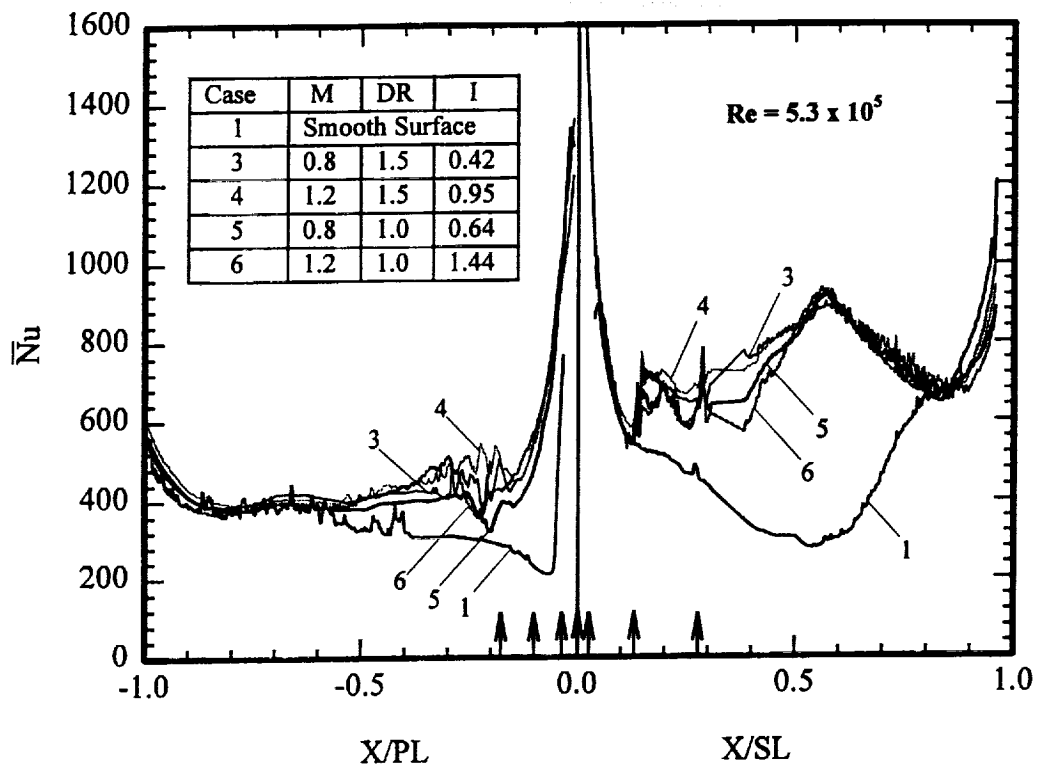


Fig.16 Effect of coolant density on spanwise-averaged Nusselt number distributions (Experiment setup 1)

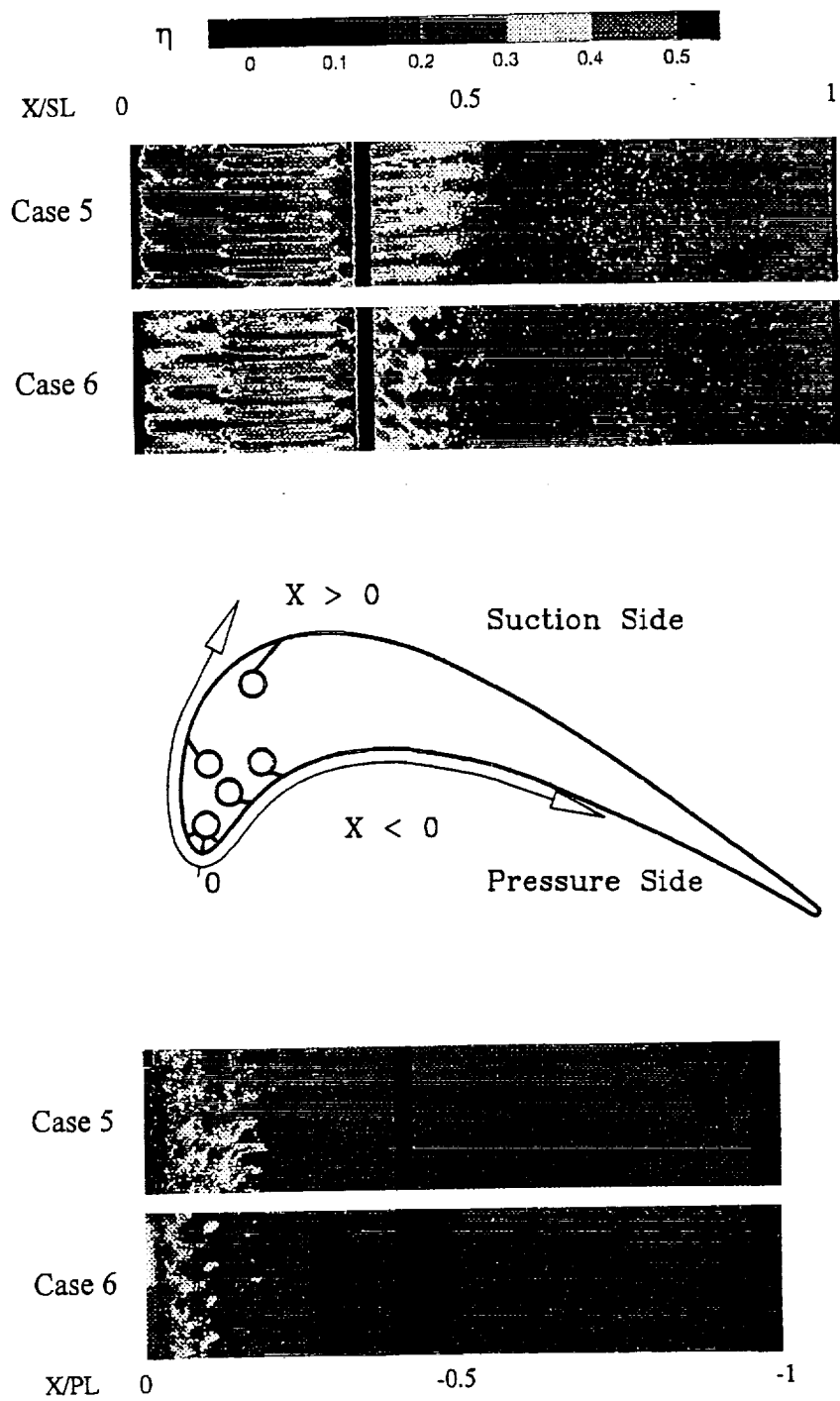


Fig.17 Effect of blowing ratio on detailed film effectiveness distributions for air injection (Experiment setup 1)

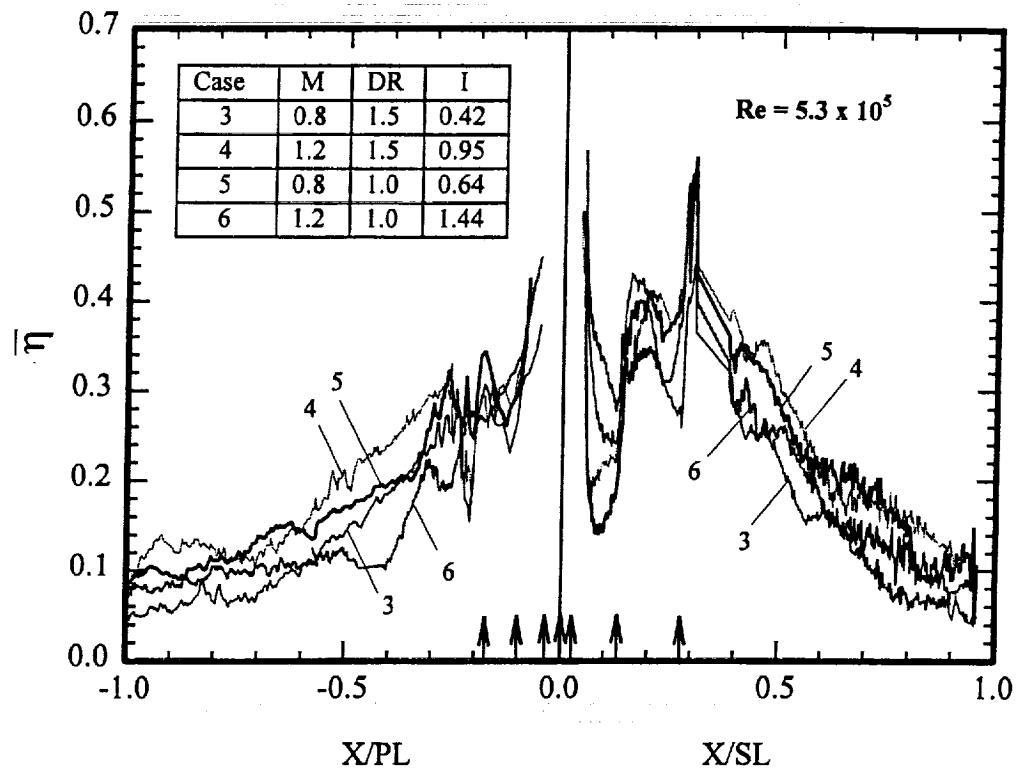


Fig.18 Effect of coolant density on spanwise-averaged film effectiveness distributions (Experiment setup 1)

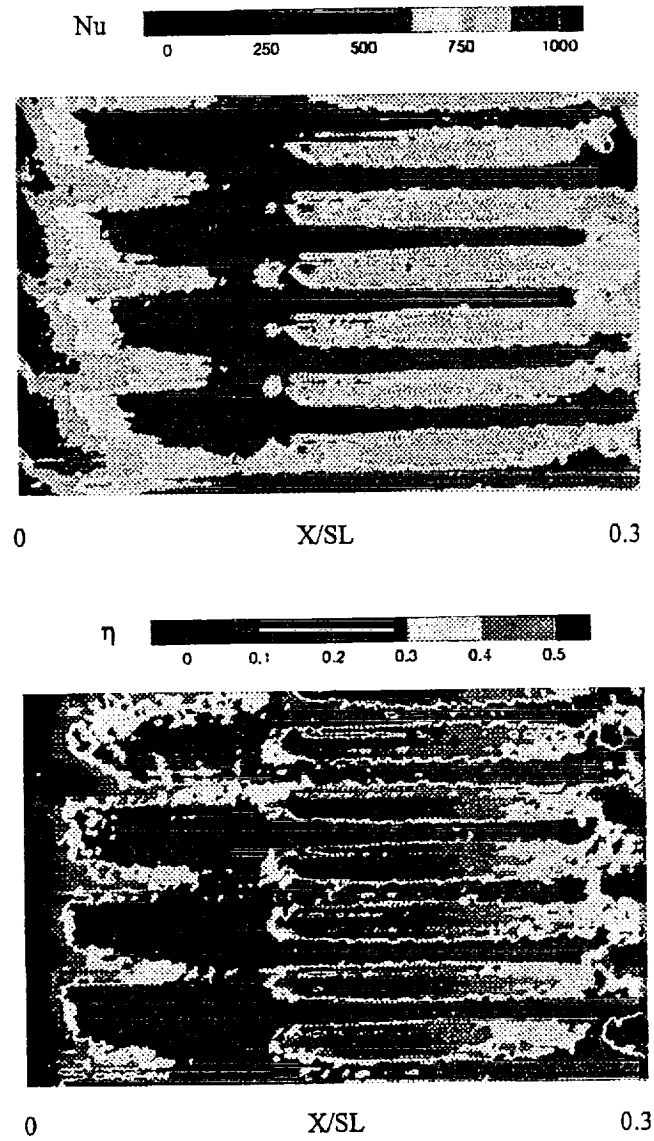


Fig.19 Detailed Nusselt number and film effectiveness distributions on the suction surface between LE and S1 rows for CO_2 injection at $M=0.8$

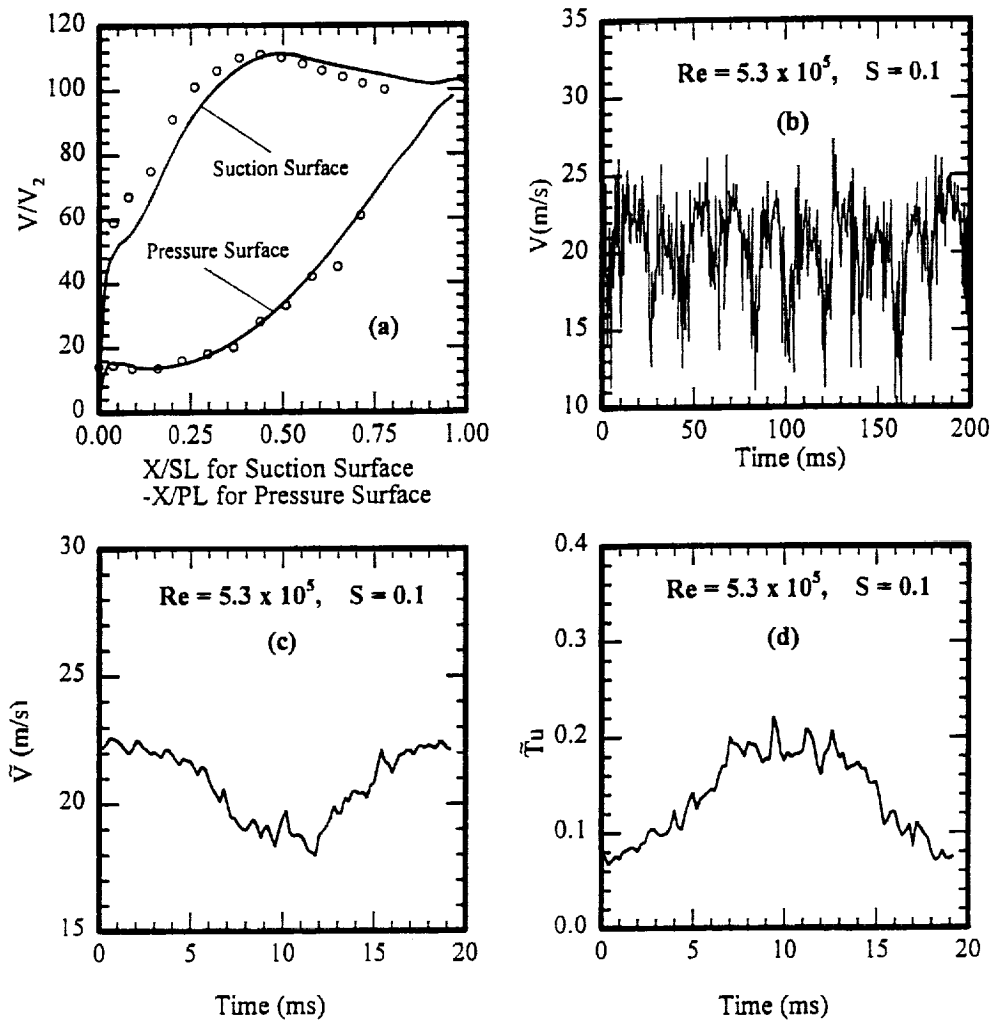


Fig.20 Local-to-exit velocity ratio (V/V_2) distributions on the test blade, Profiles for $V(t)$, \bar{V} , $\bar{T}u$, under wake effect at cascade inlet (Experiment setup 2)

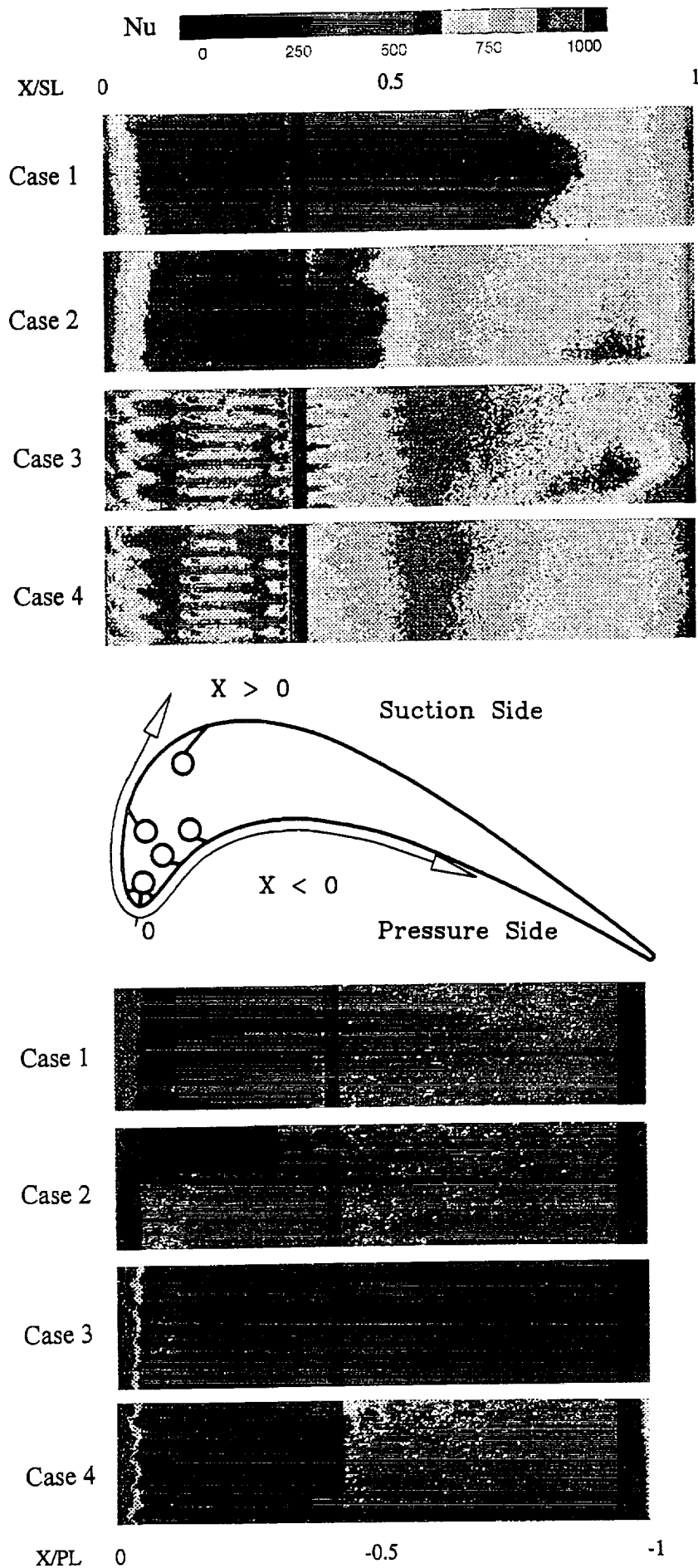


Fig.21 Effect of unsteady wake on detailed Nusselt number distributions for air injection (cases 1-4); $M=0.8$ (Experiment setup 2)

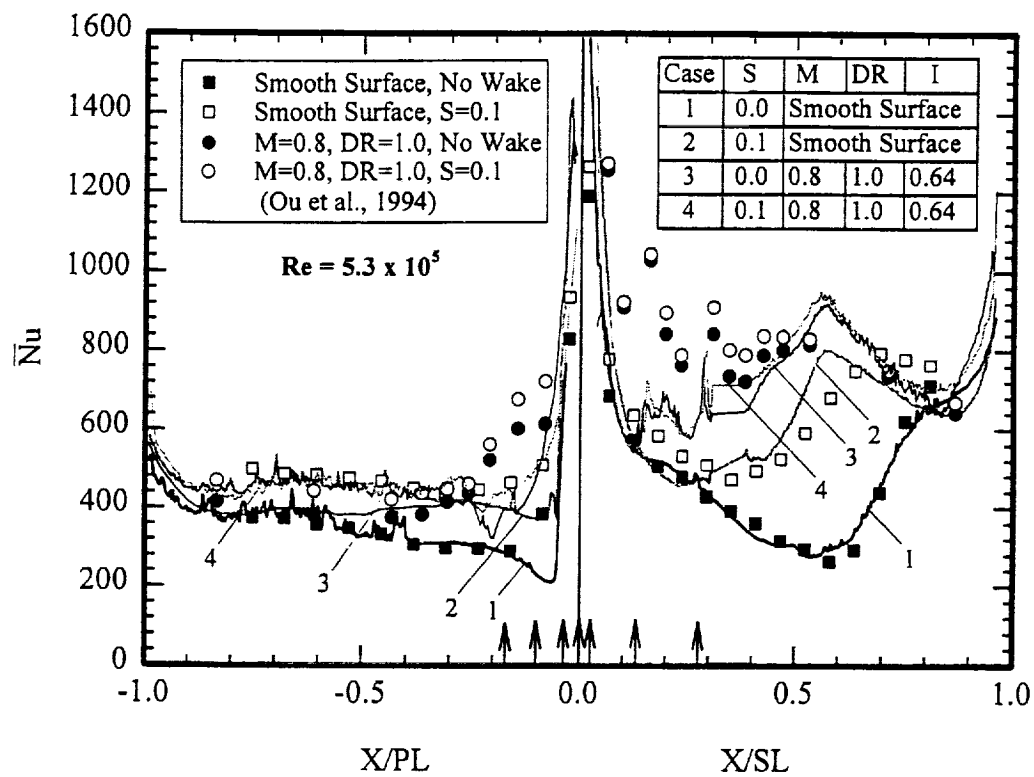


Fig.22 Effect of unsteady wake on spanwise-averaged Nusselt number distributions for air injection (cases 1-4); M=0.8 (Experiment setup 2)

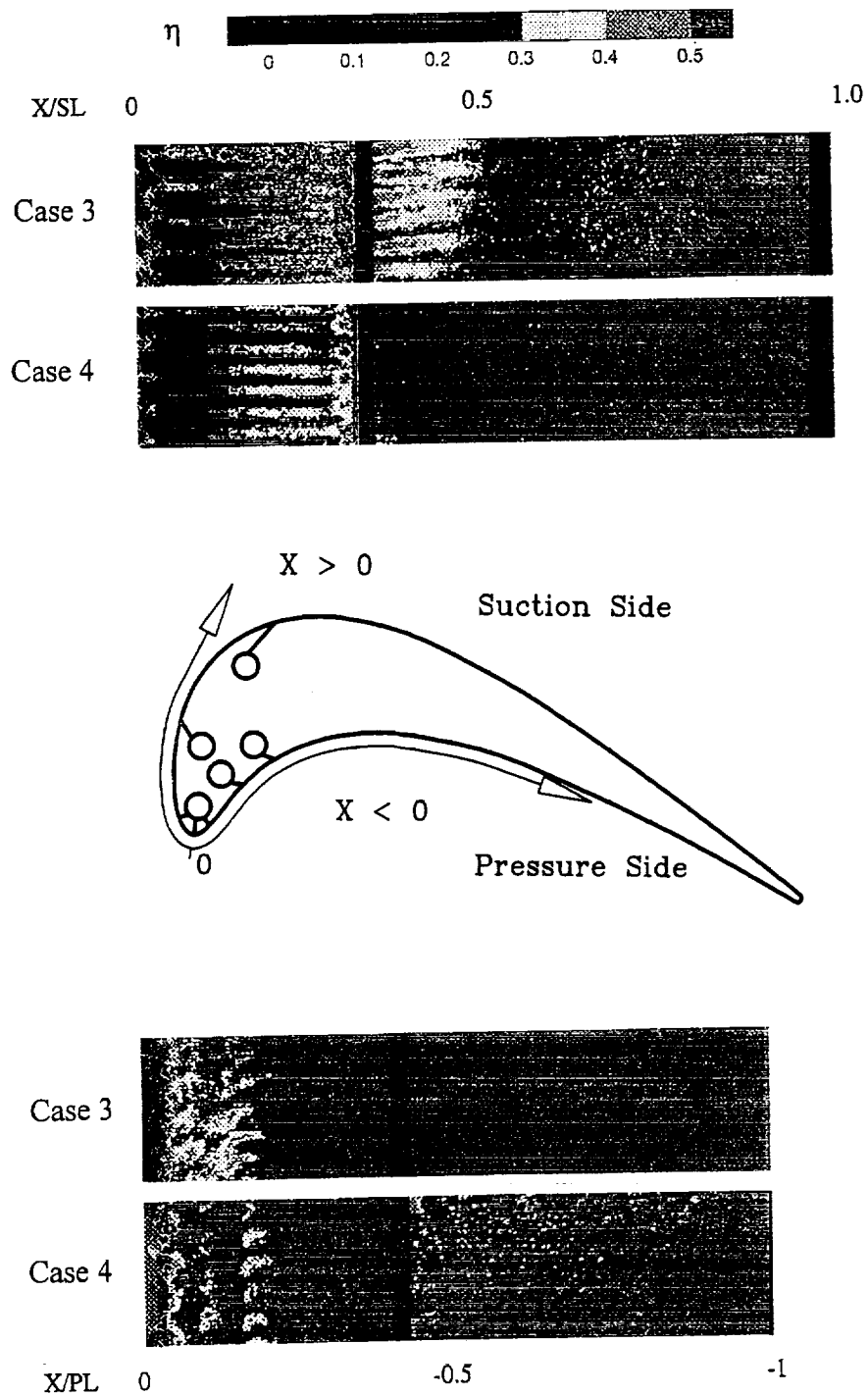


Fig.23 Effect of unsteady wake on detailed film cooling effectiveness distributions for air injection (cases 3-4); $M=0.8$ (Experiment setup 2)

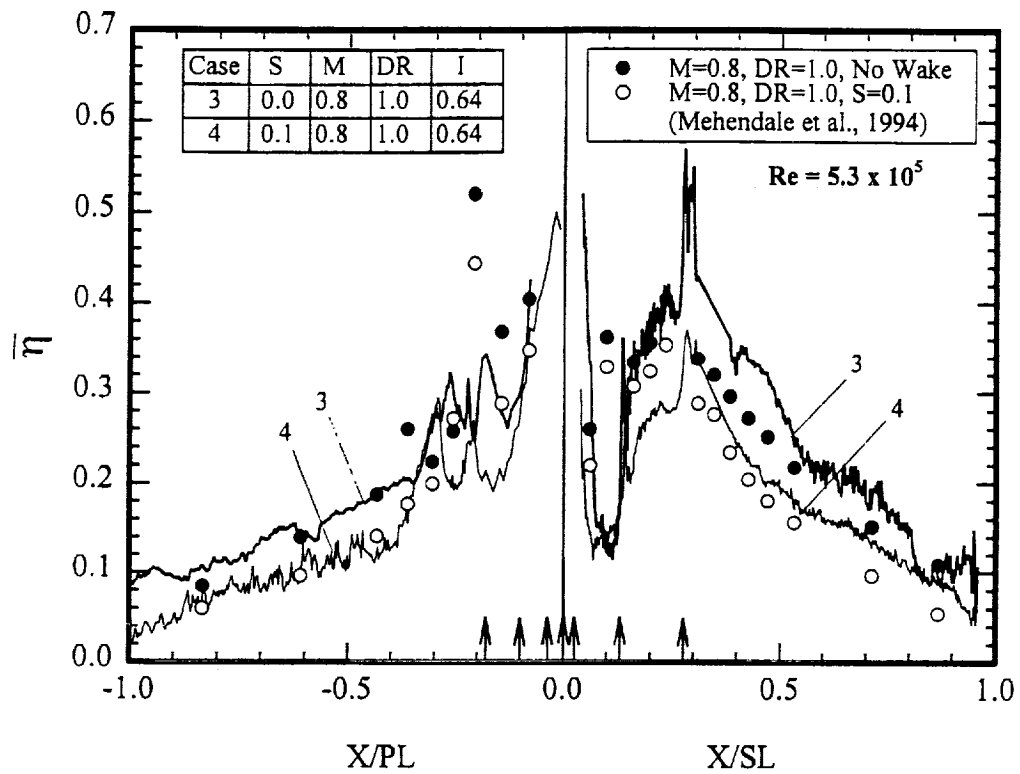


Fig.24 Effect of unsteady wake on spanwise-averaged film cooling effectiveness distributions for air injection (cases 3-4); $M=0.8$ (Experiment setup 2)

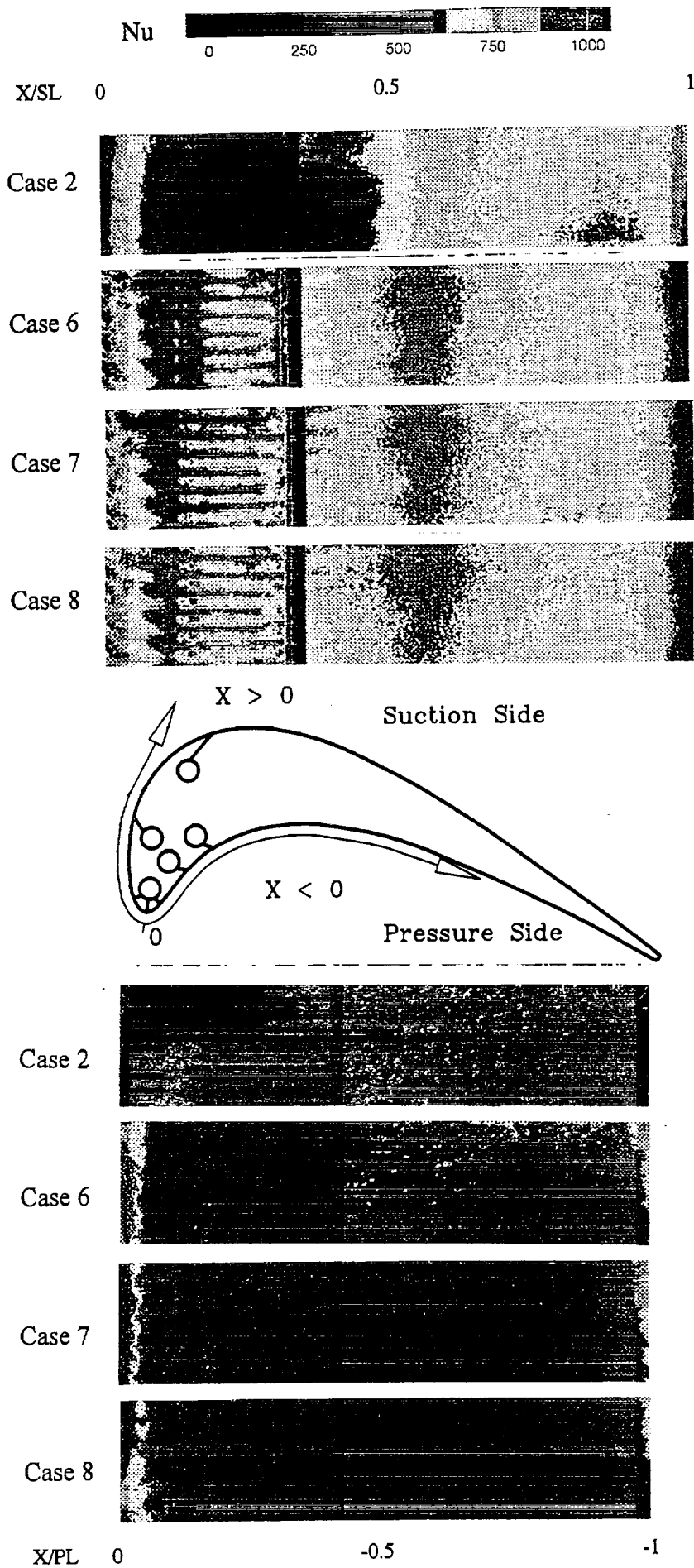


Fig.25 Effect of blowing ratio on detailed Nusselt number distributions for CO₂ injection at S=0.1 (cases 6-8) (Experiment setup 2)

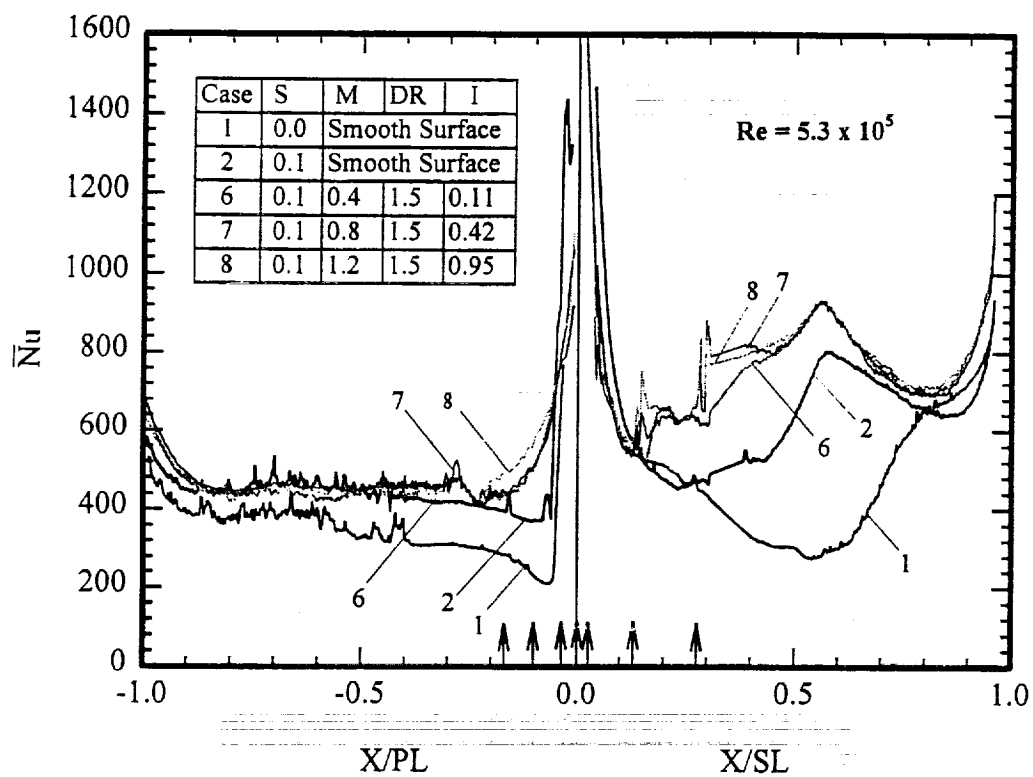


Fig.26 Effect of blowing ratio on spanwise-averaged Nusselt number distributions for CO_2 injection at $S=0.1$ (cases 6-8) (Experiment setup 2)

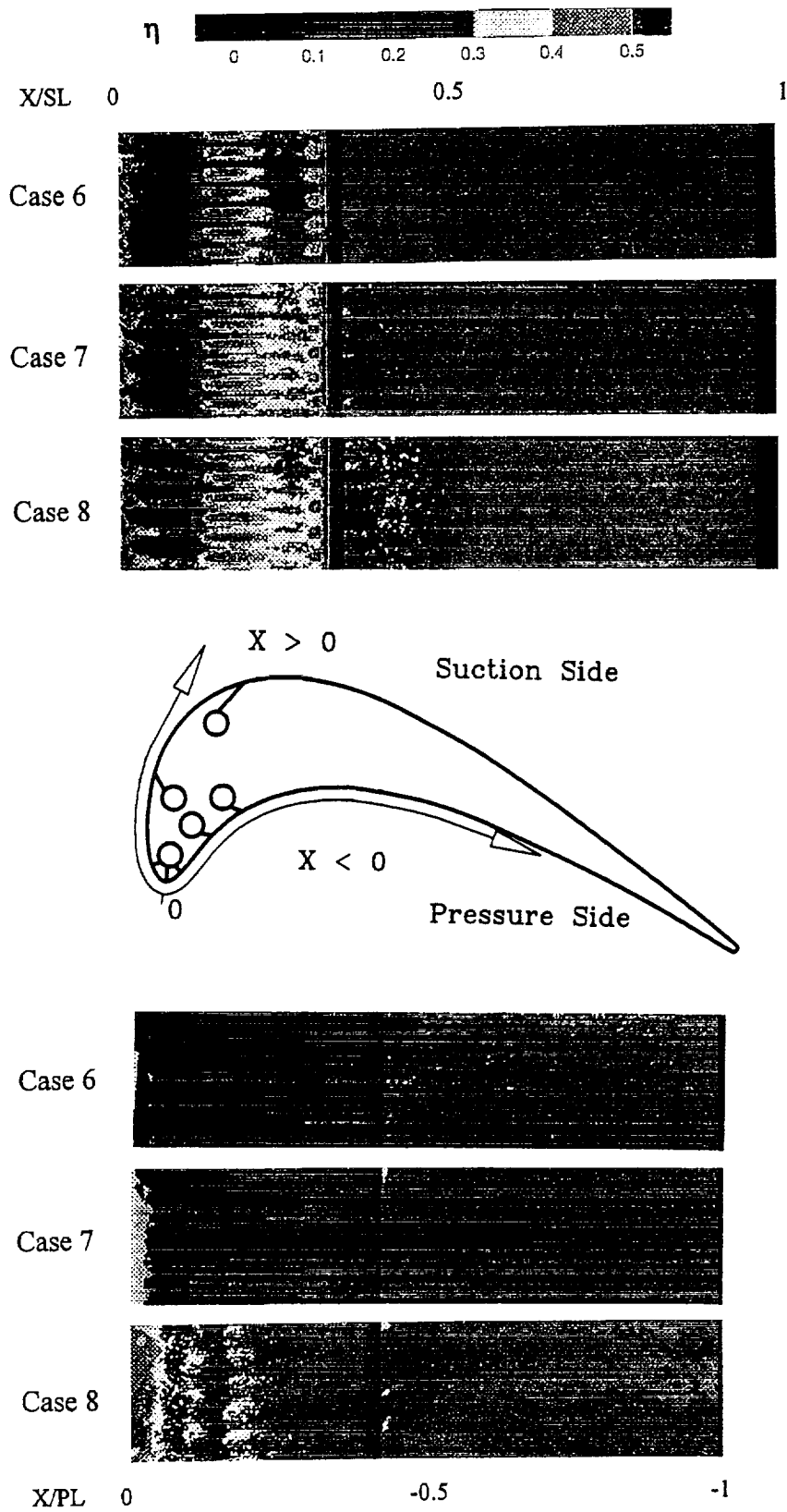


Fig.27 Effect of blowing ratio on detailed film cooling effectiveness distributions for CO_2 injection at $S=0.1$ (cases 6-8) (Experiment setup 2)

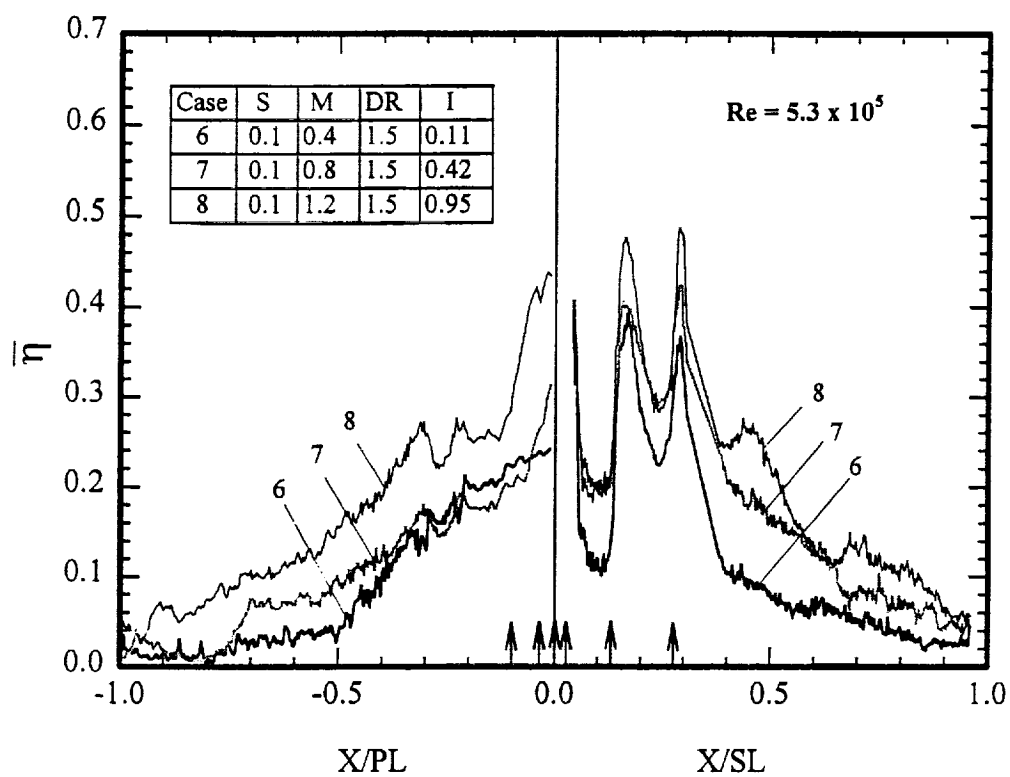


Fig.28 Effect of blowing ratio on spanwise-averaged film cooling effectiveness distributions for CO_2 injection at $S=0.1$ (cases 6-8) (Experiment setup 2)

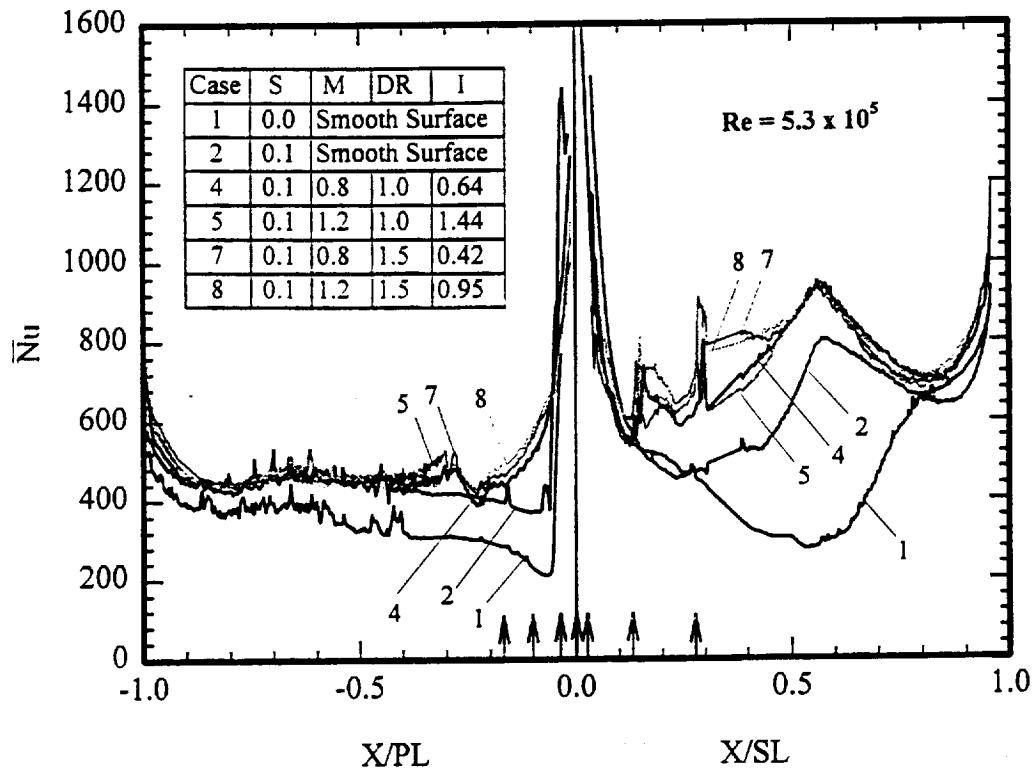


Fig.29 Effect of coolant density on spanwise-averaged Nusselt number distributions at $S=0.1$ (Experiment setup 2)

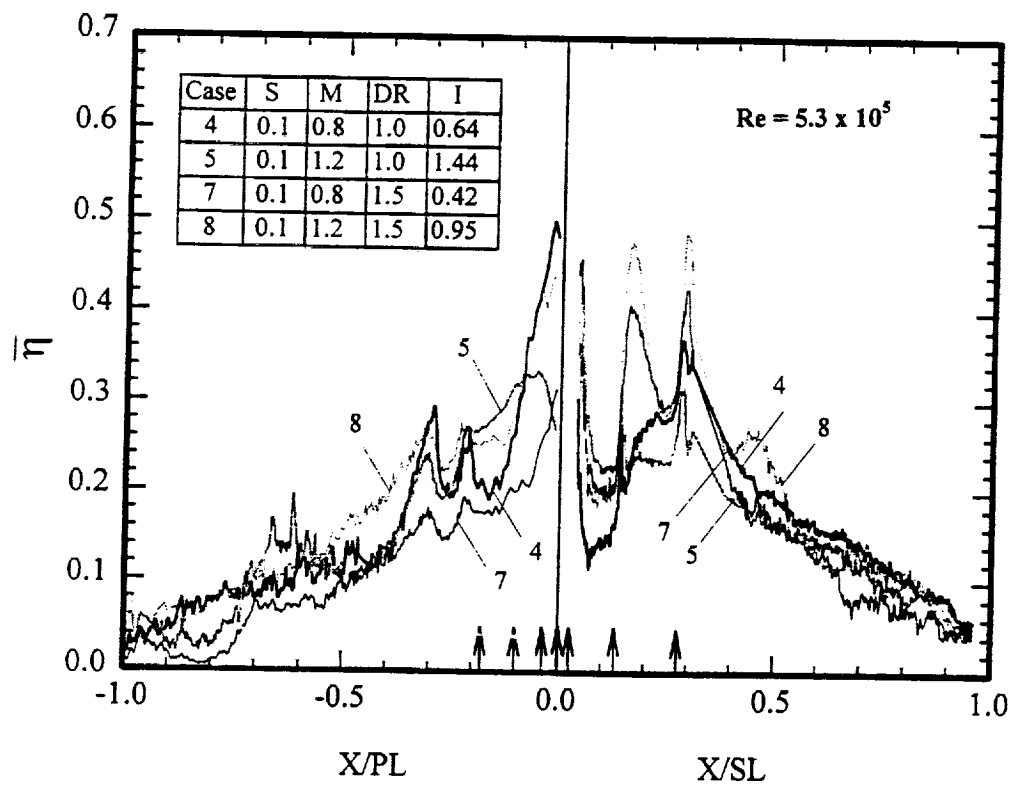


Fig.30 Effect of coolant density on spanwise-averaged film cooling effectiveness distributions at $S=0.1$ (Experiment setup 2)

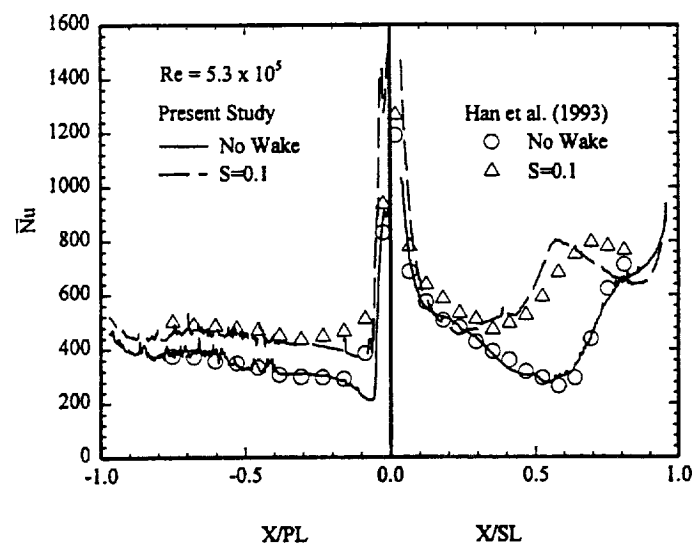


Fig.31(a) Effect of unsteady wake on spanwise-averaged Nusselt number for $Re=5.3 \times 10^5$ (Experiment setup 3, with smooth-surface turbine blade)

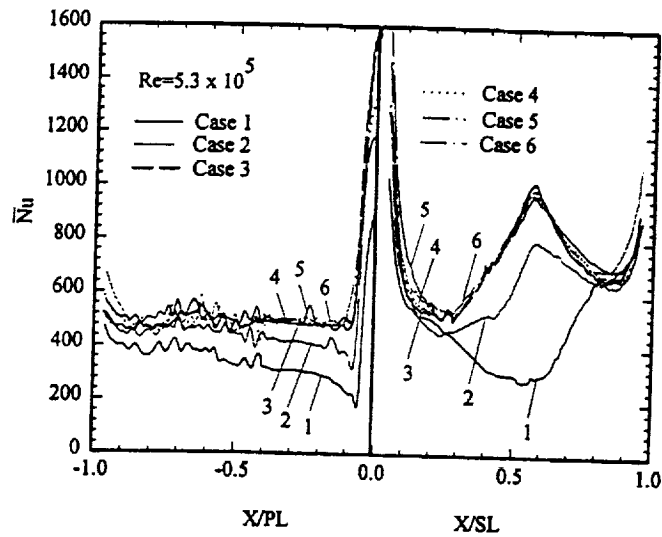


Fig.31(b) Combined effect of unsteady wake, free-stream turbulence and coolant ejection on spanwise-averaged Nusselt number for $Re=5.3 \times 10^5$ (Experiment setup 3, with smooth-surface turbine blade)

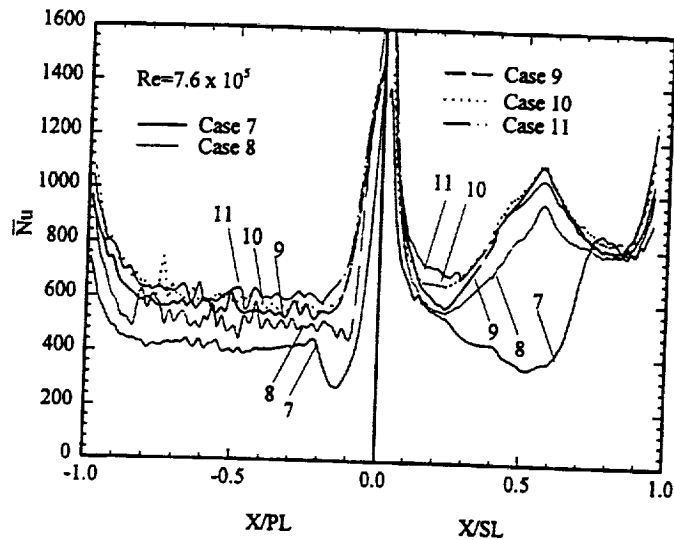


Fig.31(c) Combined effect of unsteady wake, free-stream turbulence and coolant ejection on spanwise-averaged Nusselt number for $Re=7.6 \times 10^5$ (Experiment setup 3, with smooth-surface turbine blade)

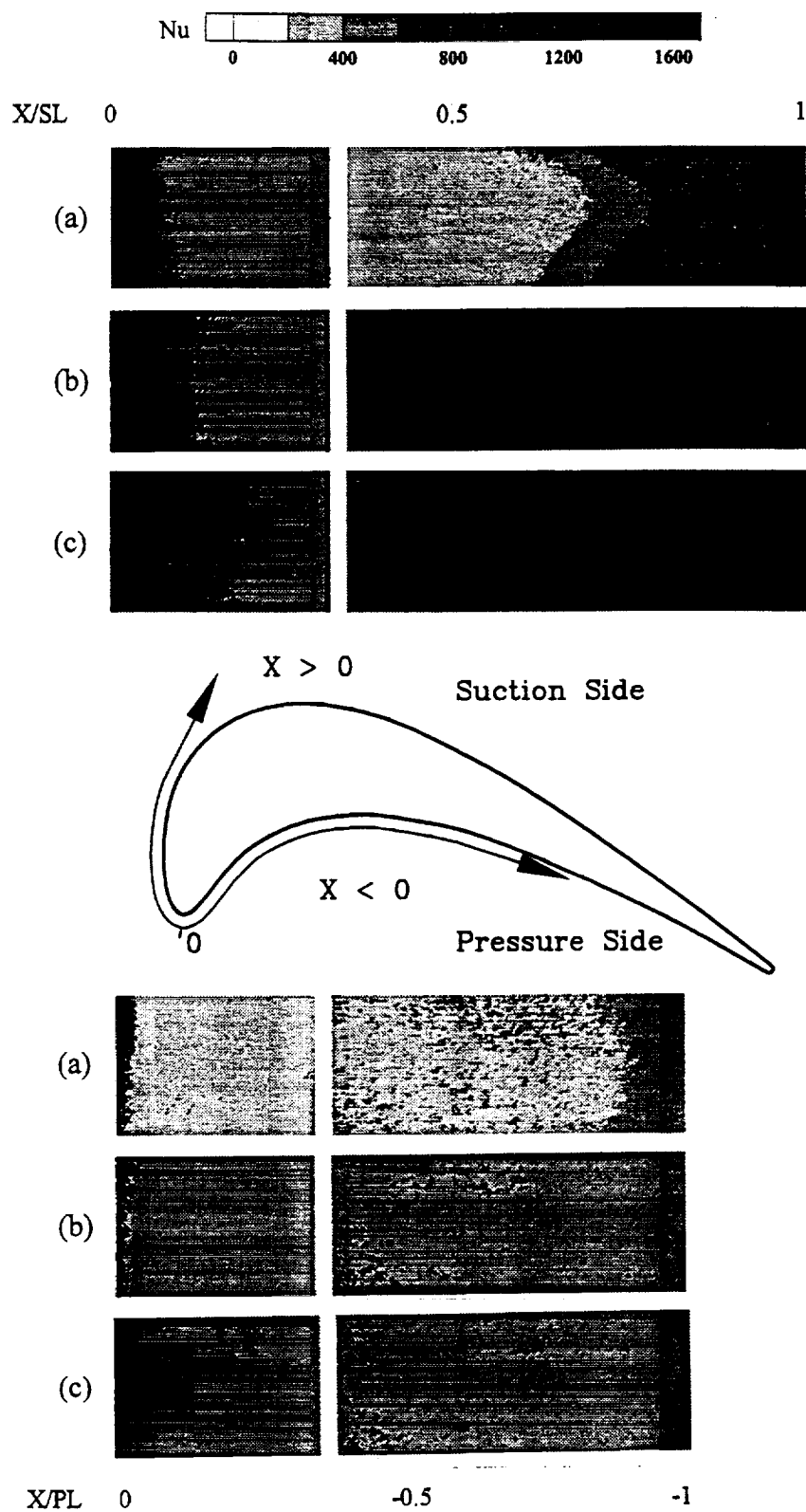


Fig.32 Detailed Nusselt number distributions for $Re=5.3 \times 10^5$: (a) Case 1, (b) Case 3, (c) Case 5. (Experiment setup 3, with smooth-surface turbine blade)

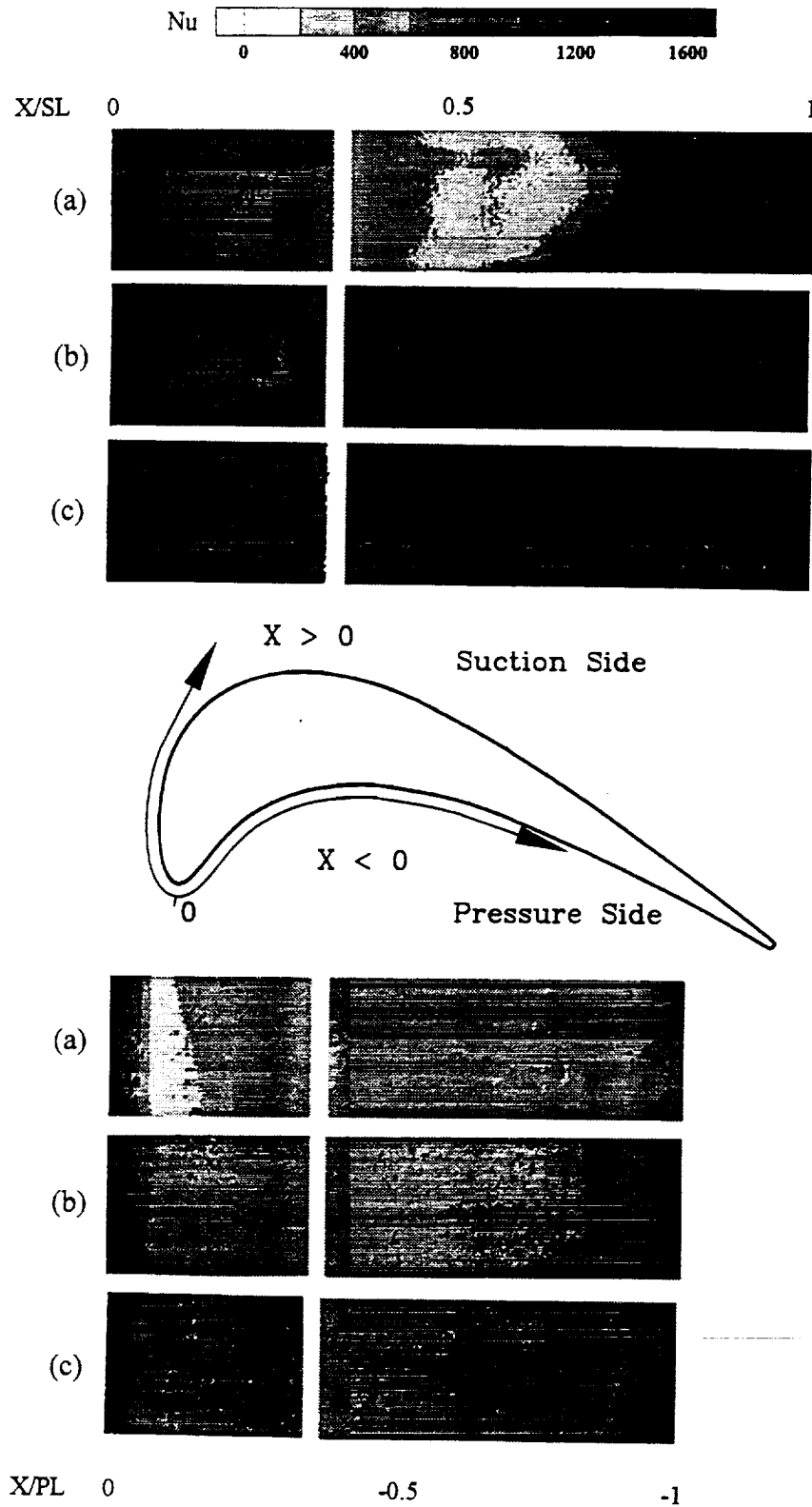


Fig.33 Detailed Nusselt number distributions for $Re=7.6 \times 10^5$: (a) Case 7, (b) Case 9, (c) Case 11. (Experiment setup 3, with smooth-surface turbine blade)

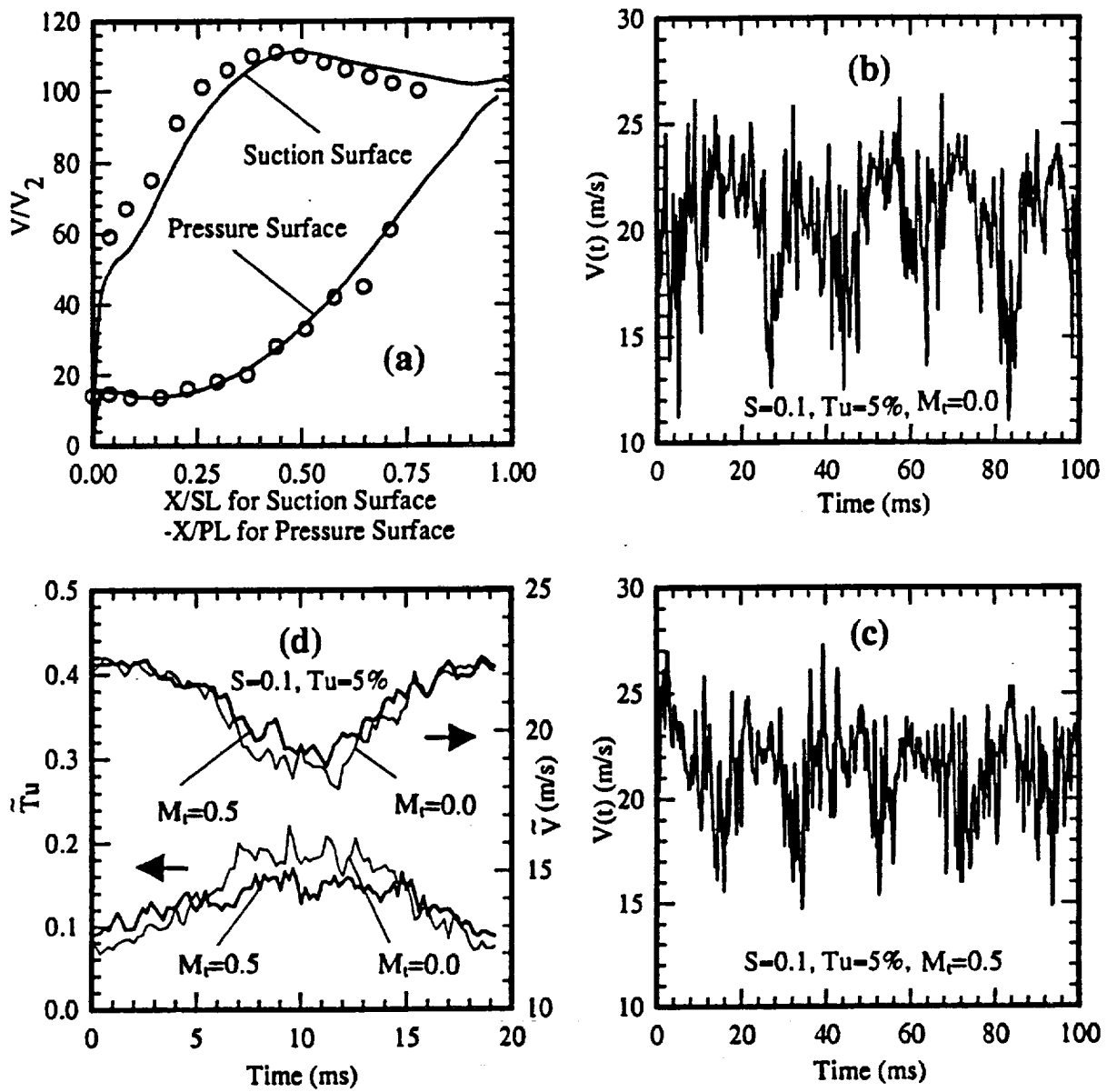


Fig.34 Local-to-exit velocity ratio (V/V_2) distributions on the test blade surface, profiles of instantaneous velocity, ensemble-averaged velocity and turbulence intensity (Experiment setup 3, with film-cooled turbine blade)

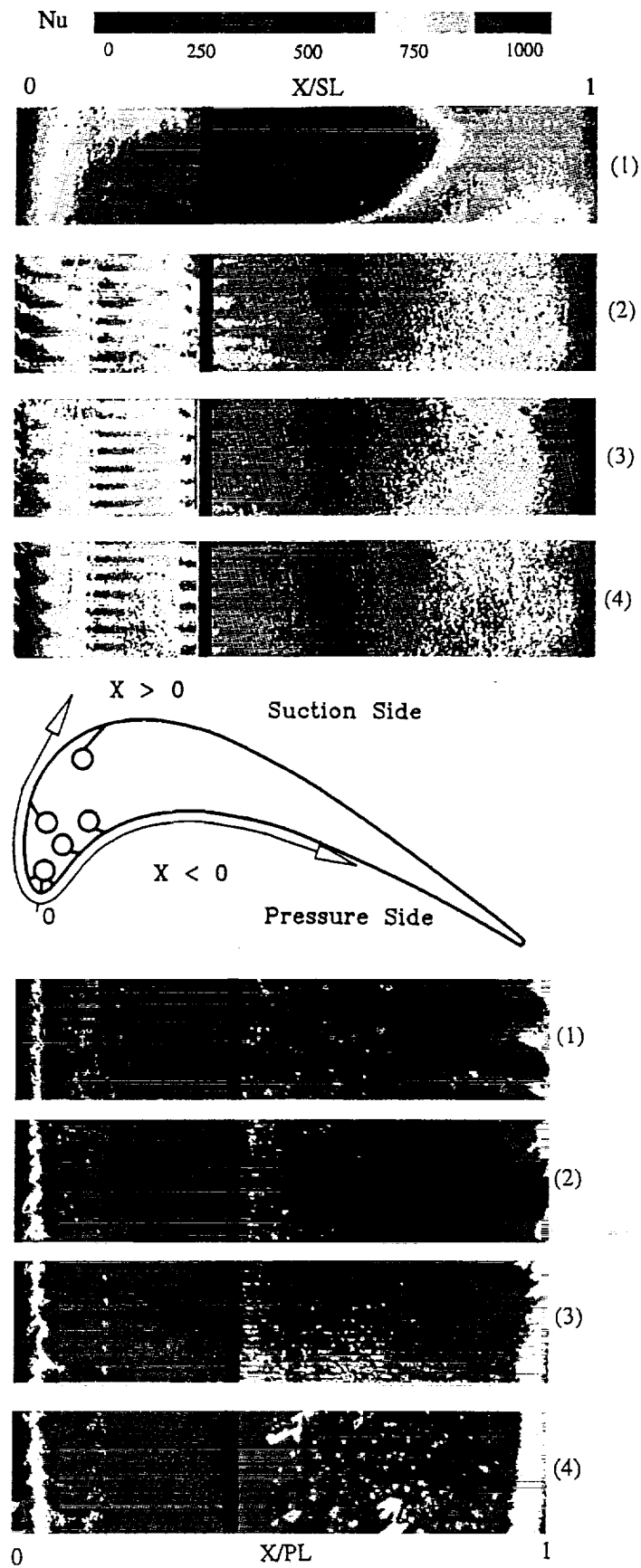


Fig.35 Detailed Nusselt number distributions for cases 1-4
(Experiment setup 3, with film-cooled turbine blade)

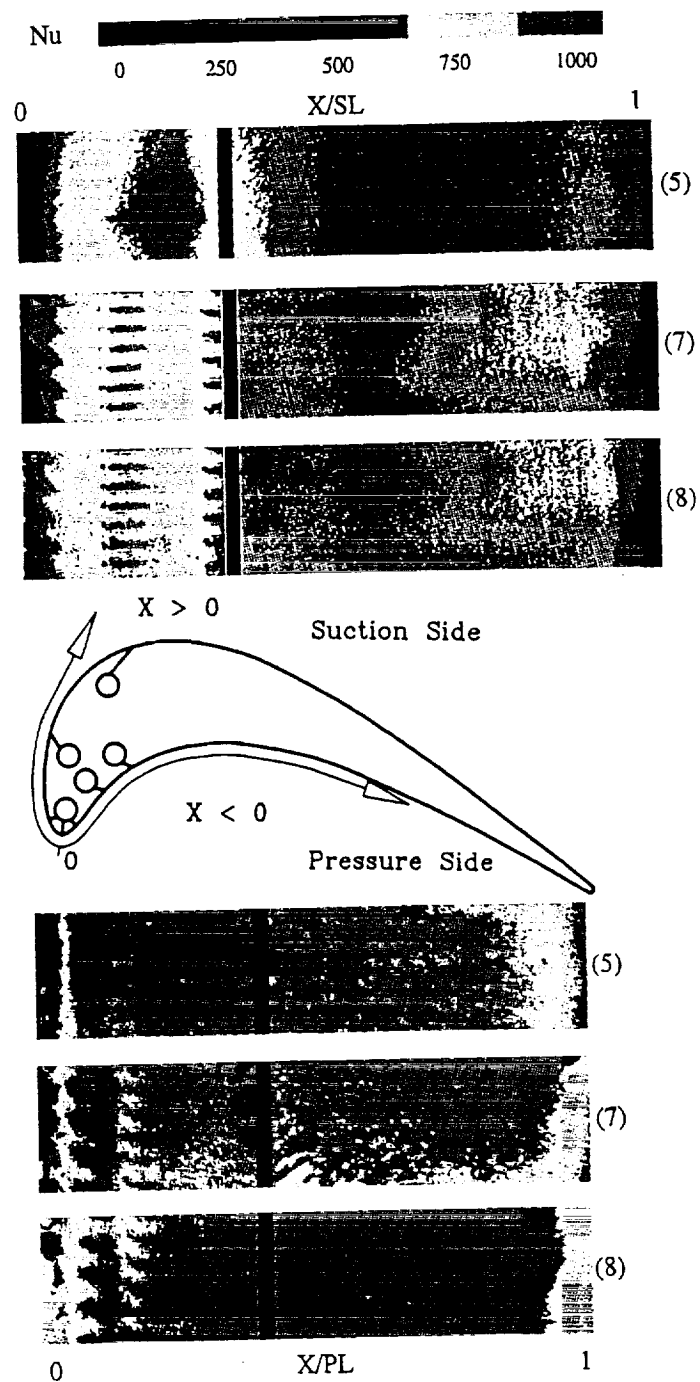


Fig.36 Detailed Nusselt number distributions for cases 5, 7 and 8
(Experiment setup 3, with film-cooled turbine blade)

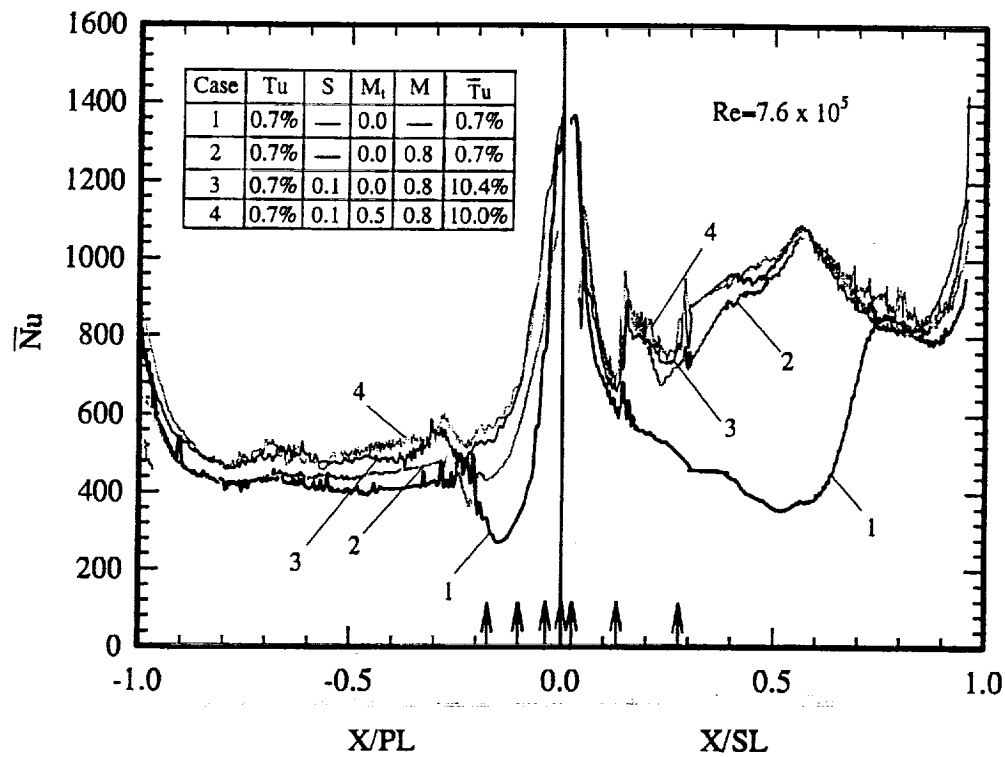


Fig.37(a) Spanwise-averaged Nusselt number distributions for cases 1-4 (Experiment setup 3, with film-cooled turbine blade)

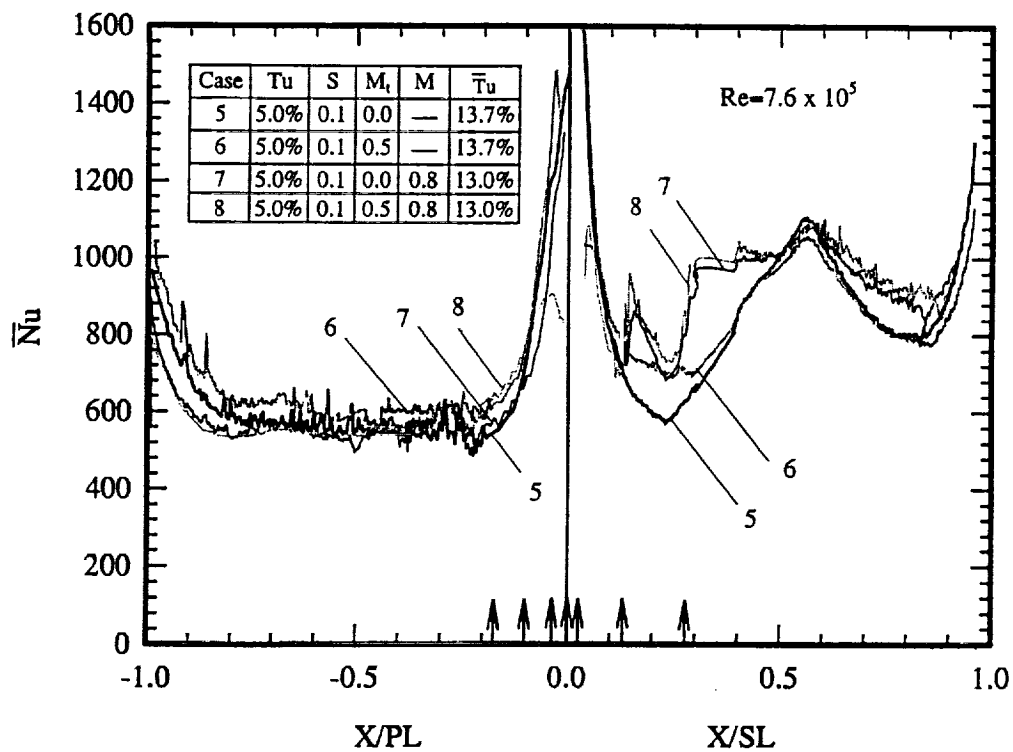


Fig.37(b) Spanwise-averaged Nusselt number distributions for cases 5-8 (Experiment setup 3, with film-cooled turbine blade)

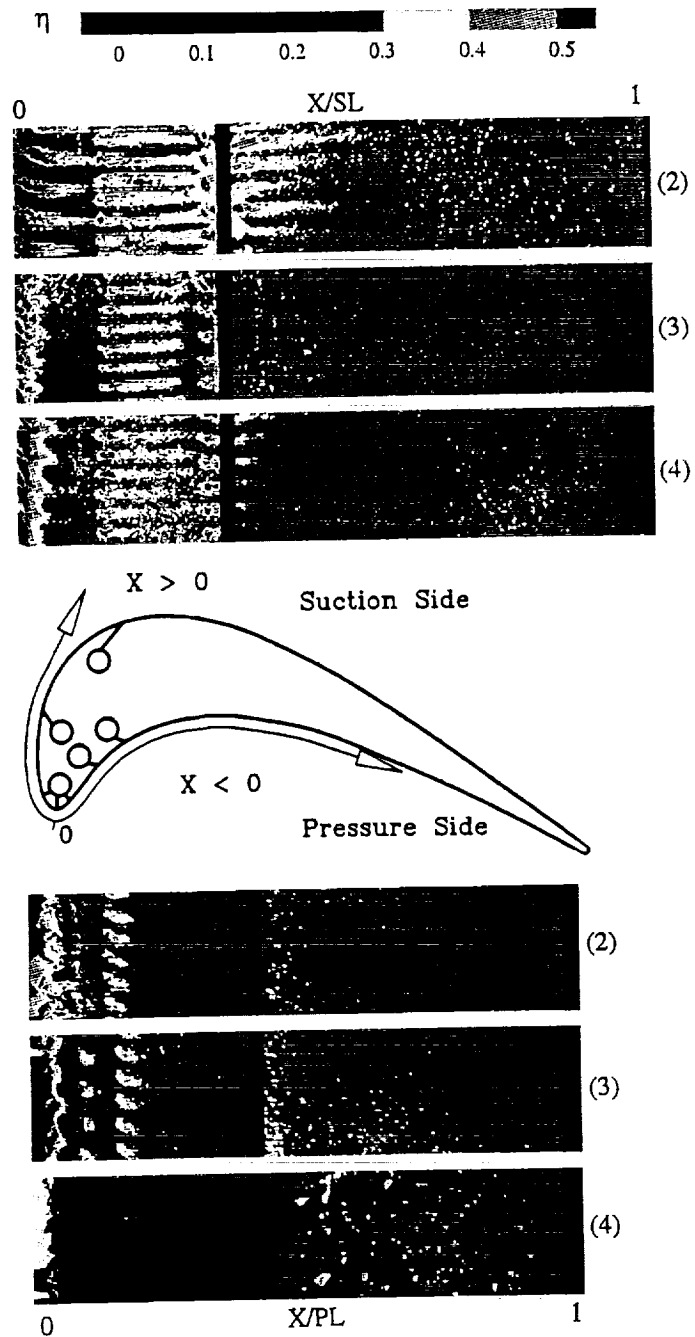


Fig.38 Detailed film effectiveness distributions for cases 2-4
(Experiment setup 3, with film-cooled turbine blade)

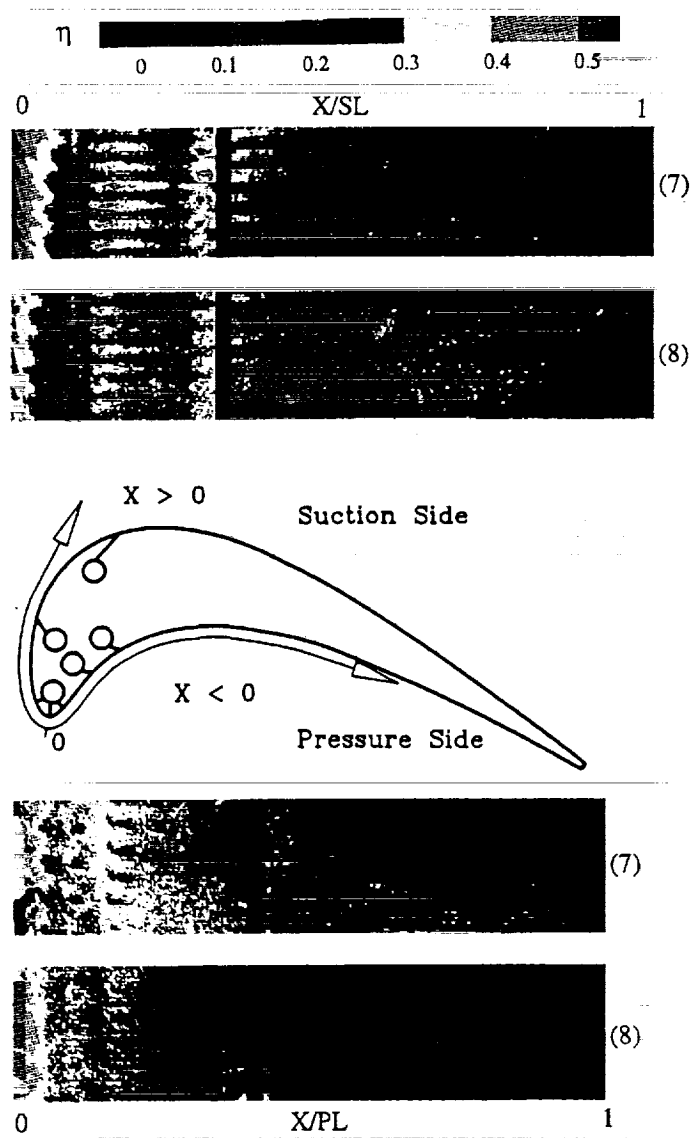


Fig.39 Detailed film effectiveness distributions for cases 7 and 8
(Experiment setup 3, with film-cooled turbine blade)

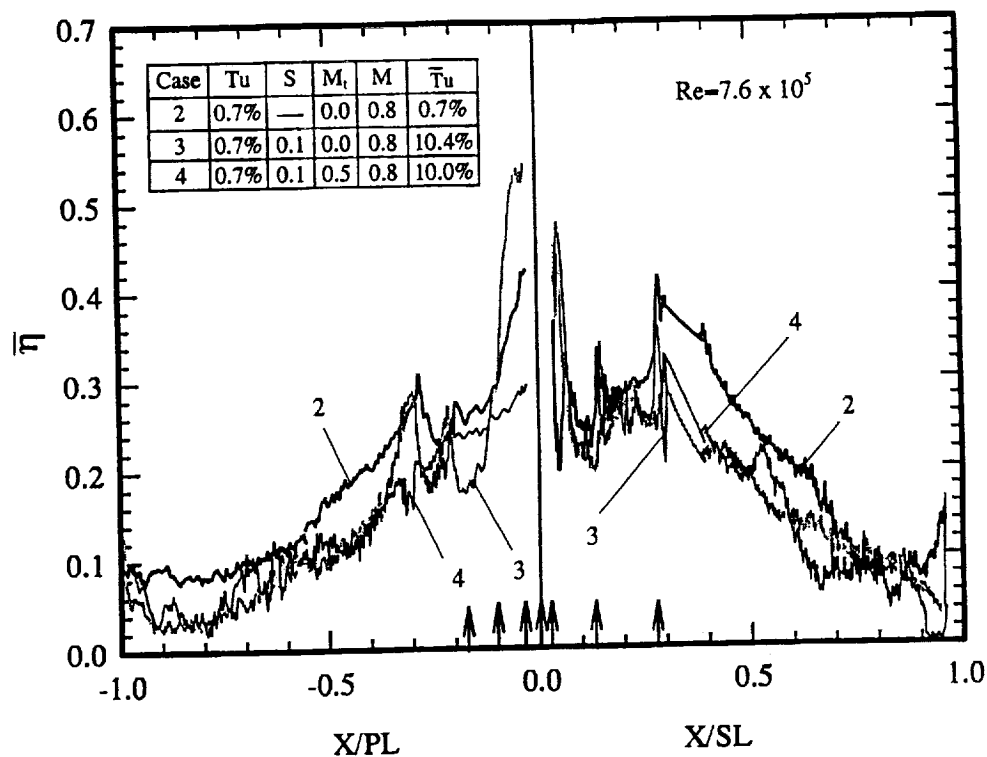


Fig.40(a) Spanwise-averaged film effectiveness distributions for cases 2-4 (Experiment setup 3, with film-cooled turbine blade)

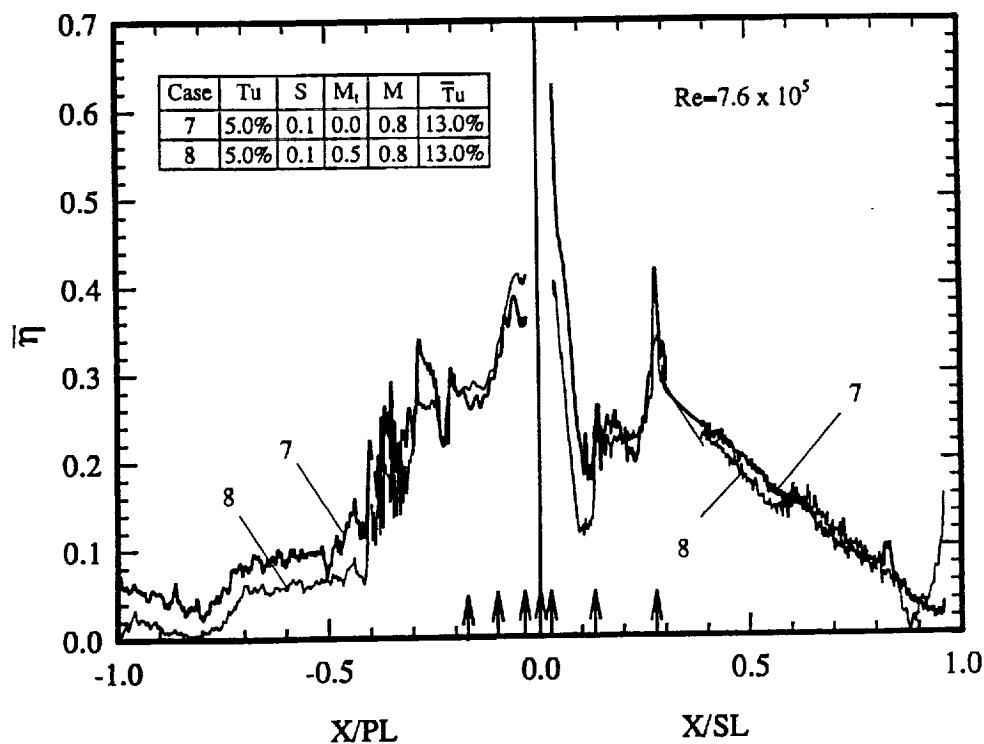


Fig.40(b) Spanwise-averaged film effectiveness distributions for cases 7-8 (Experiment setup 3, with film-cooled turbine blade)

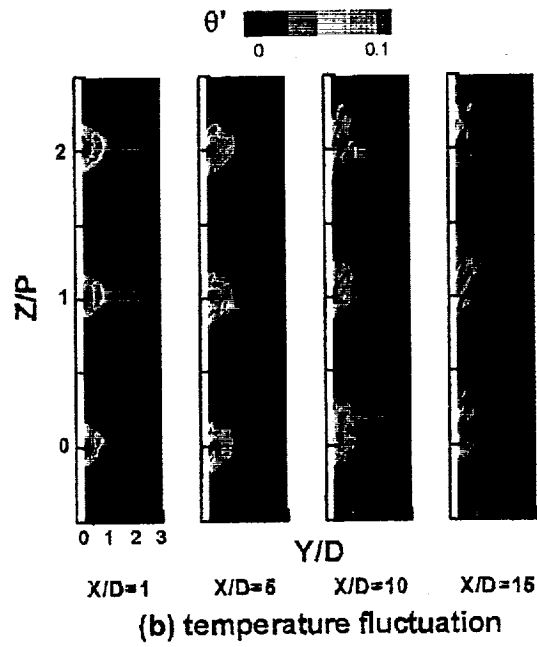
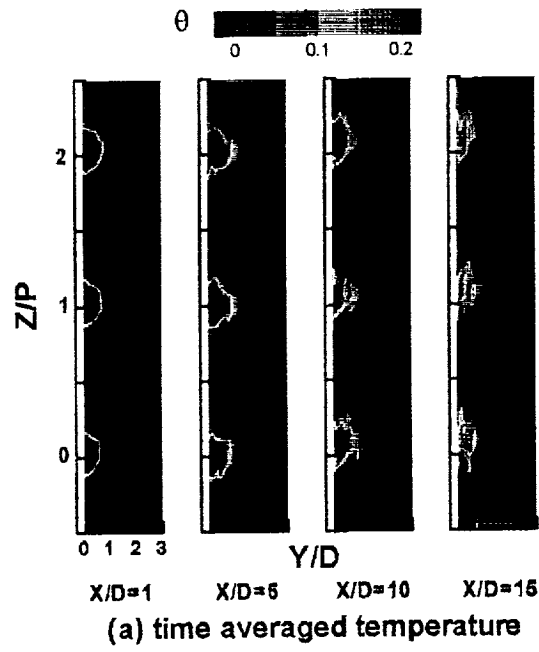


Fig.41 Film temperature field at different locations for the case of $M=0.8$ and without wake effect ($S=0$) (Experiment setup 4)

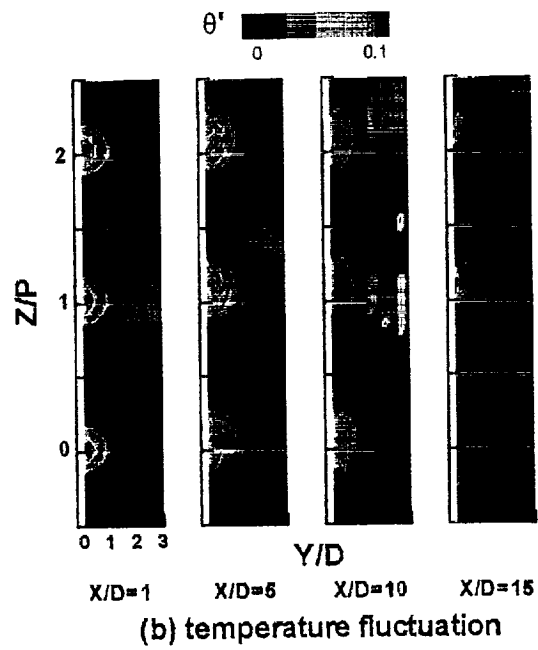
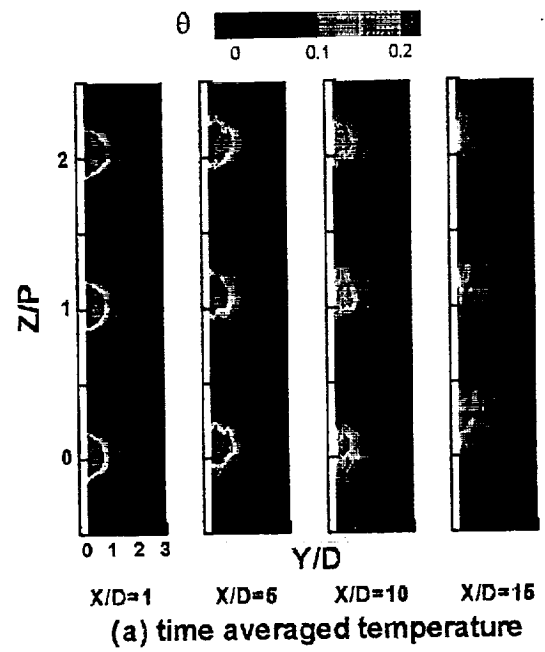
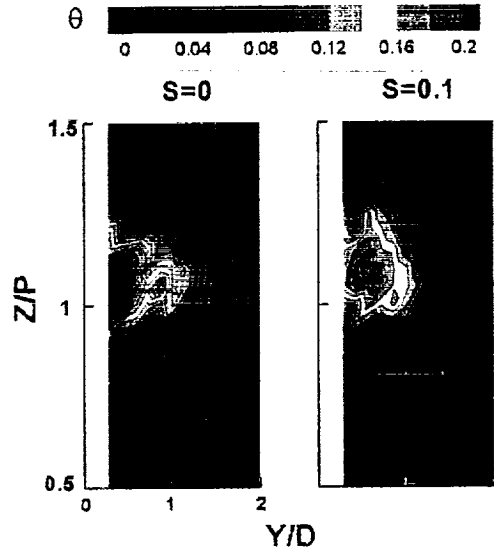
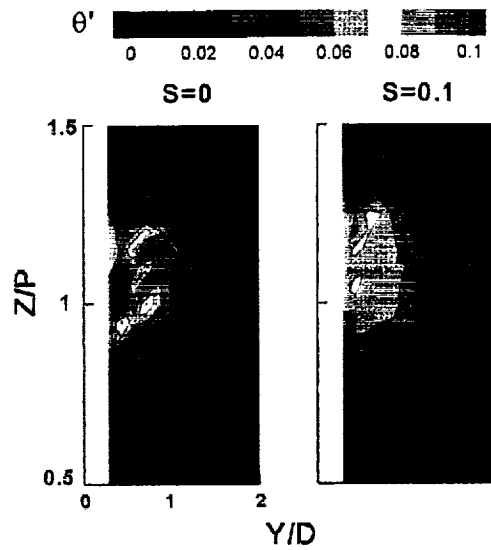


Fig.42 Film temperature field at different locations for the case of $M=0.8$ and with wake effect ($S=0.1$) (Experiment setup 4)



(a) time averaged temperature



(b) temperature fluctuation

Fig.43 Detailed Film temperature contour at $X/D=10$ for the cases of $M=0.8$, without and with unsteady wake (Experiment setup 4)

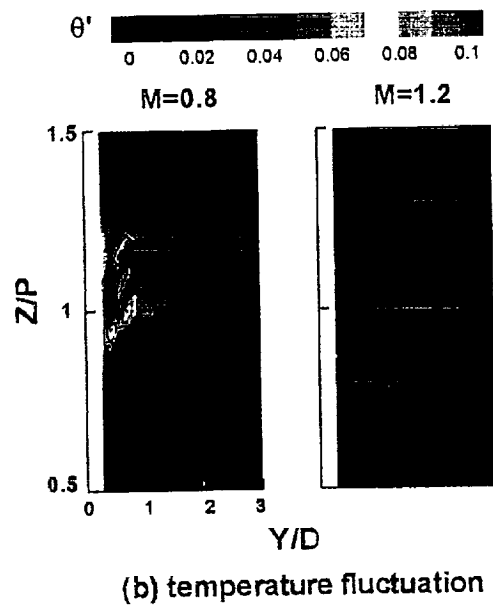
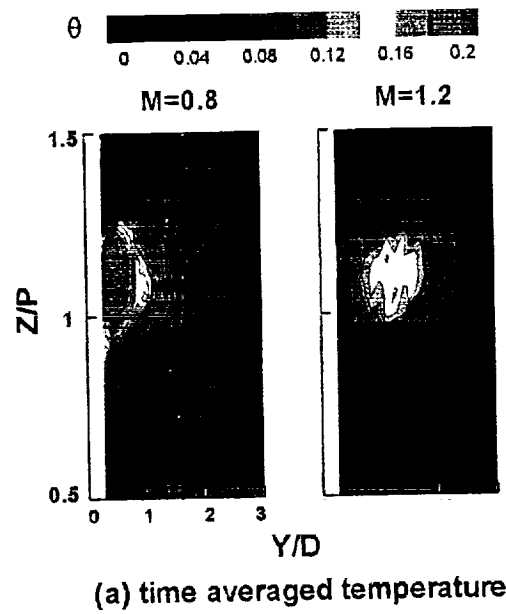


Fig.44 Effect of blowing ratio on film temperature field ($S=0$, $X/D=10$) (Experiment setup 4)

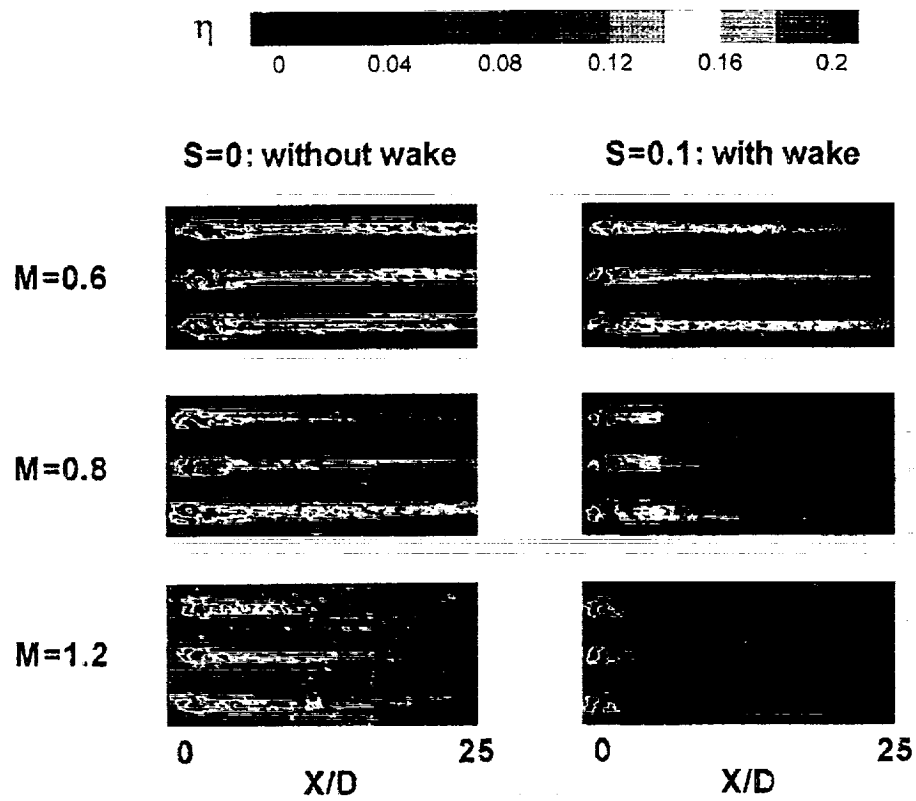


Fig.45 Effect of unsteady wake and blowing ratio on detailed film cooling effectiveness distribution (Experiment setup 4)

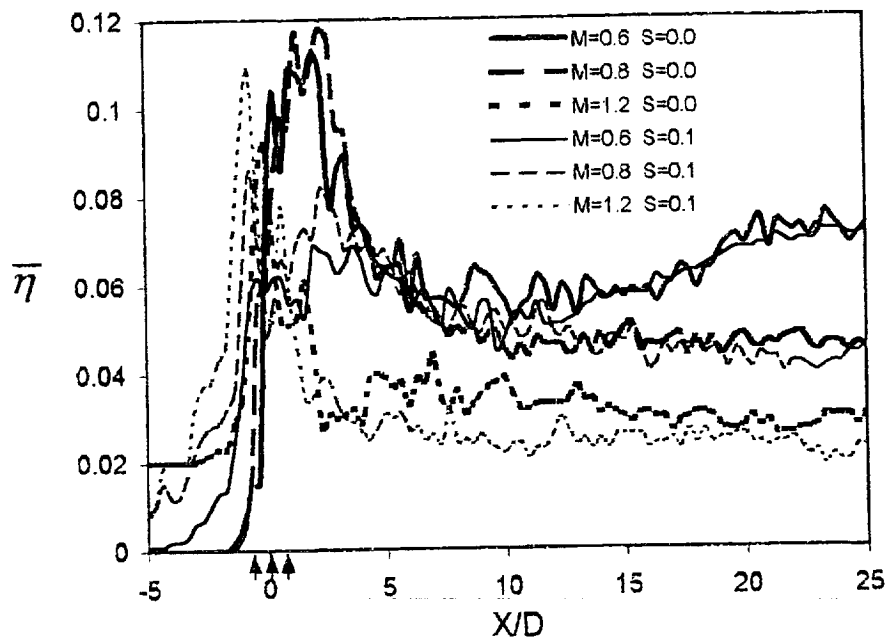
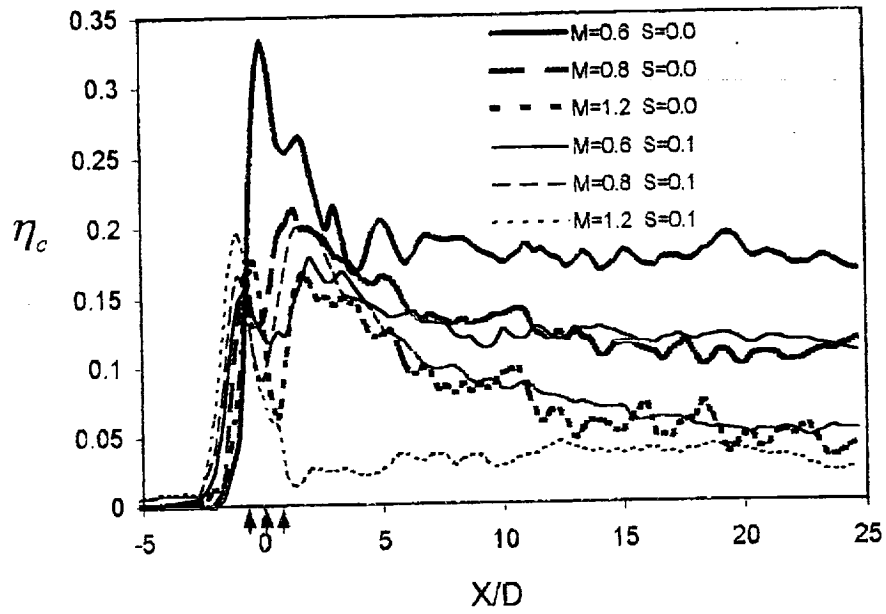


Fig.46 Film cooling effectiveness distribution (a) along film hole centerline (b) spanwise-averaged (Experiment setup 4)

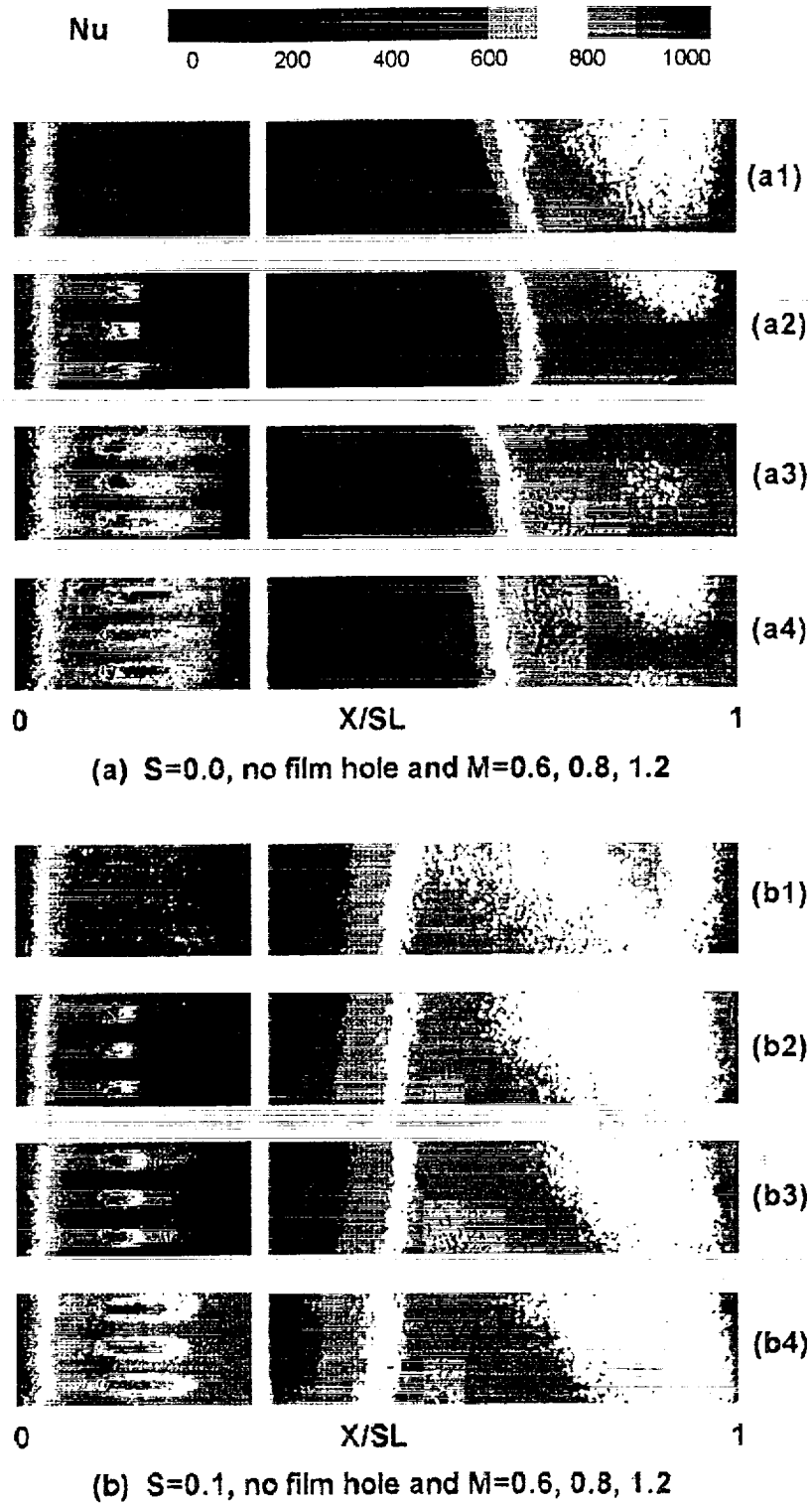


Fig.47 Detailed Nusselt number distribution for cases at different blowing ratios, with and without wake effect (Experiment setup 4)

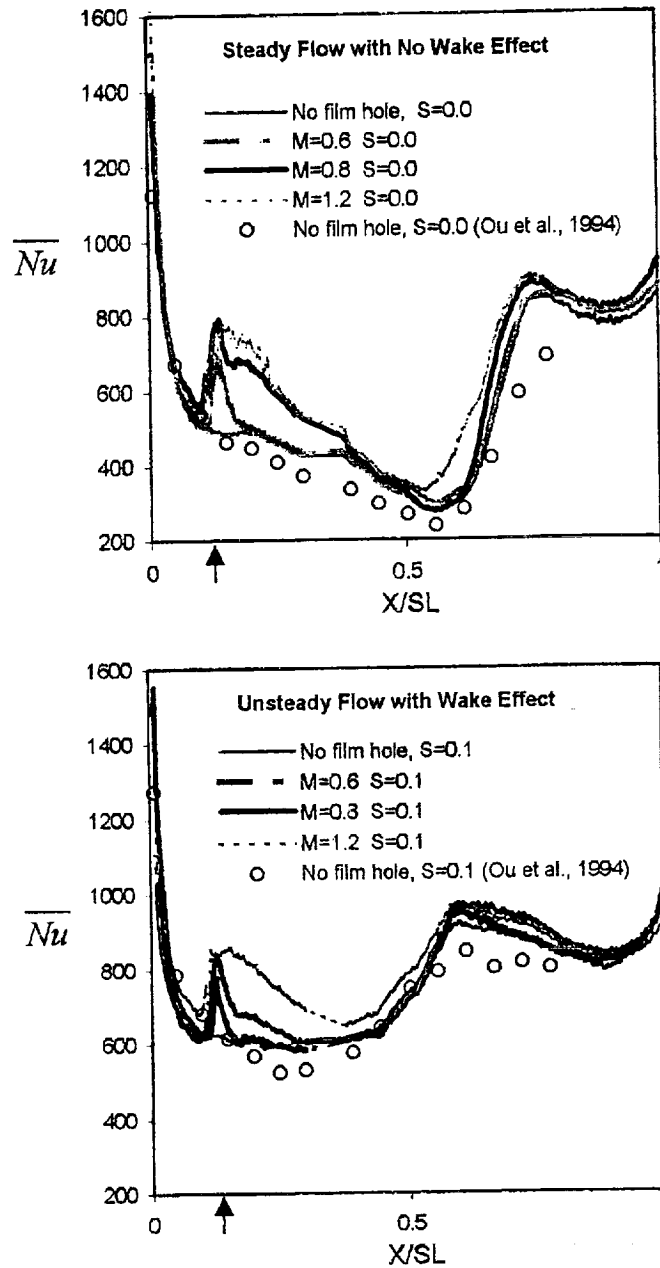


Fig.48 Spanwise-averaged Nusselt number distribution for (a)steady flow (b) unsteady flow with wake effect (Experiment setup 4)

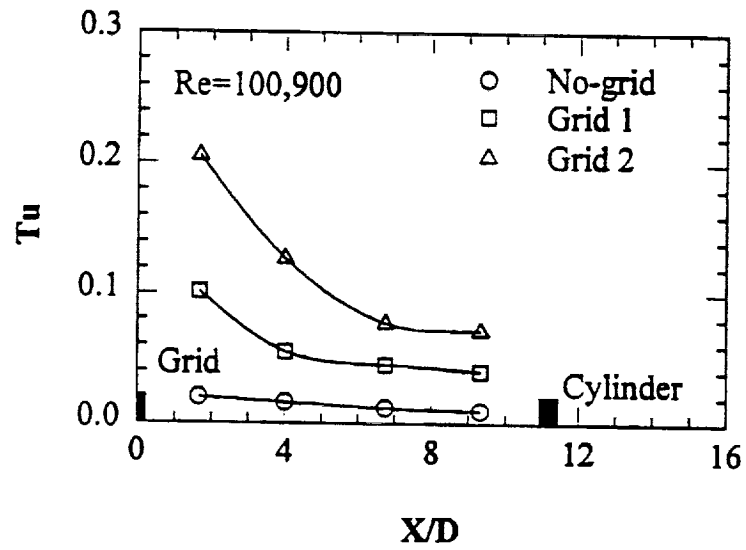


Fig.49 Streamwise turbulence distributions inside the test tunnel
(Experiment setup 5)

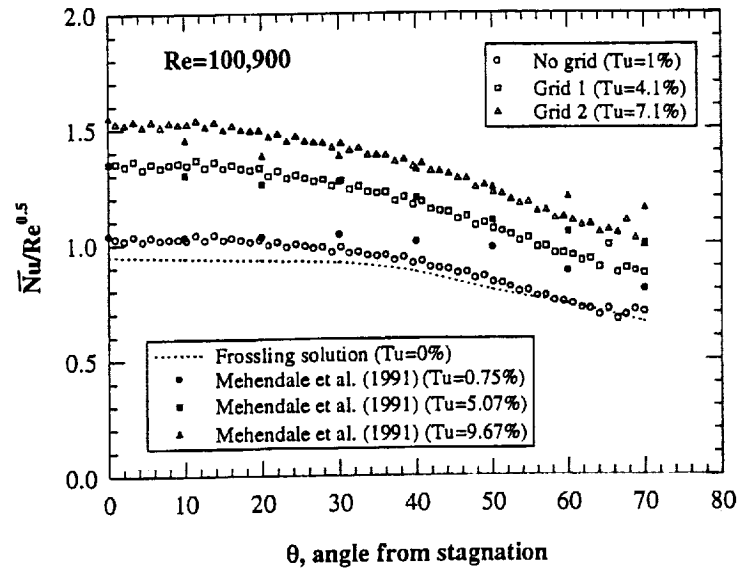


Fig.50(a) Free-stream turbulence effects on spanwise-averaged $Nu/Re^{0.5}$ distributions for a smooth surface (Experiment setup 5)

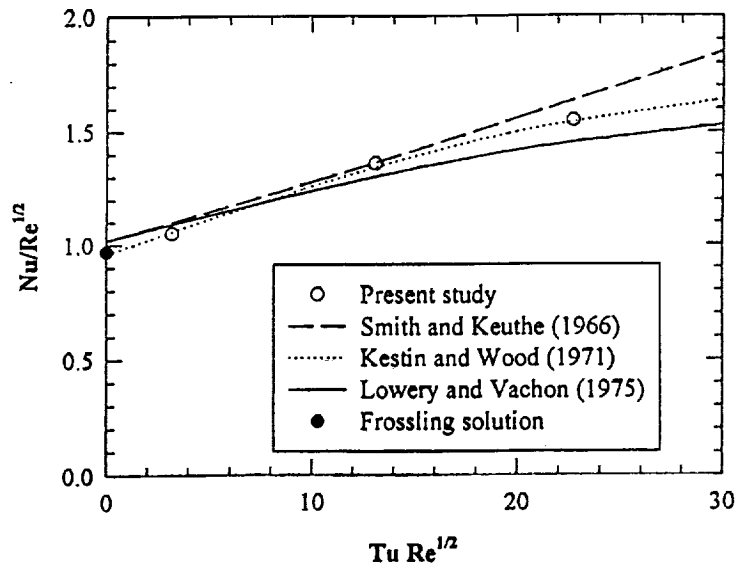


Fig.50(b) Comparison of stagnation point heat transfer results with published correlations (Experiment setup 5)

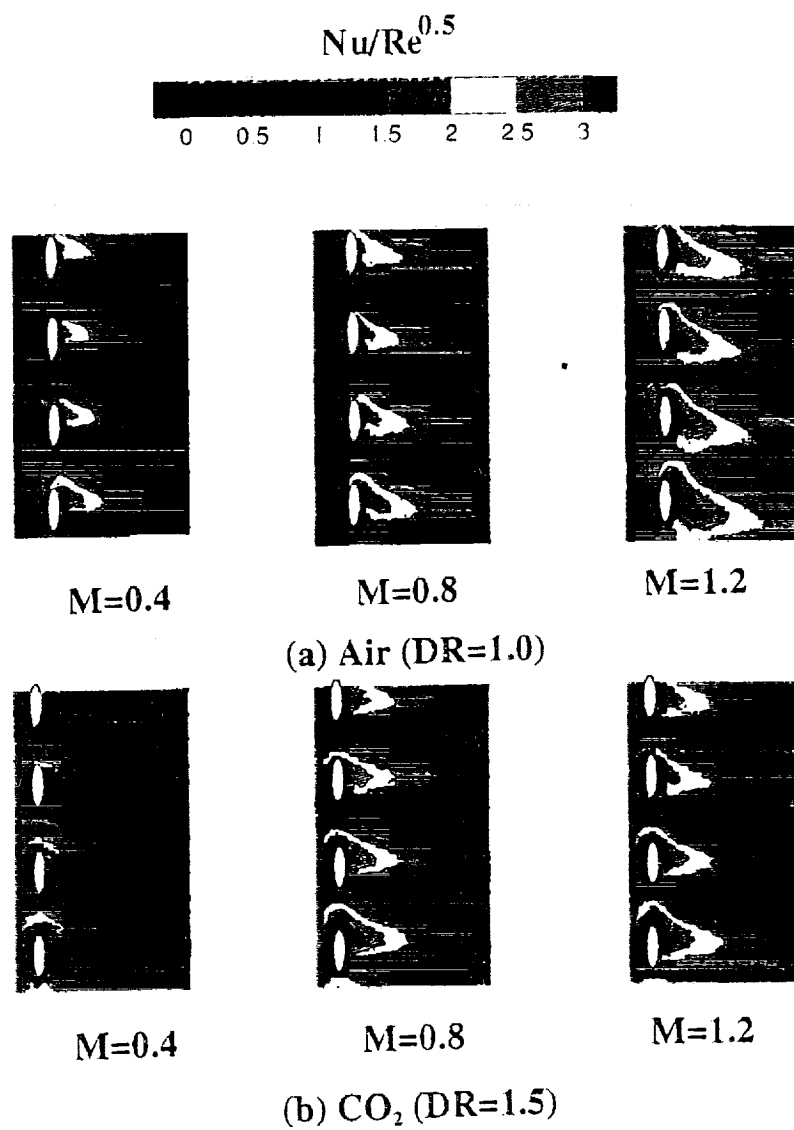


Fig.51 Effect of blowing ratio on detailed $Nu/Re^{0.5}$ distributions for air and CO₂ injection (Experiment setup 5)

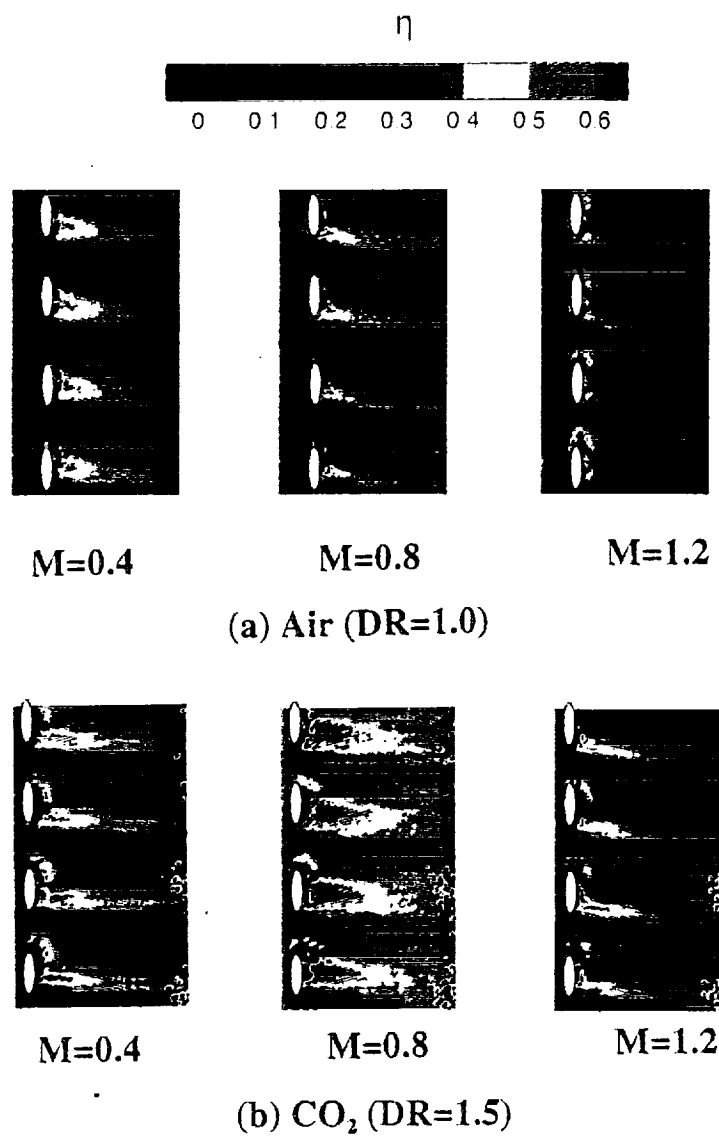


Fig.52 Effect of blowing ratio on detailed film effectiveness distributions for air and CO₂ injection (Experiment setup 5)

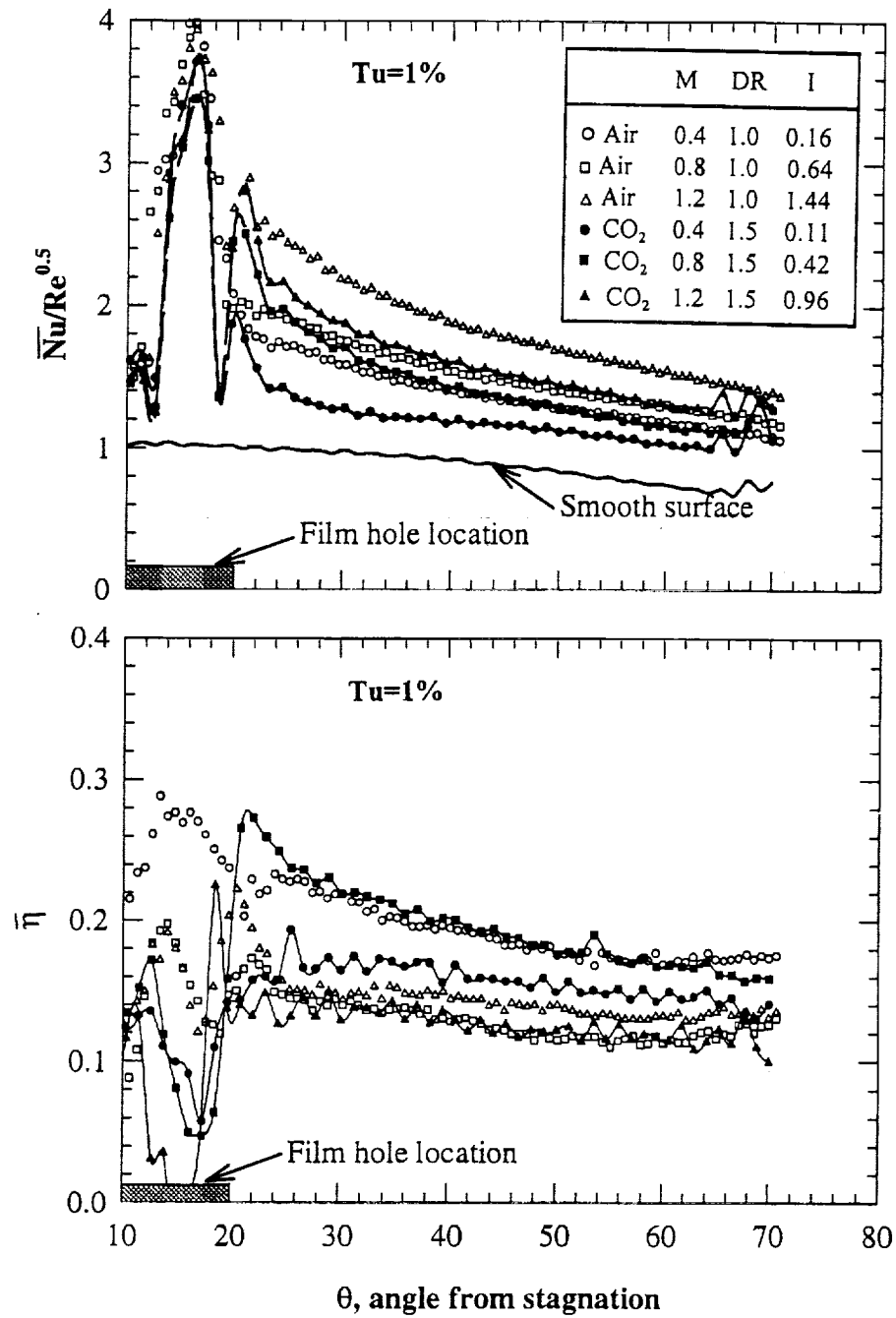


Fig.53 Effect of coolant blowing ratio and density ratio on spanwise-averaged $Nu/Re^{0.5}$ and film effectiveness distributions (Experiment setup 5)

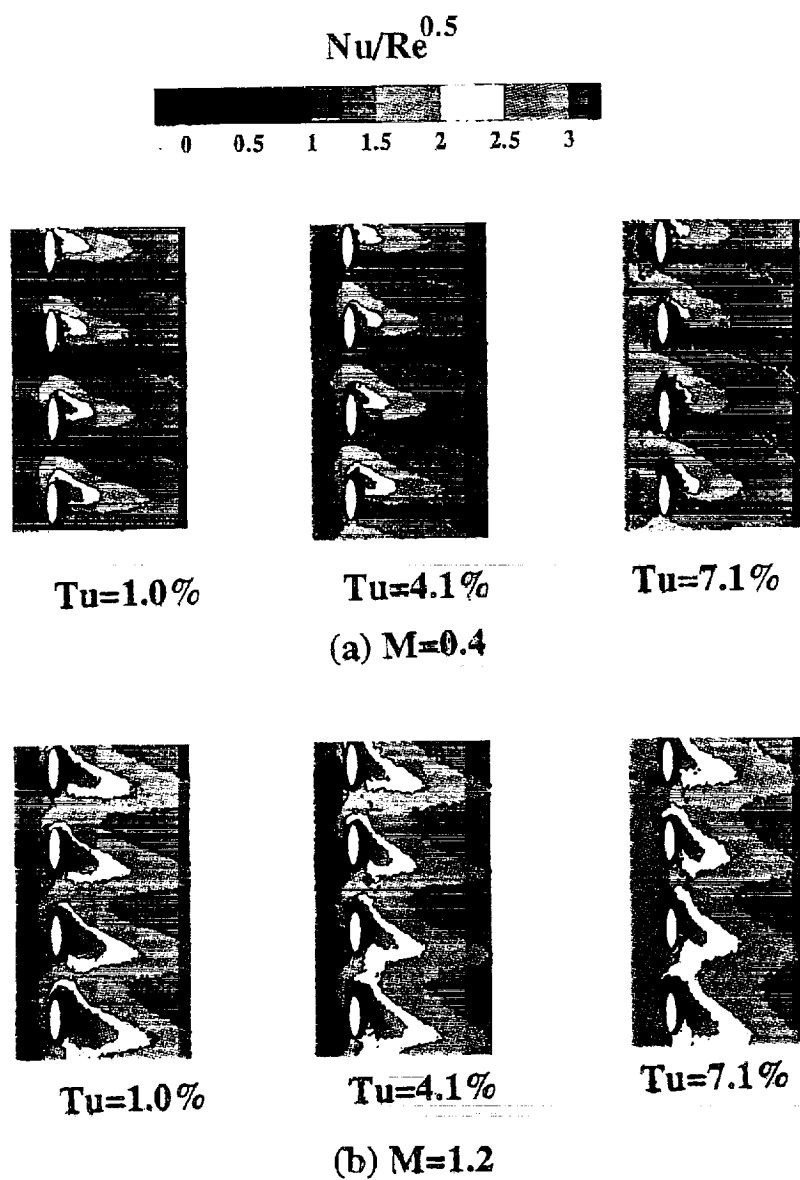


Fig.54 Effect of free-stream turbulence on detailed $Nu/Re^{0.5}$ distributions for air injection (Experiment setup 5)

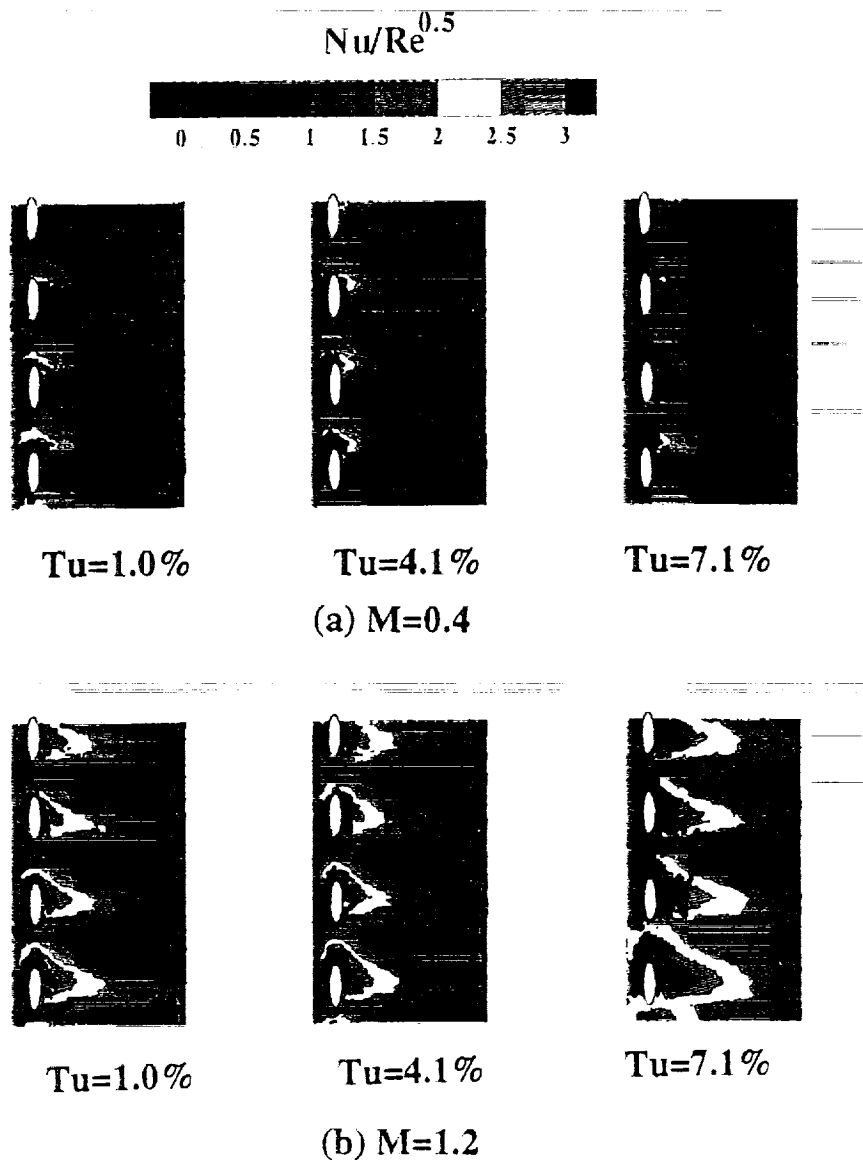


Fig.55 Effect of free-stream turbulence on detailed $Nu/Re^{0.5}$ distributions for CO_2 injection (Experiment setup 5)

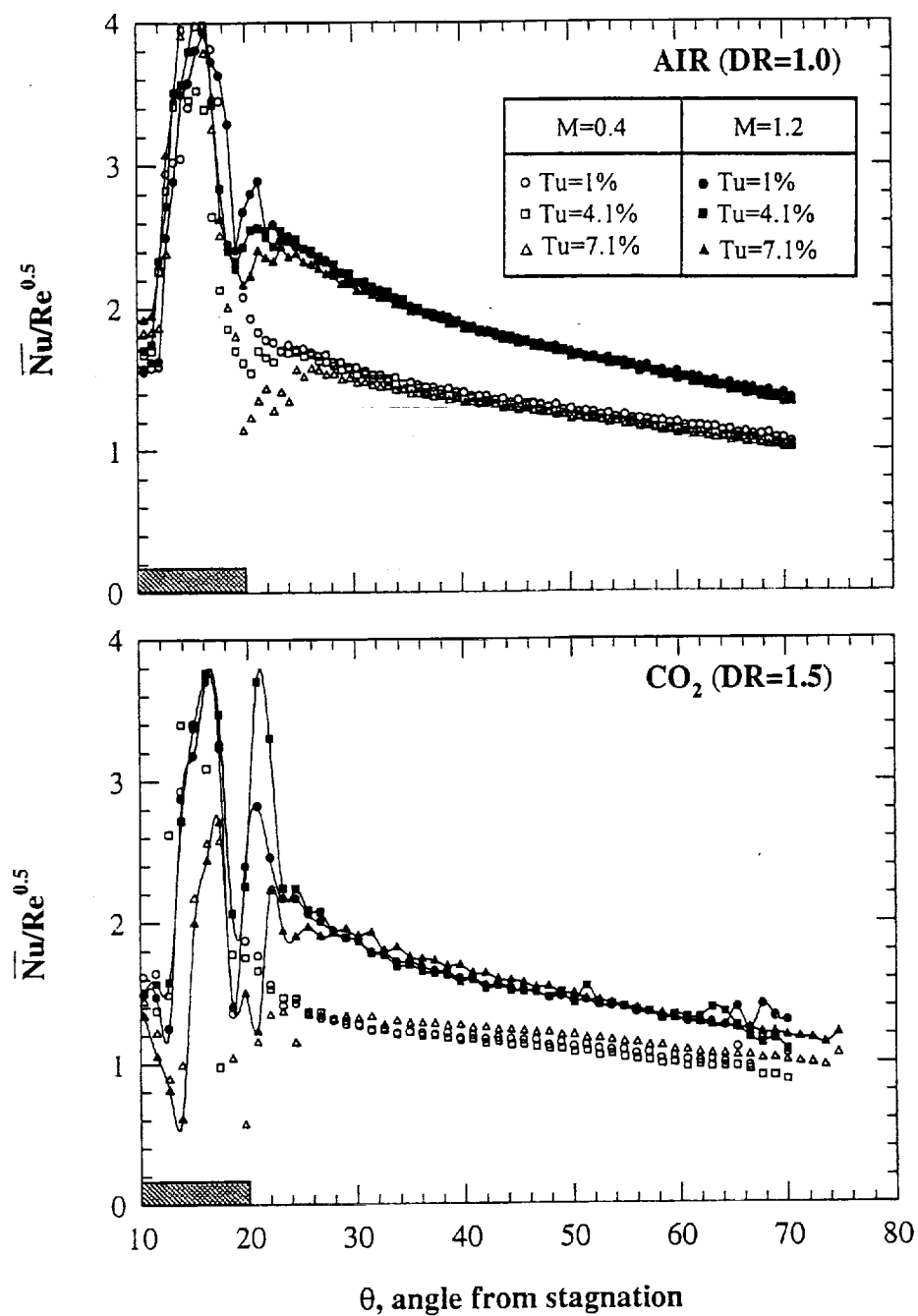


Fig.56 Effect of free-stream turbulence on spanwise-averaged $Nu/Re^{0.5}$ distributions for air and CO₂ injection (Experiment setup 5)

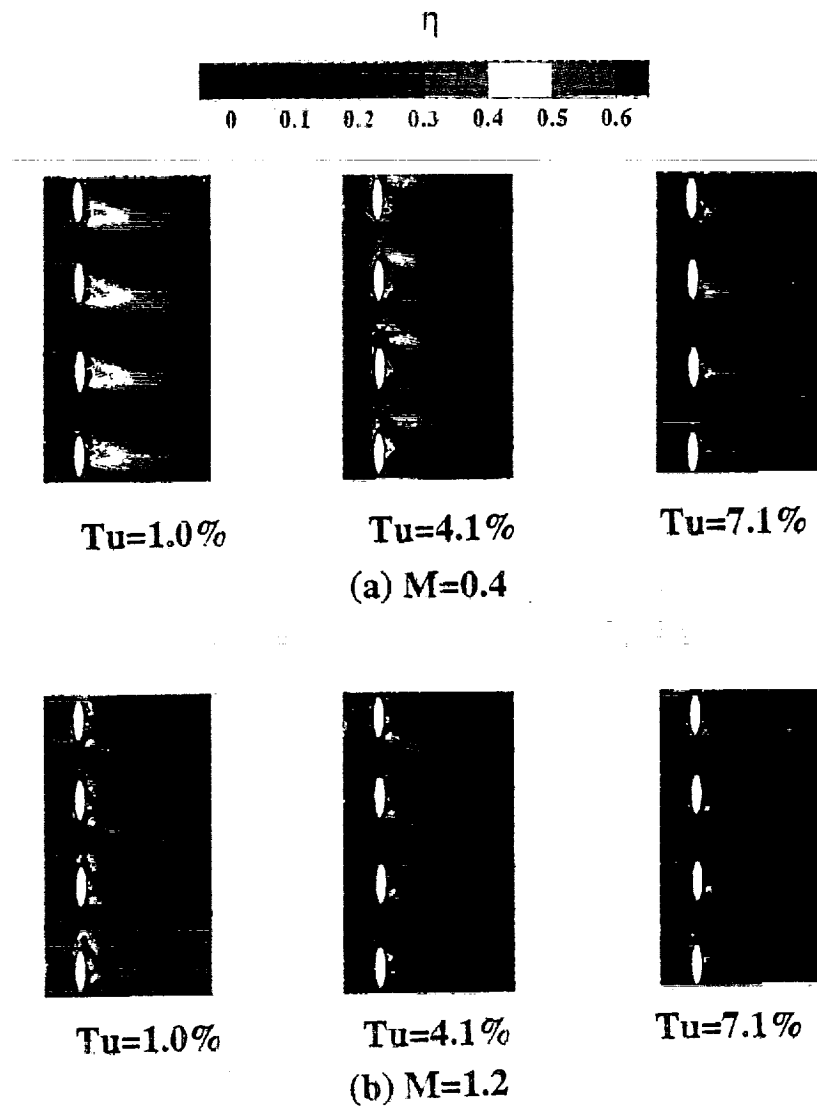


Fig.57 Effect of free-stream turbulence on detailed film effectiveness distributions for air injection (Experiment setup 5)

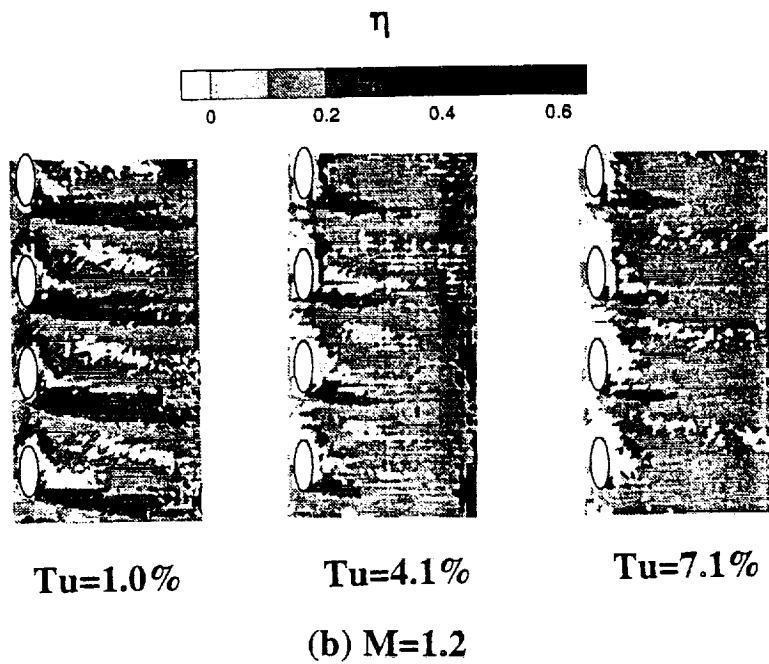
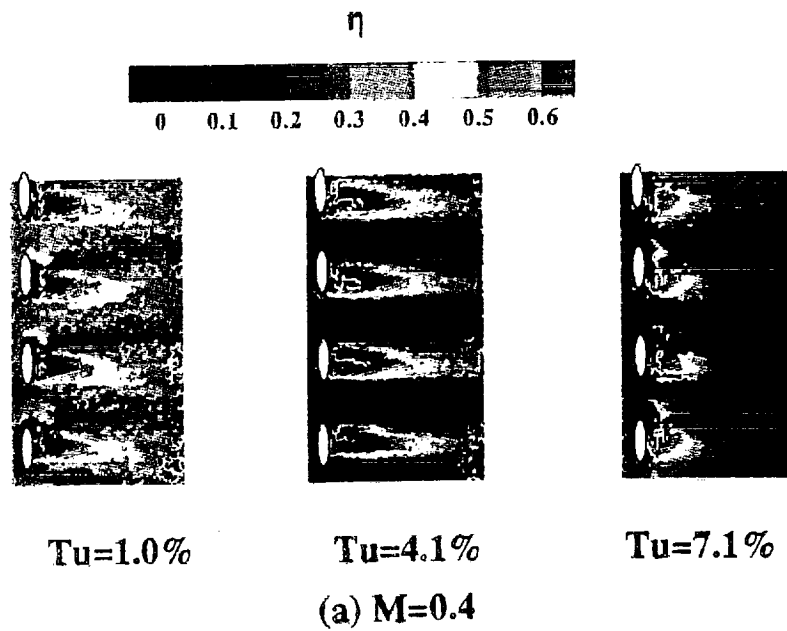


Fig.58 Effect of free-stream turbulence on detailed film effectiveness distributions for CO₂ injection (Experiment setup 5)

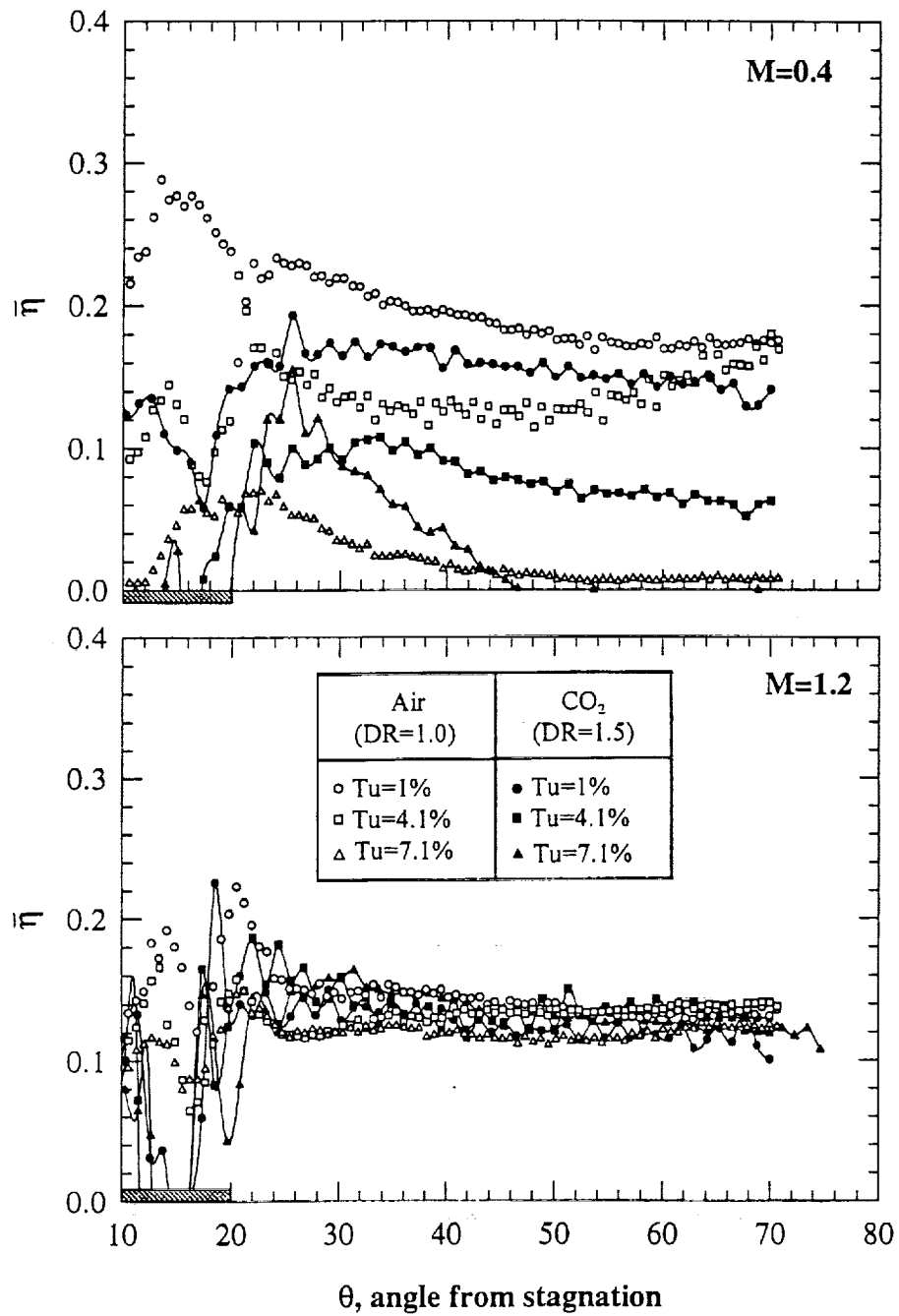


Fig.59 Effect of free-stream turbulence on spanwise-averaged film effectiveness distributions for air and CO₂ injection (Experiment setup 5)

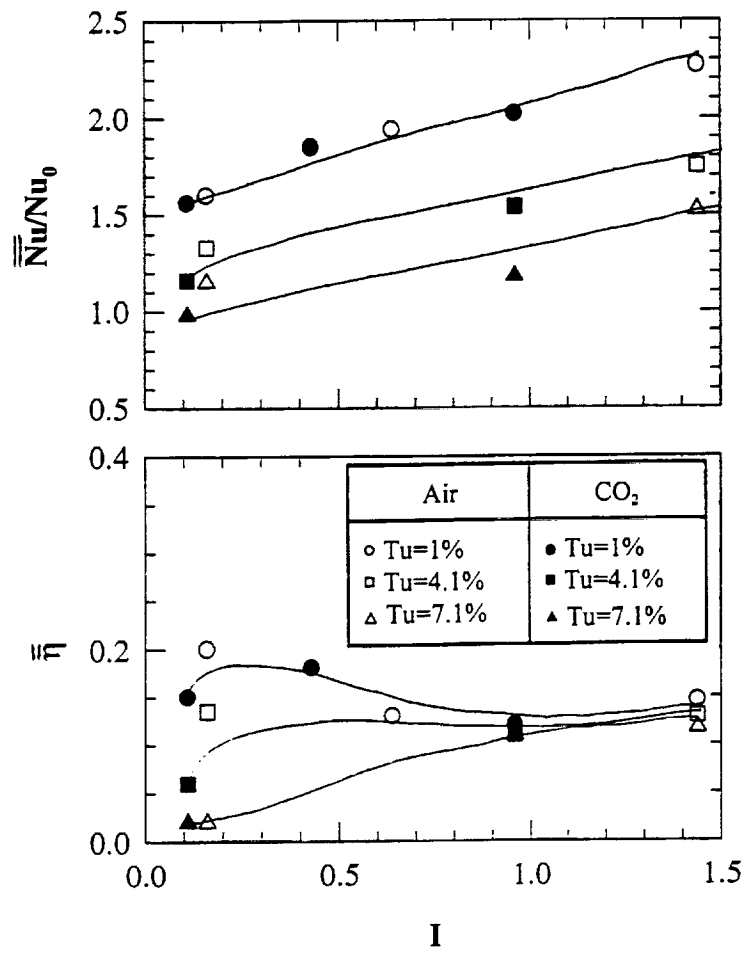


Fig.60 Variation of spatially averaged Nusselt number ratio and film effectiveness with momentum flux ratio (Experiment setup 5)

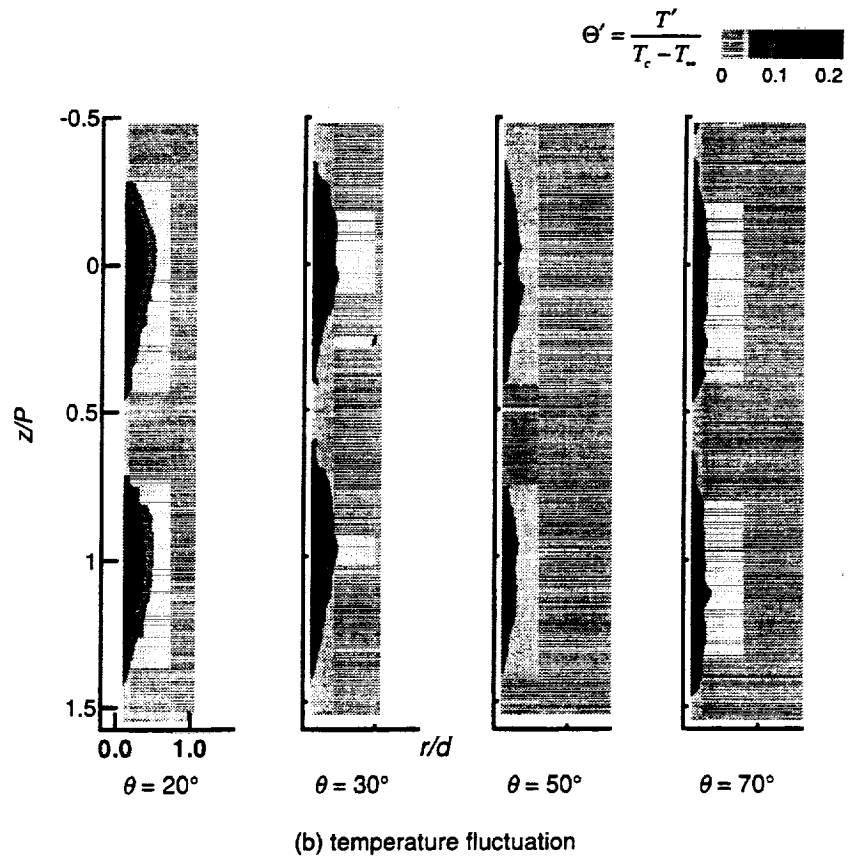
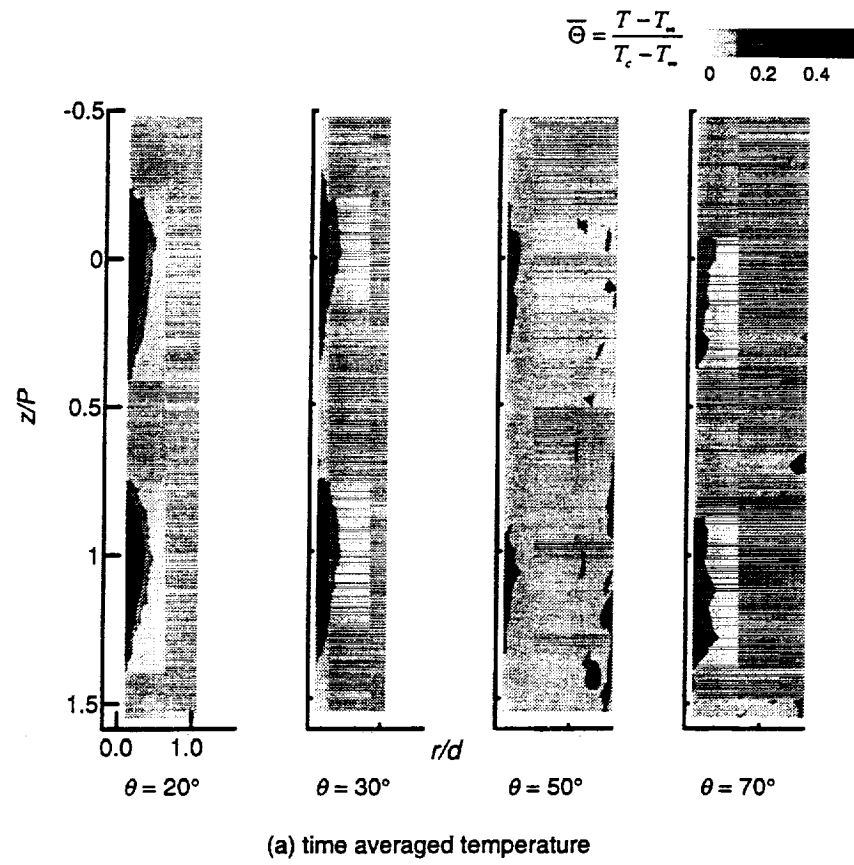
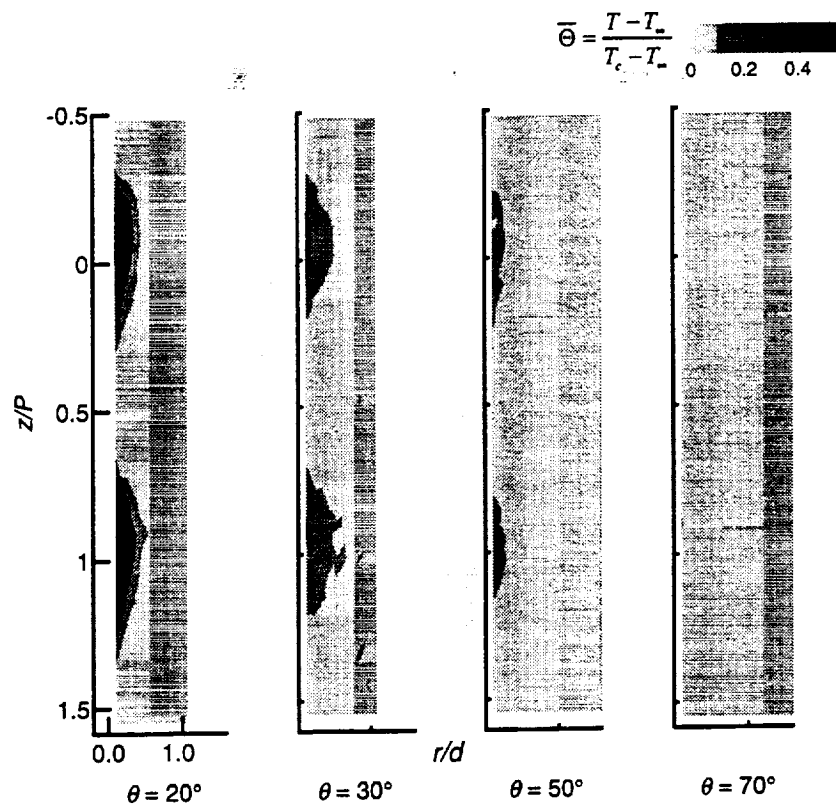
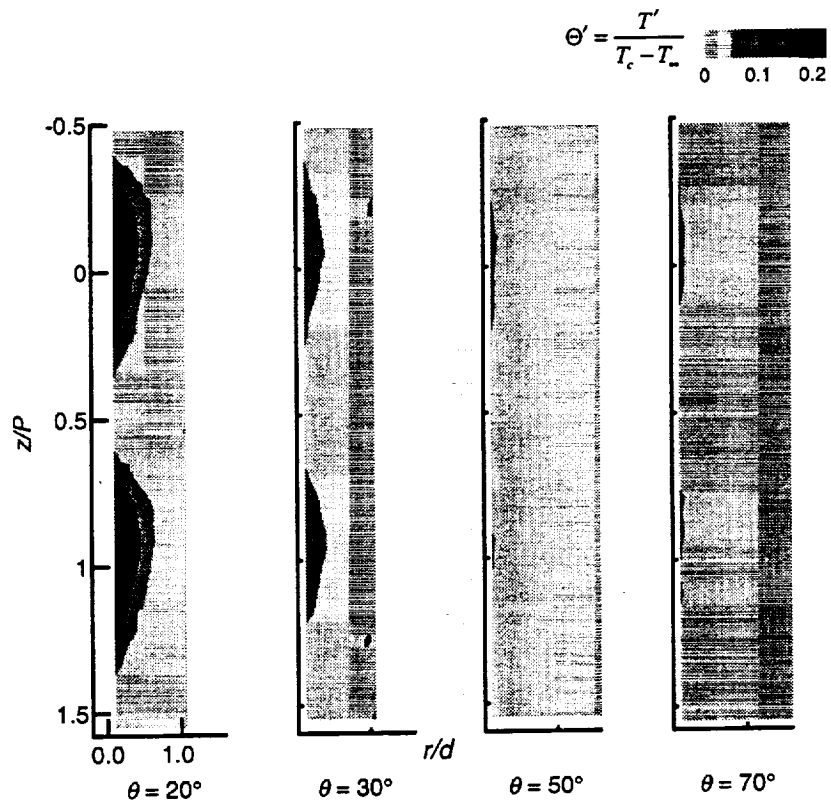


Fig.61 Film temperature distribution for $M=0.4$ and $Tu=1.0\%$
(Experiment setup 5)

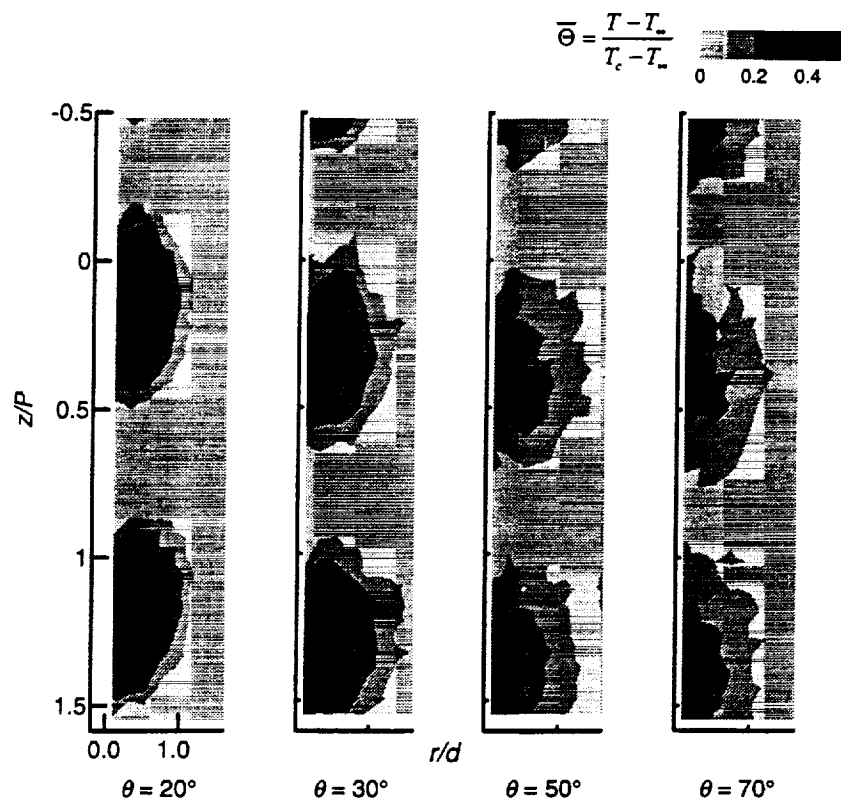


(a) time averaged temperature

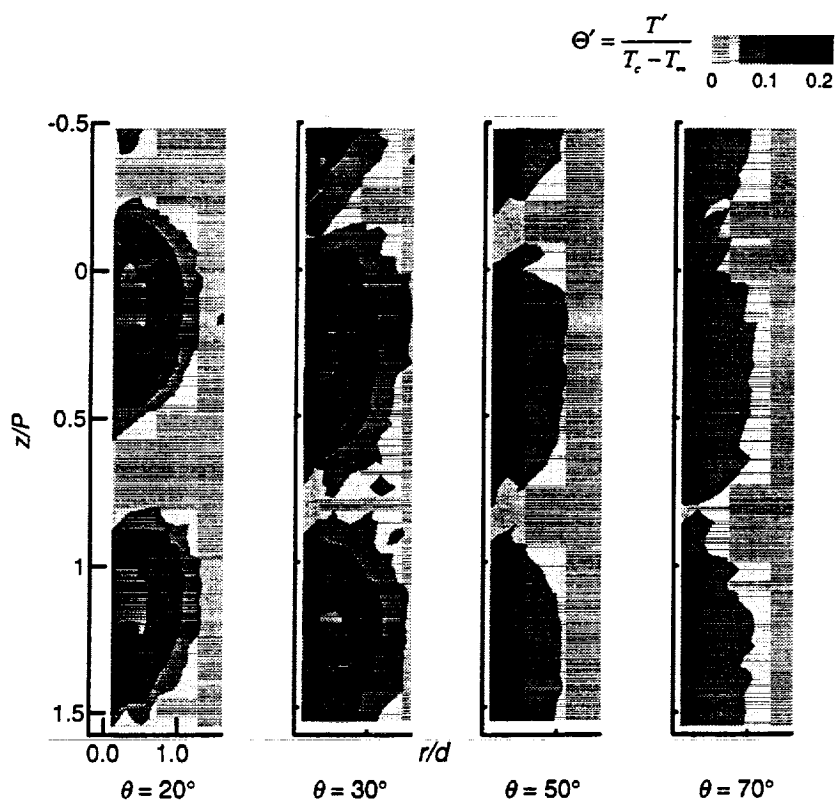


(b) temperature fluctuation

Fig.62 Film temperature distribution for $M=0.4$ and $Tu=7.1\%$
(Experiment setup 5)

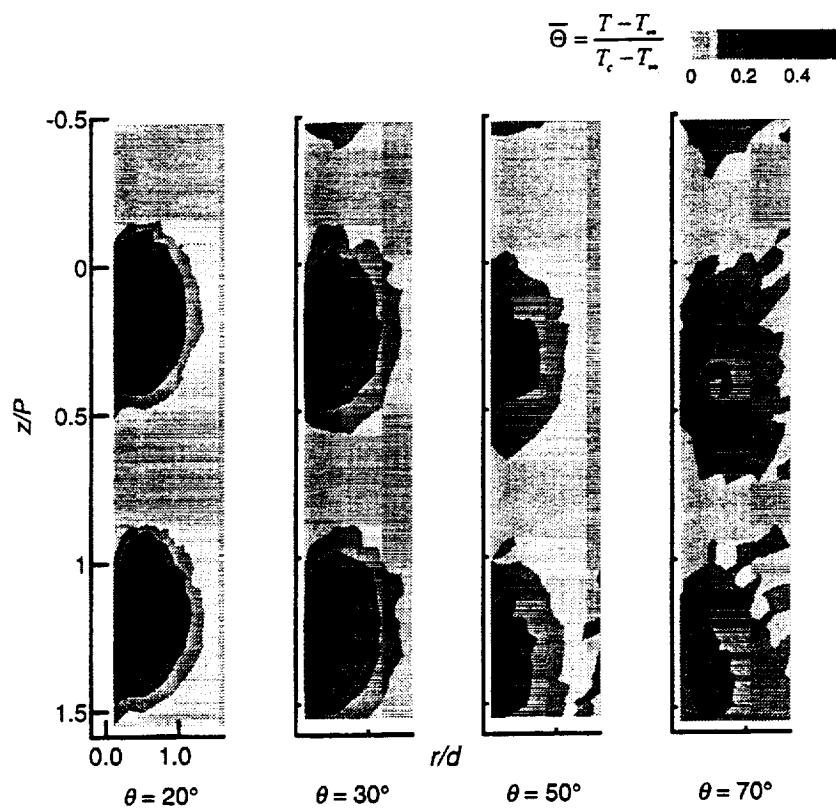


(a) time averaged temperature

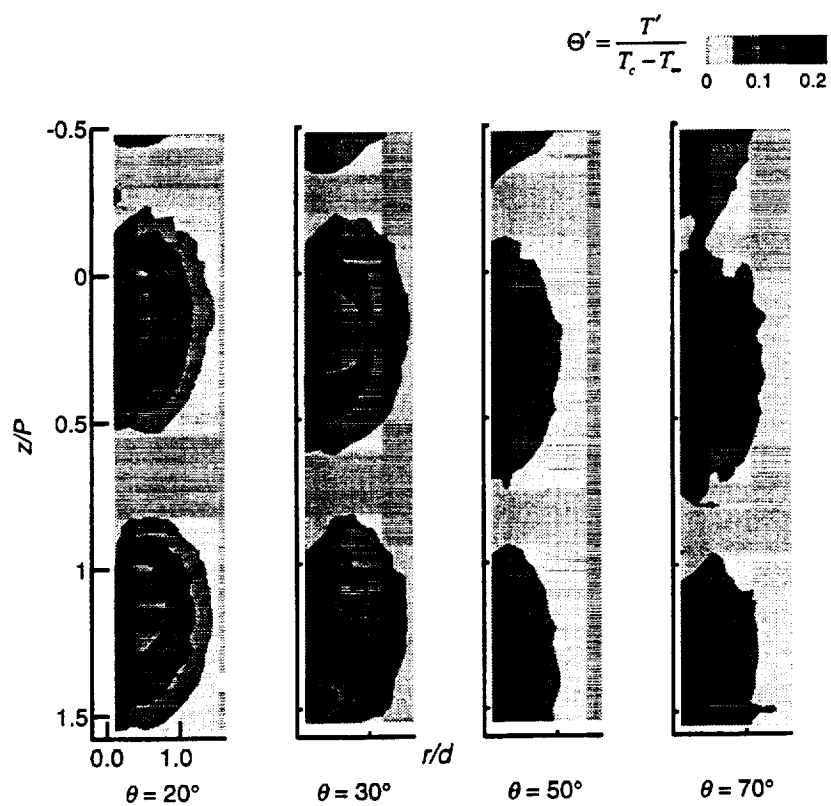


(b) temperature fluctuation

Fig.63 Film temperature distribution for $M=1.2$ and $Tu=1.0\%$
(Experiment setup 5)



(a) time averaged temperature



(b) temperature fluctuation

Fig.64 Film temperature distribution for $M=1.2$ and $Tu=7.1\%$
(Experiment setup 5)

7.2 Tabulated Spanwise-Averaged Data

Table 5. Flow Conditions for Heat Transfer/Film Effectiveness Measurement

Case No.	Re	Tu	S	M _t	Film	M	\bar{T}_u
A	5.3×10^5	0.7%	No Wake	0.0			0.70%
B		0.7%	0.1	0.0			10.4%
C		5.0%	0.1	0.0			13.7%
D		5.0%	0.1	0.25			13.4%
E		5.0%	0.1	0.50			13.0%
F		5.0%	0.1	1.00			12.7%
G	7.6×10^5	0.7%	No Wake	0.0			0.70%
H		0.7%	0.1	0.0			10.4%
I		5.0%	0.1	0.0			13.7%
J		5.0%	0.1	0.25			13.4%
K		5.0%	0.1	0.50			13.0%
L	5.3×10^5	0.7%	No Wake	0.0	Air	0.8	0.70%
M		0.7%	No Wake	0.0	Air	1.2	0.70%
N		0.7%	No Wake	0.0	CO ₂	0.4	10.4%
O		0.7%	No Wake	0.0	CO ₂	0.8	10.4%
P		0.7%	No Wake	0.0	CO ₂	1.2	10.4%
Q	7.6×10^5	0.7%	No Wake	0.0	Air	0.8	0.70%
R	5.3×10^5	0.7%	0.1	0.0	Air	0.8	10.4%
S		0.7%	0.1	0.0	Air	1.2	10.4%
T		0.7%	0.1	0.0	CO ₂	0.4	10.4%
U		0.7%	0.1	0.0	CO ₂	0.8	10.4%
V		0.7%	0.1	0.0	CO ₂	1.2	10.4%
W	7.6×10^5	0.7%	0.1	0.0	Air	0.8	10.4%
X		0.7%	0.1	0.50	Air	0.8	13.0%
Y		5.0%	0.1	0.0	Air	0.8	13.7%
Z		5.0%	0.1	0.50	Air	0.8	13.0%

Appendix 7.2 – Data for Spanwise Averaged Nusselt Number and Film Cooling Effectiveness

CASE A – Nu		0.1696	520.64	0.4284	318.10	0.6247	318.86	0.7724	607.35	0.9201	753.90	-0.1849	289.61
		0.1716	519.59	0.4316	315.54	0.6269	318.84	0.7746	610.74	0.9222	756.33	-0.1884	291.18
X/SL	Nu	0.1736	522.84	0.4348	315.03	0.6289	320.06	0.7767	612.24	0.9244	762.96	-0.1919	292.64
0.0383	1032.88	0.1756	518.36	0.4380	312.91	0.6312	322.92	0.7789	652.13	0.9266	768.46	-0.1954	293.07
0.0403	1013.91	0.1777	516.15	0.4412	312.00	0.6334	326.85	0.7811	651.83	0.9288	772.80	-0.1990	294.59
0.0424	1020.19	0.1797	518.04	0.4444	310.46	0.6356	332.64	0.7832	623.46	0.9309	777.11	-0.2025	295.75
0.0444	1012.62	0.1817	520.75	0.4476	308.61	0.6377	342.33	0.7854	644.73	0.9331	780.24	-0.2060	296.99
0.0464	966.58	0.1836	517.47	0.4508	307.75	0.6399	348.57	0.7876	631.19	0.9353	790.98	-0.2095	297.56
0.0483	932.18	0.1857	512.29	0.4540	306.68	0.6421	344.87	0.7898	632.66	0.9374	800.86	-0.2130	299.19
0.0504	906.15	0.1878	516.09	0.4572	305.79	0.6443	343.51	0.7919	649.72	0.9396	804.01	-0.2166	299.64
0.0525	885.30	0.1898	515.32	0.4987	305.41	0.6464	351.31	0.7941	652.50	0.9418	808.99	-0.2201	308.51
0.0545	857.22	0.1918	513.09	0.5008	304.25	0.6486	353.53	0.7963	657.04	0.9440	817.02	-0.2236	301.50
0.0565	839.24	0.1938	513.36	0.5031	301.46	0.6508	356.70	0.7985	661.91	0.9461	821.26	-0.2271	301.61
0.0585	818.96	0.1958	513.26	0.5053	298.85	0.6529	359.27	0.8006	663.54	0.9483	834.19	-0.2307	301.91
0.0605	796.56	0.1979	515.68	0.5074	297.37	0.6551	375.48	0.8028	643.41	0.9505	836.94	-0.2342	302.12
0.0626	772.97	0.1999	511.97	0.5096	295.85	0.6573	386.43	0.8050	643.02	0.9526	849.07	-0.2377	302.61
0.0646	755.92	0.2019	511.41	0.5118	292.56	0.6595	377.38	0.8071	663.75	0.9548	862.15	-0.2412	302.86
0.0666	745.04	0.2039	509.42	0.5138	289.77	0.6616	377.54	0.8093	667.88	0.9570	878.09	-0.2448	303.43
0.0686	725.59	0.2059	508.81	0.5161	288.35	0.6638	382.03	0.8115	651.59	0.9592	886.14	-0.2483	303.52
0.0706	711.82	0.2079	509.32	0.5183	286.55	0.6660	382.55	0.8137	654.06			-0.2518	304.56
0.0726	701.27	0.2100	505.93	0.5205	284.10	0.6681	397.75	0.8158	653.21	X/PL	Nu	-0.2553	304.69
0.0747	690.57	0.2120	501.89	0.5226	283.31	0.6703	407.56	0.8180	653.08	-0.0042	925.83	-0.2589	306.50
0.0767	682.20	0.2140	499.20	0.5248	281.48	0.6725	402.33	0.8202	681.24	-0.0127	886.81	-0.2624	307.06
0.0786	671.19	0.2160	497.58	0.5270	278.89	0.6747	407.52	0.8223	663.03	-0.0213	914.91	-0.2659	307.14
0.0807	661.61	0.2180	497.93	0.5291	277.39	0.6768	419.23	0.8245	682.77	-0.0298	829.79	-0.2694	307.59
0.0827	652.19	0.2201	496.16	0.5313	277.74	0.6790	416.54	0.8267	662.21	-0.0333	769.46	-0.2729	308.10
0.0848	643.99	0.2221	494.47	0.5335	278.27	0.6812	418.68	0.8289	662.66	-0.0369	698.85	-0.2765	308.51
0.0868	632.02	0.2241	495.32	0.5357	278.13	0.6833	418.79	0.8310	666.74	-0.0405	614.74	-0.2800	309.25
0.0888	624.35	0.2261	492.50	0.5378	275.56	0.6855	425.45	0.8332	671.09	-0.0439	524.36	-0.2835	310.16
0.0908	616.12	0.2281	490.48	0.5400	276.09	0.6877	433.87	0.8354	672.65	-0.0475	423.67	-0.2871	311.45
0.0928	614.44	0.2302	490.57	0.5422	277.86	0.6899	434.74	0.8375	670.79	-0.0510	272.79	-0.2906	311.97
0.0949	609.54	0.2302	490.09	0.5443	281.90	0.6920	434.06	0.8397	669.63	-0.0545	224.34	-0.2942	311.70
0.0969	603.95	0.2336	486.00	0.5465	281.67	0.6942	444.69	0.8419	675.53	-0.0580	213.12	-0.2976	310.90
0.0989	590.80	0.2371	480.27	0.5487	278.73	0.6964	456.49	0.8441	677.86	-0.0615	211.85	-0.3011	310.27
0.1008	588.86	0.2406	474.38	0.5509	278.35	0.6985	465.92	0.8462	675.01	-0.0651	211.50	-0.3047	310.10
0.1029	584.18	0.2441	470.24	0.5530	278.84	0.7007	460.86	0.8484	674.43	-0.0686	211.48	-0.3082	309.51
0.1050	582.09	0.2476	467.74	0.5552	281.03	0.7029	466.39	0.8506	677.53	-0.0721	211.87	-0.3117	309.25
0.1070	575.19	0.2511	467.12	0.5574	283.41	0.7050	478.52	0.8527	680.37	-0.0756	212.43	-0.3152	310.00
0.1090	570.05	0.2546	467.04	0.5596	281.45	0.7072	481.04	0.8549	682.86	-0.0791	214.43	-0.3188	309.84
0.1110	567.49	0.2581	465.72	0.5617	281.02	0.7094	495.20	0.8571	679.53	-0.0827	216.23	-0.3223	309.04
0.1130	566.01	0.2615	462.47	0.5639	287.23	0.7116	491.89	0.8593	701.20	-0.0862	218.92	-0.3258	309.26
0.1151	558.49	0.2649	465.32	0.5661	286.56	0.7138	494.55	0.8614	681.66	-0.0897	221.52	-0.3293	308.34
0.1171	557.16	0.2685	471.81	0.5682	301.91	0.7159	506.75	0.8636	684.48	-0.0932	224.19	-0.3329	308.28
0.1191	555.33	0.2720	475.55	0.5704	299.56	0.7180	508.29	0.8658	690.50	-0.0968	227.34	-0.3364	308.48
0.1211	558.12	0.2754	476.75	0.5726	301.33	0.7203	516.34	0.8679	689.76	-0.1003	231.71	-0.3400	308.69
0.1231	552.91	0.2790	451.59	0.5748	292.37	0.7224	514.09	0.8701	696.40	-0.1038	235.00	-0.3434	307.87
0.1252	545.94	0.2825	449.34	0.5769	292.32	0.7246	520.90	0.8723	698.86	-0.1073	238.36	-0.3469	308.31
0.1272	551.26	0.2860	446.93	0.5791	294.14	0.7268	523.62	0.8745	697.94	-0.1109	249.43	-0.3505	308.63
0.1292	552.31	0.2895	447.47	0.5813	292.59	0.7290	531.08	0.8766	697.82	-0.1144	260.81	-0.3540	308.51
0.1312	546.25	0.2929	447.84	0.5834	309.29	0.7310	541.62	0.8788	701.12	-0.1179	248.42	-0.3575	308.00
0.1332	540.31	0.2964	434.36	0.5856	296.11	0.7333	567.08	0.8810	705.71	-0.1214	255.65	-0.3610	307.76
0.1352	537.96	0.2999	428.37	0.5878	296.91	0.7355	546.47	0.8832	705.72	-0.1250	258.22	-0.3646	308.17
0.1373	537.32	0.3034	411.89	0.5899	299.14	0.7376	557.95	0.8853	707.30	-0.1285	260.65	-0.3681	309.14
0.1392	539.13	0.3069	404.41	0.5921	300.75	0.7398	559.13	0.8875	709.07	-0.1320	263.72	-0.3716	310.10
0.1413	536.44	0.3836	348.24	0.5943	301.85	0.7420	562.05	0.8897	710.43	-0.1355	271.78	-0.3751	309.75
0.1433	530.23	0.3868	344.49	0.5965	301.60	0.7442	565.62	0.8918	711.46	-0.1390	269.09	-0.3787	309.09
0.1453	529.54	0.3899	337.00	0.5986	300.25	0.7463	569.11	0.8940	715.29	-0.1426	266.28	-0.3822	310.19
0.1474	527.17	0.3932	333.26	0.6008	301.39	0.7485	580.14	0.8962	717.34	-0.1461	268.85	-0.3858	311.70
0.1494	526.55	0.3964	329.52	0.6029	303.46	0.7507	579.86	0.8984	721.89	-0.1496	271.23	-0.3892	319.68
0.1514	526.38	0.3996	325.77	0.6052	307.80	0.7528	580.25	0.9005	727.11	-0.1531	274.24	-0.3929	320.33
0.1534	528.68	0.4028	326.52	0.6073	320.70	0.7550	585.71	0.9027	730.50	-0.1567	286.32	-0.3963	320.83
0.1554	526.19	0.4060	327.68	0.6095	317.48	0.7572	584.51	0.9049	730.85	-0.1603	282.26	-0.3998	326.05
0.1575	521.02	0.4092	325.79	0.6117	305.99	0.7594	590.79	0.9070	733.79	-0.1637	285.00	-0.4033	329.52
0.1595	519.99	0.4124	322.90	0.6138	314.85	0.7615	594.65	0.9092	737.62	-0.1672	285.45	-0.4068	325.77
0.1615	518.45	0.4156	321.62	0.6159	312.80	0.7637	596.09	0.9114	741.59	-0.1708	284.23	-0.3969	333.26
0.1635	524.63	0.4188	319.66	0.6182	313.27	0.7659	599.89	0.9136	743.43	-0.1743	285.97	-0.3999	344.49
0.1655	521.90	0.4220	319.43	0.6204	310.71	0.7680	600.82	0.9157	746.87	-0.1778	287.22	-0.4029	327.27
0.1676	522.81	0.4252	318.72	0.6225	313.24	0.7702	619.11	0.9179	751.80	-0.1813	288.01	-0.4059	366.36

Appendix 7.2 – Data for Spanwise Averaged Nusselt Number and Film Cooling Effectiveness

-0.4090	357.32	-0.6123	420.78	-0.8157	374.28	0.0577	1077.66	0.1895	484.21	0.4303	524.25	0.5814	801.18
-0.4119	347.76	-0.6153	390.99	-0.8187	367.53	0.0596	1044.39	0.1914	482.13	0.4325	523.26	0.5836	801.98
-0.4149	359.45	-0.6183	375.15	-0.8217	361.28	0.0616	1017.66	0.1933	479.93	0.4347	525.81	0.5858	800.83
-0.4179	355.33	-0.6213	376.21	-0.8247	380.80	0.0635	982.72	0.1953	479.33	0.4370	530.92	0.5881	795.61
-0.4209	337.00	-0.6243	398.95	-0.8277	364.36	0.0654	950.28	0.1972	478.49	0.4392	533.54	0.5903	795.60
-0.4238	365.96	-0.6273	376.10	-0.8307	375.82	0.0674	924.46	0.1992	476.13	0.4414	536.50	0.5925	794.50
-0.4268	345.42	-0.6304	392.58	-0.8337	376.18	0.0693	896.63	0.2011	474.61	0.4436	537.00	0.5947	794.31
-0.4298	331.94	-0.6333	381.93	-0.8367	393.24	0.0713	872.60	0.2030	473.95	0.4459	539.42	0.5970	787.45
-0.4328	313.71	-0.6362	397.68	-0.8397	373.89	0.0732	854.01	0.2050	476.18	0.4481	546.99	0.5992	788.78
-0.4358	333.16	-0.6392	372.84	-0.8427	386.34	0.0751	831.09	0.2069	474.10	0.4503	552.63	0.6014	789.91
-0.4388	317.70	-0.6422	379.77	-0.8457	411.86	0.0771	813.81	0.2088	471.27	0.4525	555.34	0.6036	787.36
-0.4418	317.78	-0.6452	398.56	-0.8486	411.07	0.0790	795.85	0.2108	468.44	0.4547	555.52	0.6058	787.72
-0.4448	316.10	-0.6482	382.45	-0.8516	420.58	0.0810	780.07	0.2127	466.64	0.4570	558.51	0.6081	786.94
-0.4478	319.20	-0.6512	383.34	-0.8546	407.93	0.0829	764.26	0.2147	464.93	0.4592	562.26	0.6103	786.98
-0.4508	322.34	-0.6542	392.50	-0.8576	402.25	0.0848	747.11	0.2166	464.67	0.4614	566.36	0.6125	785.30
-0.4538	330.86	-0.6572	424.59	-0.8606	385.37	0.0868	735.23	0.2185	466.39	0.4636	568.11	0.6147	780.81
-0.4568	335.94	-0.6602	446.10	-0.8636	413.18	0.0887	723.45	0.2205	461.58	0.4659	572.76	0.6170	780.78
-0.4597	349.25	-0.6632	400.44	-0.8666	431.07	0.0906	712.85	0.2224	459.01	0.4681	576.56	0.6192	778.52
-0.4627	352.18	-0.6663	392.53	-0.8696	389.13	0.0926	703.09	0.2243	458.19	0.4703	577.34	0.6214	778.72
-0.4657	351.24	-0.6692	384.04	-0.8726	382.29	0.0945	694.21	0.2263	458.03	0.4725	583.67	0.6236	776.98
-0.4687	351.48	-0.6721	399.86	-0.8756	389.21	0.0965	681.94	0.2282	457.85	0.4747	589.98	0.6258	774.00
-0.4717	367.25	-0.6751	388.64	-0.8786	384.88	0.0984	669.79	0.2302	454.67	0.4770	595.88	0.6281	772.46
-0.4747	342.91	-0.6781	394.17	-0.8816	382.96	0.1003	660.18	0.2320	451.67	0.4792	599.80	0.6303	772.50
-0.4777	324.04	-0.6811	388.86	-0.8846	380.26	0.1023	654.68	0.2334	453.15	0.4814	600.33	0.6325	767.28
-0.4807	326.65	-0.6842	382.02	-0.8875	389.18	0.1042	644.17	0.2366	453.81	0.4836	602.36	0.6347	767.80
-0.4837	326.03	-0.6871	386.69	-0.8905	385.57	0.1061	632.13	0.2398	457.19	0.4859	612.37	0.6370	764.97
-0.4867	327.69	-0.6901	372.83	-0.8935	394.47	0.1081	624.31	0.2430	459.53	0.4881	616.22	0.6392	760.21
-0.4897	337.06	-0.6931	374.17	-0.8965	391.54	0.1100	617.00	0.2461	458.60	0.4903	613.61	0.6414	767.36
-0.4927	326.46	-0.6961	381.66	-0.8995	386.49	0.1120	610.55	0.2493	457.52	0.4925	619.18	0.6436	764.20
-0.4956	332.67	-0.6991	396.83	-0.9025	402.09	0.1139	605.21	0.2525	459.62	0.4947	627.04	0.6458	758.74
-0.4986	325.76	-0.7021	399.37	-0.9055	398.38	0.1158	600.03	0.2557	460.34	0.4970	634.46	0.6481	762.31
-0.5017	326.91	-0.7051	395.68	-0.9085	393.32	0.1178	594.48	0.2589	462.86	0.4992	634.75	0.6503	760.09
-0.5046	328.54	-0.7080	418.48	-0.9115	394.06	0.1197	590.04	0.2621	466.33	0.5014	641.00	0.6525	753.89
-0.5076	323.31	-0.7110	395.11	-0.9145	396.52	0.1216	587.53	0.2653	470.59	0.5036	649.97	0.6547	754.00
-0.5106	324.44	-0.7140	394.92	-0.9174	398.79	0.1236	583.77	0.2685	471.96	0.5059	656.77	0.6570	752.75
-0.5136	330.45	-0.7170	373.78	-0.9204	404.46	0.1255	581.05	0.2717	472.03	0.5081	658.53	0.6592	751.74
-0.5166	337.04	-0.7201	389.56	-0.9234	420.03	0.1275	577.43	0.2749	471.36	0.5103	665.47	0.6614	756.86
-0.5196	331.00	-0.7230	414.64	-0.9264	424.72	0.1294	573.51	0.2781	470.42	0.5125	669.56	0.6636	746.87
-0.5227	339.48	-0.7260	397.72	-0.9294	409.84	0.1313	567.23	0.2813	470.53	0.5147	676.87	0.6658	743.17
-0.5256	337.51	-0.7290	400.95	-0.9324	411.88	0.1333	563.28	0.2845	471.06	0.5170	681.30	0.6681	747.11
-0.5286	339.31	-0.7320	382.92	-0.9354	441.27	0.1352	559.54	0.2877	474.69	0.5192	689.52	0.6703	743.45
-0.5315	345.39	-0.7350	390.63	-0.9384	416.11	0.1371	556.67	0.2909	475.87	0.5214	691.83	0.6725	740.59
-0.5345	350.42	-0.7380	382.54	-0.9414	440.88	0.1391	553.39	0.2941	473.39	0.5236	699.53	0.6747	738.21
-0.5375	370.14	-0.7409	400.65	-0.9444	423.60	0.1410	549.34	0.2973	472.88	0.5259	704.42	0.6770	734.76
-0.5405	344.05	-0.7439	370.69	-0.9474	427.92	0.1430	547.50	0.3005	469.42	0.5281	713.49	0.6792	738.43
-0.5435	345.58	-0.7469	370.46	-0.9504	433.76	0.1449	542.56	0.3037	461.54	0.5303	715.82	0.6814	732.12
-0.5465	345.60	-0.7499	398.36	-0.9533	434.44	0.1468	536.60	0.3069	489.87	0.5325	721.73	0.6836	729.34
-0.5495	346.92	-0.7529	378.25	-0.9563	461.72	0.1488	531.48	0.3836	523.76	0.5347	730.89	0.6858	728.95
-0.5525	348.52	-0.7560	379.18	-0.9593	471.44	0.1507	527.43	0.3859	550.33	0.5370	738.20	0.6881	726.79
-0.5555	344.22	-0.7589	382.54	-0.9623	472.20	0.1526	523.17	0.3881	549.58	0.5392	738.31	0.6903	723.01
-0.5586	342.69	-0.7619	391.44	-0.9653	454.04	0.1546	521.95	0.3903	541.44	0.5414	745.96	0.6925	727.24
-0.5615	360.68	-0.7649	377.07	-0.9683	456.69	0.1565	518.47	0.3925	530.83	0.5436	756.81	0.6947	722.09
-0.5645	371.88	-0.7679	407.61	-0.9713	462.45	0.1585	513.95	0.3947	524.40	0.5459	763.62	0.6970	720.05
-0.5674	373.84	-0.7709	414.23			0.1604	512.36	0.3970	520.53	0.5481	763.93	0.6992	723.45
-0.5704	369.90	-0.7739	408.76			0.1623	510.24	0.3992	520.05	0.5503	770.77	0.7014	719.60
-0.5734	390.72	-0.7768	398.82			0.1643	507.96	0.4014	521.11	0.5525	778.10	0.7036	714.49
-0.5764	385.55	-0.7798	360.55			0.1662	503.66	0.4036	523.18	0.5547	786.15	0.7058	715.09
-0.5794	385.79	-0.7828	388.80			0.1682	501.74	0.4059	532.12	0.5570	785.88	0.7081	715.68
-0.5824	405.52	-0.7858	376.27			0.1701	500.67	0.4081	527.13	0.5592	790.43	0.7103	720.47
-0.5854	400.76	-0.7888	372.51			0.1720	499.33	0.4103	524.76	0.5614	791.12	0.7125	718.77
-0.5884	371.70	-0.7919	384.03			0.1740	497.67	0.4125	526.24	0.5636	792.63	0.7147	712.54
-0.5914	347.76	-0.7948	385.25			0.1759	497.51	0.4147	527.66	0.5658	794.26	0.7170	707.69
-0.5945	350.65	-0.7978	368.45			0.1778	513.63	0.4170	529.27	0.5681	799.09	0.7192	707.70
-0.5974	378.23	-0.8008	380.69			0.1798	493.35	0.4192	526.22	0.5703	805.38	0.7214	706.56
-0.6003	403.37	-0.8038	379.49			0.1817	492.07	0.4214	526.53	0.5725	801.43	0.7236	706.89
-0.6033	386.20	-0.8068	372.50			0.1837	491.18	0.4236	523.12	0.5747	800.26	0.7258	702.45
-0.6063	382.29	-0.8098	374.43			0.1856	490.46	0.4259	523.85	0.5770	801.14	0.7281	699.91
-0.6093	394.66	-0.8127	360.02			0.1875	487.66	0.4281	524.63	0.5792	801.86	0.7303	700.72

CASE B – Nu

X/SL Nu

0.0383	1468.56
0.0403	1427.25
0.0422	1367.71
0.0441	1317.00
0.0461	1281.43
0.0480	1244.83
0.0499	1211.37
0.0519	1170.95
0.0538	1134.56
0.0558	1107.06

Appendix 7.2 – Data for Spanwise Averaged Nusselt Number and Film Cooling Effectiveness

0.7325	700.27	0.8836	647.57	-0.1800	398.90	-0.4298	444.05	-0.6333	477.04	-0.8367	431.53	0.0713	824.48
0.7347	700.36	0.8858	652.00	-0.1839	398.45	-0.4328	393.32	-0.6362	475.64	-0.8397	438.45	0.0732	789.78
0.7370	694.87	0.8881	649.79	-0.1877	401.48	-0.4358	430.90	-0.6392	492.70	-0.8427	446.77	0.0751	773.79
0.7392	687.31	0.8903	648.70	-0.1916	402.73	-0.4388	456.85	-0.6422	462.68	-0.8457	441.78	0.0771	756.46
0.7414	687.73	0.8925	657.05	-0.1955	403.05	-0.4418	470.74	-0.6452	459.11	-0.8486	439.16	0.0790	741.04
0.7436	688.01	0.8947	662.17	-0.1994	401.78	-0.4448	478.51	-0.6482	467.02	-0.8516	442.06	0.0810	729.07
0.7458	688.77	0.8969	662.50	-0.2033	402.70	-0.4478	471.13	-0.6512	485.72	-0.8546	448.99	0.0829	721.70
0.7481	683.24	0.8992	663.85	-0.2072	402.83	-0.4508	495.85	-0.6542	468.70	-0.8576	454.11	0.0848	714.26
0.7503	681.12	0.9014	669.46	-0.2111	404.46	-0.4538	460.07	-0.6572	465.90	-0.8606	454.00	0.0868	702.59
0.7525	681.48	0.9036	670.47	-0.2150	405.23	-0.4568	441.73	-0.6602	480.72	-0.8636	455.24	0.0887	694.30
0.7547	683.31	0.9058	675.43	-0.2188	407.48	-0.4597	426.48	-0.6632	496.01	-0.8666	456.99	0.0906	699.59
0.7570	682.99	0.9081	678.13	-0.2227	408.02	-0.4627	413.18	-0.6662	472.51	-0.8696	461.96	0.0926	680.91
0.7592	675.64	0.9103	683.93	-0.2266	408.17	-0.4657	437.14	-0.6692	468.72	-0.8726	447.42	0.0945	670.95
0.7614	674.17	0.9125	689.88	-0.2305	409.71	-0.4687	448.74	-0.6721	458.91	-0.8756	443.69	0.0965	661.05
0.7636	671.56	0.9147	692.04	-0.2344	411.04	-0.4717	435.25	-0.6751	456.31	-0.8786	438.74	0.0984	652.44
0.7658	669.84	0.9169	694.60	-0.2383	411.52	-0.4747	454.79	-0.6781	467.55	-0.8816	439.20	0.1003	646.89
0.7681	665.11	0.9192	700.70	-0.2422	411.31	-0.4777	439.77	-0.6811	468.35	-0.8845	441.94	0.1023	636.59
0.7703	664.16	0.9214	708.53	-0.2461	411.14	-0.4807	424.43	-0.6841	456.21	-0.8875	448.99	0.1042	628.21
0.7725	667.03	0.9236	711.39	-0.2499	413.51	-0.4837	429.65	-0.6871	456.37	-0.8905	441.94	0.1061	621.08
0.7747	665.54	0.9258	721.67	-0.2538	413.45	-0.4867	439.94	-0.6901	462.01	-0.8935	443.87	0.1081	614.43
0.7770	661.93	0.9281	730.04	-0.2577	414.82	-0.4897	437.98	-0.6931	480.93	-0.8965	447.87	0.1100	609.36
0.7792	660.85	0.9303	731.20	-0.2616	414.91	-0.4927	441.40	-0.6961	480.99	-0.8995	449.11	0.1120	605.83
0.7814	666.95	0.9325	746.70	-0.2655	417.07	-0.4956	461.61	-0.6991	534.08	-0.9025	447.56	0.1139	599.80
0.7836	663.70	0.9347	751.33	-0.2694	419.60	-0.4986	460.70	-0.7021	503.14	-0.9055	448.14	0.1158	593.80
0.7858	662.02	0.9369	759.21	-0.2733	419.26	-0.5016	448.08	-0.7051	481.98	-0.9085	454.20	0.1178	594.03
0.7881	658.98	0.9392	766.61	-0.2771	418.68	-0.5046	444.45	-0.7080	473.63	-0.9115	448.64	0.1197	589.52
0.7903	661.88	0.9414	781.85	-0.2810	417.14	-0.5076	449.22	-0.7110	461.34	-0.9145	451.30	0.1216	588.51
0.7925	661.86	0.9436	792.11	-0.2849	417.99	-0.5106	435.36	-0.7140	465.58	-0.9174	460.85	0.1236	587.66
0.7947	656.07	0.9458	802.40	-0.2888	419.47	-0.5136	455.47	-0.7170	463.35	-0.9204	462.82	0.1255	587.76
0.7969	650.15	0.9481	810.85	-0.2927	419.15	-0.5166	468.48	-0.7200	450.10	-0.9234	476.00	0.1275	582.66
0.7992	651.05	0.9503	835.99	-0.2966	418.26	-0.5196	455.87	-0.7230	454.64	-0.9264	471.11	0.1294	574.00
0.8014	655.84	0.9525	856.53	-0.3005	418.68	-0.5226	448.38	-0.7260	459.32	-0.9294	464.81	0.1313	570.19
0.8036	651.63	0.9547	870.71	-0.3044	419.56	-0.5256	458.40	-0.7290	471.50	-0.9324	472.04	0.1333	569.68
0.8058	652.62	0.9569	891.76	-0.3082	418.22	-0.5286	441.43	-0.7320	470.62	-0.9354	480.98	0.1352	567.63
0.8081	648.57	0.9592	936.84	-0.3121	417.62	-0.5315	445.28	-0.7350	457.50	-0.9384	484.64	0.1371	567.54
0.8103	652.35			-0.3160	417.51	-0.5345	467.89	-0.7380	456.26	-0.9414	476.64	0.1391	566.54
0.8125	646.65			-0.3199	418.13	-0.5375	480.46	-0.7409	486.90	-0.9444	480.09	0.1410	565.88
0.8147	645.82	-0.0026	1512.74	-0.3238	417.79	-0.5405	486.76	-0.7439	509.37	-0.9474	485.50	0.1430	561.82
0.8169	649.72	-0.0090	1471.53	-0.3277	417.06	-0.5435	441.83	-0.7469	461.68	-0.9504	490.68	0.1449	557.30
0.8192	651.80	-0.0153	1321.83	-0.3316	415.98	-0.5465	450.42	-0.7499	465.13	-0.9533	494.96	0.1468	556.35
0.8214	646.64	-0.0217	1271.18	-0.3355	418.22	-0.5495	452.98	-0.7529	463.58	-0.9563	499.81	0.1488	552.81
0.8236	640.19	-0.0280	1439.44	-0.3393	421.13	-0.5525	449.63	-0.7559	452.61	-0.9593	503.11	0.1507	551.67
0.8258	647.45	-0.0344	1389.49	-0.3432	419.51	-0.5555	469.74	-0.7589	451.09	-0.9623	510.30	0.1526	550.01
0.8281	654.63	-0.0408	917.84	-0.3471	420.35	-0.5585	492.92	-0.7619	458.10	-0.9653	514.28	0.1546	549.70
0.8303	644.65	-0.0471	865.38	-0.3510	422.70	-0.5615	449.68	-0.7649	448.55	-0.9683	517.88	0.1565	546.05
0.8325	643.14	-0.0535	626.77	-0.3549	419.52	-0.5645	459.00	-0.7679	442.85	-0.9713	523.21	0.1585	543.55
0.8347	636.15	-0.0598	375.67	-0.3588	423.27	-0.5674	450.31	-0.7709	443.22			0.1604	544.41
0.8369	634.96	-0.0662	435.87	-0.3627	427.00	-0.5704	452.97	-0.7739	433.23			0.1623	543.42
0.8392	639.83	-0.0726	437.71	-0.3665	427.87	-0.5734	443.61	-0.7768	436.76			0.1643	539.14
0.8414	644.05	-0.0789	373.79	-0.3704	428.15	-0.5764	450.62	-0.7798	436.03			0.1662	538.20
0.8436	640.02	-0.0853	372.25	-0.3743	427.05	-0.5794	456.17	-0.7828	436.29			0.1682	537.98
0.8458	637.88	-0.0916	372.45	-0.3782	426.35	-0.5824	451.65	-0.7858	434.19			0.1701	539.37
0.8481	640.81	-0.0980	372.54	-0.3821	425.87	-0.5854	455.41	-0.7888	436.70			0.1720	542.08
0.8503	640.52	-0.1044	369.82	-0.3860	419.38	-0.5884	453.68	-0.7918	438.70			0.1740	539.89
0.8525	641.19	-0.1107	372.58	-0.3899	425.44	-0.5914	453.27	-0.7948	438.93			0.1759	537.94
0.8547	640.86	-0.1171	373.51	-0.3938	428.12	-0.5944	461.76	-0.7978	445.40			0.1778	538.46
0.8569	642.97	-0.1234	374.84	-0.3976	427.01	-0.5974	474.73	-0.8008	461.56			0.1798	540.44
0.8592	642.54	-0.1298	377.37	-0.3969	417.47	-0.6003	483.08	-0.8038	474.44			0.1817	541.69
0.8614	639.40	-0.1362	379.94	-0.3999	454.76	-0.6033	482.20	-0.8068	451.95			0.1837	541.41
0.8636	643.08	-0.1425	383.28	-0.4029	448.49	-0.6063	461.44	-0.8098	461.00			0.1856	538.42
0.8658	641.14	-0.1489	385.64	-0.4059	435.91	-0.6093	465.16	-0.8127	440.97			0.1875	541.35
0.8681	644.79	-0.1528	389.11	-0.4089	445.44	-0.6123	458.44	-0.8157	437.53			0.1895	538.54
0.8703	645.92	-0.1567	437.19	-0.4119	428.64	-0.6153	445.64	-0.8187	440.88			0.1914	531.34
0.8725	639.62	-0.1605	440.56	-0.4149	427.83	-0.6183	451.56	-0.8217	451.11			0.1933	531.26
0.8747	642.50	-0.1644	392.73	-0.4179	430.45	-0.6213	447.73	-0.8247	452.29			0.1953	534.83
0.8769	645.43	-0.1683	397.14	-0.4209	428.02	-0.6243	467.71	-0.8277	443.90			0.1972	534.02
0.8792	643.41	-0.1722	397.20	-0.4238	429.07	-0.6273	472.38	-0.8307	443.20			0.1992	532.58
0.8814	647.84	-0.1761	397.09	-0.4268	437.31	-0.6303	447.58	-0.8337	437.65			0.2011	533.96

CASE C – Nu

X/SL	Nu		
0.0383	1279.17	0.1701	539.37
0.0403	1238.06	0.1720	542.08
0.0422	1245.36	0.1740	539.89
0.0441	1196.39	0.1759	537.94
0.0461	1191.25	0.1778	538.46
0.0480	1177.40	0.1798	540.44
0.0499	1131.02	0.1817	541.69
0.0519	1080.25	0.1837	541.41
0.0538	1051.51	0.1856	538.42
0.0558	1008.55	0.1875	541.35
0.0577	987.28	0.1895	538.54
0.0596	975.03	0.1914	531.34
0.0616	919.74	0.1933	531.26
0.0635	898.82	0.1953	534.83
0.0654	876.16	0.1972	534.02
0.0674	851.53	0.1992	532.58
0.0693	831.96	0.2011	533.96

Appendix 7.2 – Data for Spanwise Averaged Nusselt Number and Film Cooling Effectiveness

0.2030	536.83	0.4459	771.27	0.5970	965.58	0.7481	721.20	0.8992	698.86	-0.1659	472.26	-0.4837	476.63
0.2050	535.69	0.4481	768.81	0.5992	967.43	0.7503	725.47	0.9014	700.98	-0.1695	482.47	-0.4867	457.73
0.2069	530.13	0.4503	781.29	0.6014	953.18	0.7525	712.42	0.9036	711.35	-0.1730	485.14	-0.4897	466.45
0.2088	527.47	0.4525	791.02	0.6036	955.04	0.7547	713.52	0.9058	718.44	-0.1765	481.65	-0.4927	518.19
0.2108	532.28	0.4547	790.44	0.6058	950.81	0.7570	713.67	0.9081	720.79	-0.1800	474.22	-0.4956	494.89
0.2127	532.38	0.4570	794.20	0.6081	935.70	0.7592	707.97	0.9103	723.42	-0.1836	473.27	-0.4986	500.02
0.2147	532.51	0.4592	804.68	0.6103	927.74	0.7614	705.42	0.9125	726.86	-0.1871	473.38	-0.5016	526.07
0.2166	530.13	0.4614	807.78	0.6125	928.22	0.7636	699.14	0.9147	734.52	-0.1906	474.19	-0.5046	495.94
0.2185	524.50	0.4636	803.38	0.6147	924.65	0.7658	700.41	0.9169	745.73	-0.1941	483.59	-0.5076	473.40
0.2205	523.25	0.4659	814.49	0.6170	927.52	0.7681	697.91	0.9192	753.98	-0.1977	476.48	-0.5106	473.95
0.2224	524.10	0.4681	820.93	0.6192	916.42	0.7703	694.77	0.9214	754.17	-0.2012	476.99	-0.5136	499.08
0.2243	523.01	0.4703	824.08	0.6214	915.76	0.7725	696.44	0.9236	759.90	-0.2047	477.52	-0.5166	499.21
0.2263	524.87	0.4725	822.53	0.6236	918.60	0.7747	691.82	0.9258	765.21	-0.2082	489.05	-0.5196	487.47
0.2282	522.62	0.4747	829.12	0.6258	909.14	0.7770	693.45	0.9281	773.66	-0.2117	490.64	-0.5226	436.78
0.2302	519.77	0.4770	836.29	0.6281	902.06	0.7792	689.39	0.9303	780.52	-0.2153	481.08	-0.5256	452.58
0.2302	517.79	0.4792	845.37	0.6303	903.06	0.7814	688.41	0.9325	796.26	-0.2188	480.92	-0.5286	460.20
0.2334	518.81	0.4814	848.01	0.6325	900.72	0.7836	691.36	0.9347	805.70	-0.2223	483.62	-0.5315	494.60
0.2366	527.69	0.4836	849.27	0.6347	894.22	0.7858	689.91	0.9369	815.96	-0.2258	482.27	-0.5345	511.95
0.2398	525.08	0.4859	854.86	0.6370	887.59	0.7881	682.69	0.9392	829.22	-0.2294	482.49	-0.5375	490.47
0.2430	520.91	0.4881	863.57	0.6392	878.49	0.7903	681.45	0.9414	849.58	-0.2329	481.75	-0.5405	513.67
0.2461	519.58	0.4903	861.21	0.6414	868.53	0.7925	679.68	0.9436	864.26	-0.2364	481.54	-0.5435	466.56
0.2493	520.38	0.4925	864.36	0.6436	871.30	0.7947	677.72	0.9458	873.41	-0.2399	481.39	-0.5465	446.17
0.2525	522.19	0.4947	865.91	0.6458	871.33	0.7969	680.97	0.9481	891.34	-0.2435	480.93	-0.5495	463.51
0.2557	524.93	0.4970	869.80	0.6481	861.02	0.7992	674.18	0.9503	909.81	-0.2470	480.90	-0.5525	478.38
0.2589	542.10	0.4992	873.96	0.6503	850.50	0.8014	677.72	0.9525	925.27	-0.2505	482.10	-0.5555	495.84
0.2621	542.20	0.5014	881.96	0.6525	849.49	0.8036	674.78	0.9547	940.42	-0.2540	482.44	-0.5585	516.80
0.2653	535.71	0.5036	889.21	0.6547	845.90	0.8058	672.07	0.9569	962.62	-0.2576	483.82	-0.5615	493.65
0.2685	533.73	0.5059	896.22	0.6570	838.10	0.8081	670.65	0.9592	975.46	-0.2611	482.80	-0.5645	488.54
0.2717	529.38	0.5081	896.56	0.6592	833.57	0.8103	670.64			-0.2646	482.83	-0.5674	486.60
0.2749	531.56	0.5103	898.93	0.6614	833.34	0.8125	673.26	X/PL	Nu	-0.2681	484.19	-0.5704	465.10
0.2781	538.51	0.5125	906.94	0.6636	826.24	0.8147	669.32	-0.0069	1621.73	-0.2716	481.64	-0.5734	448.86
0.2813	526.75	0.5147	912.52	0.6658	824.95	0.8169	670.59	-0.0154	1685.15	-0.2752	482.76	-0.5764	478.97
0.2845	533.30	0.5170	915.38	0.6681	824.99	0.8192	669.15	-0.0240	1637.92	-0.2787	484.05	-0.5794	488.64
0.2877	529.89	0.5192	929.37	0.6703	820.98	0.8214	667.31	-0.0326	1545.73	-0.2822	485.24	-0.5824	502.62
0.2909	530.18	0.5214	938.79	0.6725	814.57	0.8236	664.67	-0.0411	1329.28	-0.2857	485.19	-0.5854	494.39
0.2941	527.53	0.5236	939.65	0.6747	807.04	0.8258	663.08	-0.0497	1166.09	-0.2893	487.46	-0.5884	481.24
0.2973	513.15	0.5259	942.94	0.6770	795.92	0.8281	664.43	-0.0532	983.30	-0.2928	487.61	-0.5914	468.83
0.3005	506.90	0.5281	954.52	0.6792	791.63	0.8303	669.65	-0.0567	885.42	-0.2963	486.64	-0.5944	489.72
0.3037	524.23	0.5303	962.09	0.6814	797.17	0.8325	670.52	-0.0602	664.46	-0.2998	487.29	-0.5974	494.27
0.3069	546.70	0.5325	962.25	0.6836	795.40	0.8347	659.82	-0.0638	661.91	-0.3034	487.80	-0.6003	515.24
0.3836	658.78	0.5347	970.67	0.6858	792.66	0.8369	656.59	-0.0673	640.33	-0.3069	487.90	-0.6063	548.26
0.3859	671.39	0.5370	970.31	0.6881	791.69	0.8392	659.93	-0.0708	556.36	-0.3104	486.73	-0.6093	524.23
0.3881	680.18	0.5392	975.12	0.6903	786.03	0.8414	665.81	-0.0743	506.69	-0.3139	486.61	-0.6123	515.59
0.3903	714.26	0.5414	979.79	0.6925	781.52	0.8436	671.82	-0.0778	502.05	-0.3175	485.40	-0.6153	516.65
0.3925	715.20	0.5436	980.24	0.6947	775.32	0.8458	663.66	-0.0814	483.05	-0.3210	483.95	-0.6183	547.52
0.3947	719.43	0.5459	990.16	0.6970	773.66	0.8481	658.09	-0.0849	483.58	-0.3245	481.29	-0.6213	558.74
0.3970	701.39	0.5481	998.20	0.6992	773.81	0.8503	664.48	-0.0884	466.99	-0.3280	490.98	-0.6243	525.63
0.3992	709.93	0.5503	1004.51	0.7014	772.52	0.8525	670.58	-0.0919	465.33	-0.3318	495.47	-0.6273	520.07
0.4014	708.30	0.5525	1009.35	0.7036	767.39	0.8547	671.86	-0.0955	463.34	-0.3374	495.81	-0.6303	527.62
0.4036	691.04	0.5547	1010.30	0.7058	758.85	0.8569	663.75	-0.0990	465.44	-0.3809	494.66	-0.6333	528.50
0.4059	693.79	0.5570	1017.33	0.7081	755.86	0.8592	670.63	-0.1025	466.48	-0.3844	494.86	-0.6362	521.32
0.4081	732.05	0.5592	1026.12	0.7103	758.28	0.8614	673.50	-0.1060	467.54	-0.3879	493.49	-0.6392	477.22
0.4103	727.87	0.5614	1016.23	0.7125	759.06	0.8636	667.40	-0.1096	467.72	-0.3915	493.43	-0.6422	490.68
0.4125	713.53	0.5636	1013.00	0.7147	756.63	0.8658	669.07	-0.1131	466.98	-0.3950	493.06	-0.6452	531.47
0.4147	723.18	0.5658	1014.70	0.7170	750.04	0.8681	670.18	-0.1166	466.57	-0.3985	492.23	-0.6482	520.32
0.4170	718.61	0.5681	1019.23	0.7192	754.92	0.8703	675.82	-0.1201	483.41	-0.4020	492.78	-0.6512	531.64
0.4192	723.55	0.5703	1020.78	0.7214	745.76	0.8725	674.80	-0.1237	465.88	-0.4055	492.51	-0.6542	532.13
0.4214	727.32	0.5725	1022.95	0.7236	741.42	0.8747	673.75	-0.1272	466.49	-0.4091	493.17	-0.6572	535.54
0.4236	725.78	0.5747	1020.88	0.7258	741.22	0.8769	677.68	-0.1307	467.57	-0.4126	494.28	-0.6602	534.93
0.4259	726.37	0.5770	1009.27	0.7281	737.72	0.8792	682.69	-0.1342	468.36	-0.4161	493.49	-0.6632	513.96
0.4281	732.98	0.5792	1009.71	0.7303	736.93	0.8814	682.10	-0.1378	468.33	-0.4196	503.11	-0.6662	500.81
0.4303	735.66	0.5814	1010.26	0.7325	729.24	0.8836	674.33	-0.1413	468.85	-0.4232	518.22	-0.6692	483.57
0.4325	733.50	0.5836	1000.41	0.7347	733.15	0.8858	679.71	-0.1448	468.50	-0.4267	492.47	-0.6721	507.78
0.4347	735.55	0.5858	998.83	0.7370	734.43	0.8881	684.48	-0.1483	468.11	-0.4687	485.82	-0.6751	477.19
0.4370	737.96	0.5881	1005.71	0.7392	729.77	0.8903	690.58	-0.1518	469.16	-0.4717	486.90	-0.6781	508.82
0.4392	746.26	0.5903	990.00	0.7414	723.06	0.8925	687.21	-0.1554	469.66	-0.4747	526.87	-0.6811	482.33
0.4414	754.78	0.5925	982.21	0.7436	718.90	0.8947	693.63	-0.1589	471.27	-0.4777	509.94	-0.6841	488.17
0.4436	763.41	0.5947	970.15	0.7458	722.46	0.8969	700.67	-0.1624	471.95	-0.4807	466.40	-0.6871	504.41

Appendix 7.2 – Data for Spanwise Averaged Nusselt Number and Film Cooling Effectiveness

-0.6901	514.31	-0.8935	482.92	0.1081	636.23	0.2430	523.52	0.4881	832.45	0.6392	875.01	0.7903	695.23
-0.6931	524.01	-0.8965	486.72	0.1100	631.98	0.2461	521.14	0.4903	841.13	0.6414	869.30	0.7925	696.35
-0.6961	511.54	-0.8995	464.10	0.1120	627.21	0.2493	524.14	0.4925	837.84	0.6436	873.54	0.7947	696.44
-0.6991	520.45	-0.9025	473.39	0.1139	627.06	0.2525	524.62	0.4947	835.92	0.6458	870.83	0.7969	695.20
-0.7021	523.03	-0.9055	461.22	0.1158	622.95	0.2557	527.15	0.4970	849.10	0.6481	861.09	0.7992	692.45
-0.7051	511.68	-0.9085	463.43	0.1178	618.62	0.2589	532.38	0.4992	854.14	0.6503	855.13	0.8014	689.30
-0.7080	500.23	-0.9115	468.89	0.1197	617.13	0.2621	544.48	0.5014	855.69	0.6525	857.46	0.8036	688.56
-0.7110	500.94	-0.9145	470.49	0.1216	612.00	0.2653	539.50	0.5036	858.19	0.6547	858.66	0.8058	683.10
-0.7140	510.17	-0.9174	469.88	0.1236	610.07	0.2685	538.01	0.5059	865.23	0.6570	851.39	0.8081	687.99
-0.7170	498.77	-0.9204	476.23	0.1255	611.03	0.2717	542.68	0.5081	875.91	0.6592	843.61	0.8103	686.57
-0.7200	490.54	-0.9234	495.85	0.1275	627.35	0.2749	535.78	0.5103	878.18	0.6614	847.80	0.8125	689.14
-0.7230	483.84	-0.9264	490.68	0.1294	597.06	0.2781	530.86	0.5125	877.02	0.6636	842.44	0.8147	681.48
-0.7260	467.47	-0.9294	478.10	0.1313	589.62	0.2813	528.79	0.5147	883.06	0.6658	836.31	0.8169	679.74
-0.7290	474.59	-0.9324	476.49	0.1333	592.01	0.2845	535.44	0.5170	889.49	0.6681	829.59	0.8192	679.98
-0.7320	472.93	-0.9354	476.08	0.1352	589.14	0.2877	532.67	0.5192	901.70	0.6703	826.44	0.8214	682.29
-0.7350	471.79	-0.9384	484.12	0.1371	586.42	0.2909	535.97	0.5214	906.92	0.6725	831.72	0.8236	680.40
-0.7380	468.20	-0.9414	496.39	0.1391	588.48	0.2941	532.46	0.5236	909.65	0.6747	827.24	0.8258	676.67
-0.7409	503.63	-0.9444	503.08	0.1410	590.63	0.2973	539.21	0.5259	914.62	0.6770	813.73	0.8281	680.16
-0.7439	503.35	-0.9474	501.26	0.1430	583.82	0.3005	542.95	0.5281	924.59	0.6792	810.71	0.8303	689.16
-0.7469	489.77	-0.9504	501.32	0.1449	573.87	0.3037	546.70	0.5303	929.51	0.6814	806.51	0.8325	678.78
-0.7499	486.53	-0.9533	504.58	0.1468	575.42	0.3069	576.65	0.5325	936.42	0.6836	812.18	0.8347	675.12
-0.7529	472.62	-0.9563	510.49	0.1488	572.83	0.3836	659.33	0.5347	939.15	0.6858	806.05	0.8369	667.25
-0.7559	467.63	-0.9593	516.09	0.1507	568.50	0.3859	658.43	0.5370	937.11	0.6881	802.86	0.8392	663.79
-0.7589	460.60	-0.9623	520.93	0.1526	567.79	0.3881	673.84	0.5392	941.42	0.6903	800.56	0.8414	667.44
-0.7619	468.34	-0.9653	521.92	0.1546	565.10	0.3903	674.01	0.5414	952.87	0.6925	797.02	0.8436	674.17
-0.7649	483.96	-0.9683	525.80	0.1565	561.88	0.3925	688.99	0.5436	951.98	0.6947	799.07	0.8458	675.57
-0.7679	465.84	-0.9713	535.40	0.1585	560.16	0.3947	704.60	0.5459	958.72	0.6970	791.35	0.8481	668.02
-0.7709	476.03			0.1604	560.17	0.3970	745.68	0.5481	981.76	0.6992	787.82	0.8503	665.81
-0.7739	492.10			0.1623	556.65	0.3992	726.63	0.5503	979.66	0.7014	788.92	0.8525	665.50
-0.7768	468.02	CASE D – Nu		0.1643	552.91	0.4014	711.45	0.5525	983.47	0.7036	785.14	0.8547	666.64
-0.7798	473.67			0.1662	552.28	0.4036	706.68	0.5547	987.56	0.7058	782.25	0.8569	665.83
-0.7828	471.82	X/SL	Nu	0.1682	555.68	0.4059	698.34	0.5570	991.71	0.7081	775.78	0.8592	665.42
-0.7858	483.77	0.0383	1306.84	0.1701	555.23	0.4081	723.29	0.5592	990.88	0.7103	773.47	0.8614	666.37
-0.7888	470.48	0.0403	1251.89	0.1720	555.36	0.4103	741.83	0.5614	993.36	0.7125	779.29	0.8636	662.73
-0.7918	475.83	0.0422	1256.58	0.1740	554.40	0.4125	733.49	0.5636	989.55	0.7147	783.04	0.8658	665.63
-0.7948	479.20	0.0441	1228.63	0.1759	551.00	0.4147	724.58	0.5658	984.91	0.7170	777.98	0.8681	669.72
-0.7978	455.43	0.0461	1148.24	0.1778	549.88	0.4170	720.79	0.5681	991.43	0.7192	778.53	0.8703	670.01
-0.8008	460.93	0.0480	1146.04	0.1798	552.09	0.4192	712.62	0.5703	995.25	0.7214	769.51	0.8725	667.10
-0.8038	456.20	0.0499	1128.05	0.1817	550.64	0.4214	716.39	0.5725	997.36	0.7236	768.44	0.8747	664.70
-0.8068	458.20	0.0519	1071.05	0.1837	547.81	0.4236	722.58	0.5747	997.93	0.7258	764.36	0.8769	664.43
-0.8098	447.69	0.0538	1066.94	0.1856	548.88	0.4259	726.75	0.5770	991.56	0.7281	765.80	0.8792	668.18
-0.8127	469.23	0.0558	1033.13	0.1875	549.30	0.4281	722.58	0.5792	992.23	0.7303	764.03	0.8814	664.31
-0.8157	475.17	0.0577	996.38	0.1895	545.32	0.4303	725.56	0.5814	981.14	0.7325	762.68	0.8836	658.18
-0.8187	491.31	0.0596	977.93	0.1914	539.11	0.4325	723.11	0.5836	976.07	0.7347	754.47	0.8858	661.81
-0.8217	476.58	0.0616	932.18	0.1933	540.50	0.4347	729.63	0.5858	981.79	0.7370	755.66	0.8881	668.55
-0.8247	476.55	0.0635	915.44	0.1953	544.42	0.4370	727.23	0.5881	987.27	0.7392	754.04	0.8903	669.13
-0.8277	466.97	0.0654	895.47	0.1972	543.57	0.4392	736.45	0.5903	977.51	0.7414	749.89	0.8925	674.83
-0.8307	464.82	0.0674	870.29	0.1992	539.43	0.4414	742.03	0.5925	964.02	0.7436	747.56	0.8947	675.85
-0.8337	497.02	0.0693	854.19	0.2011	543.30	0.4436	748.98	0.5947	960.09	0.7458	741.60	0.8969	681.07
-0.8367	514.35	0.0713	847.67	0.2030	550.18	0.4459	750.82	0.5970	960.50	0.7481	741.15	0.8992	680.58
-0.8397	489.14	0.0732	815.52	0.2050	545.21	0.4481	755.22	0.5992	946.43	0.7503	743.01	0.9014	680.95
-0.8427	486.88	0.0751	801.93	0.2069	539.85	0.4503	762.22	0.6014	940.42	0.7525	740.93	0.9036	684.89
-0.8457	479.46	0.0771	781.56	0.2088	534.66	0.4525	768.37	0.6036	944.25	0.7547	738.13	0.9058	689.46
-0.8486	498.40	0.0790	766.78	0.2108	532.44	0.4547	773.31	0.6058	939.11	0.7570	734.12	0.9081	689.89
-0.8516	474.68	0.0810	752.98	0.2127	537.95	0.4570	777.54	0.6081	928.53	0.7592	731.01	0.9103	692.78
-0.8546	472.63	0.0829	741.97	0.2147	536.96	0.4592	780.35	0.6103	922.03	0.7614	731.61	0.9125	698.22
-0.8576	453.87	0.0848	734.75	0.2166	532.89	0.4614	788.40	0.6125	921.70	0.7636	728.96	0.9147	704.45
-0.8606	463.06	0.0868	723.77	0.2185	528.32	0.4636	790.35	0.6147	920.11	0.7658	725.35	0.9169	715.09
-0.8636	465.33	0.0887	714.63	0.2205	528.32	0.4659	790.54	0.6170	917.28	0.7681	721.41	0.9192	711.08
-0.8666	480.19	0.0906	707.89	0.2224	530.23	0.4681	797.96	0.6192	914.31	0.7703	723.69	0.9214	712.56
-0.8696	473.98	0.0926	701.18	0.2243	526.66	0.4703	801.74	0.6214	902.88	0.7725	710.92	0.9236	722.84
-0.8726	463.19	0.0945	692.31	0.2263	527.29	0.4725	804.54	0.6236	905.54	0.7747	709.14	0.9258	725.96
-0.8756	461.02	0.0965	683.42	0.2282	529.64	0.4747	806.53	0.6258	916.28	0.7770	706.06	0.9281	732.26
-0.8786	454.79	0.0984	676.65	0.2302	522.53	0.4770	817.24	0.6281	897.81	0.7792	707.11	0.9303	747.41
-0.8816	454.70	0.1003	669.41	0.2302	520.33	0.4792	826.65	0.6303	889.08	0.7814	707.12	0.9325	758.81
-0.8845	468.55	0.1023	661.38	0.2334	523.57	0.4814	828.04	0.6325	884.33	0.7836	704.67	0.9347	768.82
-0.8875	457.34	0.1042	653.41	0.2366	527.09	0.4836	836.12	0.6347	888.62	0.7858	702.90	0.9369	774.06
-0.8905	458.85	0.1061	646.60	0.2398	528.00	0.4859	827.98	0.6370	886.20	0.7881	701.38	0.9392	778.26

Appendix 7.2 – Data for Spanwise Averaged Nusselt Number and Film Cooling Effectiveness

0.9414	794.15	-0.2422	490.79	-0.4418	499.64	-0.6452	500.12	-0.8486	476.75	0.0790	938.75	0.2108	538.30
0.9436	803.38	-0.2457	489.05	-0.4448	489.24	-0.6482	477.82	-0.8516	504.97	0.0810	917.18	0.2127	540.06
0.9458	822.51	-0.2492	488.95	-0.4478	469.35	-0.6512	468.15	-0.8546	476.30	0.0829	901.33	0.2147	539.31
0.9481	834.63	-0.2527	487.85	-0.4508	471.52	-0.6542	496.91	-0.8576	478.50	0.0848	890.97	0.2166	535.46
0.9503	854.67	-0.2563	487.31	-0.4538	482.50	-0.6572	485.68	-0.8606	469.89	0.0868	876.62	0.2185	530.01
0.9525	871.02	-0.2598	486.85	-0.4568	502.49	-0.6602	513.69	-0.8636	481.41	0.0887	863.06	0.2205	525.76
0.9547	883.74	-0.2633	486.04	-0.4597	554.36	-0.6632	493.33	-0.8666	474.55	0.0906	854.07	0.2224	525.73
0.9569	891.50	-0.2668	485.71	-0.4627	547.04	-0.6662	485.19	-0.8696	478.94	0.0926	842.99	0.2243	523.01
0.9592	893.98	-0.2704	486.64	-0.4657	575.44	-0.6692	488.36	-0.8726	491.01	0.0945	831.05	0.2263	521.31
		-0.2739	486.68	-0.4687	591.05	-0.6721	498.50	-0.8756	488.80	0.0965	817.25	0.2282	520.69
X/PL	Nu	-0.2774	487.80	-0.4717	526.53	-0.6751	478.87	-0.8786	472.17	0.0984	808.58	0.2302	516.42
-0.0011	1359.71	-0.2809	486.46	-0.4747	494.02	-0.6781	495.72	-0.8816	477.14	0.1003	799.85	0.2302	515.53
-0.0096	1336.19	-0.2844	486.20	-0.4777	476.93	-0.6811	464.70	-0.8845	479.02	0.1023	786.20	0.2334	515.14
-0.0182	1285.48	-0.2880	487.30	-0.4807	430.47	-0.6841	464.28	-0.8875	477.42	0.1042	775.36	0.2366	517.40
-0.0267	1261.49	-0.2915	484.37	-0.4837	464.18	-0.6871	476.63	-0.8905	483.57	0.1061	765.11	0.2398	518.49
-0.0353	1238.99	-0.2950	485.24	-0.4867	476.38	-0.6901	497.48	-0.8935	502.44	0.1081	752.55	0.2430	516.35
-0.0438	1118.78	-0.2985	486.28	-0.4897	489.69	-0.6931	516.16	-0.8965	520.47	0.1100	746.86	0.2461	515.87
-0.0524	923.80	-0.3021	487.22	-0.4927	470.79	-0.6961	491.20	-0.8995	530.02	0.1120	740.28	0.2493	516.63
-0.0609	757.29	-0.3056	486.88	-0.4956	492.23	-0.6991	500.98	-0.9025	495.53	0.1139	734.47	0.2525	515.26
-0.0695	663.88	-0.3091	488.95	-0.4986	510.15	-0.7021	506.71	-0.9055	498.37	0.1158	725.50	0.2557	517.73
-0.0730	597.28	-0.3126	488.83	-0.5016	513.10	-0.7051	547.61	-0.9085	500.33	0.1178	719.10	0.2589	523.10
-0.0766	550.79	-0.3162	487.56	-0.5046	524.16	-0.7080	541.25	-0.9115	502.58	0.1197	716.20	0.2621	551.77
-0.0801	530.09	-0.3197	487.96	-0.5076	518.99	-0.7110	518.99	-0.9145	507.15	0.1216	710.84	0.2653	537.00
-0.0836	519.13	-0.3232	488.22	-0.5106	514.16	-0.7140	530.37	-0.9174	505.59	0.1236	706.22	0.2685	527.74
-0.0871	509.49	-0.3267	488.07	-0.5136	507.35	-0.7170	523.66	-0.9204	508.99	0.1255	704.24	0.2717	526.85
-0.0906	501.71	-0.3303	486.68	-0.5166	483.86	-0.7200	516.07	-0.9234	514.69	0.1275	742.19	0.2749	527.24
-0.0942	499.10	-0.3338	486.35	-0.5196	469.07	-0.7230	522.17	-0.9264	520.08	0.1294	767.62	0.2781	522.89
-0.0977	493.07	-0.3373	484.92	-0.5226	454.31	-0.7260	545.32	-0.9294	533.30	0.1313	695.43	0.2813	525.38
-0.1012	489.41	-0.3408	486.78	-0.5256	492.71	-0.7290	531.93	-0.9324	533.85	0.1333	670.52	0.2845	527.69
-0.1047	489.25	-0.3443	521.12	-0.5286	464.16	-0.7320	473.68	-0.9354	524.45	0.1352	665.42	0.2877	524.92
-0.1083	488.98	-0.3478	517.41	-0.5315	469.17	-0.7350	470.06	-0.9384	526.61	0.1371	664.99	0.2909	526.03
-0.1118	486.69	-0.3513	515.39	-0.5345	497.00	-0.7380	472.58	-0.9414	532.19	0.1391	665.19	0.2941	523.47
-0.1153	484.06	-0.3548	514.65	-0.5375	480.07	-0.7409	489.40	-0.9444	540.27	0.1410	661.64	0.2973	514.64
-0.1188	485.81	-0.3583	513.44	-0.5405	503.13	-0.7439	469.06	-0.9474	545.57	0.1430	653.81	0.3005	505.73
-0.1224	486.43	-0.3618	512.73	-0.5435	482.91	-0.7469	462.78	-0.9504	550.48	0.1449	644.00	0.3037	509.25
-0.1259	487.08	-0.3653	510.50	-0.5465	512.64	-0.7499	484.17	-0.9533	549.67	0.1468	640.68	0.3069	524.23
-0.1294	486.81	-0.3688	509.73	-0.5495	526.09	-0.7529	489.75	-0.9563	560.24	0.1488	634.86	0.3096	523.84
-0.1329	485.53	-0.3723	506.31	-0.5525	513.70	-0.7559	480.42	-0.9593	568.34	0.1507	628.11	0.3128	523.47
-0.1365	484.64	-0.3758	506.48	-0.5555	511.77	-0.7589	520.26	-0.9623	578.98	0.1526	624.64	0.3159	523.00
-0.1400	502.10	-0.4007	505.13	-0.5585	522.87	-0.7619	477.40	-0.9653	585.43	0.1546	623.31	0.3190	522.53
-0.1435	482.99	-0.4043	505.15	-0.5615	536.84	-0.7649	474.22	-0.9683	589.99	0.1565	617.65	0.3221	522.06
-0.1470	483.19	-0.4078	503.56	-0.5645	531.22	-0.7679	495.20	-0.9713	597.79	0.1585	611.53	0.3252	521.59
-0.1505	483.89	-0.4113	503.32	-0.5674	517.33	-0.7709	453.79			0.1604	611.44	0.3283	521.12
-0.1541	484.29	-0.4148	502.76	-0.5704	476.35	-0.7739	461.11			0.1623	608.69	0.3314	520.65
-0.1576	483.82	-0.4183	501.74	-0.5734	474.31	-0.7768	492.19			0.1643	601.43	0.3345	520.18
-0.1611	483.95	-0.4219	502.12	-0.5764	464.63	-0.7798	479.89			0.1662	597.80	0.3376	519.71
-0.1646	483.15	-0.4254	501.65	-0.5794	497.37	-0.7828	480.81			0.1682	597.58	0.3407	519.24
-0.1682	482.33	-0.4289	502.14	-0.5824	530.50	-0.7858	460.17			0.1701	596.85	0.3438	518.77
-0.1717	483.04	-0.4324	503.09	-0.5854	516.63	-0.7888	454.20			0.1720	593.41	0.3469	518.30
-0.1752	483.15	-0.4360	502.10	-0.5884	484.67	-0.7918	456.26			0.1740	593.14	0.3500	517.83
-0.1787	484.45	-0.4395	511.69	-0.5914	519.18	-0.7948	471.67			0.1759	589.39	0.3531	517.36
-0.1823	484.77	-0.4430	500.56	-0.5944	570.35	-0.7978	486.52			0.1778	585.00	0.3562	516.89
-0.1858	484.69	-0.4465	500.52	-0.5974	543.53	-0.8008	467.00			0.1798	582.76	0.3593	516.42
-0.1893	495.08	-0.3969	509.25	-0.6003	509.25	-0.8038	452.52			0.1817	583.94	0.3624	515.95
-0.1928	497.50	-0.3999	524.23	-0.6033	480.06	-0.8068	448.31			0.1837	579.90	0.3655	515.48
-0.1964	493.43	-0.4029	516.74	-0.6063	492.75	-0.8098	472.53			0.1856	575.16	0.3686	515.01
-0.1999	485.22	-0.4059	520.78	-0.6093	496.32	-0.8127	472.38			0.1875	576.23	0.3717	514.54
-0.2034	483.85	-0.4089	526.51	-0.6123	517.31	-0.8157	469.09			0.1895	571.57	0.3748	514.07
-0.2069	483.59	-0.4119	422.41	-0.6153	558.37	-0.8187	464.91			0.1914	565.43	0.3779	513.60
-0.2104	484.07	-0.4149	479.32	-0.6183	545.91	-0.8217	458.63			0.1933	560.76	0.3810	513.13
-0.2140	493.60	-0.4179	540.22	-0.6213	584.82	-0.8247	463.41			0.1953	564.08	0.3841	512.66
-0.2175	485.76	-0.4209	553.31	-0.6243	591.10	-0.8277	502.31			0.1972	561.05	0.3872	512.19
-0.2210	485.93	-0.4238	511.95	-0.6273	515.63	-0.8307	498.16			0.1992	558.12	0.3903	511.72
-0.2245	486.14	-0.4268	501.68	-0.6303	513.67	-0.8337	455.50			0.2011	558.31	0.3934	511.25
-0.2281	497.86	-0.4298	470.70	-0.6333	485.44	-0.8367	470.63			0.2030	576.28	0.3965	510.78
-0.2316	499.17	-0.4328	557.42	-0.6362	498.29	-0.8397	475.41			0.2050	556.33	0.3996	510.31
-0.2351	488.82	-0.4358	576.51	-0.6392	524.16	-0.8427	462.30			0.2069	545.14	0.4027	509.84
-0.2386	488.31	-0.4388	573.44	-0.6422	534.28	-0.8457	474.29			0.2088	541.10	0.4058	509.37

CASE E – Nu

X/SL Nu

0.0383	1610.07	0.1701	596.85	0.4081	745.10
0.0403	1552.73	0.1720	593.41	0.4103	733.92
0.0422	1578.41	0.1740	593.14	0.4125	733.59
0.0441	1511.89	0.1759	589.39	0.4147	721.90
0.0461	1510.45	0.1778	585.00	0.4170	731.05
0.0480	1413.96	0.1798	582.76	0.4192	738.15
0.0499	1385.90	0.1817	583.94	0.4214	726.98
0.0519	1340.65	0.1837	579.90	0.4236	727.69
0.0538	1281.14	0.1856	575.16	0.4259	728.03
0.0558	1269.92	0.1875	576.23	0.4281	730.30
0.0577	1241.38	0.1895	571.57	0.4303	730.27
0.0596	1201.84	0.1914	565.43	0.4325	730.39
0.0616	1152.94	0.1933	560.76	0.4347	736.16
0.0635	1145.17	0.1953	564.08	0.4370	737.98
0.0654	1101.77	0.1972	561.05	0.4392	740.14
0.0674	1071.19	0.1992	558.12	0.4414	745.58
0.0693	1053.35	0.2011	558.31	0.4436	753.69
0.0713	1044.68	0.2030	576.28	0.4459	755.87
0.0732	1002.67	0.2050	556.33	0.4481	757.40
0.0751	975.77	0.2069	545.14	0.4503	762.97
0.0771	962.22	0.2088	541.10	0.4525	772.88

Appendix 7.2 – Data for Spanwise Averaged Nusselt Number and Film Cooling Effectiveness

0.4547	777.26	0.6058	937.93	0.7570	761.08	0.9081	728.48	-0.2255	490.92	-0.4687	528.05	-0.6721	521.14
0.4570	777.03	0.6081	931.01	0.7592	755.93	0.9103	733.54	-0.2294	492.43	-0.4717	531.79	-0.6751	510.80
0.4592	783.87	0.6103	921.50	0.7614	750.31	0.9125	737.58	-0.2333	493.55	-0.4747	509.58	-0.6781	512.84
0.4614	786.78	0.6125	922.56	0.7636	748.77	0.9147	742.90	-0.2372	555.57	-0.4777	525.34	-0.6811	505.81
0.4636	793.05	0.6147	921.60	0.7658	748.88	0.9169	745.16	-0.2411	556.52	-0.4807	501.23	-0.6841	520.27
0.4659	792.48	0.6170	920.97	0.7681	744.19	0.9192	750.22	-0.2450	550.46	-0.4837	487.68	-0.6871	526.56
0.4681	803.25	0.6192	918.76	0.7703	746.20	0.9214	753.18	-0.2489	492.05	-0.4867	495.53	-0.6901	514.27
0.4703	803.94	0.6214	912.73	0.7725	739.17	0.9236	755.18	-0.2528	493.22	-0.4897	498.20	-0.6931	524.05
0.4725	805.67	0.6236	918.58	0.7747	737.95	0.9258	761.83	-0.2566	494.75	-0.4927	474.38	-0.6961	522.19
0.4747	809.29	0.6258	914.11	0.7770	741.17	0.9281	768.05	-0.2605	496.17	-0.4956	470.68	-0.6991	506.02
0.4770	815.61	0.6281	907.09	0.7792	737.87	0.9303	778.27	-0.2644	500.76	-0.4986	490.78	-0.7021	511.33
0.4792	820.39	0.6303	903.34	0.7814	733.17	0.9325	784.69	-0.2683	498.23	-0.5016	462.31	-0.7051	520.13
0.4814	822.70	0.6325	901.91	0.7836	734.89	0.9347	794.59	-0.2722	494.82	-0.5046	465.65	-0.7080	566.67
0.4836	828.72	0.6347	901.09	0.7858	734.19	0.9369	804.01	-0.2761	496.84	-0.5076	491.48	-0.7110	530.51
0.4859	826.34	0.6370	898.52	0.7881	730.41	0.9392	813.46	-0.2800	577.59	-0.5106	484.94	-0.7140	506.69
0.4881	830.91	0.6392	883.03	0.7903	731.21	0.9414	820.10	-0.2838	579.69	-0.5136	494.33	-0.7170	496.45
0.4903	841.60	0.6414	882.50	0.7925	727.74	0.9436	833.47	-0.2877	500.35	-0.5166	488.14	-0.7200	508.05
0.4925	843.59	0.6436	889.11	0.7947	729.19	0.9458	851.98	-0.2916	500.42	-0.5196	504.35	-0.7230	505.81
0.4947	838.36	0.6458	880.79	0.7969	725.72	0.9481	864.77	-0.2955	500.28	-0.5226	483.47	-0.7260	509.12
0.4970	844.65	0.6481	871.06	0.7992	722.34	0.9503	871.77	-0.2994	504.87	-0.5256	494.93	-0.7290	531.32
0.4992	850.26	0.6503	876.64	0.8014	718.74	0.9525	878.18	-0.3033	504.74	-0.5286	501.41	-0.7320	515.74
0.5014	854.08	0.6525	878.82	0.8036	715.93	0.9547	889.83	-0.3072	505.60	-0.5315	492.69	-0.7350	509.43
0.5036	859.59	0.6547	868.47	0.8058	719.95	0.9569	898.12	-0.3111	503.04	-0.5345	513.51	-0.7380	544.69
0.5059	862.29	0.6570	868.15	0.8081	716.35	0.9592	903.94	-0.3149	501.27	-0.5375	501.87	-0.7409	531.07
0.5081	867.13	0.6592	864.01	0.8103	722.20			-0.3188	498.71	-0.5405	488.19	-0.7439	519.09
0.5103	873.01	0.6614	860.84	0.8125	719.55	X/Pl	Nu	-0.3227	500.09	-0.5435	504.75	-0.7469	503.14
0.5125	873.21	0.6636	861.15	0.8147	716.32	-0.0104	1188.99	-0.3266	499.69	-0.5465	494.92	-0.7499	506.57
0.5147	878.58	0.6658	854.91	0.8169	711.72	-0.0167	1178.12	-0.3305	504.19	-0.5495	501.26	-0.7529	510.75
0.5170	883.47	0.6681	850.70	0.8192	710.08	-0.0231	1175.20	-0.3344	502.75	-0.5525	497.62	-0.7559	533.72
0.5192	888.99	0.6703	848.91	0.8214	715.97	-0.0294	1179.47	-0.3383	504.48	-0.5555	489.67	-0.7589	521.40
0.5214	893.79	0.6725	848.01	0.8236	709.62	-0.0358	1144.98	-0.3422	501.46	-0.5585	512.89	-0.7619	506.16
0.5236	898.02	0.6747	847.87	0.8258	703.69	-0.0422	1058.61	-0.3460	502.61	-0.5615	515.61	-0.7649	513.43
0.5259	902.88	0.6770	837.72	0.8281	707.27	-0.0485	1045.29	-0.3499	501.24	-0.5645	491.26	-0.7679	522.65
0.5281	900.28	0.6792	836.97	0.8303	715.17	-0.0549	1006.81	-0.3538	497.82	-0.5674	490.05	-0.7709	507.18
0.5303	911.58	0.6814	834.52	0.8325	717.72	-0.0612	889.49	-0.3577	499.15	-0.5704	504.66	-0.7739	490.22
0.5325	914.72	0.6836	836.45	0.8347	704.57	-0.0676	688.08	-0.3616	500.39	-0.5734	498.53	-0.7768	488.62
0.5347	916.42	0.6858	829.37	0.8369	698.33	-0.0740	557.75	-0.3655	499.10	-0.5764	493.84	-0.7798	491.69
0.5370	920.84	0.6881	829.84	0.8392	702.54	-0.0803	533.84	-0.3694	500.46	-0.5794	513.39	-0.7828	500.41
0.5392	929.42	0.6903	823.60	0.8414	705.13	-0.0867	522.51	-0.3732	501.34	-0.5824	507.85	-0.7858	495.64
0.5414	936.97	0.6925	824.65	0.8436	708.82	-0.0930	515.16	-0.3771	505.50	-0.5854	530.75	-0.7888	489.58
0.5436	933.53	0.6947	820.62	0.8458	703.55	-0.0994	512.94	-0.3810	507.52	-0.5884	502.97	-0.7918	493.96
0.5459	936.74	0.6970	814.83	0.8481	700.80	-0.1058	510.67	-0.3849	507.48	-0.5914	516.50	-0.7948	495.69
0.5481	951.08	0.6992	811.06	0.8503	699.17	-0.1121	508.19	-0.3888	509.56	-0.5944	529.39	-0.7978	500.51
0.5503	949.92	0.7014	809.11	0.8525	700.72	-0.1185	501.20	-0.3927	506.09	-0.5974	510.45	-0.8008	505.22
0.5525	951.63	0.7036	812.16	0.8547	700.75	-0.1248	492.42	-0.3966	507.35	-0.6003	518.57	-0.8038	509.99
0.5547	955.65	0.7058	808.25	0.8569	698.43	-0.1312	484.89	-0.4005	502.05	-0.6033	512.00	-0.8068	504.74
0.5570	956.42	0.7081	799.19	0.8592	694.86	-0.1376	483.69	-0.4043	502.26	-0.6063	509.02	-0.8098	511.23
0.5592	964.11	0.7103	798.88	0.8614	700.13	-0.1439	482.58	-0.4059	492.97	-0.6093	508.87	-0.8127	502.88
0.5614	968.23	0.7125	800.86	0.8636	698.70	-0.1478	481.54	-0.4089	483.28	-0.6123	506.70	-0.8157	496.71
0.5636	962.52	0.7147	802.04	0.8658	697.64	-0.1517	481.51	-0.4119	478.75	-0.6153	516.98	-0.8187	485.89
0.5658	965.17	0.7170	799.45	0.8681	694.88	-0.1556	482.39	-0.4149	457.22	-0.6183	493.86	-0.8217	486.58
0.5681	969.86	0.7192	794.62	0.8703	700.64	-0.1595	482.90	-0.4179	496.71	-0.6213	491.70	-0.8247	484.26
0.5703	973.26	0.7214	786.67	0.8725	701.03	-0.1634	484.82	-0.4209	555.71	-0.6243	500.30	-0.8277	485.17
0.5725	970.62	0.7236	788.13	0.8747	698.64	-0.1672	486.72	-0.4238	542.93	-0.6273	530.36	-0.8307	485.88
0.5747	966.78	0.7258	789.12	0.8769	700.83	-0.1711	485.21	-0.4268	546.33	-0.6303	518.19	-0.8337	503.68
0.5770	969.90	0.7281	787.36	0.8792	701.97	-0.1750	483.14	-0.4298	575.08	-0.6333	543.72	-0.8367	508.10
0.5792	964.79	0.7303	783.52	0.8814	700.14	-0.1789	481.24	-0.4328	518.54	-0.6362	550.04	-0.8397	507.10
0.5814	961.31	0.7325	777.59	0.8836	701.98	-0.1828	480.79	-0.4358	538.53	-0.6392	514.63	-0.8427	490.67
0.5836	959.14	0.7347	781.34	0.8858	701.84	-0.1867	481.65	-0.4388	513.24	-0.6422	522.94	-0.8457	509.25
0.5858	956.94	0.7370	776.73	0.8881	703.80	-0.1906	482.61	-0.4418	463.40	-0.6452	546.17	-0.8486	513.56
0.5881	955.28	0.7392	774.21	0.8903	710.10	-0.1944	482.45	-0.4448	454.65	-0.6482	567.97	-0.8516	508.29
0.5903	953.16	0.7414	772.84	0.8925	709.88	-0.1983	484.38	-0.4478	461.74	-0.6512	548.02	-0.8546	514.46
0.5925	949.12	0.7436	772.78	0.8947	708.87	-0.2022	487.54	-0.4508	463.08	-0.6542	547.36	-0.8576	509.99
0.5947	943.47	0.7458	768.98	0.8969	715.95	-0.2061	489.03	-0.4538	498.02	-0.6572	537.40	-0.8606	495.54
0.5970	942.94	0.7481	762.86	0.8992	719.51	-0.2100	487.12	-0.4568	504.06	-0.6602	560.98	-0.8636	495.74
0.5992	937.88	0.7503	763.07	0.9014	719.47	-0.2139	487.08	-0.4597	548.39	-0.6632	544.93	-0.8666	492.02
0.6014	930.42	0.7525	762.87	0.9036	724.62	-0.2178	487.00	-0.4627	548.10	-0.6662	505.36	-0.8696	495.45
0.6036	936.25	0.7547	761.91	0.9058	729.25	-0.2217	488.83	-0.4657	553.99	-0.6692	514.97	-0.8726	492.35

Appendix 7.2 – Data for Spanwise Averaged Nusselt Number and Film Cooling Effectiveness

-0.8756	494.33	0.1071	680.63	0.2302	545.21	0.4903	842.46	0.6414	888.72	0.7925	696.30	0.9436	973.04
-0.8786	501.62	0.1089	670.10	0.2334	547.06	0.4925	846.63	0.6436	886.74	0.7947	698.10	0.9458	981.78
-0.8816	510.04	0.1107	661.86	0.2366	549.05	0.4947	849.93	0.6458	878.08	0.7969	702.34	0.9481	998.55
-0.8845	504.82	0.1125	659.48	0.2398	547.10	0.4970	853.94	0.6481	872.16	0.7992	702.54	0.9503	1034.46
-0.8875	507.69	0.1143	651.80	0.2430	546.24	0.4992	860.53	0.6503	869.61	0.8014	697.93	0.9525	1064.04
-0.8905	498.18	0.1161	644.49	0.2461	542.51	0.5014	864.96	0.6525	865.18	0.8036	695.09	0.9547	1084.93
-0.8935	500.65	0.1178	640.15	0.2493	542.76	0.5036	872.47	0.6547	861.73	0.8058	693.85	0.9569	1114.71
-0.8965	501.26	0.1196	641.39	0.2525	544.81	0.5059	876.79	0.6570	854.70	0.8081	701.47	0.9592	1113.50
-0.8995	504.31	0.1214	639.38	0.2557	546.06	0.5081	880.83	0.6592	851.30	0.8103	701.92		
-0.9025	503.62	0.1232	637.63	0.2589	548.84	0.5103	886.77	0.6614	853.27	0.8125	699.98	X/PL	Nu
-0.9055	501.04	0.1250	633.04	0.2621	549.24	0.5125	890.79	0.6636	850.46	0.8147	696.62	-0.0223	1495.50
-0.9085	504.54	0.1268	629.46	0.2653	548.24	0.5147	896.14	0.6658	844.49	0.8169	694.81	-0.0308	1393.78
-0.9115	510.54	0.1285	630.85	0.2685	545.09	0.5170	902.73	0.6681	838.64	0.8192	698.92	-0.0394	1181.95
-0.9145	510.95	0.1303	626.81	0.2717	542.54	0.5192	908.51	0.6703	834.02	0.8214	697.06	-0.0479	967.37
-0.9174	510.98	0.1321	621.38	0.2749	542.18	0.5214	915.45	0.6725	834.80	0.8236	696.69	-0.0565	872.88
-0.9204	511.96	0.1339	612.17	0.2781	540.18	0.5236	919.43	0.6747	827.94	0.8258	694.00	-0.0651	791.89
-0.9234	515.97	0.1357	610.75	0.2813	541.38	0.5259	918.87	0.6770	821.81	0.8281	689.99	-0.0736	724.73
-0.9264	524.57	0.1375	616.50	0.2845	539.26	0.5281	932.53	0.6792	821.47	0.8303	692.45	-0.0822	659.55
-0.9294	523.97	0.1392	626.58	0.2877	538.52	0.5303	936.42	0.6814	816.57	0.8325	701.21	-0.0907	655.98
-0.9324	526.64	0.1410	636.67	0.2909	540.74	0.5325	938.75	0.6836	812.18	0.8347	699.70	-0.0993	654.15
-0.9354	534.16	0.1428	617.02	0.3836	675.63	0.5347	946.04	0.6858	808.13	0.8369	695.93	-0.1028	521.70
-0.9384	535.36	0.1446	629.21	0.3859	680.06	0.5370	956.23	0.6881	803.52	0.8392	695.11	-0.1063	521.34
-0.9414	535.58	0.1464	607.51	0.3881	681.43	0.5392	958.06	0.6903	802.04	0.8414	698.56	-0.1098	581.95
-0.9444	542.38	0.1482	600.73	0.3903	684.42	0.5414	962.10	0.6925	795.81	0.8436	700.24	-0.1134	513.82
-0.9474	545.28	0.1499	620.77	0.3925	690.86	0.5436	966.74	0.6947	795.03	0.8458	701.73	-0.1169	565.95
-0.9504	550.72	0.1553	594.77	0.3947	695.65	0.5459	963.73	0.6970	790.91	0.8481	703.81	-0.1204	482.80
-0.9533	553.87	0.1571	591.41	0.3970	699.46	0.5481	970.96	0.6992	790.22	0.8503	708.42	-0.1239	482.43
-0.9563	557.20	0.1589	589.01	0.3992	700.19	0.5503	980.89	0.7014	785.88	0.8525	711.33	-0.1275	499.07
-0.9593	564.08	0.1606	586.29	0.4014	704.07	0.5525	979.13	0.7036	785.03	0.8547	709.23	-0.1310	483.06
-0.9623	569.65	0.1624	583.97	0.4036	708.52	0.5547	978.76	0.7058	780.86	0.8569	713.76	-0.1345	490.59
-0.9653	572.27	0.1642	584.20	0.4059	711.53	0.5570	976.28	0.7081	773.54	0.8592	714.26	-0.1380	491.71
-0.9683	582.09	0.1660	585.13	0.4081	713.56	0.5592	980.98	0.7103	773.93	0.8614	715.72	-0.1416	484.91
-0.9713	585.32	0.1678	581.09	0.4103	717.72	0.5614	982.88	0.7125	773.35	0.8636	716.96	-0.1451	486.91
		0.1695	579.28	0.4125	718.36	0.5636	979.49	0.7147	769.65	0.8658	721.59	-0.1486	488.34
		0.1713	576.53	0.4147	720.38	0.5658	980.70	0.7170	766.68	0.8681	729.84	-0.1521	490.40
		0.1731	579.95	0.4170	721.83	0.5681	976.36	0.7192	767.97	0.8703	731.21	-0.1556	499.32
		0.1749	582.60	0.4192	723.52	0.5703	977.69	0.7214	767.36	0.8725	729.88	-0.1592	499.51
		0.1767	577.70	0.4214	722.51	0.5725	970.00	0.7236	755.40	0.8747	734.78	-0.1627	496.81
		0.1785	577.05	0.4236	726.11	0.5747	974.12	0.7258	756.29	0.8769	741.79	-0.1662	487.74
		0.1802	576.45	0.4259	733.15	0.5770	975.44	0.7281	752.49	0.8792	750.53	-0.1697	493.59
		0.1820	578.24	0.4281	740.04	0.5792	964.94	0.7303	747.69	0.8814	747.82	-0.1733	495.32
		0.1838	577.46	0.4303	742.24	0.5814	960.33	0.7325	743.95	0.8836	752.56	-0.1768	494.73
		0.1856	577.56	0.4325	745.58	0.5836	958.29	0.7347	737.63	0.8858	757.72	-0.1803	496.46
		0.1874	577.23	0.4347	752.25	0.5858	952.23	0.7370	741.65	0.8881	764.50	-0.1838	495.51
		0.1892	574.19	0.4370	756.16	0.5881	945.32	0.7392	741.24	0.8903	763.45	-0.1874	494.34
		0.1909	575.41	0.4392	760.79	0.5903	944.26	0.7414	737.03	0.8925	768.21	-0.1909	492.40
		0.1927	576.81	0.4414	765.36	0.5925	941.41	0.7436	733.60	0.8947	774.02	-0.1944	512.82
		0.1945	580.22	0.4436	770.23	0.5947	940.06	0.7458	732.31	0.8969	778.27	-0.1979	494.70
		0.1963	581.06	0.4459	772.09	0.5970	937.16	0.7481	731.09	0.8992	789.39	-0.2015	505.63
		0.1981	577.85	0.4481	775.58	0.5992	937.92	0.7503	729.02	0.9014	797.34	-0.2050	504.19
		0.1999	575.60	0.4503	780.52	0.6014	935.51	0.7525	723.54	0.9036	804.74	-0.2085	507.26
		0.2016	569.86	0.4525	782.08	0.6036	931.78	0.7547	720.26	0.9058	809.05	-0.2120	503.94
		0.2034	569.20	0.4547	783.74	0.6058	929.17	0.7570	722.24	0.9081	812.99	-0.2155	507.65
		0.2052	568.83	0.4570	786.88	0.6081	928.52	0.7592	721.53	0.9103	821.19	-0.2191	501.85
		0.2070	570.20	0.4592	788.81	0.6103	926.09	0.7614	718.46	0.9125	831.13	-0.2226	504.42
		0.2088	569.60	0.4614	793.33	0.6125	924.28	0.7636	711.54	0.9147	840.50	-0.2261	497.08
		0.2106	568.43	0.4636	797.96	0.6147	925.45	0.7658	712.44	0.9169	841.96	-0.2296	509.91
		0.2123	565.57	0.4659	799.26	0.6170	922.60	0.7681	709.41	0.9192	850.97	-0.2332	501.06
		0.2141	562.44	0.4681	802.12	0.6192	918.09	0.7703	709.45	0.9214	858.74	-0.2367	516.45
		0.2159	561.80	0.4703	809.71	0.6214	918.46	0.7725	705.08	0.9236	867.57	-0.2402	502.82
		0.2177	559.83	0.4725	812.27	0.6236	912.10	0.7747	709.52	0.9258	886.86	-0.2437	506.93
		0.2195	557.34	0.4747	815.49	0.6258	906.71	0.7770	707.72	0.9281	898.66	-0.2473	507.97
		0.2212	557.38	0.4770	819.07	0.6281	904.82	0.7792	706.28	0.9303	912.94	-0.2508	508.30
		0.2230	558.18	0.4792	821.80	0.6303	908.02	0.7814	703.93	0.9325	919.64	-0.2543	511.46
		0.2248	556.16	0.4814	826.53	0.6325	907.13	0.7836	703.27	0.9347	921.90	-0.2578	512.59
		0.2266	554.16	0.4836	828.73	0.6347	897.70	0.7858	707.43	0.9369	933.39	-0.2614	507.71
		0.2284	553.66	0.4859	833.96	0.6370	899.08	0.7881	702.90	0.9392	949.90	-0.2649	503.32
		0.2302	550.16	0.4881	837.55	0.6392	897.10	0.7903	698.10	0.9414	957.96	-0.2684	510.51

CASE F – Nu

X/SL Nu

0.0537	1352.18	0.1785	577.05	0.4236	726.11	0.5747	974.12	0.7258	756.29	0.8769	741.79	-0.1662	487.74
0.0554	1392.65	0.1802	576.45	0.4259	733.15	0.5770	975.44	0.7281	752.49	0.8792	750.53	-0.1697	493.59
0.0572	1379.50	0.1820	578.24	0.4281	740.04	0.5792	964.94	0.7303	747.69	0.8814	747.82	-0.1733	495.32
0.0590	1269.61	0.1838	577.46	0.4303	742.24	0.5814	960.33	0.7325	743.95	0.8836	752.56	-0.1768	494.73
0.0608	1088.33	0.1856	577.56	0.4325	745.58	0.5836	958.29	0.7347	737.63	0.8858	757.72	-0.1803	496.46
0.0626	1059.08	0.1874	577.23	0.4347	752.25	0.5858	952.23	0.7370	741.65	0.8881	764.50	-0.1838	495.51
0.0644	1014.44	0.1892	574.19	0.4370	756.16	0.5881	945.32	0.7392	741.24	0.8903	763.45	-0.1874	494.34
0.0661	1006.87	0.1909	575.41	0.4392	760.79	0.5903	944.26	0.7414	737.03	0.8925	768.21	-0.1909	492.40
0.0679	976.94	0.1927	576.81	0.4414	765.36	0.5925	941.41	0.7436	733.60	0.8947	774.02	-0.1944	512.82
0.0697	962.99	0.1945	580.22	0.4436	770.23	0.5947	940.06	0.7458	732.31	0.8969	778.27	-0.1979	494.70
0.0715	927.75	0.1963	581.06	0.4459	772.09	0.5970	937.16	0.7481	731.09	0.8992	789.39	-0.2015	505.63
0.0733	898.07	0.1981	577.85	0.4481	775.58	0.5992	937.92	0.7503	729.02	0.9014	797.34	-0.2050	504.19
0.0751	883.33	0.1999	575.60	0.4503	780.52	0.6014	935.51	0.7525	723.54	0.9036	804.74	-0.2085	507.26
0.0768	862.66	0.2016	569.86	0.4525	782.08	0.6036	931.78	0.7547	720.26	0.9058	809.05	-0.2120	503.94
0.0786	842.92	0.2034	569.20	0.4547	783.74	0.6058	929.17	0.7570	722.24	0.9081	812.99	-0.2155	507.65
0.0804	822.16	0.2052	568.83	0.4570	786.88	0.6081	928.52	0.7592	721.53	0.9103	821.19	-0.2191	501.85
0.0822	812.47	0.2070	570.20	0.4592	788.81	0.6103	926.09	0.7614	718.46	0.9125	831.13	-0.2226	504.42
0.0840	800.00	0.2088	569.60	0.4614	793.33	0.6125	924.28	0.7636	711.54	0.9147	840.50	-0.2261	497.08
0.0858	787.34	0.2106	568.43	0.4636	797.96	0.6147	925.45	0.7658	712.44	0.9169	841.96	-0.2296	509.91
0.0875	773.68	0.2123	565.57	0.4659	799.26	0.6170	922.60	0.7681	709.41	0.9192	850.97	-0.2332	501.06
0.0893	758.71	0.2141	562.44	0.4681	802.12	0.6192	918.09	0.7703	709.45	0.9214	858.74	-0.2367	516.45
0.0911	748.38	0.2159	561.80	0.4703	809.71	0.6214	918.46	0.7725	705.08	0.9236	867.57	-0.2402	502.82
0.0929	738.54	0.2177	559.83	0.4725	812.27	0.6236	912.10	0.7747	709.52	0.9258	886.86	-0.2437	506.93
0.0947	728.76	0.2195	557.34	0.4747	815.49	0.6258	906.71	0.7770	707.72	0.9281	898.66	-0.2473	507.97
0.0965	721.13	0.2212	557.38	0.4770	819.07	0.6281	904.82	0.7792	706.28	0.9303	912.94	-0.2508	508.30
0.0982	714.03	0.2230	558.18	0.4792	821.80	0.6303	908.02	0.7814	703.93	0.9325	919.64	-0.2543	511.46
0.1000	706.38	0.2248	556.16	0.4814	826.53	0.6325	907.13	0.7836	703.27	0.9347	921.90	-0.2578	512.59
0.1018	692.71	0.2266	554.16	0.4836	828.73	0.6347	897.70	0.7858	707.43	0.9369	933.39	-0.2614	507.71
0.1036	688.06	0.2284	553.66	0.4859	833.96	0.6370	899.08	0.7881	702.90	0.9392	949.90	-0.2649	503.32
0.1054	684.18	0.2302	550.16	0.4881	837.55	0.6392	897.10	0.7903	698.10	0.9414	957.96	-0.2684	510.51

Appendix 7.2 – Data for Spanwise Averaged Nusselt Number and Film Cooling Effectiveness

-0.2719	499.51	-0.4986	455.07	-0.7021	487.96	-0.9055	533.75	0.1168	629.30	0.4125	430.55	0.5636	379.87
-0.2755	497.56	-0.5016	449.30	-0.7051	497.13	-0.9085	540.65	0.1193	635.64	0.4147	428.88	0.5658	378.49
-0.2790	499.02	-0.5046	451.51	-0.7080	483.30	-0.9115	543.40	0.1218	641.40	0.4170	424.88	0.5681	378.38
-0.2825	499.60	-0.5076	453.71	-0.7110	497.13	-0.9145	551.49	0.1244	623.64	0.4192	420.90	0.5703	377.73
-0.2860	499.58	-0.5106	457.66	-0.7140	483.75	-0.9174	554.60	0.1269	607.18	0.4214	416.69	0.5725	377.11
-0.2895	498.38	-0.5136	482.08	-0.7170	482.87	-0.9204	562.86	0.1294	619.60	0.4236	413.31	0.5747	375.90
-0.2931	499.84	-0.5166	478.54	-0.7200	516.81	-0.9234	570.22	0.1319	600.07	0.4259	410.31	0.5770	380.67
-0.2966	497.92	-0.5196	481.17	-0.7230	474.82	-0.9264	574.72	0.1344	595.72	0.4281	407.42	0.5792	378.43
-0.3001	506.69	-0.5226	475.59	-0.7260	484.03	-0.9294	580.25	0.1370	617.58	0.4303	404.64	0.5814	379.12
-0.3036	496.96	-0.5256	501.54	-0.7290	477.16	-0.9324	600.67	0.1395	626.59	0.4325	401.47	0.5836	377.00
-0.3072	496.37	-0.5286	484.84	-0.7320	480.10	-0.9354	607.44	0.1420	666.68	0.4347	399.77	0.5858	381.93
-0.3107	494.47	-0.5315	479.09	-0.7350	490.61	-0.9384	617.18	0.1445	677.22	0.4370	398.65	0.5881	382.35
-0.3142	494.64	-0.5345	482.96	-0.7380	489.65	-0.9414	613.51	0.1470	632.94	0.4392	396.59	0.5903	383.25
-0.3177	494.33	-0.5375	478.45	-0.7409	488.39	-0.9444	620.57	0.1495	632.62	0.4414	396.23	0.5925	381.80
-0.3213	493.81	-0.5405	481.95	-0.7439	497.36	-0.9474	628.57	0.1521	591.12	0.4436	395.72	0.5947	382.71
-0.3248	494.89	-0.5435	465.83	-0.7469	495.82	-0.9504	639.03	0.1546	631.39	0.4459	395.13	0.5970	386.03
-0.3283	495.68	-0.5465	479.67	-0.7499	467.34	-0.9533	649.99	0.1571	628.25	0.4481	393.40	0.5992	397.71
-0.3318	494.72	-0.5495	490.47	-0.7529	466.68	-0.9563	662.28	0.1596	611.52	0.4503	391.98	0.6014	387.53
-0.3354	492.95	-0.5525	491.80	-0.7559	465.99	-0.9593	666.08	0.1621	572.50	0.4525	390.28	0.6036	396.32
-0.3389	491.29	-0.5555	495.76	-0.7589	477.64	-0.9623	679.63	0.1647	597.35	0.4547	389.09	0.6058	394.62
-0.3424	489.22	-0.5585	517.37	-0.7619	474.89	-0.9653	688.56	0.1672	591.38	0.4570	387.94	0.6081	403.18
-0.3459	487.65	-0.5615	502.14	-0.7649	475.06	-0.9683	706.12	0.1697	590.13	0.4592	387.09	0.6103	398.91
-0.3494	486.60	-0.5645	514.57	-0.7679	463.43	-0.9713	727.45	0.1722	566.10	0.4614	385.84	0.6125	400.26
-0.3530	487.19	-0.5674	520.47	-0.7709	465.86			0.1747	571.37	0.4636	385.84	0.6147	407.31
-0.3565	488.56	-0.5704	557.06	-0.7739	464.62			0.1773	566.46	0.4659	383.77	0.6170	419.02
-0.3600	489.56	-0.5734	561.37	-0.7768	486.14			0.1798	562.50	0.4681	381.39	0.6192	414.63
-0.3635	488.87	-0.5764	522.23	-0.7798	470.69			0.1823	559.96	0.4703	381.15	0.6214	416.87
-0.3671	488.95	-0.5794	493.42	-0.7828	462.01			0.1848	560.10	0.4725	381.80	0.6236	427.06
-0.3706	488.59	-0.5824	501.25	-0.7858	474.46			0.1873	561.42	0.4747	381.82	0.6258	431.04
-0.3741	487.42	-0.5854	501.89	-0.7888	461.15			0.1899	561.91	0.4770	378.57	0.6281	429.01
-0.3776	488.39	-0.5884	488.66	-0.7918	461.00			0.1924	558.60	0.4792	376.53	0.6303	430.49
-0.3812	489.06	-0.5914	491.36	-0.7948	463.11			0.1949	554.57	0.4814	374.62	0.6325	446.76
-0.3847	489.60	-0.5944	484.19	-0.7978	471.03			0.1974	554.94	0.4836	373.17	0.6347	451.04
-0.3882	489.42	-0.5974	491.13	-0.8008	464.31			0.1999	552.50	0.4859	371.91	0.6370	449.18
-0.3917	486.26	-0.6003	495.17	-0.8038	464.51			0.2025	552.07	0.4881	369.64	0.6392	452.78
-0.3953	484.64	-0.6033	485.39	-0.8068	463.58			0.2050	553.02	0.4903	367.29	0.6414	460.64
-0.3988	484.67	-0.6063	481.20	-0.8098	464.88			0.2075	556.55	0.4925	365.39	0.6436	470.18
-0.4023	505.82	-0.6093	497.55	-0.8127	466.26			0.2100	551.79	0.4947	363.72	0.6458	479.90
-0.4058	484.24	-0.6123	512.68	-0.8157	466.83			0.2125	549.16	0.4970	361.35	0.6481	480.83
-0.4094	482.52	-0.6153	498.94	-0.8187	466.70			0.2150	546.95	0.4992	361.85	0.6503	488.25
-0.4129	483.61	-0.6183	503.41	-0.8217	469.94			0.2176	545.23	0.5014	360.02	0.6525	498.70
-0.4164	482.68	-0.6213	497.15	-0.8247	466.29			0.2201	539.92	0.5036	356.75	0.6547	512.49
-0.4199	483.16	-0.6243	492.80	-0.8277	466.32			0.2226	538.47	0.5059	356.40	0.6570	513.36
-0.4234	481.26	-0.6273	499.47	-0.8307	467.95			0.2251	538.00	0.5081	356.20	0.6592	524.62
-0.4270	480.25	-0.6303	509.17	-0.8337	471.27			0.2276	537.11	0.5103	356.46	0.6614	534.22
-0.4305	479.82	-0.6333	517.89	-0.8367	472.53			0.2302	537.21	0.5125	356.47	0.6636	542.93
-0.4340	479.18	-0.6362	515.54	-0.8397	476.68			0.2302	535.08	0.5147	356.21	0.6658	549.98
-0.4375	497.68	-0.6392	496.80	-0.8427	471.68			0.2334	532.36	0.5170	354.60	0.6681	561.41
-0.4411	497.38	-0.6422	486.01	-0.8457	473.14			0.2366	531.72	0.5192	355.07	0.6703	566.93
-0.4446	498.69	-0.6452	482.75	-0.8486	476.16			0.2398	531.98	0.5214	356.63	0.6725	581.70
-0.4481	514.35	-0.6482	500.07	-0.8516	477.69			0.2430	532.06	0.5236	357.90	0.6747	594.52
-0.4516	475.42	-0.6512	504.39	-0.8546	476.60			0.2461	529.43	0.5259	356.94	0.6770	597.79
-0.4552	476.00	-0.6542	513.83	-0.8576	479.42			0.2743	501.76	0.5281	356.79	0.6792	604.02
-0.4587	475.39	-0.6572	531.87	-0.8606	481.32			0.3037	464.55	0.5303	359.83	0.6814	615.73
-0.4622	475.17	-0.6602	514.16	-0.8636	482.56			0.3069	459.20	0.5325	360.28	0.6836	637.73
-0.4657	476.44	-0.6632	506.54	-0.8666	489.42			0.3836	454.32	0.5347	361.60	0.6858	648.26
-0.4693	478.27	-0.6662	489.62	-0.8696	489.17			0.3859	451.12	0.5370	362.60	0.6881	648.80
-0.4728	478.87	-0.6692	487.79	-0.8726	490.34			0.3881	448.96	0.5392	364.03	0.6903	656.22
-0.4763	477.56	-0.6721	482.86	-0.8756	492.21			0.3903	446.27	0.5414	366.35	0.6925	675.07
-0.4717	465.35	-0.6751	498.44	-0.8786	495.68			0.3925	443.26	0.5436	369.62	0.6947	681.85
-0.4747	468.83	-0.6781	529.16	-0.8816	498.59			0.3947	441.81	0.5459	370.93	0.6970	685.33
-0.4777	476.40	-0.6811	486.96	-0.8845	499.75			0.3970	440.91	0.5481	369.50	0.6992	694.98
-0.4807	465.11	-0.6841	483.60	-0.8875	506.69			0.3992	439.72	0.5503	372.24	0.7014	713.42
-0.4837	457.31	-0.6871	480.77	-0.8905	511.78			0.4014	437.72	0.5525	374.39	0.7036	717.60
-0.4867	477.87	-0.6901	478.98	-0.8935	518.51			0.4036	437.47	0.5547	376.34	0.7058	727.22
-0.4897	463.18	-0.6931	480.57	-0.8965	519.84			0.4059	436.72	0.5570	375.01	0.7081	742.67
-0.4927	464.10	-0.6961	483.09	-0.8995	523.82			0.4081	436.12	0.5592	375.54	0.7103	753.79
-0.4956	459.10	-0.6991	483.78	-0.9025	528.96			0.4103	433.51	0.5614	382.06	0.7125	762.14

CASE G – Nu

X/SI	Nu
0.0186	1359.57
0.0186	1360.64
0.0211	1363.24
0.0236	1366.27
0.0261	1369.30
0.0286	1366.56
0.0311	1341.79
0.0337	1295.55
0.0362	1231.13
0.0387	1179.64
0.0412	1141.32
0.0437	1085.60
0.0463	1032.64
0.0488	991.57
0.0513	953.85
0.0538	925.83
0.0563	901.45
0.0589	875.60
0.0614	850.50
0.0639	827.79
0.0664	813.78
0.0689	798.79
0.0715	780.85
0.0740	761.18
0.0765	746.68
0.0790	730.96
0.0815	725.07
0.0841	720.71
0.0866	713.74
0.0891	703.36
0.0916	697.68
0.0941	695.36
0.0966	685.34
0.0992	676.39
0.1017	673.14
0.1042	676.95
0.1067	652.11
0.1092	653.67
0.1118	658.90
0.1143	633.93

Appendix 7.2 – Data for Spanwise Averaged Nusselt Number and Film Cooling Effectiveness

0.7147	770.69	0.8658	785.84	-0.1617	289.21	-0.4298	412.88	-0.6333	438.06	-0.8367	435.44	0.0577	1108.67
0.7170	782.38	0.8681	782.06	-0.1681	297.83	-0.4328	404.47	-0.6362	420.96	-0.8397	443.05	0.0596	1075.21
0.7192	790.29	0.8703	793.20	-0.1744	329.79	-0.4358	400.18	-0.6392	427.23	-0.8427	441.29	0.0616	1039.60
0.7214	800.10	0.8725	790.20	-0.1808	333.11	-0.4388	399.25	-0.6422	422.43	-0.8457	442.34	0.0635	1024.35
0.7236	797.07	0.8747	785.98	-0.1872	337.67	-0.4418	410.69	-0.6452	421.15	-0.8486	451.75	0.0654	1000.32
0.7258	798.12	0.8769	781.12	-0.1935	372.83	-0.4448	421.85	-0.6482	422.52	-0.8516	447.75	0.0674	975.90
0.7281	813.97	0.8792	785.57	-0.1974	342.13	-0.4478	406.18	-0.6512	424.74	-0.8546	441.62	0.0693	955.02
0.7303	820.44	0.8814	795.69	-0.2013	380.07	-0.4508	400.47	-0.6542	424.45	-0.8576	442.53	0.0713	935.04
0.7325	816.31	0.8836	792.84	-0.2052	417.81	-0.4538	399.62	-0.6572	427.59	-0.8606	443.30	0.0732	917.72
0.7347	817.97	0.8858	791.59	-0.2091	496.00	-0.4568	393.34	-0.6602	444.80	-0.8636	444.46	0.0751	899.08
0.7370	830.47	0.8881	792.34	-0.2130	440.23	-0.4597	394.03	-0.6632	446.37	-0.8666	446.59	0.0771	874.81
0.7392	836.45	0.8903	791.07	-0.2168	427.80	-0.4627	396.74	-0.6662	452.43	-0.8696	451.00	0.0790	857.61
0.7414	838.83	0.8925	787.77	-0.2207	463.44	-0.4657	394.36	-0.6692	439.34	-0.8726	452.59	0.0810	844.78
0.7436	837.21	0.8947	807.66	-0.2246	487.70	-0.4687	396.37	-0.6721	430.35	-0.8756	451.39	0.0829	824.26
0.7458	839.10	0.8969	793.24	-0.2285	468.98	-0.4717	402.04	-0.6751	432.76	-0.8786	451.94	0.0848	808.31
0.7481	846.99	0.8992	792.56	-0.2324	449.13	-0.4747	396.92	-0.6781	442.76	-0.8816	453.08	0.0868	796.50
0.7503	848.83	0.9014	798.95	-0.2363	497.53	-0.4777	397.54	-0.6811	456.58	-0.8845	454.00	0.0887	788.97
0.7525	847.33	0.9036	823.26	-0.2402	483.96	-0.4807	412.55	-0.6841	437.04	-0.8875	457.84	0.0906	775.80
0.7547	847.32	0.9058	820.82	-0.2441	499.20	-0.4837	412.15	-0.6871	432.08	-0.8905	460.74	0.0926	763.14
0.7570	847.29	0.9081	810.72	-0.2479	453.19	-0.4867	404.48	-0.6901	432.83	-0.8935	462.51	0.0945	756.07
0.7592	853.54	0.9103	811.71	-0.2518	428.10	-0.4897	403.59	-0.6931	434.47	-0.8965	464.21	0.0965	748.16
0.7614	858.93	0.9125	815.84	-0.2557	416.14	-0.4927	402.11	-0.6961	427.55	-0.8995	481.68	0.0984	738.95
0.7636	851.25	0.9147	816.13	-0.2596	450.54	-0.4956	395.82	-0.6991	435.25	-0.9025	539.55	0.1003	733.49
0.7658	851.88	0.9169	821.08	-0.2635	418.86	-0.4986	404.25	-0.7021	434.80	-0.9055	525.79	0.1023	725.83
0.7681	858.10	0.9192	824.99	-0.2674	419.10	-0.5016	402.46	-0.7051	429.19	-0.9085	529.95	0.1042	714.04
0.7703	858.89	0.9214	832.91	-0.2713	431.56	-0.5046	408.63	-0.7080	426.55	-0.9115	485.83	0.1061	710.87
0.7725	852.35	0.9236	835.97	-0.2752	419.88	-0.5076	399.92	-0.7110	432.71	-0.9145	492.76	0.1081	703.32
0.7747	847.35	0.9258	845.19	-0.2790	419.86	-0.5106	406.69	-0.7140	435.03	-0.9174	498.77	0.1100	695.67
0.7770	844.05	0.9281	845.20	-0.2829	471.31	-0.5136	398.80	-0.7170	431.84	-0.9204	499.39	0.1120	684.99
0.7792	854.06	0.9303	849.41	-0.2868	448.00	-0.5166	399.81	-0.7200	431.59	-0.9234	507.51	0.1139	679.47
0.7814	850.52	0.9325	856.19	-0.2907	420.90	-0.5196	401.78	-0.7230	429.91	-0.9264	513.61	0.1158	675.30
0.7836	848.26	0.9347	863.24	-0.2946	420.48	-0.5226	402.28	-0.7260	428.42	-0.9294	519.34	0.1178	672.57
0.7858	844.57	0.9369	868.79	-0.2985	430.17	-0.5256	402.35	-0.7290	429.89	-0.9324	524.91	0.1197	667.05
0.7881	840.46	0.9392	873.70	-0.3024	427.83	-0.5286	406.73	-0.7320	428.89	-0.9354	534.32	0.1216	662.63
0.7903	840.09	0.9414	880.92	-0.3062	427.81	-0.5315	401.20	-0.7350	428.66	-0.9384	540.98	0.1236	663.47
0.7925	838.15	0.9436	881.42	-0.3101	424.32	-0.5345	403.01	-0.7380	427.47	-0.9414	549.17	0.1255	660.28
0.7947	839.77	0.9458	888.11	-0.3140	420.94	-0.5375	403.51	-0.7409	415.61	-0.9444	556.20	0.1275	659.45
0.7969	838.58	0.9481	901.20	-0.3179	421.51	-0.5405	402.69	-0.7439	410.34	-0.9474	564.00	0.1294	655.48
0.7992	831.95	0.9503	914.53	-0.3218	419.81	-0.5435	410.70	-0.7469	420.22	-0.9504	569.81	0.1313	651.18
0.8014	834.64	0.9525	932.38	-0.3257	451.84	-0.5465	403.39	-0.7499	418.95	-0.9533	576.82	0.1333	649.47
0.8036	841.60	0.9547	952.30	-0.3296	418.66	-0.5495	412.10	-0.7529	412.35	-0.9563	584.97	0.1352	644.26
0.8058	843.13			-0.3335	417.54	-0.5525	434.15	-0.7559	412.54	-0.9593	593.55	0.1371	639.80
0.8081	835.53	X/PL	Nu	-0.3373	416.91	-0.5555	439.25	-0.7589	401.40	-0.9623	634.21	0.1391	635.25
0.8103	831.80	-0.0027	1363.00	-0.3412	416.71	-0.5585	413.78	-0.7619	422.82	-0.9653	641.88	0.1410	632.60
0.8125	830.43	-0.0091	1279.25	-0.3451	416.79	-0.5615	404.01	-0.7649	422.90	-0.9683	617.72	0.1430	624.20
0.8147	829.97	-0.0154	1292.29	-0.3490	415.48	-0.5645	406.10	-0.7679	417.96	-0.9713	696.04	0.1449	619.72
0.8169	829.47	-0.0218	1115.05	-0.3529	414.74	-0.5674	418.17	-0.7709	422.84	-0.9743	674.18	0.1468	613.94
0.8192	828.10	-0.0282	1053.38	-0.3568	413.85	-0.5704	429.37	-0.7739	423.94	-0.9773	726.49	0.1488	614.20
0.8214	819.71	-0.0345	808.17	-0.3607	411.99	-0.5734	409.94	-0.7768	422.00	-0.9803	706.68	0.1507	606.80
0.8236	816.82	-0.0409	760.45	-0.3646	411.39	-0.5764	408.56	-0.7798	422.46	-0.9833	731.74	0.1526	600.89
0.8258	819.76	-0.0472	705.17	-0.3684	411.20	-0.5794	412.88	-0.7828	424.00	-0.9863	755.19	0.1546	601.61
0.8281	814.16	-0.0536	576.75	-0.3723	410.68	-0.5824	406.40	-0.7858	419.28	-0.9892	738.71	0.1565	599.11
0.8303	811.62	-0.0600	567.44	-0.3762	410.00	-0.5854	425.30	-0.7888	424.99	-0.9922	768.70	0.1585	596.72
0.8325	807.77	-0.0663	468.82	-0.3801	409.62	-0.5884	420.46	-0.7918	409.37			0.1604	591.73
0.8347	805.94	-0.0727	429.23	-0.3840	410.12	-0.5914	413.30	-0.7948	410.35			0.1623	585.68
0.8369	798.19	-0.0790	408.94	-0.3879	410.01	-0.5944	410.00	-0.7978	405.10	CASE H – Nu		0.1643	583.99
0.8392	805.26	-0.0854	378.77	-0.3918	409.57	-0.5974	408.51	-0.8008	422.83			0.1662	580.85
0.8414	804.57	-0.0918	360.49	-0.3956	408.61	-0.6003	410.29	-0.8038	430.68	X/SL	Nu	0.1682	580.60
0.8436	803.49	-0.0981	343.20	-0.3995	408.72	-0.6033	412.77	-0.8068	430.36	0.0383	1551.95	0.1701	578.10
0.8458	795.29	-0.1045	328.69	-0.4034	408.31	-0.6063	413.40	-0.8098	432.01	0.0403	1411.93	0.1720	576.19
0.8481	798.34	-0.1108	316.41	-0.4073	408.85	-0.6093	429.26	-0.8127	424.64	0.0422	1330.83	0.1740	577.80
0.8503	801.92	-0.1172	303.55	-0.4112	409.56	-0.6123	419.79	-0.8157	425.85	0.0441	1297.00	0.1759	598.39
0.8525	794.51	-0.1236	290.57	-0.4151	409.30	-0.6153	443.02	-0.8187	426.81	0.0461	1256.79	0.1778	579.49
0.8547	794.43	-0.1299	280.44	-0.4190	408.68	-0.6183	443.42	-0.8217	430.78	0.0480	1226.79	0.1798	577.24
0.8569	791.43	-0.1363	274.91	-0.4229	409.52	-0.6213	417.97	-0.8247	433.21	0.0499	1199.20	0.1817	576.74
0.8592	791.61	-0.1426	271.94	-0.4267	410.45	-0.6243	425.31	-0.8277	432.80	0.0519	1170.06	0.1837	576.03
0.8614	795.33	-0.1490	271.35	-0.4306	410.46	-0.6273	425.93	-0.8307	434.65	0.0538	1145.51	0.1856	576.06
0.8636	794.33	-0.1554	273.62	-0.4268	412.15	-0.6303	419.05	-0.8337	432.72	0.0558	1136.63	0.1875	610.65

Appendix 7.2 – Data for Spanwise Averaged Nusselt Number and Film Cooling Effectiveness

0.1895	575.34	0.4303	755.31	0.5814	947.68	0.7325	809.79	0.8836	787.25	-0.1776	512.30	-0.4179	541.68
0.1914	575.40	0.4325	759.63	0.5836	944.63	0.7347	802.28	0.8858	784.57	-0.1811	517.23	-0.4209	585.35
0.1933	569.23	0.4347	763.53	0.5858	939.27	0.7370	804.83	0.8881	785.50	-0.1846	543.15	-0.4238	564.98
0.1953	567.05	0.4370	768.59	0.5881	935.11	0.7392	800.88	0.8903	782.59	-0.1881	532.19	-0.4268	520.54
0.1972	564.99	0.4392	774.55	0.5903	928.97	0.7414	797.82	0.8925	789.82	-0.1917	514.79	-0.4298	567.81
0.1992	568.98	0.4414	777.95	0.5925	923.80	0.7436	799.10	0.8947	802.66	-0.1952	534.23	-0.4328	476.71
0.2011	568.24	0.4436	783.43	0.5947	918.05	0.7458	799.09	0.8969	809.00	-0.1987	489.86	-0.4358	520.34
0.2030	566.54	0.4459	787.24	0.5970	912.21	0.7481	791.75	0.8992	818.63	-0.2022	489.26	-0.4388	497.18
0.2050	563.76	0.4481	792.50	0.5992	907.52	0.7503	792.53	0.9014	821.37	-0.2058	490.07	-0.4418	459.15
0.2069	564.36	0.4503	796.85	0.6014	903.54	0.7525	796.00	0.9036	835.44	-0.2093	480.53	-0.4448	548.69
0.2088	564.66	0.4525	801.30	0.6036	900.52	0.7547	794.33	0.9058	842.48	-0.2128	524.02	-0.4478	514.72
0.2108	563.02	0.4547	805.58	0.6058	893.65	0.7570	788.31	0.9081	853.99	-0.2163	535.87	-0.4508	511.67
0.2127	564.41	0.4570	807.77	0.6081	893.86	0.7592	788.82	0.9103	858.49	-0.2199	532.81	-0.4538	504.70
0.2147	564.63	0.4592	811.03	0.6103	887.74	0.7614	788.42	0.9125	856.01	-0.2234	522.72	-0.4568	564.96
0.2166	565.67	0.4614	813.63	0.6125	891.59	0.7636	787.51	0.9147	860.02	-0.2269	508.81	-0.4597	544.27
0.2185	563.69	0.4636	816.64	0.6147	880.41	0.7658	787.41	0.9169	864.86	-0.2304	504.22	-0.4627	535.69
0.2205	560.62	0.4659	818.56	0.6170	878.99	0.7681	787.24	0.9192	873.74	-0.2340	504.01	-0.4657	527.21
0.2224	560.09	0.4681	822.60	0.6192	876.46	0.7703	787.13	0.9214	880.58	-0.2375	484.16	-0.4687	535.26
0.2243	560.16	0.4703	825.07	0.6214	869.29	0.7725	780.32	0.9236	891.28	-0.2410	493.10	-0.4717	516.58
0.2263	558.13	0.4725	827.04	0.6236	869.66	0.7747	777.24	0.9258	897.15	-0.2445	492.56	-0.4747	494.95
0.2282	557.76	0.4747	828.93	0.6258	863.80	0.7770	782.79	0.9281	903.12	-0.2481	503.83	-0.4777	487.20
0.2302	556.31	0.4770	828.39	0.6281	861.09	0.7792	780.65	0.9303	907.84	-0.2516	481.82	-0.4807	447.84
0.2302	557.93	0.4792	830.33	0.6303	862.73	0.7814	782.27	0.9325	917.68	-0.2551	508.04	-0.4837	529.18
0.2334	559.49	0.4814	835.82	0.6325	862.86	0.7836	784.59	0.9347	922.43	-0.2586	493.45	-0.4867	502.20
0.2366	558.94	0.4836	838.36	0.6347	855.31	0.7858	777.80	0.9369	930.01	-0.2621	499.04	-0.4897	500.68
0.2398	561.33	0.4859	837.40	0.6370	848.32	0.7881	778.10	0.9392	938.49	-0.2657	490.81	-0.4927	492.74
0.2430	564.10	0.4881	839.68	0.6392	853.49	0.7903	777.54	0.9414	950.06	-0.2692	505.36	-0.4956	492.23
0.2461	565.21	0.4903	842.16	0.6414	851.26	0.7925	779.56	0.9436	962.88	-0.2727	486.13	-0.4986	474.62
0.2493	565.09	0.4925	841.46	0.6436	850.39	0.7947	785.43	0.9458	968.05	-0.2762	485.97	-0.5016	495.88
0.2525	568.15	0.4947	844.08	0.6458	848.50	0.7969	778.96	0.9481	991.31	-0.2798	485.46	-0.5046	464.46
0.2557	569.24	0.4970	847.07	0.6481	844.21	0.7992	780.87	0.9503	1010.89	-0.2833	483.65	-0.5076	463.80
0.2589	573.70	0.4992	848.32	0.6503	841.28	0.8014	777.95	0.9525	1016.66	-0.2868	487.27	-0.5106	478.03
0.2621	576.43	0.5014	854.66	0.6525	842.28	0.8036	781.36	0.9547	1028.42	-0.2903	494.53	-0.5136	470.96
0.2653	577.84	0.5036	855.88	0.6547	842.92	0.8058	780.67	0.9569	1051.26	-0.2939	489.31	-0.5166	517.30
0.2685	580.85	0.5059	858.53	0.6570	835.61	0.8081	784.52	0.9592	1083.62	-0.2974	527.62	-0.5196	502.06
0.2717	584.39	0.5081	862.66	0.6592	839.10	0.8103	785.12			-0.3009	499.86	-0.5226	477.94
0.2749	587.46	0.5103	864.98	0.6614	835.31	0.8125	785.19	X/PL	Nu	-0.3044	508.41	-0.5256	481.87
0.2781	584.47	0.5125	870.51	0.6636	835.53	0.8147	786.24	-0.0030	1651.36	-0.3080	488.49	-0.5286	486.86
0.2813	582.97	0.5147	874.05	0.6658	833.47	0.8169	784.66	-0.0115	1476.54	-0.3115	488.98	-0.5315	486.38
0.2845	582.43	0.5170	878.28	0.6681	833.49	0.8192	784.84	-0.0201	1313.79	-0.3150	488.35	-0.5345	528.91
0.2877	592.86	0.5192	879.43	0.6703	834.63	0.8214	783.46	-0.0286	1205.18	-0.3185	516.81	-0.5375	535.88
0.2909	609.95	0.5214	887.83	0.6725	829.64	0.8236	788.90	-0.0372	1170.65	-0.3220	489.12	-0.5405	529.91
0.2941	597.55	0.5236	890.92	0.6747	835.67	0.8258	784.34	-0.0457	1127.66	-0.3256	491.73	-0.5435	485.36
0.2973	597.89	0.5259	889.94	0.6770	826.86	0.8281	781.04	-0.0543	918.78	-0.3291	488.86	-0.5465	529.81
0.3005	619.92	0.5281	892.78	0.6792	829.00	0.8303	781.08	-0.0628	768.21	-0.3326	519.80	-0.5495	536.19
0.3037	590.61	0.5303	903.37	0.6814	825.38	0.8325	781.54	-0.0714	592.54	-0.3361	524.28	-0.5525	519.12
0.3069	640.96	0.5325	907.59	0.6836	825.67	0.8347	788.04	-0.0799	526.70	-0.3397	495.05	-0.5555	489.56
0.3836	693.17	0.5347	909.07	0.6858	825.39	0.8369	783.27	-0.0885	497.46	-0.3432	491.08	-0.5585	492.69
0.3859	696.61	0.5370	916.17	0.6881	821.58	0.8392	784.95	-0.0970	491.79	-0.3467	492.07	-0.5615	516.26
0.3881	692.90	0.5392	921.91	0.6903	819.49	0.8414	786.88	-0.1056	484.50	-0.3502	492.26	-0.5645	512.61
0.3903	689.46	0.5414	930.26	0.6925	823.46	0.8436	789.02	-0.1142	481.10	-0.3538	496.91	-0.5674	552.33
0.3925	692.46	0.5436	932.29	0.6947	817.16	0.8458	791.67	-0.1177	477.73	-0.3573	492.40	-0.5704	575.19
0.3947	697.54	0.5459	934.10	0.6970	821.95	0.8481	788.59	-0.1212	489.13	-0.3608	519.97	-0.5734	517.39
0.3970	702.67	0.5481	939.93	0.6992	821.01	0.8503	793.62	-0.1247	493.71	-0.3643	493.21	-0.5764	507.95
0.3992	707.89	0.5503	948.20	0.7014	823.87	0.8525	794.93	-0.1282	467.20	-0.3679	494.55	-0.5794	524.23
0.4014	712.76	0.5525	952.67	0.7036	823.67	0.8547	795.94	-0.1318	462.48	-0.3714	494.63	-0.5824	525.62
0.4036	719.35	0.5547	955.14	0.7058	818.75	0.8569	796.64	-0.1353	468.68	-0.3749	494.30	-0.5854	513.64
0.4059	722.73	0.5570	956.18	0.7081	820.07	0.8592	794.56	-0.1388	458.80	-0.3784	496.39	-0.5884	523.54
0.4081	728.02	0.5592	962.02	0.7103	817.48	0.8614	806.13	-0.1423	472.67	-0.3819	489.75	-0.5914	523.54
0.4103	729.50	0.5614	964.73	0.7125	815.41	0.8636	794.56	-0.1459	462.39	-0.3855	520.30	-0.5944	500.85
0.4125	732.93	0.5636	966.41	0.7147	810.91	0.8658	791.01	-0.1494	480.68	-0.3890	519.54	-0.5974	480.54
0.4147	736.98	0.5658	969.44	0.7170	814.85	0.8681	786.26	-0.1529	483.41	-0.3969	497.42	-0.6003	524.23
0.4170	742.22	0.5681	968.94	0.7192	817.95	0.8703	799.09	-0.1564	494.37	-0.3999	486.55	-0.6033	538.49
0.4192	744.50	0.5703	964.02	0.7214	816.02	0.8725	796.01	-0.1600	483.07	-0.4029	498.12	-0.6063	476.07
0.4214	746.29	0.5725	962.50	0.7236	813.53	0.8747	793.99	-0.1635	504.96	-0.4059	486.20	-0.6093	529.43
0.4236	749.54	0.5747	961.40	0.7258	810.82	0.8769	790.39	-0.1670	474.99	-0.4089	549.74	-0.6123	484.14
0.4259	753.04	0.5770	958.58	0.7281	810.58	0.8792	787.93	-0.1705	475.60	-0.4119	508.29	-0.6153	482.63
0.4281	752.96	0.5792	950.77	0.7303	812.36	0.8814	790.60	-0.1741	506.38	-0.4149	517.20	-0.6183	510.86

Appendix 7.2 – Data for Spanwise Averaged Nusselt Number and Film Cooling Effectiveness

-0.6213	520.01	-0.8247	593.95	0.0441	1349.77	0.2023	588.94	0.4503	941.73	0.6014	1032.41	0.7525	815.82
-0.6243	514.42	-0.8277	562.27	0.0465	1289.02	0.2046	590.37	0.4525	946.55	0.6036	1029.68	0.7547	810.57
-0.6273	486.17	-0.8307	551.66	0.0488	1240.64	0.2069	594.08	0.4547	948.03	0.6058	1025.21	0.7570	816.21
-0.6303	506.75	-0.8337	576.61	0.0511	1199.29	0.2092	589.02	0.4570	949.50	0.6081	1023.68	0.7592	807.30
-0.6333	482.87	-0.8367	502.82	0.0534	1161.85	0.2116	587.63	0.4592	953.08	0.6103	1017.41	0.7614	800.87
-0.6362	493.62	-0.8397	495.02	0.0558	1116.05	0.2139	590.06	0.4614	953.95	0.6125	1011.30	0.7636	805.77
-0.6392	512.26	-0.8427	544.52	0.0581	1088.82	0.2162	587.79	0.4636	955.43	0.6147	1005.68	0.7658	809.15
-0.6422	514.55	-0.8457	524.13	0.0604	1067.60	0.2185	584.61	0.4659	960.00	0.6170	1003.58	0.7681	802.62
-0.6452	485.58	-0.8486	523.98	0.0627	1050.54	0.2209	581.14	0.4681	962.61	0.6192	1003.25	0.7703	801.32
-0.6482	491.35	-0.8516	500.05	0.0651	1023.57	0.2232	581.14	0.4703	962.43	0.6214	997.19	0.7725	801.64
-0.6512	490.24	-0.8546	505.91	0.0674	1001.89	0.2255	580.13	0.4725	963.02	0.6236	993.04	0.7747	804.52
-0.6542	486.05	-0.8576	512.25	0.0697	986.27	0.2278	574.90	0.4747	969.86	0.6258	994.53	0.7770	800.57
-0.6572	541.70	-0.8606	509.80	0.0720	974.11	0.2302	570.65	0.4770	975.86	0.6281	992.91	0.7792	806.12
-0.6602	518.21	-0.8636	512.31	0.0744	949.42	0.2302	570.98	0.4792	976.59	0.6303	982.76	0.7814	799.90
-0.6632	542.92	-0.8666	511.92	0.0767	936.20	0.2334	575.74	0.4814	977.65	0.6325	976.81	0.7836	803.72
-0.6662	560.77	-0.8696	521.63	0.0790	917.04	0.2366	579.28	0.4836	982.46	0.6347	966.11	0.7858	796.77
-0.6692	507.13	-0.8726	517.58	0.0813	903.49	0.2398	579.80	0.4859	986.97	0.6370	965.47	0.7881	801.74
-0.6721	561.89	-0.8756	547.79	0.0837	887.28	0.2430	583.77	0.4881	989.54	0.6392	965.21	0.7903	802.90
-0.6751	543.85	-0.8786	558.53	0.0860	878.29	0.2461	588.06	0.4903	994.09	0.6414	964.05	0.7925	805.99
-0.6781	626.35	-0.8816	521.66	0.0883	857.20	0.2493	593.50	0.4925	996.07	0.6436	963.80	0.7947	804.24
-0.6811	691.76	-0.8845	530.57	0.0906	835.58	0.2525	595.75	0.4947	995.99	0.6458	950.82	0.7969	793.83
-0.6841	676.38	-0.8875	540.53	0.0930	824.58	0.2557	596.69	0.4970	1002.90	0.6481	947.08	0.7992	794.11
-0.6871	603.27	-0.8905	554.59	0.0953	817.97	0.2589	603.88	0.4992	1010.19	0.6503	941.32	0.8014	800.17
-0.6901	525.23	-0.8935	552.68	0.0976	812.05	0.2621	611.12	0.5014	1013.43	0.6525	935.68	0.8036	804.00
-0.6931	539.15	-0.8965	559.13	0.0999	805.42	0.2653	616.67	0.5036	1011.85	0.6547	935.35	0.8058	805.58
-0.6961	512.66	-0.8995	580.08	0.1023	795.20	0.2685	620.70	0.5059	1017.49	0.6570	930.57	0.8081	796.26
-0.6991	641.13	-0.9025	576.89	0.1046	787.88	0.2717	622.44	0.5081	1025.65	0.6592	928.00	0.8103	800.01
-0.7021	590.23	-0.9055	582.36	0.1069	786.85	0.2749	629.88	0.5103	1026.80	0.6614	925.05	0.8125	799.60
-0.7051	507.65	-0.9085	592.35	0.1092	779.68	0.2781	629.22	0.5125	1032.66	0.6636	924.30	0.8147	789.73
-0.7080	564.28	-0.9115	598.19	0.1116	769.38	0.2813	632.00	0.5147	1033.78	0.6658	919.19	0.8169	804.04
-0.7110	584.80	-0.9145	603.16	0.1139	759.27	0.2845	637.38	0.5170	1036.81	0.6681	916.17	0.8192	804.46
-0.7140	687.89	-0.9174	613.68	0.1162	746.67	0.2877	643.16	0.5192	1042.19	0.6703	916.28	0.8214	805.35
-0.7170	490.60	-0.9204	623.54	0.1185	739.00	0.2909	656.95	0.5214	1042.60	0.6725	911.14	0.8236	796.87
-0.7200	546.81	-0.9234	631.80	0.1209	731.11	0.2941	662.85	0.5236	1048.28	0.6747	900.78	0.8258	798.03
-0.7230	563.90	-0.9264	644.63	0.1232	727.00	0.2973	663.36	0.5259	1055.93	0.6770	904.38	0.8281	793.09
-0.7260	618.14	-0.9294	658.28	0.1255	721.76	0.3005	668.19	0.5281	1060.13	0.6792	901.43	0.8303	794.25
-0.7290	556.75	-0.9324	670.81	0.1278	710.86	0.3037	668.19	0.5303	1060.27	0.6814	894.58	0.8325	792.58
-0.7320	577.90	-0.9354	679.00	0.1302	696.36	0.3069	664.02	0.5325	1064.01	0.6836	891.07	0.8347	800.94
-0.7350	494.57	-0.9384	687.01	0.1325	691.00	0.3836	792.98	0.5347	1068.43	0.6858	891.52	0.8369	799.58
-0.7380	522.93	-0.9414	693.02	0.1348	688.72	0.3859	798.28	0.5370	1074.04	0.6881	887.91	0.8392	823.76
-0.7409	556.23	-0.9444	710.63	0.1371	681.87	0.3881	801.56	0.5392	1075.75	0.6903	884.79	0.8414	807.85
-0.7439	539.21	-0.9474	721.17	0.1395	673.31	0.3903	810.48	0.5414	1080.91	0.6925	880.45	0.8436	808.03
-0.7469	535.99	-0.9504	723.52	0.1418	667.87	0.3925	822.32	0.5436	1086.40	0.6947	877.92	0.8458	799.94
-0.7499	564.30	-0.9533	733.20	0.1441	664.28	0.3947	831.16	0.5459	1088.97	0.6970	878.05	0.8481	804.52
-0.7529	574.41	-0.9563	757.55	0.1464	657.68	0.3970	838.57	0.5481	1099.41	0.6992	876.42	0.8503	807.40
-0.7559	543.07	-0.9593	758.59	0.1488	653.36	0.3992	851.38	0.5503	1099.91	0.7014	871.60	0.8525	807.16
-0.7589	542.58	-0.9623	772.82	0.1511	646.86	0.4014	861.22	0.5525	1104.64	0.7036	861.22	0.8547	811.71
-0.7619	565.75	-0.9653	789.23	0.1534	641.47	0.4036	867.03	0.5547	1102.21	0.7058	857.97	0.8569	819.12
-0.7649	590.13	-0.9683	809.73	0.1557	644.74	0.4059	871.35	0.5570	1104.51	0.7081	856.33	0.8592	822.59
-0.7679	558.63	-0.9713	828.80	0.1581	641.97	0.4081	875.96	0.5592	1106.83	0.7103	854.90	0.8614	830.51
-0.7709	573.66	-0.9743	862.38	0.1604	637.72	0.4103	881.56	0.5614	1106.94	0.7125	851.11	0.8636	832.46
-0.7739	590.13	-0.9773	891.16	0.1627	629.90	0.4125	883.68	0.5636	1102.72	0.7147	845.67	0.8658	834.87
-0.7768	594.14	-0.9803	903.21	0.1651	632.58	0.4147	888.31	0.5658	1098.99	0.7170	850.93	0.8681	836.16
-0.7798	605.54	-0.9833	925.24	0.1674	627.97	0.4170	895.74	0.5681	1099.04	0.7192	847.42	0.8703	839.90
-0.7828	604.69	-0.9863	952.26	0.1697	628.13	0.4192	893.08	0.5703	1099.09	0.7214	846.82	0.8725	842.08
-0.7858	539.75	-0.9892	969.44	0.1720	628.06	0.4214	896.78	0.5725	1097.40	0.7236	846.95	0.8747	845.71
-0.7888	521.34	-0.9922	973.22	0.1744	620.51	0.4236	900.05	0.5747	1092.31	0.7258	846.61	0.8769	852.70
-0.7918	569.11			0.1767	618.54	0.4259	904.83	0.5770	1086.59	0.7281	841.70	0.8792	848.60
-0.7948	554.51			0.1790	618.48	0.4281	907.47	0.5792	1081.98	0.7303	827.35	0.8814	858.62
-0.7978	546.34			0.1813	617.98	0.4303	910.35	0.5814	1080.45	0.7325	828.83	0.8836	865.84
-0.8008	628.32			0.1837	615.80	0.4325	915.52	0.5836	1076.00	0.7347	822.55	0.8858	872.23
-0.8038	497.02			0.1860	613.86	0.4347	921.99	0.5858	1067.81	0.7370	824.03	0.8881	872.53
-0.8068	571.26			0.1883	605.62	0.4370	922.90	0.5881	1062.59	0.7392	820.71	0.8903	883.80
-0.8098	619.59			0.1906	601.75	0.4392	923.25	0.5903	1050.35	0.7414	825.29	0.8925	887.70
-0.8127	634.42			0.1930	601.37	0.4414	929.83	0.5925	1044.29	0.7436	818.58	0.8947	893.78
-0.8157	598.69			0.1953	603.30	0.4436	932.35	0.5947	1041.88	0.7458	820.16	0.8969	896.09
-0.8187	567.38			0.1976	600.69	0.4459	936.88	0.5970	1042.78	0.7481	816.77	0.8992	908.85
-0.8217	608.71			0.1999	592.29	0.4481	940.86	0.5992	1033.86	0.7503	810.25	0.9014	917.88

CASE I – Nu

X/SL Nu

-0.8068	571.26	0.0302	1647.27	0.1883	605.62	0.4370	922.90	0.5881	1062.59	0.7392	820.71	0.8903	883.80
-0.8098	619.59	0.0325	1586.06	0.1906	601.75	0.4392	923.25	0.5903	1050.35	0.7414	825.29	0.8925	887.70
-0.8127	634.42	0.0348	1580.53	0.1930	601.37	0.4414	929.83	0.5925	1044.29	0.7436	818.58	0.8947	893.78
-0.8157	598.69	0.0372	1498.43	0.1953	603.30	0.4436	932.35	0.5947	1041.88	0.7458	820.16	0.8969	896.09
-0.8187	567.38	0.0395	1462.61	0.1976	600.69	0.4459	936.88	0.5970	1042.78	0.7481	816.77	0.8992	908.85
-0.8217	608.71	0.0418	1400.82	0.1999	592.29	0.4481	940.86	0.5992	1033.86	0.7503	810.25	0.9014	917.88

Appendix 7.2 – Data for Spanwise Averaged Nusselt Number and Film Cooling Effectiveness

0.9036	930.18	-0.2520	580.02	-0.4897	555.24	-0.6931	576.65	-0.8965	681.85	0.0975	775.56	0.2557	665.66
0.9058	935.70	-0.2555	551.74	-0.4927	568.94	-0.6961	567.39	-0.8995	689.34	0.0998	774.24	0.2589	668.46
0.9081	938.20	-0.2590	581.25	-0.4956	580.91	-0.6991	577.98	-0.9025	687.25	0.1020	767.83	0.2621	673.81
0.9103	951.47	-0.2626	574.26	-0.4986	551.34	-0.7021	566.28	-0.9055	707.03	0.1043	762.06	0.2653	678.70
0.9125	960.31	-0.2661	518.61	-0.5016	554.77	-0.7051	578.06	-0.9085	734.55	0.1065	753.71	0.2685	679.23
0.9147	968.00	-0.2696	539.61	-0.5046	544.98	-0.7080	577.42	-0.9115	747.17	0.1088	752.70	0.2717	684.48
0.9169	980.97	-0.2731	546.22	-0.5076	556.52	-0.7110	577.29	-0.9145	742.68	0.1110	754.22	0.2749	686.13
0.9192	995.10	-0.2767	546.84	-0.5106	617.22	-0.7140	570.22	-0.9174	731.39	0.1133	749.76	0.2781	684.80
0.9214	1010.36	-0.2802	545.45	-0.5136	587.42	-0.7170	566.12	-0.9204	720.28	0.1155	739.90	0.2813	685.66
0.9236	1023.64	-0.2837	533.58	-0.5166	581.96	-0.7200	565.24	-0.9234	724.08	0.1178	732.13	0.2845	686.57
0.9258	1023.50	-0.2872	588.16	-0.5196	572.26	-0.7230	597.90	-0.9264	732.56	0.1200	728.30	0.2877	693.78
0.9281	1038.97	-0.2908	604.92	-0.5226	547.19	-0.7260	578.83	-0.9294	741.20	0.1223	723.68	0.2909	700.18
0.9303	1056.81	-0.2943	564.19	-0.5256	548.14	-0.7290	591.25	-0.9324	750.16	0.1245	719.79	0.2941	702.95
0.9325	1076.71	-0.2978	552.77	-0.5286	547.12	-0.7320	562.02	-0.9354	759.70	0.1268	723.24	0.2973	703.75
0.9347	1090.25	-0.3013	567.92	-0.5315	542.96	-0.7350	565.61	-0.9384	760.69	0.1290	716.92	0.3005	707.94
0.9369	1097.38	-0.3048	562.31	-0.5345	546.04	-0.7380	574.02	-0.9414	781.34	0.1313	707.50	0.3037	703.58
0.9392	1106.53	-0.3084	531.38	-0.5375	555.77	-0.7409	588.13	-0.9444	793.43	0.1335	701.62	0.3069	703.65
0.9414	1126.43	-0.3119	537.46	-0.5405	560.19	-0.7439	587.16	-0.9474	796.78	0.1358	699.52	0.3836	829.20
0.9436	1149.72	-0.3154	548.22	-0.5435	549.46	-0.7469	577.94	-0.9504	795.70	0.1380	697.22	0.3859	832.65
0.9458	1166.29	-0.3189	549.06	-0.5465	544.29	-0.7499	563.40	-0.9533	809.29	0.1402	689.52	0.3881	839.31
0.9481	1177.03	-0.3225	528.39	-0.5495	541.20	-0.7529	593.96	-0.9563	830.31	0.1425	685.88	0.3903	847.19
0.9503	1182.28	-0.3260	534.53	-0.5525	545.16	-0.7559	563.34	-0.9593	836.10	0.1447	683.43	0.3925	857.38
0.9525	1217.48	-0.3295	534.82	-0.5555	540.91	-0.7589	576.83	-0.9623	846.67	0.1470	683.26	0.3947	865.02
0.9547	1244.97	-0.3330	547.82	-0.5585	567.82	-0.7619	566.83	-0.9653	854.59	0.1492	679.14	0.3970	872.40
0.9569	1265.14	-0.3366	554.47	-0.5615	571.27	-0.7649	568.03	-0.9683	867.93	0.1515	675.14	0.3992	880.34
0.9592	1298.26	-0.3401	544.90	-0.5645	555.84	-0.7679	575.64	-0.9713	879.45	0.1537	671.04	0.4014	888.08
		-0.3436	568.14	-0.5674	553.72	-0.7709	570.05	-0.9743	888.73	0.1560	672.00	0.4036	894.36
		-0.3471	539.18	-0.5704	549.17	-0.7739	567.45	-0.9773	900.27	0.1582	673.70	0.4059	894.46
X/PL	Nu												
-0.0004	1479.60	-0.3507	539.05	-0.5734	539.47	-0.7768	579.58	-0.9803	910.61	0.1605	672.11	0.4081	899.14
-0.0089	1437.44	-0.3542	538.70	-0.5764	558.64	-0.7798	585.42	-0.9833	929.36	0.1627	669.17	0.4103	905.09
-0.0175	1367.31	-0.3577	536.32	-0.5794	574.71	-0.7828	583.47	-0.9863	940.31	0.1650	668.88	0.4125	912.20
-0.0261	1280.20	-0.3612	540.33	-0.5824	587.53	-0.7858	577.62	-0.9892	959.72	0.1672	666.97	0.4147	915.51
-0.0346	1219.90	-0.3647	548.53	-0.5854	581.79	-0.7888	570.68	-0.9922	963.25	0.1695	668.73	0.4170	918.09
-0.0432	1194.64	-0.3683	542.82	-0.5884	570.30	-0.7918	585.09			0.1717	668.47	0.4192	921.89
-0.0517	1109.21	-0.3718	555.31	-0.5914	559.51	-0.7948	595.33			0.1740	666.86	0.4214	922.70
-0.0603	1013.61	-0.3753	554.56	-0.5944	554.92	-0.7978	591.94			0.1762	665.68	0.4236	922.85
-0.0688	955.85	-0.3788	568.66	-0.5974	556.18	-0.8008	619.86			0.1785	667.38	0.4259	928.28
-0.0774	891.40	-0.3824	541.30	-0.6003	590.07	-0.8038	584.55			0.1807	668.76	0.4281	931.93
-0.0859	817.59	-0.3859	541.93	-0.6033	584.52	-0.8068	583.68			0.1830	667.88	0.4303	935.40
-0.0945	755.03	-0.3894	541.31	-0.6063	551.67	-0.8098	585.77			0.1852	669.73	0.4325	941.22
-0.1030	705.63	-0.3929	540.46	-0.6093	543.48	-0.8127	602.24			0.1875	665.74	0.4347	947.08
-0.1116	664.64	-0.3965	542.23	-0.6123	548.45	-0.8157	631.94			0.1897	663.29	0.4370	948.56
-0.1201	630.83	-0.4000	545.60	-0.6153	573.23	-0.8187	621.62			0.1919	661.38	0.4392	952.00
-0.1287	602.42	-0.4035	542.36	-0.6183	573.00	-0.8217	591.23			0.1942	662.76	0.4414	955.37
-0.1372	592.52	-0.4070	544.13	-0.6213	566.21	-0.8247	589.82			0.1964	667.45	0.4436	962.01
-0.1458	580.83	-0.4106	549.43	-0.6243	573.49	-0.8277	594.73			0.1987	663.91	0.4459	964.94
-0.1544	567.94	-0.4141	548.83	-0.6273	558.36	-0.8307	594.13			0.2009	660.08	0.4481	971.39
-0.1629	555.61	-0.4176	544.06	-0.6303	555.66	-0.8337	601.63			0.2032	657.49	0.4503	973.28
-0.1715	548.26	-0.4211	544.85	-0.6333	600.24	-0.8367	605.85			0.2054	664.71	0.4525	972.27
-0.1800	542.00	-0.4247	544.98	-0.6362	560.79	-0.8397	607.57			0.2077	665.22	0.4547	980.44
-0.1886	536.58	-0.4282	550.38	-0.6392	576.34	-0.8427	606.44			0.2099	661.60	0.4570	976.52
-0.1921	532.27	-0.4317	545.92	-0.6422	557.07	-0.8457	610.01			0.2122	661.98	0.4592	981.19
-0.1956	545.14	-0.4352	577.49	-0.6452	581.03	-0.8486	609.55			0.2144	664.77	0.4614	983.28
-0.1991	552.81	-0.4387	546.24	-0.6482	600.56	-0.8516	611.78			0.2167	665.46	0.4636	983.57
-0.2027	520.18	-0.4423	547.64	-0.6512	562.32	-0.8546	620.11			0.2189	661.90	0.4659	986.62
-0.2062	514.66	-0.4458	547.98	-0.6542	601.94	-0.8576	619.83			0.2212	659.57	0.4681	991.06
-0.2097	523.12	-0.4493	547.66	-0.6572	574.98	-0.8606	640.43			0.2234	662.06	0.4703	990.85
-0.2132	510.80	-0.4528	550.30	-0.6602	562.99	-0.8636	632.42			0.2257	660.99	0.4725	989.85
-0.2168	527.40	-0.4564	542.27	-0.6632	566.74	-0.8666	645.49			0.2279	658.66	0.4747	997.22
-0.2203	514.61	-0.4599	541.95	-0.6662	558.22	-0.8696	635.30			0.2302	659.66	0.4770	997.66
-0.2238	536.78	-0.4634	541.35	-0.6692	564.59	-0.8726	630.61			0.2324	656.57	0.4792	1001.19
-0.2273	542.31	-0.4687	552.23	-0.6721	570.29	-0.8756	654.19			0.2346	658.73	0.4814	995.61
-0.2308	553.00	-0.4717	555.13	-0.6751	585.66	-0.8786	649.40			0.2368	660.56	0.4836	999.87
-0.2344	540.31	-0.4747	540.21	-0.6781	582.07	-0.8816	649.46			0.2398	661.62	0.4859	1004.54
-0.2379	543.77	-0.4777	542.12	-0.6811	569.13	-0.8846	650.80			0.2430	663.04	0.4881	1006.13
-0.2414	528.90	-0.4807	552.97	-0.6841	565.87	-0.8875	652.07			0.2461	663.36	0.4903	1011.51
-0.2449	528.85	-0.4837	548.45	-0.6871	568.45	-0.8905	661.77			0.2493	663.28	0.4925	1014.77
-0.2485	569.37	-0.4867	562.73	-0.6901	569.05	-0.8935	668.05			0.2525	665.77	0.4947	1018.29

CASE J – Nu

X/SL Nu

0.0301	1435.86	0.1807	668.76	0.4281	931.93
0.0324	1517.77	0.1830	667.88	0.4303	935.40
0.0346	1457.39	0.1852	669.73	0.4325	941.22
0.0368	1437.85	0.1875	665.74	0.4347	947.08
0.0391	1392.86	0.1897	663.29	0.4370	948.56
0.0413	1307.81	0.1919	661.38	0.4392	952.00
0.0436	1252.93	0.1942	662.76	0.4414	955.37
0.0458	1214.56	0.1964	667.45	0.4436	962.01
0.0481	1180.48	0.1987	663.91	0.4459	964.94
0.0503	1136.67	0.2009	660.08	0.4481	971.39
0.0526	1099.99	0.2032	657.49	0.4503	973.28
0.0548	1073.18	0.2054	664.71	0.4525	972.27
0.0571	1041.67	0.2077	665.22	0.4547	980.44
0.0593	1013.53	0.2099	661.60	0.4570	976.52
0.0616	986.54	0.2122	661.98	0.4592	981.19
0.0638	959.28	0.2144	664.77	0.4614	983.28
0.0661	940.30	0.2167	665.46	0.4636	983.57
0.0683	929.31	0.2189	661.90	0.4659	986.62
0.0706	915.02	0.2212	659.57	0.4681	991.06
0.0728	896.98	0.2234	662.06	0.4703	990.85
0.0751	887.76	0.2257	660.99	0.4725	989.85
0.0773	874.59	0.2279	658.66	0.4747	997.22
0.0796	864.83	0.2302	659.66	0.4770	997.66
0.0818	854.67	0.2324	656.57	0.4792	1001.19
0.0841	840.15	0.2346	658.73	0.4814	995.

Appendix 7.2 – Data for Spanwise Averaged Nusselt Number and Film Cooling Effectiveness

0.4970	1018.81	0.6481	953.10	0.7992	825.39	0.9503	1137.53	-0.3337	558.80	-0.5286	600.14	-0.7320	612.74
0.4992	1022.89	0.6503	952.48	0.8014	826.06	0.9525	1155.92	-0.3372	563.52	-0.5315	598.54	-0.7350	725.08
0.5014	1027.95	0.6525	946.46	0.8036	824.66	0.9547	1179.47	-0.3407	563.58	-0.5345	603.54	-0.7380	741.41
0.5036	1023.45	0.6547	944.55	0.8058	825.15	0.9569	1202.26	-0.3443	564.16	-0.5375	600.06	-0.7409	746.10
0.5059	1030.36	0.6570	965.08	0.8081	829.73	0.9592	1239.33	-0.3478	560.57	-0.5405	617.08	-0.7439	606.93
0.5081	1032.30	0.6592	943.35	0.8103	831.31			-0.3513	564.71	-0.5435	598.53	-0.7469	595.66
0.5103	1034.23	0.6614	931.55	0.8125	829.39	X/PL	Nu	-0.3548	579.72	-0.5465	607.21	-0.7499	620.62
0.5125	1039.73	0.6636	925.60	0.8147	831.04	-0.0332	1351.71	-0.3584	567.82	-0.5495	611.09	-0.7529	616.31
0.5147	1043.55	0.6658	925.11	0.8169	826.52	-0.0418	1229.33	-0.3619	580.78	-0.5525	602.63	-0.7559	636.56
0.5170	1044.09	0.6681	917.34	0.8192	829.48	-0.0503	1112.11	-0.3654	578.64	-0.5555	600.82	-0.7589	630.01
0.5192	1048.93	0.6703	925.34	0.8214	831.54	-0.0589	1042.18	-0.3689	560.66	-0.5585	596.52	-0.7619	636.90
0.5214	1053.65	0.6725	921.07	0.8236	825.04	-0.0675	972.50	-0.3724	565.07	-0.5615	604.35	-0.7649	642.12
0.5236	1057.19	0.6747	916.48	0.8258	832.49	-0.0760	883.63	-0.3760	565.93	-0.5645	619.38	-0.7679	580.78
0.5259	1064.90	0.6770	919.97	0.8281	833.85	-0.0846	805.08	-0.3795	565.47	-0.5674	600.67	-0.7709	604.91
0.5281	1066.36	0.6792	918.52	0.8303	831.35	-0.0931	750.77	-0.3830	563.64	-0.5704	590.48	-0.7739	642.90
0.5303	1067.41	0.6814	911.82	0.8325	825.17	-0.1017	708.66	-0.3865	566.63	-0.5734	586.97	-0.7768	629.26
0.5325	1072.38	0.6836	901.37	0.8347	827.65	-0.1102	666.23	-0.3901	571.16	-0.5764	591.85	-0.7798	602.11
0.5347	1081.65	0.6858	907.36	0.8369	835.63	-0.1188	634.22	-0.3936	567.94	-0.5794	593.66	-0.7828	605.73
0.5370	1085.80	0.6881	903.47	0.8392	835.32	-0.1273	626.60	-0.3971	568.84	-0.5824	599.12	-0.7858	633.56
0.5392	1082.75	0.6903	899.90	0.8414	840.05	-0.1359	614.92	-0.4006	574.30	-0.5854	598.37	-0.7888	646.27
0.5414	1087.93	0.6925	901.01	0.8436	824.15	-0.1444	598.69	-0.4042	573.73	-0.5884	603.10	-0.7918	639.76
0.5436	1095.38	0.6947	895.45	0.8458	818.57	-0.1530	585.07	-0.4077	568.28	-0.5914	587.19	-0.7948	659.65
0.5459	1094.99	0.6970	898.48	0.8481	813.45	-0.1615	575.26	-0.4112	568.49	-0.5944	597.22	-0.7978	654.89
0.5481	1099.68	0.6992	896.72	0.8503	815.27	-0.1701	573.88	-0.4147	568.54	-0.5974	607.69	-0.8008	650.97
0.5503	1106.10	0.7014	904.00	0.8525	818.84	-0.1786	565.01	-0.3999	583.22	-0.6003	585.19	-0.8038	660.32
0.5525	1108.10	0.7036	896.44	0.8547	849.97	-0.1822	559.23	-0.3999	573.31	-0.6033	588.57	-0.8068	647.49
0.5547	1111.74	0.7058	894.85	0.8569	826.08	-0.1857	570.50	-0.4029	589.82	-0.6063	591.68	-0.8098	633.51
0.5570	1112.71	0.7081	889.14	0.8592	821.97	-0.1892	583.38	-0.4059	579.09	-0.6093	578.72	-0.8127	642.57
0.5592	1110.32	0.7103	884.50	0.8614	814.27	-0.1927	546.43	-0.4089	572.85	-0.6123	561.67	-0.8157	654.52
0.5614	1109.68	0.7125	876.01	0.8636	818.56	-0.1963	540.48	-0.4119	547.32	-0.6153	516.74	-0.8187	656.50
0.5636	1115.36	0.7147	873.88	0.8658	817.45	-0.1998	550.92	-0.4149	569.56	-0.6183	491.33	-0.8217	643.49
0.5658	1111.91	0.7170	878.98	0.8681	822.19	-0.2033	537.06	-0.4179	572.73	-0.6213	586.40	-0.8247	666.15
0.5681	1108.31	0.7192	872.63	0.8703	811.85	-0.2068	552.85	-0.4209	569.57	-0.6243	594.20	-0.8277	685.37
0.5703	1105.27	0.7214	868.48	0.8725	809.59	-0.2104	540.69	-0.4238	572.42	-0.6273	601.48	-0.8307	681.92
0.5725	1105.44	0.7236	867.36	0.8747	822.35	-0.2139	554.13	-0.4268	571.65	-0.6303	609.28	-0.8337	668.45
0.5747	1102.24	0.7258	871.14	0.8769	824.78	-0.2174	587.38	-0.4298	559.25	-0.6333	605.75	-0.8367	667.97
0.5770	1089.24	0.7281	868.40	0.8792	832.26	-0.2209	591.01	-0.4328	587.84	-0.6362	626.15	-0.8397	673.40
0.5792	1088.57	0.7303	861.31	0.8814	834.61	-0.2245	566.86	-0.4358	576.24	-0.6392	632.58	-0.8427	673.51
0.5814	1083.12	0.7325	860.89	0.8836	842.89	-0.2280	536.24	-0.4388	584.38	-0.6422	634.82	-0.8457	670.03
0.5836	1080.68	0.7347	862.58	0.8858	849.44	-0.2315	556.19	-0.4418	606.35	-0.6452	628.74	-0.8486	660.28
0.5858	1071.34	0.7370	864.24	0.8881	853.32	-0.2350	554.51	-0.4448	609.98	-0.6482	607.66	-0.8516	686.95
0.5881	1063.65	0.7392	863.29	0.8903	866.89	-0.2385	600.96	-0.4478	572.46	-0.6512	609.89	-0.8546	679.49
0.5903	1061.93	0.7414	857.54	0.8925	889.03	-0.2421	577.07	-0.4508	581.54	-0.6542	596.05	-0.8576	690.73
0.5925	1055.85	0.7436	850.34	0.8947	890.06	-0.2456	578.54	-0.4538	588.20	-0.6572	593.23	-0.8606	702.12
0.5947	1047.85	0.7458	848.10	0.8969	887.10	-0.2491	602.93	-0.4568	594.93	-0.6602	609.64	-0.8636	728.14
0.5970	1044.11	0.7481	842.34	0.8992	887.37	-0.2526	570.95	-0.4597	582.08	-0.6632	602.24	-0.8666	706.97
0.5992	1042.77	0.7503	843.50	0.9014	899.70	-0.2562	545.41	-0.4627	587.44	-0.6662	592.22	-0.8696	715.60
0.6014	1037.65	0.7525	848.32	0.9036	904.67	-0.2597	563.15	-0.4657	590.13	-0.6692	615.28	-0.8726	707.63
0.6036	1031.38	0.7547	841.29	0.9058	914.83	-0.2632	573.60	-0.4687	589.89	-0.6721	617.42	-0.8756	732.70
0.6058	1029.97	0.7570	837.46	0.9081	917.95	-0.2667	579.26	-0.4717	600.69	-0.6751	610.22	-0.8786	745.35
0.6081	1028.37	0.7592	832.95	0.9103	919.69	-0.2703	570.79	-0.4747	607.12	-0.6781	603.23	-0.8816	733.95
0.6103	1019.62	0.7614	835.91	0.9125	933.45	-0.2738	558.57	-0.4777	594.44	-0.6811	602.19	-0.8845	738.63
0.6125	1016.55	0.7636	837.09	0.9147	940.44	-0.2773	584.11	-0.4807	596.17	-0.6841	606.75	-0.8875	723.41
0.6147	1007.96	0.7658	839.31	0.9169	955.58	-0.2808	633.27	-0.4837	573.84	-0.6871	615.31	-0.8905	730.81
0.6170	1005.66	0.7681	831.81	0.9192	965.17	-0.2844	631.45	-0.4867	582.49	-0.6901	625.52	-0.8935	748.65
0.6192	1005.44	0.7703	826.03	0.9214	975.05	-0.2879	566.13	-0.4897	565.42	-0.6931	606.71	-0.8965	774.81
0.6214	999.44	0.7725	834.05	0.9236	979.53	-0.2914	584.13	-0.4927	584.14	-0.6961	609.03	-0.8995	770.53
0.6236	993.94	0.7747	833.39	0.9258	986.87	-0.2949	585.27	-0.4956	708.98	-0.6991	616.46	-0.9025	780.00
0.6258	990.21	0.7770	829.23	0.9281	1000.35	-0.2984	558.65	-0.4986	604.59	-0.7021	619.54	-0.9055	780.51
0.6281	988.47	0.7792	830.73	0.9303	1015.12	-0.3020	564.06	-0.5016	584.99	-0.7051	623.67	-0.9085	772.31
0.6303	981.48	0.7814	828.89	0.9325	1030.24	-0.3055	573.27	-0.5046	590.16	-0.7080	637.23	-0.9115	772.43
0.6325	979.93	0.7836	828.32	0.9347	1042.60	-0.3090	578.94	-0.5076	672.90	-0.7110	638.60	-0.9145	787.17
0.6347	967.01	0.7858	827.00	0.9369	1050.42	-0.3125	554.00	-0.5106	671.15	-0.7140	637.66	-0.9174	795.84
0.6370	966.42	0.7881	829.12	0.9392	1070.82	-0.3161	559.24	-0.5136	599.39	-0.7170	597.13	-0.9204	811.93
0.6392	969.99	0.7903	835.48	0.9414	1085.32	-0.3196	559.36	-0.5166	609.12	-0.7200	616.98	-0.9234	808.85
0.6414	972.13	0.7925	830.43	0.9436	1104.39	-0.3231	572.19	-0.5196	610.68	-0.7230	600.68	-0.9264	805.64
0.6436	965.15	0.7947	823.05	0.9458	1117.88	-0.3266	579.76	-0.5226	600.23	-0.7260	596.05	-0.9294	808.10
0.6458	956.29	0.7969	822.32	0.9481	1127.63	-0.3302	570.34	-0.5256	590.58	-0.7290	601.86	-0.9324	834.66

Appendix 7.2 – Data for Spanwise Averaged Nusselt Number and Film Cooling Effectiveness

-0.9354	799.05	0.1276	779.47	0.2877	700.69	0.5281	1018.95	0.6792	890.07	0.8303	776.91	-0.0655	1064.89
-0.9384	858.66	0.1297	775.84	0.2909	704.98	0.5303	1016.42	0.6814	885.62	0.8325	776.53	-0.0740	967.02
-0.9414	881.38	0.1318	778.99	0.2941	699.63	0.5325	1019.11	0.6836	875.92	0.8347	782.29	-0.0826	880.62
-0.9444	883.64	0.1339	782.30	0.2973	700.22	0.5347	1027.05	0.6858	876.92	0.8369	786.73	-0.0911	820.79
-0.9474	896.43	0.1360	772.87	0.3005	703.22	0.5370	1032.55	0.6881	871.65	0.8392	784.25	-0.0997	774.19
-0.9504	874.95	0.1381	758.95	0.3881	819.59	0.5392	1032.78	0.6903	868.32	0.8414	781.48	-0.1082	727.33
-0.9533	935.40	0.1402	761.38	0.3903	825.14	0.5414	1033.90	0.6925	861.80	0.8436	778.15	-0.1168	691.89
-0.9563	972.44	0.1423	757.95	0.3925	831.00	0.5436	1036.82	0.6947	866.53	0.8458	781.46	-0.1253	683.17
-0.9593	973.26	0.1444	752.02	0.3947	838.01	0.5459	1041.84	0.6970	865.04	0.8481	781.27	-0.1339	670.04
-0.9623	973.51	0.1464	751.20	0.3970	844.94	0.5481	1045.91	0.6992	855.69	0.8503	783.88	-0.1424	651.91
-0.9653	998.87	0.1485	747.60	0.3992	851.77	0.5503	1047.14	0.7014	856.73	0.8525	779.17	-0.1510	636.70
-0.9683	993.30	0.1506	743.28	0.4014	858.40	0.5525	1049.54	0.7036	855.77	0.8547	779.26	-0.1596	625.63
-0.9713	1008.55	0.1527	741.09	0.4036	863.42	0.5547	1048.32	0.7058	853.68	0.8569	775.26	-0.1681	623.76
-0.9743	1027.76	0.1548	741.31	0.4059	867.74	0.5570	1053.39	0.7081	855.88	0.8592	779.16	-0.1767	613.76
-0.9773	1045.35	0.1569	736.56	0.4081	873.58	0.5592	1052.26	0.7103	851.09	0.8614	777.76	-0.1802	607.12
-0.9803	1072.22	0.1590	731.51	0.4103	880.52	0.5614	1053.33	0.7125	848.97	0.8636	782.55	-0.1837	619.02
-0.9833	1068.73	0.1611	730.86	0.4125	883.79	0.5636	1057.62	0.7147	843.58	0.8658	788.25	-0.1872	632.68
-0.9863	1081.42	0.1632	735.85	0.4147	886.11	0.5658	1055.24	0.7170	846.28	0.8681	787.88	-0.1908	592.21
-0.9892	1110.48	0.1653	735.42	0.4170	890.33	0.5681	1051.60	0.7192	842.82	0.8703	790.98	-0.1943	585.43
		0.1674	735.80	0.4192	892.94	0.5703	1047.42	0.7214	831.19	0.8725	807.20	-0.1978	596.42
		0.1695	734.66	0.4214	896.70	0.5725	1049.72	0.7236	837.19	0.8747	815.00	-0.2013	581.10
		0.1716	730.11	0.4236	896.93	0.5747	1048.51	0.7258	838.81	0.8769	815.71	-0.2048	597.92
		0.1737	728.73	0.4259	898.60	0.5770	1046.93	0.7281	838.68	0.8792	809.73	-0.2084	584.42
		0.1757	732.04	0.4281	903.66	0.5792	1043.91	0.7303	831.90	0.8814	815.14	-0.2119	598.66
		0.1778	730.19	0.4303	905.26	0.5814	1037.39	0.7325	830.27	0.8836	820.59	-0.2225	611.48
		0.1799	726.43	0.4325	910.64	0.5836	1036.23	0.7347	824.57	0.8858	826.72	-0.2260	578.11
		0.1820	728.13	0.4347	916.80	0.5858	1035.27	0.7370	823.16	0.8881	830.03	-0.2295	599.33
		0.1841	728.99	0.4370	919.72	0.5881	1028.86	0.7392	829.07	0.8903	831.29	-0.2330	597.24
		0.1862	723.52	0.4392	923.57	0.5903	1020.11	0.7414	827.40	0.8925	845.59	-0.2401	620.95
		0.1883	714.94	0.4414	925.68	0.5925	1013.39	0.7436	825.74	0.8947	845.02	-0.2436	622.24
		0.1904	717.08	0.4436	927.69	0.5947	1014.38	0.7458	818.71	0.8969	842.10	-0.2471	648.17
		0.1925	722.80	0.4459	930.32	0.5970	1007.49	0.7481	823.41	0.8992	845.49	-0.2507	613.47
		0.1946	721.81	0.4481	933.07	0.5992	1002.01	0.7503	821.09	0.9014	855.91	-0.2542	585.76
		0.1967	716.19	0.4503	936.15	0.6014	997.16	0.7525	819.72	0.9036	869.16	-0.2577	604.55
		0.1988	721.88	0.4525	939.86	0.6036	995.06	0.7547	812.48	0.9058	867.15	-0.2612	615.49
		0.2009	731.94	0.4547	941.15	0.6058	990.51	0.7570	820.23	0.9081	865.77	-0.2648	621.29
		0.2030	724.80	0.4570	946.49	0.6081	992.02	0.7592	807.22	0.9103	874.92	-0.2683	611.92
		0.2050	717.62	0.4592	946.03	0.6103	986.29	0.7614	805.76	0.9125	887.16	-0.2718	598.56
		0.2071	710.33	0.4614	946.93	0.6125	981.19	0.7636	816.30	0.9147	885.04	-0.2753	625.66
		0.2092	707.36	0.4636	948.72	0.6147	975.45	0.7658	804.11	0.9169	895.25	-0.2859	605.63
		0.2113	715.25	0.4659	950.61	0.6170	971.43	0.7681	805.27	0.9192	909.83	-0.2894	624.63
		0.2134	714.09	0.4681	954.29	0.6192	976.50	0.7703	807.57	0.9214	919.41	-0.2929	625.59
		0.2155	708.55	0.4703	956.00	0.6214	970.51	0.7725	799.57	0.9236	926.04	-0.2965	596.90
		0.2176	702.34	0.4725	955.48	0.6236	971.09	0.7747	803.93	0.9258	926.10	-0.3000	602.44
		0.2197	702.50	0.4747	955.25	0.6258	967.51	0.7770	806.40	0.9281	938.42	-0.3035	612.03
		0.2218	705.37	0.4770	960.19	0.6281	965.14	0.7792	804.51	0.9303	956.32	-0.3070	617.86
		0.2239	700.55	0.4792	963.11	0.6303	959.24	0.7814	801.13	0.9325	968.15	-0.3106	590.99
		0.2260	701.65	0.4814	961.15	0.6325	950.89	0.7836	801.47	0.9347	969.10	-0.3141	596.36
		0.2281	705.12	0.4836	964.92	0.6347	948.65	0.7858	801.23	0.9369	980.60	-0.3176	596.25
		0.2302	695.36	0.4859	966.39	0.6370	943.33	0.7881	796.83	0.9392	990.73	-0.3211	609.70
		0.2323	692.31	0.4881	966.70	0.6392	948.57	0.7903	804.05	0.9414	1006.52	-0.3247	617.52
		0.2344	696.31	0.4903	969.40	0.6414	939.86	0.7925	800.94	0.9436	1017.80	-0.3282	607.28
		0.2366	700.64	0.4925	971.62	0.6436	934.32	0.7947	800.80	0.9458	1032.30	-0.3317	594.77
		0.2388	701.40	0.4947	973.17	0.6458	929.14	0.7969	792.31	0.9481	1038.00	-0.3352	599.56
		0.2409	694.66	0.4970	977.79	0.6481	927.45	0.7992	792.14	0.9503	1045.21	-0.3387	599.42
		0.2430	690.86	0.4992	982.47	0.6503	927.45	0.8014	786.85	0.9525	1061.73	-0.3423	599.82
		0.2451	694.55	0.5014	983.92	0.6525	921.28	0.8036	796.44	0.9547	1082.20	-0.3458	595.79
		0.2472	694.69	0.5036	987.24	0.6547	920.08	0.8058	798.27	0.9569	1108.01	-0.3493	599.97
		0.2493	697.67	0.5059	989.65	0.6570	916.08	0.8081	791.24	0.9592	1131.76	-0.3528	615.65
		0.2514	704.49	0.5081	991.55	0.6592	914.34	0.8103	797.10			-0.3564	602.86
		0.2535	721.10	0.5103	992.83	0.6614	912.49	0.8125	792.49	X/PL	Nu	-0.3599	616.40
		0.2556	713.51	0.5125	989.99	0.6636	909.27	0.8147	794.09	-0.0056	1456.59	-0.3634	613.92
		0.2577	710.97	0.5147	997.52	0.6658	912.20	0.8169	785.68	-0.0141	1408.68	-0.3669	594.65
		0.2598	717.80	0.5170	1001.73	0.6681	901.30	0.8192	798.08	-0.0227	1376.72	-0.3705	599.14
		0.2619	706.76	0.5192	1002.12	0.6703	908.43	0.8214	790.76	-0.0313	1484.55	-0.3740	599.84
		0.2640	699.61	0.5214	1006.24	0.6725	899.72	0.8236	790.46	-0.0398	1349.20	-0.3775	599.16
		0.2661	696.30	0.5236	1004.08	0.6747	892.68	0.8258	786.68	-0.0484	1219.49	-0.3810	597.03
		0.2682	704.93	0.5259	1014.82	0.6770	893.57	0.8281	787.00	-0.0569	1141.84	-0.3846	600.01

Appendix 7.2 – Data for Spanwise Averaged Nusselt Number and Film Cooling Effectiveness

-0.3881	604.62	-0.6692	639.22	-0.8726	697.34	0.0906	634.41	0.2224	633.42	0.4681	775.03	0.6192	857.37
-0.3916	601.02	-0.6721	647.40	-0.8756	707.24	0.0926	618.42	0.2243	613.88	0.4703	775.85	0.6214	859.39
-0.3951	601.77	-0.6751	643.32	-0.8786	698.24	0.0945	607.35	0.2263	635.90	0.4725	777.80	0.6236	880.20
-0.3986	607.34	-0.6781	644.56	-0.8816	695.54	0.0965	606.67	0.2282	647.49	0.4747	787.19	0.6258	850.58
-0.4022	606.57	-0.6811	642.04	-0.8845	715.16	0.0984	595.87	0.2302	631.76	0.4770	783.03	0.6281	839.22
-0.4057	600.63	-0.6841	641.40	-0.8875	710.80	0.1003	587.00	0.2302	596.17	0.4792	788.25	0.6303	843.55
-0.4092	600.66	-0.6871	645.90	-0.8905	719.55	0.1023	587.18	0.2334	611.06	0.4814	793.97	0.6325	835.35
-0.4127	600.52	-0.6901	632.42	-0.8935	738.90	0.1042	584.00	0.2366	593.01	0.4836	790.16	0.6347	842.57
-0.4163	606.22	-0.6931	625.21	-0.8965	748.37	0.1061	571.34	0.2398	589.84	0.4859	790.25	0.6370	824.89
-0.4198	603.00	-0.6961	627.00	-0.8995	769.20	0.1081	566.00	0.2430	587.31	0.4881	793.87	0.6392	830.07
-0.4233	634.42	-0.6991	628.41	-0.9025	761.64	0.1100	563.46	0.2461	584.25	0.4903	794.99	0.6414	823.19
-0.4268	601.49	-0.7021	618.12	-0.9055	751.22	0.1120	556.86	0.2493	580.97	0.4925	797.05	0.6436	826.65
-0.4304	602.60	-0.7051	620.52	-0.9174	881.44	0.1139	554.42	0.2525	588.17	0.4947	805.76	0.6458	820.40
-0.4339	603.40	-0.7080	622.38	-0.9204	788.75	0.1158	551.30	0.2557	576.37	0.4970	805.45	0.6481	842.11
-0.4374	603.42	-0.7110	620.64	-0.9234	800.82	0.1178	548.22	0.2589	579.42	0.4992	809.03	0.6503	841.86
-0.4409	607.43	-0.7140	627.63	-0.9264	804.15	0.1197	543.04	0.2621	582.65	0.5014	810.40	0.6525	839.70
-0.3999	584.49	-0.7170	622.32	-0.9294	806.84	0.1216	543.08	0.2653	596.28	0.5036	812.11	0.6547	835.27
-0.4418	559.89	-0.7200	623.08	-0.9324	818.85	0.1236	544.09	0.2685	615.30	0.5059	812.58	0.6570	814.84
-0.4448	566.11	-0.7230	624.72	-0.9354	822.78	0.1255	542.31	0.2717	626.81	0.5081	819.27	0.6592	825.76
-0.4478	560.83	-0.7260	635.70	-0.9384	823.67	0.1275	556.89	0.2749	632.57	0.5103	819.41	0.6614	821.81
-0.4508	564.30	-0.7290	628.30	-0.9414	838.68	0.1294	555.59	0.2781	636.81	0.5125	832.07	0.6636	836.01
-0.4538	563.66	-0.7320	629.98	-0.9444	864.41	0.1313	586.36	0.2813	664.21	0.5147	827.02	0.6658	817.69
-0.4568	576.36	-0.7350	619.35	-0.9474	876.66	0.1333	609.84	0.2845	741.50	0.5170	839.44	0.6681	805.10
-0.4597	574.90	-0.7380	616.47	-0.9504	876.35	0.1352	618.08	0.2877	784.13	0.5192	844.68	0.6703	791.45
-0.4627	568.81	-0.7409	613.76	-0.9533	896.10	0.1371	588.64	0.2909	663.22	0.5214	846.73	0.6725	815.75
-0.4657	568.18	-0.7439	612.56	-0.9563	918.38	0.1391	560.54	0.2941	653.96	0.5236	843.47	0.6747	824.02
-0.4687	573.37	-0.7469	624.44	-0.9593	916.52	0.1410	572.48	0.2973	626.97	0.5259	852.16	0.6770	811.11
-0.4717	567.25	-0.7499	633.78	-0.9623	933.03	0.1430	596.51	0.3005	634.30	0.5281	852.43	0.6792	813.35
-0.4747	585.67	-0.7529	618.20	-0.9653	936.74	0.1449	650.78	0.3037	620.55	0.5303	854.88	0.6814	812.62
-0.4777	579.47	-0.7559	615.24	-0.9683	936.83	0.1468	657.55	0.3069	642.33	0.5325	859.26	0.6836	780.65
-0.4807	635.52	-0.7589	612.44	-0.9713	956.14	0.1488	675.31	0.3836	645.45	0.5347	870.72	0.6858	775.29
-0.4837	624.59	-0.7619	620.79	-0.9743	942.69	0.1507	671.89	0.3859	652.13	0.5370	871.02	0.6881	777.16
-0.5375	618.79	-0.7649	632.30	-0.9773	971.45	0.1526	653.66	0.3881	651.93	0.5392	877.66	0.6903	780.98
-0.5405	636.41	-0.7679	622.44	-0.9803	977.94	0.1546	665.30	0.3903	651.72	0.5414	875.99	0.6925	762.27
-0.5435	594.13	-0.7709	626.90	-0.9833	1029.73	0.1565	664.33	0.3925	658.81	0.5436	894.49	0.6947	761.99
-0.5465	592.54	-0.7739	633.95	-0.9863	1031.52	0.1585	658.51	0.3947	666.04	0.5459	890.35	0.6970	768.55
-0.5495	586.28	-0.7768	615.98	-0.9892	1040.83	0.1604	644.79	0.3970	669.62	0.5481	891.15	0.6992	757.27
-0.5525	586.80	-0.7798	625.15	-0.9922	1042.14	0.1623	636.96	0.3992	672.73	0.5503	900.71	0.7014	747.49
-0.5555	579.75	-0.7828	614.27	CASE I – Nu		0.1643	631.36	0.4014	679.19	0.5525	897.95	0.7036	750.55
-0.5585	578.35	-0.7858	613.74			0.1662	628.05	0.4036	679.06	0.5547	901.90	0.7058	738.38
-0.5615	582.33	-0.7888	613.12	X/SL	Nu	0.1682	630.11	0.4059	688.89	0.5570	914.55	0.7081	746.26
-0.5645	578.19	-0.7918	627.00	0.0383	859.40	0.1701	637.44	0.4081	694.71	0.5592	910.91	0.7103	747.24
-0.5674	654.21	-0.7948	632.59	0.0403	875.57	0.1720	645.68	0.4103	695.82	0.5614	905.84	0.7125	750.70
-0.5704	618.43	-0.7978	641.08	0.0422	883.30	0.1740	632.03	0.4125	697.91	0.5636	915.84	0.7147	761.28
-0.5734	578.35	-0.8008	628.12	0.0441	886.34	0.1759	631.76	0.4147	708.36	0.5658	916.88	0.7170	762.83
-0.5764	587.30	-0.8038	620.94	0.0461	893.12	0.1778	635.81	0.4170	715.35	0.5681	913.28	0.7192	742.45
-0.5914	596.03	-0.8068	618.19	0.0480	898.98	0.1798	631.62	0.4192	720.27	0.5703	914.60	0.7214	747.88
-0.5944	590.54	-0.8098	634.03	0.0499	898.91	0.1817	636.35	0.4214	714.47	0.5725	920.42	0.7236	769.66
-0.5974	595.90	-0.8127	629.60	0.0519	890.14	0.1837	631.23	0.4236	722.66	0.5747	916.68	0.7258	772.37
-0.6003	594.49	-0.8157	637.41	0.0538	867.34	0.1856	657.15	0.4259	723.41	0.5770	914.02	0.7281	769.71
-0.6033	590.26	-0.8187	647.00	0.0558	872.48	0.1875	647.42	0.4281	732.57	0.5792	903.29	0.7303	713.06
-0.6063	644.32	-0.8217	653.82	0.0577	861.51	0.1895	675.40	0.4303	737.35	0.5814	903.10	0.7325	742.57
-0.6093	603.02	-0.8247	645.89	0.0596	857.58	0.1914	697.86	0.4325	740.51	0.5836	907.04	0.7347	753.00
-0.6123	601.64	-0.8277	646.74	0.0616	844.51	0.1933	686.10	0.4347	738.10	0.5858	891.69	0.7370	730.77
-0.6153	611.02	-0.8307	648.62	0.0635	824.26	0.1953	671.51	0.4370	746.16	0.5881	897.46	0.7392	713.81
-0.6183	651.34	-0.8337	655.43	0.0654	801.77	0.1972	680.07	0.4392	746.22	0.5903	888.73	0.7414	721.16
-0.6273	619.50	-0.8367	654.16	0.0674	781.10	0.1992	680.27	0.4414	755.96	0.5925	892.77	0.7436	725.82
-0.6303	610.94	-0.8397	674.43	0.0693	764.76	0.2011	690.02	0.4436	754.11	0.5947	880.02	0.7458	709.35
-0.6362	614.88	-0.8427	667.90	0.0713	740.12	0.2030	675.07	0.4459	755.79	0.5970	876.53	0.7481	706.32
-0.6392	621.87	-0.8457	673.65	0.0732	720.58	0.2050	673.98	0.4481	760.95	0.5992	880.27	0.7503	700.40
-0.6422	577.26	-0.8486	692.15	0.0751	711.27	0.2069	643.46	0.4503	764.18	0.6014	872.23	0.7525	696.85
-0.6452	623.24	-0.8516	685.09	0.0771	703.90	0.2088	652.42	0.4525	761.87	0.6036	881.40	0.7547	704.76
-0.6482	659.44	-0.8546	707.88	0.0790	687.49	0.2108	645.53	0.4547	764.12	0.6058	865.43	0.7570	705.78
-0.6512	623.79	-0.8576	700.23	0.0810	671.65	0.2127	649.19	0.4570	766.77	0.6081	876.97	0.7592	709.90
-0.6572	618.25	-0.8606	800.07	0.0829	665.08	0.2147	635.00	0.4592	772.30	0.6103	888.10	0.7614	715.46
-0.6602	624.02	-0.8636	698.42	0.0848	656.18	0.2166	632.86	0.4614	770.45	0.6125	871.36	0.7636	712.21
-0.6632	625.72	-0.8666	698.69	0.0868	648.82	0.2185	662.88	0.4636	773.13	0.6147	872.58	0.7658	704.91
-0.6662	618.14	-0.8696	698.45	0.0887	637.11	0.2205	640.26	0.4659	774.98	0.6170	870.98	0.7681	692.21

Appendix 7.2 – Data for Spanwise Averaged Nusselt Number and Film Cooling Effectiveness

0.7703	698.34	0.9214	875.99	-0.2901	413.97	-0.5734	384.92	-0.7768	381.22	-0.9803	533.80	0.1566	0.3900
0.7725	704.90	0.9236	885.40	-0.2936	412.13	-0.5764	385.35	-0.7798	381.66	-0.9833	539.77	0.1585	0.3800
0.7747	702.81	0.9258	887.99	-0.2971	418.67	-0.5794	386.39	-0.7828	382.65	-0.9863	548.03	0.1605	0.3860
0.7770	671.63	0.9281	899.93	-0.3007	411.43	-0.5824	386.63	-0.7858	382.69	-0.9892	555.30	0.1624	0.3890
0.7792	685.19	0.9303	916.43	-0.3042	410.25	-0.5854	386.65	-0.7888	381.53	-0.9922	561.36	0.1643	0.3900
0.7814	680.32	0.9325	923.54	-0.3077	409.75	-0.5884	387.22	-0.7918	380.43			0.1663	0.4000
0.7836	700.33	0.9347	943.32	-0.3112	409.70	-0.5914	388.25	-0.7948	380.26			0.1682	0.3780
0.7858	697.15	0.9369	954.17	-0.3148	408.82	-0.5944	389.22	-0.7978	380.54			0.1701	0.3900
0.7881	695.55	0.9392	966.34	-0.3183	406.33	-0.5974	389.99	-0.8008	381.09			0.1721	0.3960
0.7903	684.52	0.9414	980.24	-0.3218	405.06	-0.6003	390.26	-0.8038	381.32			0.1740	0.3990
0.7925	688.99	0.9436	983.67	-0.3253	404.57	-0.6033	389.81	-0.8068	383.06			0.1760	0.4001
0.7947	698.04	0.9458	1012.05	-0.3289	403.96	-0.6063	391.53	-0.8098	383.24			0.1779	0.4000
0.7969	674.37	0.9481	1057.27	-0.3324	403.33	-0.6093	391.91	-0.8127	382.94			0.1798	0.3981
0.7992	693.67	0.9503	1050.95	-0.3359	402.55	-0.6123	392.03	-0.8157	381.55			0.1818	0.4005
0.8014	681.66	0.9525	1008.47	-0.3394	401.97	-0.6153	393.29	-0.8187	382.04			0.1837	0.3980
0.8036	688.49	0.9547	1030.32	-0.3430	402.27	-0.6183	394.51	-0.8217	382.68			0.1856	0.3890
0.8058	678.98	0.9569	1149.22	-0.3465	402.28	-0.6213	396.78	-0.8247	383.83			0.1876	0.3780
0.8081	663.53	0.9592	1207.36	-0.3500	402.43	-0.6243	396.28	-0.8277	385.01			0.1895	0.3900
0.8103	656.50			-0.3535	402.62	-0.6273	396.35	-0.8307	385.70			0.1915	0.4000
0.8125	661.71	X/PL	Nu	-0.3571	403.09	-0.6303	396.04	-0.8337	385.76			0.1934	0.3998
0.8147	655.74	-0.0103	1293.93	-0.3606	403.31	-0.6333	395.90	-0.8367	386.48			0.1953	0.4100
0.8169	652.08	-0.0189	1343.11	-0.3641	403.22	-0.6362	396.95	-0.8397	386.94			0.1973	0.4092
0.8192	648.41	-0.0274	1183.71	-0.3676	402.82	-0.6392	396.57	-0.8427	387.84			0.1992	0.4110
0.8214	649.83	-0.0360	1003.79	-0.3711	403.56	-0.6422	395.30	-0.8457	388.79			0.2011	0.4056
0.8236	656.13	-0.0445	898.47	-0.3747	403.06	-0.6452	395.92	-0.8486	389.06			0.2031	0.4008
0.8258	646.12	-0.0531	773.56	-0.3782	402.65	-0.6482	397.16	-0.8516	389.24			0.2050	0.3951
0.8281	646.05	-0.0616	682.81	-0.3817	401.88	-0.6512	396.54	-0.8546	389.97			0.2070	0.3956
0.8303	645.39	-0.0702	630.46	-0.3852	401.57	-0.6542	396.65	-0.8576	390.84			0.2089	0.3896
0.8325	647.46	-0.0787	587.55	-0.3888	400.40	-0.6572	397.05	-0.8606	392.05			0.2108	0.3955
0.8347	643.29	-0.0873	528.49	-0.3923	400.67	-0.6602	396.58	-0.8636	393.32			0.2128	0.3843
0.8369	646.70	-0.0958	496.25	-0.3958	400.10	-0.6632	396.22	-0.8666	394.56			0.2147	0.3809
0.8392	652.70	-0.1044	463.16	-0.3993	399.59	-0.6662	396.70	-0.8696	396.10			0.2166	0.3866
0.8414	660.37	-0.1130	440.42	-0.4029	399.02	-0.6692	400.44	-0.8726	397.93			0.2186	0.3780
0.8436	649.46	-0.1215	425.49	-0.4064	398.36	-0.6721	397.28	-0.8756	399.42			0.2205	0.3890
0.8458	654.31	-0.1301	405.78	-0.4099	398.30	-0.6751	396.98	-0.8786	400.07			0.2225	0.3786
0.8481	659.42	-0.1386	397.39	-0.4134	398.68	-0.6781	398.42	-0.8816	401.64			0.2244	0.3799
0.8503	666.93	-0.1472	384.37	-0.4170	398.37	-0.6811	397.58	-0.8845	404.23			0.2263	0.3625
0.8525	671.59	-0.1557	397.41	-0.4205	397.76	-0.6841	396.82	-0.8875	406.47			0.2283	0.3539
0.8547	685.07	-0.1643	395.06	-0.4240	397.59	-0.6871	396.04	-0.8905	407.94			0.2302	0.3578
0.8569	681.45	-0.1728	400.23	-0.4275	397.42	-0.6901	397.17	-0.8935	410.46			0.2320	0.3592
0.8592	681.31	-0.1814	383.45	-0.4310	397.57	-0.6931	397.52	-0.8965	412.64			0.2334	0.3617
0.8614	693.28	-0.1899	358.57	-0.4346	397.82	-0.6961	396.77	-0.8995	414.92			0.2366	0.3653
0.8636	702.49	-0.1985	320.80	-0.4381	396.74	-0.6991	396.18	-0.9025	418.02			0.2398	0.3665
0.8658	710.53	-0.2020	326.85	-0.4416	396.47	-0.7021	392.81	-0.9055	421.23			0.2430	0.3659
0.8681	714.48	-0.2055	320.06	-0.4451	396.73	-0.7051	391.70	-0.9085	425.24			0.2462	0.3720
0.8703	715.86	-0.2091	335.54	-0.4487	396.97	-0.7080	391.07	-0.9115	428.13			0.2494	0.3758
0.8725	722.94	-0.2126	354.12	-0.4522	396.60	-0.7110	391.33	-0.9145	430.80			0.2526	0.3737
0.8747	719.00	-0.2161	346.68	-0.4557	396.34	-0.7140	390.60	-0.9174	434.32			0.2558	0.3751
0.8769	734.61	-0.2196	348.81	-0.4592	394.72	-0.7170	389.04	-0.9204	438.64			0.2590	0.3818
0.8792	747.67	-0.2232	380.76	-0.4628	392.64	-0.7200	388.20	-0.9234	441.87			0.2622	0.3828
0.8814	751.68	-0.2267	362.20	-0.4663	391.44	-0.7230	388.16	-0.9264	445.56			0.2654	0.3832
0.8836	756.16	-0.2302	356.26	-0.4698	389.97	-0.7260	388.83	-0.9294	448.97			0.2686	0.3946
0.8858	765.61	-0.2337	372.38	-0.4733	388.77	-0.7290	387.70	-0.9324	453.20			0.2718	0.4016
0.8881	767.93	-0.2372	383.88	-0.4769	387.50	-0.7320	384.72	-0.9354	456.41			0.2750	0.3860
0.8903	769.08	-0.2408	392.37	-0.4804	385.33	-0.7350	384.46	-0.9384	461.42			0.2782	0.4203
0.8925	778.32	-0.2443	406.41	-0.4839	384.15	-0.7380	385.66	-0.9414	464.87			0.2814	0.4807
0.8947	779.59	-0.2478	408.40	-0.4874	382.15	-0.7409	386.65	-0.9444	469.99			0.2846	0.5131
0.8969	790.27	-0.2513	419.36	-0.4910	381.10	-0.7439	386.83	-0.9474	473.04			0.2878	0.5311
0.8992	801.55	-0.2549	422.76	-0.5435	382.06	-0.7469	384.57	-0.9504	476.91			0.2910	0.4202
0.9014	804.23	-0.2584	423.05	-0.5465	381.84	-0.7499	382.98	-0.9533	482.15			0.2942	0.5410
0.9036	810.36	-0.2619	419.26	-0.5495	380.87	-0.7529	382.28	-0.9563	485.54			0.2974	0.5335
0.9058	817.55	-0.2654	414.46	-0.5525	381.78	-0.7559	381.66	-0.9593	490.87			0.3006	0.5535
0.9081	822.79	-0.2690	404.96	-0.5555	381.62	-0.7589	381.57	-0.9623	495.67			0.3038	0.5662
0.9103	828.06	-0.2725	412.86	-0.5585	382.02	-0.7619	381.22	-0.9653	501.13			0.3069	0.4338
0.9125	844.81	-0.2760	411.27	-0.5615	382.55	-0.7649	380.43	-0.9683	507.41			0.3837	0.3678
0.9147	847.17	-0.2795	417.92	-0.5645	383.24	-0.7679	380.16	-0.9713	512.89			0.3837	0.3535
0.9169	848.88	-0.2831	415.79	-0.5674	384.02	-0.7709	380.36	-0.9743	519.75			0.3859	0.3380
0.9192	866.66	-0.2866	414.50	-0.5704	385.12	-0.7739	380.76	-0.9773	526.29			0.3881	0.3345

CASE L - η

X/SL η

Appendix 7.2 – Data for Spanwise Averaged Nusselt Number and Film Cooling Effectiveness

0.3904	0.3383	0.5415	0.2397	0.6926	0.1922	0.8481	0.0899	-0.2020	0.2658	-0.4416	0.1829	-0.6631	0.1447
0.3926	0.3403	0.5437	0.2392	0.6948	0.1982	0.8503	0.0880	-0.2055	0.2457	-0.4451	0.1820	-0.6661	0.1442
0.3948	0.3254	0.5459	0.2335	0.6970	0.2047	0.8526	0.0873	-0.2090	0.2517	-0.4486	0.1829	-0.6691	0.1477
0.3970	0.3193	0.5481	0.2283	0.6992	0.1776	0.8548	0.1076	-0.2125	0.2513	-0.4521	0.1811	-0.6721	0.1434
0.3992	0.3457	0.5503	0.2421	0.7014	0.1780	0.8570	0.1052	-0.2161	0.2684	-0.4557	0.1786	-0.6751	0.1414
0.4015	0.3375	0.5526	0.2269	0.7037	0.1750	0.8592	0.1025	-0.2196	0.2898	-0.4592	0.1778	-0.6781	0.1426
0.4037	0.3403	0.5548	0.2198	0.7059	0.1702	0.8614	0.1059	-0.2231	0.3153	-0.4627	0.1786	-0.6811	0.1370
0.4059	0.3463	0.5570	0.2233	0.7081	0.1742	0.8637	0.1152	-0.2266	0.2787	-0.4662	0.1783	-0.6841	0.1376
0.4081	0.3533	0.5592	0.2277	0.7103	0.1942	0.8659	0.1000	-0.2302	0.2598	-0.4698	0.1771	-0.6871	0.1357
0.4104	0.3513	0.5615	0.2250	0.7126	0.1711	0.8681	0.0950	-0.2337	0.2683	-0.4733	0.1774	-0.6900	0.1379
0.4126	0.3433	0.5637	0.2359	0.7148	0.1851	0.8703	0.0890	-0.2372	0.2701	-0.4768	0.1779	-0.6930	0.1380
0.4148	0.3453	0.5659	0.2265	0.7170	0.1945	0.8726	0.0930	-0.2407	0.2777	-0.4803	0.1733	-0.6960	0.1368
0.4170	0.3484	0.5681	0.2209	0.7192	0.1932	0.8748	0.0880	-0.2442	0.2861	-0.4839	0.1725	-0.6990	0.1400
0.4192	0.3512	0.5703	0.2117	0.7214	0.1909	0.8770	0.0940	-0.2478	0.2798	-0.4874	0.1689	-0.7020	0.1328
0.4215	0.3438	0.5726	0.2250	0.7237	0.1990	0.8792	0.1000	-0.2513	0.2866	-0.4909	0.1718	-0.7050	0.1300
0.4237	0.3361	0.5748	0.2253	0.7259	0.1898	0.8814	0.1030	-0.2548	0.2938	-0.4944	0.1718	-0.7080	0.1309
0.4259	0.3352	0.5770	0.2175	0.7281	0.2029	0.8837	0.1100	-0.2583	0.3098	-0.4979	0.1712	-0.7110	0.1297
0.4281	0.3373	0.5792	0.1997	0.7303	0.1696	0.8859	0.1200	-0.2619	0.3177	-0.5015	0.1705	-0.7140	0.1281
0.4304	0.3361	0.5815	0.2026	0.7326	0.1902	0.8881	0.1230	-0.2654	0.3223	-0.5050	0.1700	-0.7170	0.1229
0.4326	0.3362	0.5837	0.2247	0.7348	0.2032	0.8903	0.1020	-0.2689	0.3045	-0.5085	0.1661	-0.7200	0.1215
0.4348	0.3316	0.5859	0.2168	0.7370	0.1869	0.8926	0.1000	-0.2724	0.3080	-0.5120	0.1659	-0.7230	0.1207
0.4370	0.3367	0.5881	0.2241	0.7392	0.1720	0.8948	0.1100	-0.2760	0.2918	-0.5156	0.1665	-0.7259	0.1220
0.4392	0.3281	0.5903	0.2131	0.7414	0.1727	0.8970	0.1200	-0.2795	0.2908	-0.5191	0.1654	-0.7289	0.1209
0.4415	0.3317	0.5926	0.2207	0.7437	0.1802	0.8992	0.0890	-0.2830	0.2728	-0.5226	0.1663	-0.7319	0.1115
0.4437	0.3327	0.5948	0.2031	0.7459	0.1749	0.9014	0.1040	-0.2865	0.2682	-0.5261	0.1691	-0.7349	0.1140
0.4459	0.3313	0.5970	0.2061	0.7481	0.1630	0.9037	0.0890	-0.2901	0.2752	-0.5297	0.1652	-0.7379	0.1184
0.4481	0.3308	0.5992	0.2117	0.7503	0.1582	0.9059	0.0960	-0.2936	0.2716	-0.5332	0.1649	-0.7409	0.1213
0.4503	0.3313	0.6015	0.2255	0.7526	0.1568	0.9081	0.0990	-0.2971	0.2863	-0.5367	0.1640	-0.7439	0.1204
0.4526	0.3277	0.6037	0.2082	0.7548	0.1690	0.9103	0.1100	-0.3006	0.2730	-0.5402	0.1612	-0.7469	0.1158
0.4548	0.3211	0.6059	0.1951	0.7570	0.1650	0.9126	0.1200	-0.3041	0.2646	-0.5438	0.1590	-0.7499	0.1142
0.4570	0.3271	0.6081	0.2035	0.7592	0.1716	0.9148	0.1080	-0.3077	0.2553	-0.5473	0.1583	-0.7529	0.1125
0.4592	0.3208	0.6103	0.2245	0.7614	0.1698	0.9170	0.1100	-0.3112	0.2577	-0.5508	0.1570	-0.7559	0.1123
0.4615	0.3232	0.6126	0.2113	0.7637	0.1641	0.9192	0.0990	-0.3147	0.2489	-0.5543	0.1549	-0.7588	0.1126
0.4637	0.3219	0.6148	0.2110	0.7659	0.1668	0.9214	0.1000	-0.3182	0.2375	-0.5579	0.1553	-0.7618	0.1122
0.4659	0.3206	0.6170	0.2154	0.7681	0.1555	0.9237	0.1060	-0.3218	0.2313	-0.5614	0.1545	-0.7648	0.1097
0.4681	0.3228	0.6192	0.2161	0.7703	0.1571	0.9259	0.1276	-0.3253	0.2282	-0.5649	0.1502	-0.7678	0.1080
0.4703	0.3163	0.6215	0.2178	0.7726	0.1651	0.9281	0.1308	-0.3288	0.2238	-0.5684	0.1375	-0.7708	0.1096
0.4726	0.3092	0.6237	0.2232	0.7748	0.1683	0.9303	0.1100	-0.3323	0.2140	-0.5704	0.1358	-0.7738	0.1107
0.4748	0.3135	0.6259	0.2054	0.7770	0.1485	0.9325	0.1178	-0.3359	0.2116	-0.5734	0.1359	-0.7768	0.1141
0.4770	0.3093	0.6281	0.2112	0.7792	0.1538	0.9348	0.1160	-0.3394	0.2064	-0.5764	0.1345	-0.7798	0.1139
0.4792	0.3042	0.6303	0.2106	0.7814	0.1486	0.9370	0.1219	-0.3429	0.2040	-0.5794	0.1378	-0.7828	0.1166
0.4815	0.3066	0.6326	0.2036	0.7837	0.1569	0.9392	0.1150	-0.3464	0.2011	-0.5823	0.1374	-0.7858	0.1140
0.4837	0.3062	0.6348	0.2037	0.7859	0.1541	0.9414	0.1194	-0.3500	0.2000	-0.5853	0.1388	-0.7888	0.1111
0.4859	0.3004	0.6370	0.1897	0.7881	0.1565	0.9437	0.1027	-0.3535	0.2012	-0.5883	0.1405	-0.7918	0.1118
0.4881	0.2937	0.6392	0.1928	0.7903	0.1463	0.9459	0.0780	-0.3570	0.2041	-0.5913	0.1407	-0.7947	0.1113
0.4903	0.2842	0.6415	0.1913	0.7926	0.1505	0.9481	0.0933	-0.3605	0.2059	-0.5943	0.1450	-0.7977	0.1111
0.4926	0.2921	0.6437	0.1854	0.7948	0.1571	0.9503	0.1482	-0.3640	0.2031	-0.5973	0.1453	-0.8007	0.1118
0.4948	0.2923	0.6459	0.2131	0.7970	0.1384	0.9525	0.1207	-0.3676	0.2032	-0.6003	0.1439	-0.8037	0.1116
0.4970	0.2918	0.6481	0.2175	0.7992	0.1523	0.9548	0.0420	-0.3711	0.2068	-0.6033	0.1447	-0.8067	0.1163
0.4992	0.2852	0.6503	0.2212	0.8014	0.1428	0.9570	0.0695	-0.3746	0.2027	-0.6063	0.1461	-0.8097	0.1109
0.5015	0.2837	0.6526	0.2007	0.8037	0.1499	0.9592	0.1065	-0.3781	0.2029	-0.6093	0.1468	-0.8127	0.1095
0.5037	0.2830	0.6548	0.1982	0.8059	0.1418			-0.3817	0.2004	-0.6123	0.1471	-0.8157	0.1037
0.5059	0.2721	0.6570	0.2090	0.8081	0.1284	X/PL	η	-0.3852	0.1983	-0.6153	0.1454	-0.8187	0.1011
0.5081	0.2758	0.6592	0.2045	0.8103	0.1171	-0.0787	0.4259	-0.3887	0.1967	-0.6182	0.1484	-0.8217	0.1002
0.5103	0.2696	0.6615	0.2001	0.8126	0.1206	-0.0872	0.3484	-0.3922	0.2005	-0.6212	0.1528	-0.8247	0.1015
0.5126	0.2657	0.6637	0.2184	0.8148	0.1136	-0.0958	0.3135	-0.3958	0.1980	-0.6242	0.1541	-0.8277	0.1038
0.5148	0.2688	0.6659	0.2184	0.8170	0.1089	-0.1044	0.2959	-0.3993	0.1969	-0.6272	0.1519	-0.8306	0.1058
0.5170	0.2710	0.6681	0.2155	0.8192	0.0996	-0.1129	0.2876	-0.4028	0.1948	-0.6302	0.1530	-0.8336	0.1074
0.5192	0.2718	0.6703	0.1916	0.8214	0.0992	-0.1215	0.2805	-0.4063	0.1923	-0.6332	0.1508	-0.8366	0.1064
0.5215	0.2717	0.6726	0.1899	0.8237	0.1080	-0.1300	0.2601	-0.4099	0.1921	-0.6362	0.1502	-0.8396	0.1025
0.5237	0.2596	0.6748	0.2197	0.8259	0.0972	-0.1386	0.2730	-0.4134	0.1942	-0.6392	0.1479	-0.8426	0.1026
0.5259	0.2604	0.6770	0.1988	0.8281	0.1014	-0.1471	0.2805	-0.4169	0.1957	-0.6422	0.1487	-0.8456	0.1034
0.5281	0.2561	0.6792	0.2098	0.8348	0.0911	-0.1557	0.2977	-0.4204	0.1943	-0.6452	0.1484	-0.8486	0.1004
0.5303	0.2526	0.6814	0.2146	0.8370	0.0935	-0.1642	0.3125	-0.4240	0.1929	-0.6482	0.1510	-0.8516	0.1022
0.5326	0.2399	0.6837	0.1907	0.8392	0.0936	-0.1728	0.3302	-0.4275	0.1937	-0.6512	0.1473	-0.8546	0.0999
0.5348	0.2492	0.6859	0.1955	0.8414	0.0949	-0.1813	0.3435	-0.4310	0.1930	-0.6541	0.1475	-0.8576	0.1027
0.5370	0.2471	0.6881	0.1972	0.8437	0.0878	-0.1899	0.3384	-0.4345	0.1918	-0.6571	0.1509	-0.8606	0.0998
0.5392	0.2506	0.6903	0.1870	0.8459	0.0880	-0.1984	0.2931	-0.4380	0.1857	-0.6601	0.1491	-0.8636	0.0932

Appendix 7.2 – Data for Spanwise Averaged Nusselt Number and Film Cooling Effectiveness

-0.8665	0.0897	0.0887	658.45	0.2205	628.57	0.4659	745.52	0.6170	865.34	0.7681	678.71	0.9192	783.47
-0.8695	0.0916	0.0906	645.24	0.2224	623.15	0.4681	748.54	0.6192	869.32	0.7703	678.84	0.9214	794.48
-0.8725	0.0953	0.0926	643.29	0.2243	611.64	0.4703	754.95	0.6214	858.07	0.7725	680.85	0.9236	804.62
-0.8755	0.0928	0.0945	627.88	0.2263	610.34	0.4725	755.48	0.6236	851.68	0.7747	676.93	0.9258	811.47
-0.8785	0.0897	0.0965	615.23	0.2282	607.91	0.4747	764.58	0.6258	847.10	0.7770	678.80	0.9281	820.10
-0.8815	0.0900	0.0984	600.32	0.2302	603.13	0.4770	767.63	0.6281	861.50	0.7792	674.72	0.9303	825.40
-0.8845	0.0928	0.1003	596.82	0.2302	599.34	0.4792	778.86	0.6303	842.88	0.7814	685.94	0.9325	840.20
-0.8875	0.0939	0.1023	591.28	0.2334	593.42	0.4814	785.07	0.6325	833.02	0.7836	670.77	0.9347	851.87
-0.8905	0.0920	0.1042	579.64	0.2366	597.58	0.4836	787.53	0.6347	835.24	0.7858	669.86	0.9369	872.50
-0.8935	0.0936	0.1061	572.24	0.2398	592.88	0.4859	795.82	0.6370	836.85	0.7881	684.50	0.9392	876.91
-0.8965	0.0939	0.1081	578.04	0.2430	591.88	0.4881	802.09	0.6392	834.86	0.7903	671.83	0.9414	892.67
-0.8995	0.0935	0.1100	574.36	0.2461	594.71	0.4903	806.43	0.6414	825.66	0.7925	665.29	0.9436	896.84
-0.9024	0.0955	0.1120	538.47	0.2493	592.63	0.4925	808.26	0.6436	820.70	0.7947	666.70	0.9458	907.61
-0.9054	0.0967	0.1139	527.58	0.2525	592.96	0.4947	811.67	0.6458	822.91	0.7969	674.90	0.9481	923.26
-0.9084	0.0979	0.1158	534.96	0.2557	596.22	0.4970	819.01	0.6481	835.30	0.7992	668.90	0.9503	937.29
-0.9114	0.0971	0.1178	566.88	0.2589	599.34	0.4992	828.46	0.6503	823.33	0.8014	665.20	0.9525	957.62
-0.9144	0.0961	0.1197	566.12	0.2621	602.47	0.5014	829.67	0.6525	802.42	0.8036	660.60	0.9547	969.02
-0.9174	0.0964	0.1216	544.27	0.2653	606.08	0.5036	834.11	0.6547	806.63	0.8058	658.80	0.9569	1008.57
-0.9204	0.0980	0.1236	546.50	0.2685	615.67	0.5059	844.68	0.6570	820.58	0.8081	666.00	0.9592	1115.77
-0.9234	0.0981	0.1255	548.72	0.2717	629.81	0.5081	844.26	0.6592	812.76	0.8103	667.85		
-0.9264	0.1006	0.1275	550.25	0.2749	636.72	0.5103	848.13	0.6614	793.51	0.8125	655.17	X/PL	Nu
-0.9294	0.1010	0.1294	556.32	0.2781	624.63	0.5125	853.39	0.6636	794.57	0.8147	656.75	-0.0103	1222.24
-0.9324	0.1031	0.1313	571.08	0.2813	629.36	0.5147	858.27	0.6658	802.41	0.8169	662.60	-0.0189	1105.43
-0.9353	0.1028	0.1333	601.12	0.2845	674.25	0.5170	868.44	0.6681	789.75	0.8192	662.64	-0.0274	1029.72
-0.9383	0.1037	0.1352	645.70	0.2877	704.16	0.5192	871.55	0.6703	779.13	0.8214	662.56	-0.0360	968.10
-0.9413	0.1031	0.1371	696.15	0.2909	684.90	0.5214	869.98	0.6725	772.02	0.8236	667.93	-0.0445	889.21
-0.9443	0.1058	0.1391	632.08	0.2941	597.69	0.5236	880.38	0.6747	779.66	0.8258	662.39	-0.0531	805.70
-0.9473	0.1028	0.1410	598.78	0.2973	590.68	0.5259	873.12	0.6770	778.95	0.8281	663.94	-0.0616	736.97
-0.9503	0.1034	0.1430	595.23	0.3005	603.81	0.5281	870.80	0.6792	772.90	0.8303	660.38	-0.0702	691.26
-0.9533	0.1014	0.1449	625.87	0.3037	611.23	0.5303	886.42	0.6814	772.44	0.8325	668.07	-0.0787	640.91
-0.9563	0.0966	0.1468	742.11	0.3069	615.37	0.5325	885.00	0.6836	776.42	0.8347	670.54	-0.0873	618.24
-0.9593	0.0978	0.1488	761.95	0.3836	570.04	0.5347	892.81	0.6858	773.09	0.8369	666.29	-0.0958	576.30
-0.9623	0.0950	0.1507	740.60	0.3859	583.35	0.5370	896.58	0.6881	763.31	0.8392	661.14	-0.1044	566.20
-0.9653	0.0950	0.1526	701.92	0.3881	597.78	0.5392	909.84	0.6903	758.04	0.8414	657.80	-0.1130	531.52
-0.9683	0.0963	0.1546	688.39	0.3903	593.93	0.5414	909.94	0.6925	769.25	0.8436	661.92	-0.1215	522.51
-0.9712	0.0930	0.1565	715.11	0.3925	588.56	0.5436	903.59	0.6947	764.55	0.8458	672.32	-0.1301	496.80
-0.9742	0.0932	0.1585	726.51	0.3947	596.21	0.5459	913.43	0.6970	755.80	0.8481	667.61	-0.1386	468.36
-0.9772	0.0963	0.1604	712.33	0.3970	595.35	0.5481	915.54	0.6992	756.66	0.8503	670.38	-0.1472	466.76
-0.9802	0.0957	0.1623	707.02	0.3992	610.46	0.5503	919.64	0.7014	749.78	0.8525	665.73	-0.1557	443.12
-0.9832	0.0907	0.1643	709.69	0.4014	616.94	0.5525	921.01	0.7036	743.81	0.8547	673.58	-0.1643	444.25
-0.9862	0.0902	0.1662	720.84	0.4036	624.05	0.5547	918.00	0.7058	753.25	0.8569	671.55	-0.1728	424.69
-0.9892	0.0884	0.1682	722.06	0.4059	624.48	0.5570	925.24	0.7081	735.87	0.8592	673.74	-0.1814	431.04
-0.9922	0.0847	0.1701	705.32	0.4081	634.45	0.5592	931.29	0.7103	738.43	0.8614	682.07	-0.1899	428.88
-0.9922	0.0847	0.1720	703.20	0.4103	641.68	0.5614	936.34	0.7125	733.49	0.8636	679.20	-0.1985	420.26
		0.1740	697.63	0.4125	653.87	0.5636	927.86	0.7147	735.84	0.8658	681.87	-0.2020	425.37
		0.1759	708.12	0.4147	654.90	0.5658	919.37	0.7170	728.63	0.8681	678.68	-0.2055	405.86
		0.1778	716.20	0.4170	657.17	0.5681	924.63	0.7192	726.08	0.8703	683.39	-0.2091	405.50
		0.1798	697.97	0.4192	675.84	0.5703	930.76	0.7214	723.32	0.8725	684.67	-0.2126	388.24
		0.1817	698.09	0.4214	690.18	0.5725	932.55	0.7236	728.82	0.8747	695.42	-0.2161	398.05
		0.1837	716.81	0.4236	697.80	0.5747	922.86	0.7258	719.34	0.8769	688.00	-0.2196	380.04
		0.1856	696.10	0.4259	699.88	0.5770	921.09	0.7281	713.74	0.8792	689.50	-0.2232	366.89
		0.1875	693.74	0.4281	700.38	0.5792	919.25	0.7303	733.65	0.8814	694.20	-0.2267	365.92
		0.1895	685.43	0.4303	693.38	0.5814	921.99	0.7325	717.83	0.8836	706.74	-0.2302	359.92
		0.1914	698.50	0.4325	690.77	0.5836	929.19	0.7347	711.37	0.8858	703.02	-0.2337	369.31
		0.1933	686.00	0.4347	699.56	0.5858	914.41	0.7370	702.86	0.8881	704.24	-0.2372	362.40
		0.1953	699.90	0.4370	706.95	0.5881	918.47	0.7392	716.10	0.8903	709.19	-0.2408	376.36
		0.1972	672.73	0.4392	715.28	0.5903	911.50	0.7414	711.92	0.8925	713.74	-0.2443	377.29
		0.1992	669.30	0.4414	722.94	0.5925	898.77	0.7436	696.89	0.8947	724.53	-0.2478	383.51
		0.2011	674.93	0.4436	717.97	0.5947	890.25	0.7458	697.02	0.8969	726.21	-0.2513	395.81
		0.2030	658.25	0.4459	708.52	0.5970	894.00	0.7481	694.17	0.8992	735.06	-0.2549	394.65
		0.2050	667.30	0.4481	707.71	0.5992	892.17	0.7503	692.58	0.9014	738.68	-0.2584	421.08
		0.2069	653.72	0.4503	713.90	0.6014	883.59	0.7525	693.66	0.9036	742.05	-0.2619	419.10
		0.2088	660.45	0.4525	717.27	0.6036	890.83	0.7547	688.67	0.9058	747.46	-0.2654	443.48
		0.2108	649.95	0.4547	723.01	0.6058	876.35	0.7570	688.64	0.9081	748.77	-0.2690	447.74
		0.2127	641.64	0.4570	722.87	0.6081	869.52	0.7592	698.47	0.9103	760.74	-0.2725	458.79
		0.2147	638.62	0.4592	728.41	0.6103	869.50	0.7614	684.17	0.9125	767.60	-0.2760	477.62
		0.2166	635.83	0.4614	733.41	0.6125	868.89	0.7636	686.20	0.9147	773.41	-0.2795	469.48
		0.2185	637.20	0.4636	738.26	0.6147	865.09	0.7658	679.47	0.9169	787.16	-0.2831	478.02

CASE M – Nu

X/SL	Nu
0.0519	900.21
0.0538	892.82
0.0558	865.97
0.0577	862.21
0.0596	845.81
0.0616	835.78
0.0635	819.93
0.0654	812.44
0.0674	805.17
0.0693	788.10
0.0713	762.87
0.0732	750.13
0.0751	736.31
0.0771	738.02
0.0790	716.18
0.0810	694.79
0.0829	699.76
0.0848	695.76
0.0868	674.35

Appendix 7.2 – Data for Spanwise Averaged Nusselt Number and Film Cooling Effectiveness

-0.2866	468.72	-0.5226	394.33	-0.7260	389.50	-0.9294	411.96	0.1275	0.2878	0.2750	0.3839	0.5081	0.2567
-0.2901	493.36	-0.5256	396.68	-0.7290	387.51	-0.9324	416.37	0.1294	0.2927	0.2782	0.4242	0.5103	0.2520
-0.2936	505.62	-0.5286	389.48	-0.7320	385.51	-0.9354	420.49	0.1314	0.3023	0.2814	0.4621	0.5126	0.2616
-0.2971	514.02	-0.5315	388.16	-0.7350	381.82	-0.9384	423.80	0.1333	0.3101	0.2846	0.4877	0.5148	0.2547
-0.3007	509.14	-0.5345	386.51	-0.7380	382.05	-0.9414	428.60	0.1353	0.3633	0.2878	0.4907	0.5170	0.2570
-0.3042	505.50	-0.5375	388.80	-0.7409	382.87	-0.9444	432.92	0.1372	0.3572	0.2910	0.4686	0.5192	0.2486
-0.3077	489.47	-0.5405	390.94	-0.7439	382.82	-0.9474	437.86	0.1391	0.3547	0.2942	0.4851	0.5215	0.2439
-0.3112	496.42	-0.5435	390.18	-0.7469	381.53	-0.9504	443.01	0.1411	0.3414	0.2974	0.5172	0.5237	0.2460
-0.3148	491.94	-0.5465	390.41	-0.7499	380.52	-0.9533	448.44	0.1430	0.3337	0.3006	0.5323	0.5259	0.2367
-0.3183	485.39	-0.5495	387.96	-0.7529	381.44	-0.9563	454.99	0.1449	0.3281	0.3038	0.5100	0.5281	0.2279
-0.3218	477.67	-0.5525	390.41	-0.7559	381.85	-0.9593	457.84	0.1469	0.3355	0.3069	0.3988	0.5303	0.2380
-0.3253	484.13	-0.5555	391.13	-0.7589	383.68	-0.9623	461.17	0.1488	0.3154	0.3837	0.3313	0.5326	0.2328
-0.3289	481.96	-0.5585	391.19	-0.7619	382.19	-0.9653	468.36	0.1508	0.3129	0.3837	0.3224	0.5348	0.2366
-0.3324	488.54	-0.5615	390.14	-0.7649	380.25	-0.9683	474.80	0.1527	0.3087	0.3859	0.3181	0.5370	0.2286
-0.3359	480.75	-0.5645	388.83	-0.7679	377.13	-0.9713	479.38	0.1546	0.3158	0.3881	0.3191	0.5392	0.2302
-0.3394	487.99	-0.5674	389.62	-0.7709	376.67	-0.9743	485.11	0.1566	0.3257	0.3904	0.3004	0.5415	0.2245
-0.3430	477.62	-0.5704	389.55	-0.7739	377.85	-0.9773	489.07	0.1585	0.3148	0.3926	0.2855	0.5437	0.2202
-0.3465	479.63	-0.5734	390.41	-0.7768	379.83	-0.9803	495.23	0.1605	0.3109	0.3948	0.2863	0.5459	0.2223
-0.3500	472.67	-0.5764	390.77	-0.7798	380.04	-0.9833	503.13	0.1624	0.3292	0.3970	0.2771	0.5481	0.2251
-0.3535	465.20	-0.5794	389.80	-0.7828	379.82	-0.9863	516.26	0.1643	0.3440	0.3992	0.2884	0.5503	0.2144
-0.3571	467.73	-0.5824	387.39	-0.7858	378.30	-0.9892	538.17	0.1663	0.3329	0.4015	0.2857	0.5526	0.2147
-0.3606	458.25	-0.5854	387.61	-0.7888	377.78	-0.9922	567.89	0.1682	0.3221	0.4037	0.2896	0.5548	0.2135
-0.3641	460.24	-0.5884	391.70	-0.7918	377.47			0.1701	0.3334	0.4059	0.2752	0.5570	0.2133
-0.3676	444.21	-0.5914	391.42	-0.7948	376.49			0.1721	0.3409	0.4081	0.2780	0.5592	0.2122
-0.3711	454.76	-0.5944	389.46	-0.7978	376.55			0.1740	0.3319	0.4104	0.2896	0.5615	0.2048
-0.3747	448.70	-0.5974	387.87	-0.8008	376.05			0.1760	0.3370	0.4126	0.3010	0.5637	0.2096
-0.3782	446.66	-0.6003	389.30	-0.8038	376.58			0.1779	0.3440	0.4148	0.2958	0.5659	0.2043
-0.3817	448.37	-0.6033	391.02	-0.8068	374.54			0.1798	0.3405	0.4170	0.2879	0.5681	0.1966
-0.3852	438.38	-0.6063	390.87	-0.8098	375.00			0.1818	0.3341	0.4192	0.3040	0.5703	0.2000
-0.3888	443.03	-0.6093	392.14	-0.8127	373.63			0.1837	0.3439	0.4215	0.3142	0.5726	0.2101
-0.3923	430.62	-0.6123	394.36	-0.8157	371.21			0.1856	0.3474	0.4237	0.3091	0.5748	0.2086
-0.3958	438.28	-0.6153	396.20	-0.8187	370.11			0.1876	0.3439	0.4259	0.3038	0.5770	0.1932
-0.3993	438.10	-0.6183	397.03	-0.8217	371.32			0.1895	0.3359	0.4281	0.2978	0.5792	0.1866
-0.4029	438.75	-0.6213	396.76	-0.8247	370.67			0.1915	0.3406	0.4304	0.2858	0.5815	0.1920
-0.4064	438.92	-0.6243	395.99	-0.8277	369.66			0.1934	0.3455	0.4326	0.2751	0.5837	0.2044
-0.4099	432.48	-0.6273	394.83	-0.8307	369.54			0.1953	0.3396	0.4348	0.2776	0.5859	0.1972
-0.4134	435.46	-0.6303	395.97	-0.8337	371.22			0.1973	0.3473	0.4370	0.2790	0.5881	0.1944
-0.4170	422.18	-0.6333	394.56	-0.8367	371.14			0.1992	0.3491	0.4392	0.2834	0.5903	0.1919
-0.4205	429.54	-0.6362	394.35	-0.8397	368.66			0.2011	0.3442	0.4415	0.2853	0.5926	0.1893
-0.4240	425.91	-0.6392	396.32	-0.8427	369.53			0.2031	0.3415	0.4437	0.2779	0.5948	0.1838
-0.4275	428.30	-0.6422	396.64	-0.8457	371.60			0.2050	0.3410	0.4459	0.2625	0.5970	0.1805
-0.4310	429.64	-0.6452	397.69	-0.8486	372.39			0.2070	0.3444	0.4481	0.2517	0.5992	0.1809
-0.4346	422.58	-0.6482	396.81	-0.8516	372.80			0.2089	0.3349	0.4503	0.2473	0.6015	0.1697
-0.4381	428.05	-0.6512	394.12	-0.8546	373.60			0.2108	0.3377	0.4526	0.2438	0.6037	0.1804
-0.4416	418.40	-0.6542	394.67	-0.8576	376.69			0.2128	0.3318	0.4548	0.2498	0.6059	0.1748
-0.4451	424.10	-0.6572	394.74	-0.8606	377.22			0.2147	0.3234	0.4570	0.2476	0.6081	0.1634
-0.4487	417.74	-0.6602	394.73	-0.8636	376.40			0.2166	0.3300	0.4592	0.2504	0.6103	0.1624
-0.4522	418.79	-0.6632	395.52	-0.8666	376.67			0.2186	0.3289	0.4615	0.2529	0.6126	0.1577
-0.4557	417.09	-0.6662	396.52	-0.8696	378.19			0.2205	0.3292	0.4637	0.2604	0.6148	0.1617
-0.4592	412.46	-0.6692	397.06	-0.8726	377.98			0.2225	0.3207	0.4659	0.2691	0.6170	0.1681
-0.4628	417.82	-0.6721	395.51	-0.8756	378.12			0.2244	0.3202	0.4681	0.2658	0.6192	0.1647
-0.4663	409.96	-0.6751	393.38	-0.8786	379.99			0.2263	0.3166	0.4703	0.2590	0.6215	0.1574
-0.4698	418.01	-0.6781	394.13	-0.8816	381.67			0.2283	0.3131	0.4726	0.2493	0.6237	0.1588
-0.4733	413.21	-0.6811	396.21	-0.8845	380.69			0.2302	0.3114	0.4748	0.2471	0.6259	0.1605
-0.4769	415.72	-0.6841	397.43	-0.8875	383.15			0.2320	0.3089	0.4770	0.2446	0.6281	0.1635
-0.4804	421.12	-0.6871	398.05	-0.8905	385.23			0.2334	0.3081	0.4792	0.2567	0.6303	0.1551
-0.4839	410.88	-0.6901	397.35	-0.8935	388.88			0.2366	0.3099	0.4815	0.2578	0.6326	0.1514
-0.4874	414.34	-0.6931	397.20	-0.8965	389.02			0.2398	0.3114	0.4837	0.2574	0.6348	0.1565
-0.4910	407.26	-0.6961	398.01	-0.8995	388.08			0.2430	0.3093	0.4859	0.2618	0.6370	0.1477
-0.4945	412.69	-0.6991	396.45	-0.9025	392.03			0.2462	0.3111	0.4881	0.2547	0.6392	0.1546
-0.4980	407.58	-0.7021	394.86	-0.9055	394.83			0.2494	0.3142	0.4903	0.2525	0.6415	0.1505
-0.5015	411.64	-0.7051	393.80	-0.9085	398.16			0.2526	0.3208	0.4926	0.2529	0.6437	0.1491
-0.5050	411.14	-0.7080	389.66	-0.9115	398.31			0.2558	0.3290	0.4948	0.2458	0.6459	0.1399
-0.5086	407.84	-0.7110	390.18	-0.9145	398.87			0.2590	0.3373	0.4970	0.2515	0.6481	0.1476
-0.5106	396.31	-0.7140	391.96	-0.9174	402.01			0.2622	0.3413	0.4992	0.2589	0.6503	0.1548
-0.5136	393.82	-0.7170	391.40	-0.9204	403.87			0.2654	0.3556	0.5015	0.2586	0.6526	0.1405
-0.5166	394.04	-0.7200	390.23	-0.9234	407.50			0.2686	0.3747	0.5037	0.2588	0.6548	0.1397
-0.5196	392.66	-0.7230	389.59	-0.9264	409.63			0.2718	0.3711	0.5059	0.2596	0.6570	0.1456

CASE M-η

X/SL η

0.0481	0.5673
0.0500	0.5114
0.0519	0.4726
0.0539	0.4420
0.0558	0.4303
0.0577	0.4153
0.0597	0.4068
0.0616	0.3894
0.0636	0.3840
0.0655	0.3743
0.0674	0.3775
0.0694	0.3552
0.0713	0.3605
0.0732	0.3661
0.0752	0.3578
0.0771	0.3490
0.0791	0.3531
0.0810	0.3453
0.0829	0.3507
0.0849	0.3422
0.0868	0.3323
0.0888	0.3348
0.0907	0.3379
0.0926	0.3345
0.0946	0.3328
0.0965	0.3299
0.0984	0.3202
0.1004	0.3177
0.1023	0.3198
0.1043	0.3109
0.1062	0.3066
0.1081	0.3016
0.1101	0.3052
0.1120	0.3062
0.1139	0.2973
0.1159	0.2967
0.1178	0.2931
0.1198	0.2896
0.1217	0.2819
0.1236	0.2768
0.1256	0.2855

Appendix 7.2 – Data for Spanwise Averaged Nusselt Number and Film Cooling Effectiveness

0.6592	0.1459	0.8103	0.0668			-0.3852	0.1237	-0.6482	0.1090	-0.8516	0.0863	0.0674	719.84
0.6615	0.1344	0.8126	0.0592	X/PL	η	-0.3887	0.1200	-0.6512	0.1003	-0.8546	0.0849	0.0693	703.09
0.6637	0.1370	0.8148	0.0629	-0.0872	0.3589	-0.3922	0.1142	-0.6541	0.0986	-0.8576	0.0914	0.0713	694.26
0.6659	0.1416	0.8170	0.0690	-0.0958	0.3378	-0.3958	0.1093	-0.6571	0.1061	-0.8606	0.0897	0.0732	690.58
0.6681	0.1287	0.8192	0.0701	-0.1044	0.3327	-0.3993	0.1137	-0.6601	0.1047	-0.8636	0.0886	0.0751	682.67
0.6703	0.1221	0.8214	0.0669	-0.1129	0.3201	-0.4028	0.1075	-0.6631	0.1049	-0.8665	0.0914	0.0771	673.28
0.6726	0.1198	0.8237	0.0761	-0.1215	0.3172	-0.4063	0.1005	-0.6661	0.1017	-0.8695	0.0892	0.0790	663.62
0.6748	0.1205	0.8259	0.0668	-0.1300	0.3065	-0.4099	0.1051	-0.6691	0.0974	-0.8725	0.0844	0.0810	654.10
0.6770	0.1218	0.8281	0.0666	-0.1386	0.2981	-0.4687	0.1020	-0.6721	0.0935	-0.8755	0.0801	0.0829	648.46
0.6792	0.1171	0.8303	0.0618	-0.1471	0.2950	-0.4717	0.1048	-0.6751	0.0936	-0.8785	0.0826	0.0848	644.88
0.6814	0.1211	0.8326	0.0664	-0.1557	0.2834	-0.4747	0.1098	-0.6781	0.0963	-0.8815	0.0843	0.0868	633.22
0.6837	0.1227	0.8348	0.0666	-0.1642	0.2820	-0.4776	0.1103	-0.6811	0.1041	-0.8845	0.0810	0.0887	628.95
0.6859	0.1262	0.8370	0.0663	-0.1728	0.2672	-0.4806	0.1133	-0.6841	0.1044	-0.8875	0.0813	0.0906	623.09
0.6881	0.1133	0.8392	0.0652	-0.1813	0.2660	-0.4836	0.1103	-0.6871	0.1068	-0.8905	0.0828	0.0926	614.89
0.6903	0.1131	0.8414	0.0630	-0.1899	0.2723	-0.4866	0.1121	-0.6900	0.1084	-0.8935	0.0885	0.0945	609.82
0.6926	0.1321	0.8437	0.0560	-0.1984	0.2638	-0.4896	0.1101	-0.6930	0.1063	-0.8965	0.0853	0.0965	604.78
0.6948	0.1194	0.8459	0.0679	-0.2020	0.2782	-0.4926	0.1135	-0.6960	0.1051	-0.8995	0.0803	0.0984	596.78
0.6970	0.1149	0.8481	0.0727	-0.2055	0.2698	-0.4956	0.1207	-0.6990	0.1021	-0.9024	0.0833	0.1003	593.06
0.6992	0.1204	0.8503	0.0737	-0.2090	0.2773	-0.4986	0.1176	-0.7020	0.1055	-0.9054	0.0866	0.1023	588.70
0.7014	0.1098	0.8526	0.0673	-0.2125	0.2691	-0.5016	0.1196	-0.7050	0.1063	-0.9084	0.0875	0.1042	582.09
0.7037	0.1042	0.8548	0.0642	-0.2161	0.2793	-0.5046	0.1251	-0.7080	0.0949	-0.9114	0.0829	0.1061	575.67
0.7059	0.1154	0.8570	0.0631	-0.2196	0.2797	-0.5076	0.1253	-0.7110	0.0932	-0.9144	0.0796	0.1081	575.33
0.7081	0.1030	0.8592	0.0690	-0.2231	0.2660	-0.5106	0.1237	-0.7140	0.0986	-0.9174	0.0791	0.1100	574.66
0.7103	0.1011	0.8614	0.0698	-0.2266	0.2504	-0.5135	0.1206	-0.7170	0.0931	-0.9204	0.0763	0.1120	568.28
0.7126	0.1070	0.8637	0.0629	-0.2302	0.2531	-0.5165	0.1218	-0.7200	0.0964	-0.9234	0.0794	0.1139	558.33
0.7148	0.1019	0.8659	0.0668	-0.2337	0.2451	-0.5195	0.1166	-0.7230	0.0988	-0.9264	0.0808	0.1158	550.52
0.7170	0.0981	0.8681	0.0593	-0.2372	0.2365	-0.5225	0.1182	-0.7259	0.1008	-0.9294	0.0789	0.1178	554.31
0.7192	0.0966	0.8703	0.0580	-0.2407	0.2250	-0.5255	0.1220	-0.7289	0.0986	-0.9324	0.0776	0.1197	551.27
0.7214	0.1014	0.8726	0.0619	-0.2442	0.2211	-0.5285	0.1137	-0.7319	0.1001	-0.9353	0.0799	0.1216	549.70
0.7237	0.1006	0.8748	0.0691	-0.2478	0.2136	-0.5315	0.1150	-0.7349	0.0959	-0.9383	0.0741	0.1236	548.39
0.7259	0.0903	0.8770	0.0598	-0.2513	0.2063	-0.5345	0.1082	-0.7379	0.0969	-0.9413	0.0755	0.1255	552.80
0.7281	0.0924	0.8792	0.0636	-0.2548	0.1914	-0.5375	0.1132	-0.7409	0.0991	-0.9443	0.0764	0.1275	555.28
0.7303	0.1128	0.8814	0.0674	-0.2583	0.1974	-0.5405	0.1218	-0.7439	0.0996	-0.9473	0.0752	0.1294	559.06
0.7326	0.1028	0.8837	0.0722	-0.2619	0.1905	-0.5435	0.1175	-0.7469	0.0980	-0.9503	0.0771	0.1313	564.89
0.7348	0.0972	0.8859	0.0616	-0.2654	0.1958	-0.5465	0.1151	-0.7499	0.0952	-0.9533	0.0794	0.1333	571.75
0.7370	0.0776	0.8881	0.0596	-0.2689	0.1876	-0.5494	0.1106	-0.7529	0.0982	-0.9563	0.0843	0.1352	586.44
0.7392	0.0973	0.8903	0.0635	-0.2724	0.1906	-0.5524	0.1162	-0.7559	0.0996	-0.9593	0.0787	0.1371	591.53
0.7414	0.0975	0.8926	0.0697	-0.2760	0.2002	-0.5554	0.1207	-0.7588	0.1019	-0.9623	0.0788	0.1391	562.24
0.7437	0.0811	0.8948	0.0686	-0.2795	0.1924	-0.5584	0.1165	-0.7618	0.1003	-0.9653	0.0803	0.1410	545.17
0.7459	0.0845	0.8970	0.0616	-0.2830	0.1880	-0.5614	0.1139	-0.7648	0.0972	-0.9683	0.0817	0.1430	537.16
0.7481	0.0806	0.8992	0.0771	-0.2865	0.1917	-0.5644	0.1067	-0.7678	0.0900	-0.9712	0.0809	0.1449	533.64
0.7503	0.0812	0.9014	0.0762	-0.2901	0.2131	-0.5674	0.1094	-0.7708	0.0938	-0.9742	0.0838	0.1468	544.88
0.7526	0.0799	0.9037	0.0764	-0.2936	0.2150	-0.5704	0.1076	-0.7738	0.0981	-0.9772	0.0823	0.1488	538.64
0.7548	0.0788	0.9059	0.0766	-0.2971	0.2011	-0.5734	0.1075	-0.7768	0.0996	-0.9802	0.0839	0.1507	530.39
0.7570	0.0754	0.9081	0.0747	-0.3006	0.2168	-0.5764	0.1118	-0.7798	0.1017	-0.9832	0.0865	0.1526	532.42
0.7592	0.0868	0.9103	0.0780	-0.3041	0.2136	-0.5794	0.1116	-0.7828	0.1032	-0.9862	0.0808	0.1546	529.61
0.7614	0.0688	0.9126	0.0765	-0.3077	0.2241	-0.5823	0.1071	-0.7858	0.1018	-0.9892	0.0718	0.1565	530.24
0.7637	0.0798	0.9148	0.0777	-0.3112	0.2117	-0.5853	0.1046	-0.7888	0.1045	-0.9922	0.0745	0.1585	532.07
0.7659	0.0696	0.9170	0.0774	-0.3147	0.2232	-0.5883	0.1087	-0.7918	0.0999			0.1604	530.12
0.7681	0.0654	0.9192	0.0784	-0.3182	0.2054	-0.5913	0.1088	-0.7947	0.1036			0.1623	533.25
0.7703	0.0689	0.9214	0.0847	-0.3218	0.1993	-0.5943	0.1078	-0.7977	0.1046	CASE N – Nu		0.1643	544.94
0.7726	0.0701	0.9237	0.0835	-0.3253	0.2074	-0.5973	0.1050	-0.8007	0.1038	X/SL	Nu	0.1662	562.00
0.7748	0.0748	0.9259	0.0854	-0.3288	0.1969	-0.6003	0.1042	-0.8037	0.1029	0.0383	1048.07	0.1682	570.02
0.7770	0.0746	0.9281	0.0843	-0.3323	0.1885	-0.6033	0.1048	-0.8067	0.0968	0.0403	959.64	0.1701	584.52
0.7792	0.0698	0.9303	0.0807	-0.3359	0.1852	-0.6063	0.1026	-0.8097	0.0957	0.0422	915.96	0.1720	596.28
0.7814	0.0818	0.9325	0.0861	-0.3394	0.1794	-0.6093	0.1017	-0.8127	0.0952	0.0441	949.23	0.1740	613.08
0.7837	0.0624	0.9348	0.0906	-0.3429	0.1779	-0.6123	0.1086	-0.8157	0.0915	0.0461	930.35	0.1759	618.35
0.7859	0.0651	0.9370	0.0899	-0.3464	0.1702	-0.6153	0.1099	-0.8187	0.0887	0.0480	849.64	0.1778	625.32
0.7881	0.0829	0.9392	0.0822	-0.3500	0.1659	-0.6182	0.1101	-0.8217	0.0918	0.0499	811.03	0.1798	635.42
0.7903	0.0766	0.9414	0.0906	-0.3535	0.1661	-0.6212	0.1055	-0.8247	0.0843	0.0519	803.76	0.1817	648.80
0.7926	0.0726	0.9437	0.0899	-0.3570	0.1596	-0.6242	0.1050	-0.8277	0.0881	0.0538	788.46	0.1837	649.24
0.7948	0.0764	0.9459	0.0856	-0.3605	0.1575	-0.6272	0.1039	-0.8306	0.0901	0.0558	779.43	0.1856	654.48
0.7970	0.0742	0.9481	0.0830	-0.3640	0.1512	-0.6302	0.1089	-0.8336	0.0901	0.0577	768.66	0.1875	654.85
0.7992	0.0689	0.9503	0.0825	-0.3676	0.1350	-0.6332	0.1061	-0.8366	0.0881	0.0596	755.64	0.1895	660.51
0.8014	0.0635	0.9525	0.0823	-0.3711	0.1396	-0.6362	0.1025	-0.8396	0.0827	0.0616	745.24	0.1914	663.19
0.8037	0.0565	0.9548	0.0864	-0.3746	0.1385	-0.6392	0.1076	-0.8426	0.0861	0.0635	738.33	0.1933	670.15
0.8059	0.0632	0.9570	0.0787	-0.3781	0.1340	-0.6422	0.1091	-0.8456	0.0843	0.0654	730.05	0.1953	679.60
0.8081	0.0662	0.9592	0.0746	-0.3817	0.1264	-0.6452	0.1144	-0.8486	0.0854			0.1972	681.59

Appendix 7.2 – Data for Spanwise Averaged Nusselt Number and Film Cooling Effectiveness

0.1992	679.76	0.4414	718.99	0.5925	868.11	0.7436	725.53	0.8947	731.49	-0.2478	444.12	-0.4874	398.28
0.2011	679.65	0.4436	720.73	0.5947	859.45	0.7458	739.45	0.8969	731.48	-0.2513	449.35	-0.4910	397.21
0.2030	680.82	0.4459	722.08	0.5970	852.21	0.7481	716.73	0.8992	745.15	-0.2549	452.47	-0.4945	396.07
0.2050	680.48	0.4481	721.26	0.5992	846.88	0.7503	721.05	0.9014	747.25	-0.2584	452.48	-0.4980	394.85
0.2069	676.96	0.4503	723.82	0.6014	845.76	0.7525	716.34	0.9036	757.38	-0.2619	448.38	-0.5015	393.70
0.2088	676.00	0.4525	725.96	0.6036	844.65	0.7547	713.34	0.9058	749.34	-0.2654	443.30	-0.5050	392.56
0.2108	674.00	0.4547	727.50	0.6058	844.90	0.7570	722.55	0.9081	760.45	-0.2690	433.06	-0.5086	391.22
0.2127	672.31	0.4570	725.90	0.6081	842.54	0.7592	710.01	0.9103	761.95	-0.2725	441.03	-0.5121	389.97
0.2147	671.98	0.4592	726.32	0.6103	835.15	0.7614	720.75	0.9125	769.81	-0.2760	438.81	-0.5156	389.04
0.2166	665.90	0.4614	723.37	0.6125	834.81	0.7636	730.12	0.9147	780.68	-0.2795	445.54	-0.5191	387.96
0.2185	664.63	0.4636	725.36	0.6147	837.43	0.7658	714.57	0.9169	780.61	-0.2831	443.16	-0.5227	387.38
0.2205	663.38	0.4659	726.43	0.6170	837.84	0.7681	704.05	0.9192	792.51	-0.2866	441.54	-0.5262	386.86
0.2224	663.16	0.4681	729.17	0.6192	830.87	0.7703	730.84	0.9214	791.57	-0.2901	440.78	-0.5297	385.38
0.2243	659.86	0.4703	731.80	0.6214	828.85	0.7725	720.79	0.9236	801.33	-0.2936	438.68	-0.5332	384.73
0.2263	648.83	0.4725	742.80	0.6236	833.62	0.7747	706.28	0.9258	814.66	-0.2971	444.00	-0.5368	384.49
0.2282	645.67	0.4747	740.00	0.6258	826.98	0.7770	708.90	0.9281	816.98	-0.3007	437.48	-0.5403	383.26
0.2302	643.83	0.4770	740.91	0.6281	827.15	0.7792	708.67	0.9303	828.97	-0.3042	436.00	-0.5438	382.20
0.2322	641.30	0.4792	746.67	0.6303	826.20	0.7814	717.12	0.9325	837.86	-0.3077	435.33	-0.5473	385.71
0.2344	640.85	0.4814	747.98	0.6325	825.33	0.7836	701.03	0.9347	846.65	-0.3112	434.95	-0.5508	386.58
0.2366	638.44	0.4836	747.66	0.6347	818.29	0.7858	697.46	0.9369	859.32	-0.3148	433.77	-0.5543	388.05
0.2398	637.31	0.4859	746.36	0.6370	824.07	0.7881	705.80	0.9392	869.29	-0.3183	431.12	-0.5578	386.04
0.2430	639.57	0.4881	752.49	0.6392	824.57	0.7903	729.65	0.9414	897.78	-0.3218	429.58	-0.5613	382.10
0.2461	636.25	0.4903	754.94	0.6414	812.70	0.7925	736.51	0.9436	908.22	-0.3253	428.85	-0.5648	383.40
0.2493	636.81	0.4925	756.73	0.6436	811.01	0.7947	716.76	0.9458	905.42	-0.3289	428.01	-0.5683	383.72
0.2525	636.97	0.4947	759.31	0.6458	806.89	0.7969	699.17	0.9481	912.47	-0.3324	427.10	-0.5718	385.03
0.2557	635.43	0.4970	765.04	0.6481	806.51	0.7992	713.17	0.9503	926.51	-0.3359	426.12	-0.5753	387.07
0.2589	634.26	0.4992	765.45	0.6503	811.40	0.8014	699.64	0.9525	948.02	-0.3394	425.28	-0.5788	388.92
0.2621	635.96	0.5014	765.27	0.6525	821.34	0.8036	689.88	0.9547	969.40	-0.3430	425.33	-0.5823	388.44
0.2653	635.41	0.5036	772.86	0.6547	812.69	0.8058	696.27	0.9569	974.38	-0.3465	425.09	-0.5858	386.65
0.2685	633.52	0.5059	773.75	0.6570	794.87	0.8081	699.06	0.9592	990.84	-0.3500	425.06	-0.6003	388.66
0.2717	628.18	0.5081	782.05	0.6592	801.46	0.8103	691.49			-0.3535	424.98	-0.6038	389.51
0.2749	607.43	0.5103	783.94	0.6614	810.44	0.8125	701.30	X/PL	Nu	-0.3571	425.19	-0.6063	390.98
0.2781	591.21	0.5125	781.16	0.6636	799.82	0.8147	689.41	-0.0103	1049.04	-0.3606	425.19	-0.6093	392.20
0.2813	583.22	0.5147	786.48	0.6658	794.79	0.8169	680.10	-0.0189	1028.32	-0.3641	424.91	-0.6123	391.53
0.2845	585.09	0.5170	797.56	0.6681	809.88	0.8192	680.36	-0.0274	959.08	-0.3676	424.27	-0.6153	391.27
0.2877	587.63	0.5192	800.30	0.6703	794.31	0.8214	708.37	-0.0360	888.63	-0.3711	424.77	-0.6183	393.32
0.2909	575.67	0.5214	804.24	0.6725	791.03	0.8236	688.06	-0.0445	834.99	-0.3747	424.02	-0.6213	394.56
0.2941	575.07	0.5236	810.26	0.6747	787.16	0.8258	688.14	-0.0531	759.37	-0.3782	423.42	-0.6243	395.28
0.2973	586.79	0.5259	812.53	0.6770	773.07	0.8281	690.52	-0.0616	694.98	-0.3817	422.46	-0.6273	396.03
0.3005	590.24	0.5281	814.63	0.6792	779.62	0.8303	699.63	-0.0702	653.05	-0.3852	421.88	-0.6303	393.46
0.3037	605.24	0.5303	815.89	0.6814	780.89	0.8325	704.13	-0.0787	616.15	-0.3888	420.52	-0.6333	393.15
0.3069	621.25	0.5325	816.53	0.6836	777.39	0.8347	682.08	-0.0873	562.43	-0.3923	420.53	-0.6362	393.75
0.3836	669.75	0.5347	828.12	0.6858	777.35	0.8369	684.92	-0.0958	532.18	-0.3958	419.76	-0.6392	395.40
0.3859	669.80	0.5370	829.43	0.6881	778.81	0.8392	703.23	-0.1044	500.72	-0.3993	419.02	-0.6422	395.80
0.3881	669.00	0.5392	833.51	0.6903	766.47	0.8414	691.67	-0.1130	478.11	-0.4029	418.25	-0.6452	396.38
0.3903	673.10	0.5414	833.45	0.6925	783.25	0.8436	686.66	-0.1215	463.15	-0.4064	417.42	-0.6482	398.57
0.3925	680.32	0.5436	846.21	0.6947	773.48	0.8458	675.89	-0.1301	448.24	-0.4099	417.11	-0.6512	398.81
0.3947	684.04	0.5459	857.52	0.6970	772.91	0.8481	686.29	-0.1386	434.30	-0.4134	417.24	-0.6542	403.17
0.3970	686.28	0.5481	849.47	0.6992	767.80	0.8503	701.50	-0.1472	425.83	-0.4170	416.82	-0.6572	405.63
0.3992	684.24	0.5503	857.69	0.7014	754.93	0.8525	685.50	-0.1557	428.60	-0.4205	415.95	-0.6602	403.96
0.4014	689.28	0.5525	856.64	0.7036	757.93	0.8547	679.35	-0.1643	425.76	-0.4240	415.60	-0.6632	403.05
0.4036	696.18	0.5547	867.54	0.7058	775.13	0.8569	686.01	-0.1728	430.10	-0.4275	415.23	-0.6662	402.89
0.4059	697.75	0.5570	868.38	0.7081	757.49	0.8592	696.51	-0.1814	416.02	-0.4310	415.17	-0.6692	402.95
0.4081	699.51	0.5592	870.87	0.7103	761.18	0.8614	688.03	-0.1899	384.95	-0.4346	415.16	-0.6721	403.71
0.4103	700.07	0.5614	874.31	0.7125	755.93	0.8636	700.77	-0.1985	343.38	-0.4381	413.96	-0.6751	403.89
0.4125	706.73	0.5636	881.78	0.7147	755.66	0.8658	706.06	-0.2020	348.98	-0.4416	413.46	-0.6781	403.18
0.4147	710.78	0.5658	889.39	0.7170	740.13	0.8681	693.41	-0.2055	350.25	-0.4451	413.53	-0.6811	404.11
0.4170	708.43	0.5681	874.38	0.7192	758.21	0.8703	690.42	-0.2091	363.90	-0.4487	413.48	-0.6841	405.57
0.4192	707.91	0.5703	878.00	0.7214	747.89	0.8725	691.13	-0.2126	362.90	-0.4522	412.93	-0.6871	405.18
0.4214	707.25	0.5725	879.15	0.7236	751.29	0.8747	701.69	-0.2161	358.03	-0.4557	412.55	-0.6901	404.23
0.4236	712.95	0.5747	876.71	0.7258	748.71	0.8769	714.26	-0.2196	377.40	-0.4592	410.94	-0.6931	405.48
0.4259	718.86	0.5770	874.18	0.7281	733.63	0.8792	696.56	-0.2232	404.62	-0.4628	408.82	-0.6961	406.27
0.4281	714.88	0.5792	865.80	0.7303	762.12	0.8814	698.28	-0.2267	394.68	-0.4663	407.60	-0.6991	410.70
0.4303	711.60	0.5814	867.82	0.7325	725.67	0.8836	701.73	-0.2302	391.86	-0.4698	406.16	-0.7021	405.31
0.4325	718.28	0.5836	872.01	0.7347	736.16	0.8858	722.35	-0.2337	407.52	-0.4733	404.96	-0.7051	403.33
0.4347	719.41	0.5858	873.74	0.7370	732.86	0.8881	727.57	-0.2372	423.21	-0.4769	403.67	-0.7080	402.25
0.4370	718.61	0.5881	860.13	0.7392	764.14	0.8903	717.72	-0.2408	428.15	-0.4804	401.49	-0.7110	401.54
0.4392	718.54	0.5903	857.56	0.7414	731.54	0.8925	724.75	-0.2443	437.06	-0.4839	400.32	-0.7140	401.79

Appendix 7.2 – Data for Spanwise Averaged Nusselt Number and Film Cooling Effectiveness

-0.7170	400.62	-0.9204	439.65	0.1120	0.1727	0.2494	0.2422	0.4903	0.1164	0.6415	0.0818	0.7926	0.0909
-0.7200	399.07	-0.9234	443.22	0.1139	0.1749	0.2526	0.2456	0.4926	0.1115	0.6437	0.0755	0.7948	0.0818
-0.7230	398.55	-0.9264	449.93	0.1159	0.1639	0.2558	0.2409	0.4948	0.1149	0.6459	0.0767	0.7970	0.0769
-0.7260	396.04	-0.9294	455.10	0.1178	0.1711	0.2590	0.2404	0.4970	0.1092	0.6481	0.0806	0.7992	0.0771
-0.7290	396.06	-0.9324	457.17	0.1198	0.1676	0.2622	0.2461	0.4992	0.1084	0.6503	0.0776	0.8014	0.0635
-0.7320	397.17	-0.9354	460.58	0.1217	0.1676	0.2654	0.2500	0.5015	0.1077	0.6526	0.0803	0.8037	0.0513
-0.7350	398.94	-0.9384	467.62	0.1236	0.1707	0.2686	0.2509	0.5037	0.1096	0.6548	0.0812	0.8059	0.0693
-0.7380	396.04	-0.9414	472.57	0.1256	0.1798	0.2718	0.2470	0.5059	0.1122	0.6570	0.0743	0.8081	0.0689
-0.7409	394.91	-0.9444	476.77	0.1275	0.1814	0.2750	0.2327	0.5081	0.1147	0.6592	0.0801	0.8103	0.0708
-0.7439	394.50	-0.9474	480.84	0.1294	0.1881	0.2782	0.2465	0.5103	0.1056	0.6615	0.0821	0.8126	0.0706
-0.7469	392.84	-0.9504	484.77	0.1314	0.1971	0.2814	0.2961	0.5126	0.1059	0.6637	0.0718	0.8148	0.0640
-0.7499	394.01	-0.9533	491.12	0.1333	0.2055	0.2846	0.3336	0.5148	0.1063	0.6659	0.0778	0.8170	0.0609
-0.7529	392.42	-0.9563	497.82	0.1353	0.2155	0.2878	0.3487	0.5170	0.1155	0.6681	0.0955	0.8192	0.0605
-0.7559	391.56	-0.9593	504.10	0.1372	0.2319	0.2910	0.3397	0.5192	0.1111	0.6703	0.0777	0.8214	0.0827
-0.7589	390.38	-0.9623	508.07	0.1391	0.2498	0.2942	0.3518	0.5215	0.1151	0.6726	0.0777	0.8237	0.0683
-0.7619	391.18	-0.9653	512.54	0.1411	0.2843	0.2974	0.3636	0.5237	0.1116	0.6748	0.0797	0.8259	0.0597
-0.7649	391.68	-0.9683	517.30	0.1430	0.3099	0.3006	0.3813	0.5259	0.1022	0.6770	0.0644	0.8281	0.0608
-0.7679	391.44	-0.9713	521.67	0.1449	0.3005	0.3038	0.3758	0.5281	0.1076	0.6792	0.0687	0.8303	0.0745
-0.7709	391.51	-0.9743	525.12	0.1469	0.3258	0.3069	0.3110	0.5303	0.1116	0.6814	0.0724	0.8326	0.0826
-0.7739	391.55	-0.9773	533.14	0.1488	0.3269	0.3837	0.1600	0.5326	0.1101	0.6837	0.0726	0.8348	0.0581
-0.7768	390.07	-0.9803	541.50	0.1508	0.3200	0.3837	0.1549	0.5348	0.1110	0.6859	0.0714	0.8370	0.0591
-0.7798	389.88	-0.9833	548.78	0.1527	0.3395	0.3859	0.1494	0.5370	0.1108	0.6881	0.0775	0.8392	0.0660
-0.7828	389.20	-0.9863	556.46	0.1546	0.3441	0.3881	0.1388	0.5392	0.1010	0.6903	0.0675	0.8414	0.0595
-0.7858	389.51	-0.9892	561.65	0.1566	0.3474	0.3904	0.1289	0.5415	0.0929	0.6926	0.0865	0.8437	0.0653
-0.7888	388.75	-0.9922	570.31	0.1585	0.3582	0.3926	0.1275	0.5437	0.0967	0.6948	0.0835	0.8459	0.0671
-0.7918	389.30			0.1605	0.3632	0.3948	0.1280	0.5459	0.1069	0.6970	0.0713	0.8481	0.0661
-0.7948	389.44			0.1624	0.3708	0.3970	0.1316	0.5481	0.0936	0.6992	0.0736	0.8503	0.0707
-0.7978	389.17	CASE N – n		0.1643	0.3848	0.3992	0.1324	0.5503	0.1009	0.7014	0.0726	0.8526	0.0606
-0.8008	389.02			0.1663	0.4005	0.4015	0.1307	0.5526	0.1003	0.7037	0.0729	0.8548	0.0672
-0.8038	388.38	X/SL	η	0.1682	0.4144	0.4037	0.1391	0.5548	0.1059	0.7059	0.0889	0.8570	0.0703
-0.8068	388.45	0.0384	0.5258	0.1701	0.4150	0.4059	0.1391	0.5570	0.1007	0.7081	0.0666	0.8592	0.0656
-0.8098	388.92	0.0403	0.4591	0.1721	0.4017	0.4081	0.1317	0.5592	0.1014	0.7103	0.0772	0.8614	0.0621
-0.8127	389.30	0.0422	0.4165	0.1740	0.3985	0.4104	0.1298	0.5615	0.0970	0.7126	0.0793	0.8637	0.0791
-0.8157	389.29	0.0442	0.4004	0.1760	0.3844	0.4126	0.1238	0.5637	0.1009	0.7148	0.0775	0.8659	0.0805
-0.8187	389.67	0.0461	0.3778	0.1779	0.3751	0.4148	0.1179	0.5659	0.1066	0.7170	0.0627	0.8681	0.0639
-0.8217	389.71	0.0481	0.3043	0.1798	0.3678	0.4170	0.1181	0.5681	0.0931	0.7192	0.0861	0.8703	0.0688
-0.8247	389.78	0.0500	0.2456	0.1818	0.3630	0.4192	0.1240	0.5703	0.1028	0.7214	0.0702	0.8726	0.0685
-0.8277	389.30	0.0519	0.2447	0.1837	0.3486	0.4215	0.1145	0.5726	0.0995	0.7237	0.0702	0.8748	0.0790
-0.8307	389.86	0.0539	0.2180	0.1856	0.3409	0.4237	0.1214	0.5748	0.0894	0.7259	0.0669	0.8770	0.0835
-0.8337	389.79	0.0558	0.2037	0.1876	0.3283	0.4259	0.1273	0.5770	0.0923	0.7281	0.0614	0.8792	0.0717
-0.8367	390.30	0.0577	0.1871	0.1895	0.3207	0.4281	0.1220	0.5792	0.0857	0.7303	0.0870	0.8814	0.0733
-0.8397	391.46	0.0597	0.1851	0.1915	0.3168	0.4304	0.1153	0.5815	0.0934	0.7326	0.0529	0.8837	0.0679
-0.8427	392.79	0.0616	0.1951	0.1934	0.3062	0.4326	0.1160	0.5837	0.0929	0.7348	0.0677	0.8859	0.0737
-0.8457	394.51	0.0636	0.1934	0.1953	0.3034	0.4348	0.1144	0.5859	0.0964	0.7370	0.0744	0.8881	0.0792
-0.8486	395.42	0.0655	0.1906	0.1973	0.3031	0.4370	0.1124	0.5881	0.0854	0.7392	0.0992	0.8903	0.0659
-0.8516	395.78	0.0674	0.1880	0.1992	0.3019	0.4392	0.1194	0.5903	0.0856	0.7414	0.0657	0.8926	0.0701
-0.8546	395.81	0.0694	0.1779	0.2011	0.2930	0.4415	0.1124	0.5926	0.0967	0.7437	0.0674	0.8948	0.0608
-0.8576	395.97	0.0713	0.1771	0.2031	0.2935	0.4437	0.1139	0.5948	0.0895	0.7459	0.0793	0.8970	0.0466
-0.8606	396.75	0.0732	0.1751	0.2050	0.2922	0.4459	0.1132	0.5970	0.0861	0.7481	0.0517	0.8992	0.0543
-0.8636	397.29	0.0752	0.1798	0.2070	0.2840	0.4481	0.1140	0.5992	0.0893	0.7503	0.0655	0.9014	0.0485
-0.8666	398.19	0.0771	0.1762	0.2089	0.2789	0.4503	0.1218	0.6015	0.0803	0.7526	0.0675	0.9037	0.0589
-0.8696	400.49	0.0791	0.1746	0.2108	0.2753	0.4526	0.1145	0.6037	0.0760	0.7548	0.0659	0.9059	0.0515
-0.8726	400.70	0.0810	0.1723	0.2128	0.2768	0.4548	0.1174	0.6059	0.0850	0.7570	0.0746	0.9081	0.0623
-0.8756	402.48	0.0829	0.1712	0.2147	0.2773	0.4570	0.1172	0.6081	0.0850	0.7592	0.0615	0.9103	0.0548
-0.8786	406.96	0.0849	0.1783	0.2166	0.2660	0.4592	0.1214	0.6103	0.0775	0.7614	0.0626	0.9126	0.0557
-0.8816	410.13	0.0868	0.1658	0.2186	0.2677	0.4615	0.1138	0.6126	0.0786	0.7637	0.0722	0.9148	0.0602
-0.8845	409.70	0.0888	0.1719	0.2205	0.2645	0.4637	0.1054	0.6148	0.0816	0.7659	0.0586	0.9170	0.0559
-0.8875	413.06	0.0907	0.1763	0.2225	0.2636	0.4659	0.1051	0.6170	0.0754	0.7681	0.0567	0.9192	0.0657
-0.8905	415.43	0.0926	0.1834	0.2244	0.2650	0.4681	0.1086	0.6192	0.0779	0.7703	0.0835	0.9214	0.0563
-0.8935	418.96	0.0946	0.1765	0.2263	0.2505	0.4703	0.0996	0.6215	0.0843	0.7726	0.0762	0.9237	0.0620
-0.8965	421.08	0.0965	0.1757	0.2283	0.2513	0.4726	0.1101	0.6237	0.0821	0.7748	0.0662	0.9259	0.0684
-0.8995	422.27	0.0984	0.1716	0.2302	0.2510	0.4748	0.1139	0.6259	0.0794	0.7770	0.0690	0.9281	0.0588
-0.9025	425.46	0.1004	0.1695	0.2302	0.2464	0.4770	0.1133	0.6281	0.0776	0.7792	0.0765	0.9303	0.0607
-0.9055	429.15	0.1023	0.1705	0.2334	0.2473	0.4792	0.1115	0.6303	0.0750	0.7814	0.0797	0.9325	0.0670
-0.9085	431.20	0.1043	0.1669	0.2366	0.2426	0.4815	0.1180	0.6326	0.0676	0.7837	0.0667	0.9348	0.0676
-0.9115	431.15	0.1062	0.1679	0.2398	0.2406	0.4837	0.1072	0.6348	0.0783	0.7859	0.0607	0.9370	0.0685
-0.9145	434.56	0.1081	0.1708	0.2430	0.2446	0.4859	0.1086	0.6370	0.0870	0.7881	0.0665	0.9392	0.0685
-0.9174	437.11	0.1101	0.1731	0.2462	0.2425	0.4881	0.1148	0.6392	0.0881	0.7903	0.0866	0.9414	0.0786

Appendix 7.2 – Data for Spanwise Averaged Nusselt Number and Film Cooling Effectiveness

0.9437	0.0801	-0.3359	0.1797	-0.5755	0.1142	-0.7828	0.0290	-0.9862	0.0268	0.1546	628.65	0.3903	763.41
0.9459	0.0787	-0.3394	0.1761	-0.5823	0.0980	-0.7858	0.0293	-0.9892	0.0185	0.1565	622.43	0.3925	758.34
0.9481	0.0762	-0.3429	0.1740	-0.5853	0.1006	-0.7888	0.0311	-0.9922	0.0219	0.1585	622.91	0.3947	754.01
0.9503	0.0796	-0.3464	0.1716	-0.5883	0.0954	-0.7918	0.0289			0.1604	614.00	0.3970	756.52
0.9525	0.0746	-0.3500	0.1704	-0.5913	0.0956	-0.7947	0.0286			0.1623	612.02	0.3992	754.67
0.9548	0.0839	-0.3535	0.1700	-0.5943	0.0949	-0.7977	0.0267			0.1643	613.47	0.4014	762.62
0.9570	0.0825	-0.3570	0.1707	-0.5973	0.0875	-0.8007	0.0265			0.1662	619.59	0.4036	762.12
0.9592	0.0726	-0.3605	0.1708	-0.6003	0.0861	-0.8037	0.0213			0.1682	617.89	0.4059	762.07
		-0.3640	0.1686	-0.6033	0.0886	-0.8067	0.0203			0.1701	617.00	0.4081	764.37
		-0.3676	0.1679	-0.6063	0.0905	-0.8097	0.0186			0.1720	627.07	0.4103	762.22
X/PL	η	-0.3711	0.1690	-0.6093	0.0897	-0.8127	0.0197			0.1740	634.95	0.4125	762.29
-0.0359	0.3477	-0.3746	0.1661	-0.6123	0.0901	-0.8157	0.0189			0.1759	633.41	0.4147	773.84
-0.0445	0.3478	-0.3781	0.1655	-0.6153	0.0873	-0.8187	0.0195			0.1778	638.25	0.4170	787.01
-0.0530	0.3090	-0.3817	0.1636	-0.6182	0.0907	-0.8217	0.0195			0.1798	648.81	0.4192	789.81
-0.0616	0.2992	-0.3852	0.1616	-0.6212	0.0926	-0.8247	0.0184			0.1817	654.85	0.4214	779.71
-0.0701	0.3183	-0.3887	0.1602	-0.6242	0.0929	-0.8277	0.0178			0.1837	657.62	0.4236	781.60
-0.0787	0.3078	-0.3922	0.1613	-0.6272	0.0939	-0.8306	0.0181			0.1856	657.19	0.4259	785.05
-0.0872	0.2762	-0.3958	0.1593	-0.6302	0.0883	-0.8336	0.0172			0.1875	658.88	0.4281	794.39
-0.0958	0.2620	-0.3993	0.1580	-0.6332	0.0870	-0.8366	0.0209			0.1895	672.78	0.4303	791.39
-0.1044	0.2595	-0.4028	0.1563	-0.6362	0.0857	-0.8396	0.0206			0.1914	671.11	0.4325	794.59
-0.1129	0.2558	-0.4063	0.1543	-0.6392	0.0844	-0.8426	0.0210			0.1933	677.58	0.4347	796.94
-0.1215	0.2547	-0.4099	0.1535	-0.6422	0.0876	-0.8456	0.0215			0.1953	679.21	0.4370	805.37
-0.1300	0.2469	-0.4134	0.1536	-0.6452	0.0873	-0.8486	0.0282			0.1972	678.53	0.4392	803.17
-0.1386	0.2560	-0.4169	0.1539	-0.6482	0.0896	-0.8516	0.0274			0.1992	681.37	0.4414	799.38
-0.1471	0.2618	-0.4204	0.1524	-0.6512	0.0874	-0.8546	0.0248			0.2011	682.42	0.4436	791.39
-0.1557	0.2642	-0.4240	0.1511	-0.6541	0.0967	-0.8576	0.0255			0.2030	683.79	0.4459	796.32
-0.1642	0.2693	-0.4275	0.1508	-0.6571	0.1007	-0.8606	0.0279			0.2050	680.53	0.4481	807.53
-0.1728	0.2770	-0.4310	0.1498	-0.6601	0.0990	-0.8636	0.0317			0.2069	680.69	0.4503	798.82
-0.1813	0.2827	-0.4345	0.1482	-0.6631	0.0939	-0.8665	0.0277			0.2088	679.59	0.4525	803.10
-0.1899	0.2791	-0.4380	0.1444	-0.6661	0.0938	-0.8695	0.0261			0.2108	682.17	0.4547	804.32
-0.1984	0.2499	-0.4416	0.1422	-0.6691	0.0906	-0.8725	0.0269			0.2127	681.02	0.4570	811.44
-0.2020	0.2287	-0.4451	0.1410	-0.6721	0.0953	-0.8755	0.0255			0.2147	676.09	0.4592	807.23
-0.2055	0.2209	-0.4486	0.1406	-0.6751	0.0977	-0.8785	0.0240			0.2166	673.46	0.4614	816.57
-0.2090	0.2263	-0.4521	0.1389	-0.6781	0.0955	-0.8815	0.0265			0.2185	668.63	0.4636	814.06
-0.2125	0.2202	-0.4557	0.1371	-0.6811	0.0908	-0.8845	0.0248			0.2205	673.63	0.4659	811.37
-0.2161	0.2289	-0.4592	0.1366	-0.6841	0.0924	-0.8875	0.0253			0.2224	671.74	0.4681	810.57
-0.2196	0.2529	-0.4627	0.1370	-0.6871	0.0910	-0.8905	0.0269			0.2243	668.58	0.4703	813.39
-0.2231	0.2637	-0.4662	0.1368	-0.6900	0.0955	-0.8935	0.0335			0.2263	662.70	0.4725	820.00
-0.2266	0.2476	-0.4698	0.1362	-0.6930	0.1011	-0.8965	0.0375			0.2282	654.65	0.4747	819.54
-0.2302	0.2386	-0.4733	0.1363	-0.6960	0.1003	-0.8995	0.0381			0.2302	658.56	0.4770	827.80
-0.2337	0.2376	-0.4768	0.1365	-0.6990	0.1018	-0.9024	0.0410			0.2320	655.63	0.4792	823.62
-0.2372	0.2381	-0.4803	0.1340	-0.7020	0.0965	-0.9054	0.0374			0.2334	655.32	0.4814	819.76
-0.2407	0.2406	-0.4839	0.1335	-0.7050	0.0878	-0.9084	0.0452			0.2366	654.11	0.4836	824.96
-0.2442	0.2409	-0.4874	0.1314	-0.7080	0.0865	-0.9114	0.0484			0.2398	652.82	0.4859	826.87
-0.2478	0.2350	-0.4909	0.1330	-0.7110	0.0830	-0.9144	0.0462			0.2430	651.95	0.4881	834.16
-0.2513	0.2364	-0.4944	0.1329	-0.7140	0.0802	-0.9174	0.0457			0.2461	652.56	0.4903	828.25
-0.2548	0.2388	-0.4979	0.1326	-0.7170	0.0791	-0.9204	0.0422			0.2493	651.19	0.4925	825.07
-0.2583	0.2472	-0.5015	0.1321	-0.7200	0.0703	-0.9234	0.0386			0.2525	646.72	0.4947	826.96
-0.2619	0.2509	-0.5050	0.1316	-0.7230	0.0738	-0.9264	0.0466			0.2557	643.58	0.4970	830.48
-0.2654	0.2530	-0.5085	0.1295	-0.7259	0.0676	-0.9294	0.0487			0.2589	646.48	0.4992	830.03
-0.2689	0.2400	-0.5120	0.1294	-0.7289	0.0663	-0.9324	0.0436			0.2621	645.98	0.5014	829.84
-0.2724	0.2437	-0.5156	0.1296	-0.7319	0.0621	-0.9353	0.0466			0.2653	646.40	0.5036	833.95
-0.2760	0.2321	-0.5191	0.1290	-0.7349	0.0652	-0.9383	0.0520			0.2685	650.80	0.5059	830.05
-0.2795	0.2321	-0.5226	0.1293	-0.7379	0.0613	-0.9413	0.0520			0.2717	652.52	0.5081	841.19
-0.2830	0.2228	-0.5261	0.1307	-0.7409	0.0521	-0.9443	0.0526			0.2749	637.77	0.5103	830.82
-0.2865	0.2185	-0.5297	0.1286	-0.7439	0.0504	-0.9473	0.0492			0.2781	637.17	0.5125	835.95
-0.2901	0.2224	-0.5332	0.1283	-0.7469	0.0462	-0.9503	0.0473			0.2813	643.62	0.5147	843.20
-0.2936	0.2201	-0.5367	0.1278	-0.7499	0.0488	-0.9533	0.0500			0.2845	656.47	0.5170	836.19
-0.2971	0.2263	-0.5402	0.1261	-0.7529	0.0394	-0.9563	0.0575			0.2877	677.99	0.5192	840.05
-0.3006	0.2191	-0.5438	0.1249	-0.7559	0.0350	-0.9593	0.0639			0.2909	659.44	0.5214	845.63
-0.3041	0.2140	-0.5473	0.1243	-0.7588	0.0339	-0.9623	0.0586			0.2941	651.34	0.5236	850.30
-0.3077	0.2085	-0.5508	0.1234	-0.7618	0.0372	-0.9653	0.0525			0.2973	654.50	0.5259	850.28
-0.3112	0.2088	-0.5543	0.1223	-0.7648	0.0395	-0.9683	0.0459			0.3005	666.36	0.5281	854.22
-0.3147	0.2033	-0.5579	0.1225	-0.7678	0.0374	-0.9712	0.0397			0.3037	686.98	0.5303	856.00
-0.3182	0.1971	-0.5614	0.1216	-0.7708	0.0365	-0.9742	0.0317			0.3069	690.23	0.5325	852.90
-0.3218	0.1930	-0.5649	0.1191	-0.7738	0.0385	-0.9772	0.0355			0.3836	777.48	0.5347	853.14
-0.3253	0.1907	-0.5684	0.1121	-0.7768	0.0352	-0.9802	0.0382			0.3859	766.33	0.5370	852.64
-0.3288	0.1876	-0.5719	0.1064	-0.7798	0.0341	-0.9832	0.0324			0.3881	760.48	0.5392	855.32
-0.3323	0.1816												

Appendix 7.2 – Data for Spanwise Averaged Nusselt Number and Film Cooling Effectiveness

0.5414	859.62	0.6925	793.90	0.8436	692.43	-0.1215	471.21	-0.4064	423.42	-0.6422	418.83	-0.8457	391.75
0.5436	865.04	0.6947	764.07	0.8458	672.10	-0.1301	453.57	-0.4099	422.55	-0.6452	419.52	-0.8486	391.64
0.5459	870.33	0.6970	755.64	0.8481	655.01	-0.1386	454.59	-0.4134	423.13	-0.6482	420.76	-0.8516	391.48
0.5481	874.72	0.6992	758.30	0.8503	647.07	-0.1472	439.16	-0.4170	423.34	-0.6512	420.06	-0.8546	391.87
0.5503	887.37	0.7014	762.45	0.8525	654.28	-0.1557	423.04	-0.4205	422.37	-0.6542	420.15	-0.8576	392.33
0.5525	884.79	0.7036	774.45	0.8547	657.93	-0.1643	439.92	-0.4240	422.03	-0.6572	420.59	-0.8606	393.20
0.5547	877.35	0.7058	771.63	0.8569	668.93	-0.1728	475.64	-0.4275	422.90	-0.6602	420.02	-0.8636	394.17
0.5570	878.58	0.7081	765.73	0.8592	649.36	-0.1814	504.34	-0.4310	423.46	-0.6632	419.64	-0.8666	395.00
0.5592	881.48	0.7103	753.85	0.8614	655.27	-0.1899	449.43	-0.4346	422.92	-0.6662	420.10	-0.8696	396.26
0.5614	881.46	0.7125	770.11	0.8636	679.82	-0.1985	400.12	-0.4381	422.70	-0.6692	424.11	-0.8726	397.65
0.5636	885.29	0.7147	761.56	0.8658	675.15	-0.2020	410.20	-0.4416	423.10	-0.6721	420.68	-0.8756	398.80
0.5658	881.50	0.7170	743.57	0.8681	674.43	-0.2055	419.82	-0.4451	422.05	-0.6751	420.35	-0.8786	399.07
0.5681	884.65	0.7192	752.63	0.8703	691.43	-0.2091	466.75	-0.4487	420.85	-0.6781	421.81	-0.8816	400.33
0.5703	901.80	0.7214	743.10	0.8725	667.68	-0.2126	386.68	-0.4522	420.78	-0.6811	420.95	-0.8845	402.48
0.5725	889.35	0.7236	753.96	0.8747	673.01	-0.2161	368.00	-0.4557	420.10	-0.6841	420.06	-0.8875	404.39
0.5747	885.16	0.7258	751.50	0.8769	675.94	-0.2196	385.85	-0.4592	417.86	-0.6871	419.21	-0.8905	405.50
0.5770	887.83	0.7281	769.10	0.8792	723.75	-0.2232	393.36	-0.4628	415.04	-0.6901	420.40	-0.8935	407.64
0.5792	889.60	0.7303	770.77	0.8814	677.05	-0.2267	417.48	-0.4663	414.21	-0.6931	420.80	-0.8965	409.46
0.5814	883.32	0.7325	745.64	0.8836	675.37	-0.2302	456.15	-0.4698	413.95	-0.6961	419.72	-0.8995	411.43
0.5836	877.72	0.7347	750.31	0.8858	661.74	-0.2337	454.39	-0.4733	413.69	-0.6991	418.68	-0.9025	414.10
0.5858	885.07	0.7370	725.69	0.8881	669.08	-0.2372	445.54	-0.4769	413.32	-0.7021	414.63	-0.9055	416.94
0.5881	883.69	0.7392	738.31	0.8903	683.00	-0.2408	462.33	-0.4804	412.65	-0.7051	413.03	-0.9085	420.64
0.5903	888.09	0.7414	733.08	0.8925	673.84	-0.2443	464.40	-0.4839	411.74	-0.7080	411.98	-0.9115	423.15
0.5925	869.69	0.7436	724.30	0.8947	666.57	-0.2478	468.35	-0.4874	410.21	-0.7110	411.85	-0.9145	425.45
0.5947	866.18	0.7458	718.13	0.8969	666.97	-0.2513	436.18	-0.4910	409.54	-0.7140	410.68	-0.9174	428.51
0.5970	867.81	0.7481	749.37	0.8992	681.25	-0.2549	444.59	-0.4945	407.43	-0.7170	408.54	-0.9204	432.39
0.5992	872.15	0.7503	724.96	0.9014	678.53	-0.2584	450.19	-0.4980	406.48	-0.7200	407.31	-0.9234	435.26
0.6014	869.68	0.7525	726.13	0.9036	682.36	-0.2619	458.46	-0.5015	403.33	-0.7230	406.84	-0.9264	438.53
0.6036	866.60	0.7547	709.87	0.9058	699.76	-0.2654	480.34	-0.5050	402.12	-0.7260	407.18	-0.9294	441.56
0.6058	883.33	0.7570	726.83	0.9081	695.94	-0.2690	467.57	-0.5086	401.97	-0.7290	405.56	-0.9324	445.35
0.6081	861.43	0.7592	707.87	0.9103	700.75	-0.2725	458.95	-0.5121	402.50	-0.7320	402.09	-0.9354	448.17
0.6103	862.51	0.7614	728.43	0.9125	712.30	-0.2760	446.41	-0.5156	400.18	-0.7350	401.43	-0.9384	452.70
0.6125	860.58	0.7636	746.04	0.9147	711.77	-0.2795	418.83	-0.5191	399.71	-0.7380	402.23	-0.9414	455.75
0.6147	844.21	0.7658	723.68	0.9169	723.57	-0.2831	415.56	-0.5227	400.41	-0.7409	402.85	-0.9444	460.37
0.6170	842.28	0.7681	708.64	0.9192	717.63	-0.2866	455.75	-0.5262	400.57	-0.7439	402.70	-0.9474	463.00
0.6192	841.69	0.7703	710.15	0.9214	719.94	-0.2901	480.13	-0.5297	399.86	-0.7469	399.92	-0.9504	466.37
0.6214	853.43	0.7725	678.21	0.9236	725.05	-0.2936	422.73	-0.5332	399.02	-0.7499	397.91	-0.9533	471.20
0.6236	843.66	0.7747	682.26	0.9258	736.11	-0.2971	406.25	-0.5365	404.51	-0.7529	396.74	-0.9563	474.17
0.6258	852.65	0.7770	714.11	0.9281	735.67	-0.3007	407.68	-0.5395	405.45	-0.7559	395.69	-0.9593	479.06
0.6281	852.35	0.7792	733.67	0.9303	751.89	-0.3042	409.13	-0.5425	405.22	-0.7589	395.22	-0.9623	483.34
0.6303	841.35	0.7814	727.48	0.9325	745.59	-0.3077	409.90	-0.5455	405.60	-0.7619	394.51	-0.9653	488.31
0.6325	825.91	0.7836	692.76	0.9347	756.08	-0.3112	411.37	-0.5485	406.09	-0.7649	393.25	-0.9683	494.17
0.6347	827.70	0.7858	704.36	0.9369	766.78	-0.3148	414.84	-0.5515	406.78	-0.7679	392.59	-0.9713	499.09
0.6370	848.63	0.7881	689.95	0.9392	766.12	-0.3183	417.19	-0.5545	407.58	-0.7709	392.47	-0.9743	505.42
0.6392	814.40	0.7903	727.10	0.9414	778.05	-0.3218	418.48	-0.5574	408.76	-0.7739	392.48	-0.9773	511.48
0.6414	829.53	0.7925	690.82	0.9436	787.70	-0.3253	434.66	-0.5604	408.47	-0.7768	392.50	-0.9803	518.51
0.6436	812.99	0.7947	728.02	0.9458	799.35	-0.3289	420.33	-0.5634	408.90	-0.7798	392.67	-0.9833	523.94
0.6458	819.18	0.7969	705.21	0.9481	811.23	-0.3324	436.32	-0.5664	410.00	-0.7828	393.28	-0.9863	531.61
0.6481	806.09	0.7992	704.38	0.9503	824.23	-0.3359	421.69	-0.5694	410.25	-0.7858	392.96	-0.9892	538.39
0.6503	805.50	0.8014	695.06	0.9525	822.79	-0.3394	423.42	-0.5724	410.21	-0.7888	391.35	-0.9922	543.84
0.6525	795.95	0.8036	666.65	0.9547	837.27	-0.3430	423.88	-0.5754	410.77	-0.7918	389.88		
0.6547	807.07	0.8058	679.96	0.9569	862.76	-0.3465	423.52	-0.5784	411.85	-0.7948	389.34		
0.6570	827.25	0.8081	696.30	0.9592	869.00	-0.3500	424.73	-0.5814	412.87	-0.7978	389.20		
0.6592	793.25	0.8103	672.02			-0.3535	426.01	-0.5844	413.68	-0.8008	389.43		
0.6614	819.89	0.8125	682.88			-0.3571	427.04	-0.6003	413.91	-0.8038	389.34		
0.6636	806.14	0.8147	707.12	X/PL	Nu	-0.3606	426.83	-0.6033	413.39	-0.8068	390.76	X/SL	η
0.6658	814.53	0.8169	702.58	-0.0103	1364.65	-0.3641	426.74	-0.6063	415.28	-0.8098	390.49	0.0519	0.4819
0.6681	822.50	0.8192	665.90	-0.0189	1235.09	-0.3676	426.10	-0.6093	415.58	-0.8127	389.84	0.0539	0.4395
0.6703	785.17	0.8214	656.46	-0.0274	1150.43	-0.3711	428.40	-0.6123	415.65	-0.8157	388.06	0.0558	0.4105
0.6725	791.13	0.8236	662.65	-0.0360	1047.29	-0.3747	428.59	-0.6153	417.01	-0.8187	388.21	0.0577	0.3821
0.6747	787.67	0.8258	657.21	-0.0445	970.16	-0.3782	426.62	-0.6183	418.33	-0.8217	388.44	0.0597	0.3615
0.6770	812.05	0.8281	665.02	-0.0531	863.14	-0.3817	425.74	-0.6213	420.70	-0.8247	389.22	0.0616	0.3498
0.6792	768.01	0.8303	655.19	-0.0616	778.48	-0.3852	425.34	-0.6243	420.11	-0.8277	390.12	0.0636	0.3335
0.6814	767.25	0.8325	673.83	-0.0702	705.98	-0.3888	423.53	-0.6273	420.22	-0.8307	390.48	0.0655	0.3266
0.6836	776.27	0.8347	680.89	-0.0787	655.62	-0.3923	423.81	-0.6303	419.80	-0.8337	390.12	0.0674	0.3207
0.6858	796.97	0.8369	689.26	-0.0873	619.99	-0.3958	422.50	-0.6333	419.66	-0.8367	390.52	0.0694	0.3153
0.6881	770.41	0.8392	668.20	-0.0958	579.91	-0.3993	423.78	-0.6362	420.69	-0.8397	390.59	0.0713	0.2940
0.6903	765.12	0.8414	656.08	-0.1044	527.54	-0.4029	422.60	-0.6392	420.22	-0.8427	391.11	0.0732	0.2950
				-0.1130	495.29							0.0752	0.2923

CASE O – η

Appendix 7.2 – Data for Spanwise Averaged Nusselt Number and Film Cooling Effectiveness

0.0771	0.2766	0.2089	0.3579	0.4503	0.2432	0.6015	0.1634	0.7526	0.1293	0.9037	0.0454	-0.2795	0.2369
0.0791	0.2681	0.2108	0.3625	0.4526	0.2502	0.6037	0.1711	0.7548	0.1164	0.9059	0.0505	-0.2830	0.2469
0.0810	0.2762	0.2128	0.3493	0.4548	0.2503	0.6059	0.1761	0.7570	0.1284	0.9081	0.0608	-0.2865	0.2637
0.0829	0.2640	0.2147	0.3425	0.4570	0.2539	0.6081	0.1704	0.7592	0.1125	0.9103	0.0613	-0.2901	0.2639
0.0849	0.2624	0.2166	0.3343	0.4592	0.2475	0.6103	0.1611	0.7614	0.1320	0.9126	0.0727	-0.2936	0.2402
0.0868	0.2548	0.2186	0.3288	0.4615	0.2596	0.6126	0.1627	0.7637	0.1487	0.9148	0.0634	-0.2971	0.2361
0.0888	0.2627	0.2205	0.3315	0.4637	0.2623	0.6148	0.1667	0.7659	0.1176	0.9170	0.0645	-0.3006	0.2366
0.0907	0.2618	0.2225	0.3257	0.4659	0.2555	0.6170	0.1572	0.7681	0.1152	0.9192	0.0587	-0.3041	0.2398
0.0926	0.2565	0.2244	0.3225	0.4681	0.2479	0.6192	0.1477	0.7703	0.1147	0.9214	0.0536	-0.3077	0.2349
0.0946	0.2448	0.2263	0.3155	0.4703	0.2485	0.6215	0.1506	0.7726	0.0842	0.9237	0.0527	-0.3112	0.2296
0.0965	0.2414	0.2283	0.3056	0.4726	0.2517	0.6237	0.1518	0.7748	0.1008	0.9259	0.0545	-0.3147	0.2276
0.0984	0.2474	0.2302	0.3076	0.4748	0.2458	0.6259	0.1655	0.7770	0.1270	0.9281	0.0501	-0.3182	0.2327
0.1004	0.2520	0.2302	0.3088	0.4770	0.2482	0.6281	0.1594	0.7792	0.1390	0.9303	0.0551	-0.3218	0.2313
0.1023	0.2482	0.2334	0.3056	0.4792	0.2449	0.6303	0.1490	0.7814	0.1309	0.9325	0.0452	-0.3253	0.2325
0.1043	0.2528	0.2366	0.3036	0.4815	0.2392	0.6326	0.1530	0.7837	0.1095	0.9348	0.0441	-0.3288	0.2290
0.1062	0.2442	0.2398	0.2992	0.4837	0.2379	0.6348	0.1520	0.7859	0.1287	0.9370	0.0521	-0.3323	0.2313
0.1081	0.2461	0.2430	0.2927	0.4859	0.2341	0.6370	0.1695	0.7881	0.1047	0.9392	0.0431	-0.3359	0.2216
0.1101	0.2465	0.2462	0.2936	0.4881	0.2456	0.6392	0.1546	0.7903	0.1419	0.9414	0.0434	-0.3394	0.2191
0.1120	0.2423	0.2494	0.2920	0.4903	0.2372	0.6415	0.1520	0.7926	0.1003	0.9437	0.0422	-0.3429	0.2175
0.1139	0.2376	0.2526	0.2838	0.4926	0.2332	0.6437	0.1452	0.7948	0.1327	0.9459	0.0421	-0.3464	0.2089
0.1159	0.2552	0.2558	0.2797	0.4948	0.2287	0.6459	0.1489	0.7970	0.1247	0.9481	0.0427	-0.3500	0.2122
0.1178	0.2507	0.2590	0.2814	0.4970	0.2257	0.6481	0.1386	0.7992	0.1253	0.9503	0.0494	-0.3535	0.2099
0.1198	0.2417	0.2622	0.2769	0.4992	0.2271	0.6503	0.1491	0.8014	0.1340	0.9525	0.0387	-0.3570	0.2073
0.1217	0.2425	0.2654	0.2718	0.5015	0.2233	0.6526	0.1351	0.8037	0.0973	0.9548	0.0462	-0.3605	0.2029
0.1236	0.2399	0.2686	0.2788	0.5037	0.2191	0.6548	0.1412	0.8059	0.1019	0.9570	0.0505	-0.3640	0.2011
0.1256	0.2433	0.2718	0.2814	0.5059	0.2153	0.6570	0.1483	0.8081	0.1185	0.9592	0.0479	-0.3676	0.1978
0.1275	0.2505	0.2750	0.2581	0.5081	0.2168	0.6592	0.1510	0.8103	0.1068			-0.3711	0.2017
0.1294	0.2580	0.2782	0.2915	0.5103	0.2096	0.6615	0.1564	0.8126	0.0999	X/PL	η	-0.3746	0.1997
0.1314	0.2692	0.2814	0.3557	0.5126	0.2071	0.6637	0.1488	0.8148	0.1199	-0.0530	0.3733	-0.3781	0.1968
0.1333	0.2813	0.2846	0.3882	0.5148	0.2088	0.6659	0.1464	0.8170	0.1218	-0.0616	0.3461	-0.3817	0.1945
0.1353	0.2915	0.2878	0.4043	0.5170	0.1996	0.6681	0.1601	0.8192	0.0848	-0.0701	0.3334	-0.3852	0.1930
0.1372	0.2950	0.2910	0.3970	0.5192	0.2012	0.6703	0.1384	0.8214	0.0909	-0.0787	0.3197	-0.3887	0.1887
0.1391	0.3064	0.2942	0.4062	0.5215	0.2050	0.6726	0.1324	0.8237	0.0993	-0.0872	0.3162	-0.3922	0.1926
0.1411	0.3515	0.2974	0.4150	0.5237	0.1986	0.6748	0.1436	0.8259	0.0905	-0.0958	0.3022	-0.3958	0.1872
0.1430	0.3826	0.3006	0.4373	0.5259	0.1995	0.6770	0.1578	0.8281	0.1024	-0.1044	0.2645	-0.3993	0.1870
0.1449	0.4012	0.3038	0.4467	0.5281	0.1950	0.6792	0.1329	0.8303	0.0880	-0.1129	0.2473	-0.4028	0.1836
0.1469	0.3895	0.3069	0.3645	0.5303	0.1927	0.6814	0.1295	0.8326	0.1016	-0.1215	0.2304	-0.4063	0.1855
0.1488	0.4115	0.3837	0.3232	0.5326	0.1802	0.6837	0.1400	0.8348	0.1095	-0.1300	0.2495	-0.4099	0.1847
0.1508	0.4020	0.3837	0.3022	0.5348	0.1816	0.6859	0.1522	0.8370	0.1213	-0.1386	0.2633	-0.4134	0.1807
0.1527	0.4180	0.3859	0.2990	0.5370	0.1891	0.6881	0.1386	0.8392	0.1098	-0.1471	0.2608	-0.4169	0.1761
0.1546	0.4212	0.3881	0.2853	0.5392	0.1798	0.6903	0.1338	0.8414	0.0984	-0.1557	0.2627	-0.4204	0.1746
0.1566	0.4310	0.3904	0.2914	0.5415	0.1737	0.6926	0.1561	0.8437	0.1103	-0.1642	0.2743	-0.4240	0.1781
0.1585	0.4263	0.3926	0.2813	0.5437	0.1730	0.6948	0.1349	0.8459	0.0976	-0.1728	0.2986	-0.4275	0.1822
0.1605	0.4284	0.3948	0.2817	0.5459	0.1728	0.6970	0.1334	0.8481	0.0901	-0.1813	0.3068	-0.4310	0.1778
0.1624	0.4284	0.3970	0.2828	0.5481	0.1683	0.6992	0.1218	0.8503	0.0887	-0.1899	0.2862	-0.4345	0.1741
0.1643	0.4221	0.3992	0.2728	0.5503	0.1682	0.7014	0.1253	0.8526	0.0928	-0.1984	0.2688	-0.4380	0.1710
0.1663	0.4225	0.4015	0.2787	0.5526	0.1661	0.7037	0.1347	0.8548	0.0807	-0.2020	0.2426	-0.4416	0.1694
0.1682	0.4205	0.4037	0.2751	0.5548	0.1648	0.7059	0.1484	0.8570	0.0973	-0.2055	0.2110	-0.4451	0.1661
0.1701	0.4102	0.4059	0.2713	0.5570	0.1608	0.7081	0.1451	0.8592	0.0848	-0.2090	0.1840	-0.4486	0.1626
0.1721	0.4236	0.4081	0.2702	0.5592	0.1561	0.7103	0.1375	0.8614	0.0883	-0.2125	0.1538	-0.4521	0.1611
0.1740	0.4222	0.4104	0.2711	0.5615	0.1570	0.7126	0.1531	0.8637	0.0957	-0.2161	0.1716	-0.4557	0.1563
0.1760	0.4196	0.4126	0.2622	0.5637	0.1545	0.7148	0.1370	0.8659	0.0896	-0.2196	0.1749	-0.4592	0.1527
0.1779	0.4189	0.4148	0.2563	0.5659	0.1511	0.7170	0.1282	0.8681	0.0872	-0.2231	0.1781	-0.4627	0.1475
0.1798	0.4198	0.4170	0.2556	0.5681	0.1550	0.7192	0.1415	0.8703	0.1007	-0.2266	0.1897	-0.4662	0.1494
0.1818	0.4255	0.4192	0.2494	0.5703	0.1622	0.7214	0.1254	0.8726	0.0804	-0.2302	0.2133	-0.4698	0.1489
0.1837	0.4167	0.4215	0.2475	0.5726	0.1593	0.7237	0.1253	0.8748	0.0875	-0.2337	0.2510	-0.4733	0.1532
0.1856	0.4106	0.4237	0.2459	0.5748	0.1555	0.7259	0.1339	0.8770	0.0968	-0.2372	0.2742	-0.4768	0.1535
0.1876	0.4078	0.4259	0.2475	0.5770	0.1592	0.7281	0.1499	0.8792	0.1000	-0.2407	0.2764	-0.4803	0.1545
0.1895	0.4136	0.4281	0.2541	0.5792	0.1561	0.7303	0.1434	0.8814	0.0966	-0.2442	0.2690	-0.4839	0.1521
0.1915	0.4027	0.4304	0.2520	0.5815	0.1620	0.7326	0.1278	0.8837	0.0941	-0.2478	0.2697	-0.4874	0.1515
0.1934	0.4057	0.4326	0.2569	0.5837	0.1604	0.7348	0.1389	0.8859	0.0786	-0.2513	0.2498	-0.4909	0.1509
0.1953	0.3904	0.4348	0.2622	0.5859	0.1594	0.7370	0.1274	0.8881	0.0783	-0.2548	0.2502	-0.4944	0.1453
0.1973	0.3883	0.4370	0.2525	0.5881	0.1598	0.7392	0.1321	0.8903	0.0822	-0.2583	0.2528	-0.4979	0.1443
0.1992	0.3881	0.4392	0.2544	0.5903	0.1655	0.7414	0.1198	0.8926	0.0800	-0.2619	0.2530	-0.5015	0.1399
0.2011	0.3812	0.4415	0.2553	0.5926	0.1561	0.7437	0.1350	0.8948	0.0672	-0.2654	0.2717	-0.5050	0.1372
0.2031	0.3744	0.4437	0.2500	0.5948	0.1592	0.7459	0.1200	0.8970	0.0525	-0.2689	0.2719	-0.5085	0.1385
0.2050	0.3674	0.4459	0.2451	0.5970	0.1583	0.7481	0.1322	0.8992	0.0505	-0.2724	0.2689	-0.5120	0.1400
0.2070	0.3658	0.4481	0.2492	0.5992	0.1634	0.7503	0.1240	0.9014	0.0483	-0.2760	0.2493	-0.5156	0.1361

Appendix 7.2 – Data for Spanwise Averaged Nusselt Number and Film Cooling Effectiveness

-0.5191	0.1346	-0.7140	0.0663	-0.9174	0.0615	0.1100	604.62	0.2461	666.38	0.4903	834.53	0.6414	836.79
-0.5226	0.1374	-0.7170	0.0635	-0.9204	0.0630	0.1120	597.30	0.2493	666.91	0.4925	834.87	0.6436	826.27
-0.5261	0.1391	-0.7200	0.0670	-0.9234	0.0583	0.1139	591.10	0.2525	668.10	0.4947	841.31	0.6458	851.67
-0.5297	0.1384	-0.7230	0.0705	-0.9264	0.0541	0.1158	590.62	0.2557	669.64	0.4970	837.40	0.6481	823.96
-0.5332	0.1364	-0.7259	0.0752	-0.9294	0.0568	0.1178	588.95	0.2589	675.01	0.4992	841.73	0.6503	810.93
-0.5367	0.1315	-0.7289	0.0713	-0.9324	0.0587	0.1197	586.98	0.2621	676.68	0.5014	839.87	0.6525	809.11
-0.5402	0.1328	-0.7319	0.0671	-0.9353	0.0563	0.1216	581.86	0.2653	682.06	0.5036	841.40	0.6547	813.37
-0.5438	0.1336	-0.7349	0.0654	-0.9383	0.0601	0.1236	581.91	0.2685	693.44	0.5059	841.38	0.6570	806.55
-0.5473	0.1294	-0.7379	0.0690	-0.9413	0.0585	0.1255	586.57	0.2717	688.54	0.5081	845.55	0.6592	803.12
-0.5508	0.1266	-0.7409	0.0725	-0.9443	0.0598	0.1275	591.53	0.2749	678.55	0.5103	841.65	0.6614	798.42
-0.5543	0.1243	-0.7439	0.0686	-0.9473	0.0550	0.1294	599.31	0.2781	692.46	0.5125	848.93	0.6636	826.97
-0.5579	0.1189	-0.7469	0.0677	-0.9503	0.0510	0.1313	610.17	0.2813	716.66	0.5147	855.62	0.6658	819.10
-0.5614	0.1168	-0.7499	0.0673	-0.9533	0.0509	0.1333	630.43	0.2845	750.71	0.5170	852.55	0.6681	835.74
-0.5649	0.1148	-0.7529	0.0662	-0.9563	0.0497	0.1352	675.34	0.2877	736.67	0.5192	852.49	0.6703	808.76
-0.5684	0.1181	-0.7559	0.0653	-0.9593	0.0494	0.1371	646.14	0.2909	691.80	0.5214	857.67	0.6725	790.36
-0.5719	0.1179	-0.7588	0.0668	-0.9623	0.0489	0.1391	629.06	0.2941	691.94	0.5236	862.02	0.6747	806.69
-0.5755	0.1257	-0.7618	0.0640	-0.9653	0.0478	0.1410	630.28	0.2973	714.36	0.5259	864.33	0.6770	808.05
-0.5614	0.1054	-0.7648	0.0592	-0.9683	0.0494	0.1430	655.74	0.3005	722.22	0.5281	869.23	0.6792	786.05
-0.5644	0.1044	-0.7678	0.0626	-0.9712	0.0492	0.1449	747.66	0.3037	715.23	0.5303	867.89	0.6814	778.23
-0.5674	0.1079	-0.7708	0.0675	-0.9742	0.0501	0.1468	776.65	0.3069	727.22	0.5325	869.72	0.6836	811.42
-0.5704	0.1099	-0.7738	0.0667	-0.9772	0.0495	0.1488	763.93	0.3836	722.94	0.5347	877.44	0.6858	802.60
-0.5734	0.1069	-0.7768	0.0691	-0.9802	0.0541	0.1507	746.86	0.3859	729.38	0.5370	873.00	0.6881	799.26
-0.5764	0.1068	-0.7798	0.0718	-0.9832	0.0531	0.1526	734.00	0.3881	729.56	0.5392	881.19	0.6903	815.94
-0.5794	0.1103	-0.7828	0.0769	-0.9862	0.0512	0.1546	733.13	0.3903	734.44	0.5414	883.17	0.6925	797.79
-0.5823	0.1131	-0.7858	0.0845	-0.9892	0.0489	0.1565	731.57	0.3925	736.88	0.5436	891.77	0.6947	781.68
-0.5853	0.1098	-0.7888	0.0815	-0.9922	0.0446	0.1585	713.48	0.3947	733.92	0.5459	902.26	0.6970	774.98
-0.5883	0.1082	-0.7918	0.0732			0.1604	705.42	0.3970	732.91	0.5481	896.37	0.6992	811.38
-0.5913	0.1073	-0.7947	0.0624			0.1623	715.55	0.3992	737.21	0.5503	909.01	0.7014	809.10
-0.5943	0.1060	-0.7977	0.0647			0.1643	725.08	0.4014	737.46	0.5525	916.40	0.7036	799.39
-0.5973	0.1054	-0.8007	0.0660			0.1662	716.23	0.4036	742.77	0.5547	904.65	0.7058	778.53
-0.6003	0.0996	-0.8037	0.0661			0.1682	708.49	0.4059	740.47	0.5570	905.69	0.7081	766.56
-0.6033	0.0929	-0.8067	0.0736			0.1701	714.66	0.4081	742.68	0.5592	908.45	0.7103	781.72
-0.6063	0.0940	-0.8097	0.0752			0.1720	719.75	0.4103	741.97	0.5614	918.45	0.7125	806.16
-0.6093	0.0950	-0.8127	0.0748			0.1740	717.07	0.4125	748.91	0.5636	914.87	0.7147	772.63
-0.6123	0.0993	-0.8157	0.0730			0.1759	713.59	0.4147	750.91	0.5658	909.35	0.7170	777.74
-0.6153	0.0991	-0.8187	0.0772			0.1778	719.65	0.4170	763.21	0.5681	911.89	0.7192	772.16
-0.6182	0.0997	-0.8217	0.0847			0.1798	721.17	0.4192	770.70	0.5703	923.45	0.7214	767.04
-0.6212	0.1019	-0.8247	0.0902			0.1817	715.28	0.4214	768.98	0.5725	913.39	0.7236	778.67
-0.6242	0.0993	-0.8277	0.0883			0.1837	721.56	0.4236	770.11	0.5747	913.48	0.7258	764.45
-0.6272	0.0973	-0.8306	0.0799			0.1856	718.02	0.4259	777.85	0.5770	909.28	0.7281	763.15
-0.6302	0.0963	-0.8336	0.0743			0.1875	719.10	0.4281	779.53	0.5792	914.91	0.7303	811.88
-0.6332	0.0974	-0.8366	0.0719			0.1895	714.20	0.4303	781.01	0.5814	909.02	0.7325	776.08
-0.6362	0.0973	-0.8396	0.0714			0.1914	723.09	0.4325	777.10	0.5836	896.21	0.7347	751.36
-0.6392	0.0922	-0.8426	0.0696			0.1933	728.27	0.4347	782.87	0.5858	896.81	0.7370	760.44
-0.6422	0.0919	-0.8456	0.0681			0.1953	724.44	0.4370	792.53	0.5881	903.63	0.7392	777.28
-0.6452	0.0911	-0.8486	0.0645			0.1972	723.82	0.4392	795.74	0.5903	901.69	0.7414	745.11
-0.6482	0.0896	-0.8516	0.0626			0.1992	722.85	0.4414	792.88	0.5925	889.71	0.7436	743.99
-0.6512	0.0860	-0.8546	0.0632			0.2011	722.06	0.4436	792.29	0.5947	878.11	0.7458	751.16
-0.6541	0.0835	-0.8576	0.0607			0.2030	716.29	0.4459	791.66	0.5970	886.05	0.7481	758.73
-0.6571	0.0809	-0.8606	0.0631			0.2050	711.20	0.4481	805.17	0.5992	886.80	0.7503	750.55
-0.6601	0.0831	-0.8636	0.0644			0.2069	711.99	0.4503	805.96	0.6014	870.20	0.7525	729.49
-0.6631	0.0802	-0.8665	0.0610			0.2088	708.62	0.4525	800.70	0.6036	863.99	0.7547	737.87
-0.6661	0.0818	-0.8695	0.0637			0.2108	706.73	0.4547	802.46	0.6058	860.21	0.7570	733.65
-0.6691	0.0895	-0.8725	0.0674			0.2127	703.36	0.4570	812.02	0.6081	858.99	0.7592	768.23
-0.6721	0.0854	-0.8755	0.0651			0.2147	698.66	0.4592	815.64	0.6103	862.14	0.7614	753.42
-0.6751	0.0768	-0.8785	0.0606			0.2166	697.57	0.4614	820.94	0.6125	858.83	0.7636	721.31
-0.6781	0.0825	-0.8815	0.0592			0.2185	696.90	0.4636	816.11	0.6147	851.20	0.7658	732.21
-0.6811	0.0834	-0.8845	0.0568			0.2205	693.66	0.4659	813.95	0.6170	850.19	0.7681	740.62
-0.6841	0.0820	-0.8875	0.0564			0.2224	688.94	0.4681	823.41	0.6192	852.69	0.7703	764.67
-0.6871	0.0754	-0.8905	0.0551			0.2243	683.15	0.4703	821.40	0.6214	863.64	0.7725	732.62
-0.6900	0.0777	-0.8935	0.0520			0.2263	677.54	0.4725	824.14	0.6236	842.32	0.7747	714.61
-0.6930	0.0746	-0.8965	0.0524			0.2282	677.42	0.4747	826.75	0.6258	845.41	0.7770	727.19
-0.6960	0.0758	-0.8995	0.0563			0.2302	676.79	0.4770	833.19	0.6281	858.19	0.7792	721.93
-0.6990	0.0742	-0.9024	0.0537			0.2322	672.74	0.4792	823.65	0.6303	843.04	0.7814	714.20
-0.7020	0.0648	-0.9054	0.0553			0.2344	670.22	0.4814	825.96	0.6325	846.02	0.7836	709.38
-0.7050	0.0648	-0.9084	0.0601			0.2366	670.03	0.4836	831.43	0.6347	842.13	0.7858	710.31
-0.7080	0.0685	-0.9114	0.0611			0.2398	669.97	0.4859	838.02	0.6370	836.20	0.7881	718.99
-0.7110	0.0704	-0.9144	0.0577			0.2430	667.42	0.4881	833.94	0.6392	825.14	0.7903	729.18

CASE P – Nu

X/SL Nu

Appendix 7.2 – Data for Spanwise Averaged Nusselt Number and Film Cooling Effectiveness

0.7925	716.43	0.9436	851.24	-0.3253	475.98	-0.5734	398.63	-0.7768	393.85	-0.9803	561.73	0.1508	0.3084
0.7947	717.76	0.9458	867.49	-0.3289	461.77	-0.5764	398.96	-0.7798	394.50	-0.9833	568.18	0.1527	0.3069
0.7969	719.65	0.9481	877.02	-0.3324	449.21	-0.5794	399.90	-0.7828	395.58	-0.9863	576.93	0.1546	0.3173
0.7992	702.78	0.9503	886.32	-0.3359	445.56	-0.5824	400.08	-0.7858	395.77	-0.9892	584.83	0.1566	0.3321
0.8014	699.92	0.9525	890.00	-0.3394	445.77	-0.5854	399.94	-0.7888	394.65	-0.9922	591.27	0.1585	0.3220
0.8036	707.08	0.9547	906.13	-0.3430	459.06	-0.5884	400.42	-0.7918	393.63			0.1605	0.3201
0.8058	715.58	0.9569	934.77	-0.3465	445.22	-0.5914	401.35	-0.7948	393.55			0.1624	0.3428
0.8081	712.45	0.9592	941.11	-0.3500	445.75	-0.5944	402.29	-0.7978	393.98	CASE P – η		0.1643	0.3620
0.8103	705.10			-0.3535	446.15	-0.5974	402.92	-0.8008	394.65			0.1663	0.3524
0.8125	703.96	X/PL	Nu	-0.3571	446.07	-0.6003	403.09	-0.8038	395.06	X/SL	η	0.1682	0.3429
0.8147	692.53	-0.0103	1341.18	-0.3606	458.47	-0.6033	402.49	-0.8068	396.96	0.0384	0.5002	0.1701	0.3579
0.8169	699.23	-0.0189	1262.40	-0.3641	446.32	-0.6063	404.23	-0.8098	397.18	0.0403	0.4613	0.1721	0.3686
0.8192	700.11	-0.0274	1157.24	-0.3676	444.07	-0.6093	404.47	-0.8127	397.00	0.0422	0.4604	0.1740	0.3611
0.8214	695.05	-0.0360	1020.50	-0.3711	444.95	-0.6123	404.45	-0.8157	395.69	0.0442	0.4308	0.1760	0.3692
0.8236	684.02	-0.0445	922.78	-0.3747	444.87	-0.6153	405.65	-0.8187	396.32	0.0461	0.4796	0.1779	0.3793
0.8258	709.99	-0.0531	826.71	-0.3782	438.11	-0.6183	406.84	-0.8217	397.08	0.0481	0.3941	0.1798	0.3777
0.8281	701.70	-0.0616	779.12	-0.3817	443.31	-0.6213	409.04	-0.8247	398.30	0.0500	0.3224	0.1818	0.3731
0.8303	687.67	-0.0702	699.57	-0.3852	441.40	-0.6243	408.41	-0.8277	399.72	0.0519	0.2754	0.1837	0.3861
0.8325	697.32	-0.0787	633.01	-0.3888	441.77	-0.6273	408.38	-0.8307	400.60	0.0539	0.2400	0.1856	0.3921
0.8347	692.43	-0.0873	592.05	-0.3923	441.31	-0.6303	407.98	-0.8337	400.72	0.0558	0.2318	0.1876	0.3905
0.8369	680.16	-0.0958	547.35	-0.3958	439.86	-0.6333	407.69	-0.8367	401.63	0.0577	0.2184	0.1895	0.3841
0.8392	686.50	-0.1044	539.27	-0.3993	441.45	-0.6362	408.69	-0.8397	402.19	0.0597	0.2153	0.1915	0.3914
0.8414	686.56	-0.1130	496.39	-0.4029	441.68	-0.6392	408.17	-0.8427	403.26	0.0616	0.1992	0.1934	0.3988
0.8436	696.14	-0.1215	468.93	-0.4064	439.85	-0.6422	406.76	-0.8457	404.35	0.0636	0.1973	0.1953	0.3944
0.8458	701.98	-0.1301	459.31	-0.4099	439.50	-0.6452	407.32	-0.8486	404.70	0.0655	0.1913	0.1973	0.4048
0.8481	679.06	-0.1386	454.01	-0.4134	434.44	-0.6482	408.50	-0.8516	405.04	0.0674	0.2001	0.1992	0.4087
0.8503	673.28	-0.1472	450.73	-0.4170	434.78	-0.6512	407.73	-0.8546	405.91	0.0694	0.1796	0.2011	0.4056
0.8525	679.62	-0.1557	467.74	-0.4205	441.24	-0.6542	407.71	-0.8576	406.89	0.0713	0.1949	0.2031	0.4047
0.8547	684.99	-0.1643	482.04	-0.4240	440.18	-0.6572	408.10	-0.8606	408.27	0.0732	0.2044	0.2050	0.4061
0.8569	682.50	-0.1728	477.22	-0.4275	435.88	-0.6602	407.43	-0.8636	409.73	0.0752	0.1986	0.2070	0.4115
0.8592	675.32	-0.1814	519.62	-0.4310	437.25	-0.6632	407.04	-0.8666	411.09	0.0771	0.1928	0.2089	0.4036
0.8614	674.60	-0.1899	540.57	-0.4346	443.22	-0.6662	407.44	-0.8696	412.86	0.0791	0.2039	0.2108	0.4082
0.8636	689.07	-0.1985	468.18	-0.4381	443.63	-0.6692	411.19	-0.8726	414.79	0.0810	0.1999	0.2128	0.4041
0.8658	682.93	-0.2020	501.96	-0.4416	444.55	-0.6721	407.81	-0.8756	416.49	0.0829	0.2121	0.2147	0.3971
0.8681	682.98	-0.2055	454.37	-0.4451	441.10	-0.6751	407.43	-0.8786	417.31	0.0849	0.2066	0.2166	0.4059
0.8703	691.26	-0.2091	498.42	-0.4487	441.65	-0.6781	408.79	-0.8816	419.08	0.0868	0.1992	0.2186	0.4065
0.8725	686.42	-0.2126	519.61	-0.4522	430.04	-0.6811	407.86	-0.8845	421.86	0.0888	0.2076	0.2205	0.4086
0.8747	684.08	-0.2161	521.59	-0.4557	431.20	-0.6841	406.98	-0.8875	424.33	0.0907	0.2166	0.2225	0.4017
0.8769	681.23	-0.2196	532.32	-0.4592	429.93	-0.6871	406.10	-0.8905	425.95	0.0926	0.2180	0.2244	0.4029
0.8792	687.20	-0.2232	543.09	-0.4628	422.34	-0.6901	407.18	-0.8935	428.68	0.0946	0.2204	0.2263	0.4009
0.8814	688.04	-0.2267	535.12	-0.4663	416.72	-0.6931	407.46	-0.8965	431.06	0.0965	0.2217	0.2283	0.3991
0.8836	689.04	-0.2302	495.20	-0.4698	426.97	-0.6961	406.70	-0.8995	433.61	0.0984	0.2144	0.2302	0.3990
0.8858	690.71	-0.2337	468.61	-0.4733	431.93	-0.6991	406.22	-0.9025	436.98	0.1004	0.2162	0.2302	0.3965
0.8881	688.81	-0.2372	469.16	-0.4769	437.07	-0.7021	402.91	-0.9055	440.40	0.1023	0.2234	0.2334	0.3911
0.8903	695.29	-0.2408	489.41	-0.4804	408.29	-0.7051	401.84	-0.9085	444.76	0.1043	0.2169	0.2366	0.3885
0.8925	697.29	-0.2443	479.96	-0.4839	416.72	-0.7080	401.29	-0.9115	447.86	0.1062	0.2162	0.2398	0.3854
0.8947	702.86	-0.2478	502.52	-0.4874	406.11	-0.7110	401.73	-0.9145	450.78	0.1081	0.2145	0.2430	0.3786
0.8969	710.51	-0.2513	515.35	-0.4910	410.28	-0.7140	401.17	-0.9174	454.60	0.1101	0.2235	0.2462	0.3761
0.8992	729.87	-0.2549	506.41	-0.4945	411.38	-0.7170	399.56	-0.9204	459.19	0.1120	0.2289	0.2494	0.3749
0.9014	722.10	-0.2584	514.60	-0.4980	415.56	-0.7200	398.89	-0.9234	462.70	0.1139	0.2222	0.2526	0.3775
0.9036	741.80	-0.2619	503.45	-0.5015	419.54	-0.7230	398.89	-0.9264	466.66	0.1159	0.2257	0.2558	0.3817
0.9058	732.37	-0.2654	495.66	-0.5050	419.80	-0.7260	399.77	-0.9294	470.40	0.1178	0.2256	0.2590	0.3863
0.9081	734.35	-0.2690	499.03	-0.5086	403.73	-0.7290	398.69	-0.9324	474.99	0.1198	0.2254	0.2622	0.3862
0.9103	738.09	-0.2725	489.33	-0.5121	396.24	-0.7320	395.83	-0.9354	478.46	0.1217	0.2202	0.2654	0.3974
0.9125	739.77	-0.2760	469.38	-0.5156	406.68	-0.7350	395.65	-0.9384	483.85	0.1236	0.2182	0.2686	0.4139
0.9147	746.74	-0.2795	479.08	-0.5191	389.93	-0.7380	396.98	-0.9414	487.59	0.1256	0.2324	0.2718	0.4057
0.9169	752.75	-0.2831	469.04	-0.5227	410.92	-0.7409	398.10	-0.9444	493.01	0.1275	0.2387	0.2750	0.4157
0.9192	764.23	-0.2866	479.96	-0.5262	416.82	-0.7439	398.39	-0.9474	496.41	0.1294	0.2481	0.2782	0.4558
0.9214	766.23	-0.2901	469.45	-0.5297	422.00	-0.7469	396.20	-0.9504	500.54	0.1314	0.2628	0.2814	0.4938
0.9236	771.07	-0.2936	496.81	-0.5332	416.01	-0.7499	394.72	-0.9533	506.21	0.1333	0.2755	0.2846	0.5184
0.9258	784.46	-0.2971	492.75	-0.5495	395.53	-0.7529	394.10	-0.9563	509.85	0.1353	0.3400	0.2878	0.5181
0.9281	786.82	-0.3007	484.39	-0.5525	396.34	-0.7559	393.57	-0.9593	515.65	0.1372	0.3362	0.2910	0.4897
0.9303	796.05	-0.3042	458.52	-0.5555	396.05	-0.7589	393.58	-0.9623	520.77	0.1391	0.3367	0.2942	0.5045
0.9325	801.01	-0.3077	462.59	-0.5585	396.32	-0.7619	393.34	-0.9653	526.65	0.1411	0.3245	0.2974	0.5372
0.9347	811.27	-0.3112	465.04	-0.5615	396.71	-0.7649	392.68	-0.9683	533.39	0.1430	0.3203	0.3006	0.5508
0.9369	821.44	-0.3148	491.09	-0.5645	397.27	-0.7679	392.46	-0.9713	539.24	0.1449	0.3159	0.3038	0.5220
0.9392	831.14	-0.3183	452.01	-0.5674	397.99	-0.7709	392.75	-0.9743	546.64	0.1469	0.3272	0.3069	0.4400
0.9414	846.29	-0.3218	451.22	-0.5704	399.02	-0.7739	393.33	-0.9773	553.62	0.1488	0.3079	0.3837	0.3769

Appendix 7.2 – Data for Spanwise Averaged Nusselt Number and Film Cooling Effectiveness

0.3859	0.3846	0.5370	0.2738	0.6881	0.1809	0.8392	0.1551	-0.1471	0.3031	-0.4240	0.2290	-0.6512	0.1293
0.3881	0.3902	0.5392	0.2788	0.6903	0.1972	0.8414	0.1501	-0.1557	0.2675	-0.4275	0.2380	-0.6541	0.1227
0.3904	0.3904	0.5415	0.2704	0.6926	0.1859	0.8437	0.1411	-0.1642	0.3083	-0.4310	0.2320	-0.6571	0.1194
0.3926	0.3897	0.5437	0.2691	0.6948	0.1746	0.8459	0.1452	-0.1728	0.2574	-0.4345	0.2370	-0.6601	0.1222
0.3948	0.3847	0.5459	0.2674	0.6970	0.1749	0.8481	0.1384	-0.1813	0.2934	-0.4380	0.2280	-0.6631	0.1236
0.3970	0.3802	0.5481	0.2637	0.6992	0.1932	0.8503	0.1413	-0.1899	0.2943	-0.4416	0.2260	-0.6661	0.1270
0.3992	0.3791	0.5503	0.2580	0.7014	0.1920	0.8526	0.1383	-0.1984	0.2529	-0.4451	0.2300	-0.6691	0.1360
0.4015	0.3743	0.5526	0.2671	0.7037	0.1817	0.8548	0.1335	-0.2020	0.2499	-0.4486	0.2290	-0.6721	0.1284
0.4037	0.3698	0.5548	0.2598	0.7059	0.1682	0.8570	0.1413	-0.2055	0.1896	-0.4521	0.2250	-0.6751	0.1279
0.4059	0.3637	0.5570	0.2540	0.7081	0.1674	0.8592	0.1427	-0.2090	0.1809	-0.4557	0.2240	-0.6781	0.1301
0.4081	0.3665	0.5592	0.2443	0.7103	0.1857	0.8614	0.1331	-0.2125	0.2088	-0.4592	0.2200	-0.6811	0.1253
0.4104	0.3616	0.5615	0.2550	0.7126	0.1933	0.8637	0.1349	-0.2161	0.2170	-0.4627	0.2189	-0.6841	0.1207
0.4126	0.3546	0.5637	0.2526	0.7148	0.1710	0.8659	0.1321	-0.2196	0.1982	-0.4662	0.2242	-0.6871	0.1141
0.4148	0.3359	0.5659	0.2375	0.7170	0.1767	0.8681	0.1314	-0.2231	0.2336	-0.4698	0.2239	-0.6900	0.1206
0.4170	0.3339	0.5681	0.2348	0.7192	0.1781	0.8703	0.1295	-0.2266	0.1911	-0.4733	0.2237	-0.6930	0.1215
0.4192	0.3380	0.5703	0.2396	0.7214	0.1734	0.8726	0.1281	-0.2302	0.2150	-0.4768	0.2175	-0.6960	0.1188
0.4215	0.3315	0.5726	0.2456	0.7237	0.1790	0.8748	0.1276	-0.2337	0.1972	-0.4803	0.2120	-0.6990	0.1169
0.4237	0.3421	0.5748	0.2406	0.7259	0.1742	0.8770	0.1303	-0.2372	0.2552	-0.4839	0.2010	-0.7020	0.1085
0.4259	0.3497	0.5770	0.2321	0.7281	0.1754	0.8792	0.1324	-0.2407	0.2795	-0.4874	0.1864	-0.7050	0.1066
0.4281	0.3472	0.5792	0.2338	0.7303	0.1996	0.8814	0.1285	-0.2442	0.3015	-0.4909	0.1935	-0.7080	0.1120
0.4304	0.3353	0.5815	0.2388	0.7326	0.1756	0.8837	0.1264	-0.2478	0.2769	-0.4944	0.1897	-0.7110	0.1160
0.4326	0.3413	0.5837	0.2267	0.7348	0.1540	0.8859	0.1305	-0.2513	0.2406	-0.4979	0.1979	-0.7140	0.1113
0.4348	0.3426	0.5859	0.2159	0.7370	0.1704	0.8881	0.1269	-0.2548	0.2483	-0.5015	0.2117	-0.7170	0.1111
0.4370	0.3403	0.5881	0.2280	0.7392	0.1757	0.8903	0.1240	-0.2583	0.3300	-0.5050	0.2101	-0.7200	0.1134
0.4392	0.3349	0.5903	0.2253	0.7414	0.1655	0.8926	0.1233	-0.2619	0.2900	-0.5085	0.2038	-0.7230	0.1146
0.4415	0.3372	0.5926	0.2195	0.7437	0.1663	0.8948	0.1295	-0.2654	0.3000	-0.5120	0.2009	-0.7259	0.1175
0.4437	0.3546	0.5948	0.2074	0.7459	0.1739	0.8970	0.1351	-0.2760	0.3010	-0.5156	0.2031	-0.7289	0.1216
0.4459	0.3429	0.5970	0.2123	0.7481	0.1745	0.8992	0.1293	-0.2795	0.3040	-0.5191	0.1886	-0.7319	0.1116
0.4481	0.3467	0.5992	0.2215	0.7503	0.1636	0.9014	0.1177	-0.2830	0.3000	-0.5226	0.1980	-0.7349	0.1075
0.4503	0.3511	0.6015	0.2138	0.7526	0.1471	0.9037	0.1179	-0.2865	0.3000	-0.5261	0.2027	-0.7379	0.1100
0.4526	0.3496	0.6037	0.2066	0.7548	0.1553	0.9059	0.1020	-0.2901	0.2901	-0.5297	0.2124	-0.7409	0.1128
0.4548	0.3559	0.6059	0.1976	0.7570	0.1574	0.9081	0.1079	-0.2936	0.2943	-0.5332	0.2059	-0.7439	0.1130
0.4570	0.3557	0.6081	0.2024	0.7592	0.1869	0.9103	0.1137	-0.2971	0.3003	-0.5367	0.1963	-0.7469	0.1141
0.4592	0.3487	0.6103	0.1968	0.7614	0.1680	0.9126	0.1113	-0.3006	0.2918	-0.5402	0.1785	-0.7499	0.1110
0.4615	0.3566	0.6126	0.2012	0.7637	0.1559	0.9148	0.1107	-0.3041	0.2950	-0.5438	0.1798	-0.7529	0.1142
0.4637	0.3555	0.6148	0.2142	0.7659	0.1519	0.9170	0.1084	-0.3077	0.2930	-0.5473	0.1812	-0.7559	0.1095
0.4659	0.3489	0.6170	0.1901	0.7681	0.1738	0.9192	0.1163	-0.3112	0.2960	-0.5508	0.1801	-0.7588	0.1162
0.4681	0.3533	0.6192	0.1791	0.7703	0.1848	0.9214	0.1106	-0.3147	0.2880	-0.5543	0.1725	-0.7618	0.1113
0.4703	0.3543	0.6215	0.1859	0.7726	0.1697	0.9237	0.1095	-0.3182	0.2900	-0.5579	0.1700	-0.7648	0.1134
0.4726	0.3487	0.6237	0.1863	0.7748	0.1488	0.9259	0.1169	-0.3218	0.2830	-0.5614	0.1659	-0.7678	0.1126
0.4748	0.3417	0.6259	0.1704	0.7770	0.1627	0.9281	0.1125	-0.3253	0.2830	-0.5649	0.1681	-0.7708	0.1120
0.4770	0.3358	0.6281	0.1882	0.7792	0.1624	0.9303	0.1130	-0.3288	0.2800	-0.5684	0.1807	-0.7738	0.1241
0.4792	0.3311	0.6303	0.1773	0.7814	0.1581	0.9325	0.1134	-0.3323	0.2740	-0.5719	0.1672	-0.7768	0.1264
0.4815	0.3392	0.6326	0.1874	0.7837	0.1513	0.9348	0.1125	-0.3359	0.2770	-0.5755	0.1698	-0.7798	0.1198
0.4837	0.3311	0.6348	0.1947	0.7859	0.1538	0.9370	0.1123	-0.3394	0.2700	-0.5794	0.1600	-0.7828	0.1200
0.4859	0.3285	0.6370	0.1906	0.7881	0.1613	0.9392	0.1133	-0.3429	0.2650	-0.5823	0.1568	-0.7858	0.1181
0.4881	0.3209	0.6392	0.1843	0.7903	0.1691	0.9414	0.1112	-0.3464	0.2800	-0.5853	0.1577	-0.7888	0.1250
0.4903	0.3157	0.6415	0.1938	0.7926	0.1645	0.9437	0.1023	-0.3500	0.2690	-0.5883	0.1557	-0.7918	0.1171
0.4926	0.3154	0.6437	0.1794	0.7948	0.1555	0.9459	0.1033	-0.3535	0.2650	-0.5913	0.1515	-0.7947	0.1172
0.4948	0.3195	0.6459	0.1992	0.7970	0.1530	0.9481	0.1075	-0.3570	0.2620	-0.5943	0.1517	-0.7977	0.1237
0.4970	0.3174	0.6481	0.1748	0.7992	0.1614	0.9503	0.1029	-0.3605	0.2720	-0.5973	0.1451	-0.8007	0.1249
0.4992	0.3103	0.6503	0.1737	0.8014	0.1600	0.9525	0.1021	-0.3640	0.2620	-0.6003	0.1449	-0.8037	0.1283
0.5015	0.3073	0.6526	0.1756	0.8037	0.1623	0.9548	0.1027	-0.3676	0.2550	-0.6033	0.1411	-0.8067	0.1294
0.5037	0.2980	0.6548	0.1683	0.8059	0.1675	0.9570	0.1028	-0.3711	0.2600	-0.6063	0.1468	-0.8097	0.1228
0.5059	0.2975	0.6570	0.1611	0.8081	0.1548	0.9592	0.1009	-0.3746	0.2530	-0.6093	0.1424	-0.8127	0.1258
0.5081	0.2985	0.6592	0.1730	0.8103	0.1604			-0.3781	0.2520	-0.6123	0.1397	-0.8157	0.1266
0.5103	0.2927	0.6615	0.1724	0.8126	0.1503	X/PL	η	-0.3817	0.2500	-0.6153	0.1436	-0.8187	0.1269
0.5126	0.2973	0.6637	0.1865	0.8148	0.1412	-0.0530	0.4497	-0.3852	0.2460	-0.6182	0.1459	-0.8217	0.1297
0.5148	0.2971	0.6659	0.1829	0.8170	0.1437	-0.0616	0.4296	-0.3887	0.2500	-0.6212	0.1464	-0.8247	0.1306
0.5170	0.2870	0.6681	0.1956	0.8192	0.1614	-0.0701	0.4073	-0.3922	0.2450	-0.6242	0.1456	-0.8277	0.1296
0.5192	0.2907	0.6703	0.1858	0.8214	0.1609	-0.0787	0.3804	-0.3958	0.2400	-0.6272	0.1451	-0.8306	0.1268
0.5215	0.2919	0.6726	0.1666	0.8237	0.1413	-0.0872	0.3788	-0.3993	0.2400	-0.6302	0.1411	-0.8336	0.1299
0.5237	0.2845	0.6748	0.1766	0.8259	0.1621	-0.0958	0.3294	-0.4028	0.2380	-0.6332	0.1383	-0.8366	0.1345
0.5259	0.2818	0.6770	0.1816	0.8281	0.1546	-0.1044	0.3166	-0.4063	0.2400	-0.6362	0.1406	-0.8396	0.1350
0.5281	0.2809	0.6792	0.1721	0.8303	0.1486	-0.1129	0.2906	-0.4099	0.2350	-0.6392	0.1336	-0.8426	0.1345
0.5303	0.2821	0.6814	0.1649	0.8326	0.1446	-0.1215	0.2834	-0.4134	0.2330	-0.6422	0.1295	-0.8456	0.1354
0.5326	0.2755	0.6837	0.1835	0.8348	0.1500	-0.1300	0.2941	-0.4169	0.2330	-0.6452	0.1313	-0.8486	0.1305
0.5348	0.2770	0.6859	0.1864	0.8370	0.1383	-0.1386	0.3066	-0.4204	0.2300	-0.6482	0.1329	-0.8516	0.1299

Appendix 7.2 – Data for Spanwise Averaged Nusselt Number and Film Cooling Effectiveness

-0.8546	0.1270	0.0694	929.51	0.2011	779.68	0.4436	914.25	0.5947	1034.63	0.7458	840.98	0.8969	855.69
-0.8576	0.1266	0.0713	918.09	0.2030	757.57	0.4459	916.55	0.5970	1043.81	0.7481	854.11	0.8992	859.02
-0.8606	0.1278	0.0732	906.19	0.2050	760.23	0.4481	914.74	0.5992	1032.43	0.7503	845.77	0.9014	866.64
-0.8636	0.1318	0.0752	892.69	0.2069	770.88	0.4503	912.00	0.6014	1017.90	0.7525	843.36	0.9036	878.20
-0.8665	0.1313	0.0771	874.02	0.2088	758.43	0.4525	910.99	0.6036	1004.20	0.7547	837.79	0.9058	881.38
-0.8695	0.1288	0.0791	867.09	0.2108	736.84	0.4547	913.77	0.6058	1005.06	0.7570	839.83	0.9081	884.78
-0.8725	0.1344	0.0810	850.09	0.2127	744.18	0.4570	918.82	0.6081	1008.71	0.7592	827.67	0.9103	884.53
-0.8755	0.1292	0.0829	840.63	0.2147	724.42	0.4592	917.12	0.6103	1002.60	0.7614	833.61	0.9125	884.14
-0.8785	0.1191	0.0849	826.98	0.2166	714.88	0.4614	920.46	0.6125	992.39	0.7636	838.66	0.9147	907.17
-0.8815	0.1196	0.0868	816.85	0.2185	712.93	0.4636	919.07	0.6147	993.41	0.7658	830.33	0.9169	909.92
-0.8845	0.1199	0.0888	803.65	0.2205	711.70	0.4659	917.31	0.6170	1002.15	0.7681	830.76	0.9192	922.77
-0.8875	0.1214	0.0907	791.46	0.2224	703.66	0.4681	921.56	0.6192	1002.84	0.7703	845.76	0.9214	935.91
-0.8905	0.1189	0.0926	787.58	0.2243	703.88	0.4703	919.56	0.6214	1010.22	0.7725	821.24	0.9236	934.81
-0.8935	0.1236	0.0946	781.75	0.2263	685.36	0.4725	929.46	0.6236	999.11	0.7747	830.68	0.9258	952.49
-0.8965	0.1251	0.0965	768.52	0.2282	684.46	0.4747	929.11	0.6258	994.64	0.7770	835.10	0.9281	950.51
-0.8995	0.1270	0.0984	759.11	0.2302	683.28	0.4770	939.93	0.6281	1009.37	0.7792	827.10	0.9303	961.25
-0.9024	0.1287	0.1003	747.37	0.2302	677.51	0.4792	934.90	0.6303	991.77	0.7814	815.86	0.9325	968.92
-0.9054	0.1292	0.1023	739.83	0.2334	677.12	0.4814	934.28	0.6325	974.20	0.7836	813.45	0.9347	986.00
-0.9084	0.1299	0.1042	728.73	0.2366	677.45	0.4836	939.89	0.6347	989.52	0.7858	823.55	0.9369	999.84
-0.9114	0.1321	0.1061	725.20	0.2398	680.19	0.4859	948.99	0.6370	990.01	0.7881	841.35	0.9392	1007.61
-0.9144	0.1322	0.1081	724.12	0.2430	690.04	0.4881	952.05	0.6392	975.29	0.7903	823.00	0.9414	1028.89
-0.9174	0.1359	0.1100	717.52	0.2461	697.27	0.4903	952.40	0.6414	973.70	0.7925	808.13	0.9436	1056.84
-0.9204	0.1416	0.1120	707.69	0.2493	697.09	0.4925	954.01	0.6436	986.60	0.7947	822.91	0.9458	1071.02
-0.9234	0.1384	0.1139	703.42	0.2525	700.15	0.4947	960.21	0.6458	981.81	0.7969	834.09	0.9481	1090.53
-0.9264	0.1352	0.1158	706.66	0.2557	704.11	0.4970	958.36	0.6481	963.57	0.7992	815.76	0.9503	1087.66
-0.9294	0.1334	0.1178	712.21	0.2589	710.25	0.4992	957.49	0.6503	956.78	0.8014	827.30	0.9525	1103.40
-0.9324	0.1360	0.1197	701.68	0.2621	718.22	0.5014	963.07	0.6525	966.34	0.8036	810.42	0.9547	1117.31
-0.9353	0.1337	0.1216	689.43	0.2653	718.62	0.5036	964.96	0.6547	948.55	0.8058	815.89	0.9569	1150.01
-0.9383	0.1314	0.1236	685.74	0.2685	719.11	0.5059	961.74	0.6570	964.43	0.8081	815.76	0.9592	1159.26
-0.9413	0.1239	0.1255	686.57	0.2717	725.19	0.5081	962.77	0.6592	942.32	0.8103	805.88		
-0.9443	0.1238	0.1275	695.58	0.2749	728.74	0.5103	960.92	0.6614	933.76	0.8125	820.27	X/PL	Nu
-0.9473	0.1252	0.1294	702.48	0.2781	728.41	0.5125	973.70	0.6636	945.53	0.8147	815.12	-0.0103	1071.24
-0.9503	0.1206	0.1313	704.20	0.2813	736.03	0.5147	976.77	0.6658	936.28	0.8169	832.58	-0.0188	1027.62
-0.9533	0.1209	0.1333	708.54	0.2845	739.21	0.5170	981.20	0.6681	949.26	0.8192	812.54	-0.0274	988.54
-0.9563	0.1144	0.1352	723.33	0.2877	752.43	0.5192	983.87	0.6703	941.08	0.8214	806.39	-0.0359	905.79
-0.9593	0.1137	0.1371	750.21	0.2909	773.30	0.5214	981.64	0.6725	941.49	0.8236	809.93	-0.0445	826.11
-0.9623	0.1133	0.1391	802.21	0.2941	727.69	0.5236	991.62	0.6747	961.39	0.8258	815.28	-0.0530	782.70
-0.9653	0.1162	0.1410	747.20	0.2973	735.23	0.5259	994.41	0.6770	935.48	0.8281	813.00	-0.0616	744.57
-0.9683	0.1152	0.1430	724.58	0.3005	763.56	0.5281	996.00	0.6792	927.16	0.8303	800.99	-0.0701	700.10
-0.9712	0.1080	0.1449	722.89	0.3037	732.40	0.5303	1005.54	0.6814	914.02	0.8325	822.44	-0.0787	660.72
-0.9742	0.1010	0.1468	751.17	0.3069	741.75	0.5325	1006.69	0.6836	924.66	0.8347	828.82	-0.0872	623.34
-0.9772	0.0975	0.1488	852.94	0.3836	883.77	0.5347	1010.65	0.6858	922.03	0.8369	811.52	-0.0959	584.07
-0.9802	0.1011	0.1507	883.26	0.3859	878.68	0.5370	1012.53	0.6881	917.39	0.8392	810.60	-0.1044	553.41
-0.9832	0.0983	0.1526	891.00	0.3881	874.40	0.5392	1012.54	0.6903	929.11	0.8414	821.82	-0.1130	525.94
-0.9862	0.1011	0.1546	872.84	0.3903	879.21	0.5414	1018.01	0.6925	910.41	0.8436	824.58	-0.1215	496.53
-0.9892	0.0898	0.1565	876.18	0.3925	890.88	0.5436	1025.75	0.6947	900.26	0.8458	822.69	-0.1301	482.33
-0.9922	0.0806	0.1585	889.25	0.3947	887.95	0.5459	1037.16	0.6970	883.83	0.8481	809.63	-0.1386	467.14
		0.1604	882.35	0.3970	891.46	0.5481	1037.20	0.6992	905.12	0.8503	813.03	-0.1472	459.96
		0.1623	851.56	0.3992	890.35	0.5503	1049.96	0.7014	895.05	0.8525	808.42	-0.1557	445.47
		0.1643	843.84	0.4014	882.25	0.5525	1048.01	0.7036	897.68	0.8547	822.42	-0.1643	438.12
		0.1662	838.69	0.4036	880.51	0.5547	1044.93	0.7058	883.84	0.8569	814.97	-0.1728	433.14
		0.1682	826.29	0.4059	886.04	0.5570	1052.24	0.7081	883.22	0.8592	820.19	-0.1814	434.62
		0.1701	828.07	0.4081	886.91	0.5592	1060.21	0.7103	881.33	0.8614	812.53	-0.1899	450.74
		0.1720	817.66	0.4103	887.48	0.5614	1061.52	0.7125	889.53	0.8636	817.91	-0.1985	437.27
		0.1740	826.25	0.4125	895.23	0.5636	1057.00	0.7147	877.98	0.8658	815.59	-0.2020	393.16
		0.1759	828.48	0.4147	898.58	0.5658	1055.20	0.7170	867.74	0.8681	826.25	-0.2055	379.99
		0.1778	839.54	0.4170	907.94	0.5681	1064.02	0.7192	864.94	0.8703	839.87	-0.2091	370.47
		0.1798	823.89	0.4192	907.31	0.5703	1069.40	0.7214	870.99	0.8725	845.03	-0.2126	379.41
		0.1817	833.91	0.4214	912.18	0.5725	1058.61	0.7236	888.21	0.8747	833.88	-0.2161	376.89
		0.1837	816.63	0.4236	909.21	0.5747	1058.70	0.7258	888.68	0.8769	834.61	-0.2196	364.61
		0.1856	794.85	0.4259	909.34	0.5770	1062.35	0.7281	871.31	0.8792	843.32	-0.2232	379.58
		0.1875	793.48	0.4281	907.44	0.5792	1058.14	0.7303	873.43	0.8814	834.37	-0.2267	391.23
		0.1895	787.47	0.4303	916.83	0.5814	1052.21	0.7325	871.46	0.8836	831.07	-0.2302	403.45
		0.1914	829.14	0.4325	911.71	0.5836	1052.24	0.7347	879.13	0.8858	847.81	-0.2337	412.78
		0.1933	828.85	0.4347	906.81	0.5858	1048.99	0.7370	857.29	0.8881	841.73	-0.2372	431.88
		0.1953	791.50	0.4370	917.02	0.5881	1046.51	0.7392	872.11	0.8903	843.59	-0.2408	443.28
		0.1972	792.60	0.4392	917.64	0.5903	1047.10	0.7414	857.09	0.8925	847.90	-0.2443	456.32
		0.1992	782.86	0.4414	915.90	0.5925	1037.33	0.7436	834.91	0.8947	854.27	-0.2478	467.85
CASE Q – Nu													
X/SL	Nu												
0.0384	1246.52												
0.0403	1295.13												
0.0422	1163.57												
0.0442	1098.31												
0.0461	1111.67												
0.0481	1097.14												
0.0500	1050.62												
0.0519	1041.08												
0.0539	1028.82												
0.0558	1025.45												
0.0577	1026.89												
0.0597	1015.26												
0.0616	992.16												
0.0636	979.79												
0.0655	967.43												
0.0674	937.90												

Appendix 7.2 – Data for Spanwise Averaged Nusselt Number and Film Cooling Effectiveness

-0.2513	479.91	-0.4867	436.51	-0.6901	439.69	-0.8935	467.69	0.0946	0.2505	0.2263	0.2992	0.4726	0.2644
-0.2549	490.75	-0.4897	432.95	-0.6931	441.73	-0.8965	468.92	0.0965	0.2457	0.2283	0.2986	0.4748	0.2657
-0.2584	497.27	-0.4927	436.88	-0.6961	441.72	-0.8995	471.54	0.0984	0.2520	0.2302	0.2990	0.4770	0.2623
-0.2619	508.46	-0.4956	434.11	-0.6991	441.42	-0.9025	473.16	0.1004	0.2489	0.2302	0.2972	0.4792	0.2586
-0.2654	501.86	-0.4986	433.70	-0.7021	439.82	-0.9055	474.46	0.1023	0.2504	0.2334	0.2959	0.4815	0.2591
-0.2690	493.15	-0.5016	434.87	-0.7051	437.31	-0.9085	475.95	0.1043	0.2433	0.2366	0.2929	0.4837	0.2520
-0.2725	486.20	-0.5046	435.01	-0.7080	436.09	-0.9115	478.98	0.1062	0.2461	0.2398	0.2887	0.4859	0.2551
-0.2760	474.80	-0.5076	438.20	-0.7110	433.20	-0.9145	483.22	0.1081	0.2477	0.2430	0.2947	0.4881	0.2565
-0.2795	464.15	-0.5106	438.44	-0.7140	431.33	-0.9174	487.29	0.1101	0.2473	0.2462	0.2952	0.4903	0.2569
-0.2831	475.01	-0.5136	433.71	-0.7170	429.90	-0.9204	492.31	0.1120	0.2354	0.2494	0.2941	0.4926	0.2540
-0.2866	480.97	-0.5166	438.57	-0.7200	431.13	-0.9234	498.41	0.1139	0.2423	0.2526	0.2972	0.4948	0.2565
-0.2901	475.35	-0.5196	442.82	-0.7230	432.16	-0.9264	504.97	0.1159	0.2535	0.2558	0.2995	0.4970	0.2540
-0.2936	478.25	-0.5226	437.47	-0.7260	430.71	-0.9294	511.00	0.1178	0.2564	0.2590	0.2983	0.4992	0.2491
-0.2971	475.24	-0.5256	436.40	-0.7290	430.53	-0.9324	517.43	0.1198	0.2503	0.2622	0.3032	0.5015	0.2482
-0.3007	474.72	-0.5286	436.37	-0.7320	431.45	-0.9354	522.70	0.1217	0.2430	0.2654	0.3084	0.5037	0.2457
-0.3042	474.91	-0.5315	434.00	-0.7350	429.27	-0.9384	527.65	0.1236	0.2419	0.2686	0.3117	0.5059	0.2425
-0.3077	473.65	-0.5345	437.41	-0.7380	427.66	-0.9414	535.11	0.1256	0.2375	0.2718	0.3190	0.5081	0.2412
-0.3112	470.97	-0.5375	437.66	-0.7409	427.78	-0.9444	540.61	0.1275	0.2399	0.2750	0.3226	0.5103	0.2344
-0.3148	469.66	-0.5405	440.93	-0.7439	427.16	-0.9474	549.91	0.1294	0.2444	0.2782	0.3387	0.5126	0.2385
-0.3183	468.70	-0.5435	439.38	-0.7469	426.96	-0.9504	558.70	0.1314	0.2504	0.2814	0.3818	0.5148	0.2340
-0.3218	469.11	-0.5465	441.82	-0.7499	429.62	-0.9533	569.63	0.1333	0.2541	0.2846	0.4092	0.5170	0.2398
-0.3253	468.57	-0.5495	447.67	-0.7529	425.86	-0.9563	577.01	0.1353	0.2592	0.2878	0.4110	0.5192	0.2388
-0.3289	465.15	-0.5525	447.16	-0.7559	425.60	-0.9593	579.57	0.1372	0.2756	0.2910	0.3849	0.5215	0.2342
-0.3324	463.76	-0.5555	447.06	-0.7589	423.89	-0.9623	581.06	0.1391	0.3278	0.2942	0.3630	0.5237	0.2278
-0.3359	463.33	-0.5585	442.27	-0.7619	421.87	-0.9653	586.16	0.1411	0.3299	0.2974	0.3809	0.5259	0.2321
-0.3394	465.06	-0.5615	441.78	-0.7649	421.95	-0.9683	596.09	0.1430	0.3170	0.3006	0.3785	0.5281	0.2269
-0.3430	463.90	-0.5645	443.58	-0.7679	422.48	-0.9713	607.25	0.1449	0.3108	0.3038	0.3896	0.5303	0.2322
-0.3465	462.29	-0.5674	444.58	-0.7709	424.55	-0.9743	611.42	0.1469	0.2975	0.3069	0.3790	0.5326	0.2244
-0.3500	462.98	-0.5704	442.79	-0.7739	426.01	-0.9773	617.01	0.1488	0.2875	0.3837	0.3431	0.5348	0.2284
-0.3535	463.05	-0.5734	446.10	-0.7768	425.32	-0.9803	624.17	0.1508	0.2879	0.3859	0.3439	0.5370	0.2289
-0.3571	461.34	-0.5764	440.17	-0.7798	424.68	-0.9833	628.85	0.1527	0.2997	0.3881	0.3471	0.5392	0.2228
-0.3606	462.01	-0.5794	437.06	-0.7828	422.67	-0.9863	636.94	0.1546	0.2895	0.3904	0.3476	0.5415	0.2246
-0.3641	461.40	-0.5824	441.52	-0.7858	422.73	-0.9892	647.04	0.1566	0.2802	0.3926	0.3576	0.5437	0.2243
-0.3676	457.00	-0.5854	436.76	-0.7888	423.17	-0.9922	659.39	0.1585	0.2976	0.3948	0.3501	0.5459	0.2308
-0.3711	457.24	-0.5884	435.93	-0.7918	422.72			0.1605	0.3018	0.3970	0.3498	0.5481	0.2234
-0.3747	460.04	-0.5914	436.58	-0.7948	423.83			0.1624	0.2899	0.3992	0.3392	0.5503	0.2224
-0.3782	459.95	-0.5944	438.15	-0.7978	423.22			0.1643	0.2860	0.4015	0.3268	0.5526	0.2209
-0.3817	455.11	-0.5974	437.10	-0.8008	424.06			0.1663	0.2770	0.4037	0.3264	0.5548	0.2207
-0.3852	456.05	-0.6003	434.84	-0.8038	423.58			0.1682	0.2739	0.4059	0.3337	0.5570	0.2169
-0.3888	452.50	-0.6033	437.35	-0.8068	424.26			0.1701	0.2797	0.4081	0.3307	0.5592	0.2149
-0.3923	450.71	-0.6063	439.33	-0.8098	426.82			0.1721	0.2687	0.4104	0.3164	0.5615	0.2167
-0.3958	451.25	-0.6093	438.80	-0.8127	428.21			0.1740	0.2709	0.4126	0.3108	0.5637	0.2161
-0.3993	451.93	-0.6123	442.21	-0.8157	429.57			0.1760	0.2612	0.4148	0.3066	0.5659	0.2056
-0.4029	451.91	-0.6153	438.89	-0.8187	429.67			0.1779	0.2890	0.4170	0.3051	0.5681	0.2075
-0.4064	451.20	-0.6183	447.28	-0.8217	429.90			0.1798	0.2713	0.4192	0.3021	0.5703	0.2149
-0.4099	452.33	-0.6213	440.25	-0.8247	430.20			0.1818	0.2800	0.4215	0.3061	0.5726	0.2090
-0.4134	451.85	-0.6243	445.77	-0.8277	431.33			0.1837	0.2814	0.4237	0.3034	0.5748	0.2039
-0.4170	451.51	-0.6273	437.59	-0.8307	432.00			0.1856	0.2837	0.4259	0.2999	0.5770	0.2110
-0.4205	448.62	-0.6303	438.37	-0.8337	432.81			0.1876	0.2815	0.4281	0.2953	0.5792	0.2060
-0.4240	448.36	-0.6333	440.80	-0.8367	433.18			0.1895	0.2734	0.4304	0.2979	0.5815	0.2108
-0.4275	446.56	-0.6362	441.54	-0.8397	433.82			0.1915	0.2885	0.4326	0.2916	0.5837	0.2150
-0.4310	448.82	-0.6392	441.49	-0.8427	435.83			0.1934	0.2830	0.4348	0.2878	0.5859	0.2125
-0.4346	448.94	-0.6422	442.39	-0.8457	437.36			0.1953	0.2780	0.4370	0.2914	0.5881	0.2053
-0.4381	451.24	-0.6452	441.34	-0.8486	437.77			0.1973	0.2868	0.4392	0.2871	0.5903	0.2059
-0.4416	450.30	-0.6482	445.49	-0.8516	437.94			0.1992	0.2760	0.4415	0.2854	0.5926	0.2008
-0.4451	449.00	-0.6512	448.17	-0.8546	438.76			0.2011	0.2825	0.4437	0.2922	0.5948	0.2064
-0.4487	449.25	-0.6542	443.29	-0.8576	437.77			0.2031	0.2820	0.4459	0.2825	0.5970	0.2061
-0.4522	447.10	-0.6572	443.42	-0.8606	439.07			0.2050	0.2799	0.4481	0.2770	0.5992	0.2013
-0.4557	447.57	-0.6602	444.23	-0.8636	441.86			0.2070	0.2898	0.4503	0.2757	0.6015	0.1994
-0.4592	445.43	-0.6632	443.60	-0.8666	443.16			0.2089	0.2929	0.4526	0.2704	0.6037	0.1928
-0.4628	443.37	-0.6662	441.16	-0.8696	444.08			0.2108	0.2758	0.4548	0.2768	0.6059	0.1858
-0.4663	440.30	-0.6692	445.23	-0.8726	445.52			0.2128	0.2871	0.4570	0.2717	0.6081	0.1970
-0.4687	443.96	-0.6721	445.08	-0.8756	447.95			0.2147	0.2885	0.4592	0.2672	0.6103	0.1939
-0.4717	437.06	-0.6751	439.85	-0.8786	449.24			0.2166	0.2877	0.4615	0.2730	0.6126	0.1908
-0.4747	433.62	-0.6781	438.34	-0.8816	450.59			0.2186	0.2927	0.4637	0.2763	0.6148	0.1968
-0.4777	438.52	-0.6811	439.96	-0.8845	453.64			0.2205	0.2950	0.4659	0.2685	0.6170	0.1960
-0.4807	439.85	-0.6841	440.81	-0.8875	460.62			0.2225	0.2937	0.4681	0.2631	0.6192	0.1873
-0.4837	440.76	-0.6871	439.50	-0.8905	465.80			0.2244	0.2963	0.4703	0.2608	0.6215	0.1978

CASE Q-11

X/SL η

0.0384 0.3650

0.0403 0.2422

0.0422 0.2361

0.0442 0.2451

0.0461 0.2003

0.0481 0.2116

0.0500 0.1989

0.0519 0.2096

0.0539 0.2245

0.0558 0.2441

0.0577 0.2583

0.0597 0.2614

0.0616 0.2889

0.0636 0.3040

0.0655 0.3162

0.0674 0.2881

0.0694 0.3039

0.0713 0.2891

0.0732 0.2827

0.0752 0.2721

0.0771 0.2923

0.0791 0.2921

0.0810 0.2811

0.0829 0.2704

0.0849 0.2746

0.0868 0.2828

0.0888 0.2677

0.0907 0.2497

0.0926 0.2487

Appendix 7.2 – Data for Spanwise Averaged Nusselt Number and Film Cooling Effectiveness

0.6237	0.1972	0.7748	0.0933	0.9259	0.1000	-0.3041	0.2687	-0.5438	0.1451	-0.7469	0.0927	-0.9503	0.0796
0.6259	0.1914	0.7770	0.0865	0.9281	0.0943	-0.3077	0.2650	-0.5473	0.1437	-0.7499	0.0917	-0.9533	0.0866
0.6281	0.2053	0.7792	0.0790	0.9303	0.0971	-0.3112	0.2622	-0.5508	0.1438	-0.7529	0.0825	-0.9563	0.0913
0.6303	0.1918	0.7814	0.0816	0.9325	0.0918	-0.3147	0.2553	-0.5543	0.1393	-0.7559	0.0820	-0.9593	0.0898
0.6326	0.1838	0.7837	0.0815	0.9348	0.1078	-0.3182	0.2525	-0.5579	0.1366	-0.7588	0.0841	-0.9623	0.0870
0.6348	0.1941	0.7859	0.0887	0.9370	0.1072	-0.3218	0.2517	-0.5584	0.1233	-0.7618	0.0867	-0.9653	0.0894
0.6370	0.1844	0.7881	0.0936	0.9392	0.1042	-0.3253	0.2499	-0.5614	0.1299	-0.7648	0.0882	-0.9683	0.0914
0.6392	0.1838	0.7903	0.0852	0.9414	0.1144	-0.3288	0.2471	-0.5644	0.1275	-0.7678	0.0905	-0.9712	0.0986
0.6415	0.1876	0.7926	0.0740	0.9437	0.1329	-0.3323	0.2449	-0.5674	0.1285	-0.7708	0.0928	-0.9742	0.0980
0.6437	0.1985	0.7948	0.0838	0.9459	0.1344	-0.3359	0.2425	-0.5704	0.1243	-0.7738	0.0899	-0.9772	0.0988
0.6459	0.1891	0.7970	0.0772	0.9481	0.1426	-0.3394	0.2427	-0.5734	0.1239	-0.7768	0.0907	-0.9802	0.0974
0.6481	0.1759	0.7992	0.0779	0.9503	0.1313	-0.3429	0.2381	-0.5764	0.1229	-0.7798	0.0878	-0.9832	0.0886
0.6503	0.1773	0.8014	0.0964	0.9525	0.1353	-0.3464	0.2365	-0.5794	0.1213	-0.7828	0.0824	-0.9862	0.0870
0.6526	0.1814	0.8037	0.0742	0.9548	0.1404	-0.3500	0.2350	-0.5823	0.1151	-0.7858	0.0820	-0.9892	0.0879
0.6548	0.1641	0.8059	0.0794	0.9570	0.1478	-0.3535	0.2296	-0.5853	0.1167	-0.7888	0.0824	-0.9922	0.0967
0.6570	0.1709	0.8081	0.0825	0.9592	0.1373	-0.3570	0.2266	-0.5883	0.1156	-0.7918	0.0800		
0.6592	0.1594	0.8103	0.0741			-0.3605	0.2261	-0.5913	0.1180	-0.7947	0.0821		
0.6615	0.1529	0.8126	0.0836	X/PL	η	-0.3640	0.2283	-0.5943	0.1210	-0.7977	0.0815	CASE R – Nu	
0.6637	0.1548	0.8148	0.0842	-0.0274	0.4229	-0.3676	0.2190	-0.5973	0.1163	-0.8007	0.0825	X/SL	Nu
0.6659	0.1476	0.8170	0.0913	-0.0359	0.4198	-0.3711	0.2168	-0.6003	0.1082	-0.8037	0.0819	0.0300	2170.79
0.6681	0.1551	0.8192	0.0794	-0.0445	0.3864	-0.3746	0.2180	-0.6033	0.1143	-0.8067	0.0770	0.0403	1102.93
0.6703	0.1599	0.8214	0.0870	-0.0530	0.3770	-0.3781	0.2189	-0.6063	0.1139	-0.8097	0.0819	0.0422	1011.24
0.6726	0.1562	0.8237	0.0872	-0.0616	0.3663	-0.3817	0.2104	-0.6093	0.1121	-0.8127	0.0822	0.0441	950.98
0.6748	0.1785	0.8259	0.0850	-0.0701	0.3470	-0.3852	0.2117	-0.6123	0.1163	-0.8157	0.0855	0.0461	909.13
0.6770	0.1470	0.8281	0.0857	-0.0787	0.3354	-0.3887	0.2088	-0.6153	0.1110	-0.8187	0.0863	0.0480	871.33
0.6792	0.1537	0.8303	0.0759	-0.0872	0.3169	-0.3922	0.2030	-0.6182	0.1164	-0.8217	0.0844	0.0499	852.32
0.6814	0.1455	0.8326	0.0898	-0.0958	0.2949	-0.3958	0.2017	-0.6212	0.1149	-0.8247	0.0822	0.0519	832.31
0.6837	0.1485	0.8348	0.0971	-0.1044	0.2920	-0.3993	0.2021	-0.6242	0.1137	-0.8277	0.0816	0.0538	824.73
0.6859	0.1499	0.8370	0.0873	-0.1129	0.2808	-0.4028	0.2028	-0.6272	0.1060	-0.8306	0.0821	0.0558	782.21
0.6881	0.1426	0.8392	0.0874	-0.1215	0.2739	-0.4063	0.2049	-0.6302	0.1098	-0.8336	0.0843	0.0577	757.60
0.6903	0.1568	0.8414	0.0793	-0.1300	0.2656	-0.4099	0.2074	-0.6332	0.1113	-0.8366	0.0862	0.0596	742.09
0.6926	0.1395	0.8437	0.0802	-0.1386	0.2650	-0.4134	0.2024	-0.6362	0.1111	-0.8396	0.0845	0.0616	746.84
0.6948	0.1298	0.8459	0.0820	-0.1471	0.2714	-0.4169	0.2034	-0.6392	0.1092	-0.8426	0.0847	0.0635	743.31
0.6970	0.1211	0.8481	0.0874	-0.1557	0.2658	-0.4204	0.1997	-0.6422	0.1089	-0.8456	0.0842	0.0654	727.09
0.6992	0.1339	0.8503	0.0903	-0.1642	0.2624	-0.4240	0.2021	-0.6452	0.1034	-0.8486	0.0833	0.0674	713.49
0.7014	0.1236	0.8526	0.0737	-0.1728	0.2514	-0.4275	0.1978	-0.6482	0.1117	-0.8516	0.0802	0.0693	709.75
0.7037	0.1177	0.8548	0.0842	-0.1813	0.2594	-0.4310	0.1974	-0.6512	0.1085	-0.8546	0.0803	0.0713	696.49
0.7059	0.1026	0.8570	0.0820	-0.1899	0.2707	-0.4345	0.1928	-0.6541	0.1031	-0.8576	0.0763	0.0732	679.88
0.7081	0.1192	0.8592	0.1010	-0.1984	0.2724	-0.4380	0.1941	-0.6571	0.1051	-0.8606	0.0765	0.0751	672.07
0.7103	0.1094	0.8614	0.0830	-0.2020	0.2471	-0.4416	0.1907	-0.6601	0.1028	-0.8636	0.0787	0.0771	674.98
0.7126	0.1249	0.8637	0.0773	-0.2055	0.2564	-0.4451	0.1876	-0.6631	0.1042	-0.8665	0.0808	0.0790	675.23
0.7148	0.1172	0.8659	0.0780	-0.2090	0.2355	-0.4486	0.1878	-0.6661	0.0991	-0.8695	0.0828	0.0810	669.81
0.7170	0.1047	0.8681	0.0812	-0.2125	0.2411	-0.4521	0.1841	-0.6691	0.1041	-0.8725	0.0845	0.0829	671.44
0.7192	0.1055	0.8703	0.0889	-0.2161	0.2406	-0.4557	0.1843	-0.6721	0.1035	-0.8755	0.0864	0.0848	661.05
0.7214	0.1121	0.8726	0.0970	-0.2196	0.2340	-0.4592	0.1902	-0.6751	0.0968	-0.8785	0.0868	0.0868	655.57
0.7237	0.1306	0.8748	0.0948	-0.2231	0.2362	-0.4627	0.1889	-0.6781	0.0968	-0.8815	0.0867	0.0887	643.83
0.7259	0.1223	0.8770	0.0856	-0.2266	0.2339	-0.4662	0.1812	-0.6811	0.0988	-0.8845	0.0889	0.0906	633.40
0.7281	0.0994	0.8792	0.0918	-0.2302	0.2193	-0.4698	0.1839	-0.6841	0.1002	-0.8875	0.0954	0.0926	627.77
0.7303	0.1045	0.8814	0.0866	-0.2337	0.2247	-0.4733	0.1716	-0.6871	0.1001	-0.8905	0.0976	0.0945	623.77
0.7326	0.1119	0.8837	0.0836	-0.2372	0.2341	-0.4768	0.1722	-0.6900	0.0990	-0.8935	0.0956	0.0965	611.33
0.7348	0.1128	0.8859	0.0976	-0.2407	0.2290	-0.4803	0.1778	-0.6930	0.1026	-0.8965	0.0937	0.0984	599.84
0.7370	0.0941	0.8881	0.0898	-0.2442	0.2325	-0.4839	0.1724	-0.6960	0.0982	-0.8995	0.0930	0.1003	594.68
0.7392	0.1045	0.8903	0.0842	-0.2478	0.2337	-0.4874	0.1674	-0.6990	0.1057	-0.9024	0.0918	0.1023	586.98
0.7414	0.1010	0.8926	0.0809	-0.2513	0.2370	-0.4909	0.1753	-0.7020	0.1010	-0.9054	0.0926	0.1042	584.62
0.7437	0.0876	0.8948	0.0822	-0.2548	0.2433	-0.4944	0.1715	-0.7050	0.0994	-0.9084	0.0930	0.1061	576.88
0.7459	0.0880	0.8970	0.0747	-0.2583	0.2515	-0.4979	0.1660	-0.7080	0.1012	-0.9114	0.0940	0.1081	567.68
0.7481	0.1038	0.8992	0.0752	-0.2619	0.2601	-0.5015	0.1630	-0.7110	0.0985	-0.9144	0.0934	0.1100	567.32
0.7503	0.0962	0.9014	0.0776	-0.2654	0.2632	-0.5050	0.1628	-0.7140	0.0948	-0.9174	0.0915	0.1120	561.91
0.7526	0.0894	0.9037	0.0762	-0.2689	0.2607	-0.5085	0.1715	-0.7170	0.0941	-0.9204	0.0928	0.1139	553.59
0.7548	0.0862	0.9059	0.0828	-0.2724	0.2621	-0.5120	0.1677	-0.7200	0.0971	-0.9234	0.0911	0.1158	559.97
0.7570	0.0936	0.9081	0.0819	-0.2760	0.2831	-0.5156	0.1675	-0.7230	0.1002	-0.9264	0.0921	0.1178	563.11
0.7592	0.0854	0.9103	0.0727	-0.2795	0.2915	-0.5191	0.1618	-0.7259	0.0926	-0.9294	0.0890	0.1197	556.77
0.7614	0.0902	0.9126	0.0742	-0.2830	0.3067	-0.5226	0.1538	-0.7289	0.0901	-0.9324	0.0882	0.1216	538.83
0.7637	0.0962	0.9148	0.0872	-0.2865	0.2848	-0.5261	0.1460	-0.7319	0.0895	-0.9353	0.0836	0.1236	546.90
0.7659	0.0815	0.9170	0.0915	-0.2901	0.2822	-0.5297	0.1478	-0.7349	0.0862	-0.9383	0.0800	0.1255	559.56
0.7681	0.0895	0.9192	0.0951	-0.2936	0.2778	-0.5332	0.1401	-0.7379	0.0850	-0.9413	0.0774	0.1275	559.70
0.7703	0.0937	0.9214	0.0969	-0.2971	0.2741	-0.5367	0.1438	-0.7409	0.0876	-0.9443	0.0747	0.1294	554.34
0.7726	0.0904	0.9237	0.0930	-0.3006	0.2702	-0.5402	0.1459	-0.7439	0.0877	-0.9473	0.0821		

Appendix 7.2 – Data for Spanwise Averaged Nusselt Number and Film Cooling Effectiveness

0.1313	548.25	0.2813	644.05	0.5147	871.86	0.6658	808.26	0.8169	708.41	-0.0189	985.49	-0.3641	447.85
0.1333	551.31	0.2845	641.82	0.5170	878.29	0.6681	812.10	0.8192	707.54	-0.0274	896.47	-0.3676	431.08
0.1352	559.87	0.2877	666.30	0.5192	883.73	0.6703	809.99	0.8214	705.41	-0.0360	761.29	-0.3711	452.81
0.1371	567.55	0.2909	782.62	0.5214	880.56	0.6725	811.43	0.8236	701.77	-0.0445	670.14	-0.3747	434.54
0.1391	572.90	0.2941	803.41	0.5236	888.30	0.6747	806.75	0.8258	703.08	-0.0531	624.98	-0.3782	449.22
0.1410	595.32	0.2973	677.71	0.5259	890.84	0.6770	799.32	0.8281	705.41	-0.0616	580.70	-0.3817	435.16
0.1430	650.65	0.3005	648.21	0.5281	896.91	0.6792	806.86	0.8303	704.31	-0.0702	558.35	-0.3852	437.41
0.1449	659.32	0.3037	626.15	0.5303	898.50	0.6814	796.12	0.8325	720.71	-0.0787	526.65	-0.3888	443.08
0.1468	614.00	0.3069	713.66	0.5325	910.14	0.6836	790.38	0.8347	705.65	-0.0873	526.20	-0.3923	426.81
0.1488	592.68	0.3836	712.85	0.5347	917.73	0.6858	790.31	0.8369	700.90	-0.0958	503.80	-0.3958	451.53
0.1507	610.75	0.3859	702.37	0.5370	918.35	0.6881	792.03	0.8392	704.99	-0.1044	499.48	-0.3993	439.40
0.1526	689.60	0.3881	702.54	0.5392	926.66	0.6903	786.90	0.8414	708.91	-0.1130	476.02	-0.4029	455.70
0.1546	741.15	0.3903	713.94	0.5414	928.93	0.6925	784.08	0.8436	707.08	-0.1215	480.69	-0.4064	445.55
0.1565	728.11	0.3925	712.69	0.5436	918.81	0.6947	788.63	0.8458	702.25	-0.1301	459.69	-0.4099	452.96
0.1585	701.36	0.3947	719.63	0.5459	922.47	0.6970	779.48	0.8481	705.35	-0.1386	461.45	-0.4134	453.90
0.1604	685.48	0.3970	715.34	0.5481	926.83	0.6992	782.60	0.8503	710.91	-0.1472	447.93	-0.4170	440.72
0.1623	680.92	0.3992	722.29	0.5503	930.48	0.7014	773.33	0.8525	719.56	-0.1557	434.28	-0.4205	463.48
0.1643	672.68	0.4014	727.58	0.5525	932.86	0.7036	777.81	0.8547	718.20	-0.1643	448.28	-0.4240	446.10
0.1662	676.10	0.4036	729.10	0.5547	942.22	0.7058	772.93	0.8569	718.95	-0.1728	434.89	-0.4275	465.97
0.1682	660.96	0.4059	731.46	0.5570	952.53	0.7081	768.27	0.8592	720.87	-0.1814	439.40	-0.4310	459.25
0.1701	657.51	0.4081	736.25	0.5592	940.30	0.7103	769.75	0.8614	722.05	-0.1899	431.01	-0.4346	461.80
0.1720	656.69	0.4103	733.81	0.5614	932.86	0.7125	766.20	0.8636	713.90	-0.1985	435.03	-0.4381	459.93
0.1740	654.77	0.4125	733.59	0.5636	929.46	0.7147	768.09	0.8658	722.24	-0.2020	424.01	-0.4416	453.74
0.1759	652.68	0.4147	734.19	0.5658	946.54	0.7170	764.58	0.8681	724.30	-0.2055	418.84	-0.4451	464.58
0.1778	657.89	0.4170	745.79	0.5681	940.82	0.7192	766.54	0.8703	722.96	-0.2091	407.03	-0.4487	453.69
0.1798	650.38	0.4192	743.14	0.5703	931.28	0.7214	765.38	0.8725	720.92	-0.2126	389.51	-0.4522	465.31
0.1817	649.38	0.4214	743.34	0.5725	930.37	0.7236	754.74	0.8747	724.22	-0.2161	413.68	-0.4557	453.04
0.1837	649.21	0.4236	750.07	0.5747	938.47	0.7258	750.27	0.8769	724.26	-0.2196	386.49	-0.4592	449.85
0.1856	664.70	0.4259	764.52	0.5770	944.06	0.7281	748.44	0.8792	736.07	-0.2232	393.52	-0.4628	451.16
0.1875	654.18	0.4281	753.91	0.5792	925.95	0.7303	745.21	0.8814	739.87	-0.2267	386.68	-0.4663	447.71
0.1895	645.47	0.4303	752.52	0.5814	918.99	0.7325	745.28	0.8836	743.03	-0.2302	394.03	-0.4698	443.90
0.1914	643.59	0.4325	755.05	0.5836	919.60	0.7347	743.63	0.8858	747.72	-0.2337	401.16	-0.4733	441.02
0.1933	640.69	0.4347	762.72	0.5858	928.70	0.7370	747.72	0.8881	748.90	-0.2372	395.64	-0.4769	468.03
0.1953	635.95	0.4370	766.38	0.5881	931.95	0.7392	739.62	0.8903	754.53	-0.2408	416.06	-0.4804	456.29
0.1972	630.99	0.4392	763.63	0.5903	909.76	0.7414	735.01	0.8925	761.20	-0.2443	407.73	-0.4839	463.83
0.1992	635.32	0.4414	766.00	0.5925	902.11	0.7436	731.65	0.8947	762.97	-0.2478	428.85	-0.4874	447.09
0.2011	638.22	0.4436	771.95	0.5947	902.28	0.7458	730.78	0.8969	766.68	-0.2513	427.65	-0.4910	445.26
0.2030	634.13	0.4459	786.89	0.5970	904.01	0.7481	730.22	0.8992	771.94	-0.2549	438.99	-0.4945	464.36
0.2050	632.30	0.4481	780.02	0.5992	896.23	0.7503	727.45	0.9014	774.10	-0.2584	451.53	-0.4980	451.21
0.2069	630.77	0.4503	773.96	0.6014	886.81	0.7525	727.07	0.9036	773.52	-0.2619	447.95	-0.5015	463.10
0.2088	630.87	0.4525	773.06	0.6036	886.44	0.7547	729.69	0.9058	776.07	-0.2654	469.09	-0.5050	458.78
0.2108	623.67	0.4547	777.19	0.6058	895.56	0.7570	729.33	0.9081	789.81	-0.2690	462.62	-0.5086	464.07
0.2127	623.47	0.4570	781.68	0.6081	896.16	0.7592	722.36	0.9103	789.03	-0.2725	484.48	-0.5121	458.22
0.2147	619.95	0.4592	783.16	0.6103	884.47	0.7614	716.85	0.9125	795.71	-0.2760	475.56	-0.5156	456.92
0.2166	620.17	0.4614	791.28	0.6125	884.10	0.7636	719.30	0.9147	801.42	-0.2795	481.09	-0.5191	460.83
0.2185	618.51	0.4636	795.20	0.6147	881.99	0.7658	726.54	0.9169	803.45	-0.2831	474.47	-0.5196	460.87
0.2205	612.32	0.4659	797.27	0.6170	875.38	0.7681	725.30	0.9192	808.53	-0.2866	467.80	-0.5226	450.70
0.2224	607.60	0.4681	795.98	0.6192	863.21	0.7703	715.42	0.9214	816.25	-0.2901	473.69	-0.5256	469.88
0.2243	607.60	0.4703	800.24	0.6214	872.29	0.7725	710.63	0.9236	820.58	-0.2936	453.01	-0.5286	449.85
0.2263	611.99	0.4725	809.75	0.6236	873.00	0.7747	714.13	0.9258	830.47	-0.2971	480.94	-0.5315	448.75
0.2282	601.86	0.4747	812.20	0.6258	862.43	0.7770	720.42	0.9281	841.12	-0.3007	475.45	-0.5345	460.79
0.2302	595.86	0.4770	813.96	0.6281	855.66	0.7792	709.21	0.9303	851.41	-0.3042	474.63	-0.5375	447.17
0.2302	591.77	0.4792	817.67	0.6303	852.01	0.7814	713.01	0.9325	866.01	-0.3077	457.82	-0.5405	444.46
0.2334	588.33	0.4814	822.08	0.6325	853.93	0.7836	719.83	0.9347	871.86	-0.3112	451.05	-0.5435	464.08
0.2366	589.00	0.4836	819.43	0.6347	851.78	0.7858	716.66	0.9369	877.42	-0.3148	463.92	-0.5465	458.72
0.2398	586.94	0.4859	827.47	0.6370	855.87	0.7881	706.81	0.9392	879.44	-0.3183	443.17	-0.5495	450.91
0.2430	586.48	0.4881	830.89	0.6392	842.28	0.7903	705.49	0.9414	880.39	-0.3218	454.93	-0.5525	450.58
0.2461	592.87	0.4903	834.77	0.6414	845.02	0.7925	709.70	0.9436	896.47	-0.3253	442.30	-0.5555	458.73
0.2493	597.63	0.4925	841.53	0.6436	846.60	0.7947	709.06	0.9458	916.96	-0.3289	453.64	-0.5585	453.29
0.2525	600.28	0.4947	845.30	0.6458	834.17	0.7969	706.39	0.9481	936.54	-0.3324	447.28	-0.5615	451.99
0.2557	604.28	0.4970	841.94	0.6481	830.67	0.7992	702.45	0.9503	939.73	-0.3359	440.88	-0.5645	453.92
0.2589	608.61	0.4992	842.70	0.6503	841.21	0.8014	701.17	0.9525	964.32	-0.3394	453.77	-0.5674	454.49
0.2621	608.57	0.5014	852.55	0.6525	830.46	0.8036	709.38	0.9547	1059.71	-0.3430	437.62	-0.5704	468.91
0.2653	608.18	0.5036	852.88	0.6547	825.70	0.8058	703.77	0.9569	1138.48	-0.3465	459.22	-0.5734	482.99
0.2685	610.51	0.5059	859.49	0.6570	828.14	0.8081	698.97	0.9592	1140.88	-0.3500	440.66	-0.5764	479.16
0.2717	617.05	0.5081	862.20	0.6592	828.50	0.8103	703.74			-0.3535	450.49	-0.5794	469.26
0.2749	625.08	0.5103	863.76	0.6614	820.01	0.8125	706.31	X/PL	Nu	-0.3571	438.83	-0.5824	469.55
0.2781	638.62	0.5125	864.54	0.6636	821.45	0.8147	704.91	-0.0103	1109.25	-0.3606	449.27	-0.5854	475.61

Appendix 7.2 – Data for Spanwise Averaged Nusselt Number and Film Cooling Effectiveness

-0.5884	480.65	-0.7918	416.52			0.1624	0.2332	0.3992	0.2389	0.5503	0.1717	0.7014	0.1439
-0.5914	476.82	-0.7948	430.12			0.1643	0.2318	0.4015	0.2408	0.5526	0.1662	0.7037	0.1382
-0.5944	467.75	-0.7978	425.75			0.1663	0.2387	0.4037	0.2451	0.5548	0.1695	0.7059	0.1392
-0.5974	465.11	-0.8008	428.11			0.1682	0.2434	0.4059	0.2421	0.5570	0.1681	0.7081	0.1340
-0.6003	487.79	-0.8038	425.88			0.1701	0.2503	0.4081	0.2376	0.5592	0.1732	0.7103	0.1347
-0.6033	481.50	-0.8068	428.48			0.1721	0.2553	0.4104	0.2401	0.5615	0.1659	0.7126	0.1267
-0.6063	475.86	-0.8098	422.23			0.1740	0.2623	0.4126	0.2338	0.5637	0.1643	0.7148	0.1337
-0.6093	463.79	-0.8127	428.09			0.1760	0.2483	0.4148	0.2311	0.5659	0.1641	0.7170	0.1370
-0.6123	460.96	-0.8157	424.79			0.1779	0.2498	0.4170	0.2301	0.5681	0.1712	0.7192	0.1330
-0.6153	465.85	-0.8187	429.21			0.1798	0.2592	0.4192	0.2322	0.5703	0.1644	0.7214	0.1331
-0.6183	462.02	-0.8217	433.81			0.1818	0.2664	0.4215	0.2239	0.5726	0.1663	0.7237	0.1365
-0.6213	470.89	-0.8247	428.84			0.1837	0.2669	0.4237	0.2230	0.5748	0.1642	0.7259	0.1282
-0.6243	476.33	-0.8277	432.36			0.1856	0.2612	0.4259	0.2290	0.5770	0.1735	0.7281	0.1301
-0.6273	482.08	-0.8307	427.56			0.1876	0.2565	0.4281	0.2278	0.5792	0.1680	0.7303	0.1226
-0.6303	477.66	-0.8337	426.84			0.1895	0.2703	0.4304	0.2199	0.5815	0.1588	0.7326	0.1233
-0.6333	464.68	-0.8367	429.33			0.1915	0.2713	0.4326	0.2190	0.5837	0.1660	0.7348	0.1300
-0.6362	478.70	-0.8397	435.90			0.1934	0.2686	0.4348	0.2188	0.5859	0.1636	0.7370	0.1297
-0.6392	466.15	-0.8427	433.98			0.1953	0.2697	0.4370	0.2199	0.5881	0.1675	0.7392	0.1266
-0.6422	453.48	-0.8457	439.33			0.1973	0.2717	0.4392	0.2181	0.5903	0.1704	0.7414	0.1271
-0.6452	454.77	-0.8486	447.38			0.1992	0.2676	0.4415	0.2198	0.5926	0.1658	0.7437	0.1201
-0.6482	470.05	-0.8516	451.90			0.2011	0.2780	0.4437	0.2190	0.5948	0.1713	0.7459	0.1203
-0.6512	473.82	-0.8546	432.97			0.2031	0.2806	0.4459	0.2164	0.5970	0.1579	0.7481	0.1234
-0.6542	494.60	-0.8576	434.08			0.2050	0.2797	0.4481	0.2200	0.5992	0.1564	0.7503	0.1259
-0.6572	468.62	-0.8606	444.80			0.2070	0.2753	0.4503	0.2178	0.6015	0.1624	0.7526	0.1155
-0.6602	493.79	-0.8636	462.85			0.2089	0.2830	0.4526	0.2133	0.6037	0.1622	0.7548	0.1179
-0.6632	472.99	-0.8666	455.09			0.2108	0.2750	0.4548	0.2083	0.6059	0.1543	0.7570	0.1233
-0.6662	468.58	-0.8696	450.02			0.2128	0.2742	0.4570	0.2053	0.6081	0.1566	0.7592	0.1142
-0.6692	465.17	-0.8726	448.66			0.2147	0.2782	0.4592	0.2025	0.6103	0.1592	0.7614	0.1190
-0.6721	472.43	-0.8756	442.32			0.2166	0.2812	0.4615	0.1992	0.6126	0.1595	0.7637	0.1126
-0.6751	471.43	-0.8786	442.48			0.2186	0.2812	0.4637	0.2018	0.6148	0.1592	0.7659	0.1145
-0.6781	464.98	-0.8816	453.03			0.2205	0.2896	0.4659	0.1956	0.6170	0.1575	0.7681	0.1270
-0.6811	447.38	-0.8846	446.46			0.2225	0.2904	0.4681	0.2008	0.6192	0.1567	0.7703	0.1217
-0.6841	444.59	-0.8875	445.50			0.2244	0.2855	0.4703	0.2012	0.6215	0.1536	0.7726	0.1165
-0.6871	449.56	-0.8905	454.43			0.2263	0.2882	0.4726	0.2020	0.6237	0.1591	0.7748	0.1105
-0.6901	460.58	-0.8935	461.93			0.2283	0.2871	0.4748	0.2021	0.6259	0.1546	0.7770	0.1074
-0.6931	456.40	-0.8965	461.59			0.2302	0.2845	0.4770	0.2009	0.6281	0.1565	0.7792	0.1097
-0.6961	458.57	-0.8995	461.55			0.2320	0.2813	0.4792	0.1993	0.6303	0.1559	0.7814	0.1065
-0.6991	454.27	-0.9025	459.47			0.2334	0.2825	0.4815	0.2027	0.6326	0.1541	0.7837	0.1156
-0.7021	462.89	-0.9055	461.96			0.2366	0.2768	0.4837	0.2046	0.6348	0.1501	0.7859	0.1142
-0.7051	474.07	-0.9085	463.59			0.2398	0.2809	0.4859	0.1959	0.6370	0.1574	0.7881	0.1146
-0.7080	464.85	-0.9115	465.59			0.2430	0.2773	0.4881	0.2001	0.6392	0.1576	0.7903	0.1142
-0.7110	447.11	-0.9145	465.20			0.2462	0.2783	0.4903	0.2007	0.6415	0.1498	0.7926	0.1141
-0.7140	467.70	-0.9174	469.46			0.2494	0.2809	0.4926	0.1998	0.6437	0.1606	0.7948	0.1068
-0.7170	464.82	-0.9204	478.54			0.2526	0.2834	0.4948	0.1967	0.6459	0.1591	0.7970	0.1059
-0.7200	452.16	-0.9234	486.41			0.2558	0.2815	0.4970	0.2039	0.6481	0.1515	0.7992	0.1026
-0.7230	439.08	-0.9264	485.52			0.2590	0.2821	0.4992	0.1917	0.6503	0.1528	0.8014	0.1035
-0.7260	438.95	-0.9294	490.51			0.2622	0.2891	0.5015	0.1873	0.6526	0.1584	0.8037	0.0977
-0.7290	432.68	-0.9324	495.60			0.2654	0.2935	0.5037	0.1946	0.6548	0.1557	0.8059	0.1072
-0.7320	439.65	-0.9354	498.74			0.2686	0.3011	0.5059	0.1914	0.6570	0.1511	0.8081	0.1064
-0.7350	447.68	-0.9384	504.34			0.2718	0.3129	0.5081	0.1911	0.6592	0.1629	0.8103	0.1009
-0.7380	447.86	-0.9414	508.58			0.2750	0.3330	0.5103	0.1910	0.6615	0.1552	0.8126	0.1123
-0.7409	438.74	-0.9444	511.56			0.2782	0.3553	0.5126	0.1902	0.6637	0.1492	0.8148	0.1044
-0.7439	438.04	-0.9474	515.01			0.2814	0.3688	0.5148	0.1870	0.6659	0.1582	0.8170	0.0973
-0.7469	433.44	-0.9504	520.08			0.2846	0.3702	0.5170	0.1916	0.6681	0.1483	0.8192	0.1055
-0.7499	434.80	-0.9533	526.19			0.2878	0.3611	0.5192	0.1854	0.6703	0.1514	0.8214	0.1027
-0.7529	437.12	-0.9563	534.11			0.2910	0.3536	0.5215	0.1844	0.6726	0.1410	0.8237	0.0967
-0.7559	436.79	-0.9593	538.71			0.2942	0.3325	0.5237	0.1831	0.6748	0.1495	0.8259	0.0929
-0.7589	440.26	-0.9623	541.49			0.2974	0.3356	0.5259	0.1946	0.6770	0.1512	0.8281	0.0987
-0.7619	441.87	-0.9653	546.55			0.3006	0.3402	0.5281	0.1854	0.6792	0.1412	0.8303	0.0880
-0.7649	441.23	-0.9683	549.73			0.3038	0.3630	0.5303	0.1768	0.6814	0.1498	0.8326	0.0909
-0.7679	439.63	-0.9713	556.65			0.3069	0.3420	0.5326	0.1704	0.6837	0.1446	0.8348	0.1053
-0.7709	427.58	-0.9743	567.58			0.3837	0.2573	0.5348	0.1823	0.6859	0.1375	0.8370	0.0921
-0.7739	425.28	-0.9773	578.41			0.3859	0.2569	0.5370	0.1823	0.6881	0.1418	0.8392	0.0919
-0.7768	428.94	-0.9803	607.98			0.3881	0.2566	0.5392	0.1761	0.6903	0.1456	0.8414	0.0947
-0.7798	420.54	-0.9833	649.34			0.3904	0.2501	0.5415	0.1809	0.6926	0.1356	0.8437	0.0955
-0.7828	425.21	-0.9863	683.90			0.3926	0.2521	0.5437	0.1783	0.6948	0.1402	0.8459	0.0860
-0.7858	423.80	-0.9892	709.77			0.3948	0.2446	0.5459	0.1648	0.6970	0.1486	0.8481	0.0853
-0.7888	421.82					0.3970	0.2499	0.5481	0.1714	0.6992	0.1382	0.8503	0.0876

Appendix 7.2 – Data for Spanwise Averaged Nusselt Number and Film Cooling Effectiveness

0.8526	0.0889	-0.1557	0.2012	-0.4204	0.1222	-0.6362	0.0857	-0.8396	0.0591	0.0596	857.51	0.1914	704.83
0.8548	0.0909	-0.1642	0.1903	-0.4240	0.1199	-0.6392	0.0890	-0.8426	0.0727	0.0616	844.88	0.1933	702.62
0.8570	0.0950	-0.1728	0.2022	-0.4275	0.1141	-0.6422	0.0848	-0.8456	0.0697	0.0635	809.46	0.1953	708.54
0.8592	0.0972	-0.1813	0.2138	-0.4310	0.1281	-0.6452	0.0780	-0.8486	0.0664	0.0654	812.51	0.1972	708.68
0.8614	0.0890	-0.1899	0.2022	-0.4345	0.1179	-0.6482	0.0801	-0.8516	0.0660	0.0674	806.22	0.1992	707.47
0.8637	0.0917	-0.1984	0.2137	-0.4380	0.1102	-0.6512	0.0980	-0.8546	0.0745	0.0693	799.09	0.2011	701.14
0.8659	0.0863	-0.2020	0.2324	-0.4416	0.1130	-0.6541	0.0988	-0.8576	0.0599	0.0713	777.77	0.2030	695.29
0.8681	0.0936	-0.2055	0.2452	-0.4451	0.1200	-0.6571	0.1081	-0.8606	0.0557	0.0732	766.84	0.2050	693.31
0.8703	0.0899	-0.2090	0.2699	-0.4486	0.1180	-0.6601	0.0854	-0.8636	0.0637	0.0751	758.47	0.2069	686.96
0.8726	0.0838	-0.2125	0.2478	-0.4500	0.1200	-0.6631	0.1031	-0.8665	0.0793	0.0771	747.78	0.2088	684.80
0.8748	0.0870	-0.2161	0.2413	-0.4627	0.1268	-0.6661	0.0941	-0.8695	0.0730	0.0790	740.94	0.2108	684.11
0.8770	0.0856	-0.2196	0.2464	-0.4657	0.1470	-0.6691	0.1003	-0.8725	0.0665	0.0810	738.78	0.2127	688.71
0.8792	0.0785	-0.2231	0.2450	-0.4687	0.1153	-0.6721	0.0857	-0.8755	0.0642	0.0829	731.23	0.2147	680.11
0.8814	0.0883	-0.2266	0.2424	-0.4717	0.1294	-0.6751	0.0972	-0.8785	0.0537	0.0848	714.90	0.2166	676.69
0.8837	0.0893	-0.2302	0.2105	-0.4747	0.1293	-0.6781	0.0968	-0.8815	0.0494	0.0868	704.43	0.2185	667.84
0.8859	0.0823	-0.2337	0.2252	-0.4776	0.1424	-0.6811	0.0891	-0.8845	0.0464	0.0887	697.37	0.2205	663.82
0.8881	0.0895	-0.2372	0.1991	-0.4806	0.1299	-0.6841	0.0792	-0.8875	0.0489	0.0906	683.32	0.2224	664.68
0.8903	0.0875	-0.2407	0.2015	-0.4836	0.1264	-0.6871	0.0789	-0.8905	0.0424	0.0926	674.34	0.2243	662.48
0.8926	0.0818	-0.2442	0.1967	-0.4866	0.1285	-0.6900	0.0873	-0.8935	0.0486	0.0945	657.73	0.2263	651.59
0.8948	0.0861	-0.2478	0.1928	-0.4896	0.1422	-0.6930	0.0849	-0.8965	0.0549	0.0965	653.54	0.2282	645.18
0.8970	0.0815	-0.2513	0.1995	-0.4926	0.1323	-0.6960	0.0798	-0.8995	0.0506	0.0984	647.27	0.2302	644.04
0.8992	0.0823	-0.2548	0.1919	-0.4956	0.1069	-0.6990	0.0772	-0.9024	0.0448	0.1003	647.13	0.2302	642.24
0.9014	0.0807	-0.2583	0.2085	-0.4986	0.1034	-0.7020	0.0793	-0.9054	0.0413	0.1023	633.10	0.2334	642.39
0.9037	0.0866	-0.2619	0.1947	-0.5016	0.1187	-0.7050	0.0893	-0.9084	0.0441	0.1042	625.53	0.2366	644.54
0.9059	0.0817	-0.2654	0.2035	-0.5046	0.0998	-0.7080	0.0961	-0.9114	0.0411	0.1061	618.73	0.2398	644.49
0.9081	0.0711	-0.2689	0.2009	-0.5076	0.1136	-0.7110	0.0932	-0.9144	0.0403	0.1081	614.91	0.2430	650.08
0.9103	0.0811	-0.2724	0.2070	-0.5106	0.1035	-0.7140	0.0810	-0.9174	0.0358	0.1100	611.46	0.2461	653.62
0.9126	0.0670	-0.2760	0.2101	-0.5135	0.1090	-0.7170	0.1066	-0.9204	0.0365	0.1120	615.89	0.2493	655.91
0.9148	0.0768	-0.2795	0.2222	-0.5165	0.1136	-0.7200	0.1033	-0.9234	0.0485	0.1139	618.39	0.2525	659.99
0.9170	0.0734	-0.2830	0.2370	-0.5195	0.1189	-0.7230	0.0866	-0.9264	0.0533	0.1158	603.39	0.2557	659.28
0.9192	0.0698	-0.2865	0.2592	-0.5225	0.1354	-0.7259	0.0752	-0.9294	0.0491	0.1178	594.49	0.2589	661.67
0.9214	0.0634	-0.2901	0.2908	-0.5255	0.1156	-0.7289	0.0870	-0.9324	0.0432	0.1197	600.83	0.2621	666.94
0.9237	0.0623	-0.2936	0.2944	-0.5285	0.1328	-0.7319	0.0805	-0.9353	0.0439	0.1216	609.22	0.2653	672.26
0.9259	0.0618	-0.2971	0.2841	-0.5315	0.1031	-0.7349	0.0754	-0.9383	0.0427	0.1236	610.49	0.2685	686.38
0.9281	0.0609	-0.3006	0.2754	-0.5345	0.1034	-0.7379	0.0879	-0.9413	0.0396	0.1255	602.58	0.2717	698.96
0.9303	0.0625	-0.3041	0.2750	-0.5375	0.1235	-0.7409	0.0820	-0.9443	0.0349	0.1275	600.23	0.2749	701.77
0.9325	0.0593	-0.3077	0.2760	-0.5405	0.1078	-0.7439	0.0769	-0.9473	0.0312	0.1294	607.20	0.2781	724.50
0.9348	0.0580	-0.3112	0.2623	-0.5435	0.1088	-0.7469	0.0792	-0.9503	0.0333	0.1313	616.31	0.2813	788.14
0.9370	0.0562	-0.3147	0.2600	-0.5465	0.1196	-0.7499	0.0785	-0.9533	0.0395	0.1333	628.68	0.2845	904.14
0.9392	0.0594	-0.3182	0.2476	-0.5494	0.1134	-0.7529	0.0864	-0.9563	0.0399	0.1352	642.40	0.2877	912.65
0.9414	0.0526	-0.3218	0.2447	-0.5524	0.1034	-0.7559	0.0831	-0.9593	0.0436	0.1371	674.63	0.2909	879.80
0.9437	0.0430	-0.3253	0.2366	-0.5554	0.1054	-0.7588	0.0868	-0.9623	0.0440	0.1391	742.51	0.2941	889.45
0.9459	0.0420	-0.3288	0.2356	-0.5584	0.1040	-0.7618	0.0849	-0.9653	0.0421	0.1410	750.71	0.2973	869.71
0.9481	0.0514	-0.3323	0.2187	-0.5614	0.0939	-0.7648	0.0958	-0.9683	0.0369	0.1430	680.10	0.3005	872.34
0.9503	0.0624	-0.3359	0.2197	-0.5644	0.0998	-0.7678	0.0942	-0.9712	0.0301	0.1449	665.00	0.3037	859.24
0.9525	0.0489	-0.3394	0.2180	-0.5674	0.0935	-0.7708	0.0890	-0.9742	0.0284	0.1468	703.99	0.3069	619.51
0.9548	0.0528	-0.3429	0.2032	-0.5704	0.1056	-0.7738	0.0799	-0.9772	0.0313	0.1488	769.19	0.3836	676.88
0.9570	0.0550	-0.3464	0.2012	-0.5734	0.1140	-0.7768	0.0853	-0.9802	0.0261	0.1507	813.59	0.3859	672.07
0.9592	0.0600	-0.3500	0.1848	-0.5764	0.1190	-0.7798	0.0801	-0.9832	0.0353	0.1526	777.46	0.3881	672.44
		-0.3535	0.1866	-0.5794	0.1142	-0.7828	0.0736	-0.9862	0.0364	0.1546	742.18	0.3903	672.07
		-0.3570	0.1781	-0.5823	0.1013	-0.7858	0.0797	-0.9892	0.0251	0.1565	730.47	0.3925	675.96
X/PL	η	-0.3605	0.1547	-0.5853	0.1177	-0.7888	0.0753	-0.9922	0.0217	0.1585	734.15	0.3947	679.01
-0.0103	0.4812	-0.3640	0.1738	-0.5883	0.1245	-0.7918	0.0790			0.1604	736.98	0.3970	679.90
-0.0188	0.5000	-0.3676	0.1580	-0.5913	0.1260	-0.7947	0.0720			0.1623	736.90	0.3992	684.70
-0.0274	0.4821	-0.3711	0.1587	-0.5943	0.1211	-0.7977	0.0789	CASE S – Nu					
-0.0359	0.4487	-0.3746	0.1511	-0.5973	0.1128	-0.8007	0.0731	X/SL	Nu	0.1643	728.81	0.4014	686.82
-0.0445	0.4292	-0.3781	0.1525	-0.6003	0.1115	-0.8037	0.0761			0.1662	721.18	0.4036	688.52
-0.0530	0.4112	-0.3817	0.1528	-0.6033	0.1324	-0.8067	0.0796			0.1682	732.46	0.4059	689.94
-0.0616	0.3994	-0.3852	0.1271	-0.6063	0.1075	-0.8097	0.0724	0.0383	1177.41	0.1701	733.59	0.4081	693.68
-0.0701	0.3691	-0.3887	0.1346	-0.6093	0.1048	-0.8127	0.0674	0.0403	967.13	0.1720	732.79	0.4103	694.97
-0.0787	0.3719	-0.3922	0.1312	-0.6123	0.0870	-0.8157	0.0639	0.0422	868.98	0.1740	733.83	0.4125	696.89
-0.0872	0.3133	-0.3958	0.1281	-0.6153	0.0862	-0.8187	0.0615	0.0441	864.85	0.1759	731.23	0.4147	697.07
-0.0958	0.3002	-0.3993	0.1282	-0.6182	0.1005	-0.8217	0.0637	0.0461	877.79	0.1778	734.74	0.4170	698.94
-0.1044	0.2637	-0.4028	0.1237	-0.6212	0.0940	-0.8247	0.0735	0.0480	1012.93	0.1798	726.28	0.4192	704.01
-0.1129	0.2583	-0.4063	0.1360	-0.6242	0.0904	-0.8277	0.0776	0.0499	989.31	0.1817	728.39	0.4214	706.16
-0.1215	0.2294	-0.4099	0.1239	-0.6272	0.0966	-0.8306	0.0780	0.0519	941.13	0.1837	730.78	0.4236	710.57
-0.1300	0.2238	-0.4134	0.1381	-0.6302	0.1118	-0.8336	0.0724	0.0538	892.87	0.1856	744.14	0.4259	715.26
-0.1386	0.2018	-0.4169	0.1233	-0.6332	0.0904	-0.8366	0.0606	0.0558	877.70	0.1875	721.03	0.4281	720.19
-0.1471	0.2162							0.0577	860.06	0.1895	713.51	0.4303	722.79

Appendix 7.2 – Data for Spanwise Averaged Nusselt Number and Film Cooling Effectiveness

0.4325	721.21	0.5836	916.96	0.7347	709.12	0.8858	756.69	-0.2337	422.37	-0.4733	471.01	-0.6841	489.25
0.4347	725.20	0.5858	917.76	0.7370	709.76	0.8881	759.51	-0.2372	434.62	-0.4769	451.99	-0.6871	474.81
0.4370	734.69	0.5881	920.85	0.7392	709.22	0.8903	762.29	-0.2408	424.39	-0.4804	472.48	-0.6901	478.25
0.4392	734.50	0.5903	912.32	0.7414	710.02	0.8925	770.79	-0.2443	440.55	-0.4839	455.44	-0.6931	471.31
0.4414	737.75	0.5925	904.25	0.7436	706.79	0.8947	779.23	-0.2478	431.60	-0.4874	459.30	-0.6961	473.41
0.4436	737.00	0.5947	896.66	0.7458	704.22	0.8969	781.49	-0.2513	446.06	-0.4910	456.40	-0.6991	461.31
0.4459	743.61	0.5970	894.16	0.7481	703.07	0.8992	786.90	-0.2549	444.51	-0.4945	450.96	-0.7021	467.86
0.4481	747.68	0.5992	897.27	0.7503	698.41	0.9014	789.09	-0.2584	451.85	-0.4980	469.55	-0.7051	473.45
0.4503	754.63	0.6014	897.35	0.7525	696.63	0.9036	787.86	-0.2619	462.87	-0.5015	457.74	-0.7080	483.39
0.4525	755.35	0.6036	887.47	0.7547	692.81	0.9058	798.40	-0.2654	460.31	-0.5050	462.07	-0.7110	477.78
0.4547	754.49	0.6058	881.12	0.7570	695.26	0.9081	805.09	-0.2690	479.31	-0.5086	453.00	-0.7140	457.65
0.4570	763.89	0.6081	884.15	0.7592	697.35	0.9103	812.23	-0.2725	474.98	-0.5121	454.75	-0.7170	453.64
0.4592	778.65	0.6103	885.38	0.7614	703.02	0.9125	819.24	-0.2760	492.07	-0.5156	455.24	-0.7200	464.62
0.4614	776.78	0.6125	881.62	0.7636	686.28	0.9147	823.73	-0.2795	491.62	-0.5191	451.86	-0.7230	474.29
0.4636	780.66	0.6147	874.96	0.7658	692.57	0.9169	828.08	-0.2831	490.89	-0.5227	462.88	-0.7260	462.45
0.4659	786.30	0.6170	869.96	0.7681	692.25	0.9192	835.24	-0.2866	495.34	-0.5256	456.20	-0.7290	460.13
0.4681	790.93	0.6192	876.04	0.7703	695.27	0.9214	843.82	-0.2901	477.16	-0.5286	463.86	-0.7320	442.50
0.4703	794.46	0.6214	860.44	0.7725	683.58	0.9236	848.41	-0.2936	487.53	-0.5315	451.66	-0.7350	442.27
0.4725	799.20	0.6236	856.67	0.7747	689.33	0.9258	860.96	-0.2971	485.17	-0.5345	441.19	-0.7380	454.20
0.4747	801.69	0.6258	856.97	0.7770	686.40	0.9281	870.35	-0.3007	527.06	-0.5375	437.91	-0.7409	458.18
0.4770	810.55	0.6281	859.47	0.7792	688.23	0.9303	877.82	-0.3042	521.34	-0.5405	446.20	-0.7439	455.04
0.4792	802.68	0.6303	853.77	0.7814	687.17	0.9325	891.72	-0.3077	516.16	-0.5435	457.44	-0.7469	445.53
0.4814	809.12	0.6325	838.27	0.7836	693.32	0.9347	907.30	-0.3112	508.50	-0.5465	456.84	-0.7499	449.64
0.4836	814.27	0.6347	842.35	0.7858	693.52	0.9369	923.37	-0.3148	497.27	-0.5495	465.59	-0.7529	454.34
0.4859	819.05	0.6370	840.77	0.7881	687.39	0.9392	926.57	-0.3183	514.05	-0.5525	463.94	-0.7559	453.72
0.4881	823.18	0.6392	838.73	0.7903	686.91	0.9414	930.09	-0.3218	487.13	-0.5555	457.93	-0.7589	448.51
0.4903	826.16	0.6414	825.19	0.7925	682.25	0.9436	939.98	-0.3253	504.35	-0.5585	460.08	-0.7619	451.51
0.4925	830.70	0.6436	821.68	0.7947	675.66	0.9458	954.10	-0.3289	492.63	-0.5615	458.74	-0.7649	452.63
0.4947	841.75	0.6458	830.55	0.7969	679.88	0.9481	974.36	-0.3324	496.56	-0.5645	490.06	-0.7679	454.75
0.4970	843.02	0.6481	824.24	0.7992	681.75	0.9503	984.51	-0.3359	495.63	-0.5674	452.72	-0.7709	453.60
0.4992	846.95	0.6503	815.94	0.8014	675.18	0.9525	1005.72	-0.3394	477.18	-0.5704	448.91	-0.7739	444.88
0.5014	845.37	0.6525	811.12	0.8036	678.79	0.9547	1021.38	-0.3430	495.66	-0.5734	460.87	-0.7768	442.92
0.5036	854.35	0.6547	808.01	0.8058	682.13	0.9569	1083.10	-0.3465	468.56	-0.5764	466.82	-0.7798	450.60
0.5059	861.32	0.6570	806.08	0.8081	681.41	0.9592	1195.88	-0.3500	495.26	-0.5794	465.88	-0.7828	448.08
0.5081	860.08	0.6592	807.61	0.8103	682.37			-0.3535	469.79	-0.5824	475.14	-0.7858	442.09
0.5103	864.14	0.6614	796.41	0.8125	690.00	X/PL	Nu	-0.3571	480.36	-0.5854	472.62	-0.7888	444.13
0.5125	867.27	0.6636	796.19	0.8147	688.67	-0.0103	1011.45	-0.3606	482.72	-0.5884	464.92	-0.7918	439.57
0.5147	872.82	0.6658	793.87	0.8169	687.18	-0.0189	961.54	-0.3641	473.16	-0.5914	463.28	-0.7948	442.18
0.5170	873.29	0.6681	789.01	0.8192	689.47	-0.0274	855.54	-0.3676	475.04	-0.5944	464.06	-0.7978	446.03
0.5192	881.09	0.6703	787.16	0.8214	692.49	-0.0360	770.57	-0.3711	460.20	-0.5974	477.72	-0.8008	435.46
0.5214	884.12	0.6725	780.91	0.8236	694.50	-0.0445	675.83	-0.3747	479.44	-0.6003	473.96	-0.8038	437.45
0.5236	886.14	0.6747	782.48	0.8258	692.76	-0.0531	663.09	-0.3782	454.45	-0.6033	467.59	-0.8068	449.97
0.5259	884.41	0.6770	781.80	0.8281	692.81	-0.0616	645.91	-0.3817	472.44	-0.6063	476.29	-0.8098	444.02
0.5281	890.29	0.6792	777.48	0.8303	693.21	-0.0702	620.03	-0.3852	467.51	-0.6093	497.86	-0.8127	450.28
0.5303	899.09	0.6814	769.02	0.8325	697.06	-0.0787	607.61	-0.3888	459.62	-0.6123	513.04	-0.8157	449.52
0.5325	908.13	0.6836	769.48	0.8347	698.91	-0.0873	589.81	-0.3923	476.27	-0.6153	534.31	-0.8187	448.19
0.5347	905.43	0.6858	767.34	0.8369	701.04	-0.0958	562.44	-0.3958	451.13	-0.6183	518.13	-0.8217	445.52
0.5370	912.44	0.6881	762.24	0.8392	704.11	-0.1044	550.50	-0.3993	468.50	-0.6213	479.49	-0.8247	438.48
0.5392	910.40	0.6903	761.72	0.8414	703.20	-0.1130	534.50	-0.4029	458.24	-0.6243	480.92	-0.8277	447.20
0.5414	916.56	0.6925	755.47	0.8436	703.00	-0.1215	511.04	-0.4064	472.27	-0.6273	489.11	-0.8307	442.28
0.5436	922.02	0.6947	758.50	0.8458	709.28	-0.1301	507.15	-0.4099	463.48	-0.6303	477.75	-0.8337	442.61
0.5459	923.92	0.6970	757.62	0.8481	706.78	-0.1386	489.45	-0.4134	459.70	-0.6333	484.52	-0.8367	440.36
0.5481	923.93	0.6992	752.33	0.8503	704.30	-0.1472	483.33	-0.4170	472.91	-0.6362	478.78	-0.8397	445.64
0.5503	929.30	0.7014	743.19	0.8525	710.53	-0.1557	474.67	-0.4205	456.47	-0.6392	490.22	-0.8427	452.81
0.5525	932.36	0.7036	748.62	0.8547	710.70	-0.1643	460.49	-0.4240	466.68	-0.6422	475.28	-0.8457	449.35
0.5547	930.14	0.7058	744.42	0.8569	717.07	-0.1728	469.58	-0.4275	455.20	-0.6452	485.42	-0.8486	449.94
0.5570	945.16	0.7081	739.69	0.8592	718.23	-0.1814	454.10	-0.4310	461.55	-0.6482	493.16	-0.8516	453.83
0.5592	944.74	0.7103	735.31	0.8614	721.66	-0.1899	465.17	-0.4346	453.74	-0.6512	484.91	-0.8546	447.88
0.5614	945.37	0.7125	736.79	0.8636	726.13	-0.1985	455.11	-0.4381	465.45	-0.6542	489.10	-0.8576	451.44
0.5636	935.76	0.7147	736.58	0.8658	724.84	-0.2020	453.06	-0.4416	473.47	-0.6572	509.00	-0.8606	453.43
0.5658	936.62	0.7170	730.27	0.8681	723.54	-0.2055	446.13	-0.4451	455.23	-0.6602	510.66	-0.8636	464.41
0.5681	939.36	0.7192	732.99	0.8703	728.38	-0.2091	441.19	-0.4487	468.96	-0.6632	515.02	-0.8666	458.48
0.5703	941.21	0.7214	727.17	0.8725	728.08	-0.2126	445.80	-0.4522	453.47	-0.6662	497.25	-0.8696	456.25
0.5725	929.17	0.7236	727.58	0.8747	739.03	-0.2161	430.72	-0.4557	468.32	-0.6692	491.51	-0.8726	457.50
0.5747	929.62	0.7258	726.21	0.8769	742.52	-0.2196	447.74	-0.4592	461.14	-0.6721	485.30	-0.8756	457.42
0.5770	927.36	0.7281	718.83	0.8792	737.39	-0.2232	426.77	-0.4628	459.53	-0.6751	483.69	-0.8786	454.56
0.5792	931.08	0.7303	716.15	0.8814	748.03	-0.2267	426.83	-0.4663	466.05	-0.6781	477.54	-0.8816	459.22
0.5814	925.56	0.7325	712.65	0.8836	752.99	-0.2302	428.44	-0.4698	457.02	-0.6811	463.95	-0.8845	465.41

Appendix 7.2 – Data for Spanwise Averaged Nusselt Number and Film Cooling Effectiveness

-0.8875	466.61	0.0907	0.2314	0.2225	0.2359	0.4681	0.1730	0.6192	0.1468	0.7703	0.0975	0.9214	0.0416
-0.8905	462.29	0.0926	0.2318	0.2244	0.2367	0.4703	0.1674	0.6215	0.1403	0.7726	0.0880	0.9237	0.0387
-0.8935	465.21	0.0946	0.2268	0.2263	0.2349	0.4726	0.1657	0.6237	0.1398	0.7748	0.0988	0.9259	0.0487
-0.8965	466.72	0.0965	0.2204	0.2283	0.2358	0.4748	0.1663	0.6259	0.1419	0.7770	0.0863	0.9281	0.0494
-0.8995	471.19	0.0984	0.2260	0.2302	0.2348	0.4770	0.1730	0.6281	0.1464	0.7792	0.0870	0.9303	0.0467
-0.9025	471.00	0.1004	0.2266	0.2302	0.2301	0.4792	0.1604	0.6303	0.1471	0.7814	0.0948	0.9325	0.0482
-0.9055	476.29	0.1023	0.2237	0.2334	0.2340	0.4815	0.1681	0.6326	0.1391	0.7837	0.0964	0.9348	0.0487
-0.9085	479.16	0.1043	0.2210	0.2366	0.2374	0.4837	0.1667	0.6348	0.1420	0.7859	0.0968	0.9370	0.0511
-0.9115	485.82	0.1062	0.2256	0.2398	0.2299	0.4859	0.1605	0.6370	0.1359	0.7881	0.0866	0.9392	0.0474
-0.9145	487.08	0.1081	0.2289	0.2430	0.2312	0.4881	0.1619	0.6392	0.1382	0.7903	0.0952	0.9414	0.0457
-0.9174	488.95	0.1101	0.2262	0.2462	0.2331	0.4903	0.1690	0.6415	0.1405	0.7926	0.0911	0.9437	0.0479
-0.9204	493.81	0.1120	0.2292	0.2494	0.2345	0.4926	0.1634	0.6437	0.1355	0.7948	0.0627	0.9459	0.0453
-0.9234	499.48	0.1139	0.2250	0.2526	0.2326	0.4948	0.1656	0.6459	0.1443	0.7970	0.0780	0.9481	0.0546
-0.9264	502.11	0.1159	0.2289	0.2558	0.2279	0.4970	0.1666	0.6481	0.1345	0.7992	0.0885	0.9503	0.0519
-0.9294	507.40	0.1178	0.2293	0.2590	0.2365	0.4992	0.1632	0.6503	0.1363	0.8014	0.0775	0.9525	0.0517
-0.9324	513.13	0.1198	0.2258	0.2622	0.2430	0.5015	0.1601	0.6526	0.1426	0.8037	0.0752	0.9548	0.0397
-0.9354	517.13	0.1217	0.2219	0.2654	0.2449	0.5037	0.1640	0.6548	0.1390	0.8059	0.0741	0.9570	0.0419
-0.9384	522.98	0.1236	0.2296	0.2686	0.2592	0.5059	0.1673	0.6570	0.1397	0.8081	0.0819	0.9592	0.0570
-0.9414	529.04	0.1256	0.2279	0.2718	0.2642	0.5081	0.1589	0.6592	0.1398	0.8103	0.0810		
-0.9444	535.14	0.1275	0.2254	0.2750	0.2791	0.5103	0.1660	0.6615	0.1298	0.8126	0.0758	X/PL	η
-0.9474	542.56	0.1294	0.2242	0.2782	0.3129	0.5126	0.1736	0.6637	0.1237	0.8148	0.0754	-0.0103	0.2681
-0.9504	548.01	0.1314	0.2287	0.2814	0.3148	0.5148	0.1712	0.6659	0.1211	0.8170	0.0811	-0.0188	0.2840
-0.9533	552.89	0.1333	0.2424	0.2846	0.3096	0.5170	0.1581	0.6681	0.1340	0.8192	0.0881	-0.0274	0.3034
-0.9563	558.62	0.1353	0.2558	0.2878	0.3177	0.5192	0.1679	0.6703	0.1387	0.8214	0.0810	-0.0359	0.3219
-0.9593	563.18	0.1372	0.2617	0.2910	0.2679	0.5215	0.1599	0.6726	0.1241	0.8237	0.0851	-0.0445	0.3289
-0.9623	568.21	0.1391	0.2891	0.2942	0.2529	0.5237	0.1601	0.6748	0.1208	0.8259	0.0850	-0.0530	0.3348
-0.9653	573.97	0.1411	0.3212	0.2974	0.2415	0.5259	0.1571	0.6770	0.1246	0.8281	0.0850	-0.0616	0.3288
-0.9683	576.49	0.1430	0.2878	0.3006	0.2621	0.5281	0.1579	0.6792	0.1280	0.8303	0.0837	-0.0701	0.3272
-0.9713	583.41	0.1449	0.2645	0.3038	0.2481	0.5303	0.1548	0.6814	0.1166	0.8326	0.0921	-0.0787	0.3308
-0.9743	592.87	0.1469	0.2526	0.3069	0.2732	0.5326	0.1644	0.6837	0.1156	0.8348	0.0876	-0.0872	0.3318
-0.9773	605.27	0.1488	0.2582	0.3837	0.1985	0.5348	0.1492	0.6859	0.1105	0.8370	0.0890	-0.0958	0.3181
-0.9803	623.76	0.1508	0.2658	0.3859	0.1980	0.5370	0.1600	0.6881	0.1130	0.8392	0.0992	-0.1044	0.3200
-0.9833	648.34	0.1527	0.2374	0.3881	0.1978	0.5392	0.1546	0.6903	0.1294	0.8414	0.0956	-0.1129	0.3126
-0.9863	685.74	0.1546	0.2292	0.3904	0.1969	0.5415	0.1522	0.6926	0.1121	0.8437	0.0863	-0.1215	0.3037
-0.9892	719.98	0.1566	0.2250	0.3926	0.1933	0.5437	0.1512	0.6948	0.1143	0.8459	0.0929	-0.1300	0.2938
-0.9922	750.86	0.1585	0.2312	0.3948	0.1956	0.5459	0.1503	0.6970	0.1142	0.8481	0.0866	-0.1386	0.2888
		0.1605	0.2321	0.3970	0.1916	0.5481	0.1547	0.6992	0.1173	0.8503	0.0813	-0.1471	0.2857
		0.1624	0.2351	0.3992	0.1961	0.5503	0.1582	0.7014	0.1094	0.8526	0.0886	-0.1557	0.2806
		0.1643	0.2357	0.4015	0.1915	0.5526	0.1570	0.7037	0.1240	0.8548	0.0876	-0.1642	0.2776
		0.1663	0.2258	0.4037	0.1948	0.5548	0.1490	0.7059	0.1183	0.8570	0.0927	-0.1728	0.2708
		0.1682	0.2355	0.4059	0.1922	0.5570	0.1614	0.7081	0.1175	0.8592	0.0809	-0.1813	0.2714
X/SL	η	0.1701	0.2298	0.4081	0.1886	0.5592	0.1526	0.7103	0.1222	0.8614	0.0790	-0.1899	0.2656
0.0384	0.4415	0.1721	0.2398	0.4104	0.1874	0.5615	0.1566	0.7126	0.1167	0.8637	0.0802	-0.1984	0.2670
0.0403	0.4556	0.1740	0.2405	0.4126	0.1886	0.5637	0.1549	0.7148	0.1192	0.8659	0.0666	-0.2020	0.2581
0.0422	0.4514	0.1760	0.2382	0.4148	0.1878	0.5659	0.1560	0.7170	0.1112	0.8681	0.0675	-0.2055	0.2585
0.0442	0.4583	0.1779	0.2358	0.4170	0.1856	0.5681	0.1526	0.7192	0.1259	0.8703	0.0742	-0.2090	0.2653
0.0461	0.3996	0.1798	0.2421	0.4192	0.1861	0.5703	0.1518	0.7214	0.1081	0.8726	0.0641	-0.2125	0.2674
0.0481	0.4275	0.1818	0.2374	0.4215	0.1861	0.5726	0.1446	0.7237	0.1066	0.8748	0.0727	-0.2161	0.2710
0.0500	0.3786	0.1837	0.2459	0.4237	0.1872	0.5748	0.1575	0.7259	0.1062	0.8770	0.0734	-0.2196	0.2692
0.0519	0.3499	0.1856	0.2479	0.4259	0.1950	0.5770	0.1503	0.7281	0.1042	0.8792	0.0636	-0.2231	0.2644
0.0539	0.3456	0.1876	0.2352	0.4281	0.1839	0.5792	0.1506	0.7303	0.1022	0.8814	0.0672	-0.2266	0.2472
0.0558	0.3276	0.1895	0.2362	0.4304	0.1916	0.5815	0.1498	0.7326	0.1089	0.8837	0.0628	-0.2302	0.2447
0.0577	0.2757	0.1915	0.2371	0.4326	0.1830	0.5837	0.1470	0.7348	0.0901	0.8859	0.0586	-0.2337	0.2323
0.0597	0.2759	0.1934	0.2377	0.4348	0.1710	0.5859	0.1518	0.7370	0.0971	0.8881	0.0581	-0.2372	0.2256
0.0616	0.2831	0.1953	0.2375	0.4370	0.1789	0.5881	0.1544	0.7392	0.0972	0.8903	0.0595	-0.2407	0.2195
0.0636	0.2862	0.1973	0.2366	0.4392	0.1765	0.5903	0.1490	0.7414	0.1065	0.8926	0.0554	-0.2442	0.2117
0.0655	0.2742	0.1992	0.2387	0.4415	0.1749	0.5926	0.1487	0.7437	0.1061	0.8948	0.0534	-0.2478	0.2053
0.0674	0.2625	0.2011	0.2383	0.4437	0.1706	0.5948	0.1530	0.7459	0.1018	0.8970	0.0436	-0.2513	0.2015
0.0694	0.2615	0.2031	0.2339	0.4459	0.1673	0.5970	0.1398	0.7481	0.0988	0.8992	0.0494	-0.2548	0.1980
0.0713	0.2642	0.2050	0.2343	0.4481	0.1642	0.5992	0.1458	0.7503	0.1006	0.9014	0.0516	-0.2583	0.1978
0.0732	0.2504	0.2070	0.2345	0.4503	0.1702	0.6015	0.1521	0.7526	0.0960	0.9037	0.0457	-0.2619	0.1936
0.0752	0.2432	0.2089	0.2403	0.4526	0.1708	0.6037	0.1445	0.7548	0.0873	0.9059	0.0516	-0.2654	0.1939
0.0771	0.2401	0.2108	0.2350	0.4548	0.1727	0.6059	0.1373	0.7570	0.0883	0.9081	0.0516	-0.2689	0.1910
0.0791	0.2335	0.2128	0.2385	0.4570	0.1692	0.6081	0.1410	0.7592	0.0911	0.9103	0.0514	-0.2724	0.1909
0.0810	0.2376	0.2147	0.2287	0.4592	0.1783	0.6103	0.1459	0.7614	0.1112	0.9126	0.0457	-0.2760	0.1913
0.0829	0.2360	0.2166	0.2382	0.4615	0.1794	0.6126	0.1421	0.7637	0.0858	0.9148	0.0471	-0.2795	0.1968
0.0849	0.2355	0.2186	0.2333	0.4637	0.1803	0.6148	0.1440	0.7659	0.0966	0.9170	0.0430	-0.2830	0.1956
0.0868	0.2355	0.2205	0.2370	0.4659	0.1820	0.6170	0.1348	0.7681	0.0932	0.9192	0.0405	-0.2865	0.2083

Appendix 7.2 – Data for Spanwise Averaged Nusselt Number and Film Cooling Effectiveness

-0.2901	0.2087	-0.5285	0.1378	-0.7319	0.0519	-0.9353	0.0478	0.1216	563.02	0.2653	641.59	0.5036	850.64
-0.2936	0.2124	-0.5315	0.1207	-0.7349	0.0516	-0.9383	0.0501	0.1236	553.40	0.2685	641.20	0.5059	856.59
-0.2971	0.2314	-0.5345	0.1025	-0.7379	0.0690	-0.9413	0.0504	0.1255	552.02	0.2717	630.37	0.5081	859.87
-0.3006	0.2307	-0.5375	0.0976	-0.7409	0.0678	-0.9443	0.0546	0.1275	557.08	0.2749	623.09	0.5103	857.76
-0.3041	0.2419	-0.5405	0.1052	-0.7439	0.0629	-0.9473	0.0557	0.1294	565.02	0.2781	635.88	0.5125	862.72
-0.3077	0.2327	-0.5435	0.1197	-0.7469	0.0500	-0.9503	0.0555	0.1313	564.33	0.2813	620.14	0.5147	862.10
-0.3112	0.2402	-0.5465	0.1224	-0.7499	0.0504	-0.9533	0.0544	0.1333	569.07	0.2845	609.61	0.5170	866.39
-0.3147	0.2333	-0.5494	0.1276	-0.7529	0.0544	-0.9563	0.0589	0.1352	591.18	0.2877	619.19	0.5192	868.72
-0.3182	0.2298	-0.5524	0.1236	-0.7559	0.0507	-0.9593	0.0614	0.1371	603.09	0.2909	614.90	0.5214	877.69
-0.3218	0.2248	-0.5554	0.1139	-0.7588	0.0482	-0.9623	0.0567	0.1391	577.56	0.2941	620.17	0.5236	883.71
-0.3253	0.2183	-0.5584	0.1133	-0.7618	0.0518	-0.9653	0.0519	0.1410	546.32	0.2973	619.03	0.5259	877.60
-0.3288	0.2225	-0.5614	0.1131	-0.7648	0.0504	-0.9683	0.0404	0.1430	535.02	0.3005	609.38	0.5281	878.81
-0.3323	0.2073	-0.5644	0.1509	-0.7678	0.0536	-0.9712	0.0385	0.1449	538.56	0.3037	614.45	0.5303	889.52
-0.3359	0.2093	-0.5674	0.1152	-0.7708	0.0512	-0.9742	0.0381	0.1468	557.81	0.3069	649.94	0.5325	890.54
-0.3394	0.1942	-0.5704	0.1070	-0.7738	0.0409	-0.9772	0.0470	0.1488	546.09	0.3836	760.06	0.5347	896.47
-0.3429	0.1992	-0.5734	0.1238	-0.7768	0.0380	-0.9802	0.0624	0.1507	535.98	0.3859	761.33	0.5370	898.25
-0.3464	0.1857	-0.5764	0.1391	-0.7798	0.0428	-0.9832	0.0786	0.1526	529.63	0.3881	761.99	0.5392	904.30
-0.3500	0.1862	-0.5794	0.1414	-0.7828	0.0412	-0.9862	0.0800	0.1546	519.37	0.3903	760.92	0.5414	908.00
-0.3535	0.1804	-0.5823	0.1536	-0.7858	0.0315	-0.9892	0.0770	0.1565	520.21	0.3925	763.30	0.5436	909.53
-0.3570	0.1741	-0.5853	0.1497	-0.7888	0.0376	-0.9922	0.0570	0.1585	519.48	0.3947	767.80	0.5459	914.87
-0.3605	0.1753	-0.5883	0.1266	-0.7918	0.0271			0.1604	524.61	0.3970	769.54	0.5481	917.46
-0.3640	0.1596	-0.5913	0.1241	-0.7947	0.0298			0.1623	526.61	0.3992	769.57	0.5503	914.15
-0.3676	0.1575	-0.5943	0.1292	-0.7977	0.0310			0.1643	536.80	0.4014	777.10	0.5525	919.48
-0.3711	0.1565	-0.5973	0.1398	-0.8007	0.0232			0.1662	550.88	0.4036	777.98	0.5547	921.22
-0.3746	0.1504	-0.6003	0.1309	-0.8037	0.0257			0.1682	564.63	0.4059	776.43	0.5570	921.69
-0.3781	0.1368	-0.6033	0.1290	-0.8067	0.0366			0.1701	573.26	0.4081	781.96	0.5592	927.74
-0.3817	0.1373	-0.6063	0.1387	-0.8097	0.0286			0.1720	587.64	0.4103	779.30	0.5614	929.51
-0.3852	0.1455	-0.6093	0.1574	-0.8127	0.0376			0.1740	603.54	0.4125	779.68	0.5636	926.87
-0.3887	0.1360	-0.6123	0.1767	-0.8157	0.0392			0.1759	613.91	0.4147	774.78	0.5658	924.62
-0.3922	0.1423	-0.6153	0.1952	-0.8187	0.0336			0.1778	615.88	0.4170	772.50	0.5681	929.32
-0.3958	0.1423	-0.6182	0.1747	-0.8217	0.0290			0.1798	628.31	0.4192	776.38	0.5703	928.58
-0.3993	0.1284	-0.6212	0.1359	-0.8247	0.0200			0.1817	633.87	0.4214	778.61	0.5725	926.23
-0.4028	0.1368	-0.6242	0.1334	-0.8277	0.0305			0.1837	644.99	0.4236	776.70	0.5747	912.93
-0.4063	0.1225	-0.6272	0.1401	-0.8306	0.0227			0.1856	645.10	0.4259	781.66	0.5770	916.08
-0.4099	0.1339	-0.6302	0.1286	-0.8336	0.0248			0.1875	644.70	0.4281	784.77	0.5792	918.93
-0.4134	0.1247	-0.6332	0.1389	-0.8366	0.0235			0.1895	647.23	0.4303	785.36	0.5814	917.10
-0.4169	0.1314	-0.6362	0.1325	-0.8396	0.0248			0.1914	649.60	0.4325	785.26	0.5836	902.53
-0.4204	0.1281	-0.6392	0.1423	-0.8426	0.0336			0.1933	659.17	0.4347	787.00	0.5858	903.73
-0.4240	0.1162	-0.6422	0.1270	-0.8456	0.0296			0.1953	656.81	0.4370	789.12	0.5881	906.03
-0.4275	0.1263	-0.6452	0.1377	-0.8486	0.0348			0.1972	648.29	0.4392	794.20	0.5903	896.64
-0.4310	0.1091	-0.6482	0.1420	-0.8516	0.0405			0.1992	659.53	0.4414	788.78	0.5925	888.96
-0.4345	0.1076	-0.6512	0.1356	-0.8546	0.0312			0.2011	658.96	0.4436	793.99	0.5947	886.16
-0.4380	0.1140	-0.6541	0.1432	-0.8576	0.0358			0.2030	659.11	0.4459	793.48	0.5970	888.23
-0.4416	0.1118	-0.6571	0.1606	-0.8606	0.0395			0.2050	657.47	0.4481	792.88	0.5992	886.80
-0.4451	0.1088	-0.6601	0.1671	-0.8636	0.0549			0.2069	654.67	0.4503	791.13	0.6014	880.23
-0.4486	0.1060	-0.6631	0.1684	-0.8665	0.0432			0.2088	657.82	0.4525	795.72	0.6036	873.00
-0.4521	0.1032	-0.6661	0.1438	-0.8695	0.0349			0.2108	660.83	0.4547	793.97	0.6058	875.73
-0.4557	0.0990	-0.6691	0.1347	-0.8725	0.0377			0.2127	658.60	0.4570	796.09	0.6081	877.95
-0.4592	0.1044	-0.6721	0.1316	-0.8755	0.0319			0.2147	654.63	0.4592	805.54	0.6103	873.68
-0.4627	0.0971	-0.6751	0.1317	-0.8785	0.0200			0.2166	651.73	0.4614	804.11	0.6125	869.42
-0.4662	0.1026	-0.6781	0.1223	-0.8815	0.0267			0.2185	650.70	0.4636	804.34	0.6147	862.48
-0.4698	0.1093	-0.6811	0.0995	-0.8845	0.0316			0.2205	647.66	0.4659	812.50	0.6170	862.23
-0.4733	0.1020	-0.6841	0.1210	-0.8875	0.0280			0.2224	640.33	0.4681	815.24	0.6192	863.18
-0.4768	0.1078	-0.6871	0.1050	-0.8905	0.0201			0.2243	634.34	0.4703	812.09	0.6214	853.88
-0.4803	0.1074	-0.6900	0.1179	-0.8935	0.0252			0.2263	628.61	0.4725	808.42	0.6236	844.76
-0.4839	0.1008	-0.6930	0.1086	-0.8965	0.0276			0.2282	630.53	0.4747	816.79	0.6258	833.44
-0.4874	0.0918	-0.6960	0.1109	-0.8995	0.0345			0.2302	630.21	0.4770	816.11	0.6281	839.71
-0.4909	0.0971	-0.6990	0.0987	-0.9024	0.0307			0.2320	620.64	0.4792	820.02	0.6303	833.08
-0.4944	0.0942	-0.7020	0.1021	-0.9054	0.0284			0.2334	624.61	0.4814	817.94	0.6325	828.44
-0.4979	0.1042	-0.7050	0.1090	-0.9084	0.0372			0.2366	625.36	0.4836	820.59	0.6347	819.85
-0.5015	0.1158	-0.7080	0.1190	-0.9114	0.0513			0.2398	626.21	0.4859	830.59	0.6370	825.61
-0.5076	0.1095	-0.7110	0.1128	-0.9144	0.0462			0.2430	627.47	0.4881	830.13	0.6392	826.08
-0.5106	0.1083	-0.7140	0.0858	-0.9174	0.0433			0.2461	626.00	0.4903	835.65	0.6414	817.03
-0.5135	0.1033	-0.7170	0.0789	-0.9204	0.0439			0.2493	631.18	0.4925	830.88	0.6436	817.80
-0.5165	0.1148	-0.7200	0.0863	-0.9234	0.0413			0.2525	627.53	0.4947	839.87	0.6458	815.60
-0.5195	0.1045	-0.7230	0.0988	-0.9264	0.0407			0.2557	628.41	0.4970	839.38	0.6481	818.65
-0.5225	0.1105	-0.7259	0.0898	-0.9294	0.0438			0.2589	628.62	0.4992	846.38	0.6503	808.81
-0.5255	0.1169	-0.7289	0.0846	-0.9324	0.0445			0.2621	635.04	0.5014	846.90	0.6525	808.71

CASE T – Nu

X/SL Nu

0.0383	1104.24
0.0403	961.46
0.0422	912.35
0.0441	893.83
0.0461	891.39
0.0480	844.23
0.0499	827.89
0.0519	773.70
0.0538	758.45
0.0558	731.98
0.0577	746.01
0.0596	735.64
0.0616	725.71
0.0635	730.46
0.0654	732.83
0.0674	724.88
0.0693	710.28
0.0713	702.03
0.0732	701.04
0.0751	690.97
0.0771	682.47
0.0790	678.12
0.0810	672.72
0.0829	657.26
0.0848	644.91
0.0868	636.59
0.0887	637.89
0.0906	620.70
0.0926	610.40
0.0945	602.55
0.0965	598.33
0.0984	595.90
0.1003	587.98
0.1023	578.25
0.1042	570.89
0.1061	566.24
0.1081	564.32
0.1100	572.64
0.1120	572.74
0.1139	555.57
0.1158	551.38
0.1178	565.24
0.1197	568.53

Appendix 7.2 – Data for Spanwise Averaged Nusselt Number and Film Cooling Effectiveness

0.6547	806.04	0.8058	696.31	0.9569	1099.13	-0.3465	450.13	-0.5824	426.86	-0.7858	421.63	-0.9892	664.34
0.6570	801.87	0.8081	698.37	0.9592	1203.16	-0.3500	467.65	-0.5854	424.14	-0.7888	422.01	-0.9922	687.70
0.6592	797.33	0.8103	686.85			-0.3535	449.08	-0.5884	421.99	-0.7918	430.19		
0.6614	793.16	0.8125	692.81	X/PL	Nu	-0.3571	466.04	-0.5914	432.15	-0.7948	427.15		
0.6636	801.39	0.8147	696.53	-0.0103	920.00	-0.3606	455.97	-0.5944	422.62	-0.7978	417.61	CASE T – n	
0.6658	798.19	0.8169	696.76	-0.0189	840.00	-0.3641	464.58	-0.5974	427.60	-0.8008	420.56	X/SL	η
0.6681	788.51	0.8192	697.19	-0.0274	791.00	-0.3676	461.34	-0.6003	419.89	-0.8038	422.33	0.0384	0.3840
0.6703	787.56	0.8214	694.95	-0.0360	778.49	-0.3711	451.15	-0.6033	421.49	-0.8068	434.04	0.0403	0.3841
0.6725	791.76	0.8236	702.16	-0.0445	743.15	-0.3747	469.48	-0.6063	431.06	-0.8098	447.82	0.0422	0.4072
0.6747	787.49	0.8258	699.57	-0.0531	701.19	-0.3782	447.19	-0.6093	431.30	-0.8127	457.85	0.0442	0.3898
0.6770	777.91	0.8281	700.02	-0.0616	652.55	-0.3817	469.02	-0.6123	442.73	-0.8157	442.51	0.0461	0.3612
0.6792	784.00	0.8303	703.92	-0.0702	603.86	-0.3852	451.97	-0.6153	443.12	-0.8187	438.18	0.0481	0.3550
0.6814	774.15	0.8325	704.81	-0.0787	566.04	-0.3888	462.81	-0.6183	449.72	-0.8217	434.95	0.0500	0.3284
0.6836	771.75	0.8347	709.06	-0.0873	539.24	-0.3923	454.15	-0.6213	453.30	-0.8247	438.61	0.0519	0.2533
0.6858	768.65	0.8369	706.99	-0.0958	512.00	-0.3958	452.16	-0.6243	433.02	-0.8277	434.60	0.0539	0.2048
0.6881	769.25	0.8392	705.02	-0.1044	496.64	-0.3993	466.26	-0.6273	428.60	-0.8307	443.78	0.0558	0.1677
0.6903	769.00	0.8414	707.16	-0.1130	494.67	-0.4029	441.34	-0.6303	431.29	-0.8337	433.18	0.0577	0.1468
0.6925	765.50	0.8436	713.94	-0.1215	463.65	-0.4064	467.82	-0.6333	436.55	-0.8367	431.16	0.0597	0.1592
0.6947	761.15	0.8458	718.48	-0.1301	466.39	-0.4099	452.31	-0.6362	437.69	-0.8397	431.25	0.0616	0.1419
0.6970	767.03	0.8481	709.96	-0.1386	444.81	-0.4134	464.01	-0.6392	433.62	-0.8427	442.06	0.0636	0.1448
0.6992	756.48	0.8503	708.40	-0.1472	449.17	-0.4170	453.32	-0.6422	439.28	-0.8457	439.40	0.0655	0.1548
0.7014	755.76	0.8525	713.33	-0.1557	437.51	-0.4205	451.99	-0.6452	445.20	-0.8486	440.42	0.0674	0.1506
0.7036	753.72	0.8547	719.20	-0.1643	429.56	-0.4240	467.08	-0.6482	442.44	-0.8516	446.34	0.0694	0.1514
0.7058	756.08	0.8569	717.14	-0.1728	438.70	-0.4275	441.59	-0.6512	439.57	-0.8546	450.10	0.0713	0.1343
0.7081	747.83	0.8592	719.77	-0.1814	422.52	-0.4310	467.25	-0.6542	433.34	-0.8576	447.74	0.0732	0.1396
0.7103	746.48	0.8614	726.64	-0.1899	440.93	-0.4346	449.79	-0.6572	433.80	-0.8606	473.71	0.0752	0.1294
0.7125	748.83	0.8636	731.51	-0.1985	425.91	-0.4381	469.50	-0.6602	444.71	-0.8636	471.93	0.0771	0.1120
0.7147	746.49	0.8658	732.11	-0.2020	434.19	-0.4416	454.27	-0.6632	453.28	-0.8666	463.10	0.0791	0.1141
0.7170	749.32	0.8681	732.91	-0.2055	421.98	-0.4451	457.56	-0.6662	450.55	-0.8696	452.49	0.0810	0.1189
0.7192	751.43	0.8703	738.41	-0.2091	420.47	-0.4487	465.75	-0.6692	448.65	-0.8726	450.02	0.0829	0.1273
0.7214	752.71	0.8725	739.06	-0.2126	415.00	-0.4522	447.02	-0.6721	448.78	-0.8756	463.28	0.0849	0.1094
0.7236	740.52	0.8747	746.67	-0.2161	404.14	-0.4557	469.84	-0.6751	449.17	-0.8786	455.81	0.0868	0.1054
0.7258	739.67	0.8769	752.65	-0.2196	420.18	-0.4592	448.66	-0.6781	452.03	-0.8816	467.65	0.0888	0.1273
0.7281	730.48	0.8792	751.26	-0.2232	404.63	-0.4628	461.76	-0.6811	448.85	-0.8845	460.99	0.0907	0.1111
0.7303	732.47	0.8814	758.67	-0.2267	413.80	-0.4663	451.65	-0.6841	441.46	-0.8875	462.24	0.0926	0.1142
0.7325	731.74	0.8836	761.34	-0.2302	409.12	-0.4698	450.00	-0.6871	445.73	-0.8905	465.95	0.0946	0.1062
0.7347	716.57	0.8858	770.81	-0.2337	419.72	-0.4733	451.61	-0.6901	436.00	-0.8935	480.36	0.0965	0.1123
0.7370	723.39	0.8881	770.73	-0.2372	423.81	-0.4769	441.18	-0.6931	451.76	-0.8965	476.11	0.0984	0.1202
0.7392	715.58	0.8903	777.45	-0.2408	420.62	-0.4804	458.36	-0.6961	440.41	-0.8995	487.21	0.1004	0.1214
0.7414	719.41	0.8925	785.29	-0.2443	436.95	-0.4839	439.84	-0.6991	447.12	-0.9025	481.06	0.1023	0.1125
0.7436	706.87	0.8947	787.27	-0.2478	428.16	-0.4874	457.19	-0.7021	437.29	-0.9055	487.60	0.1043	0.1051
0.7458	708.21	0.8969	798.47	-0.2513	448.33	-0.4910	441.44	-0.7051	436.07	-0.9085	481.67	0.1062	0.1084
0.7481	712.96	0.8992	801.69	-0.2549	442.38	-0.4945	449.54	-0.7080	445.19	-0.9115	481.41	0.1081	0.0999
0.7503	715.14	0.9014	800.96	-0.2584	456.22	-0.4980	448.75	-0.7110	452.83	-0.9145	490.89	0.1101	0.1065
0.7525	716.84	0.9036	806.51	-0.2619	462.29	-0.5015	433.31	-0.7140	451.42	-0.9174	495.66	0.1120	0.1086
0.7547	711.41	0.9058	809.13	-0.2654	460.80	-0.5050	446.11	-0.7170	445.64	-0.9204	497.80	0.1139	0.1257
0.7570	711.82	0.9081	819.85	-0.2690	449.52	-0.5086	438.08	-0.7200	446.41	-0.9234	497.45	0.1159	0.1099
0.7592	709.16	0.9103	825.05	-0.2725	469.95	-0.5121	450.65	-0.7230	448.54	-0.9264	498.37	0.1178	0.1049
0.7614	702.58	0.9125	834.34	-0.2760	478.12	-0.5156	434.65	-0.7260	454.84	-0.9294	504.38	0.1198	0.1131
0.7636	700.72	0.9147	835.00	-0.2795	467.11	-0.5191	448.94	-0.7290	457.34	-0.9324	509.15	0.1217	0.1186
0.7658	695.36	0.9169	842.40	-0.2831	469.10	-0.5227	443.23	-0.7320	446.54	-0.9354	518.45	0.1236	0.1173
0.7681	693.73	0.9192	848.70	-0.2866	473.50	-0.5262	438.99	-0.7350	433.44	-0.9384	522.45	0.1256	0.1239
0.7703	702.52	0.9214	856.85	-0.2901	464.74	-0.5297	440.89	-0.7380	430.04	-0.9414	526.50	0.1275	0.1246
0.7725	700.47	0.9236	868.74	-0.2936	466.58	-0.5332	425.21	-0.7409	434.46	-0.9444	533.86	0.1294	0.1374
0.7747	698.06	0.9258	876.03	-0.2971	438.87	-0.5368	438.81	-0.7439	438.67	-0.9474	538.88	0.1314	0.1412
0.7770	703.60	0.9281	886.84	-0.3007	465.96	-0.5403	430.10	-0.7469	438.99	-0.9504	546.31	0.1333	0.1507
0.7792	702.58	0.9303	889.17	-0.3042	483.45	-0.5438	434.41	-0.7499	440.85	-0.9533	551.39	0.1353	0.1627
0.7814	704.76	0.9325	902.36	-0.3077	455.72	-0.5473	421.00	-0.7529	444.92	-0.9563	556.72	0.1372	0.1981
0.7836	707.02	0.9347	916.25	-0.3112	442.48	-0.5509	422.87	-0.7559	435.84	-0.9593	562.62	0.1391	0.2522
0.7858	704.57	0.9369	939.69	-0.3148	446.65	-0.5544	430.49	-0.7589	429.82	-0.9623	572.46	0.1411	0.2769
0.7881	697.26	0.9392	951.91	-0.3183	453.97	-0.5579	418.16	-0.7619	438.95	-0.9653	578.47	0.1430	0.3087
0.7903	699.11	0.9414	954.01	-0.3218	437.27	-0.5614	423.75	-0.7649	433.48	-0.9683	584.48	0.1449	0.3158
0.7925	701.05	0.9436	960.63	-0.3253	452.21	-0.5649	420.65	-0.7679	439.93	-0.9713	592.00	0.1469	0.3441
0.7947	702.96	0.9458	975.34	-0.3289	441.52	-0.5685	431.40	-0.7709	440.92	-0.9743	601.43	0.1488	0.3553
0.7969	700.72	0.9481	990.51	-0.3324	456.20	-0.5720	423.15	-0.7739	439.16	-0.9773	612.69	0.1508	0.3529
0.7992	698.45	0.9503	1001.47	-0.3359	449.91	-0.5734	428.40	-0.7768	440.31	-0.9803	624.39	0.1527	0.3538
0.8014	693.32	0.9525	1025.96	-0.3394	452.05	-0.5764	423.58	-0.7798	437.66	-0.9833	635.08	0.1546	0.3603
0.8036	694.45	0.9547	1040.10	-0.3430	457.19	-0.5794	429.32	-0.7828	423.23	-0.9863	650.84		

Appendix 7.2 – Data for Spanwise Averaged Nusselt Number and Film Cooling Effectiveness

0.1566	0.3573	0.3926	0.1081	0.5437	0.0709	0.6948	0.0481	0.8459	0.0329	-0.1300	0.2074	-0.4099	0.0869
0.1585	0.3624	0.3948	0.1099	0.5459	0.0669	0.6970	0.0549	0.8481	0.0221	-0.1386	0.1997	-0.4134	0.1006
0.1605	0.3797	0.3970	0.1057	0.5481	0.0660	0.6992	0.0503	0.8503	0.0188	-0.1471	0.2085	-0.4169	0.0758
0.1624	0.3743	0.3992	0.1019	0.5503	0.0586	0.7014	0.0492	0.8526	0.0228	-0.1557	0.2016	-0.4204	0.0826
0.1643	0.3753	0.4015	0.1043	0.5526	0.0530	0.7037	0.0484	0.8548	0.0191	-0.1642	0.2044	-0.4240	0.0838
0.1663	0.3875	0.4037	0.1052	0.5548	0.0601	0.7059	0.0535	0.8570	0.0170	-0.1728	0.1977	-0.4275	0.0645
0.1682	0.3935	0.4059	0.1021	0.5570	0.0603	0.7081	0.0434	0.8592	0.0190	-0.1813	0.1961	-0.4310	0.0861
0.1701	0.3849	0.4081	0.1044	0.5592	0.0652	0.7103	0.0513	0.8614	0.0246	-0.1899	0.2023	-0.4345	0.0707
0.1721	0.3791	0.4104	0.0987	0.5615	0.0622	0.7126	0.0462	0.8637	0.0226	-0.1984	0.1981	-0.4380	0.0853
0.1740	0.3796	0.4126	0.1131	0.5637	0.0699	0.7148	0.0404	0.8659	0.0255	-0.2020	0.2064	-0.4416	0.0662
0.1760	0.3741	0.4148	0.1001	0.5659	0.0667	0.7170	0.0550	0.8681	0.0257	-0.2055	0.2043	-0.4451	0.0795
0.1779	0.3623	0.4170	0.0922	0.5681	0.0598	0.7192	0.0606	0.8703	0.0263	-0.2090	0.2133	-0.4477	0.0906
0.1798	0.3558	0.4192	0.0940	0.5703	0.0629	0.7214	0.0554	0.8726	0.0252	-0.2125	0.1952	-0.4507	0.0796
0.1818	0.3439	0.4215	0.0967	0.5726	0.0732	0.7237	0.0553	0.8748	0.0307	-0.2161	0.1806	-0.4537	0.0738
0.1837	0.3435	0.4237	0.1000	0.5748	0.0601	0.7259	0.0604	0.8770	0.0307	-0.2196	0.1703	-0.4567	0.0732
0.1856	0.3332	0.4259	0.1054	0.5770	0.0635	0.7281	0.0479	0.8792	0.0283	-0.2231	0.1593	-0.4597	0.0729
0.1876	0.3298	0.4281	0.0999	0.5792	0.0559	0.7303	0.0469	0.8814	0.0315	-0.2266	0.1780	-0.4627	0.0697
0.1895	0.3265	0.4304	0.0958	0.5815	0.0683	0.7326	0.0552	0.8837	0.0263	-0.2302	0.1669	-0.4657	0.0594
0.1915	0.3108	0.4326	0.1135	0.5837	0.0559	0.7348	0.0456	0.8859	0.0297	-0.2337	0.1945	-0.4687	0.0500
0.1934	0.3054	0.4348	0.1117	0.5859	0.0653	0.7370	0.0535	0.8881	0.0258	-0.2372	0.1796	-0.4717	0.0425
0.1953	0.2964	0.4370	0.0999	0.5881	0.0620	0.7392	0.0521	0.8903	0.0278	-0.2407	0.1832	-0.4747	0.0577
0.1973	0.2827	0.4392	0.1001	0.5903	0.0526	0.7414	0.0404	0.8926	0.0234	-0.2442	0.1753	-0.4776	0.0535
0.1992	0.2874	0.4415	0.0900	0.5926	0.0579	0.7437	0.0444	0.8948	0.0193	-0.2478	0.1680	-0.4806	0.0601
0.2011	0.2830	0.4437	0.0901	0.5948	0.0656	0.7459	0.0443	0.8970	0.0264	-0.2513	0.1745	-0.4836	0.0524
0.2031	0.2783	0.4459	0.0981	0.5970	0.0754	0.7481	0.0411	0.8992	0.0302	-0.2548	0.1587	-0.4866	0.0440
0.2050	0.2768	0.4481	0.0893	0.5992	0.0690	0.7503	0.0475	0.9014	0.0229	-0.2583	0.1681	-0.4896	0.0436
0.2070	0.2687	0.4503	0.0857	0.6015	0.0649	0.7526	0.0532	0.9037	0.0248	-0.2619	0.1585	-0.4926	0.0428
0.2089	0.2658	0.4526	0.0966	0.6037	0.0573	0.7548	0.0519	0.9059	0.0273	-0.2654	0.1615	-0.4956	0.0454
0.2108	0.2598	0.4548	0.0949	0.6059	0.0780	0.7570	0.0441	0.9081	0.0237	-0.2689	0.1593	-0.4986	0.0362
0.2128	0.2631	0.4570	0.0934	0.6081	0.0720	0.7592	0.0379	0.9103	0.0253	-0.2724	0.1596	-0.5016	0.0313
0.2147	0.2582	0.4592	0.0950	0.6103	0.0644	0.7614	0.0360	0.9126	0.0274	-0.2760	0.1633	-0.5046	0.0258
0.2166	0.2592	0.4615	0.0894	0.6126	0.0677	0.7637	0.0370	0.9148	0.0265	-0.2795	0.1628	-0.5076	0.0355
0.2186	0.2536	0.4637	0.0855	0.6148	0.0668	0.7659	0.0353	0.9170	0.0245	-0.2830	0.1705	-0.5106	0.0352
0.2205	0.2474	0.4659	0.0926	0.6170	0.0733	0.7681	0.0352	0.9192	0.0253	-0.2865	0.1687	-0.5135	0.0448
0.2225	0.2467	0.4681	0.0909	0.6192	0.0753	0.7703	0.0557	0.9214	0.0216	-0.2901	0.1748	-0.5165	0.0454
0.2244	0.2470	0.4703	0.0941	0.6215	0.0765	0.7726	0.0455	0.9237	0.0267	-0.2936	0.1636	-0.5195	0.0400
0.2263	0.2417	0.4726	0.0852	0.6237	0.0742	0.7748	0.0362	0.9259	0.0263	-0.2971	0.1294	-0.5225	0.0378
0.2283	0.2410	0.4748	0.0876	0.6259	0.0564	0.7770	0.0417	0.9281	0.0247	-0.3006	0.1367	-0.5255	0.0387
0.2302	0.2368	0.4770	0.0884	0.6281	0.0578	0.7792	0.0389	0.9303	0.0243	-0.3041	0.1396	-0.5285	0.0451
0.2302	0.2304	0.4792	0.0915	0.6303	0.0669	0.7814	0.0379	0.9325	0.0226	-0.3077	0.1458	-0.5315	0.0386
0.2334	0.2351	0.4815	0.0903	0.6326	0.0706	0.7837	0.0407	0.9348	0.0242	-0.3112	0.1331	-0.5345	0.0363
0.2366	0.2240	0.4837	0.0846	0.6348	0.0603	0.7859	0.0348	0.9370	0.0304	-0.3147	0.1227	-0.5375	0.0405
0.2398	0.2240	0.4859	0.0908	0.6370	0.0681	0.7881	0.0355	0.9392	0.0355	-0.3182	0.1534	-0.5405	0.0338
0.2430	0.2244	0.4881	0.0857	0.6392	0.0679	0.7903	0.0402	0.9414	0.0322	-0.3218	0.1299	-0.5435	0.0383
0.2462	0.2243	0.4903	0.0869	0.6415	0.0651	0.7926	0.0394	0.9437	0.0245	-0.3253	0.1512	-0.5465	0.0361
0.2494	0.2303	0.4926	0.0840	0.6437	0.0601	0.7948	0.0392	0.9459	0.0234	-0.3288	0.1449	-0.5494	0.0347
0.2526	0.2314	0.4948	0.0782	0.6459	0.0572	0.7970	0.0444	0.9481	0.0273	-0.3323	0.1513	-0.5524	0.0305
0.2558	0.2375	0.4970	0.0838	0.6481	0.0663	0.7992	0.0423	0.9503	0.0297	-0.3359	0.1429	-0.5554	0.0304
0.2590	0.2463	0.4992	0.0822	0.6503	0.0591	0.8014	0.0323	0.9525	0.0289	-0.3394	0.1484	-0.5584	0.0422
0.2622	0.2526	0.5015	0.0775	0.6526	0.0635	0.8037	0.0286	0.9548	0.0223	-0.3429	0.1349	-0.5614	0.0346
0.2654	0.2511	0.5037	0.0731	0.6548	0.0636	0.8059	0.0335	0.9570	0.0295	-0.3464	0.1315	-0.5644	0.0412
0.2686	0.2566	0.5059	0.0771	0.6570	0.0618	0.8081	0.0396	0.9592	0.0455	-0.3500	0.1344	-0.5674	0.0389
0.2718	0.2820	0.5081	0.0781	0.6592	0.0570	0.8103	0.0297			-0.3535	0.1285	-0.5704	0.0381
0.2750	0.2981	0.5103	0.0735	0.6615	0.0531	0.8126	0.0297	X/PL	η	-0.3570	0.1330	-0.5734	0.0380
0.2782	0.3210	0.5126	0.0816	0.6637	0.0589	0.8148	0.0316	-0.0103	0.2422	-0.3605	0.1212	-0.5764	0.0358
0.2814	0.3255	0.5148	0.0683	0.6659	0.0582	0.8170	0.0393	-0.0188	0.2378	-0.3640	0.1306	-0.5794	0.0395
0.2846	0.3585	0.5170	0.0736	0.6681	0.0583	0.8192	0.0410	-0.0274	0.2350	-0.3676	0.1161	-0.5823	0.0398
0.2878	0.3510	0.5192	0.0672	0.6703	0.0608	0.8214	0.0322	-0.0359	0.2396	-0.3711	0.1194	-0.5853	0.0387
0.2910	0.3686	0.5215	0.0762	0.6726	0.0689	0.8237	0.0294	-0.0445	0.2345	-0.3746	0.1161	-0.5883	0.0310
0.2942	0.3559	0.5237	0.0807	0.6748	0.0591	0.8259	0.0303	-0.0530	0.2325	-0.3781	0.1056	-0.5913	0.0382
0.2974	0.3304	0.5259	0.0736	0.6770	0.0494	0.8281	0.0365	-0.0616	0.2298	-0.3817	0.1153	-0.5943	0.0300
0.3006	0.3233	0.5281	0.0691	0.6792	0.0602	0.8303	0.0314	-0.0701	0.2263	-0.3852	0.0982	-0.5973	0.0324
0.3038	0.3003	0.5303	0.0702	0.6814	0.0522	0.8326	0.0265	-0.0787	0.2336	-0.3887	0.1192	-0.6003	0.0227
0.3069	0.2832	0.5326	0.0704	0.6837	0.0507	0.8348	0.0275	-0.0872	0.2299	-0.3922	0.0945	-0.6033	0.0225
0.3837	0.1208	0.5348	0.0713	0.6859	0.0595	0.8370	0.0303	-0.0958	0.2214	-0.3958	0.1096	-0.6063	0.0293
0.3859	0.1229	0.5370	0.0614	0.6881	0.0475	0.8392	0.0269	-0.1044	0.2234	-0.3993	0.1024	-0.6093	0.0287
0.3881	0.1207	0.5392	0.0641	0.6903	0.0512	0.8414	0.0304	-0.1129	0.2251	-0.4028	0.0771	-0.6123	0.0399
0.3904	0.1151	0.5415	0.0684	0.6926	0.0546	0.8437	0.0316	-0.1215	0.2089	-0.4063	0.0989	-0.6153	0.0422

Appendix 7.2 – Data for Spanwise Averaged Nusselt Number and Film Cooling Effectiveness

-0.6182	0.0444	-0.8217	0.0096	0.0480	806.29	0.1798	613.20	0.4192	805.15	0.5703	928.29	0.7214	732.96
-0.6212	0.0448	-0.8247	0.0122	0.0499	784.15	0.1817	614.57	0.4214	807.34	0.5725	914.51	0.7236	725.41
-0.6242	0.0304	-0.8277	0.0089	0.0519	747.25	0.1837	623.93	0.4236	811.01	0.5747	906.66	0.7258	725.91
-0.6272	0.0238	-0.8306	0.0136	0.0538	719.76	0.1856	626.35	0.4259	807.17	0.5770	914.22	0.7281	725.17
-0.6302	0.0255	-0.8336	0.0063	0.0558	741.11	0.1875	623.86	0.4281	809.33	0.5792	910.83	0.7303	715.92
-0.6332	0.0288	-0.8366	0.0075	0.0577	725.62	0.1895	613.01	0.4303	804.18	0.5814	916.61	0.7325	715.38
-0.6362	0.0278	-0.8396	0.0062	0.0596	717.27	0.1914	623.05	0.4325	800.80	0.5836	900.04	0.7347	714.27
-0.6392	0.0258	-0.8426	0.0116	0.0616	701.88	0.1933	636.64	0.4347	799.77	0.5858	899.81	0.7370	719.87
-0.6422	0.0302	-0.8456	0.0089	0.0635	692.88	0.1953	633.83	0.4370	806.01	0.5881	902.83	0.7392	714.71
-0.6452	0.0339	-0.8486	0.0074	0.0654	690.14	0.1972	636.68	0.4392	805.33	0.5903	893.34	0.7414	709.84
-0.6482	0.0284	-0.8516	0.0132	0.0674	687.91	0.1992	634.24	0.4414	804.91	0.5925	888.36	0.7436	704.97
-0.6512	0.0283	-0.8546	0.0148	0.0693	675.89	0.2011	637.95	0.4436	800.79	0.5947	877.76	0.7458	706.64
-0.6541	0.0214	-0.8576	0.0117	0.0713	670.78	0.2030	632.50	0.4459	796.95	0.5970	880.70	0.7481	710.06
-0.6571	0.0211	-0.8606	0.0291	0.0732	673.04	0.2050	632.52	0.4481	796.19	0.5992	876.87	0.7503	714.00
-0.6601	0.0282	-0.8636	0.0310	0.0751	663.64	0.2069	632.26	0.4503	800.46	0.6014	880.38	0.7525	705.28
-0.6631	0.0342	-0.8665	0.0205	0.0771	659.13	0.2088	636.77	0.4525	796.74	0.6036	869.63	0.7547	704.00
-0.6661	0.0333	-0.8695	0.0101	0.0790	656.41	0.2108	636.33	0.4547	800.43	0.6058	866.08	0.7570	704.41
-0.6691	0.0304	-0.8725	0.0077	0.0810	652.82	0.2127	640.93	0.4570	810.83	0.6081	876.70	0.7592	707.33
-0.6721	0.0338	-0.8755	0.0162	0.0829	637.69	0.2147	638.93	0.4592	817.08	0.6103	874.63	0.7614	704.43
-0.6751	0.0335	-0.8785	0.0088	0.0848	630.96	0.2166	632.29	0.4614	814.10	0.6125	868.66	0.7636	696.39
-0.6781	0.0350	-0.8815	0.0157	0.0868	621.23	0.2185	631.02	0.4636	814.71	0.6147	865.57	0.7658	698.49
-0.6811	0.0308	-0.8845	0.0113	0.0887	619.13	0.2205	635.25	0.4659	817.28	0.6170	863.66	0.7681	700.65
-0.6841	0.0223	-0.8875	0.0077	0.0906	605.03	0.2224	629.48	0.4681	821.19	0.6192	856.17	0.7703	693.95
-0.6871	0.0263	-0.8905	0.0065	0.0926	592.19	0.2243	619.43	0.4703	815.90	0.6214	849.17	0.7725	694.96
-0.6900	0.0215	-0.8935	0.0176	0.0945	587.48	0.2263	616.10	0.4725	816.77	0.6236	842.86	0.7747	696.76
-0.6930	0.0311	-0.8965	0.0125	0.0965	583.34	0.2282	619.13	0.4747	819.01	0.6258	845.66	0.7770	697.65
-0.6960	0.0254	-0.8995	0.0195	0.0984	579.68	0.2302	621.22	0.4770	826.80	0.6281	845.31	0.7792	705.18
-0.6990	0.0303	-0.9024	0.0124	0.1003	573.51	0.2302	616.85	0.4792	816.65	0.6303	833.41	0.7814	699.66
-0.7020	0.0225	-0.9054	0.0124	0.1023	565.84	0.2334	618.02	0.4814	819.47	0.6325	826.40	0.7836	692.89
-0.7050	0.0183	-0.9084	0.0086	0.1042	557.66	0.2366	620.84	0.4836	825.40	0.6347	830.79	0.7858	692.89
-0.7080	0.0268	-0.9114	0.0094	0.1061	560.04	0.2398	624.58	0.4859	827.79	0.6370	825.21	0.7881	695.86
-0.7110	0.0317	-0.9144	0.0135	0.1081	551.81	0.2430	629.46	0.4881	824.60	0.6392	828.18	0.7903	691.26
-0.7140	0.0284	-0.9174	0.0138	0.1100	557.78	0.2461	631.31	0.4903	834.28	0.6414	821.63	0.7925	690.58
-0.7170	0.0258	-0.9204	0.0112	0.1120	557.10	0.2493	637.11	0.4925	836.40	0.6436	823.41	0.7947	697.42
-0.7200	0.0251	-0.9234	0.0081	0.1139	542.85	0.2525	638.02	0.4947	834.11	0.6458	824.62	0.7969	697.48
-0.7230	0.0311	-0.9264	0.0088	0.1158	539.82	0.2557	638.09	0.4970	840.44	0.6481	821.83	0.7992	691.98
-0.7259	0.0360	-0.9294	0.0078	0.1178	548.83	0.2589	637.72	0.4992	842.92	0.6503	816.50	0.8014	694.97
-0.7289	0.0355	-0.9324	0.0073	0.1197	553.11	0.2621	643.16	0.5014	848.26	0.6525	808.42	0.8036	693.90
-0.7319	0.0239	-0.9353	0.0129	0.1216	543.43	0.2653	654.66	0.5036	842.84	0.6547	800.79	0.8058	692.50
-0.7349	0.0140	-0.9383	0.0124	0.1236	538.30	0.2685	660.79	0.5059	851.87	0.6570	796.99	0.8081	697.55
-0.7379	0.0142	-0.9413	0.0110	0.1255	533.15	0.2717	658.81	0.5081	853.43	0.6592	791.45	0.8103	691.59
-0.7409	0.0145	-0.9443	0.0123	0.1275	535.90	0.2749	665.85	0.5103	851.27	0.6614	780.74	0.8125	694.03
-0.7439	0.0184	-0.9473	0.0106	0.1294	546.34	0.2781	681.87	0.5125	854.83	0.6636	783.40	0.8147	691.03
-0.7469	0.0218	-0.9503	0.0110	0.1313	550.34	0.2813	772.40	0.5147	866.04	0.6658	773.45	0.8169	691.55
-0.7499	0.0228	-0.9533	0.0110	0.1333	560.39	0.2845	711.29	0.5170	865.24	0.6681	773.40	0.8192	689.96
-0.7529	0.0239	-0.9563	0.0133	0.1352	577.90	0.2877	655.45	0.5192	866.42	0.6703	768.33	0.8214	690.33
-0.7559	0.0173	-0.9593	0.0183	0.1371	612.64	0.2909	649.65	0.5214	876.24	0.6725	770.67	0.8236	696.04
-0.7588	0.0124	-0.9623	0.0204	0.1391	595.66	0.2941	651.06	0.5236	879.92	0.6747	767.01	0.8258	697.36
-0.7618	0.0158	-0.9653	0.0168	0.1410	560.05	0.2973	879.43	0.5259	880.43	0.6770	761.08	0.8281	698.14
-0.7648	0.0137	-0.9683	0.0151	0.1430	560.94	0.3005	849.81	0.5281	879.47	0.6792	759.88	0.8303	693.66
-0.7678	0.0156	-0.9712	0.0145	0.1449	589.77	0.3037	839.98	0.5303	888.06	0.6814	756.14	0.8325	695.67
-0.7708	0.0153	-0.9742	0.0163	0.1468	629.65	0.3069	789.96	0.5325	898.12	0.6836	746.73	0.8347	692.56
-0.7738	0.0134	-0.9772	0.0181	0.1488	645.13	0.3836	818.80	0.5347	898.78	0.6858	761.07	0.8369	692.74
-0.7768	0.0168	-0.9802	0.0194	0.1507	636.48	0.3859	822.04	0.5370	898.10	0.6881	755.05	0.8392	695.21
-0.7798	0.0163	-0.9832	0.0167	0.1526	631.76	0.3881	815.67	0.5392	902.76	0.6903	750.62	0.8414	700.92
-0.7828	0.0046	-0.9862	0.0204	0.1546	617.63	0.3903	813.73	0.5414	906.15	0.6925	745.12	0.8436	695.52
-0.7858	0.0048	-0.9892	0.0204	0.1565	611.77	0.3925	818.35	0.5436	907.96	0.6947	751.65	0.8458	694.66
-0.7888	0.0049	-0.9922	0.0356	0.1585	602.47	0.3947	824.02	0.5459	914.27	0.6970	753.03	0.8481	693.12
-0.7918	0.0081			0.1604	586.05	0.3970	821.34	0.5481	911.96	0.6992	743.56	0.8503	698.20
-0.7947	0.0058			0.1623	578.96	0.3992	814.14	0.5503	921.44	0.7014	743.48	0.8525	700.72
-0.7977	0.0005	CASE U – Nu		0.1643	583.20	0.4014	818.38	0.5525	923.22	0.7036	744.92	0.8547	703.29
-0.8007	0.0035			0.1662	584.47	0.4036	817.07	0.5547	921.82	0.7058	743.01	0.8569	712.21
-0.8037	0.0048	X/SL	Nu	0.1682	588.12	0.4059	817.80	0.5570	930.76	0.7081	741.62	0.8592	712.74
-0.8067	0.0132	0.0383	893.24	0.1701	592.88	0.4081	816.57	0.5592	930.10	0.7103	735.63	0.8614	714.80
-0.8097	0.0208	0.0403	833.82	0.1720	600.06	0.4103	816.02	0.5614	930.98	0.7125	739.96	0.8636	721.12
-0.8127	0.0289	0.0422	752.53	0.1740	604.03	0.4125	809.75	0.5636	923.62	0.7147	740.22	0.8658	721.48
-0.8157	0.0163	0.0441	729.32	0.1759	603.04	0.4147	805.86	0.5658	921.51	0.7170	731.27	0.8681	719.62
-0.8187	0.0131	0.0461	819.67	0.1778	606.42	0.4170	808.42	0.5681	928.76	0.7192	731.80	0.8703	722.64

Appendix 7.2 – Data for Spanwise Averaged Nusselt Number and Film Cooling Effectiveness

0.8725	726.89	-0.2126	425.46	-0.4522	455.57	-0.6662	461.16	-0.8696	463.16	0.0791	0.2123	0.2108	0.3233
0.8747	730.82	-0.2161	439.36	-0.4557	478.02	-0.6692	460.93	-0.8726	463.58	0.0810	0.2102	0.2128	0.3258
0.8769	736.80	-0.2196	449.21	-0.4592	461.29	-0.6721	461.44	-0.8756	465.79	0.0829	0.2000	0.2147	0.3217
0.8792	741.76	-0.2232	444.31	-0.4628	468.58	-0.6751	461.36	-0.8786	471.05	0.0849	0.2091	0.2166	0.3166
0.8814	746.25	-0.2267	429.62	-0.4663	456.53	-0.6781	460.25	-0.8816	474.85	0.0868	0.2042	0.2186	0.3148
0.8836	750.36	-0.2302	410.55	-0.4698	452.70	-0.6811	460.95	-0.8845	474.52	0.0888	0.2020	0.2205	0.3187
0.8858	752.84	-0.2337	421.75	-0.4733	458.93	-0.6841	462.29	-0.8875	478.58	0.0907	0.2008	0.2225	0.3120
0.8881	752.88	-0.2372	425.44	-0.4769	449.01	-0.6871	461.53	-0.8905	481.40	0.0926	0.2007	0.2244	0.3083
0.8903	761.02	-0.2408	421.71	-0.4804	462.35	-0.6901	460.20	-0.8935	485.72	0.0946	0.2056	0.2263	0.2993
0.8925	766.01	-0.2443	438.14	-0.4839	446.69	-0.6931	461.29	-0.8965	488.30	0.0965	0.1996	0.2283	0.2990
0.8947	770.32	-0.2478	431.88	-0.4874	453.55	-0.6961	462.03	-0.8995	489.87	0.0984	0.1954	0.2302	0.2995
0.8969	777.49	-0.2513	449.33	-0.4910	444.14	-0.6991	467.29	-0.9025	493.67	0.1004	0.2067	0.2302	0.2957
0.8992	779.24	-0.2549	442.82	-0.4945	448.21	-0.7021	461.25	-0.9055	498.12	0.1023	0.2005	0.2334	0.3043
0.9014	785.17	-0.2584	452.93	-0.4980	453.30	-0.7051	459.11	-0.9085	500.60	0.1043	0.1945	0.2366	0.2959
0.9036	789.66	-0.2619	463.06	-0.5015	444.33	-0.7080	458.02	-0.9115	500.76	0.1062	0.2079	0.2398	0.2900
0.9058	796.76	-0.2654	460.56	-0.5050	451.84	-0.7110	457.38	-0.9145	504.80	0.1081	0.1961	0.2430	0.2950
0.9081	804.14	-0.2690	483.10	-0.5086	443.91	-0.7140	457.77	-0.9174	507.91	0.1101	0.1968	0.2462	0.2941
0.9103	809.03	-0.2725	474.08	-0.5121	450.31	-0.7170	456.59	-0.9204	510.94	0.1120	0.1984	0.2494	0.2985
0.9125	816.15	-0.2760	509.81	-0.5156	434.23	-0.7200	454.88	-0.9234	515.31	0.1139	0.1944	0.2526	0.2956
0.9147	822.03	-0.2795	522.98	-0.5191	441.10	-0.7230	454.52	-0.9264	523.29	0.1159	0.2173	0.2558	0.2969
0.9169	824.87	-0.2831	519.96	-0.5227	443.10	-0.7260	451.72	-0.9294	529.36	0.1178	0.2007	0.2590	0.3006
0.9192	836.49	-0.2866	509.90	-0.5256	450.30	-0.7290	451.87	-0.9324	532.01	0.1198	0.1977	0.2622	0.3012
0.9214	847.20	-0.2901	469.77	-0.5286	450.16	-0.7320	453.32	-0.9354	536.16	0.1217	0.1964	0.2654	0.3088
0.9236	852.97	-0.2936	479.63	-0.5315	447.99	-0.7350	455.46	-0.9384	544.46	0.1236	0.2055	0.2686	0.3071
0.9258	860.67	-0.2971	459.10	-0.5345	448.25	-0.7380	452.24	-0.9414	550.47	0.1256	0.2004	0.2718	0.3274
0.9281	869.84	-0.3007	479.94	-0.5375	447.46	-0.7409	451.10	-0.9444	555.47	0.1275	0.1993	0.2750	0.3610
0.9303	876.51	-0.3042	491.30	-0.5405	448.04	-0.7439	450.73	-0.9474	560.36	0.1294	0.2095	0.2782	0.3823
0.9325	884.82	-0.3077	479.36	-0.5435	449.09	-0.7469	448.93	-0.9504	565.12	0.1314	0.2222	0.2814	0.3957
0.9347	899.60	-0.3112	457.35	-0.5465	448.98	-0.7499	450.49	-0.9533	572.64	0.1333	0.2393	0.2846	0.3989
0.9369	914.47	-0.3148	457.88	-0.5495	450.19	-0.7529	448.75	-0.9563	580.67	0.1353	0.2376	0.2878	0.4238
0.9392	923.12	-0.3183	464.23	-0.5525	450.63	-0.7559	447.85	-0.9593	588.18	0.1372	0.2727	0.2910	0.4239
0.9414	925.74	-0.3218	452.58	-0.5555	450.48	-0.7589	446.65	-0.9623	592.93	0.1391	0.3118	0.2942	0.4249
0.9436	936.57	-0.3253	464.07	-0.5585	450.90	-0.7619	447.70	-0.9653	598.35	0.1411	0.3117	0.2974	0.3856
0.9458	943.40	-0.3289	447.24	-0.5615	450.06	-0.7649	448.41	-0.9683	604.11	0.1430	0.3177	0.3006	0.3743
0.9481	950.29	-0.3324	463.28	-0.5645	453.76	-0.7679	448.33	-0.9713	609.33	0.1449	0.3356	0.3038	0.3621
0.9503	959.61	-0.3359	454.61	-0.5674	454.41	-0.7709	448.49	-0.9743	613.50	0.1469	0.3406	0.3069	0.3432
0.9525	985.82	-0.3394	454.32	-0.5704	455.61	-0.7739	448.65	-0.9773	623.05	0.1488	0.3542	0.3837	0.2358
0.9547	1010.64	-0.3430	463.30	-0.5734	452.90	-0.7768	447.09	-0.9803	633.10	0.1508	0.3819	0.3859	0.2370
0.9569	1066.22	-0.3465	456.33	-0.5764	447.86	-0.7798	447.05	-0.9833	641.76	0.1527	0.3900	0.3881	0.2301
0.9592	1149.17	-0.3500	471.51	-0.5794	448.99	-0.7828	446.38	-0.9863	650.91	0.1546	0.3992	0.3904	0.2256
		-0.3535	454.30	-0.5824	448.94	-0.7858	446.80	-0.9892	657.17	0.1566	0.4051	0.3926	0.2178
		-0.3571	469.10	-0.5854	450.15	-0.7888	446.06	-0.9922	667.40	0.1585	0.4077	0.3948	0.2227
		-0.3606	461.11	-0.5884	452.10	-0.7918	446.82			0.1605	0.3997	0.3970	0.2165
		-0.3641	467.40	-0.5914	453.92	-0.7948	447.16			0.1624	0.3993	0.3992	0.2055
		-0.3676	464.45	-0.5944	452.92	-0.7978	447.03			0.1643	0.4035	0.4015	0.2030
		-0.3711	450.78	-0.5974	450.49	-0.8008	446.90			0.1663	0.4020	0.4037	0.2046
		-0.3747	471.83	-0.6003	452.50	-0.8038	446.36			0.1682	0.4001	0.4059	0.2064
		-0.3782	451.84	-0.6033	453.15	-0.8068	446.55			0.0384	0.3533	0.1701	0.3941
		-0.3817	472.07	-0.6063	454.43	-0.8098	447.18			0.0403	0.3548	0.1721	0.3943
		-0.3852	453.89	-0.6093	455.43	-0.8127	447.79			0.0422	0.3633	0.1740	0.3989
		-0.3888	461.82	-0.6123	454.29	-0.8157	447.86			0.0442	0.3132	0.1760	0.3906
		-0.3923	461.25	-0.6153	453.62	-0.8187	448.43			0.0461	0.3665	0.1779	0.3898
		-0.3958	452.12	-0.6183	455.67	-0.8217	448.59			0.0481	0.3622	0.1798	0.3818
		-0.3993	485.22	-0.6213	456.73	-0.8247	448.84			0.0500	0.3379	0.1818	0.3737
		-0.4029	443.10	-0.6243	457.21	-0.8277	448.44			0.0519	0.2932	0.1837	0.3797
		-0.4064	470.93	-0.6273	457.71	-0.8307	449.23			0.0539	0.2696	0.1856	0.3809
		-0.4099	452.43	-0.6303	454.37	-0.8337	449.17			0.0558	0.2820	0.1876	0.3726
		-0.4134	469.81	-0.6333	453.68	-0.8367	449.93			0.0577	0.2534	0.1895	0.3610
		-0.4170	454.44	-0.6362	454.00	-0.8397	451.47			0.0597	0.2589	0.1915	0.3601
		-0.4205	449.30	-0.6392	455.57	-0.8427	453.11			0.0616	0.2416	0.1934	0.3593
		-0.4240	464.87	-0.6422	455.76	-0.8457	455.18			0.0636	0.2191	0.1953	0.3499
		-0.4275	446.36	-0.6452	456.03	-0.8486	456.38			0.0655	0.2212	0.1973	0.3537
		-0.4310	469.16	-0.6482	458.16	-0.8516	456.87			0.0674	0.2283	0.1992	0.3476
		-0.4346	455.07	-0.6512	458.12	-0.8546	457.17			0.0694	0.2319	0.2011	0.3455
		-0.4381	470.12	-0.6542	462.79	-0.8576	457.44			0.0713	0.2216	0.2031	0.3366
		-0.4416	462.05	-0.6572	465.29	-0.8606	458.53			0.0732	0.2263	0.2050	0.3372
		-0.4451	457.26	-0.6602	463.04	-0.8636	459.20			0.0752	0.2181	0.2070	0.3288
		-0.4487	467.81	-0.6632	461.68	-0.8666	460.37			0.0771	0.2050	0.2089	0.3275
													0.4526
													0.1804

CASE U - η

X/SL η

0.0384	0.3533
0.0403	0.3548
0.0422	0.3633
0.0442	0.3132
0.0461	0.3665
0.0481	0.3622
0.0500	0.3379
0.0519	0.2932
0.0539	0.2696
0.0558	0.2820
0.0577	0.2534
0.0597	0.2589
0.0616	0.2416
0.0636	0.2191
0.0655	0.2212
0.0674	0.2283
0.0694	0.2319
0.0713	0.2216
0.0732	0.2263
0.0752	0.2181
0.0771	0.2050

Appendix 7.2 – Data for Spanwise Averaged Nusselt Number and Film Cooling Effectiveness

0.4548	0.1810	0.6059	0.1231	0.7570	0.0794	0.9081	0.0463	-0.2689	0.1443	-0.5085	0.0966	-0.7200	0.0451
0.4570	0.1948	0.6081	0.1287	0.7592	0.0881	0.9103	0.0513	-0.2724	0.1467	-0.5120	0.0916	-0.7230	0.0487
0.4592	0.1994	0.6103	0.1277	0.7614	0.0800	0.9126	0.0495	-0.2760	0.1563	-0.5156	0.0776	-0.7259	0.0426
0.4615	0.1927	0.6126	0.1336	0.7637	0.0782	0.9148	0.0494	-0.2795	0.1504	-0.5191	0.0904	-0.7289	0.0414
0.4637	0.1904	0.6148	0.1395	0.7659	0.0793	0.9170	0.0489	-0.2830	0.1570	-0.5226	0.0799	-0.7319	0.0380
0.4659	0.1738	0.6170	0.1327	0.7681	0.0739	0.9192	0.0544	-0.2865	0.1597	-0.5261	0.0842	-0.7349	0.0414
0.4681	0.1889	0.6192	0.1252	0.7703	0.0602	0.9214	0.0545	-0.2901	0.1678	-0.5297	0.0759	-0.7379	0.0390
0.4703	0.1747	0.6215	0.1272	0.7726	0.0606	0.9237	0.0565	-0.2936	0.1688	-0.5332	0.0806	-0.7409	0.0295
0.4726	0.1785	0.6237	0.1283	0.7748	0.0695	0.9259	0.0563	-0.2971	0.1768	-0.5367	0.0833	-0.7439	0.0275
0.4748	0.1796	0.6259	0.1321	0.7770	0.0608	0.9281	0.0565	-0.3006	0.1675	-0.5402	0.0668	-0.7469	0.0262
0.4770	0.1894	0.6281	0.1279	0.7792	0.0795	0.9303	0.0539	-0.3041	0.1815	-0.5438	0.0678	-0.7499	0.0283
0.4792	0.1730	0.6303	0.1188	0.7814	0.0768	0.9325	0.0499	-0.3077	0.1718	-0.5473	0.0716	-0.7529	0.0213
0.4815	0.1684	0.6326	0.1228	0.7837	0.0675	0.9348	0.0524	-0.3112	0.1695	-0.5508	0.0687	-0.7559	0.0178
0.4837	0.1814	0.6348	0.1214	0.7859	0.0635	0.9370	0.0575	-0.3147	0.1738	-0.5543	0.0700	-0.7588	0.0158
0.4859	0.1766	0.6370	0.1068	0.7881	0.0662	0.9392	0.0600	-0.3182	0.1613	-0.5579	0.0715	-0.7618	0.0173
0.4881	0.1715	0.6392	0.1099	0.7903	0.0611	0.9414	0.0620	-0.3218	0.1700	-0.5614	0.0660	-0.7648	0.0196
0.4903	0.1756	0.6415	0.1133	0.7926	0.0677	0.9437	0.0602	-0.3253	0.1595	-0.5644	0.0787	-0.7678	0.0199
0.4926	0.1620	0.6437	0.1168	0.7948	0.0775	0.9459	0.0563	-0.3288	0.1576	-0.5674	0.0788	-0.7708	0.0166
0.4948	0.1564	0.6459	0.1087	0.7970	0.0786	0.9481	0.0561	-0.3323	0.1549	-0.5704	0.0815	-0.7738	0.0190
0.4970	0.1625	0.6481	0.1190	0.7992	0.0628	0.9503	0.0454	-0.3359	0.1497	-0.5734	0.0785	-0.7768	0.0178
0.4992	0.1678	0.6503	0.1194	0.8014	0.0737	0.9525	0.0534	-0.3394	0.1516	-0.5764	0.0756	-0.7798	0.0159
0.5015	0.1690	0.6526	0.1128	0.8037	0.0695	0.9548	0.0600	-0.3429	0.1493	-0.5794	0.0775	-0.7828	0.0117
0.5037	0.1579	0.6548	0.0924	0.8059	0.0625	0.9570	0.0571	-0.3464	0.1560	-0.5823	0.0801	-0.7858	0.0113
0.5059	0.1556	0.6570	0.0924	0.8081	0.0760	0.9592	0.0556	-0.3500	0.1449	-0.5853	0.0822	-0.7888	0.0123
0.5081	0.1693	0.6592	0.0897	0.8103	0.0713			-0.3535	0.1478	-0.5883	0.0770	-0.7918	0.0113
0.5103	0.1598	0.6615	0.0841	0.8126	0.0718	X/PL	η	-0.3570	0.1466	-0.5913	0.0772	-0.7947	0.0119
0.5126	0.1541	0.6637	0.0899	0.8148	0.0629	-0.0103	0.3140	-0.3605	0.1381	-0.5943	0.0757	-0.7977	0.0107
0.5148	0.1624	0.6659	0.0774	0.8170	0.0679	-0.0188	0.2990	-0.3640	0.1396	-0.5973	0.0688	-0.8007	0.0107
0.5170	0.1626	0.6681	0.0794	0.8192	0.0718	-0.0274	0.2699	-0.3676	0.1331	-0.6003	0.0680	-0.8037	0.0080
0.5192	0.1594	0.6703	0.0806	0.8214	0.0648	-0.0359	0.2646	-0.3711	0.1337	-0.6033	0.0698	-0.8067	0.0077
0.5215	0.1606	0.6726	0.0852	0.8237	0.0693	-0.0445	0.2535	-0.3746	0.1297	-0.6063	0.0710	-0.8097	0.0052
0.5237	0.1674	0.6748	0.0755	0.8259	0.0670	-0.0530	0.2394	-0.3781	0.1229	-0.6093	0.0709	-0.8127	0.0073
0.5259	0.1622	0.6770	0.0832	0.8281	0.0724	-0.0616	0.2179	-0.3817	0.1263	-0.6123	0.0707	-0.8157	0.0067
0.5281	0.1533	0.6792	0.0806	0.8303	0.0646	-0.0701	0.2057	-0.3852	0.1201	-0.6153	0.0675	-0.8187	0.0064
0.5303	0.1475	0.6814	0.0713	0.8326	0.0635	-0.0787	0.2078	-0.3887	0.1294	-0.6182	0.0709	-0.8217	0.0066
0.5326	0.1559	0.6837	0.0622	0.8348	0.0466	-0.0872	0.2134	-0.3922	0.1178	-0.6212	0.0717	-0.8247	0.0061
0.5348	0.1610	0.6859	0.0727	0.8370	0.0504	-0.0958	0.2007	-0.3958	0.1363	-0.6242	0.0715	-0.8277	0.0056
0.5370	0.1496	0.6881	0.0818	0.8392	0.0585	-0.1044	0.1996	-0.3993	0.1247	-0.6272	0.0719	-0.8306	0.0069
0.5392	0.1509	0.6903	0.0828	0.8414	0.0646	-0.1129	0.2046	-0.4028	0.1147	-0.6302	0.0663	-0.8336	0.0071
0.5415	0.1464	0.6926	0.0771	0.8437	0.0570	-0.1215	0.1971	-0.4063	0.1155	-0.6332	0.0648	-0.8366	0.0090
0.5437	0.1492	0.6948	0.0839	0.8459	0.0525	-0.1300	0.1852	-0.4099	0.1158	-0.6362	0.0642	-0.8396	0.0091
0.5459	0.1520	0.6970	0.0816	0.8481	0.0560	-0.1386	0.1749	-0.4134	0.1327	-0.6392	0.0620	-0.8426	0.0081
0.5481	0.1465	0.6992	0.0727	0.8503	0.0565	-0.1471	0.1844	-0.4169	0.1066	-0.6422	0.0648	-0.8456	0.0077
0.5503	0.1560	0.7014	0.0789	0.8526	0.0617	-0.1557	0.1725	-0.4204	0.1225	-0.6452	0.0644	-0.8486	0.0125
0.5526	0.1489	0.7037	0.0873	0.8548	0.0661	-0.1642	0.1792	-0.4240	0.1125	-0.6482	0.0664	-0.8516	0.0116
0.5548	0.1450	0.7059	0.0905	0.8570	0.0652	-0.1728	0.1750	-0.4275	0.1151	-0.6512	0.0643	-0.8546	0.0099
0.5570	0.1522	0.7081	0.0892	0.8592	0.0721	-0.1813	0.1767	-0.4310	0.1173	-0.6541	0.0727	-0.8576	0.0108
0.5592	0.1472	0.7103	0.0848	0.8614	0.0641	-0.1899	0.1769	-0.4345	0.1100	-0.6571	0.0764	-0.8606	0.0124
0.5615	0.1478	0.7126	0.0810	0.8637	0.0684	-0.1984	0.1767	-0.4380	0.1197	-0.6601	0.0747	-0.8636	0.0167
0.5637	0.1474	0.7148	0.0874	0.8659	0.0635	-0.2020	0.1790	-0.4416	0.1005	-0.6631	0.0703	-0.8665	0.0141
0.5659	0.1448	0.7170	0.0833	0.8681	0.0656	-0.2055	0.1823	-0.4451	0.1135	-0.6661	0.0696	-0.8695	0.0119
0.5681	0.1483	0.7192	0.0833	0.8703	0.0711	-0.2090	0.1905	-0.4486	0.1070	-0.6691	0.0663	-0.8725	0.0126
0.5703	0.1483	0.7214	0.0758	0.8726	0.0675	-0.2125	0.1854	-0.4521	0.1085	-0.6721	0.0703	-0.8755	0.0113
0.5726	0.1402	0.7237	0.0727	0.8748	0.0668	-0.2161	0.1896	-0.4557	0.1149	-0.6751	0.0729	-0.8785	0.0098
0.5748	0.1375	0.7259	0.0882	0.8770	0.0590	-0.2196	0.1931	-0.4592	0.1085	-0.6781	0.0702	-0.8815	0.0123
0.5770	0.1413	0.7281	0.0850	0.8792	0.0584	-0.2231	0.1918	-0.4627	0.1096	-0.6811	0.0657	-0.8845	0.0113
0.5792	0.1325	0.7303	0.0840	0.8814	0.0612	-0.2266	0.1818	-0.4662	0.0945	-0.6841	0.0670	-0.8875	0.0106
0.5815	0.1443	0.7326	0.0825	0.8837	0.0518	-0.2302	0.1697	-0.4698	0.1078	-0.6871	0.0652	-0.8905	0.0113
0.5837	0.1340	0.7348	0.0718	0.8859	0.0422	-0.2337	0.1751	-0.4733	0.0917	-0.6900	0.0694	-0.8935	0.0155
0.5859	0.1343	0.7370	0.0876	0.8881	0.0428	-0.2372	0.1602	-0.4768	0.1087	-0.6930	0.0754	-0.8965	0.0185
0.5881	0.1294	0.7392	0.0792	0.8903	0.0423	-0.2407	0.1627	-0.4803	0.0995	-0.6960	0.0742	-0.8995	0.0191
0.5903	0.1353	0.7414	0.0807	0.8926	0.0395	-0.2442	0.1549	-0.4839	0.0936	-0.6990	0.0756	-0.9024	0.0213
0.5926	0.1320	0.7437	0.0684	0.8948	0.0410	-0.2478	0.1524	-0.4874	0.0889	-0.7020	0.0703	-0.9054	0.0186
0.5948	0.1258	0.7459	0.0788	0.8970	0.0447	-0.2513	0.1529	-0.4909	0.0856	-0.7050	0.0618	-0.9084	0.0246
0.5970	0.1236	0.7481	0.0908	0.8992	0.0424	-0.2548	0.1452	-0.4944	0.0943	-0.7080	0.0605	-0.9114	0.0277
0.5992	0.1227	0.7503	0.1041	0.9014	0.0461	-0.2583	0.1498	-0.4979	0.0889	-0.7110	0.0572	-0.9144	0.0251
0.6015	0.1353	0.7526	0.0835	0.9037	0.0398	-0.2619	0.1455	-0.5015	0.1034	-0.7140	0.0546	-0.9174	0.0240
0.6037	0.1227	0.7548	0.0838	0.9059	0.0468	-0.2654	0.1475	-0.5050	0.0950	-0.7170	0.0539	-0.9204	0.0209

Appendix 7.2 – Data for Spanwise Averaged Nusselt Number and Film Cooling Effectiveness

-0.9234	0.0185	0.1139	576.30	0.2525	636.86	0.4947	853.34	0.6458	824.06	0.7969	705.08	0.9481	958.82
-0.9264	0.0253	0.1158	567.02	0.2557	637.62	0.4970	853.82	0.6481	820.59	0.7992	715.58	0.9503	972.52
-0.9294	0.0275	0.1178	574.55	0.2589	640.02	0.4992	849.57	0.6503	824.35	0.8014	716.31	0.9525	993.96
-0.9324	0.0240	0.1197	581.73	0.2621	644.56	0.5014	856.02	0.6525	814.43	0.8036	714.80	0.9547	1021.08
-0.9353	0.0262	0.1216	581.79	0.2653	654.52	0.5036	855.63	0.6547	815.56	0.8058	716.19	0.9569	1080.22
-0.9383	0.0293	0.1236	571.07	0.2685	667.91	0.5059	861.37	0.6570	811.26	0.8081	711.18	0.9592	1157.05
-0.9413	0.0297	0.1255	566.82	0.2717	667.32	0.5081	865.46	0.6592	807.33	0.8103	709.18		
-0.9443	0.0305	0.1275	572.31	0.2749	659.59	0.5103	867.19	0.6614	807.15	0.8125	712.13	X/PL	Nu
-0.9473	0.0276	0.1294	580.62	0.2781	669.85	0.5125	876.24	0.6636	804.46	0.8147	716.14	-0.0103	1102.53
-0.9503	0.0250	0.1313	586.44	0.2813	769.96	0.5147	872.80	0.6658	807.38	0.8169	715.73	-0.0189	905.35
-0.9533	0.0280	0.1333	592.50	0.2845	837.50	0.5170	877.71	0.6681	798.85	0.8192	711.22	-0.0274	873.73
-0.9563	0.0350	0.1352	618.99	0.2877	710.60	0.5192	881.96	0.6703	802.12	0.8214	712.17	-0.0360	830.62
-0.9593	0.0414	0.1371	662.44	0.2909	687.47	0.5214	886.60	0.6725	799.24	0.8236	711.29	-0.0445	751.23
-0.9623	0.0367	0.1391	651.98	0.2941	677.29	0.5236	881.77	0.6747	795.14	0.8258	719.18	-0.0531	681.38
-0.9653	0.0320	0.1410	615.81	0.2973	850.82	0.5259	882.30	0.6770	791.52	0.8281	714.74	-0.0616	662.36
-0.9683	0.0274	0.1430	610.97	0.3005	859.61	0.5281	891.47	0.6792	788.22	0.8303	710.52	-0.0702	645.05
-0.9712	0.0216	0.1449	634.93	0.3037	869.32	0.5303	895.15	0.6814	798.67	0.8325	714.79	-0.0787	619.04
-0.9742	0.0155	0.1468	701.51	0.3069	769.35	0.5325	893.11	0.6836	794.01	0.8347	719.53	-0.0873	599.36
-0.9772	0.0185	0.1488	755.64	0.3836	793.07	0.5347	905.44	0.6858	789.96	0.8369	715.58	-0.0958	588.92
-0.9802	0.0208	0.1507	737.03	0.3859	793.93	0.5370	910.32	0.6881	784.14	0.8392	724.96	-0.1044	557.00
-0.9832	0.0179	0.1526	718.46	0.3881	796.61	0.5392	906.30	0.6903	785.37	0.8414	722.11	-0.1130	556.18
-0.9862	0.0136	0.1546	692.23	0.3903	795.95	0.5414	916.58	0.6925	778.24	0.8436	731.69	-0.1215	532.89
-0.9892	0.0074	0.1565	696.91	0.3925	795.57	0.5436	918.63	0.6947	778.09	0.8458	732.85	-0.1301	530.37
-0.9922	0.0107	0.1585	683.56	0.3947	800.07	0.5459	925.36	0.6970	776.23	0.8481	728.43	-0.1386	510.82
		0.1604	674.83	0.3970	800.52	0.5481	917.08	0.6992	766.62	0.8503	724.29	-0.1472	506.71
		0.1623	663.15	0.3992	804.61	0.5503	920.55	0.7014	767.90	0.8525	731.14	-0.1557	494.73
		0.1643	658.35	0.4014	806.21	0.5525	927.07	0.7036	765.08	0.8547	738.21	-0.1643	481.78
		0.1662	658.18	0.4036	799.55	0.5547	921.91	0.7058	772.16	0.8569	740.21	-0.1728	490.45
		0.1682	656.20	0.4059	803.96	0.5570	931.24	0.7081	768.76	0.8592	739.21	-0.1814	475.03
		0.1701	658.13	0.4081	804.51	0.5592	935.95	0.7103	765.21	0.8614	743.64	-0.1899	480.59
		0.1720	662.82	0.4103	806.04	0.5614	931.53	0.7125	765.89	0.8636	747.26	-0.1985	470.40
		0.1740	659.37	0.4125	798.98	0.5636	920.92	0.7147	764.58	0.8658	746.25	-0.2020	471.73
		0.1759	662.72	0.4147	801.08	0.5658	922.47	0.7170	765.22	0.8681	744.48	-0.2055	461.42
		0.1778	661.88	0.4170	805.73	0.5681	935.22	0.7192	761.63	0.8703	752.47	-0.2091	448.32
		0.1798	662.98	0.4192	804.78	0.5703	931.69	0.7214	758.53	0.8725	756.83	-0.2126	448.08
		0.1817	661.56	0.4214	808.12	0.5725	923.92	0.7236	753.96	0.8747	757.28	-0.2161	432.56
		0.1837	663.66	0.4236	808.49	0.5747	912.68	0.7258	750.55	0.8769	759.89	-0.2196	448.37
		0.1856	663.91	0.4259	803.64	0.5770	913.12	0.7281	742.26	0.8792	758.90	-0.2232	418.50
		0.1875	658.11	0.4281	807.46	0.5792	913.25	0.7303	748.85	0.8814	773.00	-0.2267	425.96
		0.1895	654.07	0.4303	810.96	0.5814	912.59	0.7325	740.26	0.8836	776.80	-0.2302	422.75
		0.1914	653.68	0.4325	803.19	0.5836	900.31	0.7347	734.54	0.8858	780.17	-0.2337	420.69
		0.1933	659.39	0.4347	813.87	0.5858	899.09	0.7370	738.61	0.8881	781.87	-0.2372	432.51
		0.1953	660.76	0.4370	825.99	0.5881	902.89	0.7392	732.45	0.8903	788.71	-0.2408	414.77
		0.1972	658.57	0.4392	823.81	0.5903	900.11	0.7414	734.64	0.8925	794.68	-0.2443	440.00
		0.1992	653.07	0.4414	826.87	0.5925	892.35	0.7436	731.00	0.8947	792.59	-0.2478	430.07
		0.2011	657.13	0.4436	816.90	0.5947	882.69	0.7458	727.86	0.8969	797.25	-0.2513	444.97
		0.2030	655.93	0.4459	820.48	0.5970	886.51	0.7481	731.50	0.8992	804.92	-0.2549	440.54
		0.2050	649.14	0.4481	821.81	0.5992	890.80	0.7503	732.39	0.9014	804.37	-0.2584	445.22
		0.2069	650.16	0.4503	827.65	0.6014	881.72	0.7525	726.06	0.9036	802.72	-0.2619	459.84
		0.2088	650.52	0.4525	821.93	0.6036	873.02	0.7547	715.71	0.9058	813.06	-0.2654	452.72
		0.2108	657.21	0.4547	821.38	0.6058	869.27	0.7570	719.72	0.9081	817.99	-0.2690	473.88
		0.2127	650.06	0.4570	823.47	0.6081	875.97	0.7592	719.99	0.9103	824.75	-0.2725	464.12
		0.2147	645.18	0.4592	831.30	0.6103	874.05	0.7614	718.70	0.9125	827.45	-0.2760	482.85
		0.2166	643.85	0.4614	828.58	0.6125	870.27	0.7636	717.94	0.9147	831.09	-0.2795	477.54
		0.2185	642.53	0.4636	828.48	0.6147	864.74	0.7658	715.67	0.9169	837.89	-0.2831	478.44
		0.2205	642.66	0.4659	834.41	0.6170	863.14	0.7681	715.62	0.9192	842.88	-0.2866	477.20
		0.2224	638.36	0.4681	838.08	0.6192	861.22	0.7703	713.73	0.9214	848.55	-0.2901	459.65
		0.2243	627.77	0.4703	830.43	0.6214	851.75	0.7725	710.67	0.9236	858.26	-0.2936	468.28
		0.2263	624.46	0.4725	828.04	0.6236	847.41	0.7747	708.54	0.9258	863.28	-0.2971	449.31
		0.2282	627.44	0.4747	837.10	0.6258	844.90	0.7770	711.33	0.9281	868.23	-0.3007	475.65
		0.2302	625.04	0.4770	842.15	0.6281	851.22	0.7792	712.59	0.9303	881.86	-0.3042	480.65
		0.2302	623.37	0.4792	846.11	0.6303	836.71	0.7814	707.63	0.9325	891.23	-0.3077	458.47
		0.2334	622.67	0.4814	848.27	0.6325	832.71	0.7836	718.02	0.9347	900.70	-0.3112	452.04
		0.2366	626.28	0.4836	828.90	0.6347	836.44	0.7858	712.99	0.9369	917.14	-0.3148	442.04
		0.2398	629.18	0.4859	835.75	0.6370	833.03	0.7881	713.85	0.9392	919.65	-0.3183	460.46
		0.2430	629.04	0.4881	842.54	0.6392	831.63	0.7903	704.90	0.9414	927.65	-0.3218	431.99
		0.2461	633.82	0.4903	847.48	0.6414	824.97	0.7925	707.22	0.9436	934.11	-0.3253	451.14
		0.2493	633.61	0.4925	847.20	0.6436	824.95	0.7947	709.04	0.9458	946.38	-0.3289	432.62

Appendix 7.2 – Data for Spanwise Averaged Nusselt Number and Film Cooling Effectiveness

-0.3324	447.03	-0.5720	443.67	-0.7739	441.94	-0.9773	589.50	0.1488	0.4320	0.3837	0.2449	0.5348	0.1865
-0.3359	445.25	-0.5755	441.58	-0.7768	440.14	-0.9803	598.64	0.1508	0.4472	0.3859	0.2456	0.5370	0.1836
-0.3394	427.36	-0.5734	439.20	-0.7798	439.79	-0.9833	606.44	0.1527	0.4507	0.3881	0.2502	0.5392	0.1790
-0.3430	446.84	-0.5794	436.16	-0.7828	438.91	-0.9863	614.79	0.1546	0.4567	0.3904	0.2469	0.5415	0.1803
-0.3465	426.69	-0.5824	436.55	-0.7858	439.12	-0.9892	620.35	0.1566	0.4713	0.3926	0.2428	0.5437	0.1723
-0.3500	455.56	-0.5854	438.06	-0.7888	438.11	-0.9922	629.76	0.1585	0.4702	0.3948	0.2441	0.5459	0.1756
-0.3535	431.47	-0.5884	440.32	-0.7918	438.57			0.1605	0.4744	0.3970	0.2463	0.5481	0.1704
-0.3571	440.92	-0.5914	442.49	-0.7948	438.67			0.1624	0.4770	0.3992	0.2464	0.5503	0.1687
-0.3606	441.43	-0.5944	441.86	-0.7978	438.24			0.1643	0.4757	0.4015	0.2472	0.5526	0.1651
-0.3641	442.94	-0.5974	439.86	-0.8008	437.88			0.1663	0.4729	0.4037	0.2423	0.5548	0.1591
-0.3676	452.14	-0.6003	442.16	-0.8038	437.05			0.1682	0.4667	0.4059	0.2455	0.5570	0.1631
-0.3711	432.10	-0.6033	443.19	-0.8068	436.97			0.1701	0.4586	0.4081	0.2406	0.5592	0.1626
-0.3747	450.30	-0.6063	444.76	-0.8098	437.39			0.1721	0.4583	0.4104	0.2526	0.5615	0.1567
-0.3782	430.15	-0.6093	446.12	-0.8127	437.65			0.1740	0.4576	0.4126	0.2435	0.5637	0.1544
-0.3817	445.85	-0.6123	445.35	-0.8157	437.54			0.1760	0.4536	0.4148	0.2518	0.5659	0.1543
-0.3852	443.08	-0.6153	445.08	-0.8187	437.86			0.1779	0.4484	0.4170	0.2551	0.5681	0.1594
-0.3888	435.73	-0.6183	447.41	-0.8217	437.72			0.1798	0.4341	0.4192	0.2505	0.5703	0.1549
-0.3923	442.46	-0.6213	448.83	-0.8247	437.77			0.1818	0.4237	0.4215	0.2557	0.5726	0.1513
-0.3958	426.70	-0.6243	449.64	-0.8277	437.06			0.1837	0.4212	0.4237	0.2591	0.5748	0.1539
-0.3993	444.09	-0.6273	450.45	-0.8307	437.55			0.1856	0.4214	0.4259	0.2480	0.5770	0.1446
-0.4029	426.83	-0.6303	447.58	-0.8337	437.29			0.1876	0.4079	0.4281	0.2498	0.5792	0.1476
-0.4064	445.81	-0.6333	447.20	-0.8367	437.78			0.1895	0.4027	0.4304	0.2573	0.5815	0.1425
-0.4099	434.91	-0.6362	447.86	-0.8397	438.99			0.1915	0.3903	0.4326	0.2565	0.5837	0.1432
-0.4134	432.79	-0.6392	449.74	-0.8427	440.32			0.1934	0.3810	0.4348	0.2681	0.5859	0.1438
-0.4170	442.44	-0.6422	450.19	-0.8457	442.08			0.1953	0.3785	0.4370	0.2763	0.5881	0.1366
-0.4205	428.47	-0.6452	450.86	-0.8486	442.98			0.1973	0.3723	0.4392	0.2656	0.5903	0.1435
-0.4240	440.46	-0.6482	453.32	-0.8516	443.21			0.1992	0.3611	0.4415	0.2672	0.5926	0.1406
-0.4275	430.11	-0.6512	453.53	-0.8546	443.20			0.2011	0.3593	0.4437	0.2597	0.5948	0.1336
-0.4310	433.87	-0.6542	458.53	-0.8576	443.22			0.2031	0.3546	0.4459	0.2653	0.5970	0.1399
-0.4346	441.35	-0.6572	461.34	-0.8606	444.00			0.2050	0.3472	0.4481	0.2597	0.5992	0.1363
-0.4381	439.40	-0.6602	459.44	-0.8636	444.45			0.2070	0.3387	0.4503	0.2618	0.6015	0.1295
-0.4416	443.97	-0.6632	458.41	-0.8666	445.30			0.2089	0.3319	0.4526	0.2649	0.6037	0.1283
-0.4451	432.75	-0.6662	458.15	-0.8696	447.75			0.2108	0.3325	0.4548	0.2570	0.6059	0.1274
-0.4487	447.30	-0.6692	458.31	-0.8726	447.83			0.2128	0.3239	0.4570	0.2598	0.6081	0.1258
-0.4522	437.37	-0.6721	459.15	-0.8756	449.75			0.2147	0.3173	0.4592	0.2709	0.6103	0.1283
-0.4557	441.13	-0.6751	459.36	-0.8786	454.56			0.2166	0.3168	0.4615	0.2616	0.6126	0.1232
-0.4592	433.51	-0.6781	458.57	-0.8816	457.97			0.2186	0.3144	0.4637	0.2583	0.6148	0.1167
-0.4628	433.80	-0.6811	459.54	-0.8845	457.30			0.2205	0.3143	0.4659	0.2603	0.6170	0.1205
-0.4663	439.63	-0.6841	461.29	-0.8875	461.00			0.2225	0.3083	0.4681	0.2601	0.6192	0.1238
-0.4698	435.41	-0.6871	460.83	-0.8905	463.40			0.2244	0.3032	0.4703	0.2588	0.6215	0.1172
-0.4733	438.23	-0.6901	459.72	-0.8935	467.30			0.2263	0.2923	0.4726	0.2477	0.6237	0.1219
-0.4769	436.30	-0.6931	461.12	-0.8965	469.43			0.2283	0.2926	0.4748	0.2504	0.6259	0.1189
-0.4804	450.85	-0.6961	461.92	-0.8995	470.70			0.2302	0.2868	0.4770	0.2474	0.6281	0.1205
-0.4839	444.27	-0.6991	466.88	-0.9025	474.09			0.2320	0.2821	0.4792	0.2538	0.6303	0.1126
-0.4874	445.56	-0.7021	460.59	-0.9055	478.09			0.2334	0.2955	0.4815	0.2539	0.6326	0.1214
-0.4910	444.17	-0.7051	458.30	-0.9085	480.20			0.2366	0.2887	0.4837	0.2256	0.6348	0.1203
-0.4945	440.67	-0.7080	456.90	-0.9115	480.04			0.2398	0.2839	0.4859	0.2229	0.6370	0.1219
-0.4980	455.62	-0.7110	455.96	-0.9145	483.66			0.2430	0.2825	0.4881	0.2355	0.6392	0.1169
-0.5015	450.29	-0.7140	456.08	-0.9174	486.33			0.2462	0.2881	0.4903	0.2394	0.6415	0.1138
-0.5050	446.76	-0.7170	454.66	-0.9204	488.96			0.2494	0.2870	0.4926	0.2291	0.6437	0.1141
-0.5086	443.14	-0.7200	452.75	-0.9234	492.81			0.2526	0.2890	0.4948	0.2313	0.6459	0.1128
-0.5121	445.66	-0.7230	452.07	-0.9264	500.15			0.2558	0.2932	0.4970	0.2307	0.6481	0.1119
-0.5156	444.15	-0.7260	449.05	-0.9294	505.63			0.2590	0.3041	0.4992	0.2210	0.6503	0.1186
-0.5191	447.12	-0.7290	448.97	-0.9324	507.86			0.2622	0.3047	0.5015	0.2200	0.6526	0.1170
-0.5227	447.52	-0.7320	450.04	-0.9354	511.51			0.2654	0.3131	0.5037	0.2116	0.6548	0.1157
-0.5262	448.09	-0.7350	451.97	-0.9384	519.15			0.2686	0.3229	0.5059	0.2138	0.6570	0.1187
-0.5297	453.71	-0.7380	448.46	-0.9414	524.50			0.2718	0.3485	0.5081	0.2120	0.6592	0.1131
-0.5332	453.06	-0.7409	447.16	-0.9444	528.96			0.2750	0.3752	0.5103	0.2160	0.6615	0.1221
-0.5368	452.51	-0.7439	446.55	-0.9474	533.29			0.2782	0.3872	0.5126	0.2200	0.6637	0.1161
-0.5403	451.23	-0.7469	444.46	-0.9504	537.52			0.2814	0.4275	0.5148	0.2095	0.6659	0.1161
-0.5438	454.14	-0.7499	445.73	-0.9533	544.37			0.2846	0.4785	0.5170	0.2175	0.6681	0.1248
-0.5473	455.62	-0.7529	443.75	-0.9563	551.60			0.2878	0.4877	0.5192	0.2059	0.6703	0.1327
-0.5509	455.78	-0.7559	442.71	-0.9593	558.45			0.2910	0.4848	0.5215	0.2027	0.6726	0.1280
-0.5544	453.17	-0.7589	441.22	-0.9623	562.62			0.2942	0.4804	0.5237	0.1924	0.6748	0.1254
-0.5579	451.61	-0.7619	441.93	-0.9653	567.40			0.2974	0.4855	0.5259	0.1963	0.6770	0.1324
-0.5614	449.09	-0.7649	442.46	-0.9683	572.54			0.3006	0.4421	0.5281	0.2024	0.6792	0.1357
-0.5649	449.18	-0.7679	442.11	-0.9713	577.17			0.3038	0.4001	0.5303	0.1955	0.6814	0.1391
-0.5685	444.91	-0.7709	441.97	-0.9743	580.80			0.3069	0.3801	0.5326	0.1797	0.6837	0.1499

Appendix 7.2 – Data for Spanwise Averaged Nusselt Number and Film Cooling Effectiveness

0.6859	0.1337	0.8370	0.0936	-0.0958	0.3129	-0.3958	0.1911	-0.6093	0.1157	-0.8127	0.0650	0.0422	852.78
0.6881	0.1339	0.8392	0.1047	-0.1044	0.2825	-0.3993	0.1891	-0.6123	0.1130	-0.8157	0.0654	0.0442	821.36
0.6903	0.1351	0.8414	0.0968	-0.1129	0.2775	-0.4028	0.1845	-0.6153	0.1094	-0.8187	0.0673	0.0461	846.40
0.6926	0.1309	0.8437	0.1011	-0.1215	0.2639	-0.4063	0.1946	-0.6182	0.1135	-0.8217	0.0646	0.0481	953.57
0.6948	0.1324	0.8459	0.0948	-0.1300	0.2503	-0.4099	0.1923	-0.6212	0.1174	-0.8247	0.0615	0.0500	1032.14
0.6970	0.1398	0.8481	0.0975	-0.1386	0.2555	-0.4134	0.1833	-0.6242	0.1133	-0.8277	0.0573	0.0519	1025.47
0.6992	0.1293	0.8503	0.0890	-0.1471	0.2573	-0.4169	0.1936	-0.6272	0.1126	-0.8306	0.0573	0.0539	997.30
0.7014	0.1264	0.8526	0.0846	-0.1557	0.2636	-0.4204	0.1715	-0.6302	0.1092	-0.8336	0.0581	0.0558	967.28
0.7037	0.1227	0.8548	0.0866	-0.1642	0.2526	-0.4240	0.1827	-0.6332	0.1051	-0.8366	0.0606	0.0577	924.60
0.7059	0.1287	0.8570	0.0871	-0.1728	0.2554	-0.4275	0.1792	-0.6362	0.1038	-0.8396	0.0599	0.0597	923.80
0.7081	0.1331	0.8592	0.0856	-0.1813	0.2531	-0.4310	0.1757	-0.6392	0.1046	-0.8426	0.0584	0.0616	907.44
0.7103	0.1360	0.8614	0.0811	-0.1899	0.2478	-0.4345	0.1871	-0.6422	0.1024	-0.8456	0.0584	0.0636	913.38
0.7126	0.1384	0.8637	0.0881	-0.1984	0.2538	-0.4380	0.1799	-0.6452	0.0988	-0.8486	0.0586	0.0655	909.09
0.7148	0.1471	0.8659	0.0868	-0.2020	0.2516	-0.4416	0.1814	-0.6482	0.1040	-0.8516	0.0554	0.0674	899.75
0.7170	0.1398	0.8681	0.0800	-0.2055	0.2618	-0.4451	0.1692	-0.6512	0.0965	-0.8546	0.0537	0.0694	885.65
0.7192	0.1447	0.8703	0.0839	-0.2090	0.2637	-0.4486	0.1833	-0.6541	0.1046	-0.8576	0.0511	0.0713	862.52
0.7214	0.1228	0.8726	0.0826	-0.2125	0.2727	-0.4521	0.1718	-0.6571	0.1111	-0.8606	0.0507	0.0732	848.05
0.7237	0.1202	0.8748	0.0788	-0.2161	0.2671	-0.4557	0.1667	-0.6601	0.1030	-0.8636	0.0484	0.0752	845.81
0.7259	0.1267	0.8770	0.0790	-0.2196	0.2628	-0.4592	0.1601	-0.6631	0.1031	-0.8666	0.0500	0.0771	840.55
0.7281	0.1123	0.8792	0.0723	-0.2231	0.2615	-0.4627	0.1626	-0.6661	0.1004	-0.8695	0.0557	0.0791	824.57
0.7303	0.1263	0.8814	0.0860	-0.2266	0.2682	-0.4662	0.1713	-0.6691	0.0982	-0.8725	0.0554	0.0810	822.80
0.7326	0.1165	0.8837	0.0804	-0.2302	0.2768	-0.4698	0.1582	-0.6721	0.0981	-0.8755	0.0575	0.0829	813.31
0.7348	0.1131	0.8859	0.0813	-0.2337	0.2549	-0.4717	0.1607	-0.6751	0.0991	-0.8785	0.0645	0.0849	799.11
0.7370	0.1151	0.8881	0.0783	-0.2372	0.2584	-0.4747	0.1656	-0.6781	0.1000	-0.8815	0.0687	0.0868	784.52
0.7392	0.1106	0.8903	0.0714	-0.2407	0.2461	-0.4776	0.1730	-0.6811	0.1007	-0.8845	0.0644	0.0888	773.38
0.7414	0.1246	0.8926	0.0721	-0.2442	0.2354	-0.4806	0.1674	-0.6841	0.1037	-0.8875	0.0670	0.0907	764.14
0.7437	0.1194	0.8948	0.0619	-0.2478	0.2350	-0.4836	0.1740	-0.6871	0.1039	-0.8905	0.0655	0.0926	749.11
0.7459	0.1123	0.8970	0.0602	-0.2513	0.2326	-0.4866	0.1679	-0.6900	0.0998	-0.8935	0.0662	0.0946	739.14
0.7481	0.1185	0.8992	0.0662	-0.2548	0.2335	-0.4896	0.1637	-0.6930	0.1011	-0.8965	0.0659	0.0965	730.81
0.7503	0.1266	0.9014	0.0654	-0.2583	0.2225	-0.4926	0.1561	-0.6960	0.0966	-0.8995	0.0626	0.0984	722.44
0.7526	0.1221	0.9037	0.0557	-0.2619	0.2242	-0.4956	0.1565	-0.6990	0.1077	-0.9024	0.0642	0.1003	718.23
0.7548	0.1116	0.9059	0.0662	-0.2654	0.2235	-0.4986	0.1545	-0.7020	0.1024	-0.9054	0.0700	0.1023	711.04
0.7570	0.1066	0.9081	0.0623	-0.2689	0.2206	-0.5016	0.1568	-0.7050	0.1010	-0.9084	0.0718	0.1042	695.42
0.7592	0.1098	0.9103	0.0613	-0.2724	0.2265	-0.5046	0.1551	-0.7080	0.1024	-0.9114	0.0678	0.1061	694.59
0.7614	0.1088	0.9126	0.0574	-0.2760	0.2203	-0.5076	0.1437	-0.7110	0.1039	-0.9144	0.0679	0.1081	694.84
0.7637	0.1170	0.9148	0.0572	-0.2795	0.2281	-0.5106	0.1438	-0.7140	0.1030	-0.9174	0.0650	0.1100	680.82
0.7659	0.1069	0.9170	0.0542	-0.2830	0.2271	-0.5135	0.1434	-0.7170	0.1031	-0.9204	0.0637	0.1120	680.70
0.7681	0.1145	0.9192	0.0498	-0.2865	0.2414	-0.5165	0.1461	-0.7200	0.1014	-0.9234	0.0591	0.1139	692.34
0.7703	0.1108	0.9214	0.0454	-0.2901	0.2476	-0.5195	0.1483	-0.7230	0.1021	-0.9264	0.0590	0.1158	684.22
0.7726	0.1103	0.9237	0.0510	-0.2936	0.2556	-0.5225	0.1520	-0.7259	0.0900	-0.9294	0.0553	0.1178	670.71
0.7748	0.1083	0.9259	0.0444	-0.2971	0.2594	-0.5255	0.1497	-0.7289	0.0874	-0.9324	0.0488	0.1197	666.60
0.7770	0.1151	0.9281	0.0419	-0.3006	0.2560	-0.5285	0.1460	-0.7319	0.0864	-0.9353	0.0402	0.1216	673.37
0.7792	0.1055	0.9303	0.0492	-0.3041	0.2724	-0.5315	0.1385	-0.7349	0.0904	-0.9383	0.0396	0.1236	680.85
0.7814	0.1032	0.9325	0.0449	-0.3077	0.2602	-0.5345	0.1339	-0.7379	0.0858	-0.9413	0.0344	0.1255	670.71
0.7837	0.1134	0.9348	0.0433	-0.3112	0.2713	-0.5375	0.1308	-0.7409	0.0866	-0.9443	0.0309	0.1275	662.33
0.7859	0.1051	0.9370	0.0384	-0.3147	0.2684	-0.5405	0.1239	-0.7439	0.0868	-0.9473	0.0323	0.1294	660.13
0.7881	0.1046	0.9392	0.0377	-0.3182	0.2599	-0.5435	0.1265	-0.7469	0.0899	-0.9503	0.0258	0.1313	665.52
0.7903	0.1025	0.9414	0.0485	-0.3218	0.2555	-0.5465	0.1278	-0.7499	0.0851	-0.9533	0.0282	0.1333	675.62
0.7926	0.1067	0.9437	0.0387	-0.3253	0.2549	-0.5494	0.1211	-0.7529	0.0784	-0.9563	0.0321	0.1352	679.45
0.7948	0.0981	0.9459	0.0362	-0.3288	0.2500	-0.5524	0.1198	-0.7559	0.0765	-0.9593	0.0362	0.1371	694.34
0.7970	0.0946	0.9481	0.0424	-0.3323	0.2497	-0.5554	0.1191	-0.7588	0.0796	-0.9623	0.0370	0.1391	733.35
0.7992	0.1112	0.9503	0.0448	-0.3359	0.2553	-0.5584	0.1238	-0.7618	0.0883	-0.9653	0.0400	0.1410	779.71
0.8014	0.1149	0.9525	0.0462	-0.3394	0.2333	-0.5614	0.1292	-0.7648	0.0916	-0.9683	0.0388	0.1430	723.25
0.8037	0.1131	0.9548	0.0492	-0.3429	0.2473	-0.5644	0.1310	-0.7678	0.0927	-0.9712	0.0395	0.1449	721.26
0.8059	0.1087	0.9570	0.0525	-0.3464	0.2284	-0.5674	0.1307	-0.7708	0.0908	-0.9742	0.0399	0.1468	729.50
0.8081	0.1068	0.9592	0.0396	-0.3500	0.2387	-0.5704	0.1280	-0.7738	0.0842	-0.9772	0.0455	0.1488	783.36
0.8103	0.1098			-0.3535	0.2264	-0.5734	0.1207	-0.7768	0.0837	-0.9802	0.0468	0.1507	878.89
0.8126	0.1131	X/PL	η	-0.3570	0.2227	-0.5764	0.1173	-0.7798	0.0810	-0.9832	0.0419	0.1526	880.24
0.8148	0.1186	-0.0103	0.4339	-0.3605	0.2222	-0.5794	0.1221	-0.7828	0.0768	-0.9862	0.0440	0.1546	850.42
0.8170	0.1122	-0.0188	0.4390	-0.3640	0.2236	-0.5823	0.1149	-0.7858	0.0768	-0.9892	0.0435	0.1565	816.95
0.8192	0.0988	-0.0274	0.4255	-0.3676	0.2314	-0.5853	0.1189	-0.7888	0.0747	-0.9922	0.0499	0.1585	814.30
0.8214	0.1031	-0.0359	0.4042	-0.3711	0.2224	-0.5883	0.1228	-0.7918	0.0733			0.1604	817.29
0.8237	0.1048	-0.0445	0.4226	-0.3746	0.2224	-0.5913	0.1272	-0.7947	0.0742			0.1623	810.17
0.8259	0.1101	-0.0530	0.4130	-0.3781	0.2113	-0.5943	0.1253	-0.7977	0.0747	CASE W – Nu			
0.8281	0.1020	-0.0616	0.4007	-0.3817	0.2036	-0.5973	0.1169	-0.8007	0.0738	X/SL	Nu	0.1643	806.16
0.8303	0.0924	-0.0701	0.3773	-0.3852	0.2196	-0.6003	0.1144	-0.8037	0.0723	0.0384	887.21	0.1701	799.51
0.8326	0.0892	-0.0787	0.3554	-0.3887	0.1987	-0.6033	0.1175	-0.8067	0.0657	0.0403	897.93	0.1720	800.91
0.8348	0.0980	-0.0872	0.3303	-0.3922	0.2060	-0.6063	0.1146	-0.8097	0.0669				

Appendix 7.2 – Data for Spanwise Averaged Nusselt Number and Film Cooling Effectiveness

0.1740	799.40	0.4125	956.95	0.5636	1088.01	0.7147	867.01	0.8658	848.42	-0.2020	530.54	-0.4416	486.18
0.1759	797.57	0.4147	943.99	0.5658	1078.47	0.7170	867.09	0.8681	847.58	-0.2055	520.88	-0.4451	489.36
0.1778	808.45	0.4170	954.42	0.5681	1083.57	0.7192	865.09	0.8703	859.68	-0.2091	514.03	-0.4487	488.60
0.1798	803.91	0.4192	954.55	0.5703	1082.94	0.7214	865.26	0.8725	865.11	-0.2126	507.08	-0.4522	490.63
0.1817	803.38	0.4214	949.71	0.5725	1078.05	0.7236	853.81	0.8747	873.11	-0.2161	500.51	-0.4557	495.76
0.1837	799.40	0.4236	959.62	0.5747	1069.88	0.7258	849.10	0.8769	878.74	-0.2196	503.34	-0.4592	492.16
0.1856	800.86	0.4259	942.59	0.5770	1074.12	0.7281	853.26	0.8792	877.22	-0.2232	483.89	-0.4628	494.66
0.1875	797.13	0.4281	942.05	0.5792	1079.90	0.7303	843.79	0.8814	884.11	-0.2267	490.05	-0.4663	492.72
0.1895	795.39	0.4303	943.69	0.5814	1073.51	0.7325	848.59	0.8836	890.97	-0.2302	471.77	-0.4698	489.50
0.1914	790.30	0.4325	948.75	0.5836	1059.79	0.7347	850.48	0.8858	897.20	-0.2337	491.05	-0.4733	486.50
0.1933	781.24	0.4347	954.04	0.5858	1058.23	0.7370	839.92	0.8881	892.88	-0.2372	481.44	-0.4769	484.72
0.1953	783.91	0.4370	952.14	0.5881	1063.40	0.7392	834.12	0.8903	901.69	-0.2408	483.83	-0.4804	487.21
0.1972	789.64	0.4392	950.99	0.5903	1046.61	0.7414	839.85	0.8925	911.90	-0.2443	494.31	-0.4839	486.14
0.1992	791.81	0.4414	953.42	0.5925	1042.08	0.7436	827.99	0.8947	914.58	-0.2478	485.72	-0.4874	489.67
0.2011	791.49	0.4436	947.09	0.5947	1020.24	0.7458	822.61	0.8969	928.07	-0.2513	510.67	-0.4910	483.32
0.2030	788.66	0.4459	940.41	0.5970	1032.69	0.7481	829.95	0.8992	933.13	-0.2549	494.33	-0.4945	475.09
0.2050	790.48	0.4481	934.02	0.5992	1043.84	0.7503	828.66	0.9014	938.41	-0.2584	514.65	-0.4980	479.18
0.2069	785.35	0.4503	941.30	0.6014	1029.23	0.7525	822.01	0.9036	936.73	-0.2619	518.74	-0.5015	480.82
0.2088	777.37	0.4525	942.40	0.6036	1018.09	0.7547	829.24	0.9058	943.82	-0.2654	523.68	-0.5050	481.11
0.2108	774.33	0.4547	943.20	0.6058	1014.36	0.7570	823.22	0.9081	958.87	-0.2690	541.48	-0.5086	483.91
0.2127	779.85	0.4570	943.61	0.6081	1031.96	0.7592	832.88	0.9103	961.08	-0.2725	535.39	-0.5121	487.63
0.2147	779.44	0.4592	950.57	0.6103	1026.79	0.7614	824.53	0.9125	968.14	-0.2760	560.64	-0.5156	480.65
0.2166	774.72	0.4614	952.79	0.6125	1017.95	0.7636	822.19	0.9147	973.05	-0.2795	541.24	-0.5191	474.90
0.2185	763.82	0.4636	955.60	0.6147	999.50	0.7658	818.96	0.9169	983.46	-0.2831	565.96	-0.5227	474.09
0.2205	758.43	0.4659	959.98	0.6170	1003.20	0.7681	836.69	0.9192	991.57	-0.2866	549.34	-0.5262	473.16
0.2224	758.31	0.4681	953.75	0.6192	1003.19	0.7703	823.18	0.9214	1002.78	-0.2901	548.56	-0.5297	476.10
0.2243	762.37	0.4703	949.95	0.6214	989.97	0.7725	825.06	0.9236	1011.93	-0.2936	552.51	-0.5332	477.17
0.2263	757.04	0.4725	959.27	0.6236	981.34	0.7747	819.95	0.9258	1022.01	-0.2971	538.77	-0.5368	478.93
0.2282	747.01	0.4747	961.74	0.6258	987.55	0.7770	820.99	0.9281	1032.23	-0.3007	562.54	-0.5403	477.52
0.2302	740.66	0.4770	955.40	0.6281	992.01	0.7792	836.08	0.9303	1038.08	-0.3042	554.69	-0.5438	475.14
0.2302	736.47	0.4792	949.68	0.6303	980.17	0.7814	822.18	0.9325	1050.58	-0.3077	587.53	-0.5473	474.38
0.2334	734.47	0.4814	959.64	0.6325	976.55	0.7836	824.62	0.9347	1065.35	-0.3112	523.27	-0.5509	476.67
0.2366	735.38	0.4836	968.35	0.6347	971.70	0.7858	817.77	0.9369	1088.03	-0.3148	525.78	-0.5544	478.09
0.2398	733.03	0.4859	974.58	0.6370	963.99	0.7881	816.36	0.9392	1096.10	-0.3183	536.03	-0.5579	478.31
0.2430	732.79	0.4881	977.43	0.6392	967.89	0.7903	812.51	0.9414	1095.58	-0.3218	513.98	-0.5614	479.37
0.2461	731.02	0.4903	974.75	0.6414	954.67	0.7925	810.33	0.9436	1105.44	-0.3253	525.16	-0.5649	479.21
0.2493	733.66	0.4925	985.85	0.6436	958.21	0.7947	822.46	0.9458	1123.35	-0.3289	499.04	-0.5685	477.79
0.2525	735.89	0.4947	983.08	0.6458	955.89	0.7969	817.79	0.9481	1139.08	-0.3324	523.40	-0.5720	476.23
0.2557	731.22	0.4970	982.19	0.6481	958.64	0.7992	816.15	0.9503	1146.85	-0.3359	509.70	-0.5755	476.47
0.2589	736.13	0.4992	983.33	0.6503	942.27	0.8014	815.90	0.9525	1172.99	-0.3394	507.70	-0.5764	484.14
0.2621	739.79	0.5014	994.63	0.6525	925.61	0.8036	818.94	0.9547	1211.09	-0.3430	510.27	-0.5794	490.35
0.2653	744.45	0.5036	997.90	0.6547	936.75	0.8058	824.86	0.9569	1307.84	-0.3465	488.17	-0.5824	497.31
0.2685	760.79	0.5059	998.38	0.6570	936.05	0.8081	817.62	0.9592	1418.33	-0.3500	513.79	-0.5854	488.41
0.2717	767.70	0.5081	1001.54	0.6592	937.29	0.8103	818.13			-0.3535	481.74	-0.5884	479.23
0.2749	782.66	0.5103	1001.66	0.6614	925.82	0.8125	819.39	X/PL	Nu	-0.3571	505.79	-0.5914	477.76
0.2781	768.57	0.5125	1006.18	0.6636	932.56	0.8147	822.42	-0.0103	1341.97	-0.3606	489.94	-0.5944	481.13
0.2813	786.94	0.5147	1008.49	0.6658	922.99	0.8169	817.61	-0.0188	1284.11	-0.3641	498.35	-0.5974	492.87
0.2845	855.91	0.5170	1008.50	0.6681	918.36	0.8192	819.88	-0.0274	1197.03	-0.3676	475.05	-0.6003	496.01
0.2877	893.05	0.5192	1019.02	0.6703	907.31	0.8214	816.49	-0.0359	1171.04	-0.3711	466.39	-0.6033	497.72
0.2909	858.32	0.5214	1028.88	0.6725	898.50	0.8236	821.12	-0.0445	1081.75	-0.3747	491.00	-0.6063	500.70
0.2941	803.93	0.5236	1023.12	0.6747	904.81	0.8258	816.71	-0.0530	966.84	-0.3782	487.16	-0.6093	504.31
0.2973	772.46	0.5259	1020.30	0.6770	903.48	0.8281	814.83	-0.0616	913.57	-0.3817	502.17	-0.6123	527.89
0.3005	791.20	0.5281	1028.21	0.6792	903.42	0.8303	818.66	-0.0701	872.94	-0.3852	480.03	-0.6153	520.72
0.3037	859.52	0.5303	1042.30	0.6814	899.87	0.8325	821.15	-0.0787	818.00	-0.3888	477.41	-0.6183	495.55
0.3069	879.72	0.5325	1044.78	0.6836	892.90	0.8347	822.20	-0.0872	740.97	-0.3923	476.78	-0.6213	494.86
0.3836	950.88	0.5347	1042.70	0.6858	903.58	0.8369	822.36	-0.0959	682.32	-0.3958	479.96	-0.6243	495.22
0.3859	954.36	0.5370	1056.13	0.6881	896.10	0.8392	821.89	-0.1044	653.57	-0.3993	490.53	-0.6273	499.80
0.3881	947.52	0.5392	1051.95	0.6903	878.54	0.8414	820.46	-0.1130	624.48	-0.4029	486.04	-0.6303	490.95
0.3903	956.51	0.5414	1061.68	0.6925	876.97	0.8436	822.80	-0.1215	602.43	-0.4064	486.49	-0.6333	505.93
0.3925	961.35	0.5436	1067.04	0.6947	897.31	0.8458	823.79	-0.1301	593.26	-0.4099	478.28	-0.6362	484.10
0.3947	957.43	0.5459	1073.04	0.6970	885.11	0.8481	823.21	-0.1386	566.90	-0.4134	487.91	-0.6392	490.29
0.3970	959.85	0.5481	1071.08	0.6992	869.07	0.8503	821.91	-0.1472	569.92	-0.4170	489.20	-0.6422	512.25
0.3992	964.12	0.5503	1081.01	0.7014	871.05	0.8525	832.64	-0.1557	538.78	-0.4205	485.11	-0.6452	518.96
0.4014	958.37	0.5525	1081.00	0.7036	870.89	0.8547	841.31	-0.1643	530.93	-0.4240	488.53	-0.6482	502.16
0.4036	956.35	0.5547	1084.50	0.7058	868.93	0.8569	842.24	-0.1728	535.79	-0.4275	478.37	-0.6512	497.40
0.4059	958.21	0.5570	1082.94	0.7081	868.86	0.8592	839.03	-0.1814	524.80	-0.4310	484.11	-0.6542	500.13
0.4081	964.08	0.5592	1085.41	0.7103	876.46	0.8614	838.10	-0.1899	533.21	-0.4346	483.01	-0.6572	514.76
0.4103	959.47	0.5614	1087.51	0.7125	868.92	0.8636	841.65	-0.1985	521.50	-0.4381	493.78	-0.6602	503.87

Appendix 7.2 – Data for Spanwise Averaged Nusselt Number and Film Cooling Effectiveness

-0.6632	516.67	-0.8666	503.76	0.0771	0.2444	0.2089	0.2751	0.4530	0.2170	0.6040	0.1330	0.7550	0.1070
-0.6662	508.20	-0.8696	504.64	0.0791	0.2275	0.2108	0.2732	0.4550	0.2080	0.6060	0.1420	0.7570	0.0933
-0.6692	495.55	-0.8726	506.57	0.0810	0.2355	0.2128	0.2728	0.4570	0.2060	0.6080	0.1470	0.7590	0.1060
-0.6721	516.50	-0.8756	510.54	0.0829	0.2307	0.2147	0.2767	0.4590	0.2100	0.6100	0.1360	0.7610	0.1130
-0.6751	493.42	-0.8786	509.16	0.0849	0.2238	0.2166	0.2841	0.4610	0.2110	0.6130	0.1370	0.7640	0.1080
-0.6781	494.14	-0.8816	515.66	0.0868	0.2337	0.2186	0.2791	0.4640	0.2120	0.6150	0.1260	0.7660	0.1030
-0.6811	485.04	-0.8845	524.98	0.0888	0.2297	0.2205	0.2787	0.4660	0.2060	0.6170	0.1380	0.7680	0.1160
-0.6841	480.41	-0.8875	527.89	0.0907	0.2200	0.2225	0.2747	0.4680	0.2030	0.6190	0.1330	0.7700	0.1020
-0.6871	489.07	-0.8905	529.44	0.0926	0.2153	0.2244	0.2864	0.4700	0.2060	0.6210	0.1350	0.7730	0.1130
-0.6901	496.87	-0.8935	525.19	0.0946	0.2229	0.2263	0.2940	0.4730	0.1980	0.6240	0.1250	0.7750	0.1080
-0.6931	496.01	-0.8965	533.11	0.0965	0.2227	0.2283	0.2958	0.4750	0.2020	0.6260	0.1320	0.7770	0.0971
-0.6961	486.92	-0.8995	530.45	0.0984	0.2215	0.2302	0.2892	0.4770	0.2010	0.6280	0.1280	0.7790	0.1020
-0.6991	484.46	-0.9025	538.28	0.1004	0.2207	0.2302	0.2830	0.4790	0.1870	0.6300	0.1360	0.7810	0.1020
-0.7021	483.88	-0.9055	537.20	0.1023	0.2234	0.2334	0.2764	0.4810	0.1970	0.6330	0.1410	0.7840	0.0963
-0.7051	485.77	-0.9085	541.68	0.1043	0.2111	0.2366	0.2755	0.4840	0.1940	0.6350	0.1430	0.7860	0.0956
-0.7080	492.11	-0.9115	544.04	0.1062	0.2131	0.2398	0.2684	0.4860	0.1950	0.6370	0.1290	0.7880	0.0934
-0.7110	500.68	-0.9145	546.75	0.1081	0.2223	0.2430	0.2621	0.4880	0.1960	0.6390	0.1390	0.7900	0.0936
-0.7140	497.27	-0.9174	551.13	0.1101	0.2108	0.2462	0.2572	0.4900	0.1920	0.6410	0.1460	0.7930	0.0971
-0.7170	492.15	-0.9204	552.72	0.1120	0.2090	0.2494	0.2578	0.4930	0.1950	0.6440	0.1350	0.7950	0.0988
-0.7200	491.08	-0.9234	556.18	0.1139	0.2168	0.2526	0.2534	0.4950	0.1970	0.6460	0.1390	0.7970	0.0925
-0.7230	482.35	-0.9264	567.04	0.1159	0.2191	0.2558	0.2446	0.4970	0.1880	0.6480	0.1410	0.7990	0.0935
-0.7260	475.61	-0.9294	570.54	0.1178	0.2138	0.2590	0.2479	0.4990	0.1940	0.6500	0.1250	0.8010	0.0930
-0.7290	481.86	-0.9324	579.94	0.1198	0.2084	0.2622	0.2543	0.5010	0.1900	0.6530	0.1290	0.8040	0.0918
-0.7320	488.28	-0.9354	583.11	0.1217	0.2007	0.2654	0.2461	0.5040	0.1850	0.6550	0.1330	0.8060	0.0846
-0.7350	476.95	-0.9384	591.48	0.1236	0.2122	0.2686	0.2491	0.5060	0.1830	0.6570	0.1290	0.8080	0.0844
-0.7380	484.52	-0.9414	600.01	0.1256	0.2072	0.2718	0.2478	0.5080	0.1820	0.6590	0.1360	0.8100	0.0861
-0.7409	479.91	-0.9444	607.98	0.1275	0.2015	0.2750	0.2611	0.5100	0.1750	0.6610	0.1300	0.8130	0.0917
-0.7439	481.32	-0.9474	621.29	0.1294	0.2003	0.2782	0.2424	0.5130	0.1710	0.6640	0.1410	0.8150	0.0903
-0.7469	471.14	-0.9504	628.60	0.1314	0.1980	0.2814	0.2434	0.5150	0.1740	0.6660	0.1240	0.8170	0.0848
-0.7499	472.43	-0.9533	631.68	0.1333	0.1974	0.2846	0.2549	0.5170	0.1760	0.6680	0.1270	0.8190	0.0839
-0.7529	477.35	-0.9563	638.33	0.1353	0.2052	0.2878	0.2797	0.5190	0.1700	0.6700	0.1250	0.8210	0.0888
-0.7559	483.01	-0.9593	649.91	0.1372	0.2072	0.2910	0.2704	0.5210	0.1660	0.6730	0.1180	0.8240	0.0952
-0.7589	477.67	-0.9623	655.34	0.1391	0.2045	0.2942	0.2353	0.5240	0.1680	0.6750	0.1190	0.8260	0.0936
-0.7619	463.68	-0.9653	665.92	0.1411	0.2397	0.2974	0.2129	0.5260	0.1640	0.6770	0.1170	0.8280	0.0952
-0.7649	473.48	-0.9683	679.76	0.1430	0.2274	0.3006	0.2200	0.5280	0.1690	0.6790	0.1170	0.8300	0.0966
-0.7679	467.98	-0.9713	683.85	0.1449	0.2358	0.3038	0.3158	0.5300	0.1670	0.6810	0.1140	0.8330	0.0868
-0.7709	464.44	-0.9743	685.27	0.1469	0.2287	0.3069	0.2856	0.5330	0.1620	0.6840	0.1160	0.8350	0.0919
-0.7739	462.49	-0.9773	693.89	0.1488	0.2421	0.3840	0.2090	0.5350	0.1540	0.6860	0.1200	0.8370	0.0953
-0.7768	461.81	-0.9803	705.93	0.1508	0.2841	0.3860	0.2130	0.5370	0.1620	0.6880	0.1260	0.8390	0.0953
-0.7798	462.42	-0.9833	721.34	0.1527	0.2730	0.3880	0.2080	0.5390	0.1550	0.6900	0.1090	0.8410	0.0861
-0.7828	460.83	-0.9863	733.55	0.1546	0.2426	0.3900	0.2160	0.5410	0.1450	0.6930	0.1020	0.8440	0.0813
-0.7858	465.82	-0.9892	769.69	0.1566	0.2258	0.3930	0.2180	0.5440	0.1540	0.6950	0.1170	0.8460	0.0799
-0.7888	460.47	-0.9922	813.62	0.1585	0.2254	0.3950	0.2170	0.5460	0.1530	0.6970	0.1140	0.8480	0.0893
-0.7918	465.04			0.1605	0.2277	0.3970	0.2130	0.5480	0.1520	0.6990	0.1070	0.8500	0.0946
-0.7948	464.84			0.1624	0.2306	0.3990	0.2210	0.5500	0.1550	0.7010	0.1080	0.8530	0.0917
-0.7978	460.65			0.1643	0.2391	0.4010	0.2110	0.5530	0.1450	0.7040	0.1140	0.8550	0.0924
-0.8008	472.99			0.1663	0.2369	0.4040	0.2090	0.5550	0.1500	0.7060	0.1100	0.8570	0.0859
-0.8038	473.14			0.1682	0.2320	0.4060	0.2160	0.5570	0.1410	0.7080	0.1120	0.8590	0.0827
-0.8068	471.75			0.1701	0.2437	0.4080	0.2160	0.5590	0.1430	0.7100	0.1190	0.8610	0.0752
-0.8098	469.95			0.1721	0.2459	0.4100	0.2220	0.5610	0.1410	0.7130	0.1060	0.8640	0.0769
-0.8127	477.37			0.1740	0.2469	0.4130	0.2210	0.5640	0.1470	0.7150	0.1060	0.8660	0.0760
-0.8157	478.39			0.1760	0.2462	0.4150	0.2240	0.5660	0.1380	0.7170	0.1120	0.8680	0.0683
-0.8187	479.42			0.1779	0.2590	0.4170	0.2250	0.5680	0.1370	0.7190	0.1050	0.8700	0.0796
-0.8217	481.20			0.1798	0.2562	0.4190	0.2190	0.5700	0.1410	0.7210	0.1110	0.8730	0.0762
-0.8247	477.17			0.1818	0.2555	0.4210	0.2220	0.5730	0.1420	0.7240	0.1100	0.8750	0.0696
-0.8277	475.89			0.1837	0.2552	0.4240	0.2200	0.5750	0.1450	0.7260	0.1020	0.8770	0.0744
-0.8307	482.67			0.1856	0.2544	0.4260	0.2050	0.5770	0.1400	0.7280	0.1090	0.8790	0.0650
-0.8337	486.80			0.1876	0.2545	0.4280	0.2010	0.5790	0.1440	0.7300	0.1010	0.8810	0.0623
-0.8367	482.42			0.1895	0.2596	0.4300	0.2050	0.5810	0.1430	0.7330	0.1050	0.8840	0.0666
-0.8397	482.77			0.1915	0.2677	0.4330	0.2160	0.5840	0.1460	0.7350	0.1110	0.8860	0.0671
-0.8427	485.95			0.1934	0.2582	0.4350	0.2240	0.5860	0.1430	0.7370	0.1060	0.8880	0.0569
-0.8457	491.04			0.1953	0.2567	0.4370	0.2200	0.5880	0.1430	0.7390	0.1080	0.8900	0.0567
-0.8486	489.90			0.1973	0.2613	0.4390	0.2250	0.5900	0.1390	0.7410	0.1030	0.8930	0.0600
-0.8516	491.02			0.1992	0.2673	0.4410	0.2250	0.5930	0.1420	0.7440	0.1050	0.8950	0.0566
-0.8546	495.08			0.2011	0.2707	0.4440	0.2180	0.5950	0.1350	0.7460	0.1010	0.8970	0.0593
-0.8576	495.09			0.2031	0.2707	0.4460	0.2140	0.5970	0.1470	0.7480	0.1010	0.8990	0.0622
-0.8606	504.64			0.2050	0.2752	0.4480	0.2080	0.5990	0.1460	0.7500	0.1000	0.9010	0.0649
-0.8636	505.52			0.2070	0.2813	0.4500	0.2160	0.6010	0.1350	0.7530	0.0994	0.9040	0.0552

CASE W – η

X/SI η

Appendix 7.2 – Data for Spanwise Averaged Nusselt Number and Film Cooling Effectiveness

0.9060	0.0608	-0.2720	0.1970	-0.5120	0.1040	-0.7230	0.0497	-0.9260	0.0346	0.1158	707.39	0.2557	764.94
0.9080	0.0643	-0.2760	0.1950	-0.5160	0.1030	-0.7260	0.0377	-0.9290	0.0348	0.1178	705.76	0.2589	763.13
0.9100	0.0589	-0.2790	0.1960	-0.5190	0.0982	-0.7290	0.0436	-0.9320	0.0374	0.1197	703.50	0.2621	763.70
0.9130	0.0551	-0.2830	0.2200	-0.5230	0.0859	-0.7320	0.0444	-0.9350	0.0391	0.1216	694.24	0.2653	757.58
0.9150	0.0540	-0.2870	0.2400	-0.5260	0.0926	-0.7350	0.0398	-0.9380	0.0416	0.1236	700.04	0.2685	774.69
0.9170	0.0577	-0.2900	0.2730	-0.5300	0.0827	-0.7380	0.0487	-0.9410	0.0437	0.1255	690.30	0.2717	805.36
0.9190	0.0494	-0.2940	0.2740	-0.5330	0.0866	-0.7410	0.0484	-0.9440	0.0434	0.1275	696.75	0.2749	841.52
0.9210	0.0537	-0.2970	0.2880	-0.5370	0.1040	-0.7440	0.0509	-0.9470	0.0514	0.1294	698.58	0.2781	847.44
0.9240	0.0534	-0.3010	0.2830	-0.5400	0.1030	-0.7470	0.0411	-0.9500	0.0579	0.1313	714.41	0.2813	834.37
0.9260	0.0516	-0.3040	0.2850	-0.5440	0.0985	-0.7500	0.0448	-0.9530	0.0572	0.1333	738.73	0.2845	848.83
0.9280	0.0492	-0.3080	0.2750	-0.5470	0.0900	-0.7530	0.0476	-0.9560	0.0571	0.1352	788.49	0.2877	926.34
0.9300	0.0416	-0.3110	0.2750	-0.5510	0.0937	-0.7560	0.0431	-0.9590	0.0587	0.1371	850.79	0.2909	947.45
0.9330	0.0436	-0.3150	0.2720	-0.5540	0.0935	-0.7590	0.0428	-0.9620	0.0566	0.1391	787.18	0.2941	900.31
0.9350	0.0445	-0.3180	0.2450	-0.5580	0.0991	-0.7620	0.0358	-0.9650	0.0609	0.1410	746.05	0.2973	888.23
0.9370	0.0431	-0.3220	0.2720	-0.5610	0.0974	-0.7650	0.0522	-0.9680	0.0622	0.1430	754.95	0.3005	874.55
0.9390	0.0377	-0.3250	0.2350	-0.5650	0.0992	-0.7680	0.0422	-0.9710	0.0584	0.1449	814.72	0.3037	882.25
0.9410	0.0373	-0.3290	0.2410	-0.5680	0.0963	-0.7710	0.0393	-0.9740	0.0491	0.1468	936.73	0.3069	886.15
0.9440	0.0327	-0.3320	0.2170	-0.5700	0.0993	-0.7740	0.0375	-0.9770	0.0526	0.1488	968.18	0.3836	934.39
0.9460	0.0384	-0.3360	0.2180	-0.5730	0.1010	-0.7770	0.0396	-0.9800	0.0549	0.1507	928.46	0.3859	936.00
0.9480	0.0390	-0.3390	0.2190	-0.5760	0.0965	-0.7800	0.0375	-0.9830	0.0692	0.1526	922.27	0.3881	933.93
0.9500	0.0388	-0.3430	0.2070	-0.5790	0.1110	-0.7830	0.0319	-0.9860	0.0692	0.1546	912.43	0.3903	927.81
0.9530	0.0385	-0.3460	0.2090	-0.5820	0.1100	-0.7860	0.0366	-0.9890	0.0979	0.1565	880.36	0.3925	932.67
0.9550	0.0530	-0.3500	0.1840	-0.5850	0.0999	-0.7890	0.0302	-0.9920	0.1270	0.1585	888.38	0.3947	933.98
0.9570	0.1010	-0.3530	0.1900	-0.5880	0.0982	-0.7920	0.0352			0.1604	878.47	0.3970	937.41
0.9590	0.1540	-0.3570	0.1900	-0.5910	0.0906	-0.7950	0.0339			0.1623	867.11	0.3992	936.49
		-0.3610	0.1750	-0.5940	0.0789	-0.7980	0.0266			0.1643	850.54	0.4014	946.37
		-0.3640	0.1650	-0.5970	0.0893	-0.8010	0.0326			0.1662	847.99	0.4036	952.89
		-0.3680	0.1540	-0.6000	0.0947	-0.8040	0.0317			0.1682	865.69	0.4059	952.53
		-0.3710	0.1620	-0.6030	0.0947	-0.8070	0.0276			0.1701	861.37	0.4081	953.38
		-0.3750	0.1450	-0.6060	0.0958	-0.8100	0.0248			0.1720	840.00	0.4103	960.40
		-0.3780	0.1750	-0.6090	0.0934	-0.8130	0.0360			0.1740	836.66	0.4125	967.88
		-0.3820	0.1540	-0.6120	0.1090	-0.8160	0.0312			0.1759	860.42	0.4147	964.50
		-0.3850	0.1570	-0.6150	0.1070	-0.8190	0.0320			0.1778	851.05	0.4170	964.15
		-0.3890	0.1530	-0.6180	0.0864	-0.8220	0.0333			0.1798	848.51	0.4192	959.95
		-0.3920	0.1340	-0.6210	0.0752	-0.8250	0.0273			0.1817	839.90	0.4214	955.00
		-0.3960	0.1570	-0.6240	0.0736	-0.8280	0.0281			0.1837	843.23	0.4236	961.52
		-0.3990	0.1370	-0.6270	0.0840	-0.8310	0.0336			0.1856	865.18	0.4259	964.14
		-0.4030	0.1490	-0.6300	0.0747	-0.8340	0.0374			0.1875	839.85	0.4281	967.53
		-0.4060	0.1260	-0.6330	0.0904	-0.8370	0.0294			0.1895	824.56	0.4303	968.81
		-0.4100	0.1310	-0.6360	0.0699	-0.8400	0.0314			0.1914	834.62	0.4325	976.42
		-0.4130	0.1400	-0.6390	0.0765	-0.8430	0.0336			0.1933	831.86	0.4347	977.66
		-0.4170	0.1240	-0.6420	0.0899	-0.8460	0.0320			0.1953	850.02	0.4370	974.21
		-0.4200	0.1440	-0.6450	0.0828	-0.8490	0.0269			0.1972	823.68	0.4392	976.29
		-0.4240	0.1350	-0.6480	0.0771	-0.8520	0.0273			0.1992	822.25	0.4414	986.49
		-0.4270	0.1360	-0.6510	0.0656	-0.8550	0.0320			0.2011	834.45	0.4436	985.27
		-0.4310	0.1190	-0.6540	0.0634	-0.8580	0.0323			0.2030	846.32	0.4459	982.81
		-0.4350	0.1220	-0.6570	0.0653	-0.8610	0.0377			0.2050	829.28	0.4481	987.07
		-0.4380	0.1320	-0.6600	0.0654	-0.8640	0.0303			0.2069	835.86	0.4503	982.18
		-0.4420	0.1250	-0.6630	0.0656	-0.8670	0.0302			0.2088	844.14	0.4525	984.77
		-0.4450	0.1350	-0.6660	0.0681	-0.8700	0.0244			0.2108	839.81	0.4547	977.53
		-0.4490	0.1060	-0.6690	0.0569	-0.8730	0.0269			0.2127	812.25	0.4570	974.40
		-0.4520	0.1150	-0.6720	0.0716	-0.8760	0.0280			0.2147	790.05	0.4592	987.54
		-0.4560	0.1040	-0.6750	0.0655	-0.8790	0.0235			0.2166	792.04	0.4614	992.86
		-0.4590	0.1090	-0.6780	0.0653	-0.8820	0.0283			0.2185	789.81	0.4636	982.86
		-0.4630	0.1140	-0.6810	0.0586	-0.8840	0.0327			0.2205	786.19	0.4659	985.31
		-0.4660	0.1230	-0.6840	0.0487	-0.8870	0.0363			0.2224	772.19	0.4681	990.65
		-0.4700	0.1220	-0.6870	0.0528	-0.8900	0.0345			0.2243	773.95	0.4703	999.18
		-0.4730	0.1080	-0.6900	0.0583	-0.8930	0.0259			0.2263	801.26	0.4725	1002.48
		-0.4770	0.1100	-0.6930	0.0511	-0.8960	0.0313			0.2282	784.10	0.4747	999.06
		-0.4800	0.1010	-0.6960	0.0491	-0.8990	0.0238			0.2302	793.70	0.4770	1003.71
		-0.4840	0.1000	-0.6990	0.0463	-0.9020	0.0267			0.2320	760.65	0.4792	1010.82
		-0.4870	0.1060	-0.7020	0.0483	-0.9050	0.0262			0.2334	777.23	0.4814	1001.80
		-0.4910	0.0962	-0.7050	0.0525	-0.9080	0.0279			0.2366	768.07	0.4836	1003.53
		-0.4940	0.1060	-0.7080	0.0540	-0.9110	0.0284			0.2398	758.39	0.4859	1004.03
		-0.4980	0.0909	-0.7110	0.0561	-0.9140	0.0289			0.2430	760.08	0.4881	999.07
		-0.5010	0.1060	-0.7140	0.0603	-0.9170	0.0307			0.2461	742.15	0.4903	1000.09
		-0.5050	0.0933	-0.7170	0.0592	-0.9200	0.0261			0.2493	747.39	0.4925	1001.44
		-0.5090	0.0938	-0.7200	0.0611	-0.9230	0.0258			0.2525	761.84	0.4947	1002.52

Appendix 7.2 – Data for Spanwise Averaged Nusselt Number and Film Cooling Effectiveness

0.4970	1006.55	0.6481	992.33	0.7992	914.73	0.9503	997.31	-0.3359	532.32	-0.5764	477.66	-0.7798	477.45
0.4992	1005.61	0.6503	985.40	0.8014	919.03	0.9525	1007.68	-0.3394	533.82	-0.5794	480.21	-0.7828	463.30
0.5014	1002.39	0.6525	997.93	0.8036	862.43	0.9547	1020.07	-0.3430	538.88	-0.5824	475.56	-0.7858	460.65
0.5036	1004.22	0.6547	971.64	0.8058	871.86	0.9569	1029.13	-0.3465	529.61	-0.5854	477.96	-0.7888	471.98
0.5059	1005.44	0.6570	964.35	0.8081	920.51	0.9592	1051.50	-0.3500	549.21	-0.5884	479.64	-0.7918	458.87
0.5081	1011.41	0.6592	963.72	0.8103	908.68			-0.3535	526.47	-0.5914	485.67	-0.7948	459.16
0.5103	1013.10	0.6614	970.81	0.8125	883.65			-0.3571	545.38	-0.5944	496.70	-0.7978	463.24
0.5125	1014.92	0.6636	966.24	0.8147	856.65	X/PL	Nu	-0.3606	532.74	-0.5974	500.54	-0.8008	470.73
0.5147	1027.90	0.6658	948.32	0.8169	851.69	-0.0103	1245.86	-0.3641	541.77	-0.6003	489.71	-0.8038	471.56
0.5170	1024.09	0.6681	945.75	0.8192	870.65	-0.0188	1175.94	-0.3676	537.09	-0.6033	482.50	-0.8068	481.79
0.5192	1028.91	0.6703	966.02	0.8214	856.29	-0.0274	1104.66	-0.3711	524.25	-0.6063	474.55	-0.8098	478.39
0.5214	1025.40	0.6725	955.63	0.8236	865.09	-0.0359	1082.64	-0.3747	544.65	-0.6093	475.04	-0.8127	474.40
0.5236	1036.70	0.6747	935.27	0.8258	850.87	-0.0445	1029.02	-0.3782	517.93	-0.6123	481.29	-0.8157	472.88
0.5259	1040.22	0.6770	953.58	0.8281	850.53	-0.0530	966.78	-0.3817	542.31	-0.6153	475.01	-0.8187	475.96
0.5281	1037.50	0.6792	967.05	0.8303	880.06	-0.0616	896.17	-0.3852	521.72	-0.6183	489.41	-0.8217	490.10
0.5303	1040.00	0.6814	936.36	0.8325	874.50	-0.0701	825.96	-0.3888	533.36	-0.6213	512.59	-0.8247	489.19
0.5325	1043.41	0.6836	948.47	0.8347	857.89	-0.0787	771.27	-0.3923	522.59	-0.6243	514.03	-0.8277	482.76
0.5347	1047.19	0.6858	964.62	0.8369	834.79	-0.0872	732.16	-0.3958	519.50	-0.6273	509.05	-0.8307	473.83
0.5370	1053.96	0.6881	983.24	0.8392	845.10	-0.0959	692.70	-0.3993	534.87	-0.6303	513.42	-0.8337	477.24
0.5392	1055.71	0.6903	977.11	0.8414	847.19	-0.1044	669.33	-0.4029	505.48	-0.6333	520.18	-0.8367	477.86
0.5414	1047.54	0.6925	914.12	0.8436	833.86	-0.1130	664.33	-0.4064	534.97	-0.6362	504.34	-0.8397	481.06
0.5436	1057.26	0.6947	937.31	0.8458	829.03	-0.1215	620.52	-0.4099	516.39	-0.6392	488.35	-0.8427	481.49
0.5459	1073.97	0.6970	923.75	0.8481	835.46	-0.1301	621.99	-0.4134	529.02	-0.6422	475.04	-0.8457	488.68
0.5481	1062.35	0.6992	926.93	0.8503	850.15	-0.1386	591.18	-0.4170	516.04	-0.6452	482.54	-0.8486	483.82
0.5503	1065.04	0.7014	925.38	0.8525	836.00	-0.1472	595.03	-0.4205	513.74	-0.6482	471.48	-0.8516	497.25
0.5525	1063.51	0.7036	932.39	0.8547	830.67	-0.1557	577.68	-0.4240	530.14	-0.6512	473.42	-0.8546	499.85
0.5547	1071.10	0.7058	922.86	0.8569	845.67	-0.1643	565.32	-0.4275	500.41	-0.6542	492.87	-0.8576	503.68
0.5570	1071.73	0.7081	928.36	0.8592	856.15	-0.1728	575.46	-0.4310	528.83	-0.6572	500.97	-0.8606	496.51
0.5592	1079.17	0.7103	928.72	0.8614	845.18	-0.1814	552.54	-0.4346	508.28	-0.6602	496.11	-0.8636	501.93
0.5614	1077.08	0.7125	908.05	0.8636	860.90	-0.1899	574.78	-0.4381	529.81	-0.6632	492.32	-0.8666	511.62
0.5636	1071.98	0.7147	910.82	0.8658	848.97	-0.1985	553.49	-0.4416	511.92	-0.6662	493.66	-0.8696	520.50
0.5658	1077.42	0.7170	924.48	0.8681	843.62	-0.2020	562.58	-0.4451	514.90	-0.6692	499.84	-0.8726	523.66
0.5681	1075.95	0.7192	934.10	0.8703	845.39	-0.2055	545.06	-0.4487	523.39	-0.6721	513.16	-0.8756	529.06
0.5703	1065.13	0.7214	921.07	0.8725	837.90	-0.2091	541.58	-0.4522	501.64	-0.6751	519.95	-0.8786	524.66
0.5725	1064.55	0.7236	930.53	0.8747	842.09	-0.2126	532.92	-0.4557	526.49	-0.6781	521.35	-0.8816	530.11
0.5747	1077.17	0.7258	955.82	0.8769	847.34	-0.2161	517.54	-0.4592	502.86	-0.6811	525.43	-0.8845	535.43
0.5770	1066.56	0.7281	910.24	0.8792	849.77	-0.2196	536.48	-0.4592	502.86	-0.6811	525.43	-0.8845	535.43
0.5792	1056.52	0.7303	906.33	0.8814	862.00	-0.2232	515.20	-0.4628	517.64	-0.6841	533.42	-0.8875	537.65
0.5814	1051.42	0.7325	882.55	0.8836	842.32	-0.2267	525.40	-0.4663	506.32	-0.6871	523.14	-0.8905	545.05
0.5836	1059.73	0.7347	911.78	0.8858	861.39	-0.2302	518.02	-0.4698	504.55	-0.6901	525.21	-0.8935	550.78
0.5858	1071.98	0.7370	903.47	0.8881	867.06	-0.2337	530.01	-0.4733	506.36	-0.6931	526.42	-0.8965	554.65
0.5881	1056.95	0.7392	905.07	0.8903	887.81	-0.2372	533.79	-0.4769	494.79	-0.6961	521.41	-0.8995	556.27
0.5903	1044.01	0.7414	906.37	0.8925	879.44	-0.2408	528.45	-0.4804	514.07	-0.6991	540.24	-0.9025	559.28
0.5925	1047.83	0.7436	907.92	0.8947	869.80	-0.2443	547.51	-0.4839	493.41	-0.7021	514.48	-0.9055	562.65
0.5947	1044.71	0.7458	911.24	0.8969	868.28	-0.2478	535.04	-0.4874	512.88	-0.7051	497.79	-0.9085	567.15
0.5970	1047.63	0.7481	913.95	0.8992	867.39	-0.2513	558.88	-0.4910	495.30	-0.7080	502.38	-0.9115	571.50
0.5992	1029.91	0.7503	898.15	0.9014	888.64	-0.2549	550.11	-0.4945	504.45	-0.7110	513.49	-0.9145	574.75
0.6014	1022.89	0.7525	918.56	0.9036	895.09	-0.2584	565.93	-0.4980	503.61	-0.7140	506.22	-0.9174	579.11
0.6036	1031.90	0.7547	899.74	0.9058	896.31	-0.2619	572.00	-0.5015	486.29	-0.7170	507.70	-0.9204	586.18
0.6058	1042.43	0.7570	910.33	0.9081	885.46	-0.2654	568.87	-0.5050	500.77	-0.7200	507.33	-0.9234	593.10
0.6081	1023.64	0.7592	919.42	0.9103	866.83	-0.2690	593.88	-0.5086	491.84	-0.7230	503.93	-0.9264	601.28
0.6103	1024.32	0.7614	906.69	0.9125	873.87	-0.2725	578.63	-0.5121	505.91	-0.7260	507.85	-0.9294	606.59
0.6125	1029.87	0.7636	886.09	0.9147	882.87	-0.2760	602.00	-0.5156	488.00	-0.7290	504.85	-0.9324	615.74
0.6147	1025.76	0.7658	935.45	0.9169	884.67	-0.2795	588.79	-0.5191	504.12	-0.7320	501.01	-0.9354	624.80
0.6170	1023.60	0.7681	895.90	0.9192	876.67	-0.2831	598.65	-0.5227	497.78	-0.7350	489.04	-0.9384	633.73
0.6192	1022.22	0.7703	856.82	0.9214	880.56	-0.2866	576.46	-0.5262	491.84	-0.7380	481.53	-0.9414	647.10
0.6214	1023.56	0.7725	882.59	0.9236	896.16	-0.2901	564.59	-0.5305	502.43	-0.7409	486.86	-0.9444	659.17
0.6236	1030.38	0.7747	883.35	0.9258	910.99	-0.2936	565.62	-0.5345	502.36	-0.7439	487.55	-0.9474	668.83
0.6258	1010.19	0.7770	870.87	0.9281	915.60	-0.2971	530.87	-0.5385	492.11	-0.7469	491.04	-0.9504	676.32
0.6281	1013.85	0.7792	872.28	0.9303	925.18	-0.3007	562.37	-0.5425	488.01	-0.7499	489.32	-0.9533	684.63
0.6303	1006.87	0.7814	883.54	0.9325	925.23	-0.3042	582.27	-0.5465	468.56	-0.7529	496.09	-0.9563	693.34
0.6325	1011.57	0.7836	873.42	0.9347	934.94	-0.3077	547.74	-0.5505	480.23	-0.7559	482.35	-0.9593	706.41
0.6347	1009.50	0.7858	865.47	0.9369	950.13	-0.3112	530.72	-0.5545	463.85	-0.7589	484.48	-0.9623	720.65
0.6370	1002.57	0.7881	855.79	0.9392	964.10	-0.3148	534.68	-0.5585	464.59	-0.7619	503.20	-0.9653	733.30
0.6392	999.46	0.7903	898.26	0.9414	971.48	-0.3183	542.36	-0.5615	455.62	-0.7649	484.60	-0.9683	748.58
0.6414	1003.42	0.7925	933.19	0.9436	974.92	-0.3218	521.33	-0.5645	459.42	-0.7679	481.05	-0.9713	761.99
0.6436	988.17	0.7947	874.08	0.9458	980.18	-0.3253	538.13	-0.5674	461.45	-0.7709	468.11	-0.9743	775.20
0.6458	982.85	0.7969	896.41	0.9481	987.99	-0.3289	524.33	-0.5704	460.19	-0.7739	467.28	-0.9773	790.27
						-0.3324	540.76	-0.5734	469.00	-0.7768	479.81	-0.9803	804.05

Appendix 7.2 – Data for Spanwise Averaged Nusselt Number and Film Cooling Effectiveness

-0.9833	819.39	0.1530	0.3120	0.3880	0.2390	0.5390	0.2100	0.6900	0.1020	0.8410	0.0614	-0.1300	0.2450
-0.9863	832.97	0.1550	0.2950	0.3900	0.2410	0.5410	0.1960	0.6930	0.0709	0.8440	0.0579	-0.1390	0.2380
-0.9892	847.04	0.1570	0.2500	0.3930	0.2420	0.5440	0.2050	0.6950	0.0918	0.8460	0.0463	-0.1470	0.2460
-0.9922	863.15	0.1590	0.2760	0.3950	0.2440	0.5460	0.2030	0.6970	0.0828	0.8480	0.0481	-0.1560	0.2400
		0.1600	0.2780	0.3970	0.2400	0.5480	0.1870	0.6990	0.0797	0.8500	0.0586	-0.1640	0.2430
		0.1620	0.2710	0.3990	0.2360	0.5500	0.1870	0.7010	0.0895	0.8530	0.0714	-0.1730	0.2370
		0.1640	0.2550	0.4010	0.2320	0.5530	0.1830	0.7040	0.0915	0.8550	0.0675	-0.1810	0.2360
		0.1660	0.2560	0.4040	0.2320	0.5550	0.1760	0.7060	0.0698	0.8570	0.0756	-0.1900	0.2410
		0.1680	0.2740	0.4060	0.2260	0.5570	0.1650	0.7080	0.0753	0.8590	0.0701	-0.1980	0.2370
		0.1700	0.2660	0.4080	0.2280	0.5590	0.1830	0.7100	0.0780	0.8610	0.0673	-0.2020	0.2440
		0.1720	0.2530	0.4100	0.2240	0.5610	0.1830	0.7130	0.0779	0.8640	0.0825	-0.2050	0.2420
		0.1740	0.2570	0.4130	0.2200	0.5640	0.1790	0.7150	0.0753	0.8660	0.0685	-0.2090	0.2490
		0.1760	0.2640	0.4150	0.2130	0.5660	0.1790	0.7170	0.0794	0.8680	0.0669	-0.2130	0.2290
		0.1780	0.2680	0.4170	0.2210	0.5680	0.1740	0.7190	0.0930	0.8700	0.0698	-0.2160	0.2130
		0.1800	0.2730	0.4190	0.2240	0.5700	0.1780	0.7210	0.0730	0.8730	0.0671	-0.2200	0.2060
		0.1820	0.2630	0.4210	0.2240	0.5730	0.1730	0.7240	0.0728	0.8750	0.0670	-0.2230	0.1910
		0.1840	0.2710	0.4240	0.2190	0.5750	0.1790	0.7260	0.0791	0.8770	0.0594	-0.2270	0.2130
		0.1860	0.2890	0.4260	0.2140	0.5770	0.1710	0.7280	0.0706	0.8790	0.0604	-0.2300	0.2030
		0.1880	0.2750	0.4280	0.2160	0.5790	0.1740	0.7300	0.0790	0.8810	0.0627	-0.2340	0.2330
		0.1900	0.2640	0.4300	0.2130	0.5810	0.1570	0.7330	0.0678	0.8840	0.0594	-0.2370	0.2210
		0.1910	0.2640	0.4330	0.2080	0.5840	0.1510	0.7350	0.0870	0.8860	0.0562	-0.2410	0.2240
		0.1930	0.2590	0.4350	0.2120	0.5860	0.1610	0.7370	0.0703	0.8880	0.0554	-0.2440	0.2170
		0.1950	0.2640	0.4370	0.2080	0.5880	0.1490	0.7390	0.0774	0.8900	0.0604	-0.2480	0.2110
		0.1970	0.2720	0.4390	0.2080	0.5900	0.1360	0.7410	0.0841	0.8930	0.0598	-0.2510	0.2160
		0.1990	0.2500	0.4410	0.2060	0.5930	0.1330	0.7440	0.0921	0.8950	0.0489	-0.2550	0.2020
		0.2010	0.2410	0.4440	0.1920	0.5950	0.1290	0.7460	0.0876	0.8970	0.0454	-0.2580	0.2100
		0.2030	0.2460	0.4460	0.1940	0.5970	0.1270	0.7480	0.0743	0.8990	0.0399	-0.2620	0.2020
		0.2050	0.2360	0.4480	0.1990	0.5990	0.1260	0.7500	0.0860	0.9010	0.0424	-0.2650	0.2040
		0.2070	0.2620	0.4500	0.1980	0.6010	0.1120	0.7530	0.0915	0.9040	0.0378	-0.2690	0.2010
		0.2090	0.2540	0.4530	0.1990	0.6040	0.1150	0.7550	0.0668	0.9060	0.0333	-0.2720	0.2020
		0.2110	0.2700	0.4550	0.2020	0.6060	0.1230	0.7570	0.0748	0.9080	0.0268	-0.2760	0.2050
		0.2130	0.2390	0.4570	0.1970	0.6080	0.1200	0.7590	0.0880	0.9100	0.0088	-0.2790	0.2050
		0.2150	0.2500	0.4590	0.2020	0.6100	0.1260	0.7610	0.0869	0.9130	0.0078	-0.2830	0.2110
		0.2170	0.2380	0.4610	0.2040	0.6130	0.1050	0.7640	0.0819	0.9150	0.0058	-0.2870	0.2080
		0.2190	0.2520	0.4640	0.1920	0.6150	0.1050	0.7660	0.1210	0.9170	0.0059	-0.2900	0.2110
		0.2210	0.2530	0.4660	0.2010	0.6170	0.1120	0.7680	0.1040	0.9190	0.0035	-0.2940	0.1980
		0.2220	0.2460	0.4680	0.1920	0.6190	0.0917	0.7700	0.0753	0.9210	0.0017	-0.2970	0.1590
		0.2240	0.2580	0.4700	0.1910	0.6210	0.0905	0.7730	0.0858	0.9240	0.0050	-0.3010	0.1670
		0.2260	0.2660	0.4730	0.1840	0.6240	0.0982	0.7750	0.0903	0.9260	0.0083	-0.3040	0.1710
		0.2280	0.2610	0.4750	0.1890	0.6260	0.1030	0.7770	0.0805	0.9280	0.0032	-0.3080	0.1770
		0.2300	0.2650	0.4770	0.1870	0.6280	0.1010	0.7790	0.0842	0.9300	0.0064	-0.3110	0.1660
		0.2320	0.2620	0.4790	0.1830	0.6300	0.0878	0.7810	0.0863	0.9330	0.0035	-0.3150	0.1530
		0.2330	0.2840	0.4810	0.1830	0.6330	0.0827	0.7840	0.0740	0.9350	0.0051	-0.3180	0.1910
		0.2370	0.2610	0.4840	0.1920	0.6350	0.0931	0.7860	0.0763	0.9370	0.0051	-0.3220	0.1630
		0.2400	0.2590	0.4860	0.1930	0.6370	0.0786	0.7880	0.0672	0.9390	0.0087	-0.3250	0.1900
		0.2430	0.2530	0.4880	0.1920	0.6390	0.0707	0.7900	0.0806	0.9410	0.0077	-0.3290	0.1840
		0.2460	0.2470	0.4900	0.1870	0.6410	0.0876	0.7930	0.1010	0.9440	0.0054	-0.3320	0.1920
		0.2490	0.2580	0.4930	0.1940	0.6440	0.0823	0.7950	0.0643	0.9460	0.0040	-0.3360	0.1840
		0.2530	0.2600	0.4950	0.1830	0.6460	0.0855	0.7970	0.0794	0.9480	0.0044	-0.3390	0.1880
		0.2560	0.2550	0.4970	0.1980	0.6480	0.0882	0.7990	0.0914	0.9500	0.0072	-0.3430	0.1770
		0.2590	0.2570	0.4990	0.1890	0.6500	0.0670	0.8010	0.1040	0.9530	0.0124	-0.3460	0.1720
		0.2620	0.2560	0.5010	0.1980	0.6530	0.0844	0.8040	0.0759	0.9550	0.0174	-0.3500	0.1760
		0.2650	0.2520	0.5040	0.1900	0.6550	0.0747	0.8060	0.0897	0.9570	0.0224	-0.3530	0.1710
		0.2690	0.2630	0.5060	0.2010	0.6570	0.0683	0.8080	0.0937	0.9590	0.0342	-0.3570	0.1740
		0.2720	0.2670	0.5080	0.2050	0.6590	0.0586	0.8100	0.0773			-0.3610	0.1640
		0.2750	0.2840	0.5100	0.1940	0.6610	0.0602	0.8130	0.0634	X/PL	η	-0.3640	0.1720
		0.2780	0.3110	0.5130	0.2120	0.6640	0.0634	0.8150	0.0683	-0.0274	0.2940	-0.3680	0.1590
		0.2810	0.3530	0.5150	0.2100	0.6660	0.0619	0.8170	0.0588	-0.0359	0.2920	-0.3710	0.1590
		0.2850	0.3560	0.5170	0.2110	0.6680	0.0594	0.8190	0.0589	-0.0445	0.2870	-0.3750	0.1580
		0.2880	0.3360	0.5190	0.2100	0.6700	0.0819	0.8210	0.0469	-0.0530	0.2790	-0.3780	0.1490
		0.2910	0.3050	0.5210	0.2130	0.6730	0.0786	0.8240	0.0555	-0.0616	0.2710	-0.3820	0.1570
		0.2940	0.2780	0.5240	0.2220	0.6750	0.0705	0.8260	0.0405	-0.0701	0.2640	-0.3850	0.1410
		0.2970	0.3040	0.5260	0.2210	0.6770	0.0758	0.8280	0.0419	-0.0787	0.2670	-0.3890	0.1600
		0.3010	0.3090	0.5280	0.2140	0.6790	0.0771	0.8300	0.0501	-0.0872	0.2630	-0.3920	0.1380
		0.3040	0.3120	0.5300	0.2170	0.6810	0.0709	0.8330	0.0599	-0.0958	0.2560	-0.3960	0.1480
		0.3070	0.3200	0.5330	0.2240	0.6840	0.0726	0.8350	0.0520	-0.1040	0.2580	-0.3990	0.1450
		0.3840	0.2350	0.5350	0.2140	0.6860	0.0775	0.8370	0.0500	-0.1130	0.2590	-0.4030	0.1170
		0.3860	0.2350	0.5370	0.2090	0.6880	0.0794	0.8390	0.0525	-0.1210	0.2460	-0.4060	0.1410

Appendix 7.2 – Data for Spanwise Averaged Nusselt Number and Film Cooling Effectiveness

-0.4100	0.1280	-0.6390	0.0811	-0.8430	0.0310	0.0616	1014.17	0.1933	775.28	0.4347	999.30	0.5858	1071.44
-0.4130	0.1400	-0.6420	0.0591	-0.8460	0.0378	0.0636	1008.32	0.1953	768.82	0.4370	998.83	0.5881	1064.43
-0.4170	0.1170	-0.6450	0.0666	-0.8490	0.0342	0.0655	994.04	0.1972	768.79	0.4392	994.31	0.5903	1061.61
-0.4200	0.1210	-0.6480	0.0489	-0.8520	0.0420	0.0674	986.99	0.1992	760.65	0.4414	1000.74	0.5925	1070.04
-0.4240	0.1260	-0.6510	0.0525	-0.8550	0.0439	0.0694	976.64	0.2011	756.26	0.4436	1011.82	0.5947	1066.35
-0.4270	0.1000	-0.6540	0.0698	-0.8580	0.0463	0.0713	970.75	0.2030	753.24	0.4459	999.40	0.5970	1053.81
-0.4310	0.1280	-0.6570	0.0792	-0.8610	0.0403	0.0732	959.13	0.2050	747.19	0.4481	996.41	0.5992	1042.46
-0.4350	0.1130	-0.6600	0.0675	-0.8640	0.0425	0.0752	937.90	0.2069	744.31	0.4503	1003.53	0.6014	1041.37
-0.4380	0.1230	-0.6630	0.0659	-0.8670	0.0490	0.0771	927.62	0.2088	735.18	0.4525	994.53	0.6036	1051.43
-0.4420	0.1080	-0.6660	0.0669	-0.8700	0.0565	0.0791	917.69	0.2108	725.25	0.4547	996.11	0.6058	1040.03
-0.4450	0.1170	-0.6690	0.0736	-0.8730	0.0571	0.0810	906.60	0.2127	718.15	0.4570	991.03	0.6081	1031.47
-0.4490	0.1160	-0.6720	0.0880	-0.8760	0.0633	0.0829	887.51	0.2147	718.65	0.4592	1000.29	0.6103	1039.83
-0.4520	0.1050	-0.6750	0.0931	-0.8790	0.0518	0.0849	871.36	0.2166	712.28	0.4614	998.22	0.6125	1035.14
-0.4560	0.1200	-0.6780	0.0897	-0.8820	0.0508	0.0868	862.48	0.2185	705.48	0.4636	995.23	0.6147	1027.08
-0.4590	0.1030	-0.6810	0.0928	-0.8840	0.0553	0.0888	851.78	0.2205	699.51	0.4659	999.78	0.6170	1028.09
-0.4630	0.1240	-0.6840	0.1050	-0.8870	0.0501	0.0907	841.82	0.2224	702.63	0.4681	1005.00	0.6192	1034.00
-0.4660	0.1080	-0.6870	0.0918	-0.8900	0.0532	0.0926	829.03	0.2243	697.67	0.4703	1008.49	0.6214	1027.36
-0.4700	0.1110	-0.6900	0.0920	-0.8930	0.0549	0.0946	818.07	0.2263	693.63	0.4725	1010.14	0.6236	1023.60
-0.4730	0.1110	-0.6930	0.0920	-0.8960	0.0553	0.0965	808.98	0.2282	688.26	0.4747	1011.35	0.6258	1015.38
-0.4770	0.1120	-0.6960	0.0872	-0.8990	0.0518	0.0984	804.48	0.2302	685.14	0.4770	1006.91	0.6281	1010.53
-0.4800	0.1180	-0.6990	0.1090	-0.9020	0.0421	0.1003	798.06	0.2302	681.84	0.4792	1012.09	0.6303	1026.53
-0.4840	0.1110	-0.7020	0.0909	-0.9050	0.0373	0.1023	786.06	0.2334	686.28	0.4814	1010.19	0.6325	1014.01
-0.4870	0.1290	-0.7050	0.0694	-0.9080	0.0330	0.1042	775.61	0.2366	689.36	0.4836	1008.96	0.6347	1013.41
-0.4910	0.1160	-0.7080	0.0774	-0.9110	0.0310	0.1061	769.69	0.2398	691.55	0.4859	1006.05	0.6370	1003.56
-0.4940	0.1220	-0.7110	0.0919	-0.9140	0.0297	0.1081	761.86	0.2430	696.31	0.4881	1003.46	0.6392	1014.13
-0.4980	0.1250	-0.7140	0.0864	-0.9170	0.0296	0.1100	746.16	0.2461	702.00	0.4903	1005.91	0.6414	1002.52
-0.5010	0.1070	-0.7170	0.0810	-0.9200	0.0343	0.1120	739.45	0.2493	707.43	0.4925	1010.40	0.6436	996.16
-0.5050	0.1220	-0.7200	0.0814	-0.9230	0.0364	0.1139	738.63	0.2525	713.15	0.4947	1013.66	0.6458	992.55
-0.5090	0.1190	-0.7230	0.0753	-0.9260	0.0442	0.1158	740.79	0.2557	718.69	0.4970	1008.45	0.6481	992.64
-0.5120	0.1220	-0.7260	0.0774	-0.9290	0.0461	0.1178	731.90	0.2589	724.90	0.4992	1009.08	0.6503	990.06
-0.5160	0.1140	-0.7290	0.0742	-0.9320	0.0502	0.1197	723.62	0.2621	734.83	0.5014	1012.36	0.6525	982.78
-0.5190	0.1290	-0.7320	0.0662	-0.9350	0.0543	0.1216	718.86	0.2653	751.24	0.5036	1013.27	0.6547	983.83
-0.5230	0.1250	-0.7350	0.0529	-0.9380	0.0606	0.1236	715.41	0.2685	774.48	0.5059	1017.88	0.6570	980.22
-0.5260	0.1110	-0.7380	0.0471	-0.9410	0.0673	0.1255	714.72	0.2717	800.82	0.5081	1012.37	0.6592	981.52
-0.5300	0.1310	-0.7410	0.0480	-0.9440	0.0726	0.1275	720.25	0.2749	797.27	0.5103	1017.88	0.6614	975.87
-0.5330	0.1020	-0.7440	0.0485	-0.9470	0.0750	0.1294	724.75	0.2781	809.67	0.5125	1020.43	0.6636	975.28
-0.5370	0.1170	-0.7470	0.0534	-0.9500	0.0750	0.1313	743.04	0.2813	836.07	0.5147	1029.22	0.6658	966.58
-0.5400	0.0949	-0.7500	0.0601	-0.9530	0.0734	0.1333	779.12	0.2845	880.77	0.5170	1028.91	0.6681	961.87
-0.5440	0.0955	-0.7530	0.0691	-0.9560	0.0695	0.1352	736.10	0.2877	900.49	0.5192	1028.59	0.6703	971.36
-0.5470	0.1040	-0.7560	0.0517	-0.9590	0.0737	0.1371	723.03	0.2909	896.53	0.5214	1030.41	0.6725	961.21
-0.5510	0.0936	-0.7590	0.0531	-0.9620	0.0802	0.1391	724.32	0.2941	897.23	0.5236	1034.08	0.6747	959.35
-0.5540	0.1140	-0.7620	0.0630	-0.9650	0.0826	0.1410	738.35	0.2973	901.02	0.5259	1039.31	0.6770	963.47
-0.5580	0.1030	-0.7650	0.0505	-0.9680	0.0894	0.1430	772.01	0.3005	917.27	0.5281	1040.12	0.6792	958.05
-0.5610	0.1110	-0.7680	0.0483	-0.9710	0.0896	0.1449	803.82	0.3037	931.56	0.5303	1041.40	0.6814	965.74
-0.5650	0.1010	-0.7710	0.0339	-0.9740	0.0919	0.1468	811.18	0.3069	974.07	0.5325	1050.74	0.6836	959.48
-0.5680	0.1040	-0.7740	0.0300	-0.9770	0.0959	0.1488	838.69	0.3836	967.64	0.5347	1051.36	0.6858	968.43
-0.5720	0.0990	-0.7770	0.0441	-0.9800	0.0945	0.1507	838.41	0.3859	968.82	0.5370	1054.11	0.6881	952.24
-0.5750	0.0977	-0.7800	0.0431	-0.9830	0.0960	0.1526	848.47	0.3881	966.92	0.5392	1052.13	0.6903	955.99
-0.5790	0.0892	-0.7830	0.0242	-0.9860	0.0886	0.1546	862.32	0.3903	968.11	0.5414	1055.70	0.6925	949.16
-0.5820	0.0834	-0.7860	0.0216	-0.9890	0.0917	0.1565	860.76	0.3925	972.91	0.5436	1058.29	0.6947	946.70
-0.5850	0.0871	-0.7890	0.0294	-0.9920	0.0930	0.1585	860.30	0.3947	972.43	0.5459	1067.95	0.6970	940.51
-0.5880	0.0890	-0.7920	0.0200			0.1604	846.55	0.3970	982.64	0.5481	1073.85	0.6992	932.12
-0.5910	0.1010	-0.7950	0.0204			0.1623	852.34	0.3992	994.48	0.5503	1070.13	0.7014	928.15
-0.5940	0.1120	-0.7980	0.0276			0.1643	848.46	0.4014	995.54	0.5525	1076.95	0.7036	919.58
-0.5970	0.1040	-0.8010	0.0348			0.1662	848.93	0.4036	997.26	0.5547	1084.49	0.7058	930.95
-0.6000	0.0942	-0.8040	0.0352			0.1682	836.05	0.4059	992.78	0.5570	1084.78	0.7081	937.11
-0.6030	0.0882	-0.8070	0.0450			0.1701	826.98	0.4081	995.41	0.5592	1080.11	0.7103	929.97
-0.6060	0.0712	-0.8100	0.0381			0.1720	822.47	0.4103	998.66	0.5614	1077.63	0.7125	925.94
-0.6090	0.0721	-0.8130	0.0334			0.1740	820.85	0.4125	1002.95	0.5636	1089.58	0.7147	922.77
-0.6120	0.0694	-0.8160	0.0293			0.1759	816.90	0.4147	1006.93	0.5658	1085.40	0.7170	926.77
-0.6150	0.0592	-0.8190	0.0329			0.1778	815.70	0.4170	999.54	0.5681	1082.37	0.7192	925.48
-0.6180	0.0775	-0.8220	0.0441			0.1798	808.74	0.4192	993.83	0.5703	1081.18	0.7214	932.12
-0.6210	0.1070	-0.8250	0.0371			0.1817	801.04	0.4214	994.74	0.5725	1098.88	0.7236	949.42
-0.6240	0.1070	-0.8280	0.0337			0.1837	797.73	0.4236	998.42	0.5747	1093.61	0.7258	934.21
-0.6270	0.1060	-0.8310	0.0246			0.1856	792.79	0.4259	998.04	0.5770	1085.75	0.7281	924.82
-0.6300	0.1160	-0.8340	0.0282			0.1875	783.27	0.4281	997.22	0.5792	1083.20	0.7303	912.20
-0.6330	0.1230	-0.8370	0.0314			0.1895	782.78	0.4303	993.60	0.5814	1073.79	0.7325	913.29
-0.6360	0.1080	-0.8400	0.0320			0.1914	782.39	0.4325	998.54	0.5836	1087.23	0.7347	916.76

CASE Y – Nu

X/SL Nu

0.0384	1037.12	0.1701	826.98	0.4081	995.41	0.5592	1080.11	0.7103	929.97
0.0403	1035.96	0.1720	822.47	0.4103	998.66	0.5614	1077.63	0.7125	925.94
0.0422	1034.85	0.1740	820.85	0.4125	1002.95	0.5636	1089.58	0.7147	922.77
0.0442	1033.95	0.1759	816.90	0.4147	1006.93	0.5658	1085.40	0.7170	926.77
0.0461	1032.93	0.1778	815.70	0.4170	999.54	0.5681	1082.37	0.7192	925.48
0.0481	1032.00	0.1798	808.74	0.4192	993.83	0.5703	1081.18	0.7214	932.12
0.0500	1031.34	0.1817	801.04	0.4214	994.74	0.5725	1098.88	0.7236	949.42
0.0519	1030.66	0.1837	797.73	0.4236	998.42	0.5747	1093.61	0.7258	934.21
0.0539	1030.29	0.1856	792.79	0.4259	998.04	0.5770	1085.75	0.7281	924.82
0.0558	1027.33	0.1875	783.27	0.4281	997.22	0.5792	1083.20	0.7303	912.20
0.0577	1021.74	0.1895	782.78	0.4303	993.60	0.5814	1073.79	0.7325	913.29
0.0597	1017.54	0.1914	782.39	0.4325	998.54	0.5836	1087.23	0.7347	916.76

Appendix 7.2 – Data for Spanwise Averaged Nusselt Number and Film Cooling Effectiveness

0.7370	923.44	0.8881	937.89	-0.2372	516.73	-0.4657	543.01	-0.6692	569.45	-0.8726	571.48	0.0771	0.3370
0.7392	907.24	0.8903	942.78	-0.2408	504.83	-0.4687	532.66	-0.6721	569.79	-0.8756	575.50	0.0791	0.3240
0.7414	912.76	0.8925	937.71	-0.2443	535.96	-0.4717	530.93	-0.6751	570.41	-0.8786	576.14	0.0810	0.3120
0.7436	909.25	0.8947	938.08	-0.2478	524.92	-0.4747	541.79	-0.6781	573.96	-0.8816	584.41	0.0829	0.2910
0.7458	915.04	0.8969	943.74	-0.2513	552.50	-0.4777	534.76	-0.6811	569.93	-0.8845	584.82	0.0849	0.2750
0.7481	911.81	0.8992	949.53	-0.2549	550.76	-0.4807	540.11	-0.6841	560.52	-0.8875	586.79	0.0868	0.2660
0.7503	904.41	0.9014	965.51	-0.2584	565.49	-0.4837	534.34	-0.6871	565.93	-0.8905	590.71	0.0888	0.2520
0.7525	911.08	0.9036	972.74	-0.2619	581.98	-0.4867	524.83	-0.6901	552.61	-0.8935	600.76	0.0907	0.2420
0.7547	918.47	0.9058	974.25	-0.2654	577.06	-0.4897	520.24	-0.6931	553.35	-0.8965	602.37	0.0926	0.2330
0.7570	917.13	0.9081	965.64	-0.2690	604.89	-0.4927	510.65	-0.6961	558.38	-0.8995	608.13	0.0946	0.2270
0.7592	919.45	0.9103	967.22	-0.2725	596.15	-0.4956	504.26	-0.6991	567.16	-0.9025	610.54	0.0965	0.2220
0.7614	906.03	0.9125	983.76	-0.2760	624.90	-0.4986	502.17	-0.7021	555.11	-0.9055	619.09	0.0984	0.2180
0.7636	890.92	0.9147	995.24	-0.2795	612.93	-0.5016	499.05	-0.7051	553.61	-0.9085	611.66	0.1000	0.2140
0.7658	887.39	0.9169	1001.32	-0.2831	620.11	-0.5046	496.05	-0.7080	565.18	-0.9115	611.26	0.1020	0.2050
0.7681	890.22	0.9192	999.67	-0.2866	611.18	-0.5076	511.48	-0.7110	574.88	-0.9145	623.36	0.1040	0.1980
0.7703	898.50	0.9214	1007.82	-0.2901	602.15	-0.5106	515.79	-0.7140	573.10	-0.9174	629.40	0.1060	0.1870
0.7725	898.02	0.9236	1027.55	-0.2936	609.85	-0.5136	531.90	-0.7170	565.73	-0.9204	632.13	0.1080	0.1880
0.7747	897.40	0.9258	1040.26	-0.2971	572.47	-0.5166	531.97	-0.7200	566.65	-0.9234	631.67	0.1100	0.2200
0.7770	885.35	0.9281	1049.69	-0.3007	610.28	-0.5196	527.15	-0.7230	569.41	-0.9264	632.80	0.1120	0.2280
0.7792	890.47	0.9303	1057.64	-0.3042	607.44	-0.5226	529.26	-0.7260	577.40	-0.9294	640.47	0.1140	0.2090
0.7814	901.60	0.9325	1069.80	-0.3077	611.40	-0.5256	528.27	-0.7290	580.59	-0.9324	646.57	0.1160	0.1830
0.7836	902.03	0.9347	1085.05	-0.3112	588.29	-0.5286	529.72	-0.7320	566.91	-0.9354	658.34	0.1180	0.1790
0.7858	890.21	0.9369	1097.82	-0.3148	579.19	-0.5315	522.42	-0.7350	550.32	-0.9384	663.42	0.1200	0.1930
0.7881	894.13	0.9392	1111.14	-0.3183	595.99	-0.5345	526.47	-0.7380	545.89	-0.9414	668.57	0.1220	0.1910
0.7903	901.05	0.9414	1118.67	-0.3218	568.60	-0.5375	526.46	-0.7409	551.54	-0.9444	677.92	0.1240	0.1920
0.7925	895.96	0.9436	1124.81	-0.3253	578.55	-0.5405	526.94	-0.7439	556.81	-0.9474	684.33	0.1260	0.1780
0.7947	898.33	0.9458	1142.93	-0.3289	561.88	-0.5435	535.15	-0.7469	557.27	-0.9504	693.75	0.1280	0.1940
0.7969	888.33	0.9481	1150.72	-0.3324	581.97	-0.5465	533.52	-0.7499	559.63	-0.9533	700.13	0.1290	0.2070
0.7992	902.04	0.9503	1180.77	-0.3359	567.96	-0.5495	535.89	-0.7529	564.77	-0.9563	706.99	0.1310	0.2050
0.8014	878.91	0.9525	1184.18	-0.3394	549.09	-0.5525	532.68	-0.7559	553.37	-0.9593	714.44	0.1330	0.2370
0.8036	872.46	0.9547	1201.87	-0.3430	576.63	-0.5555	532.95	-0.7589	545.71	-0.9623	726.91	0.1350	0.2050
0.8058	885.32	0.9569	1223.53	-0.3465	532.25	-0.5585	540.70	-0.7619	546.67	-0.9653	734.55	0.1370	0.2480
0.8081	895.69	0.9592	1260.60	-0.3500	583.19	-0.5615	536.40	-0.7649	550.39	-0.9683	742.13	0.1390	0.2610
0.8103	890.63			-0.3535	558.50	-0.5645	541.58	-0.7679	545.28	-0.9713	751.73	0.1410	0.2440
0.8125	864.58	X/PL	Nu	-0.3571	577.18	-0.5674	538.11	-0.7709	544.53	-0.9743	763.75	0.1430	0.2280
0.8147	876.01	-0.0103	1324.68	-0.3606	556.10	-0.5704	527.99	-0.7739	545.29	-0.9773	778.02	0.1450	0.2130
0.8169	865.78	-0.0188	1235.82	-0.3641	575.30	-0.5734	533.95	-0.7768	547.21	-0.9803	792.91	0.1470	0.1890
0.8192	872.82	-0.0274	1183.59	-0.3676	573.39	-0.5764	530.51	-0.7798	544.93	-0.9833	806.42	0.1490	0.2220
0.8214	878.42	-0.0359	1121.91	-0.3711	522.56	-0.5794	528.24	-0.7828	535.63	-0.9863	826.46	0.1510	0.2260
0.8236	881.28	-0.0445	985.40	-0.3747	562.77	-0.5824	542.38	-0.7858	534.55	-0.9892	843.63	0.1530	0.2160
0.8258	879.88	-0.0530	890.33	-0.3782	497.85	-0.5854	538.89	-0.7888	534.51	-0.9922	873.31	0.1550	0.2200
0.8281	880.48	-0.0616	830.06	-0.3817	540.02	-0.5884	536.19	-0.7918	535.15	-0.9892	584.83	0.1570	0.2280
0.8303	876.78	-0.0701	771.90	-0.3852	522.05	-0.5914	549.10	-0.7948	532.11	-0.9922	591.27	0.1590	0.2350
0.8325	872.26	-0.0787	739.69	-0.3888	529.26	-0.5944	536.98	-0.7978	530.20			0.1600	0.2350
0.8347	858.50	-0.0872	694.57	-0.3923	529.93	-0.5974	543.23	-0.8008	533.97			0.1620	0.2460
0.8369	849.28	-0.0959	693.57	-0.3969	510.44	-0.6003	533.51	-0.8038	534.70	CASE Y-η		0.1640	0.2490
0.8392	849.47	-0.1044	661.62	-0.3999	533.04	-0.6033	535.49	-0.8068	542.23	X/SL	η	0.1660	0.2410
0.8414	841.39	-0.1130	655.22	-0.4029	561.95	-0.6063	547.62	-0.8098	559.72	0.0384	0.6270	0.1680	0.2430
0.8436	829.89	-0.1215	622.43	-0.4059	559.17	-0.6093	540.71	-0.8127	563.24	0.0403	0.6090	0.1700	0.2410
0.8458	845.11	-0.1301	628.51	-0.4089	568.55	-0.6123	554.96	-0.8157	550.13	0.0422	0.5710	0.1720	0.2300
0.8481	859.48	-0.1386	599.39	-0.4119	567.60	-0.6153	548.87	-0.8187	556.01	0.0442	0.5260	0.1740	0.2370
0.8503	862.42	-0.1472	601.35	-0.4149	584.83	-0.6183	557.61	-0.8217	552.20	0.0461	0.4990	0.1760	0.2380
0.8525	855.10	-0.1557	582.73	-0.4179	581.55	-0.6213	563.16	-0.8247	556.92	0.0481	0.4780	0.1780	0.2490
0.8547	861.26	-0.1643	563.91	-0.4209	583.04	-0.6243	546.92	-0.8277	551.81	0.0500	0.4600	0.1800	0.2500
0.8569	877.05	-0.1728	582.52	-0.4238	562.44	-0.6273	543.91	-0.8307	563.46	0.0519	0.4540	0.1820	0.2540
0.8592	873.09	-0.1814	564.27	-0.4268	560.12	-0.6303	547.79	-0.8337	550.00	0.0539	0.4510	0.1840	0.2370
0.8614	885.03	-0.1899	570.07	-0.4298	574.70	-0.6333	554.52	-0.8367	547.39	0.0558	0.4430	0.1860	0.2400
0.8636	887.00	-0.1985	558.56	-0.4328	566.43	-0.6362	555.92	-0.8397	547.60	0.0577	0.4370	0.1880	0.2420
0.8658	902.83	-0.2020	563.69	-0.4358	573.31	-0.6392	550.82	-0.8427	561.32	0.0597	0.4320	0.1900	0.2360
0.8681	906.74	-0.2055	548.73	-0.4388	578.81	-0.6422	557.88	-0.8457	557.85	0.0616	0.4260	0.1930	0.2360
0.8703	903.60	-0.2091	541.68	-0.4418	571.64	-0.6452	565.46	-0.8486	559.21	0.0636	0.4190	0.1950	0.2360
0.8725	906.94	-0.2126	517.84	-0.4448	560.68	-0.6482	551.47	-0.8516	566.66	0.0655	0.4060	0.1970	0.2290
0.8747	912.70	-0.2161	494.12	-0.4478	562.04	-0.6512	556.44	-0.8546	571.48	0.0674	0.3980	0.1990	0.2240
0.8769	913.91	-0.2196	513.73	-0.4508	553.73	-0.6542	549.88	-0.8576	568.42	0.0694	0.3870	0.2010	0.2250
0.8792	914.26	-0.2232	485.03	-0.4538	546.83	-0.6572	550.76	-0.8606	590.29	0.0713	0.3790	0.2030	0.2200
0.8814	909.73	-0.2267	507.30	-0.4568	548.48	-0.6602	564.81	-0.8636	587.03	0.0732	0.3680	0.2050	0.2210
0.8836	914.10	-0.2302	489.09	-0.4597	554.60	-0.6632	564.74	-0.8666	587.06	0.0752	0.3480	0.2070	0.2220
0.8858	930.03	-0.2337	507.54	-0.4627	547.51	-0.6662	571.54	-0.8696	574.57				

Appendix 7.2 – Data for Spanwise Averaged Nusselt Number and Film Cooling Effectiveness

0.2090	0.2110	0.4530	0.2130	0.6040	0.1490	0.7550	0.0869	0.9060	0.0335	-0.2720	0.3170	-0.4960	0.0834
0.2110	0.1980	0.4550	0.2190	0.6060	0.1520	0.7570	0.0900	0.9080	0.0294	-0.2760	0.3210	-0.4990	0.0826
0.2130	0.2090	0.4570	0.2130	0.6080	0.1490	0.7590	0.0901	0.9100	0.0245	-0.2790	0.3290	-0.5020	0.0739
0.2150	0.2120	0.4590	0.2170	0.6100	0.1550	0.7610	0.0878	0.9130	0.0284	-0.2830	0.3390	-0.5050	0.0707
0.2170	0.2060	0.4610	0.2140	0.6130	0.1530	0.7640	0.0858	0.9150	0.0303	-0.2870	0.3110	-0.5080	0.0831
0.2190	0.2100	0.4640	0.2110	0.6150	0.1480	0.7660	0.0785	0.9170	0.0308	-0.2900	0.2630	-0.5110	0.0881
0.2210	0.2070	0.4660	0.2060	0.6170	0.1520	0.7680	0.0772	0.9190	0.0265	-0.2940	0.2520	-0.5140	0.1010
0.2220	0.2120	0.4680	0.2080	0.6190	0.1560	0.7700	0.0861	0.9210	0.0230	-0.2970	0.2190	-0.5170	0.1040
0.2240	0.2020	0.4700	0.2070	0.6210	0.1490	0.7730	0.0800	0.9240	0.0251	-0.3010	0.2410	-0.5200	0.0969
0.2260	0.2080	0.4730	0.2070	0.6240	0.1520	0.7750	0.0944	0.9260	0.0259	-0.3040	0.2520	-0.5230	0.0985
0.2280	0.1980	0.4750	0.2050	0.6260	0.1520	0.7770	0.0859	0.9280	0.0267	-0.3080	0.2610	-0.5260	0.0975
0.2300	0.2040	0.4770	0.1970	0.6280	0.1410	0.7790	0.0823	0.9300	0.0238	-0.3110	0.2470	-0.5290	0.0991
0.2300	0.1980	0.4790	0.2030	0.6300	0.1540	0.7810	0.0794	0.9330	0.0267	-0.3150	0.2180	-0.5310	0.0945
0.2330	0.2020	0.4810	0.2050	0.6330	0.1450	0.7840	0.0832	0.9350	0.0252	-0.3180	0.2350	-0.5340	0.0967
0.2370	0.2090	0.4840	0.2050	0.6350	0.1480	0.7860	0.0768	0.9370	0.0172	-0.3220	0.2260	-0.5370	0.0976
0.2400	0.2230	0.4860	0.2030	0.6370	0.1380	0.7880	0.0735	0.9390	0.0217	-0.3250	0.2340	-0.5400	0.0953
0.2430	0.2350	0.4880	0.2030	0.6390	0.1450	0.7900	0.0682	0.9410	0.0198	-0.3290	0.1930	-0.5430	0.0984
0.2460	0.2310	0.4900	0.2020	0.6410	0.1420	0.7930	0.0720	0.9440	0.0200	-0.3320	0.2210	-0.5460	0.0966
0.2490	0.2470	0.4930	0.2000	0.6440	0.1450	0.7950	0.0785	0.9460	0.0253	-0.3360	0.2030	-0.5490	0.0974
0.2530	0.2440	0.4950	0.1980	0.6460	0.1360	0.7970	0.0780	0.9480	0.0250	-0.3390	0.1950	-0.5520	0.0937
0.2560	0.2570	0.4970	0.1950	0.6480	0.1410	0.7990	0.0795	0.9500	0.0224	-0.3430	0.2460	-0.5550	0.0928
0.2590	0.2770	0.4990	0.1920	0.6500	0.1340	0.8010	0.0775	0.9530	0.0190	-0.3460	0.1900	-0.5580	0.0969
0.2620	0.2880	0.5010	0.1950	0.6530	0.1320	0.8040	0.0789	0.9550	0.0251	-0.3500	0.2910	-0.5610	0.0928
0.2650	0.2990	0.5040	0.1920	0.6550	0.1360	0.8060	0.0830	0.9570	0.0214	-0.3530	0.2050	-0.5640	0.1010
0.2690	0.2960	0.5060	0.1970	0.6570	0.1260	0.8080	0.0843	0.9590	0.0285	-0.3570	0.2560	-0.5670	0.0968
0.2720	0.3150	0.5080	0.1880	0.6590	0.1180	0.8100	0.0833			-0.3610	0.2300	-0.5700	0.0896
0.2750	0.3620	0.5100	0.1900	0.6610	0.1170	0.8130	0.0732	X/PL	η	-0.3640	0.2520	-0.5730	0.0927
0.2780	0.4100	0.5130	0.1910	0.6640	0.1240	0.8150	0.0849	-0.0274	0.3630	-0.3680	0.2540	-0.5760	0.0945
0.2810	0.4120	0.5150	0.1900	0.6660	0.1200	0.8170	0.0803	-0.0359	0.3620	-0.3710	0.1910	-0.5790	0.0928
0.2850	0.3740	0.5170	0.1850	0.6680	0.1220	0.8190	0.0771	-0.0445	0.3660	-0.3750	0.2510	-0.5820	0.1010
0.2880	0.3480	0.5190	0.1880	0.6700	0.1260	0.8210	0.0969	-0.0530	0.3850	-0.3780	0.1530	-0.5850	0.0996
0.2910	0.3160	0.5210	0.1830	0.6730	0.1180	0.8240	0.1000	-0.0616	0.3800	-0.3820	0.2070	-0.5880	0.0939
0.2940	0.3270	0.5240	0.1870	0.6750	0.1110	0.8260	0.1000	-0.0701	0.3530	-0.3850	0.1640	-0.5910	0.1010
0.2970	0.3330	0.5260	0.1820	0.6770	0.1160	0.8280	0.0941	-0.0787	0.3650	-0.3890	0.1780	-0.5940	0.0885
0.3010	0.3200	0.5280	0.1850	0.6790	0.1090	0.8300	0.0954	-0.0872	0.3250	-0.3920	0.1870	-0.5970	0.0911
0.3040	0.2990	0.5300	0.1820	0.6810	0.1180	0.8330	0.1010	-0.0958	0.3180	-0.3970	0.2040	-0.6000	0.0821
0.3070	0.2760	0.5330	0.1830	0.6840	0.1130	0.8350	0.0930	-0.1040	0.2950	-0.4000	0.2190	-0.6030	0.0849
0.3840	0.2400	0.5350	0.1750	0.6860	0.1140	0.8370	0.0869	-0.1130	0.2930	-0.4030	0.2240	-0.6060	0.0891
0.3860	0.2410	0.5370	0.1740	0.6880	0.1090	0.8390	0.0772	-0.1210	0.2750	-0.4060	0.2010	-0.6090	0.0839
0.3880	0.2370	0.5390	0.1760	0.6900	0.1110	0.8410	0.0716	-0.1300	0.2740	-0.4090	0.1580	-0.6120	0.0975
0.3900	0.2400	0.5410	0.1780	0.6930	0.1200	0.8440	0.0577	-0.1390	0.2610	-0.4120	0.1230	-0.6150	0.0936
0.3930	0.2410	0.5440	0.1660	0.6950	0.1200	0.8460	0.0576	-0.1470	0.2740	-0.4150	0.1150	-0.6180	0.0997
0.3950	0.2380	0.5460	0.1620	0.6970	0.1110	0.8480	0.0588	-0.1560	0.2650	-0.4180	0.1180	-0.6210	0.0993
0.3970	0.2380	0.5480	0.1670	0.6990	0.1070	0.8500	0.0632	-0.1640	0.2600	-0.4210	0.1320	-0.6240	0.0884
0.3990	0.2370	0.5500	0.1700	0.7010	0.1040	0.8530	0.0583	-0.1730	0.2710	-0.4240	0.1160	-0.6270	0.0862
0.4010	0.2280	0.5530	0.1630	0.7040	0.0941	0.8550	0.0581	-0.1810	0.2810	-0.4270	0.1180	-0.6300	0.0903
0.4040	0.2360	0.5550	0.1630	0.7060	0.1030	0.8570	0.0526	-0.1900	0.2750	-0.4300	0.1330	-0.6330	0.0939
0.4060	0.2370	0.5570	0.1610	0.7080	0.1030	0.8590	0.0479	-0.1980	0.2850	-0.4330	0.1320	-0.6360	0.0906
0.4080	0.2310	0.5590	0.1680	0.7100	0.0990	0.8610	0.0557	-0.2020	0.2990	-0.4360	0.1380	-0.6390	0.0843
0.4100	0.2260	0.5610	0.1660	0.7130	0.0979	0.8640	0.0543	-0.2050	0.2930	-0.4390	0.1580	-0.6420	0.0857
0.4130	0.2250	0.5640	0.1590	0.7150	0.0978	0.8660	0.0577	-0.2090	0.3060	-0.4420	0.1460	-0.6450	0.0910
0.4150	0.2300	0.5660	0.1590	0.7170	0.1020	0.8680	0.0510	-0.2130	0.2780	-0.4450	0.1410	-0.6480	0.0838
0.4170	0.2270	0.5680	0.1600	0.7190	0.1050	0.8700	0.0444	-0.2160	0.2230	-0.4480	0.1430	-0.6510	0.0833
0.4190	0.2240	0.5700	0.1580	0.7210	0.0960	0.8730	0.0410	-0.2200	0.2350	-0.4510	0.1340	-0.6540	0.0785
0.4210	0.2300	0.5730	0.1580	0.7240	0.1000	0.8750	0.0467	-0.2230	0.2240	-0.4540	0.1270	-0.6570	0.0777
0.4240	0.2290	0.5750	0.1620	0.7260	0.0949	0.8770	0.0423	-0.2270	0.2180	-0.4570	0.1320	-0.6600	0.0893
0.4260	0.2300	0.5770	0.1590	0.7280	0.0895	0.8790	0.0418	-0.2300	0.2210	-0.4600	0.1230	-0.6630	0.0875
0.4280	0.2300	0.5790	0.1550	0.7300	0.0947	0.8810	0.0362	-0.2340	0.2280	-0.4630	0.1170	-0.6660	0.0938
0.4300	0.2220	0.5810	0.1470	0.7330	0.0911	0.8840	0.0361	-0.2370	0.2460	-0.4660	0.1080	-0.6690	0.0917
0.4330	0.2240	0.5840	0.1590	0.7350	0.0850	0.8860	0.0389	-0.2410	0.2550	-0.4690	0.1050	-0.6720	0.0929
0.4350	0.2270	0.5860	0.1520	0.7370	0.0997	0.8880	0.0339	-0.2440	0.2930	-0.4720	0.0962	-0.6750	0.0950
0.4370	0.2310	0.5880	0.1490	0.7390	0.0913	0.8900	0.0395	-0.2480	0.2860	-0.4750	0.1110	-0.6780	0.0954
0.4390	0.2180	0.5900	0.1500	0.7410	0.0952	0.8930	0.0341	-0.2510	0.3030	-0.4780	0.0989	-0.6810	0.0889
0.4410	0.2190	0.5930	0.1530	0.7440	0.0942	0.8950	0.0369	-0.2550	0.3000	-0.4810	0.1150	-0.6840	0.0802
0.4440	0.2240	0.5950	0.1580	0.7460	0.0958	0.8970	0.0344	-0.2580	0.3120	-0.4840	0.1100	-0.6870	0.0826
0.4460	0.2180	0.5970	0.1510	0.7480	0.0913	0.8990	0.0309	-0.2620	0.3050	-0.4870	0.1040	-0.6900	0.0765
0.4480	0.2170	0.5990	0.1450	0.7500	0.0911	0.9010	0.0363	-0.2650	0.3120	-0.4900	0.1020	-0.6930	0.0798
0.4500	0.2200	0.6010	0.1450	0.7530	0.0900	0.9040	0.0339	-0.2690	0.3120	-0.4930	0.0885	-0.6960	0.0816

Appendix 7.2 – Data for Spanwise Averaged Nusselt Number and Film Cooling Effectiveness

-0.6990	0.0834	-0.9020	0.0528	0.1004	757.96	0.2302	730.03	0.4792	1016.71	0.6303	1047.08	0.7814	925.82
-0.7020	0.0769	-0.9050	0.0525	0.1023	753.91	0.2334	734.81	0.4815	1012.12	0.6326	1038.08	0.7837	919.84
-0.7050	0.0727	-0.9080	0.0515	0.1043	750.67	0.2366	736.82	0.4837	1010.87	0.6348	1026.05	0.7859	921.01
-0.7080	0.0833	-0.9110	0.0526	0.1062	740.70	0.2398	732.50	0.4859	1002.77	0.6370	1027.63	0.7881	919.23
-0.7110	0.0860	-0.9140	0.0544	0.1081	742.80	0.2430	731.55	0.4881	1009.21	0.6392	1086.49	0.7903	929.58
-0.7140	0.0825	-0.9170	0.0559	0.1101	709.86	0.2462	734.55	0.4903	1007.53	0.6415	1054.29	0.7926	928.73
-0.7170	0.0793	-0.9200	0.0535	0.1120	688.26	0.2494	744.08	0.4926	1010.72	0.6437	1046.26	0.7948	924.61
-0.7200	0.0764	-0.9230	0.0480	0.1139	699.54	0.2526	759.30	0.4948	1012.90	0.6459	1020.95	0.7970	930.06
-0.7230	0.0801	-0.9260	0.0451	0.1159	720.79	0.2558	748.40	0.4970	1006.94	0.6481	1015.39	0.7992	923.74
-0.7260	0.0783	-0.9290	0.0462	0.1178	721.23	0.2590	752.95	0.4992	1003.95	0.6503	1023.01	0.8014	905.96
-0.7290	0.0790	-0.9320	0.0460	0.1198	707.12	0.2622	765.19	0.5015	1012.07	0.6526	1019.07	0.8037	906.32
-0.7320	0.0680	-0.9350	0.0531	0.1217	694.90	0.2654	784.25	0.5037	1007.85	0.6548	1035.50	0.8059	913.49
-0.7350	0.0572	-0.9380	0.0529	0.1236	698.23	0.2686	811.91	0.5059	1011.94	0.6570	1031.30	0.8081	936.56
-0.7380	0.0536	-0.9410	0.0519	0.1256	707.79	0.2718	852.92	0.5081	1008.66	0.6592	1026.41	0.8103	933.26
-0.7410	0.0552	-0.9440	0.0550	0.1275	714.03	0.2750	862.25	0.5103	1014.81	0.6615	1011.95	0.8126	900.85
-0.7440	0.0584	-0.9470	0.0542	0.1294	715.37	0.2782	827.93	0.5126	1022.43	0.6637	1005.06	0.8148	897.46
-0.7470	0.0588	-0.9500	0.0570	0.1314	752.29	0.2814	865.79	0.5148	1027.38	0.6659	1012.70	0.8170	905.36
-0.7500	0.0593	-0.9530	0.0561	0.1333	843.61	0.2846	980.77	0.5170	1029.51	0.6681	999.56	0.8192	914.97
-0.7530	0.0549	-0.9560	0.0579	0.1353	875.80	0.2878	961.95	0.5192	1029.03	0.6703	1000.33	0.8214	915.31
-0.7560	0.0482	-0.9590	0.0610	0.1372	778.78	0.2910	967.00	0.5215	1025.33	0.6726	991.07	0.8237	920.13
-0.7590	0.0434	-0.9620	0.0633	0.1391	758.63	0.2942	946.64	0.5237	1023.43	0.6748	1001.33	0.8259	924.05
-0.7620	0.0451	-0.9650	0.0604	0.1411	816.96	0.2974	983.45	0.5259	1022.58	0.6770	1000.79	0.8281	927.82
-0.7650	0.0505	-0.9680	0.0565	0.1430	894.53	0.3006	950.00	0.5281	1025.07	0.6792	1005.68	0.8303	935.19
-0.7680	0.0442	-0.9710	0.0553	0.1449	958.35	0.3038	960.00	0.5303	1033.77	0.6814	988.52	0.8326	920.49
-0.7710	0.0423	-0.9740	0.0539	0.1469	951.05	0.3069	1000.00	0.5326	1041.81	0.6837	988.57	0.8348	914.46
-0.7740	0.0440	-0.9770	0.0580	0.1488	941.94	0.3837	990.30	0.5348	1041.29	0.6859	1005.34	0.8370	911.66
-0.7770	0.0435	-0.9800	0.0604	0.1508	920.67	0.3859	991.02	0.5370	1044.95	0.6881	988.91	0.8392	916.59
-0.7800	0.0423	-0.9830	0.0568	0.1527	917.90	0.3881	991.87	0.5392	1041.60	0.6903	980.47	0.8414	904.98
-0.7830	0.0333	-0.9860	0.0579	0.1546	897.62	0.3904	994.38	0.5415	1046.00	0.6926	967.55	0.8437	898.79
-0.7860	0.0309	-0.9890	0.0593	0.1566	884.32	0.3926	998.05	0.5437	1046.98	0.6948	968.20	0.8459	906.70
-0.7890	0.0319	-0.9920	0.0707	0.1585	879.35	0.3948	1002.55	0.5459	1065.86	0.6970	970.41	0.8481	924.17
-0.7920	0.0287			0.1605	865.30	0.3970	1017.83	0.5481	1068.06	0.6992	972.06	0.8503	925.72
-0.7950	0.0251			0.1624	873.69	0.3992	1024.19	0.5503	1065.77	0.7014	956.32	0.8526	899.09
-0.7980	0.0227	CASE Z – Nu		0.1643	876.69	0.4015	1041.44	0.5526	1065.53	0.7037	953.62	0.8548	904.07
-0.8010	0.0274			0.1663	889.47	0.4037	1038.73	0.5548	1083.12	0.7059	965.49	0.8570	922.01
-0.8040	0.0262	X/SL	Nu	0.1682	854.14	0.4059	1015.76	0.5570	1080.62	0.7081	971.70	0.8592	904.49
-0.8070	0.0317	0.0384	948.44	0.1701	850.20	0.4081	1021.02	0.5592	1068.37	0.7103	968.41	0.8614	896.77
-0.8100	0.0416	0.0403	956.67	0.1721	834.07	0.4104	1025.50	0.5615	1070.34	0.7126	948.26	0.8637	888.14
-0.8130	0.0458	0.0422	1029.28	0.1740	844.64	0.4126	1030.86	0.5637	1074.56	0.7148	963.63	0.8659	893.37
-0.8160	0.0358	0.0442	1073.42	0.1760	839.17	0.4148	1032.02	0.5659	1079.19	0.7170	969.65	0.8681	888.99
-0.8190	0.0350	0.0461	1085.06	0.1779	833.19	0.4170	1029.24	0.5681	1083.95	0.7192	940.66	0.8703	882.27
-0.8220	0.0357	0.0481	1086.69	0.1798	830.60	0.4192	1015.87	0.5703	1081.05	0.7214	977.76	0.8726	870.66
-0.8250	0.0383	0.0500	1079.49	0.1818	818.21	0.4215	1018.45	0.5726	1096.16	0.7237	985.90	0.8748	852.76
-0.8280	0.0332	0.0519	1059.89	0.1837	827.72	0.4237	1021.81	0.5748	1086.51	0.7259	981.40	0.8770	852.11
-0.8310	0.0369	0.0539	1031.77	0.1856	815.04	0.4259	1014.54	0.5770	1088.75	0.7281	946.34	0.8792	851.13
-0.8340	0.0300	0.0558	1042.07	0.1876	807.09	0.4281	1012.53	0.5792	1084.26	0.7303	939.24	0.8814	853.96
-0.8370	0.0297	0.0577	1023.85	0.1895	817.20	0.4304	1021.29	0.5815	1086.68	0.7326	941.73	0.8837	864.76
-0.8400	0.0278	0.0597	999.36	0.1915	806.93	0.4326	1021.76	0.5837	1094.55	0.7348	943.75	0.8859	882.72
-0.8430	0.0369	0.0616	982.33	0.1934	814.21	0.4348	1013.29	0.5859	1075.42	0.7370	935.97	0.8881	905.71
-0.8460	0.0345	0.0636	970.24	0.1953	797.09	0.4370	1012.16	0.5881	1093.66	0.7392	933.06	0.8903	903.28
-0.8490	0.0383	0.0655	942.39	0.1973	798.83	0.4392	1020.32	0.5903	1072.86	0.7414	950.46	0.8926	905.51
-0.8520	0.0418	0.0674	925.01	0.1992	791.29	0.4415	1015.04	0.5926	1062.73	0.7437	941.00	0.8948	907.08
-0.8550	0.0450	0.0694	906.22	0.2011	786.63	0.4437	1019.27	0.5948	1071.43	0.7459	937.16	0.8970	915.57
-0.8580	0.0451	0.0713	892.18	0.2031	794.06	0.4459	1008.27	0.5970	1089.90	0.7481	945.70	0.8992	928.74
-0.8610	0.0615	0.0732	885.39	0.2050	791.03	0.4481	1010.89	0.5992	1062.99	0.7503	946.13	0.9014	959.59
-0.8640	0.0621	0.0752	877.30	0.2070	806.04	0.4503	1013.38	0.6015	1070.81	0.7526	946.28	0.9037	979.34
-0.8670	0.0547	0.0771	860.16	0.2089	777.74	0.4526	1011.46	0.6037	1103.31	0.7548	949.95	0.9059	981.62
-0.8700	0.0471	0.0791	849.40	0.2108	780.76	0.4548	997.01	0.6059	1059.69	0.7570	939.99	0.9081	979.89
-0.8730	0.0431	0.0810	843.01	0.2128	777.73	0.4570	1000.86	0.6081	1045.17	0.7592	940.30	0.9103	981.23
-0.8760	0.0439	0.0829	831.21	0.2147	762.30	0.4592	1011.23	0.6103	1049.77	0.7614	944.73	0.9126	990.10
-0.8790	0.0367	0.0849	813.09	0.2166	755.99	0.4615	1014.58	0.6126	1069.59	0.7637	938.93	0.9148	997.23
-0.8820	0.0413	0.0868	805.90	0.2186	751.89	0.4637	1007.11	0.6148	1053.26	0.7659	925.08	0.9170	1003.07
-0.8840	0.0393	0.0888	793.59	0.2205	741.93	0.4659	1015.43	0.6170	1048.00	0.7681	913.88	0.9192	1005.34
-0.8870	0.0376	0.0907	784.37	0.2225	746.38	0.4681	1017.38	0.6192	1056.15	0.7703	915.08	0.9214	1015.15
-0.8900	0.0395	0.0926	773.04	0.2244	744.25	0.4703	1016.58	0.6215	1054.18	0.7726	922.45	0.9237	1028.59
-0.8930	0.0474	0.0946	762.20	0.2263	745.43	0.4726	1016.50	0.6237	1050.07	0.7748	920.99	0.9259	1044.32
-0.8960	0.0491	0.0965	762.65	0.2283	740.41	0.4748	1011.79	0.6259	1030.92	0.7770	905.20	0.9281	1051.58
-0.8990	0.0519	0.0984	757.16	0.2302	733.63	0.4770	1016.87	0.6281	1032.39	0.7792	925.13	0.9303	1061.19

Appendix 7.2 – Data for Spanwise Averaged Nusselt Number and Film Cooling Effectiveness

0.9325	1070.01	-0.3080	592.69	-0.5405	537.43	-0.7439	540.52	-0.9473	671.90	0.1290	0.1530	0.2780	0.3310
0.9348	1081.56	-0.3110	584.04	-0.5435	538.66	-0.7469	538.34	-0.9503	677.63	0.1310	0.1690	0.2810	0.3370
0.9370	1105.05	-0.3150	570.87	-0.5465	538.61	-0.7499	540.13	-0.9533	686.67	0.1330	0.2250	0.2850	0.3390
0.9392	1118.00	-0.3180	594.31	-0.5494	540.02	-0.7529	538.04	-0.9563	696.27	0.1350	0.2450	0.2880	0.3060
0.9414	1125.40	-0.3220	557.15	-0.5524	540.53	-0.7559	537.04	-0.9593	705.34	0.1370	0.2300	0.2910	0.2910
0.9437	1131.95	-0.3250	581.62	-0.5554	540.36	-0.7588	535.61	-0.9623	711.04	0.1390	0.2260	0.2940	0.2890
0.9459	1141.26	-0.3290	557.38	-0.5584	540.86	-0.7618	536.80	-0.9653	717.47	0.1410	0.2400	0.2970	0.3060
0.9481	1159.13	-0.3320	575.64	-0.5614	539.80	-0.7648	537.69	-0.9683	724.41	0.1430	0.2530	0.3010	0.2910
0.9503	1179.84	-0.3360	573.11	-0.5644	544.27	-0.7678	537.62	-0.9712	730.67	0.1450	0.2600	0.3040	0.2940
0.9525	1191.23	-0.3390	549.77	-0.5674	544.98	-0.7708	537.75	-0.9742	735.72	0.1470	0.2320	0.3070	0.2800
0.9548	1195.76	-0.3430	574.57	-0.5704	546.51	-0.7738	538.00	-0.9772	747.10	0.1490	0.2380	0.3840	0.2200
0.9570	1215.89	-0.3460	548.40	-0.5734	543.21	-0.7768	536.14	-0.9802	759.16	0.1510	0.2340	0.3860	0.2190
0.9592	1264.40	-0.3500	585.16	-0.5764	537.19	-0.7798	536.04	-0.9832	769.54	0.1530	0.2240	0.3880	0.2230
		-0.3530	553.91	-0.5794	538.51	-0.7828	535.23	-0.9862	780.55	0.1550	0.2120	0.3900	0.2300
		-0.3570	565.82	-0.5823	538.50	-0.7858	535.80	-0.9892	788.05	0.1570	0.2050	0.3930	0.2270
X/PL	Nu	-0.3610	566.21	-0.5853	539.86	-0.7888	534.93	-0.9922	800.28	0.1590	0.2060	0.3950	0.2270
-0.0103	831.33	-0.3640	567.78	-0.5883	542.27	-0.7918	535.76			0.1600	0.2100	0.3970	0.2370
-0.0188	843.08	-0.3680	579.38	-0.5913	544.47	-0.7947	536.19			0.1620	0.2190	0.3990	0.2220
-0.0274	879.01	-0.3710	553.36	-0.5943	543.23	-0.7977	536.06			0.1640	0.2270	0.4010	0.2240
-0.0359	905.82	-0.3750	576.48	-0.5973	540.31	-0.8007	535.92			0.1660	0.2250	0.4040	0.2270
-0.0445	899.45	-0.3780	550.39	-0.6003	542.73	-0.8037	535.21			0.1680	0.2160	0.4060	0.2200
-0.0530	897.39	-0.3820	570.22	-0.6033	543.47	-0.8067	535.44			0.1700	0.2170	0.4080	0.2250
-0.0616	884.70	-0.3850	566.42	-0.6063	544.94	-0.8097	536.24			0.1720	0.2020	0.4100	0.2180
-0.0701	861.06	-0.3890	556.68	-0.6093	546.19	-0.8127	536.94			0.1740	0.2160	0.4130	0.2150
-0.0787	825.70	-0.3920	565.12	-0.6123	544.83	-0.8157	537.07			0.1760	0.2160	0.4150	0.2180
-0.0872	798.70	-0.3960	544.68	-0.6153	544.04	-0.8187	537.70			0.1780	0.2210	0.4170	0.2180
-0.0958	784.02	-0.3990	566.65	-0.6182	546.44	-0.8217	537.92			0.1800	0.2250	0.4190	0.2160
-0.1040	741.12	-0.4030	544.40	-0.6212	547.77	-0.8247	538.21			0.1820	0.2260	0.4210	0.2140
-0.1130	739.14	-0.4060	568.33	-0.6242	548.27	-0.8277	537.74			0.1840	0.2230	0.4240	0.2190
-0.1210	707.78	-0.4100	554.09	-0.6272	548.94	-0.8306	538.65			0.1860	0.2200	0.4260	0.2160
-0.1300	703.71	-0.4130	551.24	-0.6302	544.95	-0.8336	538.60			0.1880	0.2230	0.4280	0.2110
-0.1390	677.34	-0.4170	563.25	-0.6332	544.06	-0.8366	539.55			0.1900	0.2260	0.4300	0.2140
-0.1470	671.37	-0.4200	545.18	-0.6362	544.53	-0.8396	541.37			0.1910	0.2230	0.4330	0.2120
-0.1560	654.95	-0.4240	560.29	-0.6392	546.38	-0.8426	543.27			0.1930	0.2300	0.4350	0.2120
-0.1640	637.30	-0.4270	546.82	-0.6422	546.52	-0.8456	545.87			0.1950	0.2230	0.4370	0.2060
-0.1730	648.29	-0.4310	551.33	-0.6452	546.88	-0.8486	547.30			0.1970	0.2210	0.4390	0.2110
-0.1810	627.39	-0.4350	560.62	-0.6482	549.45	-0.8516	547.93			0.1990	0.2170	0.4410	0.2060
-0.1900	634.20	-0.4380	557.90	-0.6512	549.39	-0.8546	548.22			0.2010	0.2190	0.4440	0.2050
-0.1980	620.39	-0.4420	563.48	-0.6541	555.02	-0.8576	548.48			0.2030	0.2230	0.4460	0.2000
-0.2020	621.65	-0.4450	549.00	-0.6571	558.01	-0.8606	549.78			0.2050	0.2280	0.4480	0.2030
-0.2050	607.58	-0.4490	567.18	-0.6601	555.29	-0.8636	550.60			0.2070	0.2350	0.4500	0.2030
-0.2090	589.97	-0.4520	554.39	-0.6631	553.62	-0.8665	552.09			0.2090	0.2200	0.4530	0.2020
-0.2130	589.26	-0.4560	558.89	-0.6661	553.01	-0.8695	555.40			0.2110	0.2200	0.4550	0.1910
-0.2160	568.49	-0.4590	549.29	-0.6691	552.76	-0.8725	555.90			0.2130	0.2310	0.4570	0.2000
-0.2200	588.70	-0.4630	549.65	-0.6721	553.32	-0.8755	558.52			0.2150	0.2250	0.4590	0.1970
-0.2230	549.15	-0.4660	557.02	-0.6751	553.22	-0.8785	564.80			0.2170	0.2220	0.4610	0.1960
-0.2270	558.58	-0.4700	551.66	-0.6781	551.94	-0.8815	569.43			0.2190	0.2270	0.4640	0.1930
-0.2300	554.03	-0.4730	555.24	-0.6811	552.71	-0.8845	569.04			0.2210	0.2230	0.4660	0.2030
-0.2340	551.01	-0.4806	539.63	-0.6841	554.36	-0.8875	573.90			0.2220	0.2280	0.4680	0.1960
-0.2370	566.18	-0.4836	539.85	-0.6871	553.44	-0.8905	577.29			0.2240	0.2230	0.4700	0.1920
-0.2410	542.54	-0.4866	538.51	-0.6900	551.81	-0.8935	582.44			0.2260	0.2320	0.4730	0.1960
-0.2440	575.15	-0.4896	539.52	-0.6930	553.08	-0.8965	585.53			0.2280	0.2270	0.4750	0.1870
-0.2480	561.82	-0.4926	538.45	-0.6960	554.04	-0.8995	587.32			0.2300	0.2280	0.4770	0.1840
-0.2510	580.92	-0.4956	537.15	-0.6990	560.33	-0.9024	591.94			0.2320	0.2240	0.4790	0.1810
-0.2550	574.81	-0.4986	537.94	-0.7020	553.03	-0.9054	597.26			0.2330	0.2270	0.4810	0.1880
-0.2580	580.43	-0.5016	541.14	-0.7050	550.63	-0.9084	600.28			0.2370	0.2260	0.4840	0.1920
-0.2620	599.15	-0.5046	543.01	-0.7080	549.25	-0.9114	600.45			0.2400	0.2330	0.4860	0.1770
-0.2650	589.54	-0.5076	540.93	-0.7110	548.44	-0.9144	605.31			0.2430	0.2360	0.4880	0.1820
-0.2690	616.58	-0.5106	541.93	-0.7140	548.93	-0.9174	609.00			0.2460	0.2300	0.4900	0.1810
-0.2720	603.62	-0.5135	540.36	-0.7170	547.49	-0.9204	612.67			0.2490	0.2430	0.4930	0.1810
-0.2760	627.51	-0.5165	540.08	-0.7200	545.51	-0.9234	617.89			0.2530	0.2420	0.4950	0.1730
-0.2790	620.28	-0.5195	540.43	-0.7230	544.98	-0.9264	627.48			0.2560	0.2430	0.4970	0.1760
-0.2830	621.01	-0.5225	541.16	-0.7259	541.71	-0.9294	634.82			0.2590	0.2540	0.4990	0.1760
-0.2870	619.09	-0.5255	540.19	-0.7289	541.87	-0.9324	637.96			0.2620	0.2620	0.5010	0.1750
-0.2900	595.90	-0.5285	540.02	-0.7319	543.59	-0.9353	642.91			0.2650	0.2700	0.5040	0.1720
-0.2940	606.72	-0.5315	537.39	-0.7349	546.14	-0.9383	652.89			0.2690	0.2690	0.5060	0.1740
-0.2970	581.84	-0.5345	537.76	-0.7379	542.30	-0.9413	660.02			0.2720	0.2850	0.5080	0.1650
-0.3010	615.47	-0.5375	536.78	-0.7409	540.93	-0.9443	666.06			0.2750	0.3210	0.5100	0.1640
-0.3040	621.60												

CASE Z – η

X/SL η

0.0384	0.4050
0.0403	0.3960
0.0422	0.4020
0.0442	0.3920
0.0461	0.3780
0.0481	0.3640
0.0500	0.3480
0.0519	0.3350
0.0539	0.3170
0.0558	0.3220
0.0577	0.3110
0.0597	0.2960
0.0616	0.2860
0.0636	0.2780
0.0655	0.2600
0.0674	0.2480
0.0694	0.2340
0.0713	0.2230
0.0732	0.2170
0.0752	0.2100
0.0771	0.1940
0.0791	0.1850
0.0810	0.1780
0.0829	0.1670
0.0849	0.1530
0.0868	0.1470
0.0888	0.1350
0.0907	0.1280
0.0926	0.1230
0.0946	0.1170
0.0965	0.1220
0.0984	0.1190
0.1000	0.1200
0.1020	0.1220
0.1040	0.1250
0.1060	0.1140
0.1080	0.1220
0.1100	0.1320
0.1120	0.1240
0.1140	0.1210
0.1160	0.1210
0.1180	0.1260
0.1200	0.1300
0.1220	0.1250
0.1240	0.1330
0.1260	0.1330
0.1280	0.1460

Appendix 7.2 – Data for Spanwise Averaged Nusselt Number and Film Cooling Effectiveness

0.5130	0.1700	0.6640	0.1340	0.8150	0.0631	-0.0274	0.4120	-0.3680	0.1860	-0.5760	0.0622	-0.7800	0.0120
0.5150	0.1770	0.6660	0.1400	0.8170	0.0692	-0.0359	0.4080	-0.3710	0.1260	-0.5790	0.0637	-0.7830	0.0084
0.5170	0.1740	0.6680	0.1340	0.8190	0.0678	-0.0445	0.4130	-0.3750	0.1870	-0.5820	0.0661	-0.7860	0.0079
0.5190	0.1720	0.6700	0.1360	0.8210	0.0639	-0.0530	0.4110	-0.3780	0.1180	-0.5850	0.0678	-0.7890	0.0089
0.5210	0.1600	0.6730	0.1300	0.8240	0.0654	-0.0616	0.4020	-0.3820	0.1760	-0.5880	0.0634	-0.7920	0.0081
0.5240	0.1570	0.6750	0.1370	0.8260	0.0703	-0.0701	0.3830	-0.3850	0.1360	-0.5910	0.0636	-0.7950	0.0086
0.5260	0.1560	0.6770	0.1330	0.8280	0.0683	-0.0787	0.3660	-0.3890	0.1070	-0.5940	0.0621	-0.7980	0.0077
0.5280	0.1570	0.6790	0.1330	0.8300	0.0682	-0.0872	0.3450	-0.3920	0.1430	-0.5970	0.0563	-0.8010	0.0079
0.5300	0.1580	0.6810	0.1240	0.8330	0.0692	-0.0958	0.3310	-0.3960	0.1110	-0.6000	0.0556	-0.8040	0.0056
0.5330	0.1570	0.6840	0.1240	0.8350	0.0593	-0.1040	0.3060	-0.3990	0.1520	-0.6030	0.0572	-0.8070	0.0056
0.5350	0.1490	0.6860	0.1360	0.8370	0.0622	-0.1130	0.3030	-0.4030	0.1970	-0.6060	0.0581	-0.8100	0.0035
0.5370	0.1480	0.6880	0.1210	0.8390	0.0596	-0.1210	0.2920	-0.4060	0.1640	-0.6090	0.0580	-0.8130	0.0051
0.5390	0.1490	0.6900	0.1210	0.8410	0.0535	-0.1300	0.2820	-0.4090	0.1060	-0.6120	0.0577	-0.8160	0.0046
0.5410	0.1480	0.6930	0.1170	0.8440	0.0508	-0.1390	0.2850	-0.4120	0.0737	-0.6150	0.0550	-0.8190	0.0044
0.5440	0.1460	0.6950	0.1190	0.8460	0.0567	-0.1470	0.2860	-0.4150	0.0617	-0.6180	0.0580	-0.8220	0.0045
0.5460	0.1490	0.6970	0.1170	0.8480	0.0653	-0.1560	0.2910	-0.4180	0.0633	-0.6210	0.0588	-0.8250	0.0042
0.5480	0.1520	0.6990	0.1270	0.8500	0.0619	-0.1640	0.2820	-0.4210	0.0698	-0.6240	0.0584	-0.8280	0.0039
0.5500	0.1500	0.7010	0.1110	0.8530	0.0466	-0.1730	0.2850	-0.4240	0.0698	-0.6270	0.0588	-0.8310	0.0050
0.5530	0.1410	0.7040	0.1170	0.8550	0.0482	-0.1810	0.2830	-0.4270	0.0711	-0.6300	0.0541	-0.8340	0.0052
0.5550	0.1450	0.7060	0.1180	0.8570	0.0483	-0.1900	0.2790	-0.4300	0.0701	-0.6330	0.0527	-0.8370	0.0067
0.5570	0.1440	0.7080	0.1170	0.8590	0.0324	-0.1980	0.2830	-0.4330	0.0758	-0.6360	0.0526	-0.8400	0.0068
0.5590	0.1460	0.7100	0.1180	0.8610	0.0248	-0.2020	0.2820	-0.4360	0.0747	-0.6390	0.0504	-0.8430	0.0058
0.5610	0.1460	0.7130	0.1100	0.8640	0.0236	-0.2050	0.2900	-0.4390	0.0907	-0.6420	0.0526	-0.8460	0.0055
0.5640	0.1380	0.7150	0.1220	0.8660	0.0249	-0.2090	0.2860	-0.4420	0.0855	-0.6450	0.0524	-0.8490	0.0094
0.5660	0.1380	0.7170	0.1210	0.8680	0.0242	-0.2130	0.2830	-0.4450	0.0834	-0.6480	0.0542	-0.8520	0.0088
0.5680	0.1470	0.7190	0.1080	0.8700	0.0245	-0.2160	0.2700	-0.4480	0.0822	-0.6510	0.0523	-0.8550	0.0072
0.5700	0.1460	0.7210	0.1240	0.8730	0.0134	-0.2200	0.2560	-0.4510	0.0798	-0.6540	0.0595	-0.8580	0.0081
0.5730	0.1490	0.7240	0.1280	0.8750	0.0070	-0.2230	0.2350	-0.4540	0.0782	-0.6570	0.0628	-0.8610	0.0093
0.5750	0.1390	0.7260	0.1210	0.8770	0.0041	-0.2270	0.2230	-0.4570	0.0783	-0.6600	0.0614	-0.8640	0.0129
0.5770	0.1450	0.7280	0.1010	0.8790	0.0028	-0.2300	0.2280	-0.4600	0.0693	-0.6630	0.0575	-0.8670	0.0108
0.5790	0.1340	0.7300	0.1100	0.8810	0.0048	-0.2340	0.2390	-0.4630	0.0671	-0.6660	0.0569	-0.8700	0.0090
0.5810	0.1380	0.7330	0.1000	0.8840	0.0115	-0.2370	0.2740	-0.4660	0.0602	-0.6690	0.0540	-0.8730	0.0094
0.5840	0.1500	0.7350	0.1030	0.8860	0.0171	-0.2410	0.2560	-0.4690	0.0659	-0.6720	0.0574	-0.8760	0.0083
0.5860	0.1450	0.7370	0.0956	0.8880	0.0200	-0.2440	0.2700	-0.4720	0.0666	-0.6750	0.0597	-0.8790	0.0070
0.5880	0.1570	0.7390	0.0982	0.8900	0.0161	-0.2480	0.2620	-0.4750	0.0697	-0.6780	0.0574	-0.8820	0.0094
0.5900	0.1410	0.7410	0.1060	0.8930	0.0125	-0.2510	0.2680	-0.4780	0.0657	-0.6810	0.0534	-0.8840	0.0085
0.5930	0.1320	0.7440	0.0972	0.8950	0.0202	-0.2550	0.2690	-0.4810	0.0714	-0.6840	0.0546	-0.8870	0.0077
0.5950	0.1430	0.7460	0.0992	0.8970	0.0200	-0.2580	0.2610	-0.4840	0.0704	-0.6870	0.0530	-0.8900	0.0085
0.5970	0.1530	0.7480	0.1020	0.8990	0.0234	-0.2620	0.2630	-0.4870	0.0687	-0.6900	0.0566	-0.8930	0.0116
0.5990	0.1470	0.7500	0.1020	0.9010	0.0340	-0.2650	0.2620	-0.4900	0.0732	-0.6930	0.0618	-0.8960	0.0141
0.6010	0.1590	0.7530	0.1010	0.9040	0.0349	-0.2690	0.2600	-0.4930	0.0663	-0.6960	0.0610	-0.8990	0.0146
0.6040	0.1700	0.7550	0.1050	0.9060	0.0375	-0.2720	0.2650	-0.4960	0.0615	-0.6990	0.0621	-0.9020	0.0164
0.6060	0.1540	0.7570	0.0858	0.9080	0.0410	-0.2760	0.2610	-0.4990	0.0641	-0.7020	0.0573	-0.9050	0.0140
0.6080	0.1490	0.7590	0.0859	0.9100	0.0398	-0.2790	0.2670	-0.5020	0.0653	-0.7050	0.0503	-0.9080	0.0190
0.6100	0.1530	0.7610	0.0980	0.9130	0.0357	-0.2830	0.2660	-0.5050	0.0683	-0.7080	0.0490	-0.9110	0.0216
0.6130	0.1650	0.7640	0.1020	0.9150	0.0348	-0.2870	0.2770	-0.5080	0.0642	-0.7110	0.0462	-0.9140	0.0195
0.6150	0.1570	0.7660	0.0989	0.9170	0.0374	-0.2900	0.2550	-0.5110	0.0672	-0.7140	0.0441	-0.9170	0.0184
0.6170	0.1590	0.7680	0.0859	0.9190	0.0345	-0.2940	0.2600	-0.5140	0.0638	-0.7170	0.0435	-0.9200	0.0158
0.6190	0.1490	0.7700	0.0868	0.9210	0.0367	-0.2970	0.2120	-0.5170	0.0684	-0.7200	0.0360	-0.9230	0.0140
0.6210	0.1460	0.7730	0.0918	0.9240	0.0388	-0.3010	0.2140	-0.5200	0.0638	-0.7230	0.0389	-0.9260	0.0195
0.6240	0.1470	0.7750	0.0964	0.9260	0.0444	-0.3040	0.2000	-0.5230	0.0620	-0.7260	0.0337	-0.9290	0.0215
0.6260	0.1480	0.7770	0.0799	0.9280	0.0459	-0.3080	0.2020	-0.5260	0.0633	-0.7290	0.0328	-0.9320	0.0185
0.6280	0.1490	0.7790	0.0921	0.9300	0.0516	-0.3110	0.1820	-0.5290	0.0658	-0.7320	0.0299	-0.9350	0.0203
0.6300	0.1520	0.7810	0.0840	0.9330	0.0536	-0.3150	0.1660	-0.5310	0.0655	-0.7350	0.0329	-0.9380	0.0227
0.6330	0.1500	0.7840	0.0843	0.9350	0.0544	-0.3180	0.1950	-0.5340	0.0616	-0.7380	0.0312	-0.9410	0.0232
0.6350	0.1410	0.7860	0.0860	0.9370	0.0659	-0.3220	0.1540	-0.5370	0.0604	-0.7410	0.0229	-0.9440	0.0239
0.6370	0.1410	0.7880	0.0840	0.9390	0.0757	-0.3250	0.2010	-0.5400	0.0593	-0.7440	0.0212	-0.9470	0.0215
0.6390	0.1680	0.7900	0.0825	0.9410	0.0745	-0.3290	0.1410	-0.5430	0.0570	-0.7470	0.0204	-0.9500	0.0193
0.6410	0.1550	0.7930	0.0835	0.9440	0.0738	-0.3320	0.1890	-0.5460	0.0600	-0.7500	0.0221	-0.9530	0.0217
0.6440	0.1600	0.7950	0.0763	0.9460	0.0757	-0.3360	0.1670	-0.5490	0.0594	-0.7530	0.0164	-0.9560	0.0276
0.6460	0.1420	0.7970	0.0855	0.9480	0.0859	-0.3390	0.1410	-0.5520	0.0584	-0.7560	0.0138	-0.9590	0.0333
0.6480	0.1410	0.7990	0.0755	0.9500	0.0969	-0.3430	0.1860	-0.5550	0.0569	-0.7590	0.0119	-0.9620	0.0292
0.6500	0.1410	0.8010	0.0701	0.9530	0.1040	-0.3460	0.1380	-0.5580	0.0553	-0.7620	0.0131	-0.9650	0.0254
0.6530	0.1440	0.8040	0.0772	0.9550	0.1080	-0.3500	0.2200	-0.5610	0.0537	-0.7650	0.0149	-0.9680	0.0216
0.6550	0.1550	0.8060	0.0849	0.9570	0.1210	-0.3530	0.1570	-0.5640	0.0648	-0.7680	0.0153	-0.9710	0.0167
0.6570	0.1530	0.8080	0.0893	0.9590	0.1540	-0.3570	0.1820	-0.5670	0.0649	-0.7710	0.0123	-0.9740	0.0117
0.6590	0.1490	0.8100	0.0832			-0.3610	0.1850	-0.5700	0.0673	-0.7740	0.0145	-0.9770	0.0142
0.6610	0.1380	0.8130	0.0555	X/PL	η	-0.3640	0.1940	-0.5730	0.0646	-0.7770	0.0138	-0.9800	0.0161

Appendix 7.2 – Data for Spanwise Averaged Nusselt Number and Film Cooling Effectiveness

-0.9830	0.0139
-0.9860	0.0104
-0.9890	0.0055
-0.9920	0.0084

REPORT DOCUMENTATION PAGE			Form Approved OMB No. 0704-0188	
Public reporting burden for this collection of information is estimated to average 1 hour per response, including the time for reviewing instructions, searching existing data sources, gathering and maintaining the data needed, and completing and reviewing the collection of information. Send comments regarding this burden estimate or any other aspect of this collection of information, including suggestions for reducing this burden, to Washington Headquarters Services, Directorate for Information Operations and Reports, 1215 Jefferson Davis Highway, Suite 1204, Arlington, VA 22202-4302, and to the Office of Management and Budget, Paperwork Reduction Project (0704-0188), Washington, DC 20503.				
1. AGENCY USE ONLY (Leave blank)	2. REPORT DATE February 2000	3. REPORT TYPE AND DATES COVERED Final Contractor Report		
4. TITLE AND SUBTITLE Unsteady High Turbulence Effects on Turbine Blade Film Cooling Heat Transfer Performance Using a Transient Liquid Crystal Technique		5. FUNDING NUMBERS WU-714-01-4A-00 NAG3-1656		
6. AUTHOR(S) J.C. Han, S.V. Ekkad, H. Du, and S. Teng				
7. PERFORMING ORGANIZATION NAME(S) AND ADDRESS(ES) Texas A&M University College Station, Texas 77843-3123		8. PERFORMING ORGANIZATION REPORT NUMBER E-12173		
9. SPONSORING/MONITORING AGENCY NAME(S) AND ADDRESS(ES) National Aeronautics and Space Administration John H. Glenn Research Center at Lewis Field Cleveland, Ohio 44135-3191		10. SPONSORING/MONITORING AGENCY REPORT NUMBER NASA CR-2000-209929		
11. SUPPLEMENTARY NOTES Project Manager, Philip Poinatte, Turbomachinery and Propulsion Systems Division, NASA Glenn Research Center, organization code 5820, (216) 433-5898.				
12a. DISTRIBUTION/AVAILABILITY STATEMENT Unclassified - Unlimited Subject Categories: 02, 07, and 34 This publication is available from the NASA Center for AeroSpace Information, (301) 621-0390.		12b. DISTRIBUTION CODE Distribution: Nonstandard		
13. ABSTRACT (Maximum 200 words) Unsteady wake effect, with and without trailing edge ejection, on detailed heat transfer coefficient and film cooling effectiveness distributions is presented for a downstream film-cooled gas turbine blade. Tests were performed on a five-blade linear cascade at an exit Reynolds number of 5.3×10^5 . Upstream unsteady wakes were simulated using a spoke-wheel type wake generator. Coolant blowing ratio was varied from 0.4 to 1.2; air and CO ₂ were used as coolants to simulate different density ratios. Surface heat transfer and film effectiveness distributions were obtained using a transient liquid crystal technique; coolant temperature profiles were determined with a cold wire technique. Results show that Nusselt numbers for a film cooled blade are much higher compared to a blade without film injection. Unsteady wake slightly enhances Nusselt numbers but significantly reduces film effectiveness versus no wake cases. Nusselt numbers increase only slightly but film cooling effectiveness increases significantly with increasing blowing ratio. Higher density coolant (CO ₂) provides higher effectiveness at higher blowing ratios ($M = 1.2$) whereas lower density coolant (Air) provides higher effectiveness at lower blowing ratios ($M = 0.8$). Trailing edge ejection generally has more effect on film effectiveness than on the heat transfer, typically reducing film effectiveness and enhancing heat transfer. Similar data is also presented for a film cooled cylindrical leading edge model.				
14. SUBJECT TERMS Film cooling; Heat transfer; Gas turbine; Heat transfer; Turbulent heat transfer; Turbomachinery; Heat transfer coefficient		15. NUMBER OF PAGES 227		
		16. PRICE CODE All		
17. SECURITY CLASSIFICATION OF REPORT Unclassified	18. SECURITY CLASSIFICATION OF THIS PAGE Unclassified	19. SECURITY CLASSIFICATION OF ABSTRACT Unclassified	20. LIMITATION OF ABSTRACT	